THE DETERMINATION OF SURFACE DEFORMATIONS BY HOLOGRAPHIC-ELECTRO-OPTICAL PROCESSING

by

© K. REZAI, M. Eng.

A thesis submitted to the Faculty of Graduate Studies and Research in partial fulfillment of the requirements for the Degree of Doctor of Philosophy

Micromechanics of Solids Laboratory
Department of Mechanical Engineering
McGill University
Montreal, Quebec
Canada

May 1981

Department of
Mechanical Engineering

Ph.D. Thesis
May 1981

ABSTRACT

This thesis is concerned with the experimental determination of surface displacements of material foils by means of an automatic evaluation of the holographic interferograms obtained in testing. The experimental work utilizes a newly developed method referred to as the "holographic-electro-optical" technique that employs a specially designed microcomputer unit. The experimental procedure and the microcomputer organization are fully described. The application of this technique is illustrated by the evaluation of strain field and thickness changes at a large number of points on both sides of a commercial newsprint paper sample subjected to uniaxial loads. Furthermore, a new quantity called the "volumetric mass density" is introduced for this material for the first time that is experimentally evaluated and correlated to the obtained strain field. In the conclusion of this thesis general remarks concerning the holographic-electro-optical technique are given and the obtained results for the newsprint sample and future research are indicated.

Département de
génie mécanique

Thèse Doctorale
Mai 1981

RÉSUMÉ

L'objet de cette thèse est la détermination expérimentale des déplacements à la surface d'une feuille par l'utilisation de l'holographie interférométrique comprenant une étape de reconstruction automatisée. Cette technique, appelée "holographic-electro-optical" a nécessité la conception d'un microprocesseur; celui-ci, de même que son incorporation à la nouvelle méthode son présentés en détail. En guise d'exemple, cette méthode est utilisée pour la détermination des déformations et de la variation de l'épaisseur d'un échantillon de papier journal, de fabrication commerciale, assujetti à des tensions uniaxiales. De plus, l'auteur définit une nouvelle quantité, la "densité volumique de masse", pour la première fois dans le cas du papier. Celle-ci, evaluée à partir de données experimentales, est correlée au champ des déformations. En conclusion de cette thèse, l'auteur fait quelques remarques générales concernant la technique "holographic-electro-optical", résume les résultats obtenus dans le cas du papier journal, et suggère des développements futurs.

ACKNOWLEDGEMENTS

The author wishes to express his sincere appreciation to his supervisor, Professor D.R. Axelrad. The successful completion of this thesis was due, in large part, to his constant encouragement and many useful suggestions which arose from discussions throughout the course of this work.

Special thanks are due to Professor J.W. Provan, who has contributed in many ways to the completion of this work, and to Dr. D. Atack, for his support and interest in this investigation.

The acknowledgements are further extended to Mr. S. Syed, who spent long days helping me with the construction and programming of the microcomputer unit, to Mr. B. Alaghehband for his useful ideas regarding the correlation coefficients and also to Mr. L. Achard, who supplied the French version of the Abstract.

Finally, sincere thanks are due to Mrs. V.R. Read, who did an excellent job in typing this thesis.

TABLE OF CONTENTS

LIST OF NOTATIONS

A	Absorbance of X-ray film
A_{ij}	Reconstruction geometry matrix
$\langle A \rangle^s$	Film absorbance averaged on step s of the handsheet
c	Exposure coefficient
$\hat{i},\hat{j},\hat{k}$	Unit vectors of the cartesian frame XYZ
$\underset{\sim}{k}_i$	Light propagation vectors
$\beta_{k_1,..}$	Correlation coefficients for row β of the paper sample
ℓ_i, m_i, n_i	Quantities contributing to the elements of A_{ij}
H_m	Mass of handsheet in a given area
N_m	Mass of newsprint paper in a given area
α_m	Mass of the sample at an observation point α
n	Number of observation points
$N-N_i$	Fringe number - fringenumber in the scanning direction i
$\underset{\sim}{r}$, $\underset{\sim}{R}$	Position vectors
R	Radius of the observation point
t	time - exposure time
H_T	Transmission factor for handsheet
N_T	Transmission factor for newsprint
$\underset{\sim}{u}$	General deformation vector
$\alpha u^{L,R}_{x,y,z}$	Components of deformation for point α of the sample in the directions X,Y or Z corresponding to the left side (L) or the right side (R) of the sample.

α_w	Basis weight (area mass density) at point α
$\langle w \rangle^s$	Basis weight averaged on step s of the hand-sheet
$\alpha_x, \alpha_y, \alpha_z$	Coordinates of an observation point α
α, β, γ	Angles between the scanning directions
δ	Phase difference
δ_r	Constant phase difference
$\alpha_{\varepsilon}{}^{R,L}_{xx,yy}$	xx or yy strain components for point α of the paper sample corresponding to the left side (L) or the right side (R) of the sample
θ	Angle between the sample and the holographic plate
$\kappa_{1,..,4}$	Correlation coefficients for the entire sample
λ	Laser wavelength
μ_x	Mean value of the random variable X
μ	Absorption coefficient
α_ρ	Volumetric mass density at point α of the paper sample
α_{ρ_u}	Value of α_ρ in the undeformed state
σ_x^2	Variance of the random variable X
σ_{xy}	Covariance of the random variables X and Y
$\phi(\cdot)$	Correlation function
ϕ_{o1} ; ϕ_{o2}	Light phase

LIST OF ILLUSTRATIONS

LIST OF TABLES

Chapter I

INTRODUCTION

It is well known that engineering materials have two distinct features. First, there exists a multitude of singular surfaces (interfaces) within a finite volume of the macroscopic material body, and second, the elements of the microstructure of real materials show random geometrical and physical characteristics. The very existence of the interfaces representing in fact the interaction zones between the elements of the microstructure renders the analysis of the response behaviour on the basis of continuum theory impossible. It has also been recognized that models, which comply with the axiomatics of continuum theory do not, in most cases, reflect the experimental observations of the behaviour of discrete materials.

The analytical aspects of various classes of discrete solids have been discussed in reference [1]. It has also been shown for a certain class of fibrous materials that their response behaviour can be modelled on the basis of the micromechanics theory [2].

It is the main aim of the present investigation to introduce a new holographic-electro-optical measurement technique, which by means of a fully computerized arrangement permits the assessment of the three-dimensional deformation field of these

thin foil materials with a microstructure. The method to be discussed in this thesis is applicable to various classes of materials, such as crystalline solids, composites and fibrous networks. In developing this technique, it has been found convenient to use the existing experimental set-up that has been designed for testing cellulose networks, in particular[3,4].

In view of the importance of newsprint paper in the papermaking industry, the new measurement technique will be illustrated by observations and measurements concerning newsprint paper. Another aspect of this thesis is concerned with the well known term "basis weight", which is employed in the paper industry and which defines the weight of the paper sheet per unit area. It has been found from the present investigation that it is more significant for the overall strength characteristics of a paper sheet to use a modified parameter, which will be referred to, in this thesis, as the "volumetric mass density (VMD)". Hence, it is one of the aims in the present work to assess the validity of this parameter in the description of the mechanical response behaviour of newsprint paper. For this particular material, the methods employed for the verification of the parameter is accomplished by means of Beta-radiography and double-sided

holographic interferometry (DSHI). It is the author's belief that the experimental procedure can also be employed for other thin foil materials such as metallic and/or polymeric structures.

The holographic interferometry technique has been developed over a number of years in the Micromechanics of Solids Laboratory [5], in order to evaluate the three-dimensional surface deformations of thin foils. It was then extended to the measurements of the occurring deformation field on both sides of thin foils in a sequential manner, such that the deformation history of the foil materials can also be obtained [4]. By means of this technique, it is possible to assess the local deformation components with very high accuracy (fractions of a micrometer). However, with the requirement of a large number of observations corresponding to a large number of surface points on both sides of a foil, it is evident that the test set-up has to be extended to a completely automated observation procedure. Hence, the main body of the thesis deals with this automated technique, which generally is applicable to any type of foil material and which permits the required data to be obtained from the produced interferograms.

It is to be noted that this new technique can be used for any arbitrary number of points on the object to be analyzed

and that all the measurements can be performed automatically in a self-consistent manner. As mentioned above, in order to illustrate this new technique tests were performed on newsprint paper sheets. In doing so, it was found useful, not only to assess the deformation field of the sample under a given load and controlled environmental conditions, but also to investigate the local behaviour of extremely small areas of the test sample by using scanning electron microscopy and the information obtained from Beta-radiography. Hence, in the discussion of the experimental results, an attempt is made in this thesis to relate the VMD (volumetric mass density) to the occurring deformations under a given load and hence to the local thickness. It is important that such considerations lead to a strength characteristic of the material sheet, which is significant to its overall response behaviour.

The structure of the thesis is as follows: Chapter II considers briefly the proposed models for the mechanical response of paper. The definition and meaning of volumetric mass density in relation to fibrous networks is also discussed. Chapter III deals in detail with the Sequential-DSHI technique (Sequential double-sided holographic interferometry) as well as the general analytical approach for the evaluation of the obtained interferograms. Chapter IV is concerned with the actual experi-

mental set up and the adopted method of investigation. The microcomputer organization and its application to the determination of the three-dimensional deformation field on both sides of thin foils (newsprint paper sheet) is fully described. The microcomputer design itself, and the necessary programming for the performance of the test are given in Appendices I and II. The newly developed optical technique of local thickness measurement and area mass density measurement are also discussed in Chapter IV, whilst the discussion of the obtained results is given in Chapter V. Finally, the concluding remarks and the indication of the future research are the subject matter of Chapter VI.

Chapter II

DISCUSSION ON THE RESPONSE BEHAVIOUR OF THIN FOILS WITH PARTICULAR REFERENCE TO FIBROUS NETWORKS

2.1 Introduction

Although macroscopic observations do not reflect the mechanical behaviour of fibrous networks, many investigators in this field have nevertheless attempted to explain the mechanical response behaviour of such systems in terms of macroscopic quantities [6-13]. The proposed analytical models in this context as well as the experimental observations are mainly concerned with the mechanical strength of the paper sheets. In the context of the present thesis, Page [14], Kallmes [15-17], Lyne [18] and others have proposed that paper weakness is associated with areas whose grammage is below the basis weight of the test sheet. In the case of newsprint, which is the material being considered in this thesis, this statement was confirmed by Moffat, et al.[19]. In these references test methods were employed to measure the basic parameters related to the paper strength. However, more recently, distinct emphasis has been made on the contribution of microstructural effects to the overall response behaviour of fibrous networks [20-24]. Thus, the currently held view is that the physical properties of individual fibres in the paper

sheet, their orientation with respect to the application of the load as well as the mutual bonding are the most significant parameters related to the strength of the material. Erickson [25] employed three layered samples, each layer being made of a different type of fibre and found that the selection of the layers affect the physical properties of the sheet. Stockmann [26] made the observation that a sheet of highly oriented fibres is much stronger than the one with uniform fibre orientation. In some other cases more attention was paid to the response of the single fibre and bonding. Thus, for instance, Kallmes, et al.[27] considered different strains induced in the free portion of a fibre segment than in the bonded part. On the assumption that their response is the same to an applied load, he found the variations in the sheet moduli, primarily, caused by the change in the fibre modulus. Somewhat similar models and experiments are due to Perkins, et al.[28] and Hollmark, et al[29] with the conclusion that the physical properties of the paper sheet are strongly influenced by the presence of the microstructure.

As mentioned previously, since these studies follow the classical continuum theory, the fibrous networks with a random arrangement of fibres and random bonding makes it impossible to

derive a response behaviour on the basis of macroscopic quantities. Hence, an analytical model attempting to describe the mechanical response should include the deformational behaviour and failure characteristics of bonded areas between overlapping fibres, the behaviour of the fibres themselves and its relation to the volumetric mass density of the paper sheet - the basic approach to such models from a micromechanics point of view is given by Axelrad [1] and in particular in references [30,31].

2.2 General Formulation - Material Modelling

To mention briefly the material modelling from the point of view of the micromechanics theory, a similar view is taken in the above mentioned references [1,30,31] as proposed earlier in [32-38]. The probabilistic concepts and statistical considerations introduced by the micromechanics theory have been used to represent the response behaviour of a cellulose network.

In particular, by using the principles of the micromechanics theory, Haddad [31] was able to consider the response behaviour of a two dimensional sheet (2-D sheet) of a random network of cellulose fibres. His formulation and modelling of the response of paper sheets took into consideration the characteristics of free fibre segments and the occurrence of the so-called "relative bonding areas in overlapping fibres". The investigation

showed the response of a real fibrous network with randomly arranged fibres and inter-fibre bonds, in contrast to the proposed theories by Kallmes, Corte and Bernier [32-36], whose model was based on an assumed random geometry of the 2-D sheet as a further step towards a proper modelling of the 2-D sheet. Wahren [39] introduced a random geometry of fibrous network by using the Monte-Carlo computing technique. From all these investigations, it appeared that one of the fundamental characteristics required in the modelling of the response behaviour of the paper sheet is the so-called "basis weight" of the material under consideration. It has been found important, during the investigations carried out in the Micromechanics of Solids Laboratory and in particular, in the context of the present work, to introduce the fundamental quantity of volumetric mass density instead. It is considered that this quantity, in relation to the occurring variation of the local thickness in a paper sheet can be directly correlated with the induced strain field caused by the application of a uniaxial load on the paper sheet. This will be treated in the subsequent sections of this thesis. The following sections (2.3 and 2.4) are concerned with the definitions and the corresponding testing procedures of the quantity w (basis weight) of the paper sheet.

2.3 Significance of the Basis Weight - Material Characteristics

Taking into consideration the present effort of assessing the strength characteristics of a fibrous network and in particular one of the cellulosic type, the overall mechanical strength must include not only the strength of an individual fibre, but also the fibre-fibre bonds, as well as the existence of a certain pore volume in the real sheet. The failure of a network can thus be ascribed, primarily, to the bond failure and to the failure of the individual fibres. With the application of probabilistic concepts to the behaviour of fibrous networks, hydrogen-bond failure of cellulosic networks has been studied by Axelrad [40]. Single fibre failure has been investigated by Page [41,42]. In all these papers, parameters like the number of bonds in an overlapping area and the number of intercepting fibres in a 2-D sheet play a significant role indicating that these quantities require a proper definition of the basis weight.

It is of utmost importance to note that the present work stresses the fact to use, instead of the commonly used basis weight definition, which is a weight per unit area, the necessity to introduce the volumetric mass density. Other reasons for introducing this material characteristic are the great variety of test procedures to establish it and not to standardize the procedure

in the performance of the necessary test. Furthermore, since real sheets consist of several layers of 2-D sheets, which form a given thickness, that has been observed to vary during the application of a load, requires the introduction of the VMD. The standard definition of the basis weight, as discussed in this section, is given below.

First, it is usual to define the structure of the paper in terms of a 2-D sheet, and secondly, to take the mass of the paper as a projection on an arbitrary plane as indicated in Fig.2.1.

Hence, the area mass density (basis weight) is defined by,

$$w = \frac{m}{a} \qquad - (2.1)$$

The simple experimental technique known as Beta-radiography, which serves to obtain the basis weight of a given sheet material is indicated below. However, in order to compare the basis weight of the given sheet of the material with a standard hand-sheet as carried out in this investigation, the sketch of the Beta-radiography technique is shown in Fig.2.2.

It is seen that the basis weight or the projection of the actual mass on the observing medium depends on the amount of Beta rays transmitted through the sheet. This can be expressed simply by,

$$\text{Transmittance: } \left.\begin{aligned} H_T &= f\,(H_m) \quad \text{for handsheet} \\ N_T &= f\,(N_m) \quad \text{for newsprint} \end{aligned}\right\} \quad - (2.2)$$

where the function f is of the exponential form. It is assumed that the transmittance of both materials and hence their response to the Beta-ray correspond to an approximately equal fibre structure.

As shown by Norman and Wahren [43], the X-ray film indicated in Fig.2.2 absorbs the Beta-rays over a certain period of time. In general, radioactive decay is a statistical phenomenon valid for a large number of particles, the radiation of which may be considered as a continuous wave with a constant amplitude and energy flux. One can define, in the case of a thin paper sample, the transmittance in the following form:

$$T = f(m) = e^{-\mu w} \quad - (2.3)$$

in which T is the transmission factor, μ is absorption coefficient and w is the basis weight of the sample. According to Norman and Wahren [43], this semi-empirical form is valid for the basis weight corresponding to 3-4 times of the half thickness of the paper sheet. At higher values of the basis weight, the rate of absorption increases to a maximum, which is reached, approximately, to 7-8 times of the half thickness of the sheet. It is to be noted that the

half thickness, is a function of the energy of the incident radiation and for the standard radioactive material C-14 is of the order of 30 g/m^2. Hence, one can expect a limit of the exponential absorption to be between 90-120 g/m^2. However, the directly measurable quantity is not the transmittance, but the absorption of the developed film, which is given by,

$$A = \ln \left(\frac{1}{T}\right) \qquad - (2.4)$$

If in the test procedure, the linear range of the X-ray film is used, the film absorbance will be proportional to the amount of radiations transmitted by the paper sample and hence, to the exposure time t and the above transmission factor T. It follows that the relation between these parameters can be given by,

$$A = c.t.e^{-\mu w} + A_\infty \qquad - (2.5)$$

in which A_∞ represents the absorbance of an exposed part of the film corresponding to an infinitely high basis weight, whilst c denotes an exposure coefficient and μ is the above absorption coefficient. Relation (2.5) can also be expressed for convenience as,

$$\ln (A - A_\infty) = \ln ct - \mu w \qquad - (2.6)$$

The above relation can be verified experimentally and is usually

employed in the standard assessment of the basis weight of paper sheets. Since it is the main aim in this thesis, to establish a more accurate technique for the assessment of the w both by definition and measurement, a modified procedure for the measurement of w will be given in Section 4.4.

2.4 Definition of the Volumetric Mass Density

It has been pointed out before that a more accurate quantity, required in the characterization of the strength of a fibrous network is the VMD or more briefly, denoted by $^{\alpha}\rho$ indicating that it is meant to be a "local quantity". This quantity can then be used to follow the statistics of the entire paper sample. Thus, consider the model for a small volume of a fibrous network, which has the VMD $^{\alpha}\rho$ ($\alpha = 1,\ldots,N$) as indicated in Fig. 2.3.

This density refers to a cylinder of radius R so that it is defined by,

$$^{\alpha}\rho = \frac{\alpha_m}{\pi R^2} \cdot \alpha_\tau^{-1} \qquad - (2.7)$$

where α is an index ($\alpha = 1,\ldots,N$), referring in micromechanics to an element of the structure, so that a large number of such elements can be accounted for, in a statistical approach. Referring to the previous given definition, the standard basis weight (area

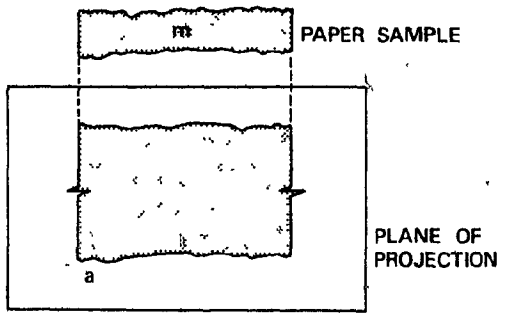

FIG. 2.1 AREA MASS DENSITY OF FIBROUS NETWORKS $w = \frac{m}{a}$

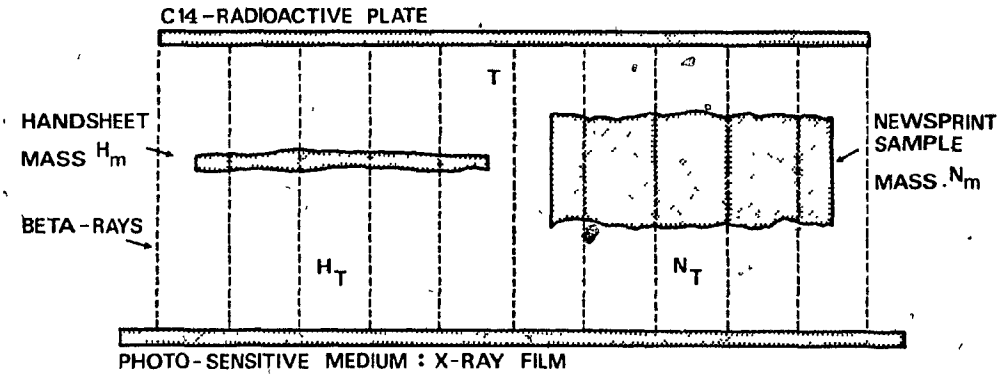

FIG. 2.2 SCHEMATICS OF BETA-RADIOGRAPHY TECHNIQUE.

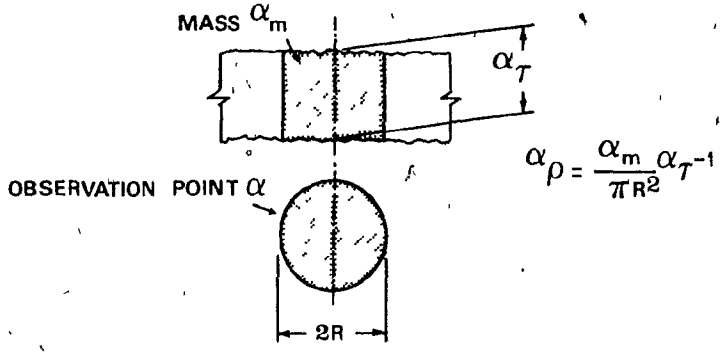

FIG. 2.3 MODEL FOR THE VOLUMETRIC MASS DENSITY .

mass density) is α_w in [g/m^2]. Then, since the local thickness is α_τ in [m], the volumetric mass density, (VMD), by (2.7) is,

$$\alpha_\rho \triangleq \alpha_w \cdot \alpha_\tau^{-1} \quad [g/m^3] \qquad (2.8)$$

This definition will be maintained throughout the thesis. However, it is to be understood that this definition conforms to a "static test procedure", i.e. for conditions, which comply with the undeformed paper sample. It is obvious, since α_ρ will vary over the whole sample and a distribution function of this quantity will be established. This will be further discussed in section 3.3. of the thesis.

In this context, a further clarification as to the necessity of the VMD measurements, in the present work, is as follows. In general, the variance of the DMD (distribution of the area mass density) of a random sheet can be predicted from the knowledge of the fibre length, fibre weight per unit length and mean weight [44,45]. As shown in reference [46], a testing procedure has been devised in the form of a "Beta-ray scanner", that permits the assessment of the α_w - distribution for paper sheets, which agrees fairly well with the predicted DMD mentioned in references [44,45]. However, these considerations, although of great practical value, do not take into account the basis quantity, i.e.

the dependence on the paper thickness, which is subject to a variation under the application of a stress. Hence, in the present investigation it was considered that, at least, during the steady-state deformation of the paper sheet, one can assume α_w to remain, essentially, constant and to permit the variation of α_τ, in order to establish a correlation between the VMD, as defined by (2.8) and the holographically evaluated strain field.

The use of the DMD technique mentioned in reference [46] could further the determination of α_ρ and its correlation to the occurring deformations. It will be further discussed in Chapter VI of this thesis concerned with concluding remarks and future research.

Based on the definition of VMD (relation (2.8)), its change due to the paper thickness at the undeformed and deformed states, as obtained from the subsequent holographic interferometry analysis, and on the assumption that α_w remains constant during the steady-state deformation, it can be stated that this change is given by,

$$\Delta^{\alpha}\rho = - \frac{\alpha_w}{\alpha_{\tau_u} \cdot \alpha_{\tau_D}} \Delta^{\alpha}\tau \quad , \quad \Delta^{\alpha}\tau = {}^{\alpha}\tau_D - {}^{\alpha}\tau_u \qquad - (2.9)$$

in which, ${}^{\alpha}\tau_D$ and ${}^{\alpha}\tau_u$ correspond to the local paper thickness in

the deformed and undeformed states, respectively. $\Delta^{\alpha}\tau$ can be assessed experimentally, directly from the deformation vector components in the z-direction (out-of-plane direction of the sample), i.e.

$$\Delta^{\alpha}\tau = {}^{\alpha}u_z^R - {}^{\alpha}u_z^L \qquad - (2.9)$$

as will be discussed in Chapter IV in detail. The surface displacement vector ${}^{\alpha}\underset{\sim}{u}$, in general, is obtained by DSHI-technique. The experimental procedure of which is also dealt with in Chapter III, where superscripts R and L refer to the right hand and left hand sides of the sheet.

The required techniques of assessing the strain components and the $\Delta^{\alpha}\tau$ as well as their correlation to the volumetric mass density ${}^{\alpha}\rho$ will be discussed, in detail, in the subsequent chapters of the thesis.

Chapter III

GENERAL REMARKS ON THE TEST PROCEDURES

3.1 Introduction

It has been stressed in the foregoing chapters that one of the aims of the present investigation is to establish, accurately, the variation of thickness of thin foils, when subjected to external load. This thickness variation has been investigated in this thesis, in order to establish its relation to the VMD of the foil material, in particular, the material investigated is that of newsprint paper.

Over the years, a method of surface deformations on thin foils has been developed in the Micromechanics of Solids Laboratory, known as DSHI-technique (double-sided holographic interferometry), which is a general method valid for any type of thin foil of material specimen. The application of this method to thin foils and in particular to the assessment of the induced strain field requires a large number of readings to be carried out over both sides of the sample, in a self consistent manner. Therefore, an automated test procedure was required. This procedure, in the case of a newsprint paper sample has been taken in the following steps:

1) The evaluation of the surface deformation of thin foils of materials by the use of an automated

holographic interferometry technique and read-out.

2) The measurement of the local VMD of the material, which is generally applicable to fibrous networks or crytalline solids.

The holographic electro-optical technique according to (1) and the determination of the VMD according to (2) are, then, the subject matter of this chapter.

It should be noted that in the description of the procedure, the designation of an "observation point" will be frequently made. However, it is necessary to clarify this notation from the beginning, since the holographic interferometry technique used in determining deformations at such points does not occur on the same scale as the corresponding observations concerned with the VMD. Hence, for the holographic interferometry method an observation point is typically of the finite size and of the order of 500 μm diameter (see Fig.3.1). Within the experimental set-up for the VMD, an observation point corresponds, however, to a diameter of 250 μm. It is assumed throughout the thesis that the variation of the structure due to such difference is negligible and hence, the readings can be taken, on average, to correspond to the larger size of the observation point, in accordance to the holographic interferometry technique. This assumption is due to the present restriction in the availability of instrumentation and their

resolution, employed in this investigation. The difference in scale does not include noticeable errors of numerical values in the VMD that correspond to the diameter of 500 μm and that, which corresponds to the actual diameter of 250 μm. This assumption is valid for all practical purposes and has been verified by the results of Beta-radiography technique.

3.2 Holographic Interferometry

As already discussed in previous publications [3,4,5], the evaluation of surface deformations of thin foils is based on the interference pattern of wavefronts, due to the observation between an undeformed and a deformed state of material. Such observations can be made by using the technique of single doubly-exposed holograms, as discussed below.

3.2.1 Single Doubly-Exposed Holograms

The general set-up for single holographic interferometry is indicated in Fig.3.2. Thus, using a laser source, which emits a coherent light beam of a specific wavelength. This beam is split into two beams, which are filtered and expanded by means of spatial filters. As can be seen from the arrangement, one beam illuminates the object and is called the "object beam". The other beam illuminates the entire surface of the holographic plate. This beam is called the "reference beam". Thus, each

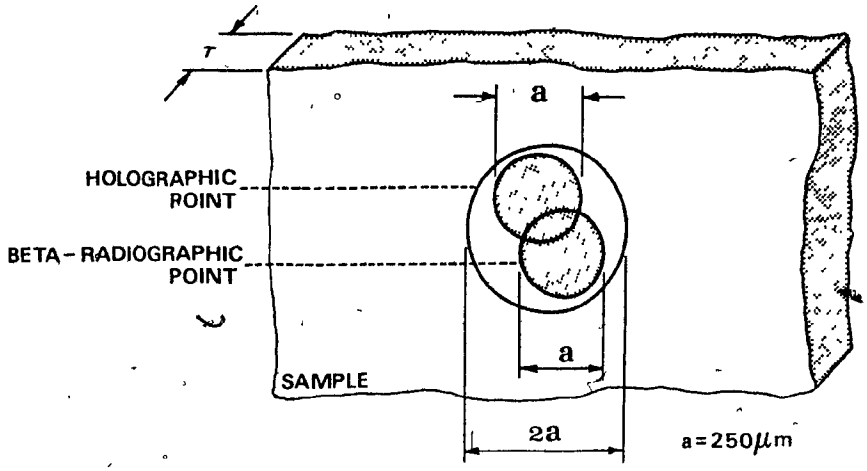

FIG. 3.1 EXPERIMENTAL « OBSERVATION POINT ».

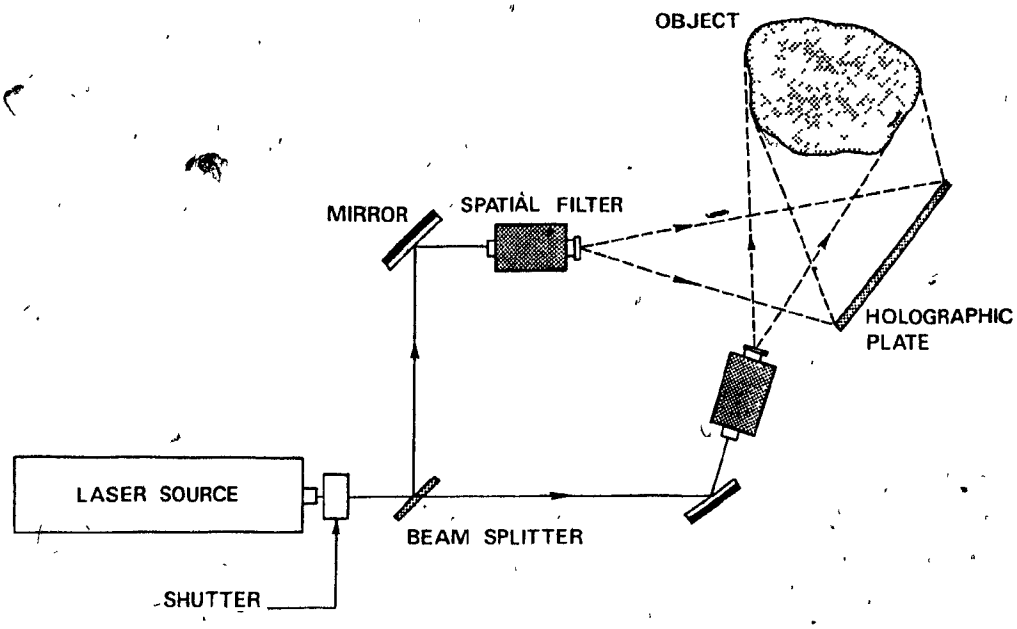

FIG. 3.2 SINGLE HOLOGRAPHIC INTERFEROMETRY SET-UP.

exposure on the holographic plate contains both the object and the reference beams.

The basic concept of holography is that, illumination of the produced interferogram, by a beam, which is conjugate to the reference beam, produces an exact duplication of the object beam and hence, an image of the object is made possible.

In the double exposure technique, the plate is exposed twice. This corresponds to a first exposure in the undeformed state and another in the deformed state of the material. It is of utmost importance that, for both exposures, all test conditions must be maintained unchanged, so that only the object beam itself changes by the effect of the occurring deformations of the sheet sample. Illuminating the doubly-exposed hologram (interferogram) will, therefore, permit the "reconstruction" of the image of the object as well as a fringe pattern arising from the interference of the object beams. It is evident that the analysis of the induced fringe pattern is directly related to the occurring deformation of the object between the two exposures[47-49]. This will be discussed in more detail below.

3.2.2 Surface Deformations and Fringe Interpretation

In later sections of this thesis, interferograms obtained

by holographic interferometry technique will be discussed. Hence, for the understanding of the interferometry technique discussed below, it may be instructive to mention, briefly, how fringe patterns are produced. For this purpose consider Fig. 3.3 concerned with the deformation of the material specimen. Here, the surface topography of the material foil is described in the deformed and undeformed states.

Considering, now, two arbitrary points A and B in the undeformed state which are moved to new locations A' and B', due to the deformation of the sample, then the light rays being propagated from the light source S are scattered from these points. The radiations scattered from points A and A' yield an interference at a fixed observation point P, which appears in the form of a localized fringe pattern. A localized fringe pattern is one, when projected on a screen, possesses high contrast and brightness. Similarly, the light beams being scattered from points A' and B' will also interfere. The random microstructure of the object surface implies random radiations at given points. Their interference produces a "non-localized high-frequency fringe pattern", which has little effect on the localized fringe pattern associated with the points A and A'. Thus, the localized or the "visible fringe pattern" at the observation point P is primarily due to the relative dis-

placement of the corresponding points of the sample surface in the undeformed and deformed states.

These general conditions are indicated in Fig. 3.3, in which $\underset{\sim}{r}_i$ are the position vectors of the surface points and $\underset{\sim}{R}$ is the position vector of the observation point, $\underset{\sim}{k}_1$, $\underset{\sim}{k}_3$ are the illuminating beam light propagation vectors, whilst $\underset{\sim}{k}_2$ and $\underset{\sim}{k}_4$ are the scattered light propagation vectors. It is seen from the geometry that the phases ϕ_{01} and ϕ_{02} along the paths of $\underset{\sim}{k}_1\underset{\sim}{k}_2$ and $\underset{\sim}{k}_3\underset{\sim}{k}_4$, respectively, may be expressed in the following manner [47-49]:

$$\phi_{01} = \underset{\sim}{k}_1 \cdot \underset{\sim}{r}_1 + \underset{\sim}{k}_2 \cdot (\underset{\sim}{R} - \underset{\sim}{r}_1) + \delta_r \qquad - (3.1)$$

$$\phi_{02} = \underset{\sim}{k}_3 \cdot \underset{\sim}{r}_3 + \underset{\sim}{k}_4 \cdot (\underset{\sim}{R} - \underset{\sim}{r}_3) + \delta_r$$

where δ_r is a constant phase difference of the radiation reflected from the corresponding points A and A'. The propagation vectors can also be written as:

$$\underset{\sim}{k}_i = k \cdot \hat{k}_i = \frac{2\Pi}{\lambda} \hat{k}_i \; ; \; i = 1,\ldots,4 \qquad - (3.2)$$

where λ is the wavelength of the light and $\hat{k}_i$ are the unit vectors of the light wave propagation. Similarly, the vectors $\underset{\sim}{k}_3$ and $\underset{\sim}{k}_4$ can be expressed by:

$$\underset{\sim}{k}_3 = \underset{\sim}{k}_1 + \Delta\underset{\sim}{k}_1 \qquad - (3.3)$$

$$\underset{\sim}{k}_4 = \underset{\sim}{k}_2 + \Delta\underset{\sim}{k}_2$$

It has been shown in reference [5] that the phase difference $\delta = \phi_{01} - \phi_{02}$ is a direct measure of the displacement $\underset{\sim}{u}$ of an arbitrary point on the surface of the sample. Hence, in view of the above relations, one may write that:

$$\delta = (\underset{\sim}{k}_1 - \underset{\sim}{k}_2) \cdot (\underset{\sim}{r}_1 - \underset{\sim}{r}_3) - \Delta\underset{\sim}{k}_1 \cdot \underset{\sim}{r}_3 - \Delta\underset{\sim}{k}_2 \cdot (\underset{\sim}{R} - \underset{\sim}{r}_3) \quad - (3.4)$$

Since the displacements are usually very small, compared with the magnitude of the position vectors, one can write that the surface deformation vectors $\underset{\sim}{u}$ is given by:

$$\underset{\sim}{r}_1 \ , \ \underset{\sim}{r}_3 \gg \underset{\sim}{u} = \underset{\sim}{r}_3 - \underset{\sim}{r}_1 \quad - (3.5)$$

Furthermore, the quantities $\Delta\underset{\sim}{k}_1$ and $\Delta\underset{\sim}{k}_2$ are perpendicular to $\underset{\sim}{r}_3$ and $\underset{\sim}{R} - \underset{\sim}{r}_3$, respectively and thus the dot products in relation (3.4) vanish, so that the following form is obtained:

$$\delta = (\underset{\sim}{k}_1 - \underset{\sim}{k}_2) \cdot (\underset{\sim}{r}_1 - \underset{\sim}{r}_3) = - (\underset{\sim}{k}_1 - \underset{\sim}{k}_2) \cdot \underset{\sim}{u} \quad - (3.6)$$

The above form is the basic relation required for the analysis of deformations in any holographic interferogram of a diffusely reflecting surface.

It was mentioned earlier in section 3.2.1 that a holographic interferogram is formed by exposing a holographic plate twice, once in the undeformed state of the material, then in the deformed

state. The evaluation of the obtained interferograms, for the general case, was first introduced by Leigh and Upatnieks[50]. Their technique is employed, where the fringe pattern is due to a "real time" or a double exposure arrangement. The three-dimensional surface deformation in both these cases can be evaluated by either using several holograms as suggested by Ennos[51] or a single interferogram technique suggested by Alexandrov and Bonch-Bruevich[52]. The first method requires the identification of a zeroth-order fringe on the image plane, i.e. a fringe that remains fixed relative to the object surface, when the observer is in motion. This, however, in the case of complicated fringe pattern cannot be achieved. The second method is rather simpler than the first and hence, is frequently used if the main purpose is the determination of three-dimensional surface deformations (see, for example, references 53-55). However, in the present investigation, a somewhat different technique has been used, which will be discussed in more detail later in this thesis.

It should be noted that upon looking at any "image point", i.e. any point on the reconstructed image, through an interferogram, the fringe pattern shifts, when the position of the observer is changed. This shifting fringe pattern is then a measure of the phase difference δ (relation (3.6)). Since the latter is $\delta = 2\pi N$, N being the number of fringes that move past the image

point, one can express relation (3.6) also by:

$$\delta = -(\underset{\sim}{k}_1 - \underset{\sim}{k}_2) \cdot \underset{\sim}{u} = 2\Pi N \qquad - (3.7)$$

The above equation related the components of the deformation vector $\underset{\sim}{u}$ to the fringe number N directly. Obviously, in order to compute the three components of $\underset{\sim}{u}$ this relation is not sufficient and two more similar relations are required, in order to construct a system of three simultaneous equations for three components of $\underset{\sim}{u}$, i.e. u_x, u_y and u_z. For this purpose, consider Fig. 3.4a, where $\underset{\sim}{k}_1$ denotes the propagation vector of the illumination light and $\underset{\sim}{k}_2 \ldots \underset{\sim}{k}_5$ the vectors of the light rays being scattered in these directions at point A. Then, for the assessment of the three-dimensional deformation vector $\underset{\sim}{u}$ and the required additional relations of (3.7), one can take any combination of the difference vectors $A_1, \ldots, A_6$ as shown in the figure. This results in determining additional relations to (3.7) in the chosen directions, so that for a three-dimensional assessment of the deformation vector $\underset{\sim}{u}$, one can choose any three non-collinear directions. Thus, by evaluating the fringe number N on moving the illumination point A (Fig.3.4b) in one of the chosen "scanning directions" one relation of type (3.7) is obtained for this direction. The angles between the scanning directions, together with the knowledge of the directions of the vectors $\underset{\sim}{k}_1, \ldots, \underset{\sim}{k}_5$ as well as the evaluated

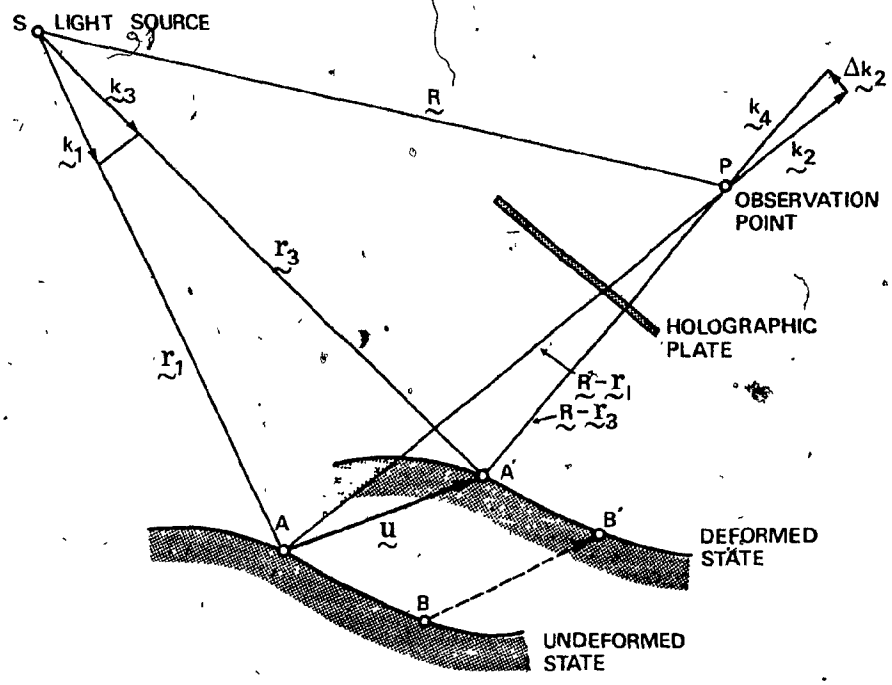

FIG. 3.3 SURFACE TOPOGRAPHY AND GEOMETRY OF LIGHT BEAM FOR THE GENERAL CASE OF HOLOGRAPHIC INTERFEROMETRY.

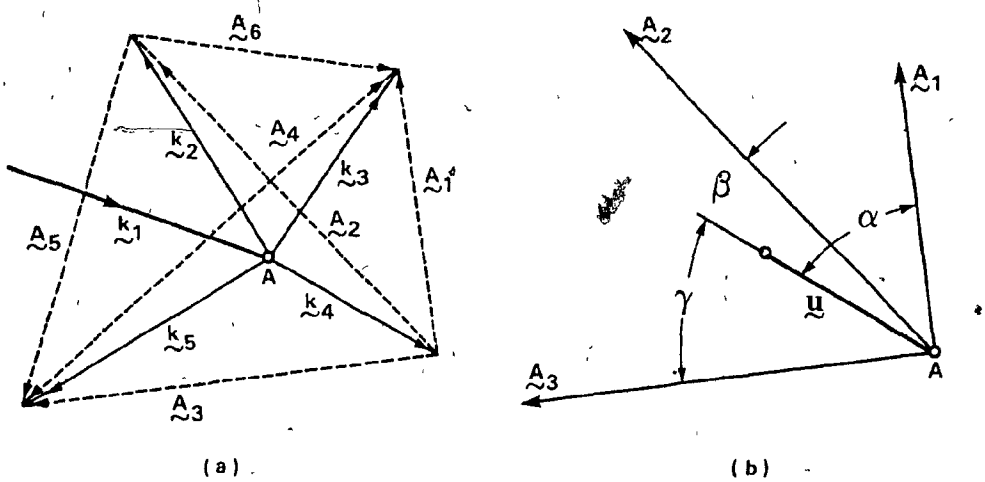

FIG. 3.4 THREE SCANNING DIRECTIONS.

fringe numbers and the wavelength of the illumination light are sufficient to completely determine the components of $\underset{\sim}{u}$. This has been discussed in detail in reference [5].

3.2.3 The DSHI-Method (Formation Stage)

Holographic interferometry technique as mentioned in the previous sections is usually employed in investigations of surface deformations of thin foils. The materials commonly used are plastics, metals and composites. However, in the case of fibrous materials, like newsprint paper, it has been found more necessary to extend the technique to a so-called "double-sided holographic interferometry (DSHI) technique". It has been shown in the past [4] that paper samples and samples of similar structured materials exhibit a considerable out-of-plane motion during the application of a uniaxial tensile load. Hence, some components of the evaluated deformation vector are combined with out-of-plane motion. Once a double-sided technique is employed, this difficulty is considerably reduced. Furthermore, one can, at the same time, evaluate the changes of thickness of the sample foil under stress, which is of considerable importance. Thus, a method developed in this laboratory, known as the "sequential-DSHI technique". This technique consists of two distinct stages, namely a formation and a reconstruction stage. The formation

stage was first performed by Peralta-Fabi [4] and its explanation is given below. The reconstruction stage has been fully automated by the author of the present thesis, since it was one of the main objectives in this work. This will be discussed in detail in Chapter IV. This technique is useful when the deformation history of the sample foil is to be taken into account. The optical arrangements that are required as well as the control of the set-up will be discussed in detail in the subsequent chapter.

As indicated in Fig. 3.5, the method employs four holographic plate holders, two on each side of the sample. This permits one to form, simultaneously, one interferogram on each side of the sample. Further interferograms are taken at certain time intervals in a sequential manner. The double exposure permits each holographic plate to be exposed to two successive configurations of the sample surface at two different times. Hence, they record the deformations. It should be noted that the existence of two plates on each side makes it possible to form "two successive interferograms" in a manner so that they are exposed in one common exposure. A set of sequential interferograms can therefore be produced. In order to illustrate this technique the following steps have to be considered in order to obtain a sequence of interferograms of a paper sample, the deformational behaviour of which is indicated in Fig. 3.6:

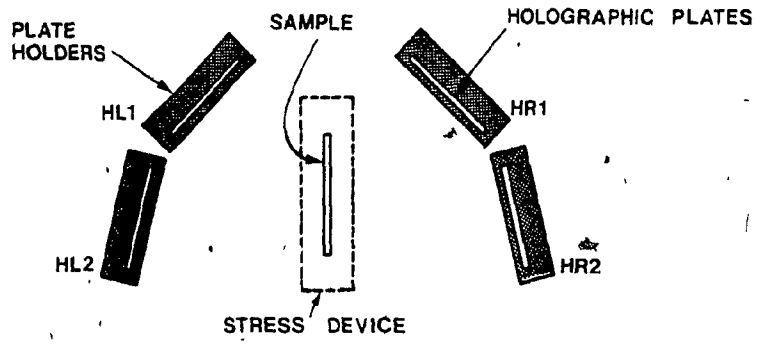

FIG. 3.5 POSITIONS OF THE HOLOGRAPHIC PLATES IN THE SEQUENTIAL-DSHI – FORMATION STAGE.

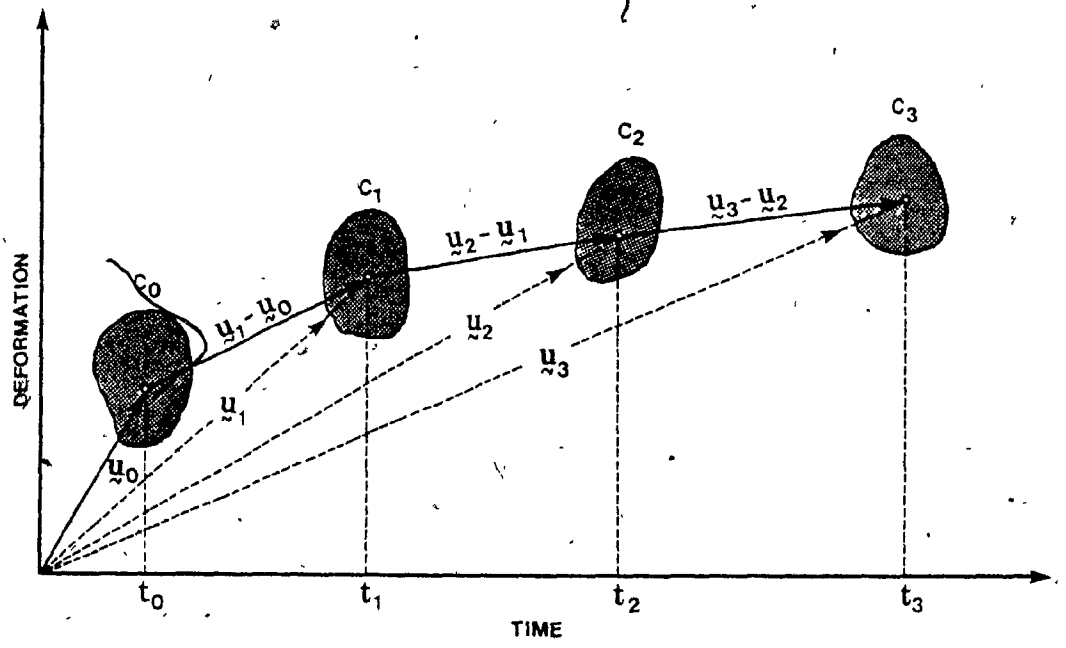

FIG. 3.6 DEFORMATIONAL HISTORY OF AN ARBITRARY OBJECT.

1) At time $t=t_o$, the plate holders HR1 (right hand side) and HL1 (left hand side) are loaded with unexposed holographic plates. HR2 and HL2 are left empty.
2) The first exposure E1 at time $t=t_o$ is carried out.
3) Plate holders HR2 and HL2 are loaded with unexposed plates.
4) The second exposure E2 at time $t=t_1$ is carried out. Note that during the time $t_o \rightarrow t_1$ the sample has deformed. The plates in the holders HR1 and HL1 have, therefore, two exposures E1 and E2. E2 is common to the plates in holders HR2 and HL2.
5) The doubly-exposed plates are removed from HR1 and HL1 and replaced by new plates.
6) The third exposure E3 is performed at time $t=t_2$. Now, the plates in HR2 and HL2 have received two exposures E2 and E3, whereby E3 is common to the new plates of HR2 and HL2.
7) Doubly exposed plates are removed from HR2 and HL2.
8) The fourth exposure E4 is carried out at time $t=t_3$.
9) Finally, the doubly-exposed plates are removed from HR1 and HL1.

In this manner, one can continue the test to obtain more sequential interferograms. In the present investigation, the surface deformations of both sides of a newsprint paper sample were evaluated at eight successive times by adopting the sequential DSHI

technique, details of which are discussed in Chapter IV.

3.2.4 Reconstruction Stage of Interferograms

Although the formation of interferograms (double-exposed holograms) has been discussed above for the case of the sequential DSHI-method the reconstruction of these interferograms will be discussed below. It is valid for any type of interferogram. The technique employed was first introduced by Fosati-Bellani and Sona [53] and is, in the present work, fully automated. Hence, in presenting the general reconstruction technique in this section, the actual computerized set-up will be discussed in detail in Chapter IV and Appendix I.

Once an interferogram is produced it is necessary to establish the geometrical arrangement between the holographic plate and the sample in order to reconstruct an exact image of the sample, i.e. the exact angle of the interferogram plate relative to the foil sample position and the distance between the centers of the plate and the sample. In this manner the interferogram can be considered to be a permanent record of the deformational behaviour of the sample and the subsequent reconstruction of the plate becomes independent of the specific conditions for the sample itself.

Generally, if an interferogram of a stressed foil sample is

illuminated by the reference beam, a "virtual image" of the sample and the induced fringe pattern can be observed by looking through the interferogram plate (see Fig. 3.7a). This means that, for an observer as indicated in the figure, the virtual image appears in the free space on the illuminated side of the plate. A "real image" can be reconstructed by illuminating the plate with the conjugate reference beam (mirror image of the beam). This image can, then, be projected onto a screen (see Fig. 3.7b).

It should be noted that there are two ways of counting the number of fringes. First, when considering the virtual image, the observer must move along some predetermined direction and hence, count the fringe number occurring at any arbitrary point of the object. Second, in dealing with the "real image", the direction of illumination is changed, whilst the observer remains in a fixed position. This position corresponds, then, to the chosen arbitrary point of the object. The second procedure is used in the present work, which has been fully automated. In this arrangement three directions $O'P^1$, $O'P^2$ and $O'P^3$ are chosen (Fig. 3.8), so that the point O' corresponds to the center of the interferogram plate. The deformation components can, then, be evaluated with respect to a fixed cartesian frame XYZ with its origin at the center of the real image plane. An arbitrary

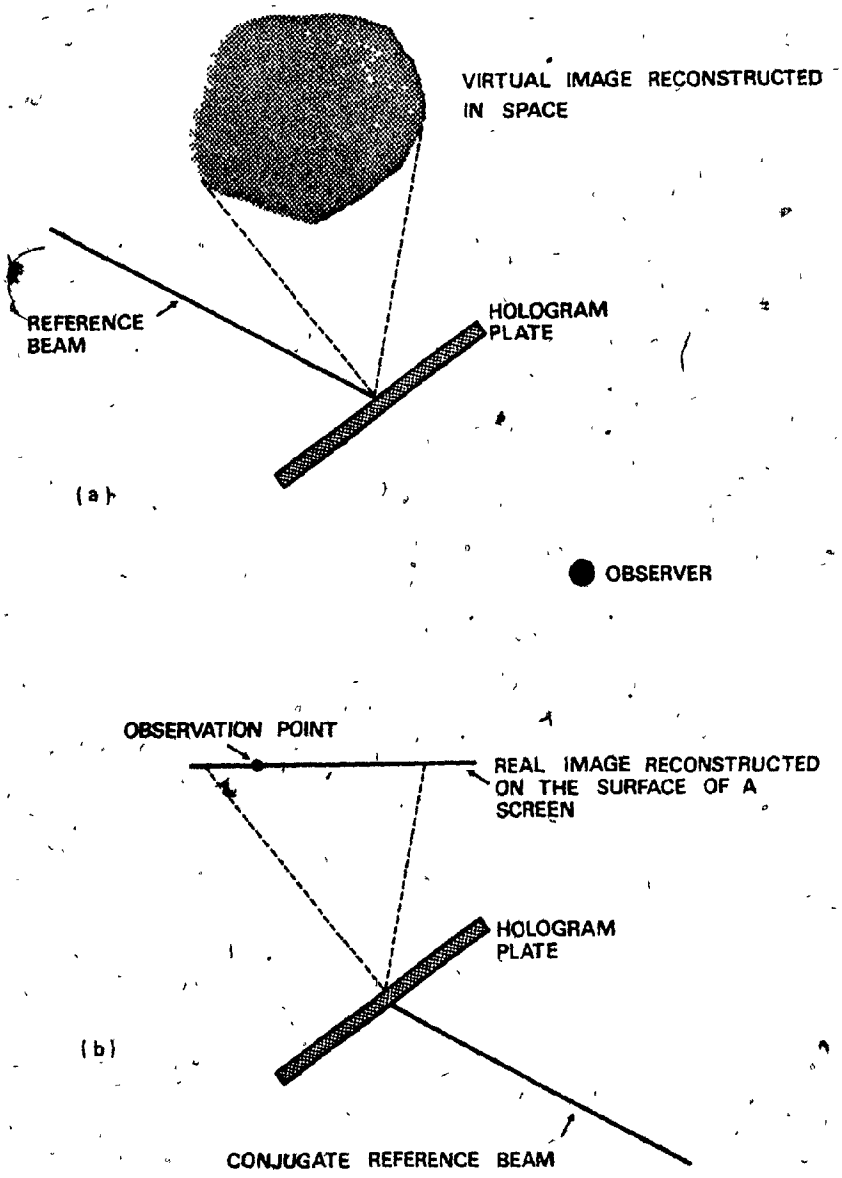

FIG. 3.7 RECONSTRUCTION OF THE VIRTUAL AND REAL IMAGES.

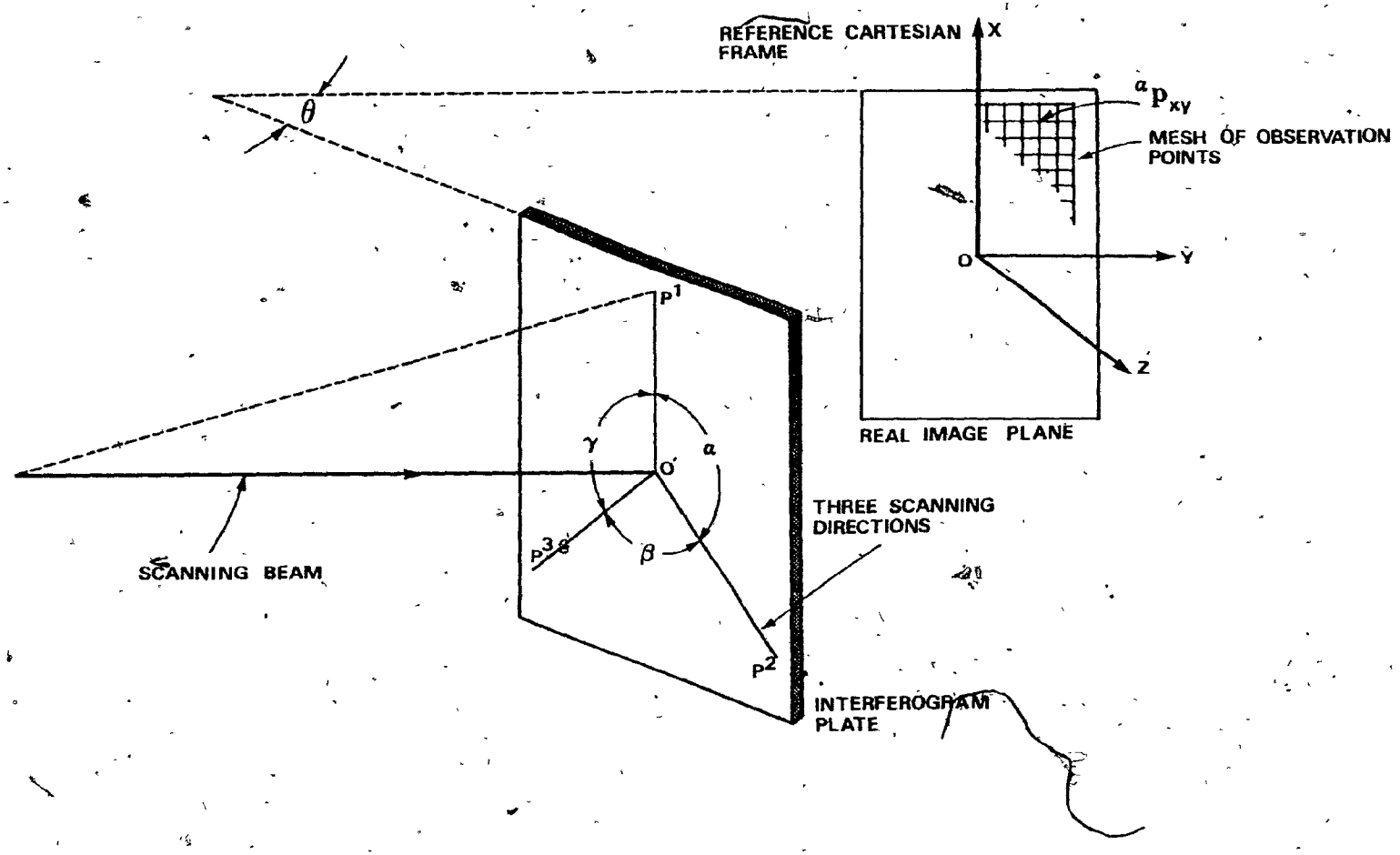

FIG. 3.8 GENERAL RECONSTRUCTION GEOMETRY OF INTERFEROGRAMS.

observation point ${}^{\alpha}P_{xy}$ can be considered on the real image plane. The location of this point is, therefore, identified within the XYZ frame. As it was mentioned above, one may count the fringe numbers at such a point ${}^{\alpha}P_{xy}$ by sweeping the conjugate reference beam on the interferogram plate along the directions $O'P^1$, $O'P^2$ and $O'P^3$. In doing so, the key relation (3.7) given previously becomes, in the view of the geometry of Fig.3.8 as follows:

$$\begin{bmatrix} x_0 - x_1 & y_0 - y_1 & z_0 - z_1 \\ x_0 - x_2 & y_0 - y_2 & z_0 - x_2 \\ x_0 - x_3 & y_0 - y_3 & z_0 - x_3 \end{bmatrix} \begin{bmatrix} \hat{i} \\ \hat{j} \\ \hat{k} \end{bmatrix} \left[\hat{i}, \hat{j}, \hat{k} \right] \begin{bmatrix} u_x \\ u_y \\ u_z \end{bmatrix} = \pm\lambda \begin{bmatrix} N_1 \\ N_2 \\ N_3 \end{bmatrix} \quad - (3.8)$$

in which the first matrix represents the illumination direction with reference to XYZ frame, $\hat{i}$,$\hat{j}$ and $\hat{k}$ are the unit vectors of this coordinate system. The second column vector is the displacement vector, which is also measured with respect to the XYZ frame. Finally, the vector on the right hand side of the relation is a fringe number vector, the components of which N_1, N_2 and N_3 are associated with the "scanning directions $O'P^1$, $O'P^2$ and $O'P^3$", respectively. Alternatively, one may write equation (3.8) in a briefer form as:

$$[A]\,[u] = \pm\lambda\,[N] \qquad - (3.9)$$

or, by solving for [u]:

$$[u] = \pm\lambda\,[A]^{-1}\,[N] \qquad - (3.10)$$

where:

$$A_{ij} : [A] = \begin{bmatrix} \ell_0 - \ell_1 & m_0 - m_1 & n_0 - n_1 \\ \ell_0 - \ell_2 & m_0 - m_2 & n_0 - n_2 \\ \ell_0 - \ell_3 & m_0 - m_3 & n_0 - n_3 \end{bmatrix} \qquad - (3.11)$$

It is seen that the elements of the above matrix are the direction cosines of the light wave vectors with respect to the XYZ coordinate system. The indices 0,1,2 and 3 refer to points O', P^1, P^2 and P^3, respectively. One can, then, introduce the quantities ℓ_i, m_i and n_i (i=0,1,2,3) that are directly obtainable from the geometry of the reconstruction set-up. For this purpose the following relations can be used:

$$\ell_i = \pm \frac{\alpha_x - x_i}{[(x_i - \alpha_x)^2 + (y_i - \alpha_y)^2 + z_i^2]^{\frac{1}{2}}}$$

$$m_i = \pm \frac{\alpha_y - y_i}{[(x_i - \alpha_x)^2 + (y_i - \alpha_y)^2 + z_i^2]^{\frac{1}{2}}} \qquad - (3.12)$$

$$n_i = \pm \frac{z_i}{[(x_i - \alpha_x)^2 + (y_i - \alpha_y)^2 + z_i^2]^{\frac{1}{2}}}$$

where α_x and α_y are the actual coordinates of an observation point αP on the real image plane of the test sample.

From the above relations it is seen that, in order to obtain the components of the deformation field at any point of the sample, one

needs to scan the interferogram plate in the three pre-determined directions $O'P^1$, $O'P^2$ and $O'P^3$ and count the number of fringes passing over the point ${}^{\alpha}P$, whilst the plate is being scanned. The obtained fringe numbers and the geometry of the reconstruction set-up are sufficient to evaluate the three deformation components of the sample at an arbitrary observation point. However, it should be mentioned that the choice of the angle θ in the formation stage and the angles α, β and γ in the reconstruction stage are of utmost importance in order to obtain accurate results in the fringe number reading procedure. In general, the angle θ should be chosen so that the image distortion is minimized. Similarly, α, β and γ should be selected in such a way that a larger number of fringes pass over the observation point. In the present work these quantities were optimized by considering some trial and error analysis. Thus; the angle θ for the four plate holders HR1, HL1, HR2 and HL2 (Fig. 3.5) were, then, found to be 65°, 63.5°, 51° and 49°, respectively. It was also found that in the present case of interferograms $\alpha=\beta=\gamma=120°$ lead to optimum results.

Finally, it should be noted that the angle θ and the distance OO', i.e. the distance between the geometrical centers of the interferogram and the real image plane, must be identical to those of the formation set-up, in order to reconstruct an exact size of the object. However, one may choose OO' different from that of

the formation set-up. In that case, a magnification factor has to be involved in the relations (3.8-3.12).

3.3 On the Determination of the Volumetric Mass Density

It was mentioned earlier in Section 2.4, in dealing with the definition of the volumetric mass density (VMD), that the VMD is obtained by measuring, directly, the mass and the thickness of the sample foil at any point of interest. Therefore, measurement techniques have been developed in this investigation to evaluate these quantities independently by means of non-destructive methods. The experimental techniques will be discussed in detail in Chapter IV. Since it was recognized that the local VMD $^{\alpha}\rho$ is an important strength characteristic of the fibrous networks, a correlation of this measured quantity with the occurring strain field becomes important. The corresponding calculations of such correlations are given in the discussion of the obtained experimental results in Chapter V.

Chapter IV

INVESTIGATION OF NEWSPRINT PAPER

4.1 Introduction

The sequential holographic technique has been discussed in the previous chapter. This chapter deals with the actual experimental set-up, that can be applied to any fibrous material. However, the technique to be discussed refers mainly to the testing of newsprint paper. Sections 1 and 2 of this chapter deal with the formation stage and the reconstruction stage, required in sequential DSHI-technique. Section 3 is concerned with the determination of the basis weight α_w of this type of paper. For this purpose the conventional Beta-radiography method has been modified, that is, used in conjunction with scanning electron microscopy measurements. In Section 4 a newly developed optical technique is discussed, which permits the measurement of the "local thickness" of the paper sample. This is required in order to establish a correlation between the volumetric mass density of the paper sample with the induced strain field as mentioned in the previous chapters.

4.2 Sequential DSHI - Formation Set-up

The formation set-up is shown in the photograph Fig.4.1 and the schematics of the set-up is indicated in Fig.4.2. It

FIG. 4.1 PHOTOGRAPH OF THE SEQUENTIAL - DSHI TECHNIQUE – FORMATION SETUP.

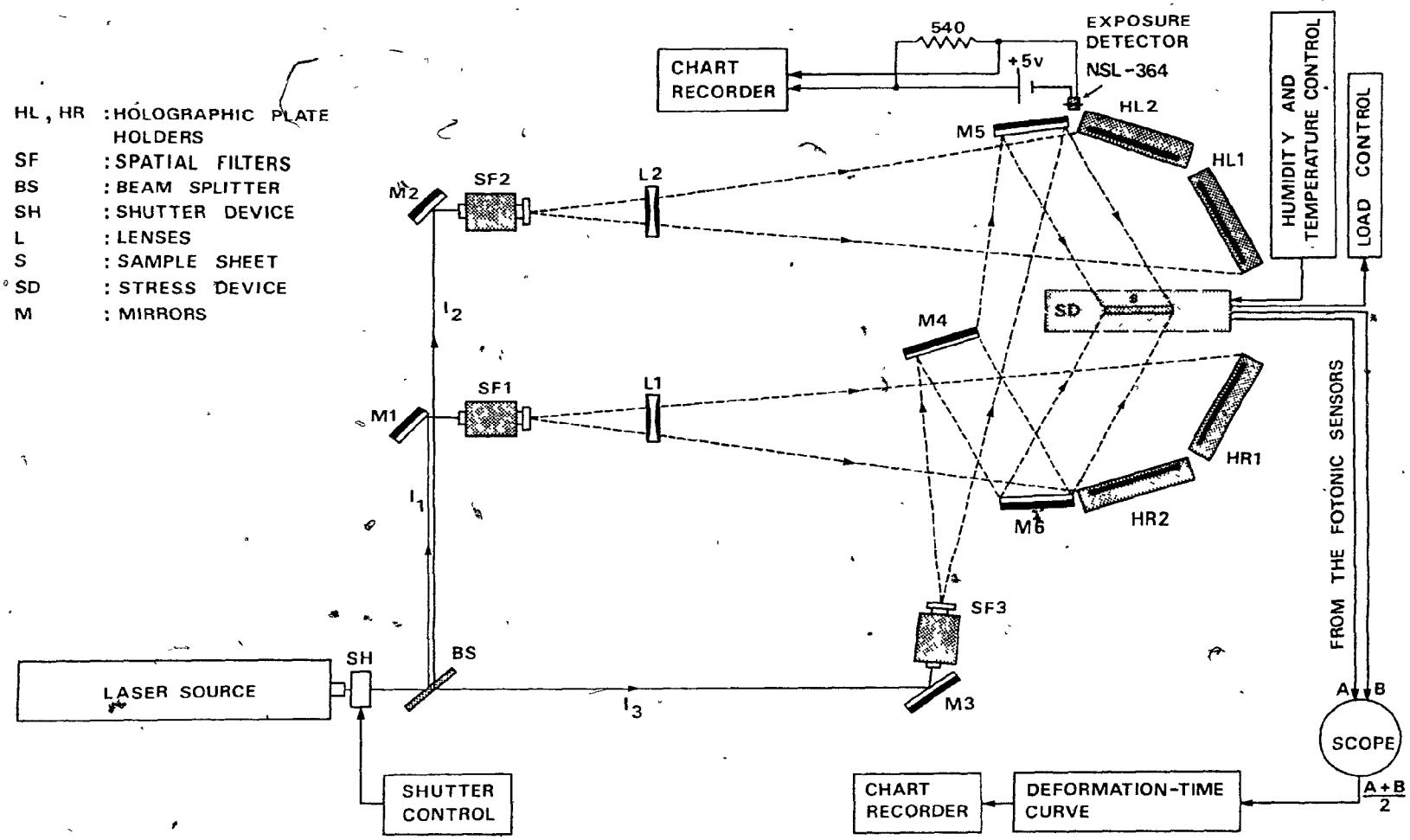

FIG. 4.2 SCHEMATICS OF INTERFEROGRAM FORMATION SET-UP IN SEQUENTIAL DSHI-METHOD.

can be seen that the newsprint paper sample with the dimensions 55 mm x 96 mm is positioned in a stress device (SD). On each side of the SD there are two holographic plate holders for sequential interferometry. As mentioned before, each holographic plate has to be exposed to a reference beam and to an object beam, simultaneously. Thus, using a tunable coherent laser source for the supply of a light beam, the latter emits a beam of 1.5 mm diameter at 640 mw power in the blue range (λ=4880Å). This beam is split into three major beams, I_1, I_2 and I_3 by means of a beam splitter (BS). The reflectivity of the beam splitter is adjustable. It is adjusted in such a manner that $I_1=I_2$. The beams I_1 and I_2 are directed towards spatial filters SF1 and SF2, each of which is equipped with a 50 µm precision pinhole. However, it is necessary to expand the beams so that they cover the entire surfaces of the plates. The lenses L1 and L2 are used to adjust the uniformity of the incident light beams over the plates and also to obtain the required intensity for proper interferograms. The beams leaving these filters have uniform wavefronts and are, thus, referred to as the reference beams. On the other hand, beam I_3 is also expanded by spatial filter SF3, whose pinhole size is 25 µm. The wave front of the expanded beam is divided into two by mirror M4. Each of these beams is collected by mirrors M5 and M6, which then illuminate the

two sides of the paper sample. The paper sample, in turn, diffusely scatters the wave fronts of these two beams. The scattered beams on each side of the sample are called the object beams. On each side of the arrangement, the reference beam and the object beam interfere with each other in space and overlap. The position of the plate holders is significant and must be chosen so that the plates receive the interference pattern. The appropriate exposure times, to obtain high accuracy interferograms must also be chosen at certain time intervals (see Section 4.2.3).

4.2.1 Loading and Environmental Control

The mechanical response behaviour of a material, in general, depends on the loading and specific environmental conditions. In the present case, for the testing of paper samples, a mechanical device referred to as the "stress device" was used to apply a constant uniaxial load on the paper sample. A photograph of this device is shown in Fig. 4.3, whilst its schematic drawing is given in Fig. 4.4. Although the design itself is rather simple, a few aspects of it, in particular with respect to the holographic interferometry, should be mentioned. The first one is the loading arrangement, which eliminates all the rigid body motion of the stress device within the accuracy of the inter-

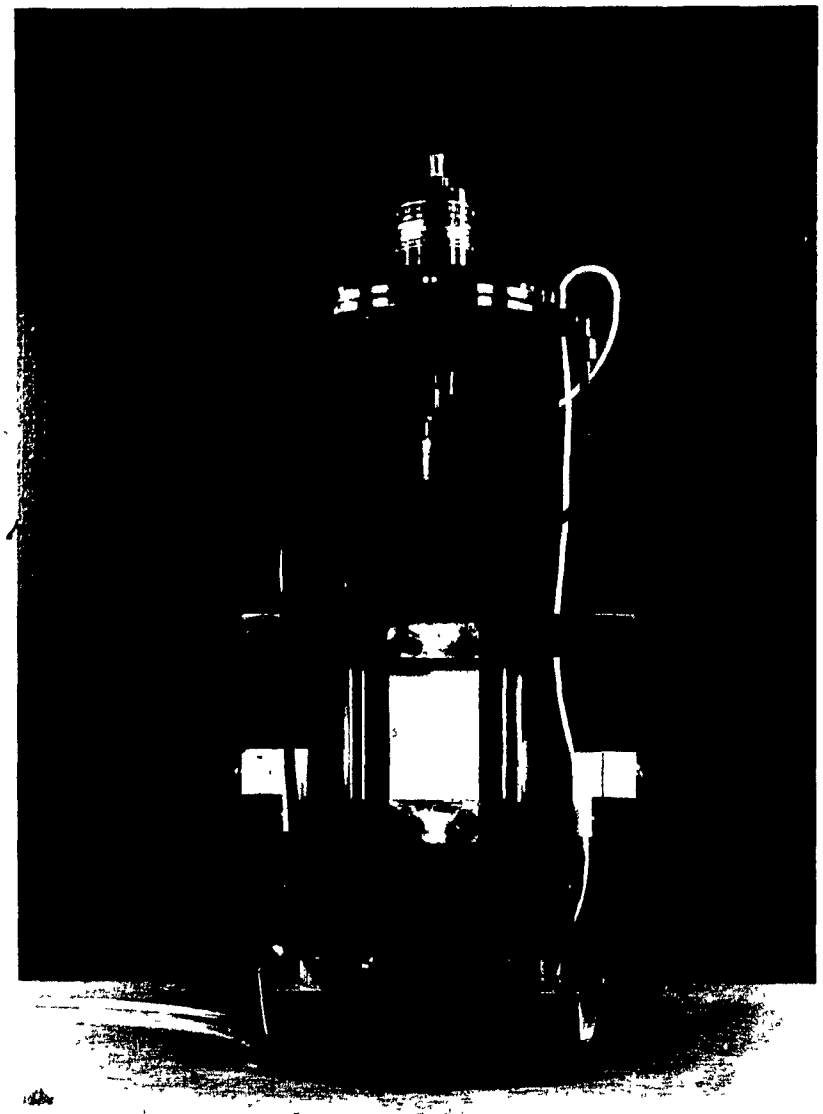

FIG. 4.3 PHOTOGRAPH OF THE STRESS DEVICE.

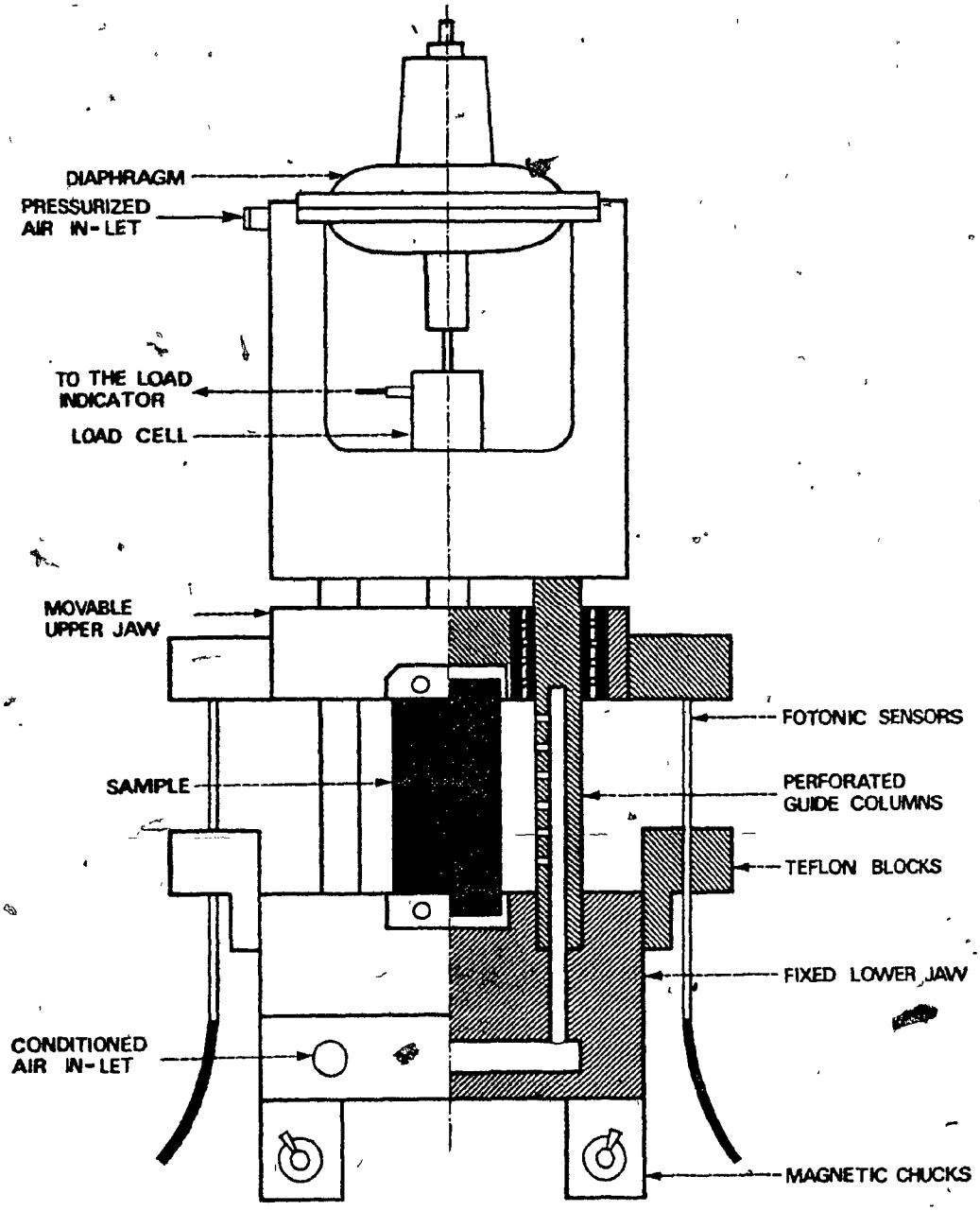

FIG. 4.4 SCHEMATIC DIAGRAM OF THE LOAD DEVICE.

ferometry, i.e. up to λ=4880Å. This is particularly important for holographic interferometry measurements, since the elements of the apparatus must not experience any rigid body motion of magnitudes greater than the wavelength of the coherent light source. In dealing with this requirement a proper load application in the present set-up was achieved by means of a pneumatic diaphragm, as shown in Fig. 4.4. The latter is mounted rigidly onto the frame of the apparatus and connected by a pivot arrangement directly onto a load cell with a capacity of 45 kg. In addition, the diaphragm is pressurized through a set of air valves. The air pressure is maintained at a constant level by employing a search tank, equipped with a feedback, control and pressure indicators. The pressure in the diaphragm is, then, transmitted to the movable jaw of the device through the load cell. The load cell is connected to a transducer, the response of which is obtained within an accuracy of ±25g and lies within its linear range. The stress device ensures, further, a linear vertical motion of the upper jaw that holds the upper end of the paper sample. Both the fixed and the movable jaws have been mounted onto two hollow cylindrical columns with a high quality surface finish. The movable jaw is able to slide linearly along the two guide columns by the aid of precision linear ball bearings for the uniaxial load applications. The two hollow columns are

perforated to permit the entrance of air with a specific humidity and at a controlled temperature. The latter is controlled by means of a humidifying chamber (Fig. 4.5). This device is capable of supplying a constant air flow at a preset humidity and temperature. In the present investigation a humidity of 50% ± 1% and a controlled temperature of 24.5°C ± 0.5°C were employed.

For the maintenance of these environmental conditions on the paper sample, the SD is designed so that an isolating glass cage can be mounted. Thus, a chamber is produced that encloses the sample and the perforated surfaces of the columns. The pre-conditioned air is then permitted to flow inside the chamber and maintain the sample at the required environmental conditions. The size of the chamber, on the other hand, is such that the disturbance due to the air flow is minimized. This has been checked from the holographic interferometry observations. Obviously, if the air circulation around the sample is too large, a substantially distorted fringe pattern could develop. The glasses, enclosing the chamber are optically flat so that they induce no noticeable diffraction in the object beams. Equal attention has been paid to the mounting of the paper sample, so that no-slip conditions prevail, whilst they are gripped within the two jaws of the stress device.

FIG. 4.5 PHOTOGRAPH OF THE HUMIDITY AND TEMPERATURE CONTROL CHAMBER .

It has been stated earlier that the fringe pattern produced on the real image plane is as a result of the deformation of the sample. Thus, a readable and clear fringe pattern will depend on the amount by which the sample is deformed between the two holographic exposures. A too compact or a too separated fringe pattern is generally too difficult to be analyzed. Hence, it is essential to carry out tests so that a readable fringe pattern is obtained. This has been achieved by controlling the vertical motion of the upper jaw corresponding to a macroscopic deformation of the paper sample, and holographic observations have indicated that good fringe patterns can be obtained if the motion of the upper jaw is within the range of 5-12 μm. In order to register this motion of the upper jaw, two fotonic sensors have been employed. Each one of them is attached to one side of the apparatus by means of a teflon block which permits a fine adjustment of the sensor probe. The tips of the probes are preset at close contact to the upper jaw surfaces to follow its motion. An oscilloscope and a chart recorder were put in line with the fotonic sensors to register their average outputs. During the performance of the holographic interferometry experiment oscilloscope observations then monitor the exposure intervals. For a more accurate timing of the exposures a digital shutter device could be used, which, during the performance of the present investigations, was

not available. In addition, a chart recorder was also used to register the macroscopic deformation-time curve of the paper sample. Fig. 4.6 shows the fotonic sensors output of the present arrangement for the case of the newsprint paper sample In this context, an "exposure detector" (Fig. 4.2 top) was employed to produce signals that corresponded to the exposures, which were simultaneously registered to the motion of the upper jaw. Thus, it was possible to measure the required time interval with an accuracy of 1 second. It is further important to note that for a proper formation set-up, vibrations caused by surroundings have to be completely eliminated. Thus, previous tests required the design of a carefully adjusted vibration isolation system which was available during the performance of the present work (see reference [5]).

Finally, in order to eliminate any vibrations during the tests, it is important that the stress device, the holographic plate holders and all the optical components are firmly positioned. For this purpose all the devices and optical components were attached to the vibration-free holographic table by means of magnetic chucks.

4.2.2 Holographic Plates and Their Chemical Treatment

The production of good interferograms is an essential step in the assessment of the deformation field of thin foils. A high

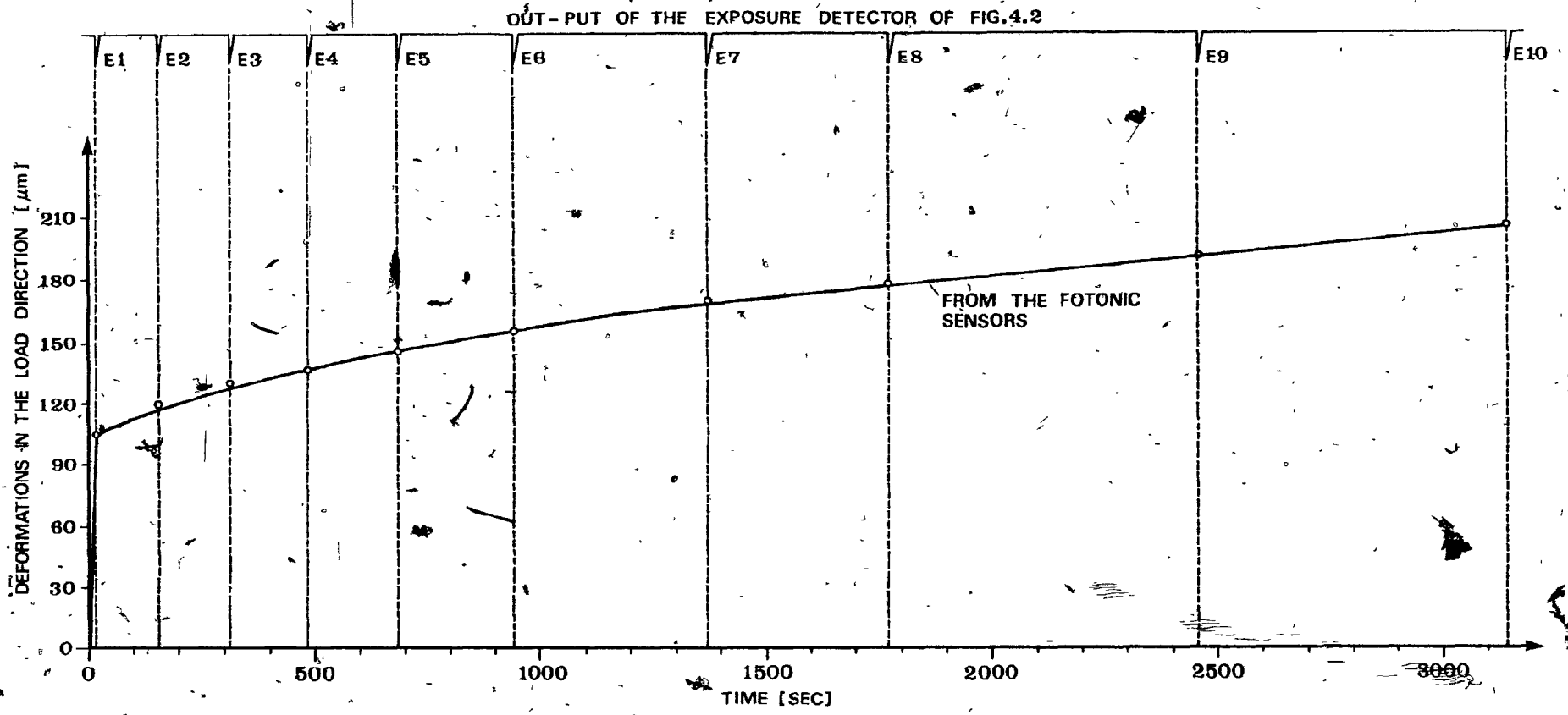

FIG. 4.6 OVERALL DEFORMATION OF SAMPLE #38 IN THE DIRECTION OF 82 N UNIAXIAL TENSILE LOAD.

quality interferogram is the one which, during reconstruction, can produce a fringe pattern with high contrast and brightness. This depends on several factors such as the ratio of the reference beam intensity to that of the object beam, the even distribution of the photosensitive emulsion over the holographic plate and also, the development of the plates.

Holographic observations, in the case of newsprint paper samples, showed that a ratio of 5:1 for the reference beam intensity to that of the object beam, gives the optimum brightness and contrast in fringe patterns. This confirms the argument given in reference [48]. It was also found that Kodak 125-02 high-speed holographic plates (size 13 x 10 cm) have good resolution and gave accurate holograms.

In the present thesis, for the development of holographic plates, Kodak developer D-19 and Kodak Rapid Fixer were used. The holographic plates were immersed in D-19 for 5 minutes with continuous agitation, then fixed in rapid fixer and finally, placed in a hypo-cleaning agent for one minute. In order to remove the chemical deposits of the development process, the plates were also washed in 20°C running water for 20 minutes. Finally, they were immersed in an ethyl-alcohol bath for one minute for the removal of the water, then dried in a low-turbulent air jet.

Obviously, the emulsions undergo some shrinkage due to the developing process itself. However, since it effects both the object beams (each due to one exposure) in the same way, no distortion or inaccuracy is induced in the fringe pattern during the reconstruction stage.

4.2.3 Deformational Behaviour of a Newsprint Paper Sample

For the purpose of investigating the deformational behaviour of newsprint paper samples, 20 interferograms were produced from the final sample that had been subjected to 82N uniaxial tensile load. The complete test duration was 52.5 minutes. The interferograms were produced so that 10 of them correspond to each side of the paper sample. Thus, in accordance with Fig.4.6, each pair of interferograms correspond to one point of the deformation curve. This curve was obtained from the analysis of the previously discussed arrangement using the fotonic sensor devices.

It can be seen from Fig.4.6 that the first three exposures correspond to the transient behaviour during the deformation process. It is important to note that, due to this transient behaviour, the first pair of interferograms had to be discarded, since they resulted in somewhat unreadable fringe patterns. The same was observed at the end of the steady-state deformations, so that the last pair of interferograms had to be equally eliminated. In this context, it may be mentioned that it is possible to

produce the required fringe patterns also for these points on the deformation-time curve with an automatic control and high speed shutter device which, again, was not available at the time of the present investigation. However, this is discussed in the last chapter of this thesis concerned with future research suggestions.

4.3 Reconstruction Set up

After the formation of interferograms has been completed, the reconstruction stage of the obtained interferograms must be considered. The method discussed in this section follows the general discussion of Chapter III. Hence, the interferograms that were produced in positions HR1, HR2, HL1 and HL2, shown in Fig.4.2 are reconstructed in the same way as already indicated by Fig.3.8. It is evident that reconstruction geometries for these interferograms will only differ in the angle θ and the distance OO' (Fig.3.8). However, in order to avoid any confusion in the directions of the deformation components to be evaluated, it is necessary to adopt a sign convention for each side of the sample. This is discussed in the following section.

4.3.1 Sign Convention and Reconstruction Geometries

Considering Fig.4.7, which indicates the finite thickness of the paper sample, the two sides of the latter are denoted by the

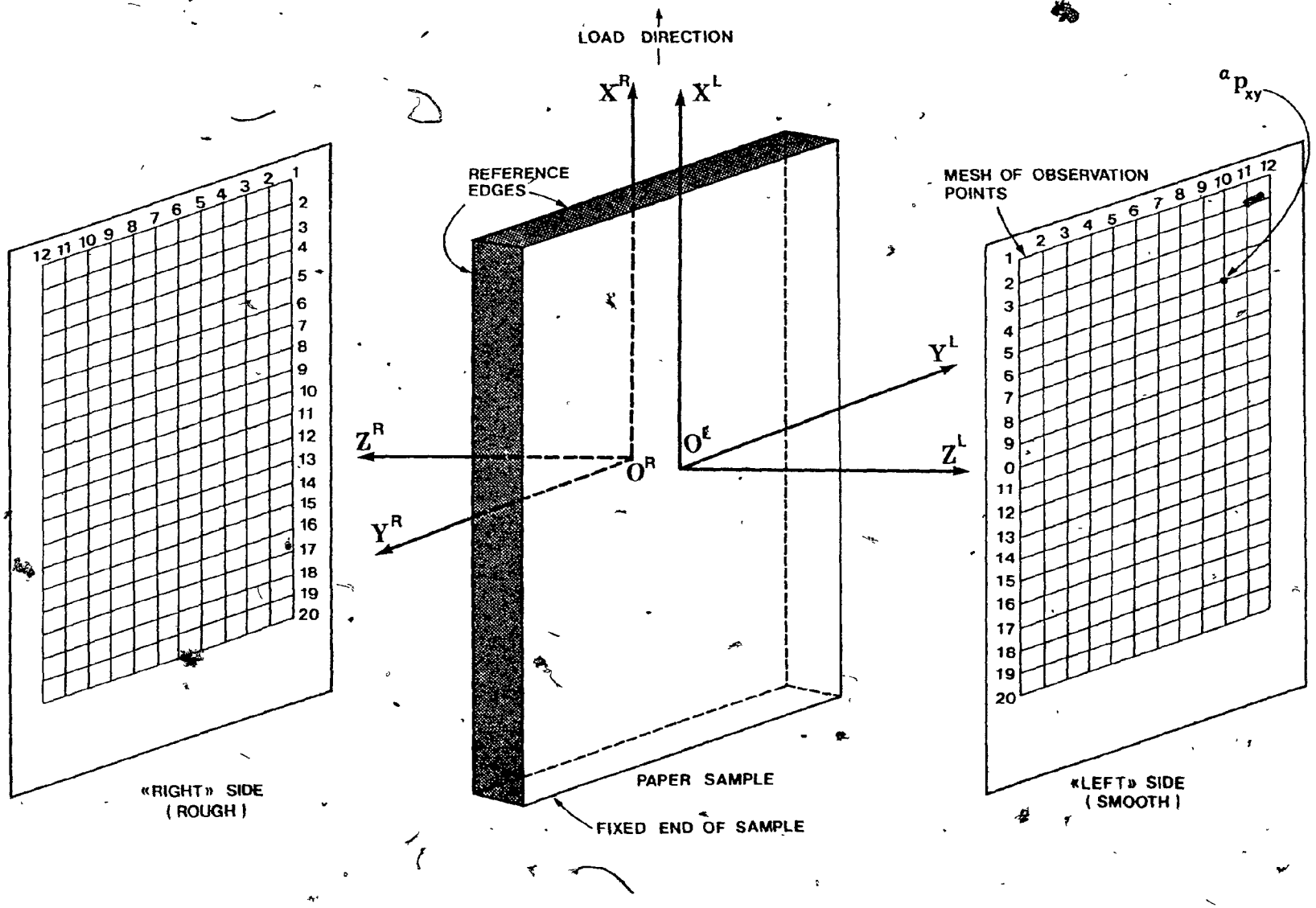

FIG. 4.7 REFERENCE FRAMES FOR «RIGHT» AND «LEFT» SIDES OF PAPER SAMPLE.

"right side (R)" and the "left side (L)", respectively. Usually, in the formation of paper webs, one side of the sheet appears to be smoother than the other side. In the present work, careful attention was paid to distinguish these two sides in all stages of the investigation. Therefore, the rough side of the sample was called the "right side (R)" and correspondingly, the smoother side (L).

It is seen from Fig. 4.6, that the paper sample has been loaded in the machining direction. On each side of the sample one cartesian frame is chosen. The origin of the frames are at the geometrical centers of the two sides of the sample. Hence, the load direction is that of the +X-direction, the transverse direction corresponds to the +Y-direction and the out-of-plane motion to the +Z-direction. On this basis, the reconstruction geometrics of the interferograms which are produced in the position of the plate holders HR1, HR2, HL1 and HL2, are illustrated by Fig.4.8.

On each side of the sample a mesh of observation points has been selected as shown. The size of the mesh covered 20 rows by 12 columns. This provided altogether, 240 observations points, which were 4 mm apart in both the X and Y directions. Finally, it should be mentioned that, for the purpose of measurements, the paper samples were cut to size with the precision of +0.01 mm.

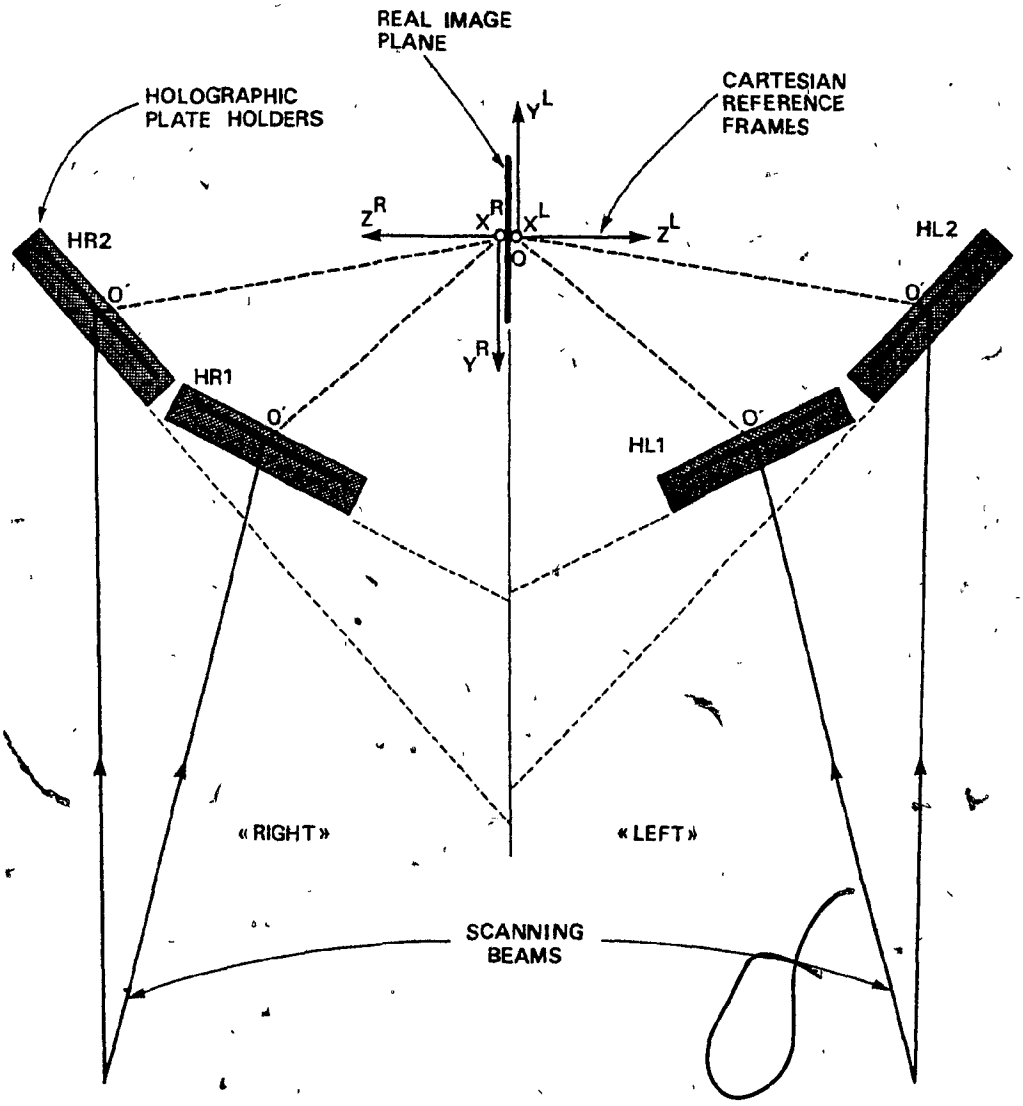

FIG. 4.8 RECONSTRUCTION GEOMETRIES OF THE «RIGHT»-AND «LEFT»-HAND SIDES INTERFEROGRAMS.

Then two edges were chosen as the reference edges. In all experiments concerning the thickness measurements and Beta-radiography, great care was taken to maintain these edges in the undisturbed sample.

4.3.2 Electro-Optical Reconstruction Technique

The technique required in the reconstruction stage of interferograms is shown in Fig.4.9 and also in the form of a block diagram in Fig.4.10. The lower part of the figure represents the reconstruction geometry employed as shown earlier in Fig.3.8. The following devices have been used in this arrangement:

4.3.2.1. Scanning Device

A photograph of this device is given in Fig.4.11. In addition, a diagrammatic sketch of this device, which has been firmly located on the holographic table by magnetic chucks, is shown in Fig.4.12a, whilst the scanning mirror arrangement is indicated in Fig.4.12b.

The optical flat mirror has, on the top face, a reflective surface. This mirror is mounted in a preset groove of a cylindrical piece, so that the reflective surface can be adjusted by means of three set screws, whilst the mirror itself is held by the pressure of a helical spring (Fig.4.12b). The cylindrical

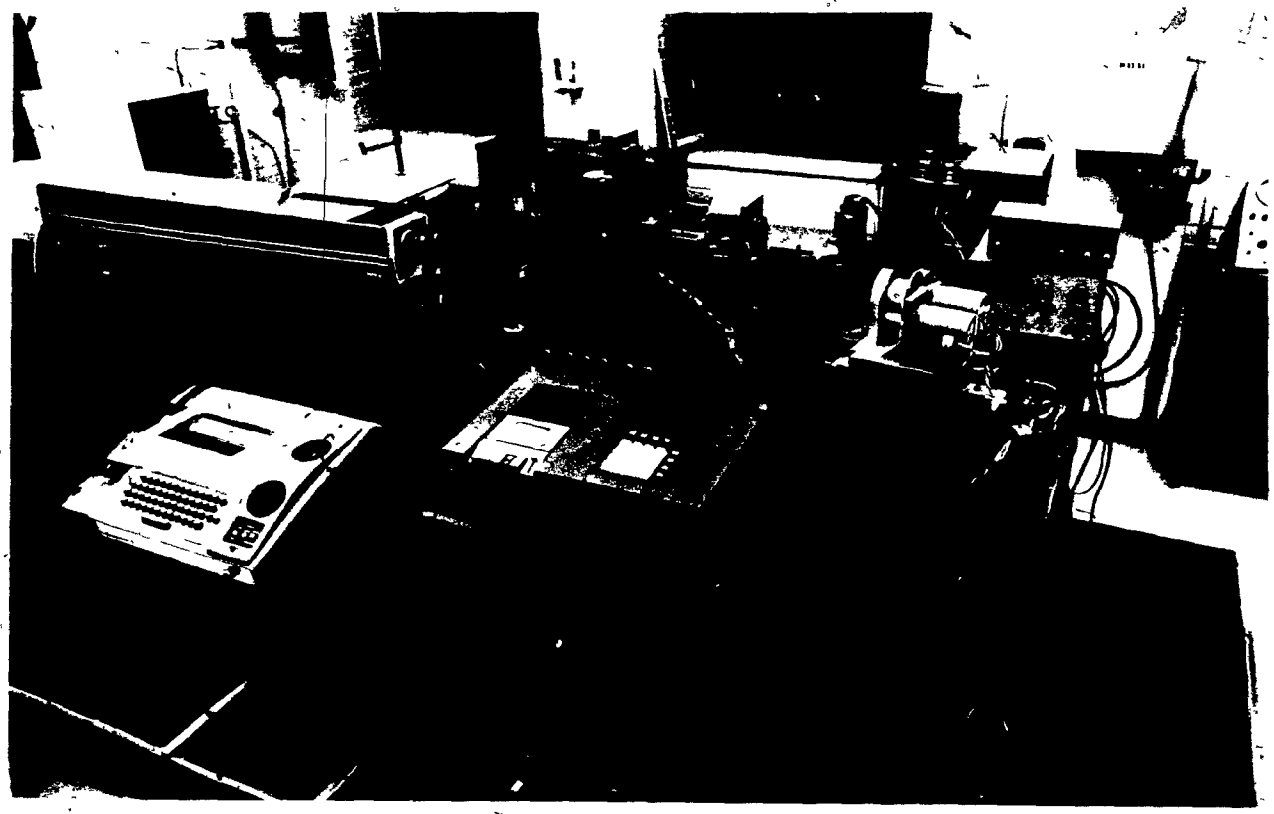

FIG. 4.9 PHOTOGRAPH OF THE AUTOMATED RECONSTRUCTION TECHNIQUE.

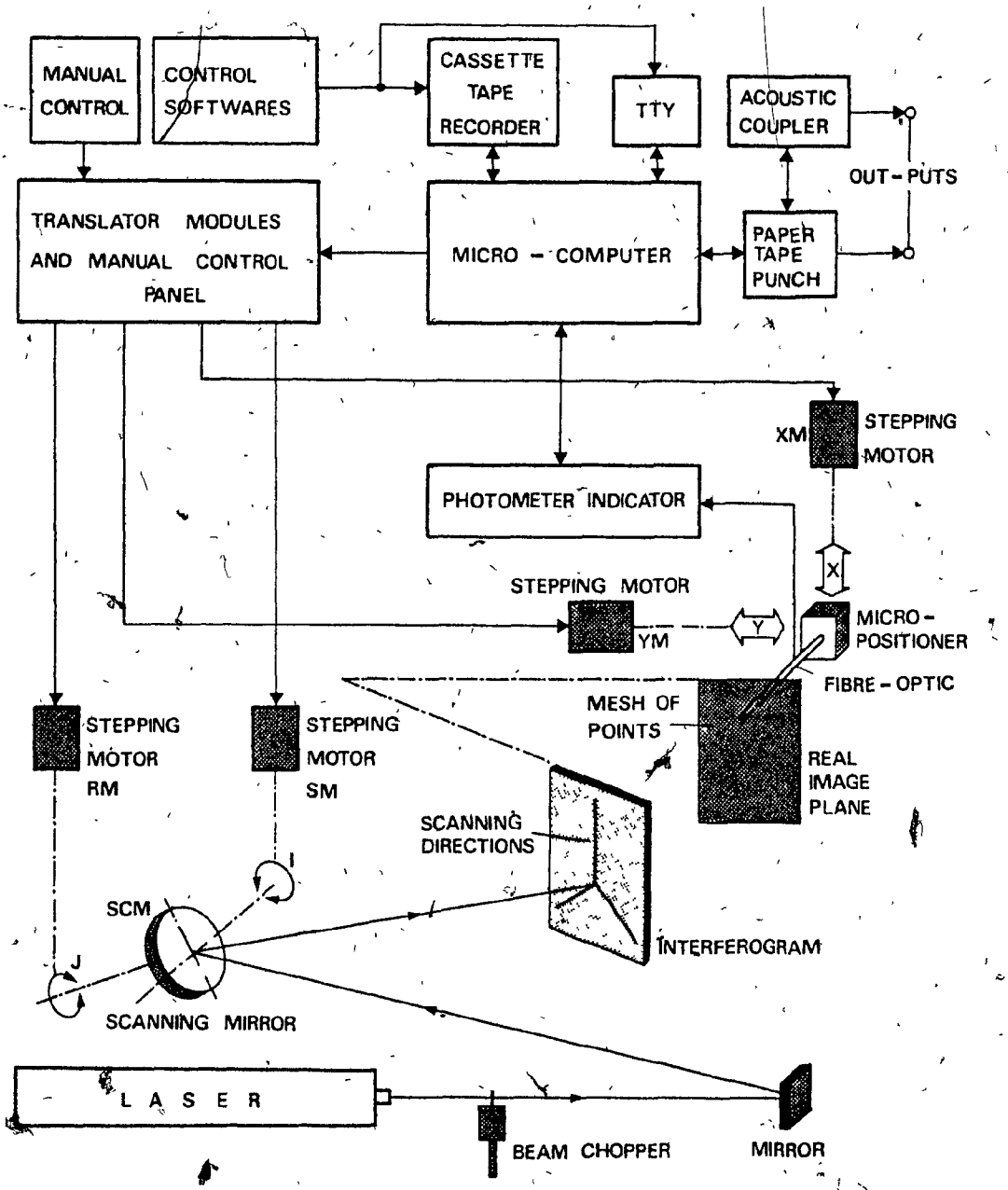

FIG. 4.10 - BLOCK DIAGRAM OF THE AUTOMATED RECONSTRUCTION STAGE.

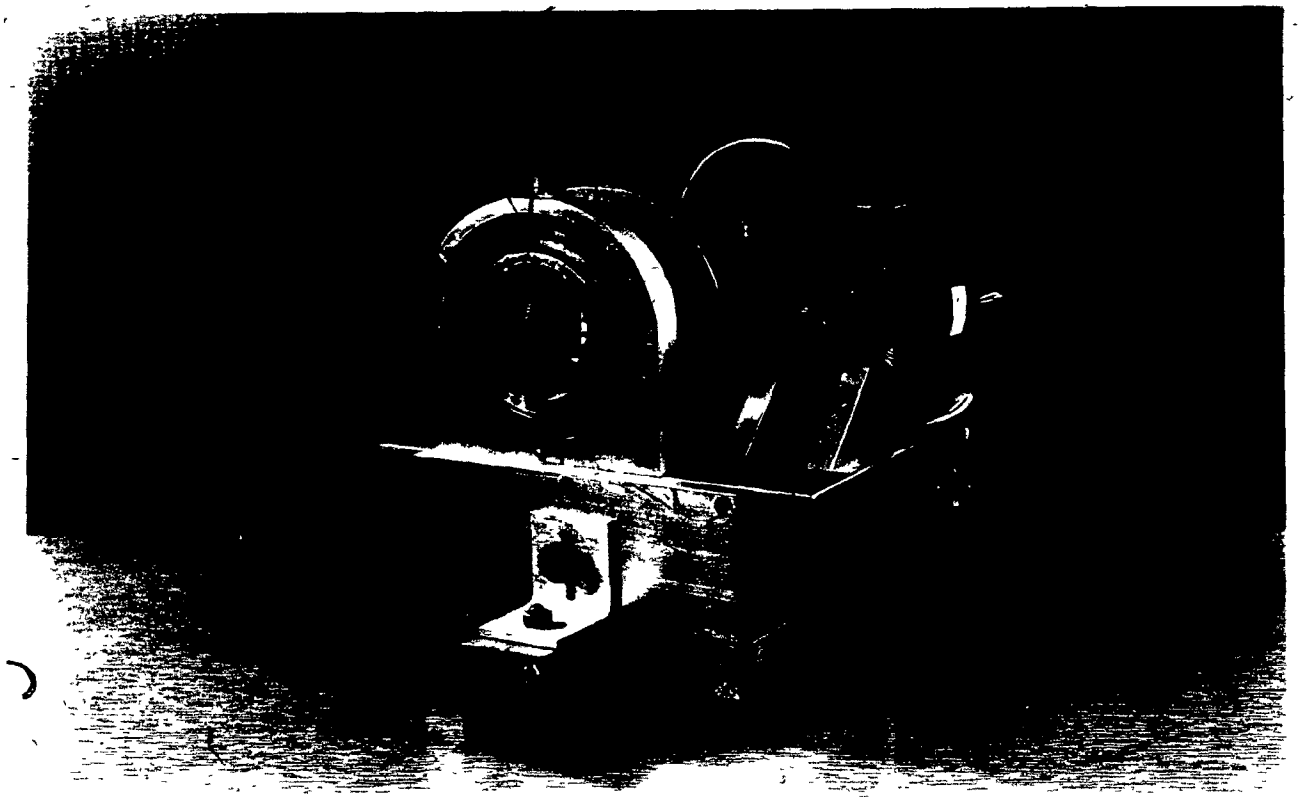

FIG. 4.11 PHOTOGRAPH OF THE SCANNING DEVICE.

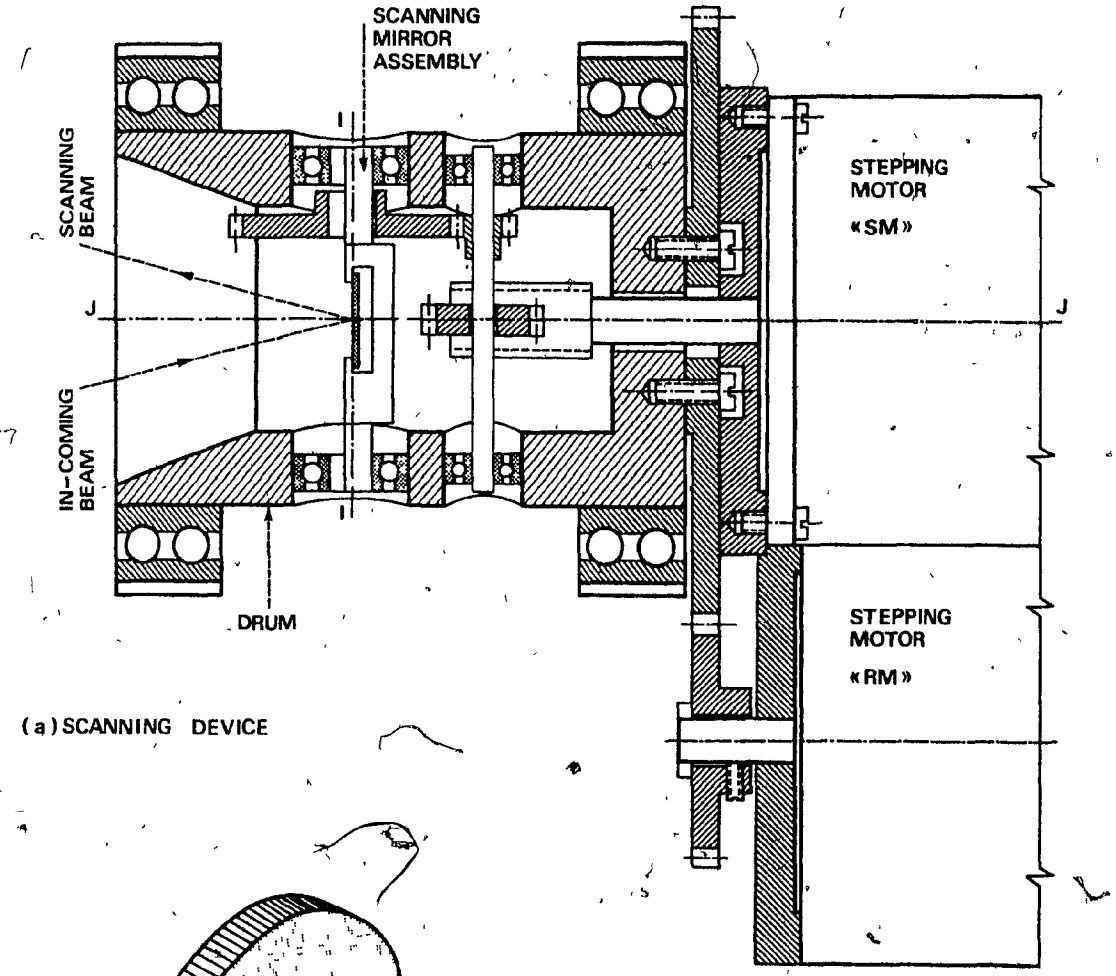

(a) SCANNING DEVICE

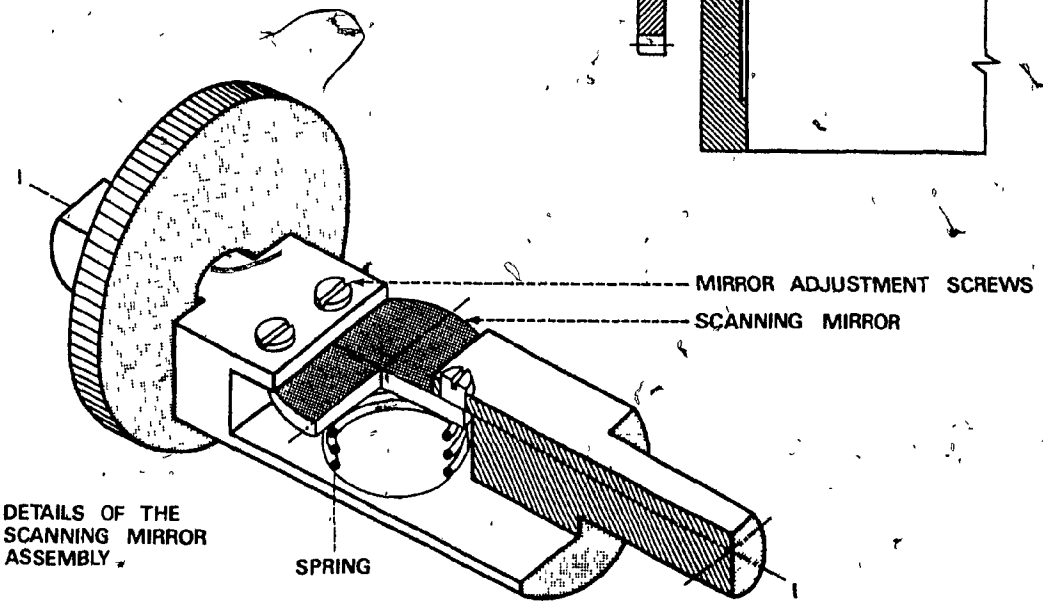

(b) DETAILS OF THE SCANNING MIRROR ASSEMBLY

FIG. 4.12 SCHEMATIC DRAWING OF THE SCANNING DEVICE.

piece is permitted to rotate about its "I-I axis". This piece is then mounted inside a "drum" (Fig.4.12a), which is supported by two high precision ball bearings. The incoming laser beam is reflected by the scanning mirror to the interferogram plate. Hence, one can sweep the beam along the predetermined "scanning direction" on the interferogram by rotating the cylindrical piece about the I-I axis. Any scanning direction, in turn, can be chosen by a simple rotation of the drum. This scanning device is further automated by using digital controlled stepping motors, one of which is employed to rotate the drum (motor RM) and the other to rotate the cylindrical piece (motor SM) (Fig.4.12a).

It should be noted that careful centering of the mirror support with respect to the J-J axis has been observed. Furthermore, the mirror mounting permitted a fine adjustment of the mirror so that on illuminating the mirror with a beam perpendicular to the mirror surface, deviations of the reflected beam from the normal to the surface did not exceed 0.01 degrees.

4.3.2.2 X-Y Positioner

A photograph and a drawing sketch of this apparatus are shown in Figs.4.13, 4.14a,b, respectively. As can be seen from the automated reconstruction stage (Fig.4.10), this device is used to position a fibre optic at any point of the mesh of observation points. The latter is predetermined on the real image plane.

FIG. 4.13 PHOTOGRAPH OF THE X-Y POSITIONER.

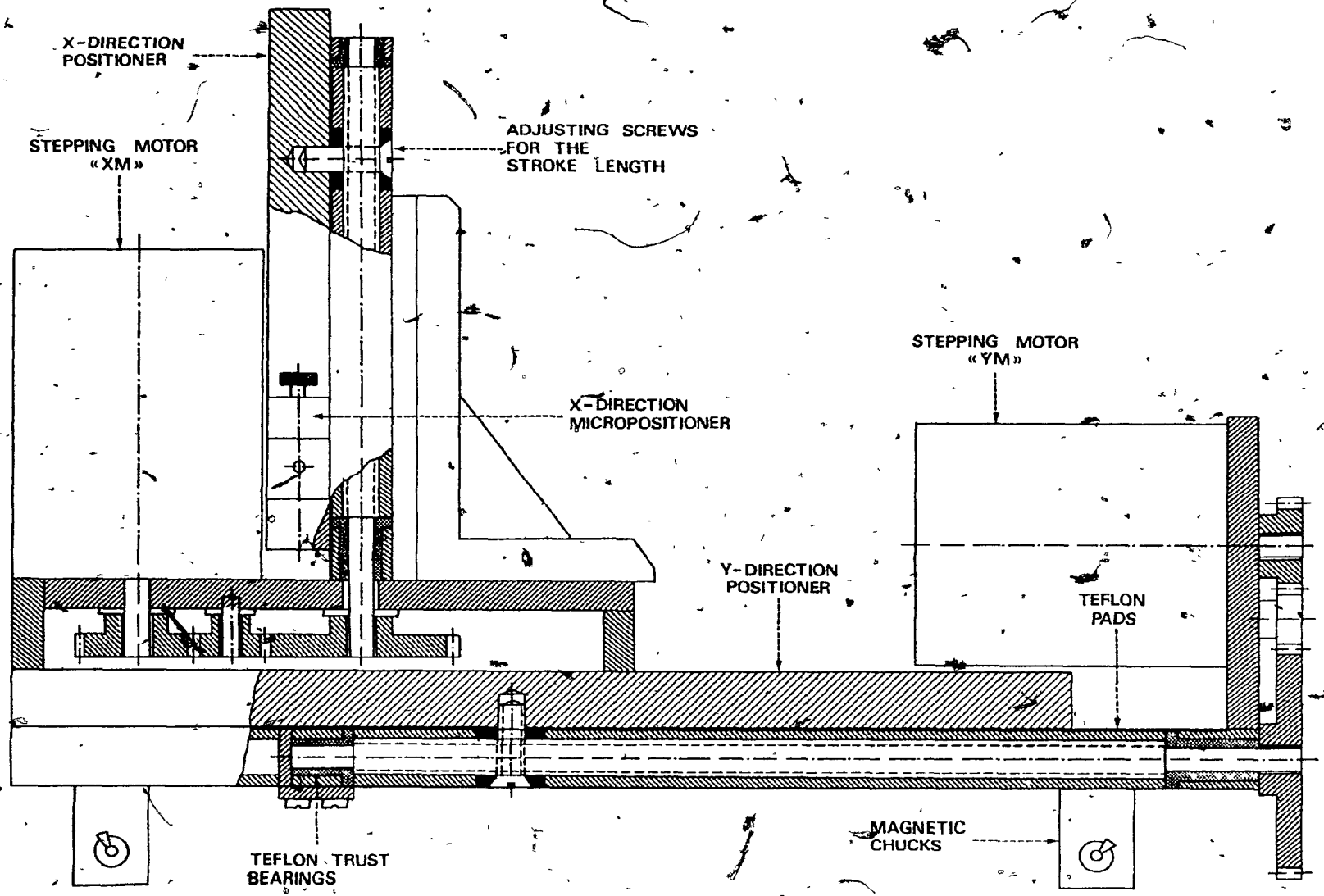

FIG. 4.14a X-Y POSITIONER — GENERAL SCHEMATICS.

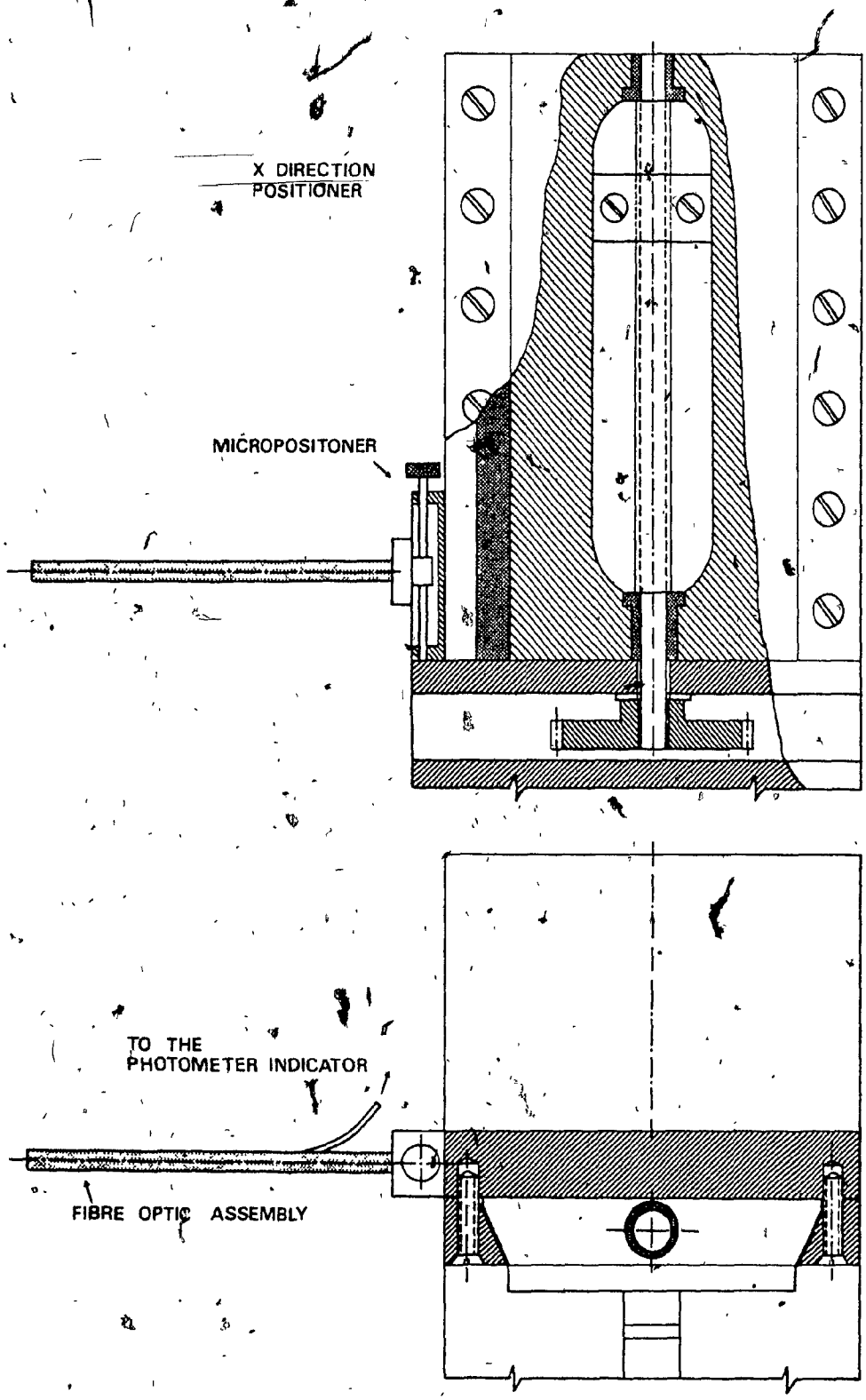

FIG. 4.14b X-Y POSITIONER – VERTICAL SLIDER AND THE FIBRE OPTIC ASSEMBLY.

The X-Y positioner consists of two sliders whose smooth and low friction linear motions are ensured by teflon pads (see fig. 4.14a). The linear motions were supplied by unified square-threaded shafts. The latter are supported by brass thrust bearings and are again driven by digital controlled stepping motors. In this context, motor YM is used to drive the horizontal slider, while motor XM is employed to drive the vertical one. The vertical slider, in turn, carries an assembly for the fibre optic (Fig.4.14b), which is called the "vertical micro-positioner". This positioner is required in the beginning of the X-Y motions, in order to preset the initial condition from the edge of the paper sample as mentioned previously.

4.3.2.3 Photometer Indicator

Since, for the fringe evaluation of the obtained interferograms a measurement of the light intensities is required, a photometer indicator (Zeiss, Model PMI-1 type) is included in the reconstruction set-up. This instrument measures the light intensities that are associated with the fringe intensities. The latter is carried by the fibre optic from the real image plane to the photometer. In this manner, the intensity measurement distinguishes the darkest area of the fringe pattern, which is defined as "no transparency" from the brighter areas, up to

"full transparency". This instrument permits, therefore, to record the changes in light intensities during the scanning of the interferograms and are used as an input to the subsequently discussed microcomputer. - It has been found in the present investigation, that for high contrast between bright and dark fringes, the setting of the range of transparency was extended from a 0-100 (standard) to 20-470. This permitted optimum contrast of the fringe pattern in the reconstruction of the obtained interferograms and their evaluation.

4.3.2.4 Microcomputer

It has been mentioned earlier that the read-out of a great number of observation points on the surface of the paper sample requires an automatic procedure to facilitate the corresponding evaluation of surface deformations. This has been achieved by introducing a "microprocessing" apparatus or microcomputer, discussed in this section. It can be seen from Fig.4.10, that an automatic reconstruction and read-out is made possible by this equipment, which was designed and built by the author of this thesis in the Micromechanics Laboratory of this University. In the following section, a description of the automatic reconstruction technique, using the devices discussed in 4.3.2.1-3 in conjunction with the microcomputer will be given, whilst the

construction details are given in Appendix I and the required program listing in Appendix II.

In general, the automatic reconstruction technique, required for the evaluation of the obtained interferograms, consists of the following parts:

1) the automatic scanning of the interferograms in three predetermined scanning directions,
2) measurements of the interferogram transparency (i.e. the light intensity associated with the fringe patterns) at each observation point,
3) the storage of these transparency measurements in the form of permanent records,
4) the evaluation of the fringe numbers from these permanent records and, finally,
5) the evaluation of the induced deformation field and the corresponding strain field.

Thus, the function of the microcomputer is concerned with parts (1), (2) and (3) above, whilst parts (4) and (5) are carried out by the main computer of this University. A general discussion of (4) and (5) will be given in Section 4.3.4, dealing with the evaluation of the fringe numbers.

Considering again the block diagram of Fig.4.10, where the interferogram is shown in position, then, as mentioned earlier, the

interferogram is scanned in three scanning directions by the scanning device, whilst the latter is driven by stepping motors SM and RM. Thus, the real image of the paper sample and the induced fringe pattern is reconstructed on a real image plane. Then, in order to measure the interferogram transparency, the photometer indicator and a fibre optic are used. The latter is positioned at a point on the mesh of observation points on the real image plane, by means of the X-Y positioner, which is driven, again, by stepping motors XM and YM. Thus, one important function of the microcomputer becomes, to activate the four stepping motors SM, RM, XM and YM, in such a way that, for each observation point on the mesh, the interferogram is scanned along the three scanning directions. Obviously, these four motors must run in a certain sequence. In the present work, this sequence is referred to as the "scanning technique", and will be outlined below. The next important function of the microcomputer, related to part (3), is to store the obtained results of the transparency measurements. For this purpose the photometer indicator is interfaced to the microcomputer so that the data, corresponding to the transparency measurements, are transferred from the photometer into the memory board of the microcomputer. The content of the memory can be sent into the main computer of the University (temporary storage) by means of

an acoustic coupler (Fig.4.10 top) or it can be punched onto paper tape by a punching unit (permanent storage).

The microcomputer itself is programmed to produce the above functions. This control program consists of two major routines, one of which is used to initialize the test conditions and the other to perform the scanning technique and the data storage. These routines, which are recorded on a conventional cassette tape, are designed in a general manner, such that the scanning directions, the rate of transparency measurements for the scanning directions, number of rows and columns of the mesh of observations points and the mesh size can be preset for the microcomputer operation. Furthermore, it can be seen from Fig. 4.10, that another feature of this equipment is the special interfacing of the stepping motors to the microcomputer. The latter permits the manual control of the motors in order to rectify initial testing conditions.

4.3.3 Automatic Scanning Technique

With reference to Fig.3.8, which has been used to discuss the general method of scanning, it becomes necessary to explain, in this section, the modified geometry used for the automatic scanning procedure. Thus, as shown in Fig.4.15a, the start point for the automatic scanning should be O' and any end point for scanning P^1, P^2 and P^3. However, it is apparent that by

scanning in the direction $O'P^2$, for example, a fraction of a bright or dark fringe may be missed in the counting. Hence, the scanning geometry scheme, indicated in Fig.4.15b, has been adopted which overcomes the difficulty of measuring the fractional fringe numbers. This way, the scanning lengths have been enlarged from both ends, i.e. from point O' to O" and P' to A. Similarly, for the two other directions, from O' to C and from P^2 to B, and O' to D and P^3 to E, respectively. These extensions in the lengths of scanning have been chosen in such a manner that at least one whole fringe will fall onto the length, thus permitting to evaluate an accurate number of fringes within the lengths $O'P^1$, $O'P^2$ and $O'P^3$, respectively. These extensions and fringe number evaluation in terms of the extended scanning lengths in mm is indicated in Fig. 4.15C.

After the modified scanning lengths are defined for the microcomputer the first direction to be considered in the scanning routine is O"A (Fig.4.16). Hence, the conjugate reference beam reflected by the scanning mirror from the laser source to the interferogram (Fig.4.10) is focused onto the starting point O". The scanning procedure, following the scheme of Fig. 4.16, is carried out automatically by means of the following steps:

a - the beam scans the plate in the direction 1 (motor SM),

b - it is then rotated to point B (motor RM),

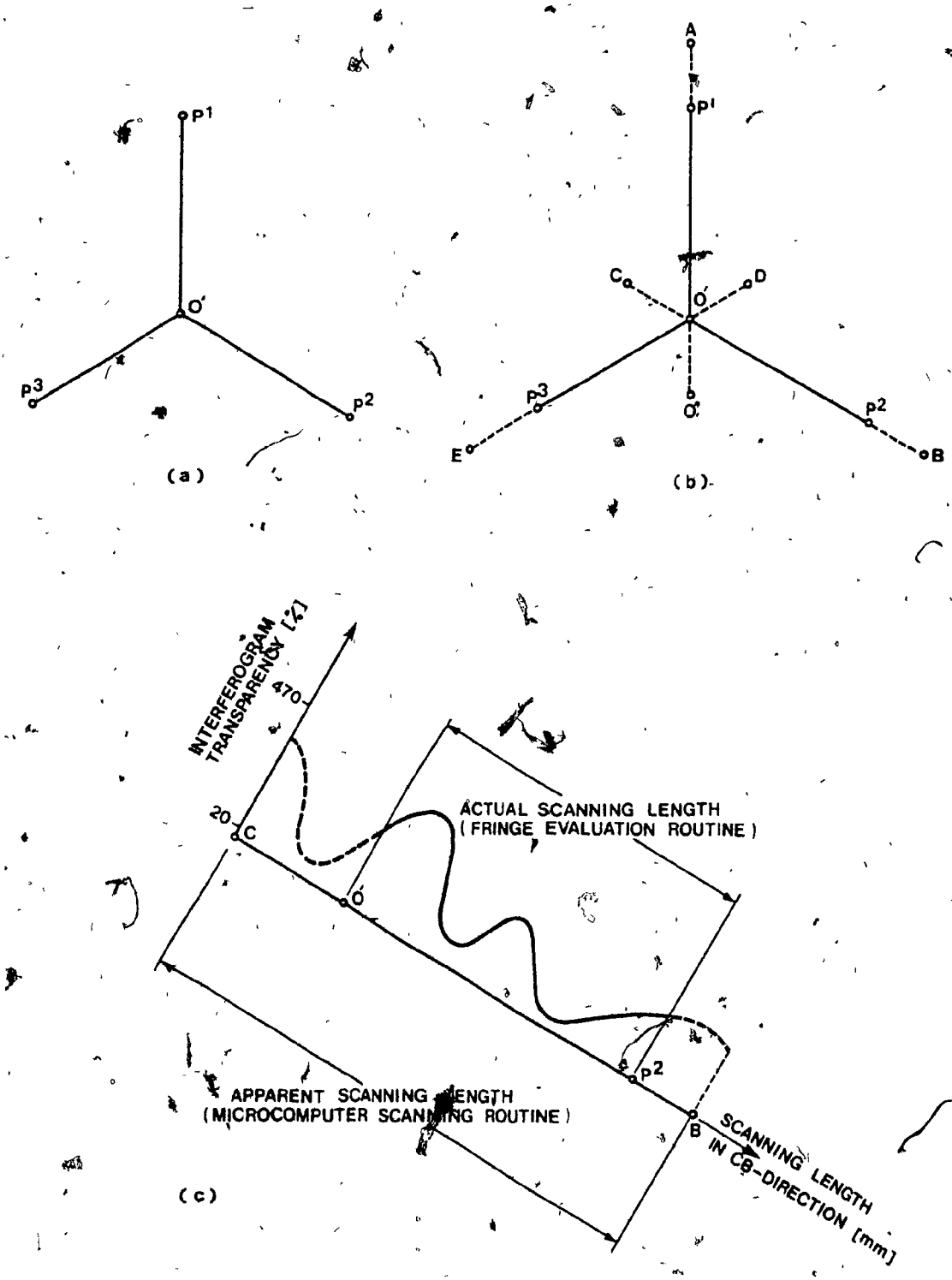

FIG. 4.15 THREE SCANNING LENGTHS.

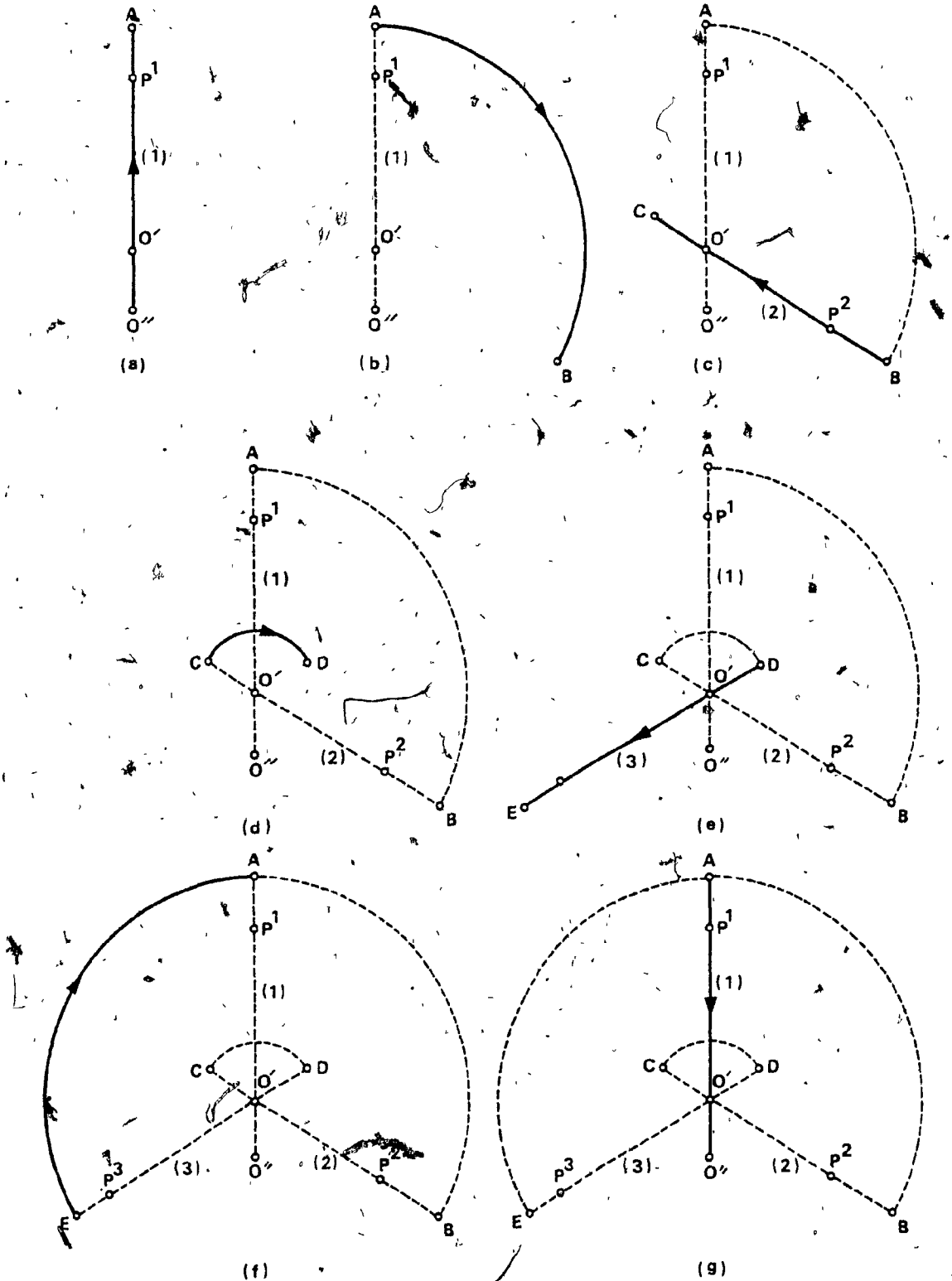

FIG. 4.16 AUTOMATED SCANNING PROCEDURE.

c - it then scans the plate in the direction 2 (motor SM),

d - it is rotated again to point D (motor RM),

e - and then scans the plate in direction 3 (motor SM).

f - In order to begin the procedure for the neighbouring observation point, the beam is rotated to point A on the first scanning direction (motor RM), and

g - the beam is moved back to the starting point O" (motor SM).

It should be noted that according to (4.3.2.3) the fibre optic required to transmit the light intensity of the measured fringes is, during the time of scanning, positioned at the observation point ${}^{\alpha}P_{xy}$ on the mesh. Thus, the transparency measurements are carried out by the photometer indicator in a continuous way with respect to the prescribed scanning directions. The data storage is then performed parallel to the steps (a), (c) and (e).

For a neighbouring observation point on the mesh the above procedure has to be repeated. As mentioned earlier in this chapter, for each side of the paper sample 240 observation points have been considered. It was also mentioned that the fibre optic is positioned at each of the points by the X-Y positioner. In general, the sequence of points to be analyzed is of no importance in the reconstruction method. However, from the point of view of

the microcomputer programming it was found more practical to select the observation points in a sequence, as shown in Fig. 4.17. Hence, these points are numbered from 1 to 240 in going from row 1 - 20. The first observation point is then point 1, and the final is 240. Once all the points have been observed the microcomputer moves the fibre optic back to the starting point 1 and stands by until the next is considered. At this point of the discussion it is useful to mention again that the vertical micropositioner of Fig. 4.14b is employed for accurately positioning point 1. It should also be mentioned that the tables of points in Fig. 4.17 is equally valid for interferograms of the "right" side of the paper sample only. For the left side ones, a mirror image of Fig. 4.17 is to be used. However, in the evaluation of the thickness variations from the αu_z^R and αu_z^L deformation components, careful attention has been paid to consider the analogous point on the two sides of the paper sample.

It should be noted that the above discussed automatic scanning technique is quite general. Hence, a larger number of mesh points and hence, scanning length can be preset. The general flow chart of this scanning technique is shown in Fig. 4.18. It also serves as the required flow chart for the programming. In this context, it is important to mention two other aspects of the microcomputer system.

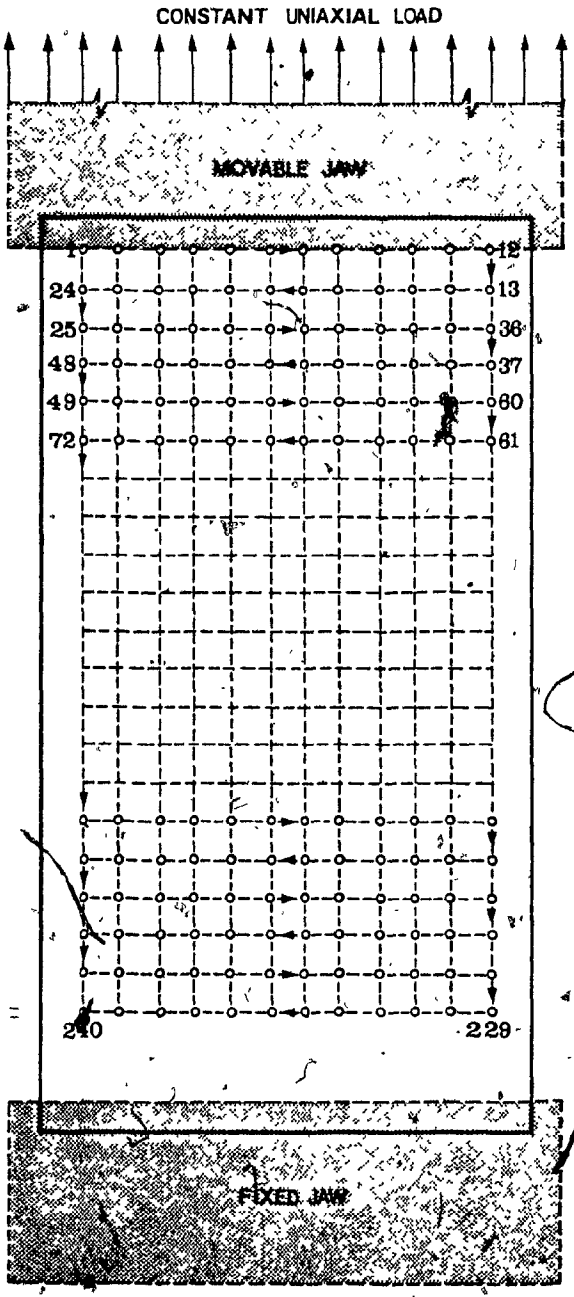

FIG. 4.17 SEQUENCE OF THE OBSERVATION POINTS IN THE MICRO-COMPUTER SOFTWARE ROUTINES.

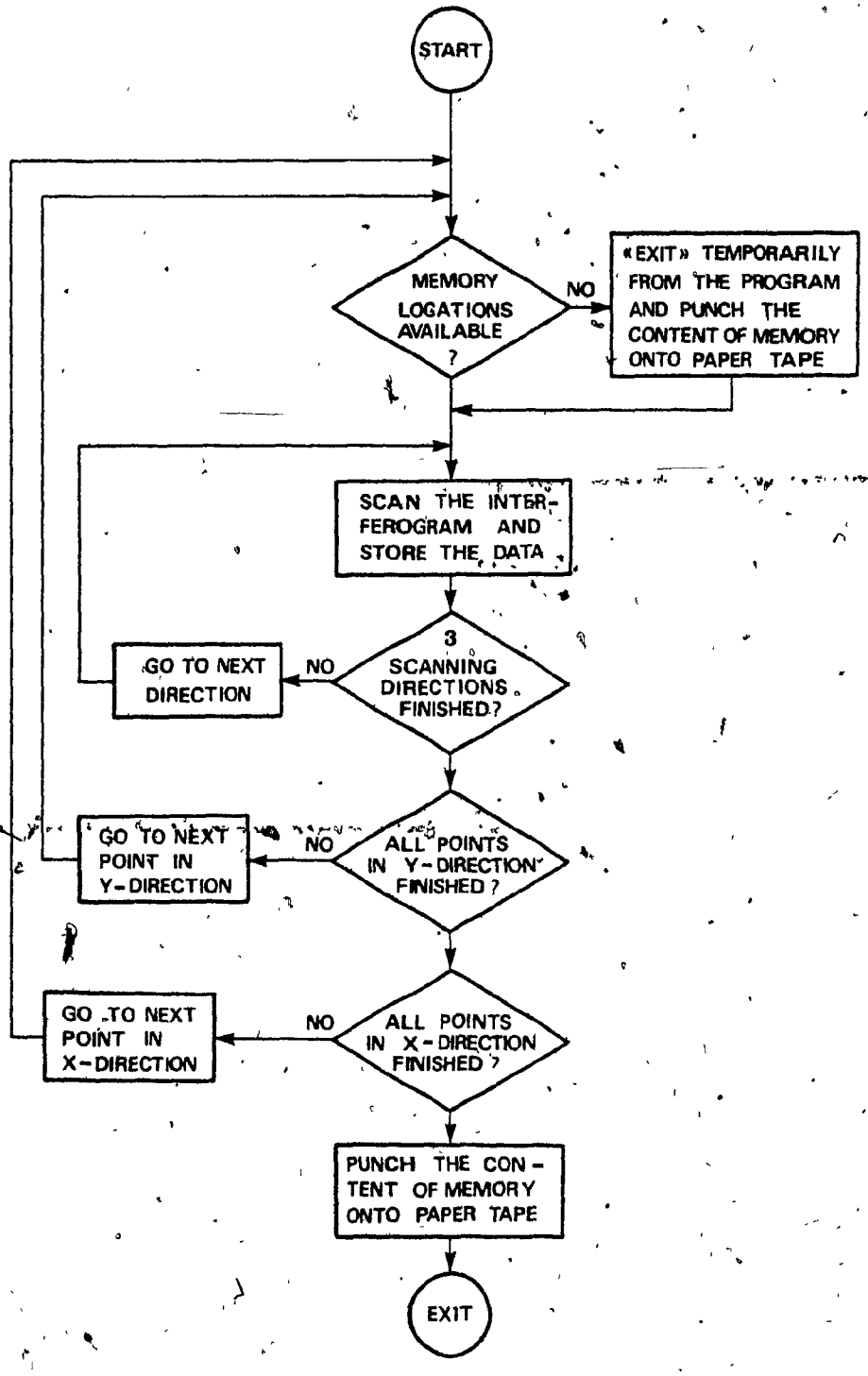

FIG. 4.18 SUMMARIZED FLOW-CHART OF THE MICROCOMPUTER SOFTWARE ROUTINES (SEE ALSO APPENDIX II).

The first aspect deals with the memory allocation for storing the "raw data", i.e. the results of the transparency measurement. As an example, considering the reconstruction results of the interferograms of newsprint paper samples, then for each scanning direction 30 transparency measurements have been carried out at a rate of 10 readings/second. A minimum of 120 bytes (1 byte in this system = 4 bits) memory locations have been assigned to the storage of the results. Hence, noting that there are 240 observation points to be analyzed with 3 scanning directions for each point, a minimum memory of 86.4K bytes had to be assigned to each interferogram evaluation. However, since the present system had been equipped with a 4K byte external memory that is capable of storing the raw data for 11 points only, it has become necessary to employ a loop within the microcomputer program (Fig. 4.18), so that a much larger number of points and their corresponding reading can be accommodated. The function of this loop is to examine the availability of memory locations within the scanning technique. Once the limit of the external memory is reached the computer is executing a "temporary EXIT". It therefore punches the complete memory content onto a paper tape and returns afterwards to the point of observation corresponding to the "temporary EXIT" in the routine. Thus, by inserting such a loop the 240 observation points and their readings are accommodated. This also applies to

a much larger number of points. Thus, a 1000 or more points on each side of the paper sample could be arranged this way.

The second aspect is concerned with the synchronization of the reading and the storage of the raw data with the scanning motor action. Since the raw data is obtained by means of the photometer indicator the latter had to be interfaced with the microcomputer, such that the raw data flow rate can be extended within a range of 10 - 60 measurements/second. This makes the design of the microcomputer and the synchronization procedure fairly flexible, so that this system can also be used for various structured foil materials.

4.3.4. Evaluation of Fringe Numbers

The raw data stored on the paper tape represents the photometer output. Generally, it is possible to plot this data on a "CALCOM" plotter unit and to produce curves that correspond to the fringe patterns, so that counting of the fringe numbers can be carried out directly from these curves. However, for a large number of observation points, it was necessary to evaluate the fringe numbers by applying a "finite difference technique" to the obtained data. For this purpose, the computational procedure outlined by Fig. 4.19 has been adopted.

In this context, the paper tape of each obtained interferogram has been fed into the "MUSIC" system (McGill University Systems for

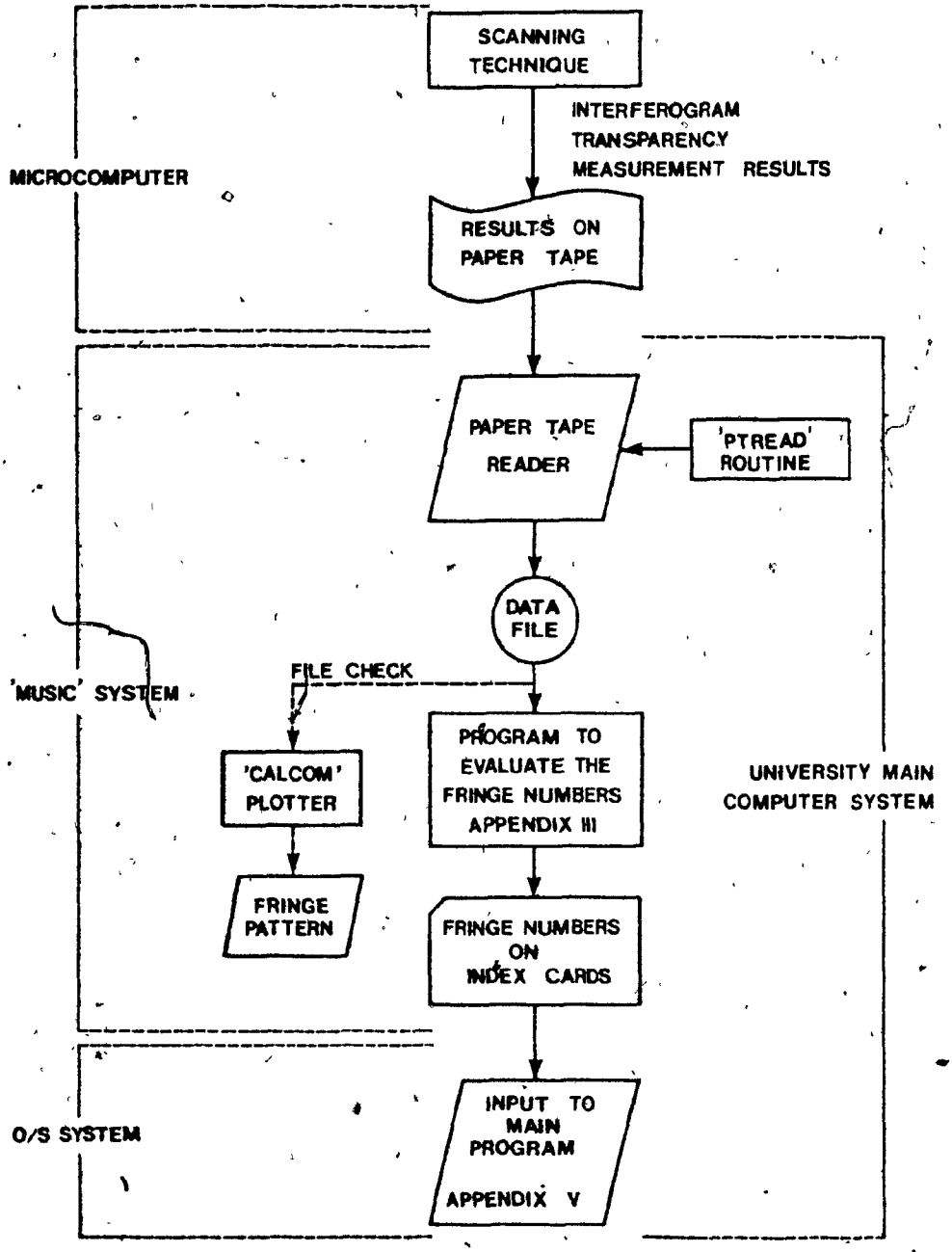

FIG. 4.19 FLOW CHART FOR THE PROCESS OF FRINGE NUMBER EVALUATION.

Interactive Computing), in order to create a data file. Then, within the same system, a computer program has been employed, together with the data file, from which the fringe numbers were evaluated and punched onto index cards, (Appendix III). The latter were then used in the "main Fortran program" for the evaluation of the deformation field. The corresponding program listing is given in Appendix V.

4.3.5 Statement of Accuracy

During the course of this investigation great attention has been paid to minimize the experimental errors. The major error sources are associated with presetting the reconstruction geometry and the mechanical devices in fringe number reading.

The inaccuracies due to the scanning device and the X-Y positioner arise in presetting some geometrical conditions, such as the scanning lengths, the angles between the scanning directions and the positions of the observation points themselves. To eliminate as far as possible these error sources, the two ends of each scanning length have been preset by means of photoresistors, so that the fringe numbers were counted within an accuracy better than ±0.1 of a bright fringe. The latter corresponds to an average accuracy of ±0.05 μm in the deformation evaluation. The X-Y positioner has also been capable of positioning the fibre optic at the observation point within an accuracy of ±0.012 mm.

A further source of experimental error is the image aberration during the scanning of the interferograms. Aberrations will occur when the position of the scanning beam is not identical to the mirror image of the reference beam[47,54]. In this context, since the present set-up permits fringe evaluation with an accuracy up to ±0.1 of a fringe, the possible aberration would be within this range of accuracy. These aberrations, however, can be accounted for in the fringe numbers evaluation by employing some correction factors. In the present work the geometrical arrangement of the scanning beams has been carefully observed. Thus, no correction factor was required.

4.4 Mass Distribution Measurement

The random arrangement of fibres in a paper sheet and their uneven distribution produce a variation in the local thickness. It has been mentioned earlier that this mass distribution and the nonuniform thickness of the sheet are major characteristics for the mechanical response behaviour for such networks. Hence, the determination of these characteristics and their relation to the deformational behaviour of the paper sample are the most important objectives in the present study. As mentioned in Chapter II, the conventional technique used in testing paper has been modified so that "local mass" measurements and the thickness measurements can be performed in accordance with the requirements -

stated in Chapter II. Hence, first the method of Beta-radiography will be discussed below, whilst the local thickness measurement technique will be described in Section 4.5 of this Chapter.

4.4.1 Beta-radiography

Among the various techniques for establishing mass distribution in paper samples such as "weighting" or the method by "light transmission", Beta-radiography was developed in the 1960's by The British Paper and Board Manufacturers' Research Association. Since then, the method has been studied and rectified [57-64] and today it is considered as a proper tool in the determination of mass distribution.

In employing Beta-radiography technique, the radioactive sources available are Krypton-85, Promethium-147 and Carbon-14, which can penetrate through paper samples of basis weight 2250, 400 and 240 g/m^2, respectively. Since, in accordance with the given definition of the basis weight (Chapter II) of newsprint paper, which in this investigation is of the order of 85 g/m^2, the radioactive source C-14 was found suitable for the present technique. For the experiment itself, the C-14 radioactive material has been embedded in a clear plastic plate of 1 mm thickness. The plates used in the experimental procedure were of the size 7 x 12 cm. This size was considered large enough to cover the entire surface of the paper sample and the required

reference handsheet. As mentioned in Chapter II, the simultaneous radiation of the paper sample and the handsheet is necessary. As shown in Fig. 2.2, dealing with the general Beta-radiography technique, the actual arrangement for the performed test series is given in the next two sections.

4.4.2 Experimental Set-up

The actual Beta-radiography arrangement that has been used for the present study is shown in Fig. 4.20. This figure shows that a paper sample and a "multi-step strip" of a handsheet are positioned on each side of the C-14 plate. Thus, they are sandwiched between two unexposed X-ray film plates. In order to maintain proper contact of these two paper samples and the multi-step strip handsheet, two foam pads were inserted between the set-up base plate and the light insulation box, as shown in the figure. Using this arrangement, the paper samples were exposed to the Beta-radiations in the insulated box for 150 ± 1 minutes. The exposure time was chosen to obtain the required contrast and resolution of the Beta-radiograms. At the end of the exposure time the obtained radiograms were developed in a conventional manner.

4.4.3 Evaluation of Beta-radiograms.

In the present investigation the Beta-radiograms of more than 60 newsprint paper samples have been studied. For the purpose of

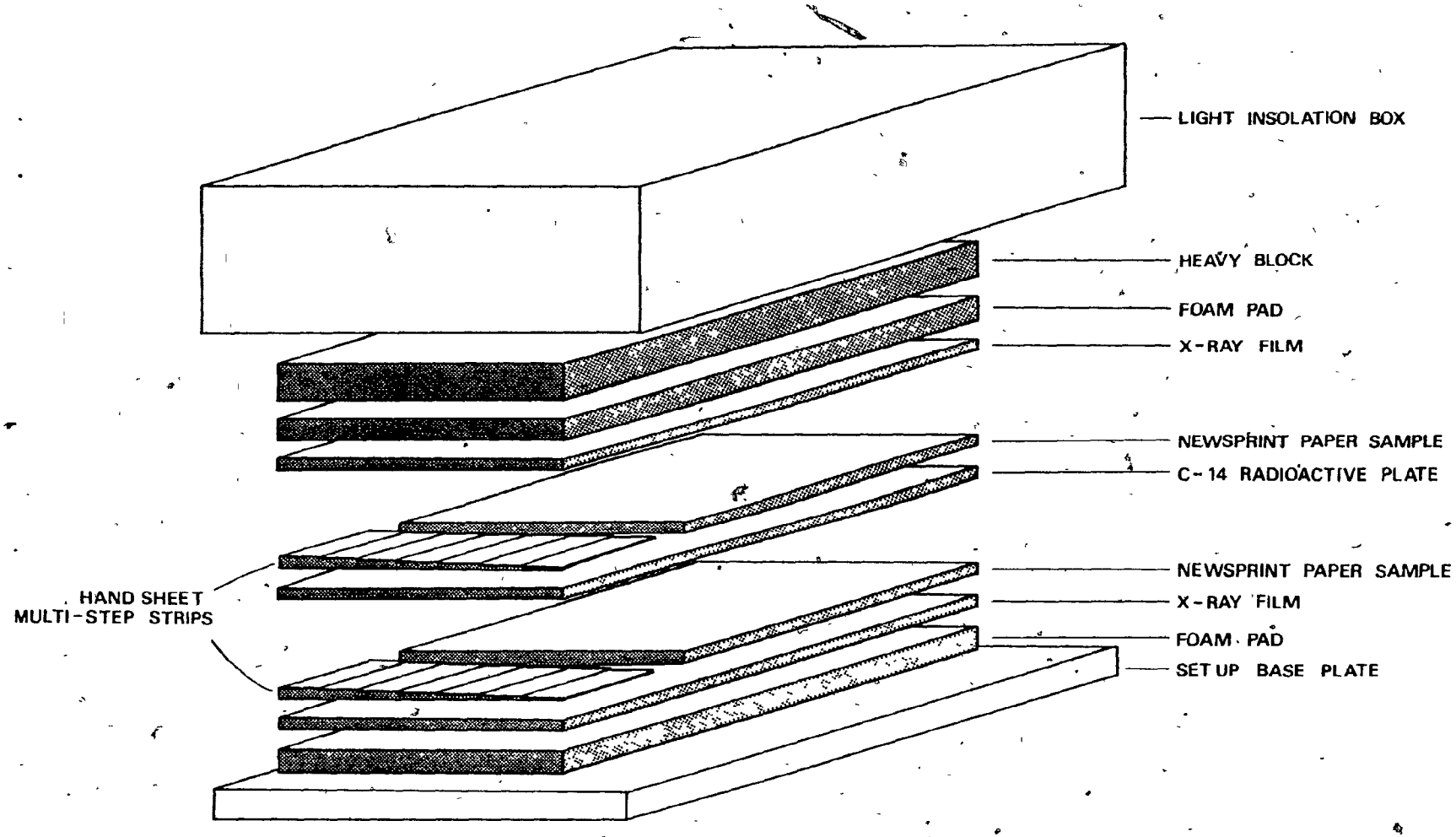

FIG. 4.20 BETA-RADIOGRAPHY – EXPERIMENTAL SET UP.

sequential-DSHI method and corresponding thickness measurement of the paper samples, only a certain number of the paper samples were considered for the experimental data. Thus, in the following presentation the results will refer to a particular sample of the totally tested paper samples.

It was stated in Chapter II that the amount of absorption of Beta-rays by the X-ray film over a given area is proportional to the rays that are transmitted through the sample (Equation 2.4) and where the latter is a function of the mass of the test sample (Equation 2.2). It is evident that, for the evaluation of the Beta-radiogram film, the relation between the film absorbance and the actual mass distribution within the paper sample is required. It has been found convenient to determine such a relation from a direct measurement technique that was developed in this laboratory. Thus, a handsheet of the paper material with a known basis weight of approximately 10 g/m^2 for the comparison with the absorbance of the Beta-radiogram of actual newsprint was employed. Due to the knowledge of the basis weight of the handsheet, the direct measurement of the basis weight of the newsprint sample becomes possible. Hence, a "calibration curve" using the handsheet was obtained in the following way.

A strip of the handsheet was produced in seven steps so that each step contained a double layer of handsheet. This is indicated

in the diagrammatic sketch of Fig. 4.21 and the actual Beta-radiogram for this calibration procedure is shown in Fig. 4.22. In this manner, the basis weight of the strip is equivalent to 20, 40,...,140 g/m^2 by considering steps 1,2,...,7, respectively. Since the strip and the paper sample are exposed to the Beta-rays together it is possible, by analyzing the Beta-radiogram, to determine the average film absorbance (in percentage) over the area of each step. These absorbance measurements have been carried out by means of a microdensitometer discussed subsequently. Thus, for each step of the handsheet strip, the average basis weight $\langle w \rangle^s$ and the corresponding film absorbance on average $\langle A \rangle^s$ were obtained. The superscript refers to steps s=1,2,...,7, as indicated in Fig. 4.21. The calibration curve obtained in this manner is shown in Fig. 4.23. The validity of this curve is based on the assumption that the handsheet and the newsprint sample are of approximately the same structural composition.

Before dealing with the actual evaluation of the basis weight at a given point α of the material sample, which will be required for the correlation of the measured mass density and the induced strain field, it is necessary to clarify the insertion of the scanning electron microscopy (SEM) observation into the evaluation. Since the handsheet material supplied by the Pulp and Paper Research Institute of Canada (PPRIC) was approximately a basis weight of 10 g/m^2, a verification of a similar microstructure with the tested

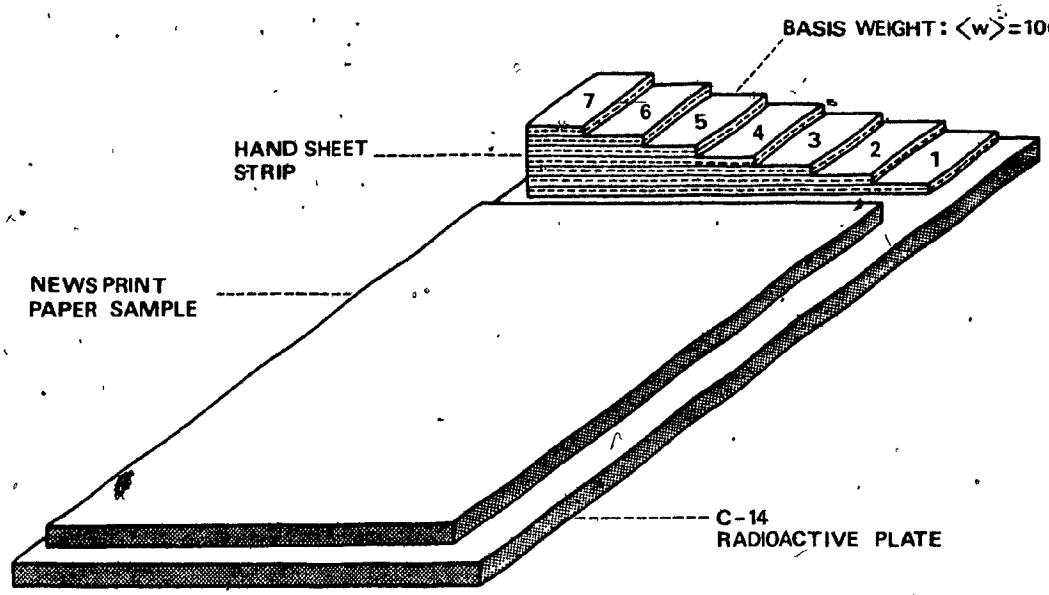

FIG. 4.21 PAPER SAMPLE AND THE HAND SHEET STRIP IN POSITION

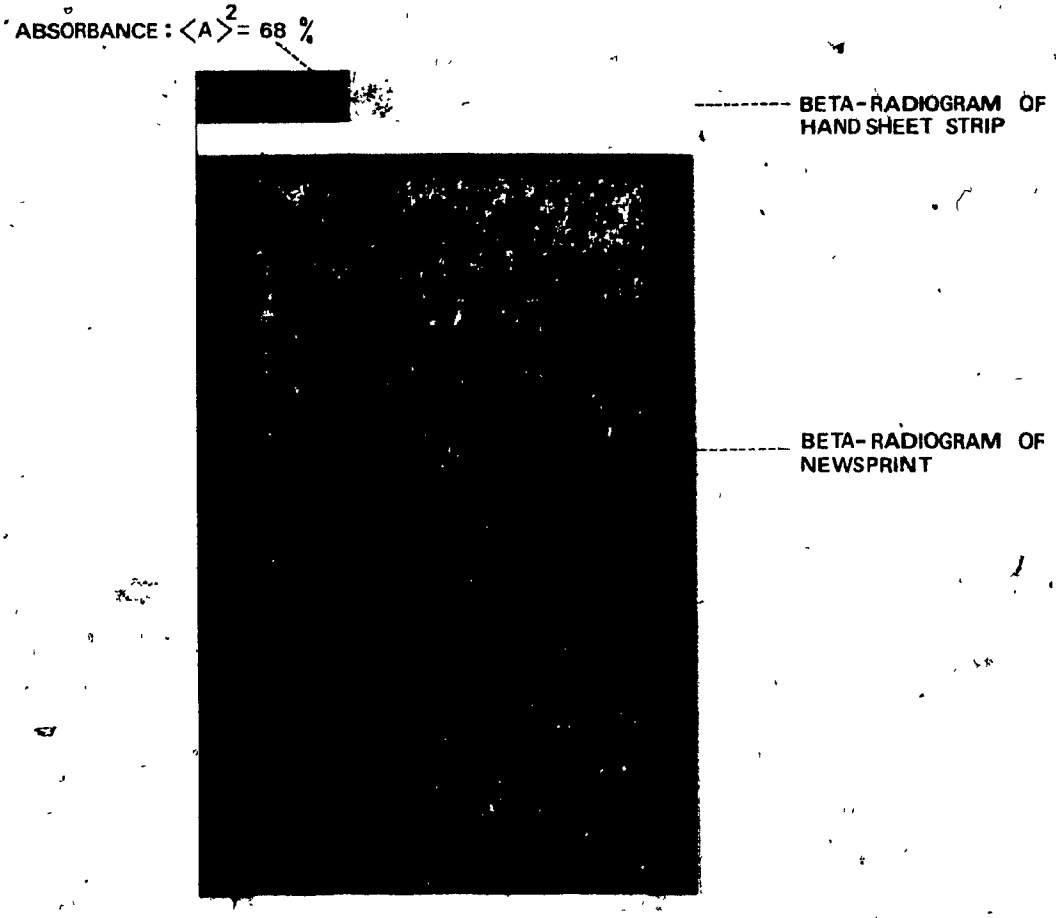

FIG. 4.22 PHOTOGRAPH OF THE TESTED BETA-RADIOGRAM

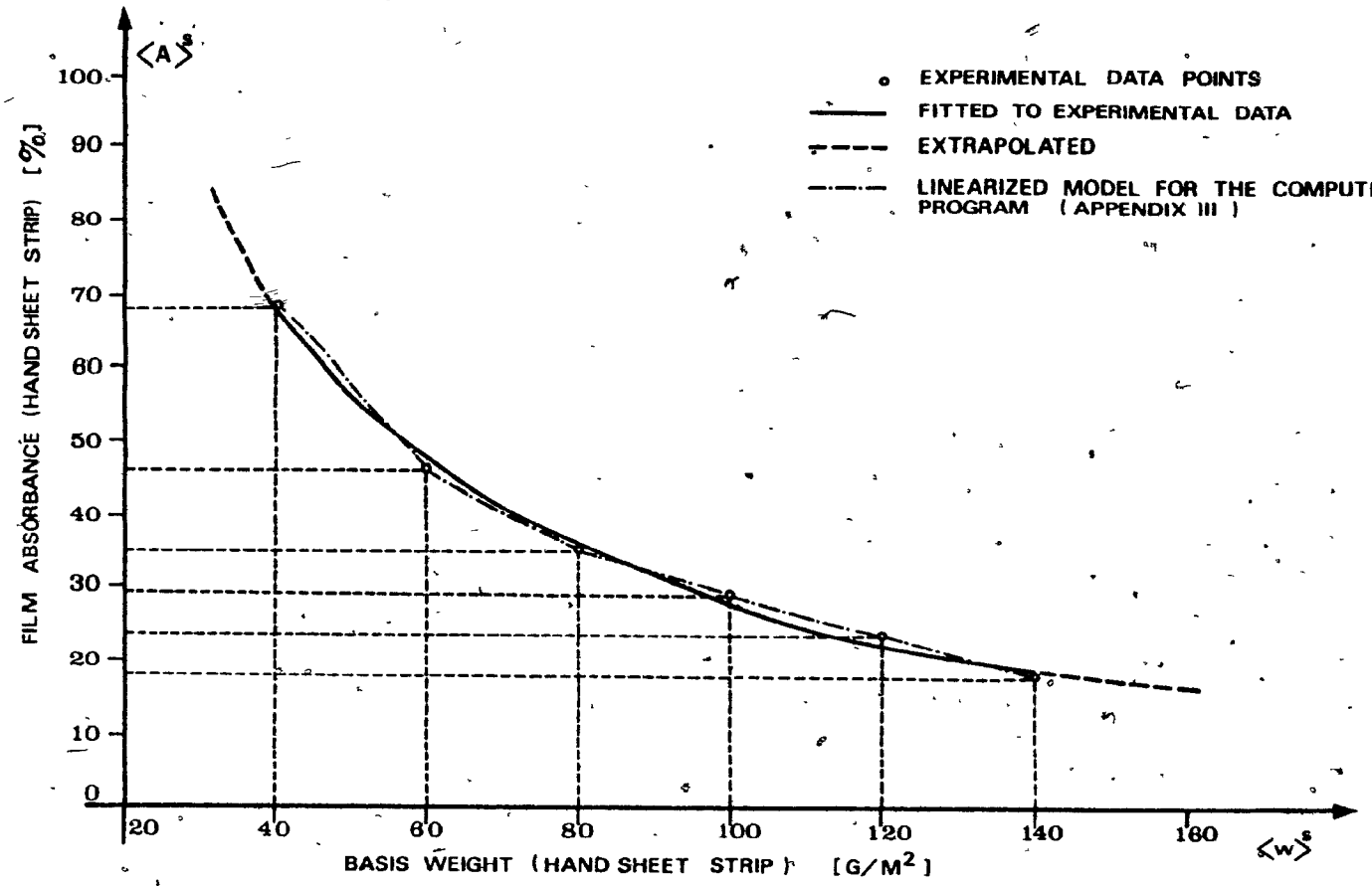

FIG. 4-23 BETA-RADIOGRAPHY CALIBRATION CURVE

newsprint sample, 8 randomly chosen areas of the handsheet (0.55 mm x 0.55 mm) were subjected to observation in the SEM. This resulted in a typical microstructural arrangement as shown in Fig. 4.24. To check on the given basis weight value the total length of fibres within the viewing area of each micrograph was measured. Since the mass density of the handsheet fibres themselves for this material was established to be 1.55×10^{-4} g/m, the basis weight in this manner was calculated and the result was 9.58 g/m^2. Allowing for a possible shrinkage of the fibres in the high vacuum system of the SEM chamber, the above value is very close to that given by PPRIC. For the calibration the average value of the basis weight was therefore taken to be 10 g/m^2. In order to use the handsheet as a calibration material the uniformity of the absorbance was also checked. In comparison to the actual newsprint Beta-radiogram, the calibration strip material was found to have a uniform film absorbance (see Fig. 4.22).

For the actual measurements of the absorbance by means of "microdensitometer", the latter fulfills two functions. The first function is to permit, optically, a reference light to illuminate the Beta-radiogram film to be investigated over an area of 0.25 mm in diameter, corresponding to the area of an observation point explained earlier in Fig. 3.1. Thus, the light which is transmitted by the film is measured by the

ACTUAL AREA : 0.55mm x 0.55mm

FIG. 4.24 TYPICAL SCANNING ELECTRON MICROGRAPH OF HAND SHEET - MAGNIFICATION : 180X

optical arrangement and compared to the reference beam. This results in the output of the instrument, giving the absorbance of the film at the illuminated point α of the film. The second function of the instrument is the plotting of the obtained absorbances by means of a mechanical device. This stage consists of two moving tables, the motions of which are synchronized. One of the tables is made of transparent glass, holding the sample under the optics. Then, upon each reciprocal motion of the table, the illuminating light beam scans the film along a scanning line of 0.25 mm thickness. On the other table a chart is provided and a plotting pen unit. Hence, on scanning the film in a certain direction, the output from the optical arrangement is plotted with respect to a chosen position of the observation point on the scanning line. Thus, the film corresponding to the handsheet was scanned over the strip length and the average absorbance for each step on the strip was calculated. For the actual newsprint sample film, again 240 points were considered and the obtained Beta-radiogram was scanned along 12 columns in the arrangement of Figs. 4.7 and 4.17. A typical result for this scanning is given in Fig. 4.25. In this manner, 12 curves were obtained, corresponding to 240 measured absorbance values. The scanning procedure was carried out so that the position of the scanning lines and the 20 observation points for each line were preset within an experimental accuracy of ±50 μm. This was

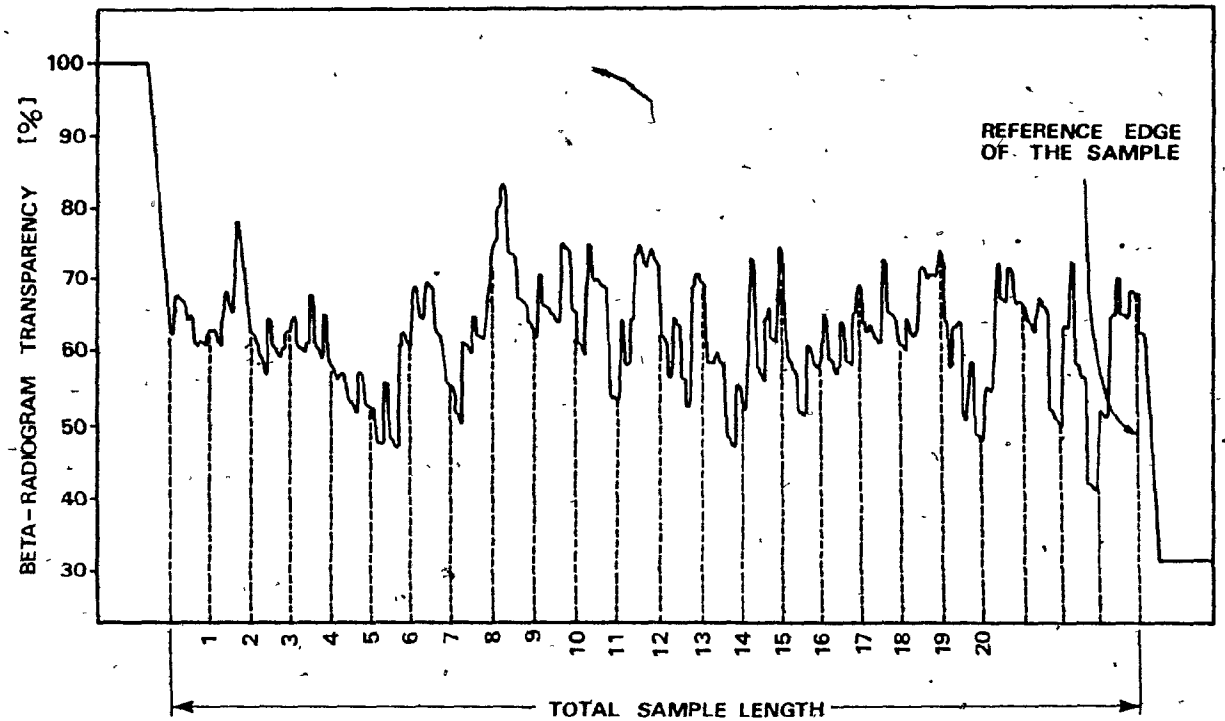

FIG. 4.25 TYPICAL MASS MEASUREMENT CURVE OBTAINED FROM SCANNING THE BETA-RADIOGRAM ALONG ONE COLUMN OF THE MESH.

achieved by using the radiographic images of the two reference edges of the carefully cut paper sample.

The results obtained from the curve indicated in Fig. 4.23 were then fed into a computer program by linearizing this curve in the manner indicated in that figure. The computer results corresponding to the calculated basis weight for the 240 points on a newsprint paper sample are shown in Appendix V.

4.5 Local Thickness Measurement

It is well known in paper manufacturing that the local thickness of paper is a function of the formation process. The techniques conventionally used for measuring the thickness of paper samples and its possible variation, when subjected to external load, is given in references [65-68]. However, no attempt was made previously to develop a measurement technique that corresponds to the local assessment of the paper thickness. The technique used by the author for the first time in this thesis is one using an optical sensor device and which permits highly accurate thickness measurements to be performed.

The diagrammatic sketch of the "fotonic sensor" device in this new measurement technique is indicated in Fig. 4.26. This device consists of a light source, mounted together with a photocell, a light probe and an amplifier. The light probe consists of a number of fibre bundles in a random arrangement. The inner

bundle (see also magnification in Fig. 4.26b) transmits the light rays from the light source to the object surface. However, since the surface of the paper sample is not sufficiently reflective, an "adaptor" was designed and mounted on to the probe. This adaptor has an accurately machined tip of 0.25 mm diameter, the purpose of which will be discussed below. The outer fibre bundle collects the reflected light from the object surface and sends it to the photocell. Hence, the difference between the transmitted and reflected light intensities can be obtained from the photocell and amplified for accurate measurements. The difference of these intensities is a function of the gap size of the light probe tip and the test surface. This function is characterized by the output characteristic curve of the device, shown in Fig. 4.27.

For the actual performed test, due to the chosen range of the gap sizes, only the linear range on the output curve has been used (region bounded by points A and B in Fig. 4.27). Since the newsprint paper sample, in general, vary in colour and surface morphology, the above mentioned adaptor has been designed in such a manner as to permit the tip of the adaptor to trace the sample surface profile during the scanning procedure. It should be noted that the actual reflected light is due to the highly polished inside surface of the adaptor (Fig. 4.28b) and is obtained by the transverse movement of the paper sample

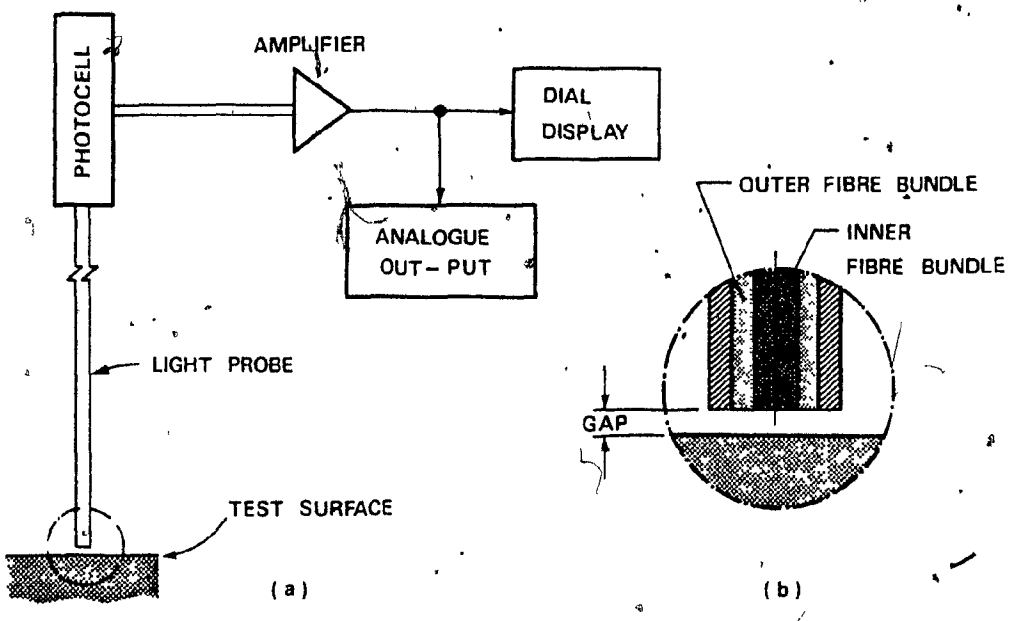

FIG.4.26 SCHEMATICS OF A FOTONIC SENSOR.

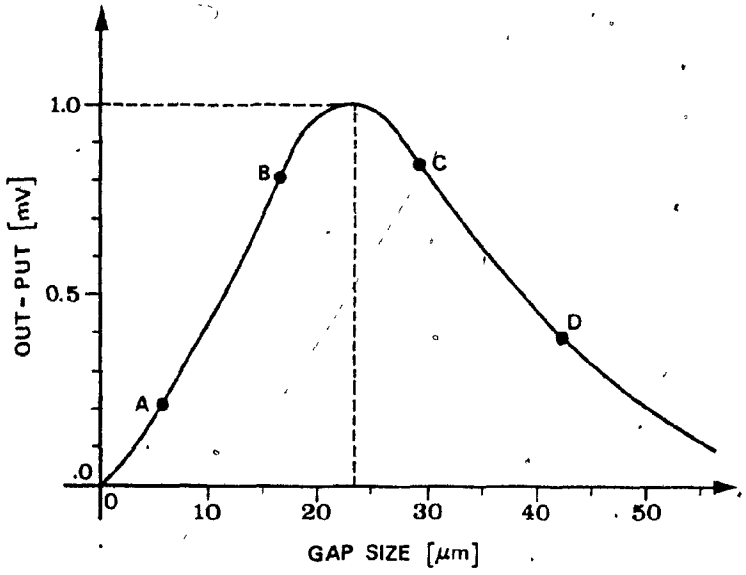

FIG.4.27 OUT-PUT CHRACTERISTICS OF THE FOTONIC SENSOR.

relative to the adaptor tip. Thus, the surface topology of the sample uses a mechanical scanning and the inside surface of the adaptor for the optical transmission. In this manner, an in situ testing procedure of the paper sample can be carried out free of the specific state of the paper. For the actual holographic testing of the paper sample it may be recalled that great care had to be taken in observing the 50% relative humidity during the testing. In using this device it was not necessary to renew the proper humidity arrangement, since the paper sample itself during the Beta-radiography was, to a certain extent, dried out. In this manner an irregularity in the paper sample profile is reflected in a preset gap size.

The actual experimental set-up is indicated in Fig. 4.28. The paper sample is positioned with its left side (smooth side) on a reference glass plate which is firmly fixed onto a heavy block. This block, in turn, can be adjusted to a supporting table which permits a sideway motion. In accordance with the scanning procedure mentioned previously by transversing the paper sample relative to the fixed adaptor top, the changes in the gap size and hence, in the reflected light intensities were obtained. Again, for high accuracy, the end points of each scanning line were chosen with reference to the edges of the tested sample. It should be noted that after the

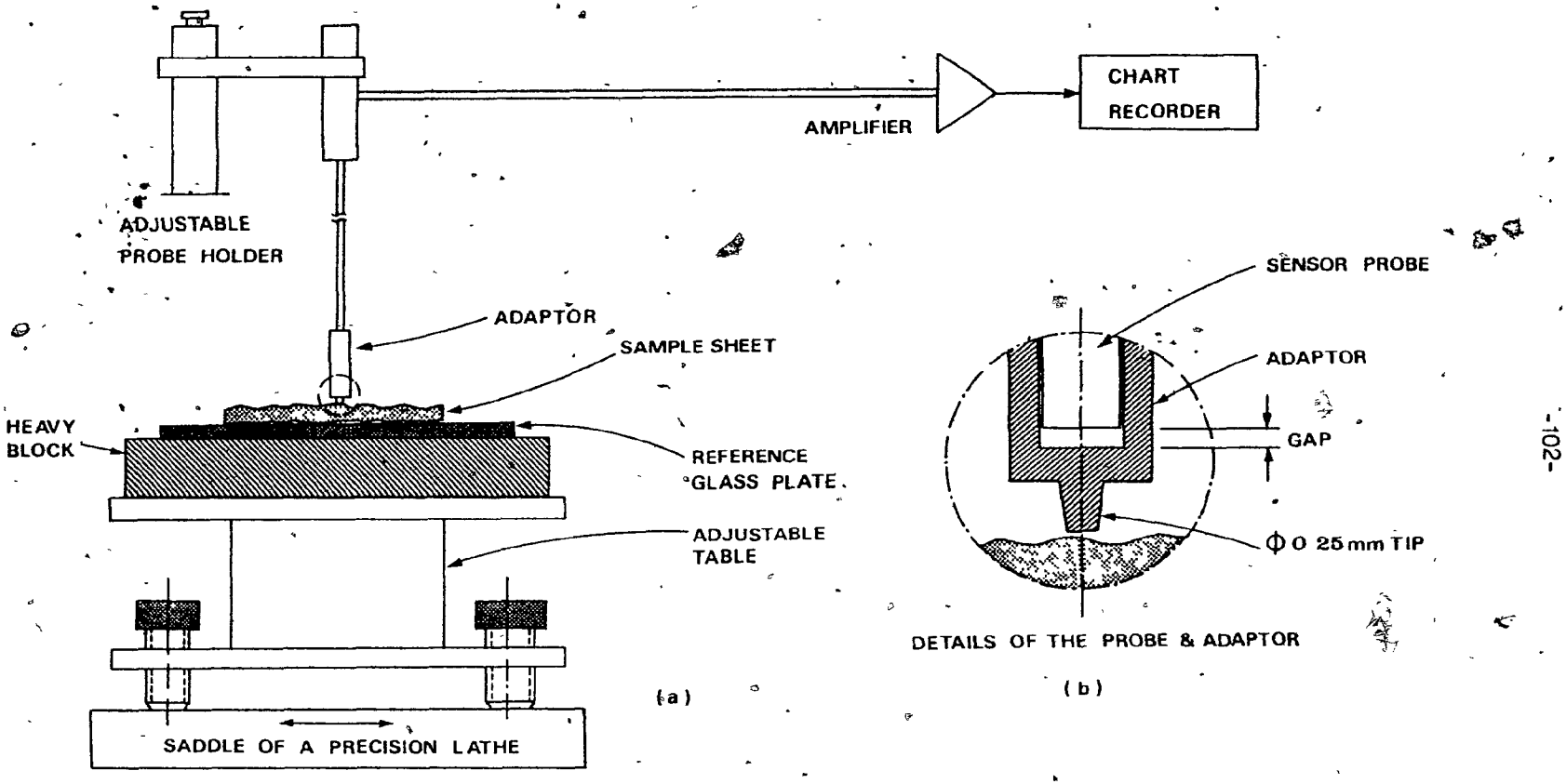

FIG.4.28 SCHEMATICS OF THE THICKNESS MEASURMENT SET-UP.

scanning of the paper sample was completed the same scanning lines were used to scan the reference glass plate itself. Thus, the difference between the profiles, following the paper sample and that of the reference glass in view of the identical presetting of the fotonic sensor and adaptor, were obtained. Evidently, this difference is a direct measurement of the thickness of the paper sample. A typical result obtained in this manner is indicated in Fig. 4.29, whilst a micrograph of the adaptor to a magnification of 14X in SEM is shown in Fig. 4.30.

Finally, it should be noted that the actual thickness measurement required for the assessment of the VMD (α_ρ) is tabulated in Appendix IV together with the α_w and α_τ itself.

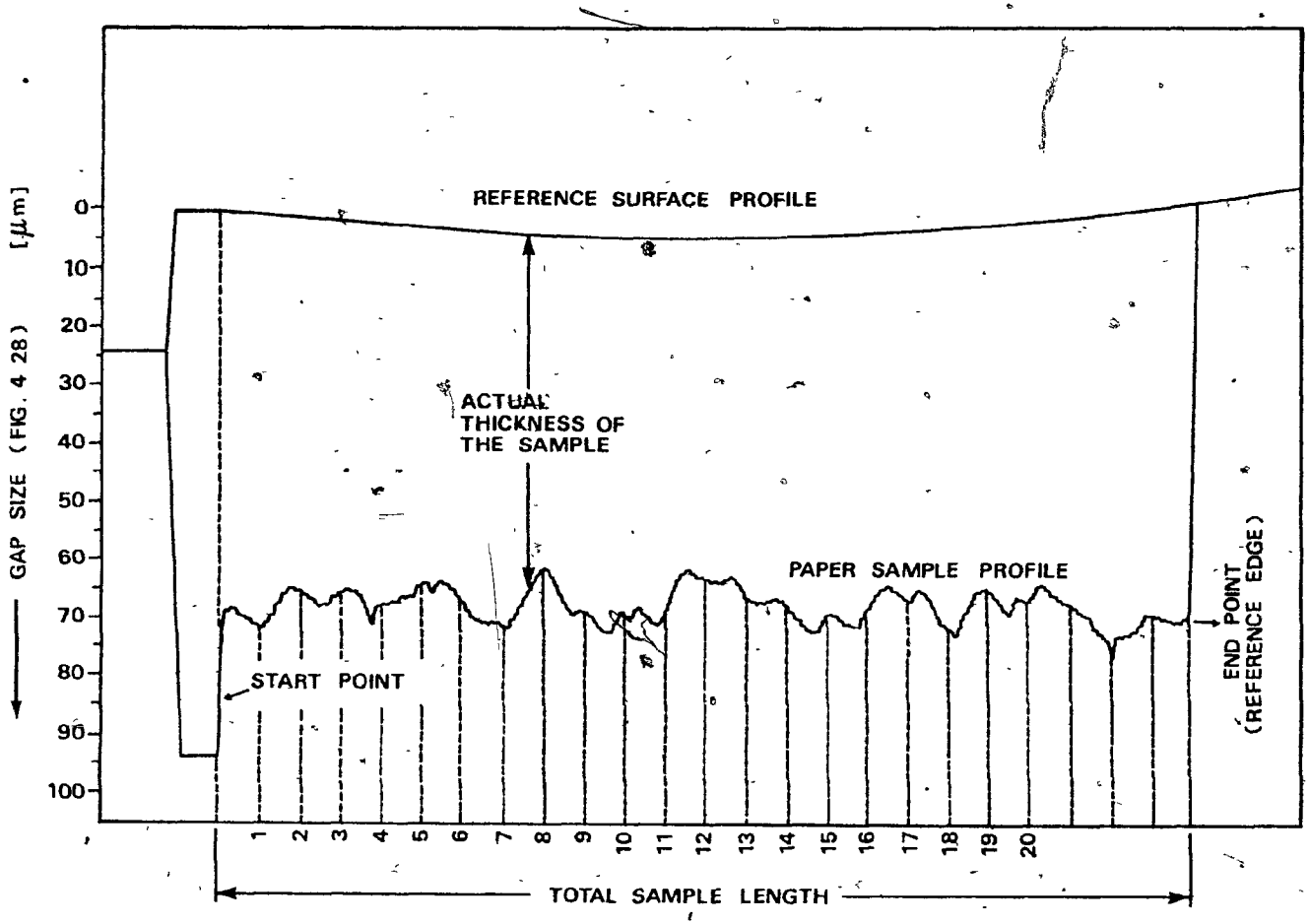

FIG. 4.29 TYPICAL THICKNESS MEASUREMENT CURVE OBTAINED FROM SCANNING THE PAPER SAMPLE ALONG A COLUMN OF THE MESH.

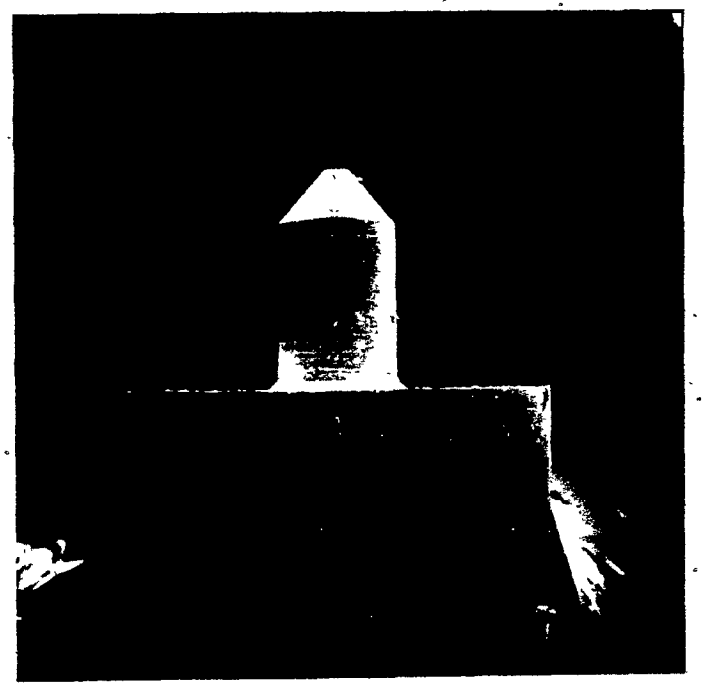

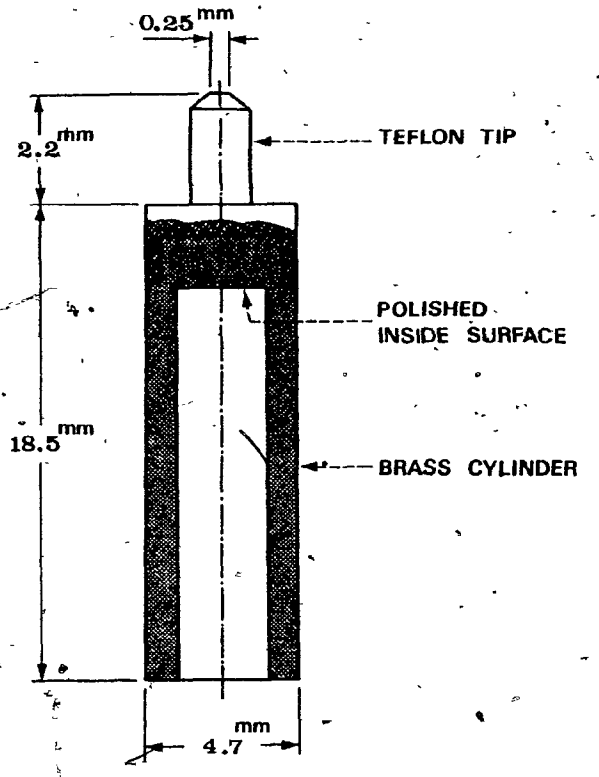

FIG. 4.30 SCANNING ELECTRON MICROGRAPH OF THE FOTONIC SENSOR ADAPTOR TIP - MAG. 14 X.

Chapter V

EXPERIMENTAL RESULTS AND DISCUSSION

5.1 Introduction

The volumetric mass density of fibrous networks has been discussed in Chapter II. The two stages of holographic interferometry, namely the sequential-DSHI formation stage and the general reconstruction stage, have been discussed in Chapter III. The newly developed reconstruction technique, i.e. the holographic-electro-optical technique as well as the actual experimental set up for obtaining the deformation field of newsprint paper samples and, in particular, the experimental assessment of the volumetric mass density for this material have been the subject-matter of Chapter IV. This chapter is concerned with the discussion of the holographic-electro-optical technique and the actual experimental results that have been obtained from this technique for newsprint as well as the Beta-radiography and thickness measurement tests.

5.2 Holographic-Electro-Optical Technique

Before discussing the holographic-electro-optical technique for the evaluation of interferograms it is necessary first to make some remarks on the sequential-DSHI method itself. This method of obtaining chainwise interferograms is applicable to

most engineering materials when their deformational history is in question. Formation of interferograms that have a readable fringe pattern depends on several factors such as the nature of the material, the angles between the holographic plates and the reference beam, and the ratio between the light intensities of the reference and object beams. The deformations of solid materials such as metallic foils produce more distinct and parallel fringe patterns than materials with weaker structure such as paper samples. Thus, the optical arrangement and the exposure intervals for a given sample should be optimized so that localized fringe patterns are obtained.

As already mentioned in Chapter IV of this thesis, 16 readable interferograms have been selected from the complete test series of newsprint paper samples which were subjected to 82 N uniaxial tensile load at the conditions of 50% relative humidity and 23.5°C temperature. These interferograms correspond to the measurements on both sides of the paper sample, i.e. eight interferograms for each side. Photographs of the typical interferograms corresponding to the "right" and "left" sides of the tested newsprint paper sample are shown in Figs. 5.1 and 5.2 respectively. It can be noted that the upper part of these figures show a distinct fringe pattern which is also occurring on the upper jaw. Hence, fringes are straight parallel lines indicating the rigid

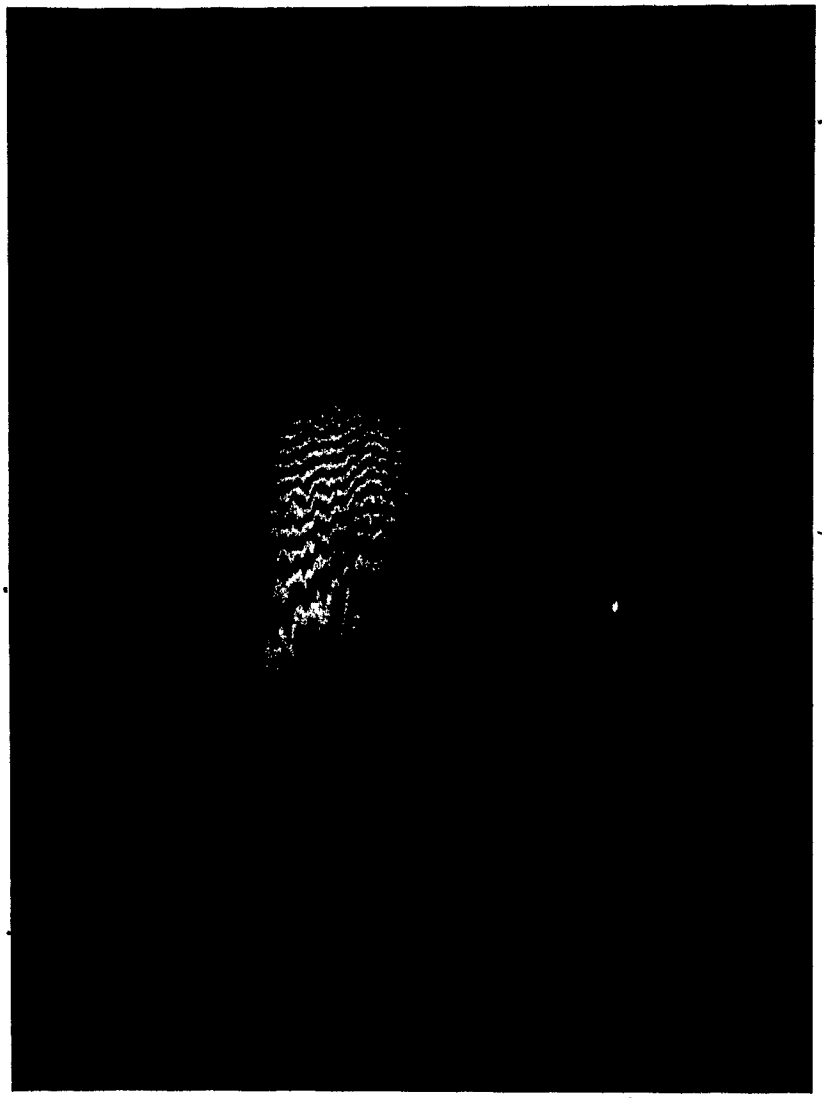

FIG. 5.1 PHOTOGRAPH OF INTERFEROGRAM OF NEWSPRINT PAPER. (SIZE 55mm x 96mm) AT TIME $t = 302$ SEC AFTER LOAD APPLICATION.

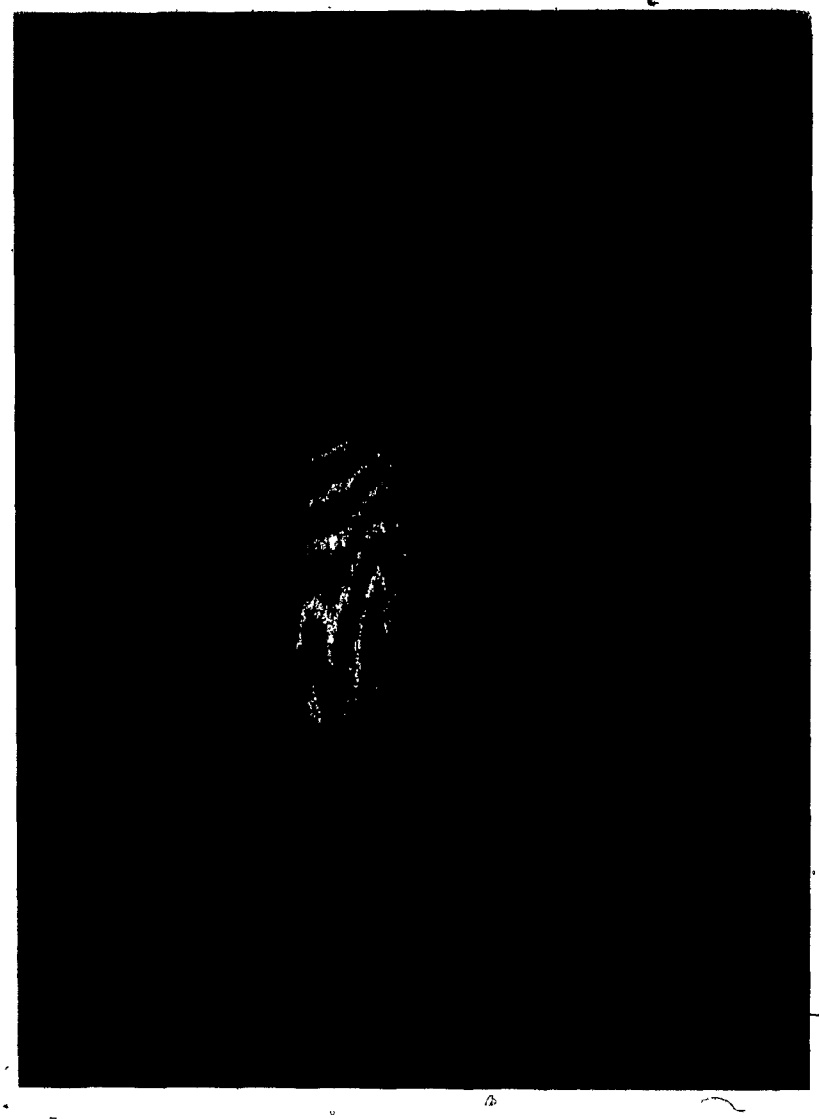

FIG. 5.2 PHOTOGRAPH OF INTERFERAM FROM THE « LEFT » SIDE OF NEWSPRINT PAPER (SIZE 55mm x 96mm) AT TIME $t = 302$ SEC AFTER LOAD APPLICATION.

body motion of the upper jaw. The wavy fringe pattern on the paper sample surface is caused by the three-dimensional displacement of the surface points clearly indicating that a bowing-out effect occurs in spite of a strictly uniaxial load application. The lower parts in the photographs, however, show the holographic images of the lower jaw. There is no fringe to be observed, thus the required rigidity of the lower or fixed jaw was obtained.

The readable fringe patterns of Figs. 5.1 and 5.2 have been obtained by selecting a ratio of 5:1 between the light intensity of the reference beam to that of the object beam and also by controlling the rigid uniaxial motion of the upper jaw so that the motion of the latter lies in the range of 5 - 12 μm. It can also be seen from the above figures that the fringes are not uniformly distributed over the image plane. The upper part of the image contains more distinct fringes than the lower part. Those points of the paper sample adjacent to the lower jaw experience no deformation, whilst those adjacent to the upper jaw have a deformation equivalent to the total macroscopic deformation of the sample, i.e. the displacement of the upper jaw. The displacements of the upper jaw, however, have been measured by fotonic sensor devices. A comparison of the fotonic sensor output and holographic-electro-optical readings will be given in the subsequent section.

All the 16 obtained interferograms of the tested newsprint paper sample have been evaluated according to the scanning procedure discussed in Chapter IV. First, the fringe numbers were evaluated. The procedure of fringe number evaluation has been designed so that any number of fringes greater than 1 passing in front of an image point or observation point can be evaluated within an accuracy of ±0.1 of a fringe. During reconstruction the newsprint interferograms showed a non-countable number of fringes on the lower portion of the images. Thus, the lowest row of the mesh of observation points was selected 12 mm above the lower jaw (see Fig. 4.17), so that by scanning the interferograms in any of the three scanning directions a minimum of one complete fringe was observed passing in front of the observation points on this row. A detailed discussion of the accuracy of the holographic-electro-optical technique has been given in Section 4.3.5 of Chapter IV. However, the displacements of the upper jaw as predicted by this technique are compared to those measured macroscopically by the fotonic sensors.

5.3 Experimental Results from the Holographic-Electro-Optical Technique

For the actual evaluation of the required surface deformation fields the obtained fringe numbers were fed into the main

program (Appendix V), which includes the evaluation of deformations, strains, thickness changes and the correlation coefficients. The flow chart for the main program is given in Fig. 5.3, whilst the source listing and the corresponding output results are given in Appendix V.

It should be noted that the program in accordance with Fig. 5.3 is designed for a general procedure that permits, in conjunction with the holographic-electro-optical routine, any arbitrary interferogram to be evaluated for an arbitrary number of observation points. The input to this program consists of the test information, i.e. the number of interferograms, the number of observation points (statement 27), the reconstruction geometrical data and the fringe numbers (statements 56,60). Hence, solving the key relations (3.10 - 3.12), the program is able to evaluate the components of the deformations at any observation point on the sample surfaces. A typical table of the deformation evaluation that corresponds to the interferogram 2L is given in Table (5.1), where the notation (2L) is referred to the interferogram on the left side (L) of the paper sample at time t(H2)= 302 sec. In this table the coordinates of the observation points are given in millimeters, whilst the three deformation components are given in microns. The corresonding tables for the remaining 15 interferograms are given in Appendix V.

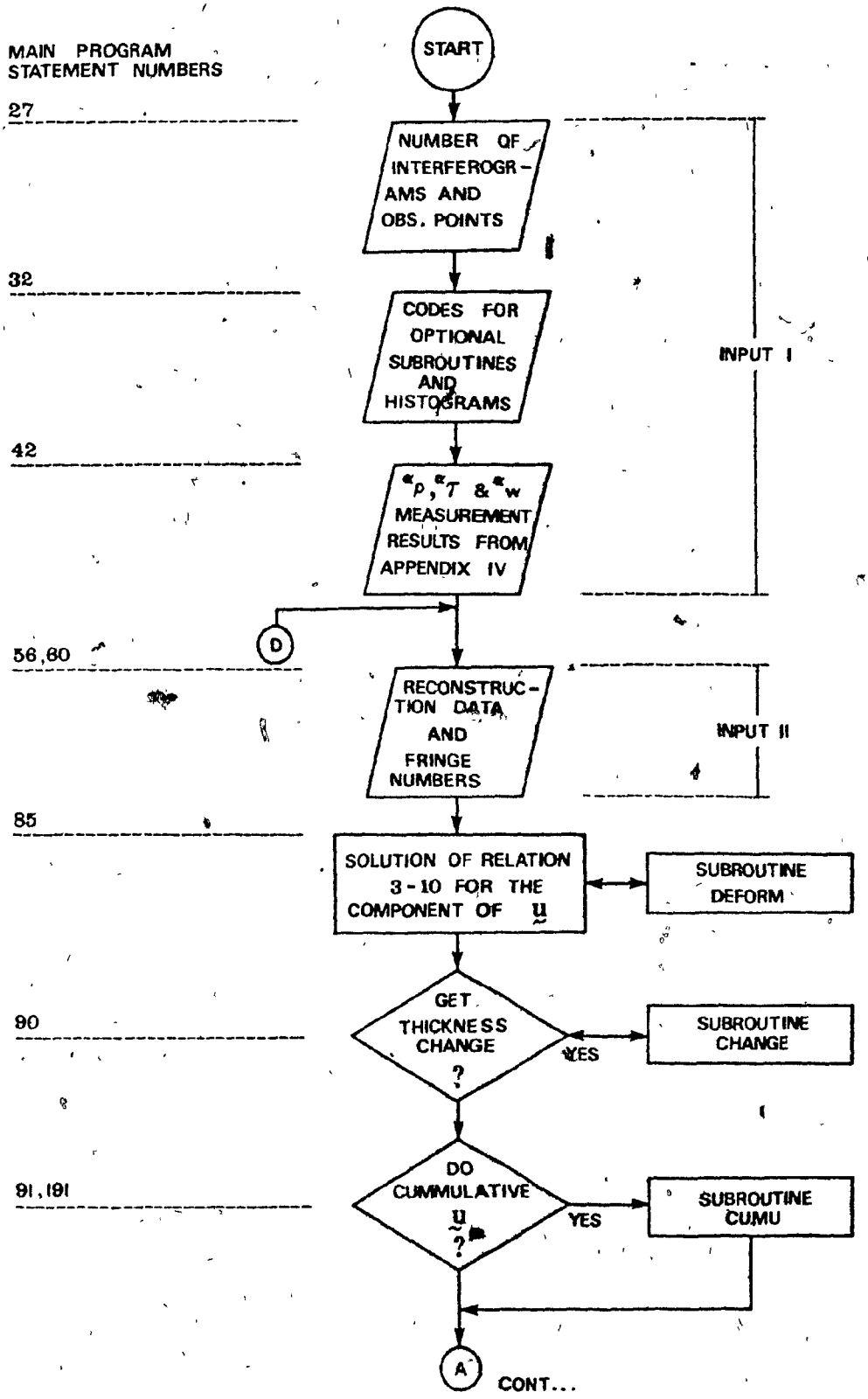

FIG. 5.3 FLOW CHART OF THE MAIN COMPUTER PROGRAM FOR EVALUATION OF DEFORMATIONS, STRAINS, THICKNESS CHANGE AND CORRELATION COEFFICIENTS.

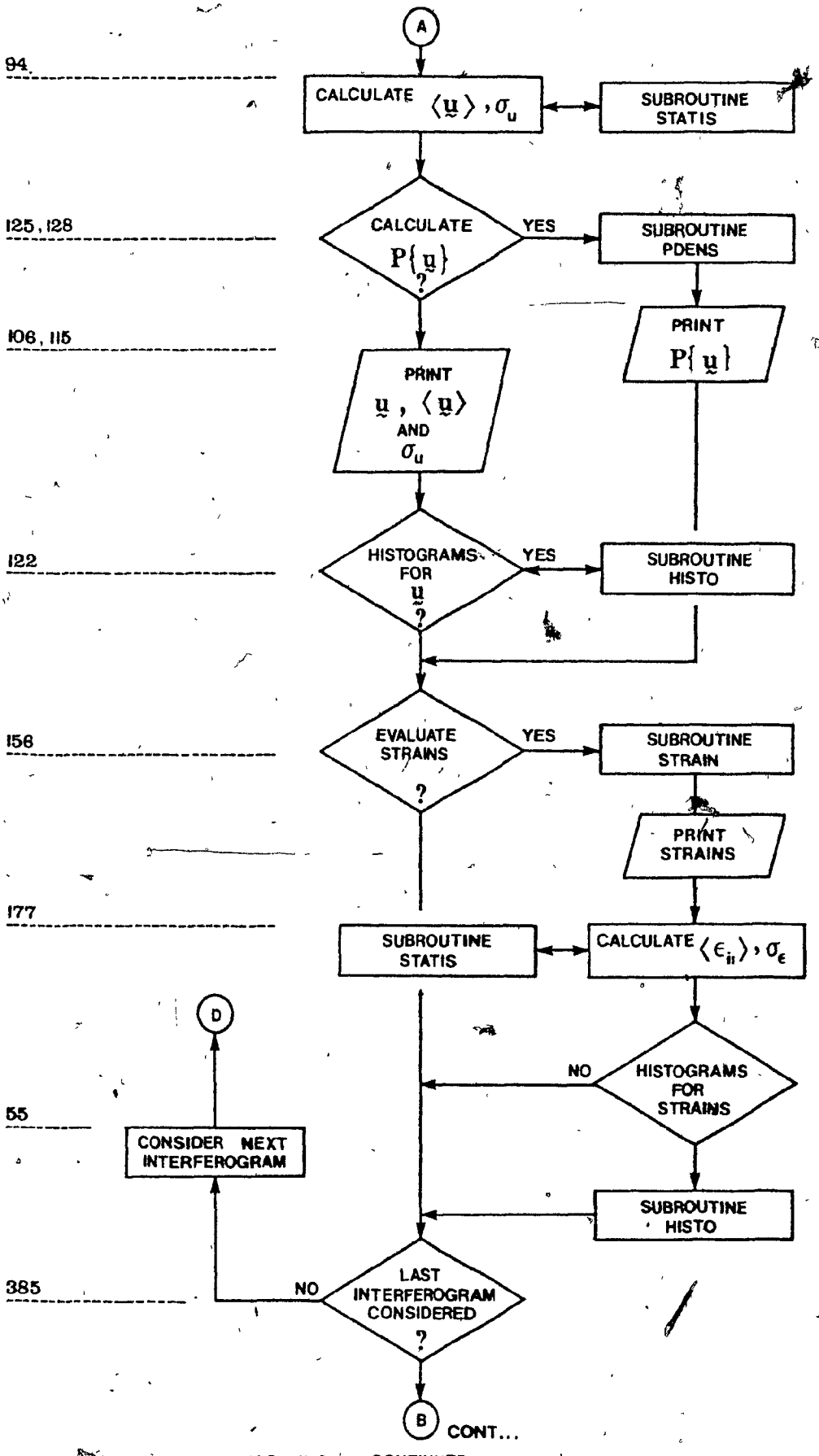

FIG. 5.3 CONTINUED.

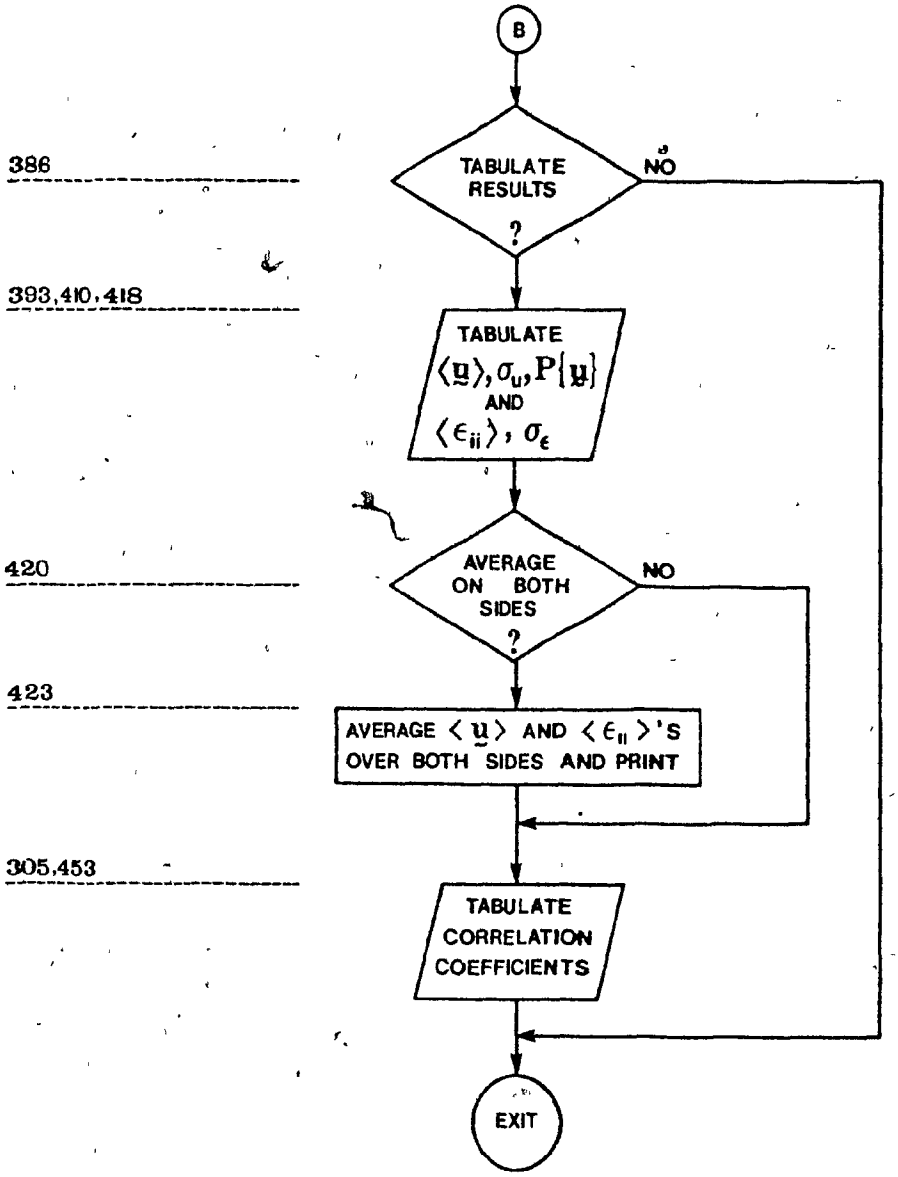

463	SUBROUTINE DEFORM
487	SUBROUTINE STATIS
504	SUBROUTINE PDENS
518	SUBROUTINE CUMU
550	SUBROUTINE STRAIN
562	SUBROUTINE CHANGE
605	SUBROUTINE HISTO
639	SUBROUTINE CROLAT

FIG. 5.3 CONTINUED.

RECONSTRUCTION RESULTS OF INTERFEROGRAM (2L) OF THE NEWS-PRINT PAPER SAMPLE #38 CUMMULATIVE DEFORMATION)

CO-ORDINATES X	CO-ORDINATES Y	DEFORMATIONS X	DEFORMATIONS Y	DEFORMATIONS Z
44.0	-22.0	0.2591D 02	-0.1980D 00	-0.1147D 02
44.0	-18.0	0.2682D 02	0.1305D 02	-0.6631D 01
44.0	-14.0	0.2612D 02	-0.6302D 01	0.2177D 02
44.0	-10.0	0.2459D 02	-0.2497D 01	-0.1323D 02
44.0	-6.0	0.2575D 02	0.2355D 02	-0.6024D 01
44.0	-2.0	0.2700D 02	0.5174D 01	0.1500D 01
44.0	2.0	0.2532D 02	-0.1197D 02	0.5536D 01
44.0	6.0	0.2593D 02	-0.2963D 02	-0.2699D 01
44.0	10.0	0.2566D 02	0.4940D 00	0.2828D 02
44.0	14.0	0.2572D 02	0.2113D 02	0.2215D 02
44.0	18.0	0.2708D 02	0.1481D 01	-0.8489D 01
44.0	22.0	0.2504D 02	-0.1672D 02	0.2450D 01
40.0	-22.0	0.2447D 02	-0.5684D 01	-0.1152D 02
40.0	-18.0	0.2602D 02	-0.5283D 01	0.1276D 02
40.0	-14.0	0.2519D 02	0.1831D 02	0.3399D 02
40.0	-10.0	0.2569D 02	-0.3063D 01	-0.1777D 01
40.0	-6.0	0.2655D 02	0.2344D 02	-0.6013D 00
40.0	-2.0	0.2551D 02	-0.5042D 01	0.2363D 02
40.0	2.0	0.2575D 02	-0.5544D 01	0.2146D 02
40.0	6.0	0.2608D 02	-0.5908D 01	-0.2670D 00
40.0	10.0	0.2439D 02	-0.2103D 01	-0.1084D 02
40.0	14.0	0.2467D 02	0.1105D 02	0.2461D 02
40.0	18.0	0.2671D 02	0.3671D 01	0.3814D 01
40.0	22.0	0.2559D 02	0.1962D 02	0.1033D 02
36.0	-22.0	0.2602D 02	0.3425D 02	-0.6607D 01
36.0	-18.0	0.2569D 02	0.1182D 02	0.1872D 02
36.0	-14.0	0.2350D 02	-0.1603D 01	-0.1983D 02
36.0	-10.0	0.2608D 02	0.1676D 01	0.8227D 01
36.0	-6.0	0.2632D 02	0.2039D 02	0.7101D 01
36.0	-2.0	0.2363D 02	0.1288D 02	-0.8011D 01
36.0	2.0	0.2281D 02	-0.1402D 02	-0.2440D 02
36.0	6.0	0.2151D 02	-0.1994D 02	0.1972D 02
36.0	10.0	0.2217D 02	0.2659D 01	-0.9026D 01
36.0	14.0	0.2367D 02	0.1702D 01	0.1257D 02
36.0	18.0	0.2321D 02	0.3189D 01	0.1006D 02
36.0	22.0	0.2439D 02	0.8733D 01	0.9358D 01
32.0	-22.0	0.2089D 02	-0.8146D 01	-0.5858D 01
32.0	-18.0	0.2488D 02	-0.1737D 02	0.2161D 02
32.0	-14.0	0.2317D 02	0.1474D 02	0.1441D 02
32.0	-10.0	0.2468D 02	0.2499D 02	0.1097D 02
32.0	-6.0	0.2250D 02	-0.1099D 02	0.9650D 01
32.0	-2.0	0.2355D 02	-0.3668D 01	-0.9002D 01
32.0	2.0	0.2202D 02	-0.8446D 01	0.4007D 01
32.0	6.0	0.2323D 02	-0.2993D 02	0.6544D 01
32.0	10.0	0.2317D 02	-0.1389D 02	0.6484D 01
32.0	14.0	0.2279D 02	0.1654D 02	-0.6192D 01
32.0	18.0	0.2564D 02	0.1561D 02	0.1030D 02
32.0	22.0	0.2198D 02	-0.7157D 01	-0.3020D 02
28.0	-22.0	0.2097D 02	-0.1971D 02	-0.2642D 02
28.0	-18.0	0.2253D 02	-0.1038D 02	-0.1918D 01
28.0	-14.0	0.2434D 02	0.2622D 02	0.3034D 01
28.0	-10.0	0.2006D 02	-0.4115D 01	-0.5742D 01
28.0	-6.0	0.2149D 02	-0.3859D 01	0.1832D 02
28.0	-2.0	0.2476D 02	0.1877D 02	-0.1722D 01
28.0	2.0	0.1866D 02	-0.2139D 01	0.9897D 01
28.0	6.0	0.2295D 02	-0.6041D 01	0.3897D 02
28.0	10.0	0.2086D 02	-0.3207D 00	0.1778D 02
28.0	14.0	0.2236D 02	0.9426D 01	-0.6846D 01
28.0	18.0	0.2104D 02	0.2151D 02	-0.2176D 02
28.0	22.0	0.2227D 02	-0.1847D 02	0.1059D 02

TABLE (5.1). Holographic-electro-optical results obtained from evaluating interferogram (2L) of the tested newsprint paper at time t=302 sec.

24.0	-22.0	0.2309D 02	-0.9814D 01	-0.1706D 02	
24.0	-18.0	0.2241D 02	0.1371D 01	0.4933D 01	
24.0	-14.0	0.2154D 02	0.1240D 02	-0.8417D 01	
24.0	-10.0	0.2087D 02	-0.7985D 01	0.2570D 02	
24.0	-6.0	0.2004D 02	-0.6647D 01	0.1288D 02	
24.0	-2.0	0.2126D 02	0.1420D 01	-0.2320D 02	
24.0	2.0	0.2427D 02	0.5534D 01	0.1122D 02	
24.0	6.0	0.2062D 02	0.8846D 01	0.1141D 02	
24.0	10.0	0.1930D 02	0.7186D 01	-0.3720D 01	
24.0	14.0	0.2255D 02	-0.5346D 01	-0.3208D 02	
24.0	18.0	0.1824D 02	-0.4929D 00	-0.4264D 01	
24.0	22.0	0.2277D 02	0.8815D 01	0.4508D 00	
20.0	-22.0	0.2141D 02	0.9396D 01	-0.1867D 02	
20.0	-18.0	0.1809D 02	-0.1621D 02	0.2071D 02	
20.0	-14.0	0.2135D 02	0.1348D 02	0.2703D 01	
20.0	-10.0	0.1918D 02	0.1089D 02	-0.1383D 02	
20.0	-6.0	0.1950D 02	0.1550D 02	-0.1686D 02	
20.0	-2.0	0.2068D 02	-0.1779D 02	0.1258D 02	
20.0	2.0	0.1875D 02	0.1662D 01	0.1960D 02	
20.0	6.0	0.2110D 02	-0.1040D 02	-0.2385D 01	
20.0	10.0	0.2263D 02	0.1028D 02	0.2112D 01	
20.0	14.0	0.1923D 02	0.2759D 02	0.2283D 02	
20.0	18.0	0.1822D 02	-0.3987D 01	0.1405D 02	
20.0	22.0	0.2002D 02	0.1376D 02	0.7510D 01	
16.0	-22.0	0.2201D 02	0.9026D-01	0.3084D 02	
16.0	-18.0	0.2002D 02	-0.1217D 02	0.6612D 01	
16.0	-14.0	0.1706D 02	0.2045D 01	-0.1613D 02	
16.0	-10.0	0.2003D 02	0.9313D 01	0.5205D 01	
16.0	-6.0	0.1864D 02	-0.1915D 02	0.8053D 01	
16.0	-2.0	0.1814D 02	-0.4041D 01	0.1440D 02	
16.0	2.0	0.2186D 02	0.5082D 01	0.2512D 02	
16.0	6.0	0.1804D 02	0.6275D 01	-0.1428D 01	
16.0	10.0	0.1802D 02	0.2040D 02	-0.1389D 02	
16.0	14.0	0.1966D 02	-0.2872D 02	0.1106D 01	
16.0	18.0	0.1904D 02	-0.1533D 01	0.7703D 01	
16.0	22.0	0.2046D 02	0.2232D 02	0.2359D 02	
12.0	-22.0	0.1910D 02	-0.7101D 01	0.2758D 02	
12.0	-18.0	0.1807D 02	0.6447D 00	0.1177D 02	
12.0	-14.0	0.2017D 02	-0.2010D 02	-0.6592D 01	
12.0	-10.0	0.2073D 02	0.1106D 02	-0.3600D 01	
12.0	-6.0	0.1867D 02	-0.1953D 02	-0.1064D 02	
12.0	-2.0	0.1778D 02	-0.3561D 01	-0.8173D 01	
12.0	2.0	0.1755D 02	0.5135D 01	-0.5880D 00	
12.0	6.0	0.1958D 02	-0.4223D 01	-0.1231D 02	
12.0	10.0	0.1691D 02	-0.5820D 01	-0.7211D 01	
12.0	14.0	0.2018D 02	0.2148D 02	0.1734D 02	
12.0	18.0	0.1795D 02	-0.4410D 01	0.7675D 01	
12.0	22.0	0.2301D 02	0.1121D 02	0.2997D 02	
8.0	-22.0	0.2169D 02	0.2836D 02	-0.2434D 00	
8.0	-18.0	0.1746D 02	0.3244D 01	0.1274D 02	
8.0	-14.0	0.1952D 02	0.4723D 01	-0.2826D 01	
8.0	-10.0	0.2032D 02	0.1006D 02	0.7215D 01	
8.0	-6.0	0.1542D 02	-0.1772D 02	0.6833D 01	
8.0	-2.0	0.1735D 02	-0.2120D 02	-0.4254D 01	
8.0	2.0	0.1701D 02	0.7894D 01	0.7864D 01	
8.0	6.0	0.1961D 02	-0.1456D 02	0.6500D 01	
8.0	10.0	0.1935D 02	-0.1103D 02	-0.2104D 02	
8.0	14.0	0.1558D 02	-0.8634D 01	-0.1480D 02	
8.0	18.0	0.1715D 02	-0.1466D 01	-0.3103D 02	
8.0	22.0	0.1999D 02	-0.5598D 00	-0.2914D 01	
4.0	-22.0	0.1662D 02	-0.1122D 02	0.4203D 01	
4.0	-18.0	0.1675D 02	0.8746D 01	0.1631D 02	
4.0	-14.0	0.1516D 02	-0.1612D 02	-0.4152D 01	
4.0	-10.0	0.1951D 02	0.1474D 02	0.2779D-01	
4.0	-6.0	0.1580D 02	-0.1256D 02	-0.1828D 02	
4.0	-2.0	0.1807D 02	0.2303D 02	-0.1844D 02	
4.0	2.0	0.2127D 02	0.2494D 02	0.8705D 01	
4.0	6.0	0.1591D 02	-0.2035D 02	0.4774D 01	
4.0	10.0	0.1794D 02	-0.8557D 00	-0.9613D 01	
4.0	14.0	0.1589D 02	-0.1914D 02	-0.8130D 01	
4.0	18.0	0.2009D 02	-0.1161D 01	0.3379D 02	
4.0	22.0	0.1563D 02	0.1952D 02	0.2863D 02	

TABLE (5.1) contd.

0.0	-22.0	0.1487D 02	-0.9905D 01	-0.2222D 02	
0.0	-18.0	0.1547D 02	0.1941D 02	-0.5362D 01	
0.0	-14.0	0.1511D 02	-0.1107D 02	0.1803D 02	
0.0	-10.0	0.1597D 02	-0.3569D 01	-0.6105D 01	
0.0	-6.0	0.1569D 02	-0.2236D 01	0.3530D 00	
0.0	-2.0	0.1813D 02	0.1059D 01	-0.2225D 02	
0.0	2.0	0.1663D 02	0.3460D 01	-0.2616D 02	
0.0	6.0	0.1891D 02	-0.9685D 00	0.8722D 01	
0.0	10.0	0.1432D 02	0.4720D 01	0.1072D 02	
0.0	14.0	0.1493D 02	-0.1032D 02	0.1500D 02	
0.0	18.0	0.1746D 02	-0.2588D 02	0.3061D 01	
0.0	22.0	0.1671D 02	0.8356D 01	0.1824D 02	
-4.0	-22.0	0.1617D 02	-0.4720D 01	0.7488D 01	
-4.0	-18.0	0.1559D 02	0.1925D 02	-0.2303D 01	
-4.0	-14.0	0.1509D 02	-0.1328D 02	-0.1551D 01	
-4.0	-10.0	0.1819D 02	0.1692D 02	-0.7797D 00	
-4.0	-6.0	0.1406D 02	-0.5604D 01	-0.6498D 01	
-4.0	-2.0	0.1694D 02	-0.1881D 02	0.2630D 02	
-4.0	2.0	0.1741D 02	-0.1351D 02	-0.1645D 01	
-4.0	6.0	0.1491D 02	-0.2243D 02	0.2366D 02	
-4.0	10.0	0.1462D 02	0.1061D 02	0.6940D 01	
-4.0	14.0	0.1513D 02	-0.4775D 01	0.1434D 02	
-4.0	18.0	0.1354D 02	-0.4448D 01	-0.1756D 02	
-4.0	22.0	0.1587D 02	-0.6190D 01	0.6383D 01	
-8.0	-22.0	0.1534D 02	-0.2516D 01	0.1125D 00	
-8.0	-18.0	0.1683D 02	-0.5904D 01	-0.3580D 02	
-8.0	-14.0	0.1777D 02	0.1325D 01	0.6568D 01	
-8.0	-10.0	0.1508D 02	0.5884D 00	-0.2314D 02	
-8.0	-6.0	0.1402D 02	-0.1010D 02	0.6937D 01	
-8.0	-2.0	0.1402D 02	-0.1742D 02	-0.2352D 02	
-8.0	2.0	0.1524D 02	0.2726D 02	-0.1685D 01	
-8.0	6.0	0.1585D 02	0.7366D 01	0.6175D 01	
-8.0	10.0	0.1585D 02	0.2517D 02	-0.3235D 01	
-8.0	14.0	0.1669D 02	-0.2155D 02	0.9051D 01	
-8.0	18.0	0.1427D 02	-0.2614D 02	-0.2263D 02	
-8.0	22.0	0.1712D 02	-0.2858D 02	0.1146D 02	
-12.0	-22.0	0.1419D 02	-0.1635D 01	-0.1496D 02	
-12.0	-18.0	0.1508D 02	0.6603D 01	0.1205D 02	
-12.0	-14.0	0.1829D 02	0.1195D 02	-0.2278D 02	
-12.0	-10.0	0.1531D 02	0.2950D 02	0.1236D 02	
-12.0	-6.0	0.1457D 02	0.1135D 02	0.2309D 01	
-12.0	-2.0	0.1518D 02	-0.2601D 02	0.4349D 00	
-12.0	2.0	0.1519D 02	-0.5561D 01	-0.1857D 01	
-12.0	6.0	0.1443D 02	-0.1038D 02	-0.2164D 02	
-12.0	10.0	0.1403D 02	-0.2220D 02	0.2935D 01	
-12.0	14.0	0.1396D 02	-0.1026D 01	0.1133D 02	
-12.0	18.0	0.1755D 02	0.8836D 01	-0.1323D 02	
-12.0	22.0	0.1556D 02	0.6766D 01	-0.3566D 02	
-16.0	-22.0	0.1328D 02	-0.9711D 01	0.3670D 02	
-16.0	-18.0	0.1536D 02	-0.3246D-01	-0.1462D 02	
-16.0	-14.0	0.1299D 02	0.1149D 02	0.3287D 02	
-16.0	-10.0	0.1462D 02	-0.2034D 01	-0.4854D 01	
-16.0	-6.0	0.1704D 02	0.4430D 01	0.4430D 01	
-16.0	-2.0	0.1513D 02	-0.1502D 02	0.3011D 02	
-16.0	2.0	0.1453D 02	0.7230D 01	0.2836D 02	
-16.0	6.0	0.1317D 02	0.1792D 02	0.1236D 02	
-16.0	10.0	0.1653D 02	-0.1411D 02	0.1571D 02	
-16.0	14.0	0.1530D 02	-0.8139D-01	0.1629D 02	
-16.0	18.0	0.1495D 02	-0.4880D 01	-0.1212D 02	
-16.0	22.0	0.1524D 02	-0.2935D 02	-0.1404D 01	
-20.0	-22.0	0.1372D 02	-0.9356D 01	0.9275D 01	
-20.0	-18.0	0.1580D 02	0.1392D 02	-0.1295D 02	
-20.0	-14.0	0.1385D 02	0.2785D 02	-0.3815D 01	
-20.0	-10.0	0.1311D 02	-0.1569D 02	0.1864D 02	
-20.0	-6.0	0.1516D 02	-0.2698D 01	0.6735D 01	
-20.0	-2.0	0.1379D 02	-0.7865D 01	0.1999D 02	
-20.0	2.0	0.1337D 02	-0.2205D 02	0.2946D 02	
-20.0	6.0	0.1750D 02	-0.1654D 01	0.8071D 01	
-20.0	10.0	0.1218D 02	-0.8789D 01	-0.9742D 01	
-20.0	14.0	0.1379D 02	0.2252D 02	0.1258D 02	
-20.0	18.0	0.1475D 02	0.6160D 01	0.2533D 02	
-20.0	22.0	0.1357D 02	-0.1079D 02	0.7375D 01	

TABLE (5.1) contd.

*	-24.0	-22.0	*	0.1368D 02	0.4827D 01	0.5876D 01	*
*	-24.0	-18.0	*	0.1399D 02	-0.6204D 01	-0.1740D 02	*
*	-24.0	-14.0	*	0.1243D 02	0.7906D 01	-0.4476D 01	*
*	-24.0	-10.0	*	0.1475D 02	0.2853D 02	0.2074D 02	*
*	-24.0	-6.0	*	0.1186D 02	0.4218D 01	-0.9967D 01	*
*	-24.0	-2.0	*	0.1255D 02	-0.9424D 01	0.5222D 01	*
*	-24.0	2.0	*	0.1147D 02	-0.3201D 02	-0.6901D 01	*
*	-24.0	6.0	*	0.1135D 02	0.9029D 00	-0.1274D 02	*
*	-24.0	10.0	*	0.1353D 02	-0.9278D 01	0.1319D 02	*
*	-24.0	14.0	*	0.1474D 02	0.1709D 02	0.1840D 02	*
*	-24.0	18.0	*	0.1234D 02	-0.2216D 02	-0.1389D 01	*
*	-24.0	22.0	*	0.1266D 02	-0.7529D 01	0.3670D 02	*
*	-28.0	-22.0	*	0.1426D 02	0.2928D 02	0.1844D 02	*
*	-28.0	-18.0	*	0.1155D 02	-0.1284D 02	-0.1887D 02	*
*	-28.0	-14.0	*	0.1293D 02	0.9420D 01	-0.2985D 02	*
*	-28.0	-10.0	*	0.1298D 02	0.1889D 01	0.1574D 02	*
*	-28.0	-6.0	*	0.1106D 02	-0.3793D 01	0.3230D 01	*
*	-28.0	-2.0	*	0.1223D 02	0.1800D 02	0.7619D 01	*
*	-28.0	2.0	*	0.1238D 02	0.6735D 01	0.1428D 02	*
*	-28.0	6.0	*	0.1192D 02	-0.2684D 02	-0.1434D 02	*
*	-28.0	10.0	*	0.1154D 02	-0.9759D 01	-0.1126D 02	*
*	-28.0	14.0	*	0.1387D 02	-0.5226D 01	0.3833D 01	*
*	-28.0	18.0	*	0.9989D 01	-0.3081D 02	0.6752D 01	*
*	-28.0	22.0	*	0.1278D 02	-0.8284D 01	-0.6434D 01	*
*	-32.0	-22.0	*	0.1325D 02	0.3635D 01	-0.6656D 01	*
*	-32.0	-18.0	*	0.1234D 02	-0.5489D 01	-0.2057D 01	*
*	-32.0	-14.0	*	0.1125D 02	0.2630D 02	0.2836D 02	*
*	-32.0	-10.0	*	0.1143D 02	-0.9264D 01	0.7949D 01	*
*	-32.0	-6.0	*	0.1263D 02	-0.1234D 01	0.1839D 02	*
*	-32.0	-2.0	*	0.1049D 02	-0.1021D 02	0.8880D 01	*
*	-32.0	2.0	*	0.1205D 02	-0.2530D 02	-0.1922D 02	*
*	-32.0	6.0	*	0.1110D 02	0.1256D 02	-0.5003D 01	*
*	-32.0	10.0	*	0.1096D 02	-0.9943D 00	0.1847D 02	*
*	-32.0	14.0	*	0.1274D 02	-0.1606D 02	-0.4152D 00	*
*	-32.0	18.0	*	0.1064D 02	-0.2378D 02	-0.3422D 01	*
*	-32.0	22.0	*	0.1120D 02	-0.2343D 02	0.1938D 02	*

STATISTICAL RESULTS:

	MEAN VALUE	STANDARD DEVIATION
X-DIRECTION	0.783D 02	0.446D 01
Y-DIRECTION	-0.661D 00	0.142D 02
Z-DIRECTION	0.267D 01	0.152D 02

From this table it can be readily seen that the points closer to the upper jaw have experienced more deformations in the load direction than those on the lower rows of the paper sample. The load direction components of deformations for each row of the paper web have been averaged on both sides (i.e. $^{\beta}< {}^{\alpha}u_x^R , {}^{\alpha}u_x^L >$; $\alpha = 1,2,\ldots, 12$ and β: column index = $1,2,\ldots, 20$) and plotted in Fig. 5.4. The plot of Fig.5.4 shows the values of $^{\beta}< {}^{\alpha}u_x >$ that are averaged on both sides of the sample with respect to the distance of the corresponding row β from the lower (fixed) jaw. It can be seen that by extrapolating this curve between X=-44 mm and X=- 32 mm a nonlinear deformation $^{\alpha}u_x$ along the sample is obtained, which indicates that the lower portion of the sample has deformed considerably. However, by considering the corresponding interferograms that are similar to those shown in Figs. 5.1 and 5.2, it can be observed that the fringe pattern in this region of the paper sample is different from that of the upper part. The fringes closer to the upper jaw are more distinct and straight, whilst those close to the lower jaw are contour-shaped and indicate excessive bowing-out effect of the paper sample in that region. It is this author's belief that this non-uniformity in the fringe formation and the corresponding deformation field should deal with the boundary effects of the

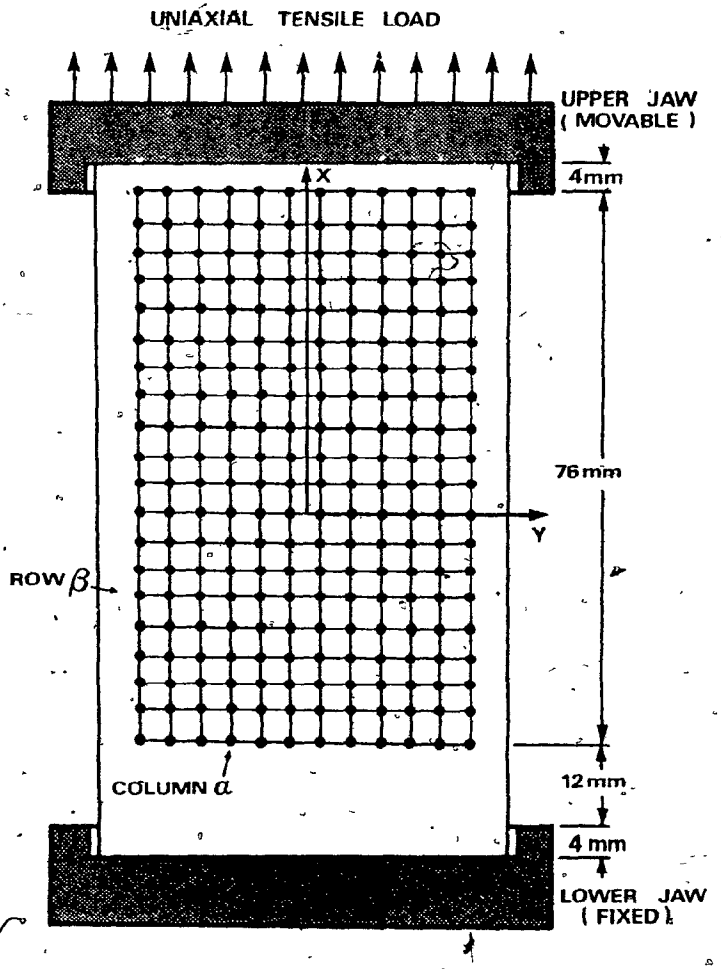

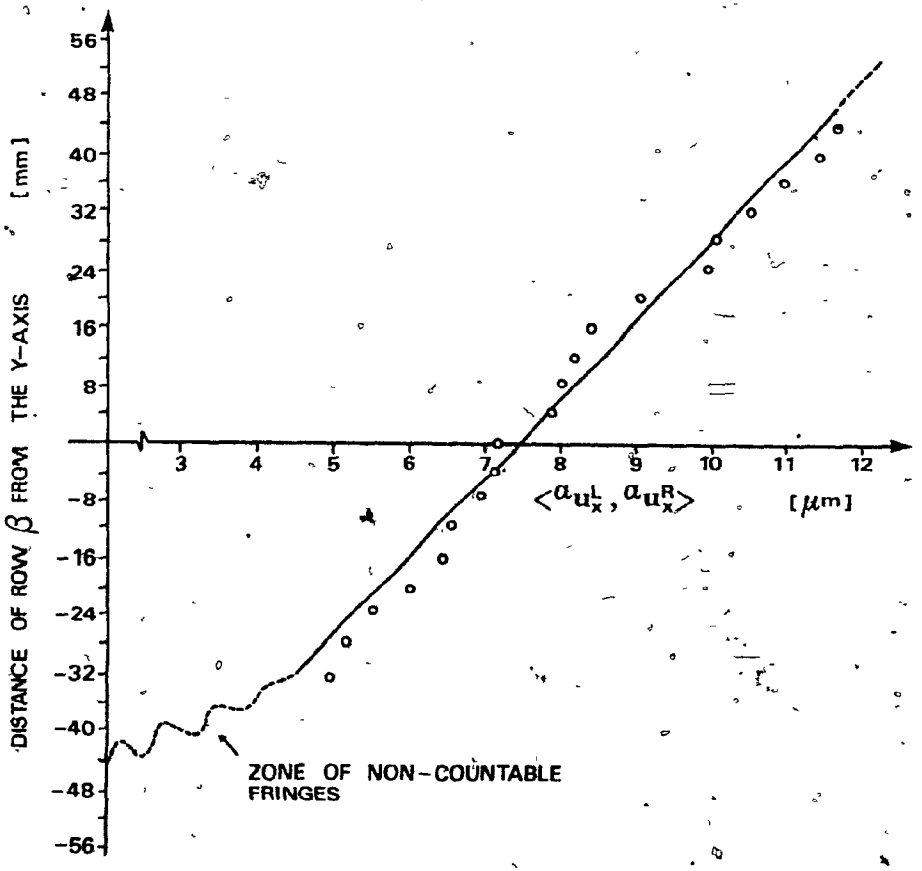

FIG. 5.4 HOLOGRAPHIC-ELECTRO-OPTICAL RESULTS OF $\langle {}^{a}u_x \rangle$ FOR EACH ROW OF THE TESTED NEWSPRINT SAMPLE AT TIME H2 .

lower jaw and the presently developed technique as well as the known conventional techniques are unable to evaluate accurately any fringes within such areas.

In dealing with the comparison of the holographic-electro-optical test results with the fotonic sensor output, since the first row of the observation points (i.e. $\beta=1$ and $\alpha=1,2...,12$) are in contact with the upper jaw, the mean value of the deformation on this row is equivalent to the macroscopic displacement of the upper jaw. Thus, the values of $^{\beta=1}\langle {}^{\alpha}u_x \rangle$ at each time instant have been obtained. These values as well as the fotonic sensors output have been plotted with respect to time in Fig. 5.5. The origin of the displacement axis has been shifted from 105 μm (see also Fig. 4.6) to zero, because no holographic observations could have been made during the 105 μm macroscopic displacement of the upper jaw. A comparison of the two curves indicate that although the holographic test and the fotonic sensors readings have been carried out independently, their difference after approximately 40 minutes does not exceed 4% of the magnitude of the measured quantity. The latter is within the frame of the engineering standards.

The next step in the main program is to perform the statistical analysis of the deformation field. By this is meant the determination of the first moment $\langle {}^{\alpha}\underset{\sim}{u} \rangle$ and the second moment $\langle ({}^{\alpha}\underset{\sim}{u})^2 \rangle$;

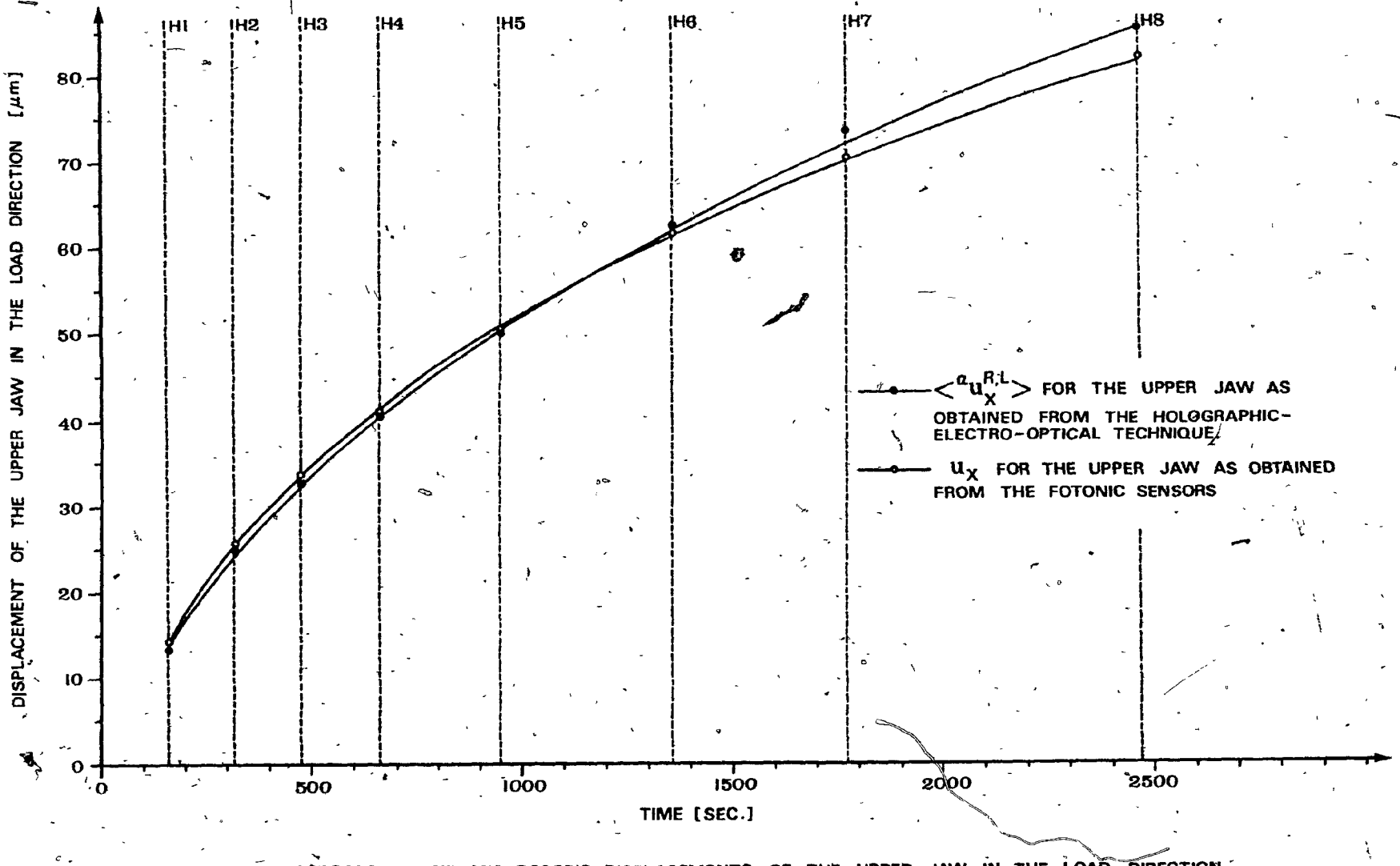

FIG. 5.5 MACROSCOPIC AND MICROSCOPIC DISPLACEMENTS OF THE UPPER JAW IN THE LOAD DIRECTION

$\alpha=1,2,\ldots,240$ for all the observation points at each time instant (statements 85, 94, 122). The overall microscopic deformational behaviour of the tested newsprint is given in Fig. 5.6, in which the values of $<{}^{\alpha}u_x^R>$ and $<{}^{\alpha}u_x^L>$ have been plotted with respect to time. In this figure points H1, H2,..., H8 indicated the time instants at which the interferograms are obtained. It is further of interest to note again that due to the rapid failure of the weaker bonds between the overlapped fibres and the alignment of fibres in the direction of the load application, the paper microstructure becomes rather unstable during the time 0 - H1. The instability of the microstructure has been observed in the interferogram that corresponds to this time interval. Although the permissible macroscopic displacement of the upper jaw has been carefully controlled at all times (see Section 4.2.1), but the compact and non-localized fringe pattern on the real image plane have indicated unusual deformations of the paper sample. Thus, the point H1 at time $t_1=164$ sec. had to be considered as the starting point of the observable microscopic deformational behaviour of the paper sample under investigation. Further examination of the obtained curve in Fig. 5.6 shows that the newsprint paper exhibits creep behaviour very similar to other solid materials.

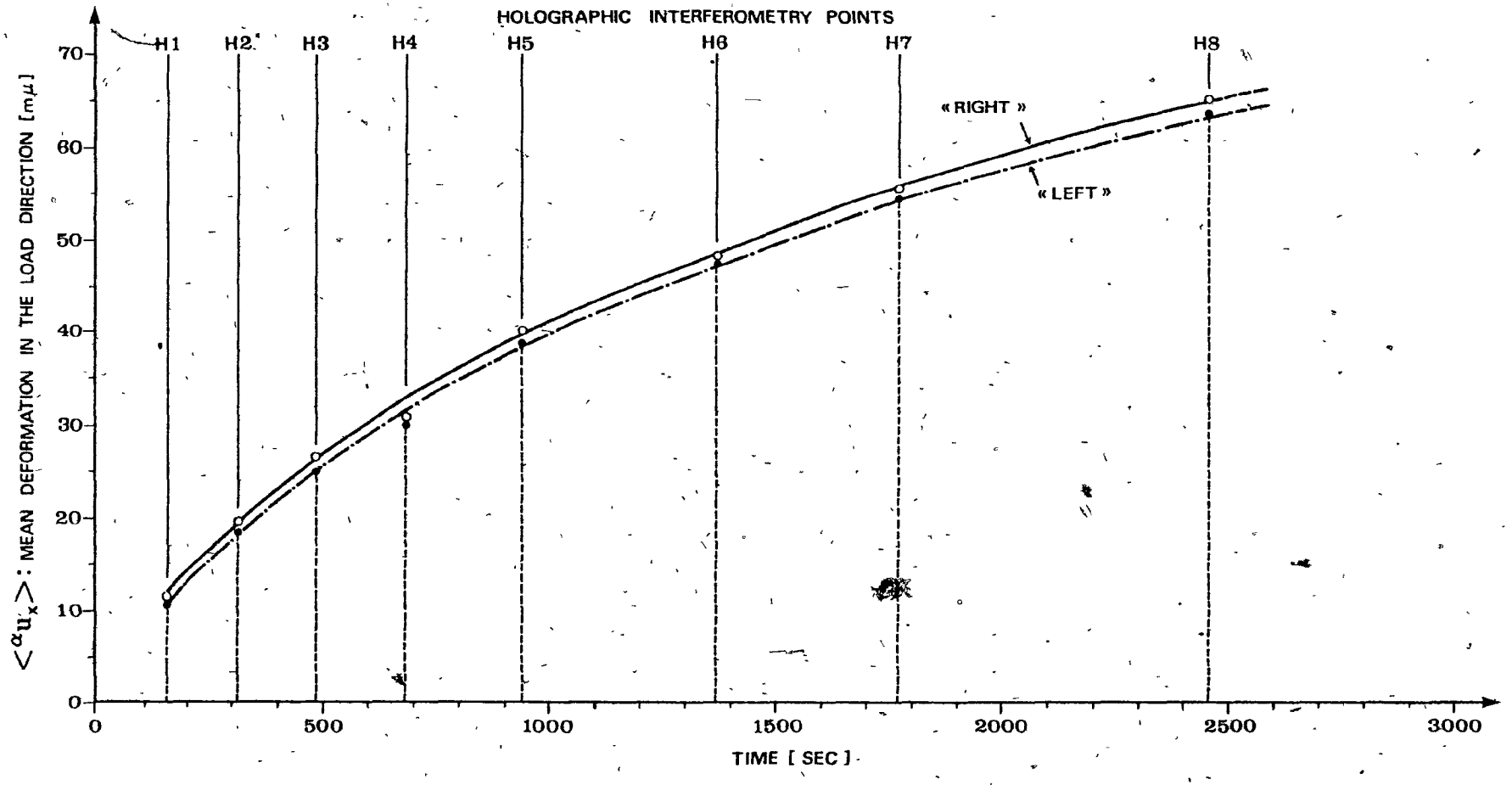

FIG.5.6 MICROSCOPIC DEFORMATIONS OF SAMPLE #38 IN THE DIRECTION OF LOAD FROM RIGHT AND LEFT INTERFEROGRAM READINGS.

However, this particular structured solid shows a far more extended stage of steady-state creep than usually encountered in other engineering materials. This can be ascribed to the unwoven microstructure, the motion of which is predominantly indicated by the hydrogen bonding between overlapping fibres [70].

The first and second moments of the typical interferogram 2L for all 240 observation points have also been tabulated in Table (5.1). Examination of the values in this table shows wider deviations of the $^{\alpha}u_y^R$ and $^{\alpha}u_z^R$ components from their mean values than that of the $^{\alpha}u_x^R$ component. This, however, signifies the magnitude of the out-of-plane motion of the sample, which is believed to be due to the straightening out of the fibres that are misaligned with respect to the load application direction. In order to show the distribution of these deformation components, some typical histograms of the obtained deformation field at points H2, H4 and H6 are given in Figs. 5.7-5.12. Among other tested known distributions such as Poisson and Binominal, these histograms showed a distinct Gaussian character of the deformation distributions on the surfaces of the paper sample.

Whilst the above information is of utmost importance, the next steps considered in the main program are the evaluation of the strain field (statement 156) and the thickness variation of the paper web during each time interval (statement 90). For the

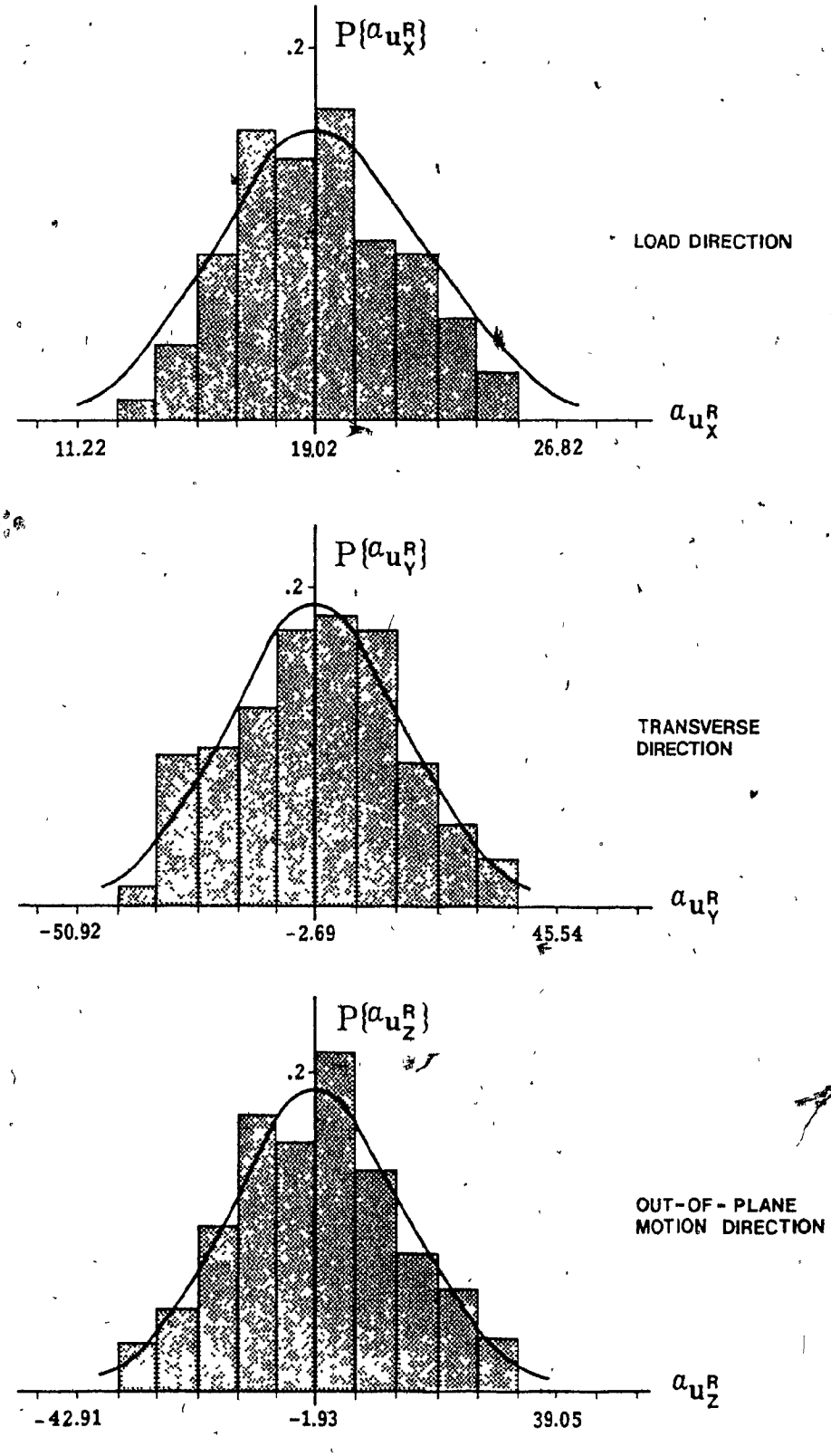

FIG. 5.7 HISTOGRAMS AND GAUSSIAN DISTRIBUTIONS OF DEFORMATIONS AT TIME $t = 302$ SEC FOR THE «RIGHT» SIDE OF PAPER SAMPLE.

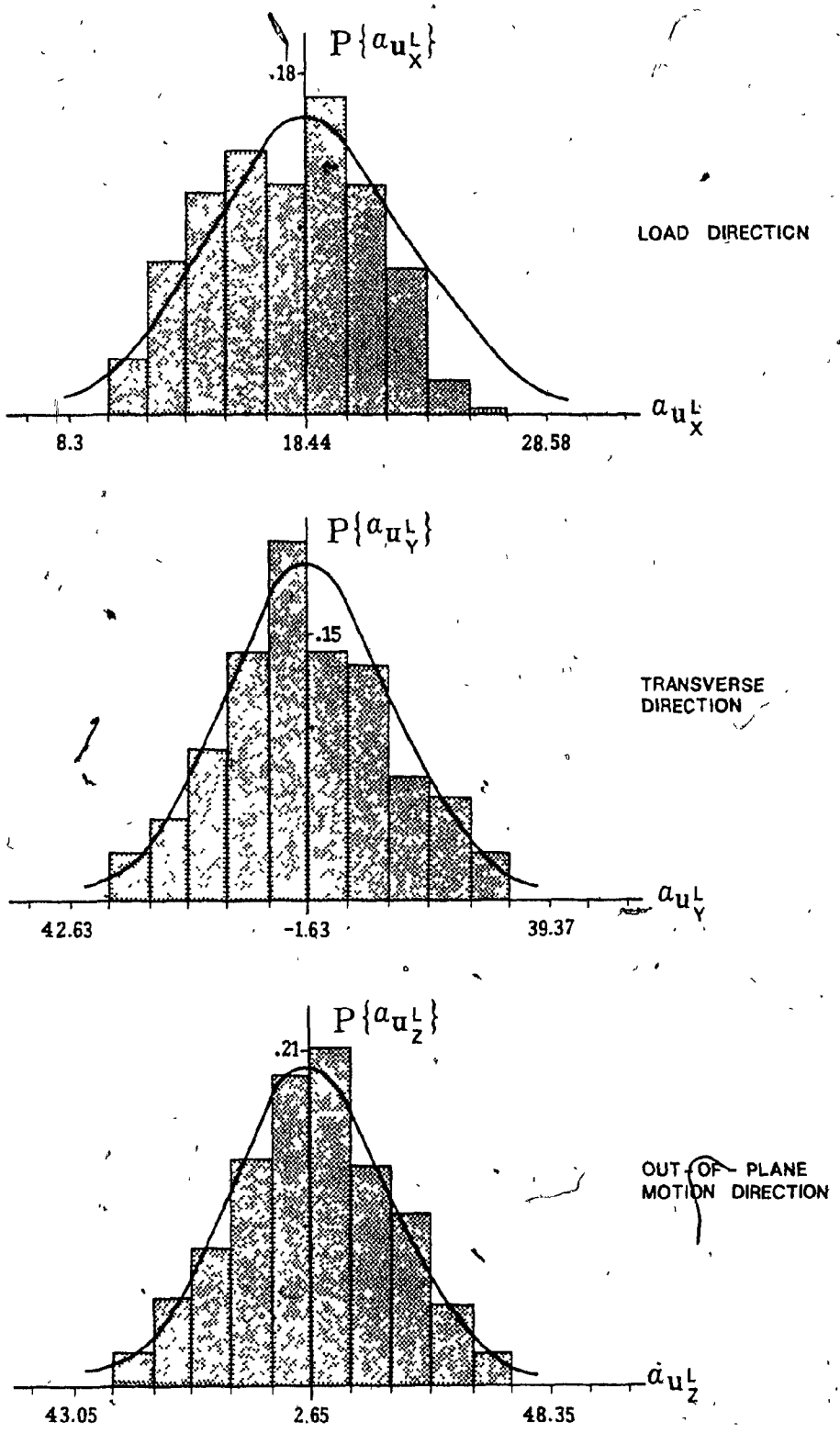

FIG. 5.8 HISTOGRAMS AND GAUSSIAN DISTRIBUTIONS OF DEFORMATIONS AT TIME = 302 SEC FOR THE «LEFT» SIDE OF PAPER SAMPLE.

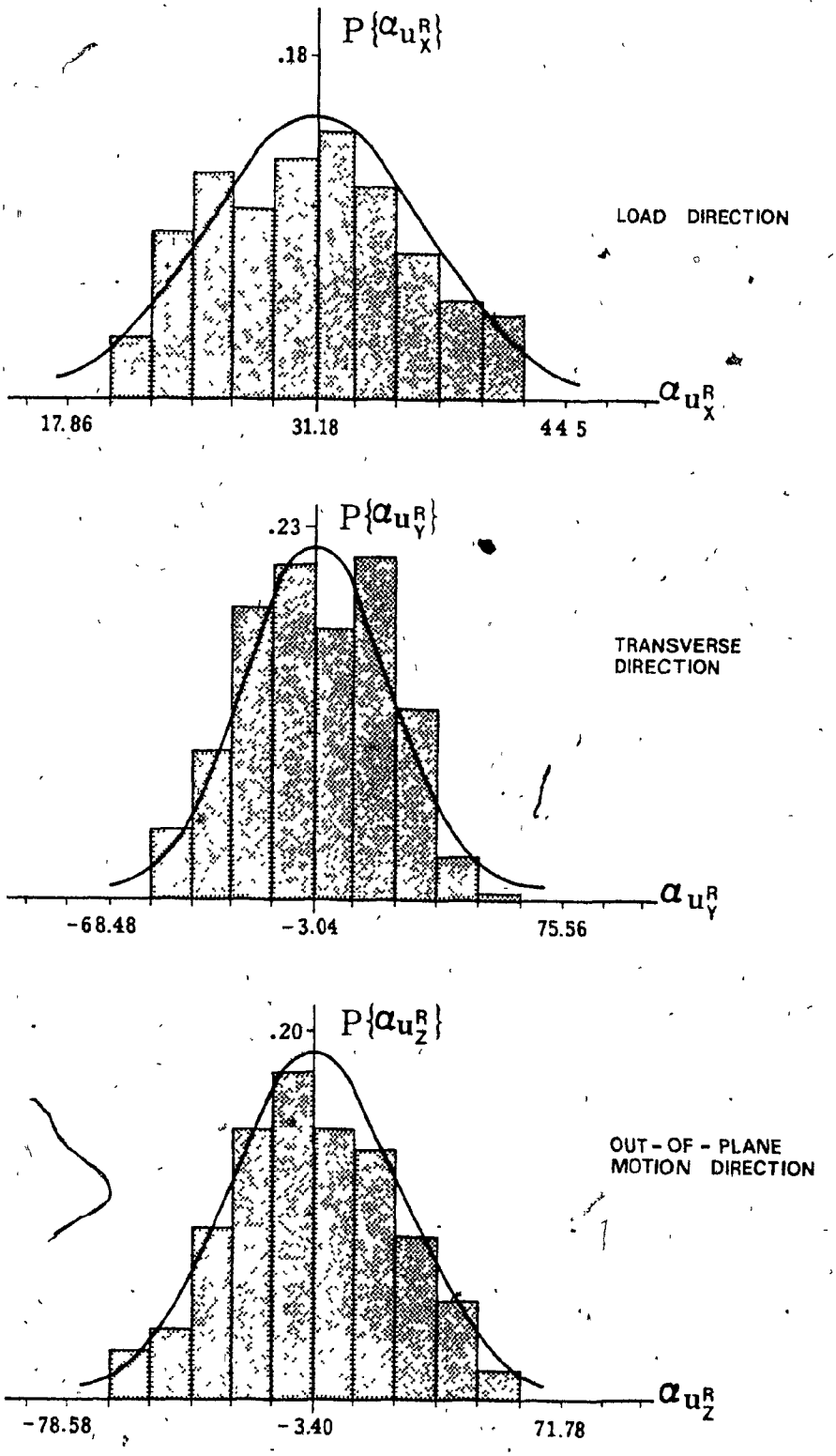

FIG. 5.9 HISTOGRAMS AND GAUSSIAN DISTRIBUTIONS OF DEFORMATIONS AT TIME $t = 674$ SEC FOR THE « RIGHT » SIDE OF PAPER SAMPLE.

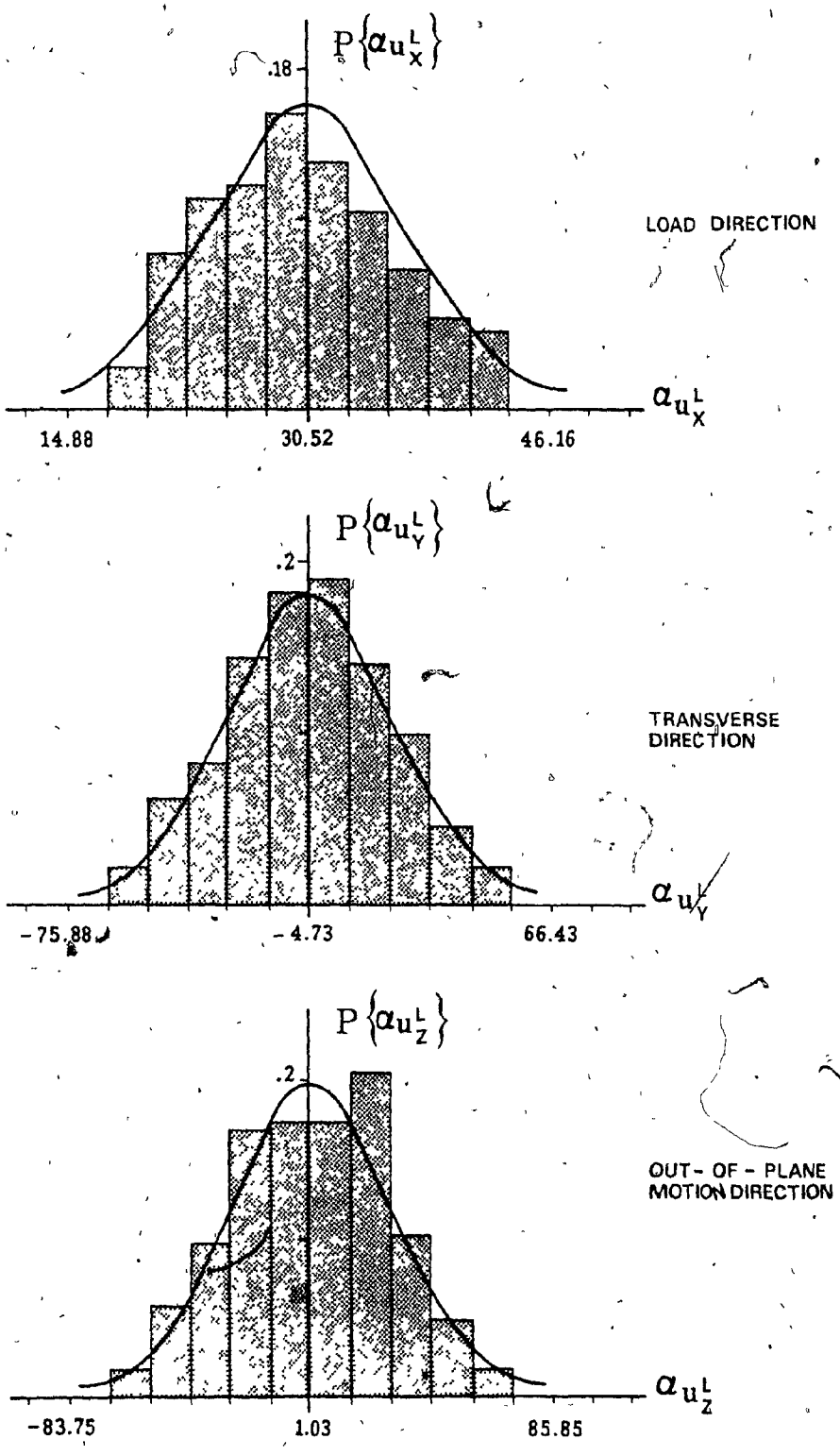

FIG. 5.10 HISTOGRAMS AND GAUSSIAN DISTRIBUTIONS OF DEFORMATIONS AT TIME TIME $t = 674$ SEC FOR THE « LEFT » SIDE OF PAPER SAMPLE.

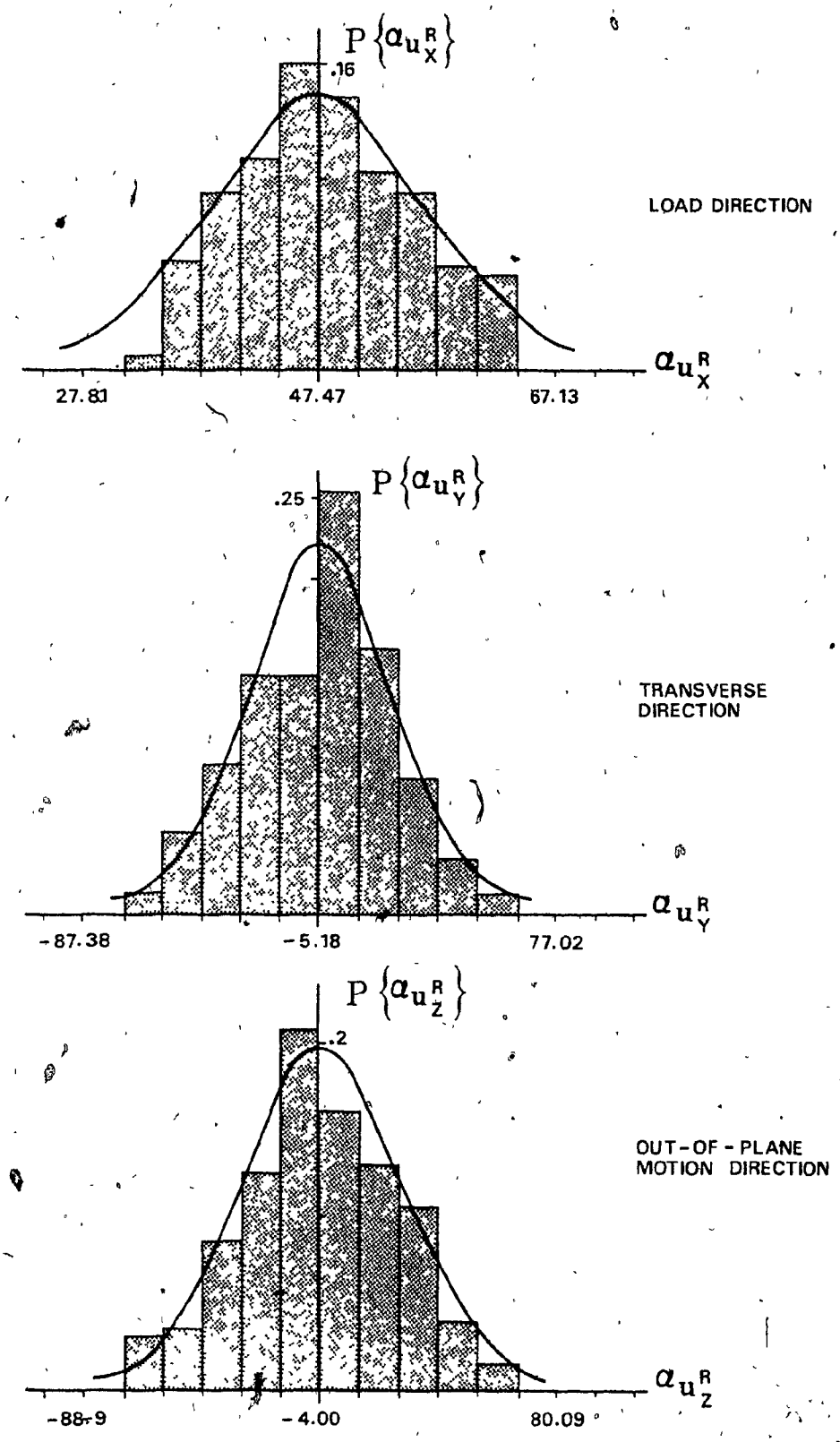

FIG. 5.11 HISTOGRAMS AND GAUSSIAN DISTRIBUTIONS OF DEFORMATIONS AT TIME t=1374 SEC FOR THE « RIGHT » SIDE OF PAPER SAMPLE.

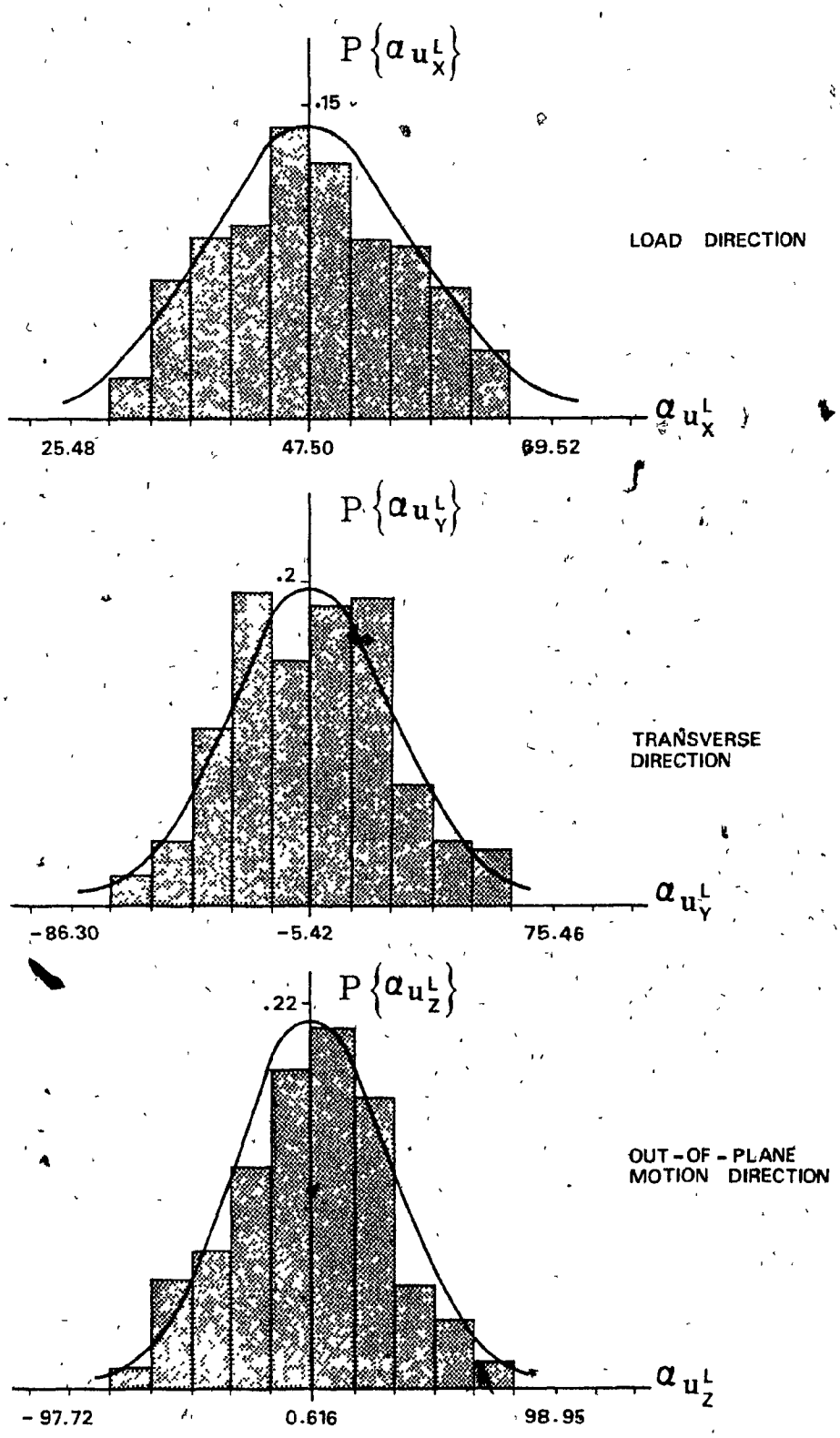

FIG. 5.12 HISTOGRAMS AND GAUSSIAN DISTRIBUTIONS OF DEFOMATIONS AT TIME $t = 1374$ SEC FOR THE « LEFT » SIDE OF PAPER SAMPLE.

purpose of the strain assessment the relation in accordance with the small strain theory has been used, i.e.

$$\varepsilon_{ij} = \tfrac{1}{2}\left(\frac{\partial u_i}{\partial x_j} + \frac{\partial u_j}{\partial x_i}\right) \approx \tfrac{1}{2}\left(\frac{\Delta u_i}{\Delta x_j} + \frac{\Delta u_j}{\Delta x_i}\right) \qquad - (5.1)$$

where $\partial u_m/\partial x_n$ is a continuous deformation gradient. In the present strain evaluation this gradient is considered to be equivalent to $\Delta u_m/\Delta x_n$. Thus, the diagonal elements of ε_{ij} are the strains in the load direction and the transverse direction. These elements are as follows:

$$\varepsilon_{xx} = \tfrac{1}{2}\left(\frac{\Delta u_x}{\Delta x} + \frac{\Delta u_x}{\Delta x}\right) = \frac{\Delta u_x}{\Delta x}$$

$$\varepsilon_{yy} = \ldots\ldots\ldots\ldots = \frac{\Delta u_y}{\Delta y} \qquad - (5.2)$$

Thus, using the deformation vector, relations (5.2) and the corresponding "subroutine strain" of the main program, permitted the evaluation of the strain components ε_{xx} and ε_{yy}. The values of the strain components for all observation points are tabulated for each interferogram. These tables are given in the computer listing of Appendix V. However, in order to show the microscopic creep curve of the tested newsprint paper sample, the values of $\langle\varepsilon_{xx}\rangle$ that are averaged over the entire sample points are plotted with respect to time in Fig.5.13. Since the main objective in

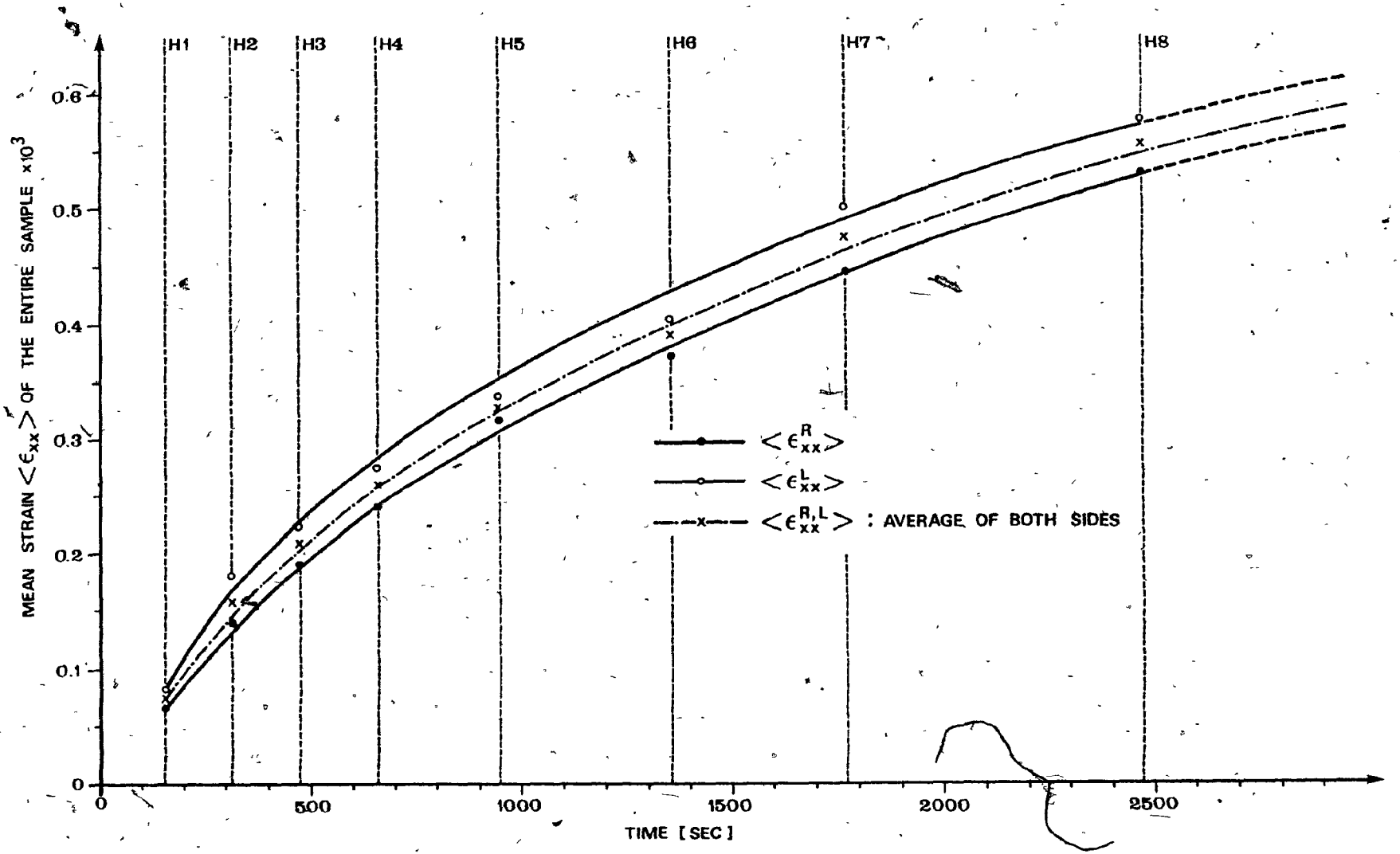

FIG. 5.13 MICROSCOPIC CREEP CURVE OF THE TESTED NEWSPRINT PAPER SAMPLE.

the interpretation of the results is to correlate the evaluated strain field to the volumetric mass density, no further analysis of the creep behaviour of the newsprint paper sample is necessary.

In dealing with the local thickness changes, it was mentioned in Chapter II of this thesis that the latter can be obtained from the following relation:

$$\Delta^{\alpha}\tau = {}^{\alpha}u_z^R - {}^{\alpha}u_z^L \quad ; \quad \alpha = 1, 2, \ldots, 240$$

where ${}^{\alpha}u_z^R$ and ${}^{\alpha}u_z^L$ are the deformation components in the out-of-plane motion direction. It should be noticed that in this relation both of the deformation components are measured with respect to an arbitrary Z-axis. However, since the deformation evaluation in this thesis is with respect to Z^R and Z^L axes (see Fig. 4.7), whilst $Z^R = -Z^L$, thus the above relation can be rewritten in the following form:

$$\Delta^{\alpha}\tau = {}^{\alpha}u_{zR}^R + {}^{\alpha}u_{zL}^L \qquad (5.3)$$

The solution of the above relation for $\Delta^{\alpha}\tau$ has been carried out in "Subroutine CHANGE" of the main program. Thus, at each time instant, first the deformation field is evaluated for both sides of the paper sample, then only the ${}^{\alpha}u_{zR}^R$ and ${}^{\alpha}u_{zL}^L$ components have been considered in the "Subroutine CHANGE" for the evaluation of the corresponding $\Delta^{\alpha}\tau$. A typical table of results is given in Table (5.2). The

EVALUATED THICKNESS CHANGES (MICRONS)
(COLUMNS: 1- 6)

	1	2	3	4	5	6
1	1.62	-0.05	-1.77	-3.16	1.74	0.91
2	-1.55	3.89	4.23	-3.68	-3.44	2.60
3	3.45	2.37	1.20	3.45	-3.01	2.52
4	2.35	-2.70	0.43	-3.46	2.34	0.87
5	4.19	-1.22	3.89	2.85	-1.71	0.79
6	-2.04	1.26	-0.18	0.76	-0.19	1.66
7	2.54	4.20	3.87	4.39	-3.48	-2.04
8	-1.35	-2.17	3.18	0.12	-0.34	-2.52
9	4.09	-2.38	-0.29	3.21	-2.30	-3.32
10	-0.29	-1.41	-3.00	3.83	-0.15	-3.91
11	3.66	-3.84	0.18	4.52	-2.71	-0.68
12	-2.42	3.73	0.72	-0.03	3.75	-2.29
13	2.98	-2.70	2.53	4.02	-2.85	3.55
14	4.45	-3.21	-1.32	4.27	1.00	-3.44
15	2.21	-2.88	-1.89	1.05	-3.34	4.37
16	3.12	-1.83	4.04	-2.20	0.82	-2.28
17	3.98	1.09	-1.44	0.22	-2.61	-2.31
18	-3.02	0.05	1.80	2.85	-2.04	-0.34
19	-3.04	0.88	3.76	-2.98	0.49	0.71
20	3.63	-0.49	-0.28	0.71	2.37	-1.35

(COLUMNS: 7-12)

	7	8	9	10	11	12
1	-3.54	-0.75	3.51	-2.21	2.87	-2.77
2	-3.09	1.63	-2.78	0.99	1.26	-1.32
3	-1.87	3.08	-3.00	1.48	-2.93	-0.36
4	-3.17	2.52	-3.79	0.49	0.88	-2.04
5	4.41	3.43	-0.98	-1.23	1.49	3.68
6	-2.54	-1.19	-1.69	-1.69	-2.34	-2.46
7	0.33	-3.66	4.30	0.18	-3.17	4.23
8	-2.93	1.27	-0.59	-2.69	-1.31	1.56
9	4.74	4.12	-2.03	3.41	4.22	-2.46
10	3.88	4.29	-0.38	1.99	-2.21	-2.77
11	0.35	2.24	-1.42	1.68	-2.19	-3.96
12	0.47	1.66	-1.75	3.73	-2.52	0.33
13	0.96	-2.90	2.16	-0.07	-2.16	2.84
14	-3.11	1.72	-2.11	2.76	-0.21	1.09
15	-2.52	-0.73	0.77	4.60	-1.88	-3.76
16	0.08	-0.30	2.09	1.99	-2.07	-1.96
17	2.96	-3.47	-2.23	0.41	-3.48	1.10
18	1.84	3.15	-0.39	-2.77	0.32	1.51
19	-0.16	-0.71	2.31	1.75	-2.59	-2.75
20	0.94	4.13	2.13	4.29	-3.39	4.26

Table (5.2) Thickness variations of the tested newsprint paper sample at time t=H2 as obtained from Holographic-electro-optical technique.

remaining results are correspondingly tabulated in Appendix V. In these tables, the negative values of $\Delta^{\alpha}\tau$ indicate the thickness reduction of the paper web at a point α, whose location is specified by the row and column numbers of the mesh of observation points, and the positive values the increase of the web thickness at the specified points.

A paper subjected to strain, in general, undergoes different thickness variations. Some investigators [69] believe that the thickness increase of the web during stretching of the paper is due to lateral contraction, whilst some others [65] have argued that the thickness increase is as a result of the straightening out of the fibres oriented in the direction of the load application. Based on the observations that have been made in the present investigation, it is difficult to make a firm statement in dealing with this phenomenon. However, the author of this thesis believes that the thickness increase is due to both straightening out of some fibres when getting aligned in the load direction and the partial or total failure of the bonding between the fibres. It has been observed experimentally [70] that before the final rupture occurs in a bonded area between two fibre segments, the bonded area rotates around the direction of the load application and therefore increase the web thickness in that particular point. It is evident that these changes in the thickness induce changes

in the volumetric mass density $^{\alpha}\rho$ of the web. On the other hand, since the deformational behaviour of the paper sample has been evaluated at eight successive time instants, the corresponding thickness variations and the $^{\alpha}\rho$ values of each of these time instants have been numerically evaluated. Hence, the subject matter of the following sections is an attempt to correlate $^{\alpha}\rho$ and the strain field at each time instant. However, before dealing with the derivations of such correlations, it should be mentioned that the results from the Beta-radiography correspond to time t=o, i.e. prior to the actual loading of the paper sample. The distribution of these results is also shown in Fig. 5.14.

5.4 Thickness and VMD Measurement Results

The results of the thickness measurements are tabulated in the computer output of Appendix IV as well as the results for the evaluated VMD. The $^{\alpha}\tau$ measurements have been carried out on the "rough side" or the right side of the sample. Since the "smooth side" of the paper is maintained in close contact with the reference glass plate by means of the calibrated weight of the fotonic sensor's adaptor, thus it is assumed that only the measurements from the right side represent the thickness of the sample. Once again, the thickness measurement results were found to be close to a Gaussian distribution (See Fig. 5.15).

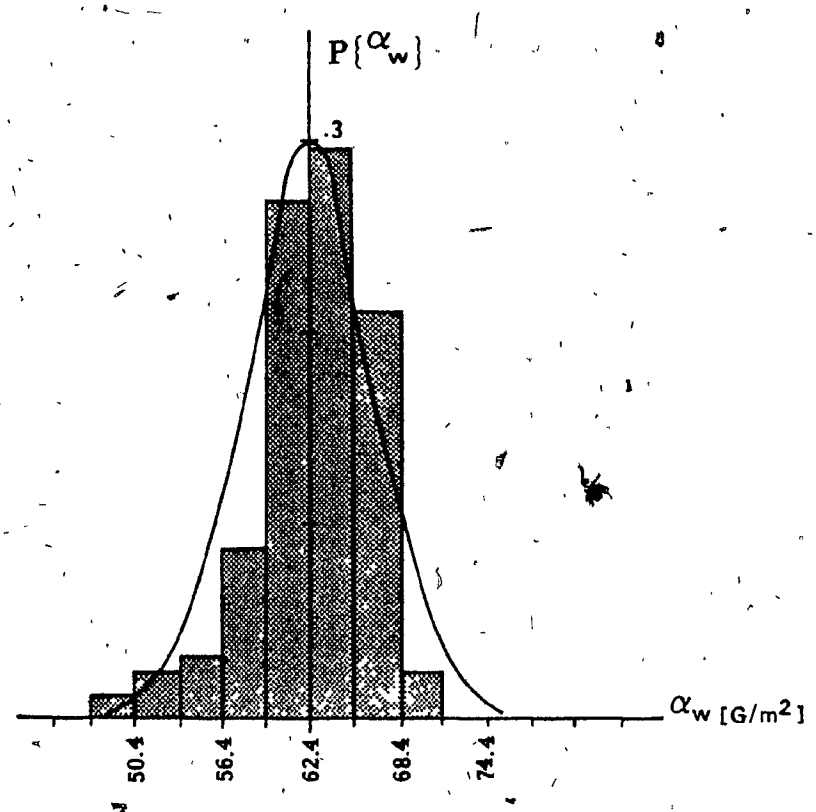

FIG. 5.14 DISTRIBUTION OF THE LOCAL AREA MASS DENSITY OF THE NEWSPRINT PAPER SAMPLE AT TIME t = 0.

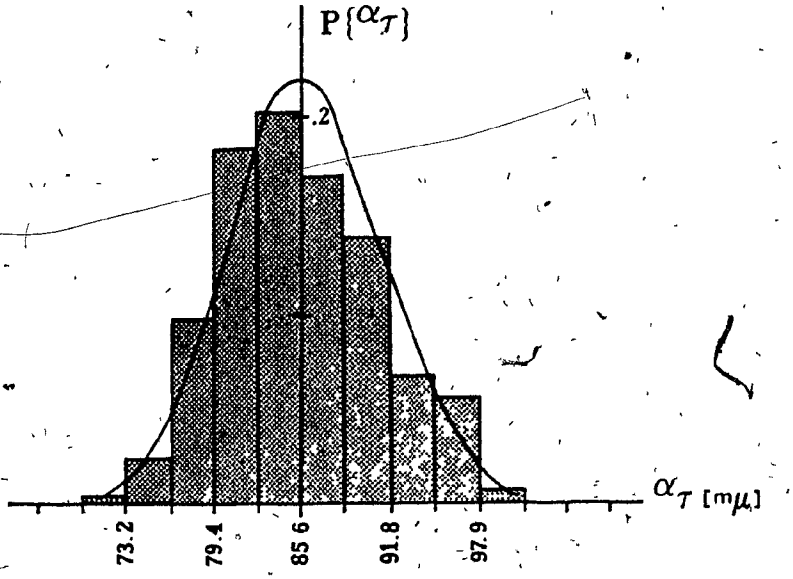

FIG. 5.15 DISTRIBUTION OF THE LOCAL THICKNESS OF THE NEWSPRINT PAPER SAMPLE AT TIME t = 0.

The $^{\alpha}\tau$ measurements have been carried out before subjecting the paper sample to uniaxial load, thus they correspond to the state of the web at time t=o. Then using relation (2.7), i.e.

$$^{\alpha}\rho = {}^{\alpha}w \cdot {}^{\alpha}\tau^{-1}$$

The obtained values of $^{\alpha}w$ and $^{\alpha}\tau$ at time t=o have been substituted in the above relation in order to obtain the values of $^{\alpha}\rho$ at the specified observation points α. Once the paper sample undergoes the load application, the above quantities, i.e. $^{\alpha}w$ and $^{\alpha}\tau$ change. The assessment of the variations of $^{\alpha}w$ required a fast Beta-radiographic technique to be applied parallel to the holographic test. This, however, could not be achieved with the existing equipment, but can be improved as discussed in Chapter VI concerned with the proposed future research. Thus, it has been assumed that the changes in $^{\alpha}\rho$ were caused mainly by the changes in $^{\alpha}\tau$. Thus, for each time instant H1,..., H8 the new thickness and the new VMD have been evaluated. These results do not appear in the computer evaluation of Appendix V, instead the correlation coefficients between $^{\alpha}\rho$ and $^{\alpha}\varepsilon_{xx}$ and/or $^{\alpha}\varepsilon_{yy}$ at times H1-H8 have been established and given in this Appendix.

5.5 On the Correlation Coefficients

In general, consider two random variables X_i and Y_i, i=1,2,..,N, where each of these variables can be considered as one of the

experimentally obtained quantities, i.e. $X_i \equiv {}^{\alpha}\rho$, $Y_i \equiv {}^{\alpha}\varepsilon_{xx}$; $i = 1,2,\ldots, 209$. The number 209 here corresponds to the total number of strains. Let μ_x and μ_y be the first moments of X_i and Y_i, respectively. Then:

$$\mu_x = E\{X_i\} = \frac{1}{n} \sum_{i=1}^{n} X_i$$

$$\mu_y = E\{Y_i\} = \frac{1}{n} \sum_{i=1}^{n} Y_i$$

Then from the probability theory, the quantity $E\{(X_i-\mu_x)^a(Y_i-\mu_y)^b\}$ is known as the (a+b)th central moment of X_i and Y_i[71,72]. However, for a more complete description, the second central moments are important, i.e.

$$E\{(X_i-\mu_x)(X_i-\mu_x)\} = \sum_{i=1}^{n} (X_i-\mu_x)^2 = \sigma_x^2 \text{ variance of } X_i$$

$$E\{(Y_i-\mu_y)(Y_i-\mu_y)\} = \sum_{i=1}^{n} (Y_i-\mu_y)^2 = \sigma_y^2 \text{ variance of } Y_i \qquad - (5.4)$$

$$E\{(X_i-\mu_x)(Y_i-\mu_y)\} = \sigma_{xy} \qquad \text{covariance of } X_i \text{ and } Y_i$$

If the two random variables are independent, it can be shown that [73]:

$$E\{(X_i-\mu_x)(Y_i-\mu_y)\} = E\{(X_i-\mu_x)\} \cdot E\{(Y_i-\mu_y)\} = 0 \qquad - (5.5)$$

The theoretical covariance is the limiting value of the observed covariance of a frequency distribution defined as:

$$\sigma_{xy} = \lim_{n\to\infty} \left[\sum_{i=1}^{n} (X_i-\mu_x)\,(Y_i-\mu_y) \right] \Big/ n \qquad - (5.6)$$

where, for real experiments $n\to\infty$ signifies a large number of trials. Thus, the covariance of random variables may be used to find the way these variables are related to each other. For this purpose, a more convenient factor known as the correlation coefficient is defined by:

$$k(X,Y) = \left[\sum (X_i-\mu_x)(Y_i-\mu_y) \right] \Big/ \left[\sum (X_i-\mu_x)^2 \cdot \sum (Y_i-\mu_y)^2 \right]^{\frac{1}{2}} - (5.5)$$

which is the normalized form of the covariance. By referring to equation (5.4), it should be mentioned that these relations are valid for a large number of observations, i.e. $n\to\infty$, otherwise the obtained values of σ_x, σ_y and σ_{xy}, in general, become smaller than their actual values[74]. Thus, for large values of n, the correlation coefficient becomes:

$$\kappa\,(X,Y) = \sigma_{xy}/\sigma_x \cdot \sigma_y \qquad - (5.8)$$

The correlation coefficient is a dimensionless quantity which can, therefore, be used with certain reservations as an absolute measure of the relationship between the two variables[73]. If X and Y

are independent then their covariance and their correlation coefficient are zero. If large values of X tend to be accompanied by large values of Y and vice versa, then their covariance and correlation coefficient will be positive; in the extreme case when one variable is completely determined by the other one in such a way that the points (x_i, y_i); $x_i \epsilon X$ and $y_i \epsilon Y$ lie exactly on a straight line with a positive slope, the correlation coefficient attains its largest possible value of +1. On the other hand, if large values of X tend to be accompanied by small values of Y and vice versa, their covariance and correlation coefficient will be negative; in the extreme case when the points (x_i, y_i) lie exactly on a straight line with a negative slope, the correlation coefficient attains its smallest possible value of -1. Provided that the relationship between the two variables is approximately linear, the correlation coefficient provides a reasonable measure of the degree of association between them, but may underestimate it if their relationship is non-linear.

In dealing with the experimental results of a newsprint paper sample, the correlation coefficients of quantities ${}^{\alpha}\rho$, ${}^{\alpha}\varepsilon_{xx}$, ${}^{\alpha}\varepsilon_{yy}$ and ${}^{\alpha}w$ can be computed for all points α; $\alpha=1,2\ldots,209$. These coefficients can also be obtained for points along each row or each column of the mesh of points on paper. For this purpose, for convenience, a different indexing for the quantities should be

made. For example, ${}^{\alpha\beta}\rho$ or ${}^{\alpha\beta}\varepsilon_{xx}$ indicate the volumetric mass density and the xx-strain components of a point whose location is specified by β^{th} row and α^{th} column. Thus, $\beta=1,2,\ldots,19$ and $\alpha=1,2,\ldots,11$, whilst in the case of ${}^{\alpha}\rho$ or ${}^{\alpha}\varepsilon_{xx}$, $\alpha=1,2,\ldots,209$ is referred to the entire sample. In this context relation (5.7) can be employed for each row or column of the sample, whilst equation (5.8) is for the entire sample. Thus, the following relations can be established:

$$\left.\begin{aligned} \beta_{k_1} : {}^{\beta}k({}^{\alpha\beta}\rho, {}^{\alpha\beta}\varepsilon_{xx}) = \Big[\sum_{\alpha=1}^{11} ({}^{\alpha\beta}\rho - \langle {}^{\alpha\beta}\rho \rangle)({}^{\alpha\beta}\varepsilon_{xx} - \langle {}^{\alpha\beta}\varepsilon_{xx} \rangle)\Big] \Big/ \\ \Big[\sum_{\alpha=1}^{11} ({}^{\alpha\beta}\rho - \langle {}^{\alpha\beta}\rho \rangle)^2 \cdot \sum_{\alpha=1}^{11} ({}^{\alpha\beta}\varepsilon_{xx} - \langle {}^{\alpha\beta}\varepsilon_{xx} \rangle)^2\Big]^{\frac{1}{2}} \\ \beta_{k_2} : {}^{\beta}k\ ({}^{\alpha\beta}\rho, {}^{\alpha\beta}\varepsilon_{yy}) \\ \beta_{k_3} : {}^{\beta}k\ ({}^{\alpha\beta}w, {}^{\alpha\beta}\varepsilon_{xx}) \quad ; \quad \beta = 1,2,\ldots,19 \\ \beta_{k_4} : {}^{\beta}k\ ({}^{\alpha\beta}w, {}^{\alpha\beta}\varepsilon_{yy}) \end{aligned}\right\} \quad (5.9)$$

Then, for the entire sample, the correlation coefficients are as follows:

$$\kappa_1 : \kappa({}^{\alpha}\rho, {}^{\alpha}\varepsilon_{xx}) = \sigma_{({}^{\alpha}\rho, {}^{\alpha}\varepsilon_{xx})} \Big/ \sigma_{{}^{\alpha}\rho} \cdot \sigma_{{}^{\alpha}\varepsilon_{xx}}$$

$$\kappa_2 : \kappa({}^{\alpha}\rho, {}^{\alpha}\varepsilon_{yy}) = \ldots$$

$$\kappa_3 : \kappa({}^{\alpha}w, {}^{\alpha}\varepsilon_{xx}) = \ldots \qquad \text{- (5.10)}$$

$$\kappa_4 : \kappa({}^{\alpha}w, {}^{\alpha}\varepsilon_{yy}) = \ldots \qquad ; \ \alpha = 1,2,\ldots, 209$$

It should be mentioned that the strain components in the above relations represent the mean values of the two sides of the paper sample, i.e.

$${}^{\alpha}\varepsilon_{\ell\ell} = \tfrac{1}{2} ({}^{\alpha}\varepsilon^{R}_{\ell\ell} + {}^{\alpha}\varepsilon^{L}_{\ell\ell}) \qquad ; \qquad \alpha = 1,2,\ldots, 209$$

or

$${}^{\alpha\beta}\varepsilon_{\ell\ell} = \tfrac{1}{2} ({}^{\alpha\beta}\varepsilon^{R}_{\ell\ell} + {}^{\alpha\beta}\varepsilon^{L}_{\ell\ell}) \qquad ; \qquad \beta = 1,\ldots, 19 \ , \ \alpha = 1,\ldots, 11$$

The experimental results obtained at each time instant H1,..., H8 have been substituted into the above relations and the computed correlation coefficients have been tabulated in Appendix V. For the purpose of interpretation of these results, a typical table is given in Table (5.3), which shows the correlation coefficients $\beta_{k_1},\ldots,\beta_{k_4}$ and $\kappa_1,\ldots,\kappa_4$ as obtained from relations (5.7) and (5.8), respectively at time t=H2. Again, in this table, the negative correlation coefficients indicate that the larger values

i	i_{k_1}	i_{k_2}	i_{k_3}	i_{k_4}
1	0.571	0.443	-0.034	0.301
2	-0.308	-0.285	-0.429	-0.094
3	-0.582	0.020	-0.453	0.110
4	0.294	0.324	0.187	0.209
5	-0.410	-0.257	-0.190	-0.297
6	-0.280	-0.138	-0.043	0.202
7	-0.063	0.051	0.003	-0.103
8	0.686	0.430	0.657	0.261
9	-0.157	0.508	-0.207	0.075
10	0.017	0.276	0.090	0.238
11	0.298	-0.034	-0.148	-0.382
12	0.383	0.292	0.225	0.097
13	-0.478	0.511	-0.329	0.195
14	0.005	0.323	-0.275	0.094
15	-0.135	-0.057	-0.164	-0.077
16	-0.091	0.174	0.158	-0.197
17	0.230	-0.206	0.090	-0.570
18	-0.318	0.480	-0.536	0.462
19	-0.325	0.213	-0.334	0.452

K_1	K_2	K_3	K_4
-0.061	0.176	-0.041	0.050

TABLE (5.3). Correlation coefficients at time t=H2.

of strains are associated with the smaller values of the volumetric mass density or the basis weight. Furthermore, from the obtained results, the following general conclusions can be made:

1. The low values of $\kappa_1,\ldots,\kappa_4$ indicate that the strain field is not linearly related to the volumetric mass density and the basis weight. They also indicate that the strain field cannot be directly related to $^{\alpha}\rho$ or $^{\alpha}w$ and that other influencing quantities such as the bonding between the fibres should also be considered.

The variations of $\kappa_1,\ldots,\kappa_4$ with time are given in Figs. 5.16 and 5.17. The fluctuations of these correlation coefficients are mainly due to the instability of the microstructure of the paper web. The latter is, however, caused by rapid failure of the weaker bonds and fibres. Once the load is carried by the stronger ones, the correlation coefficients will approach to their steady mean values (dashed lines in Figs. 5.16-17). It can be seen from these figures that κ_1 and κ_2, i.e. the correlation coefficients between $^{\alpha}\rho$ and $^{\alpha}\varepsilon_{\ell\ell}$, are slightly higher than κ_3 and κ_4 for $^{\alpha}w$ and $^{\alpha}\varepsilon_{\ell\ell}$. This difference is due to the inclusion of the quantity thickness $^{\alpha}\tau$ in the determination of $^{\alpha}\rho$, confirming that $^{\alpha}\rho$ is a more meaningful quantity to be considered in formulating the strength characteristic of fibrous networks. In dealing with the correlation

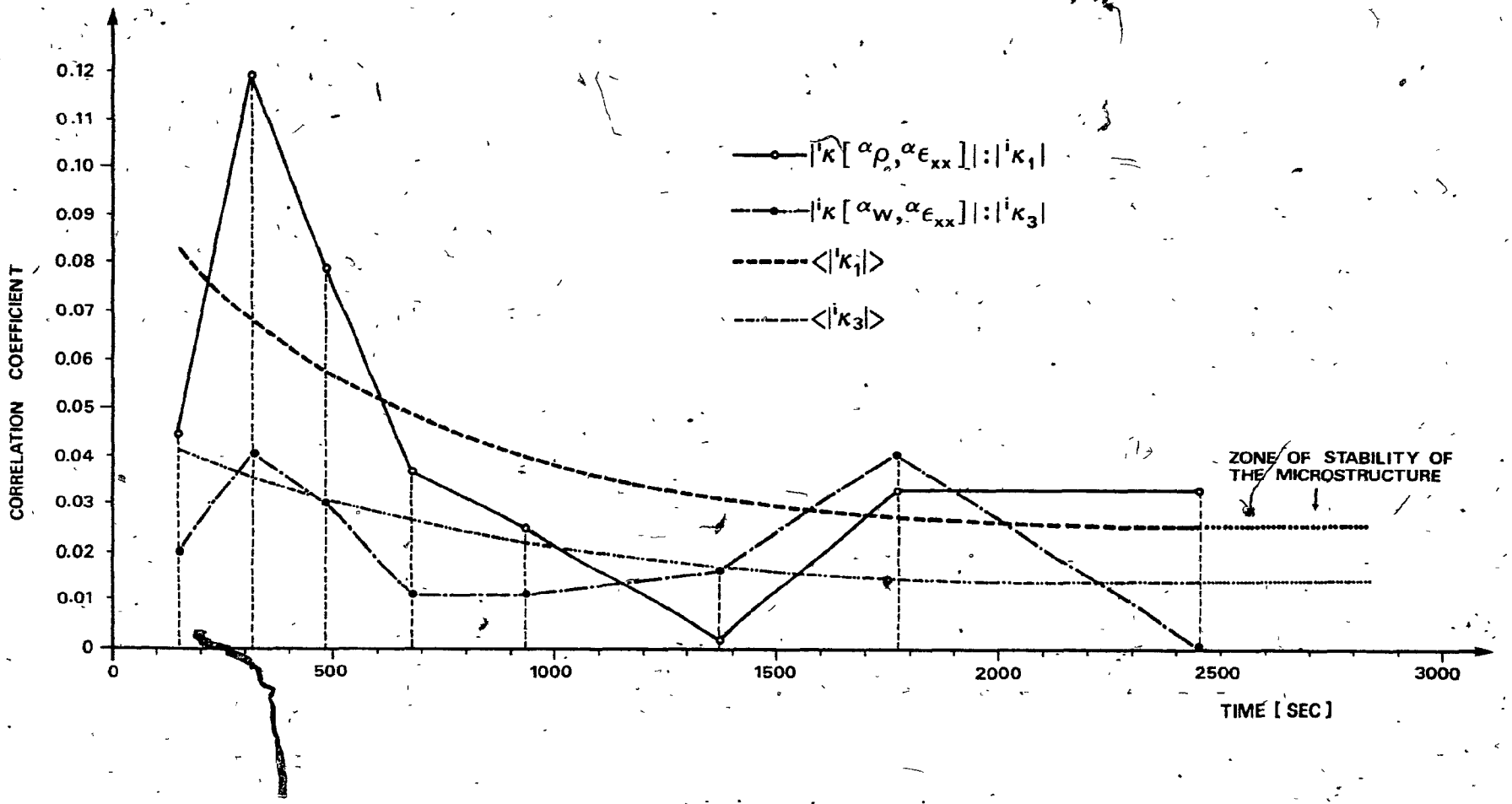

FIG. 5.16 VARIATIONS OF $\langle|^i\kappa_1|\rangle$ AND $\langle|^i\kappa_3|\rangle$ WITH TIME.

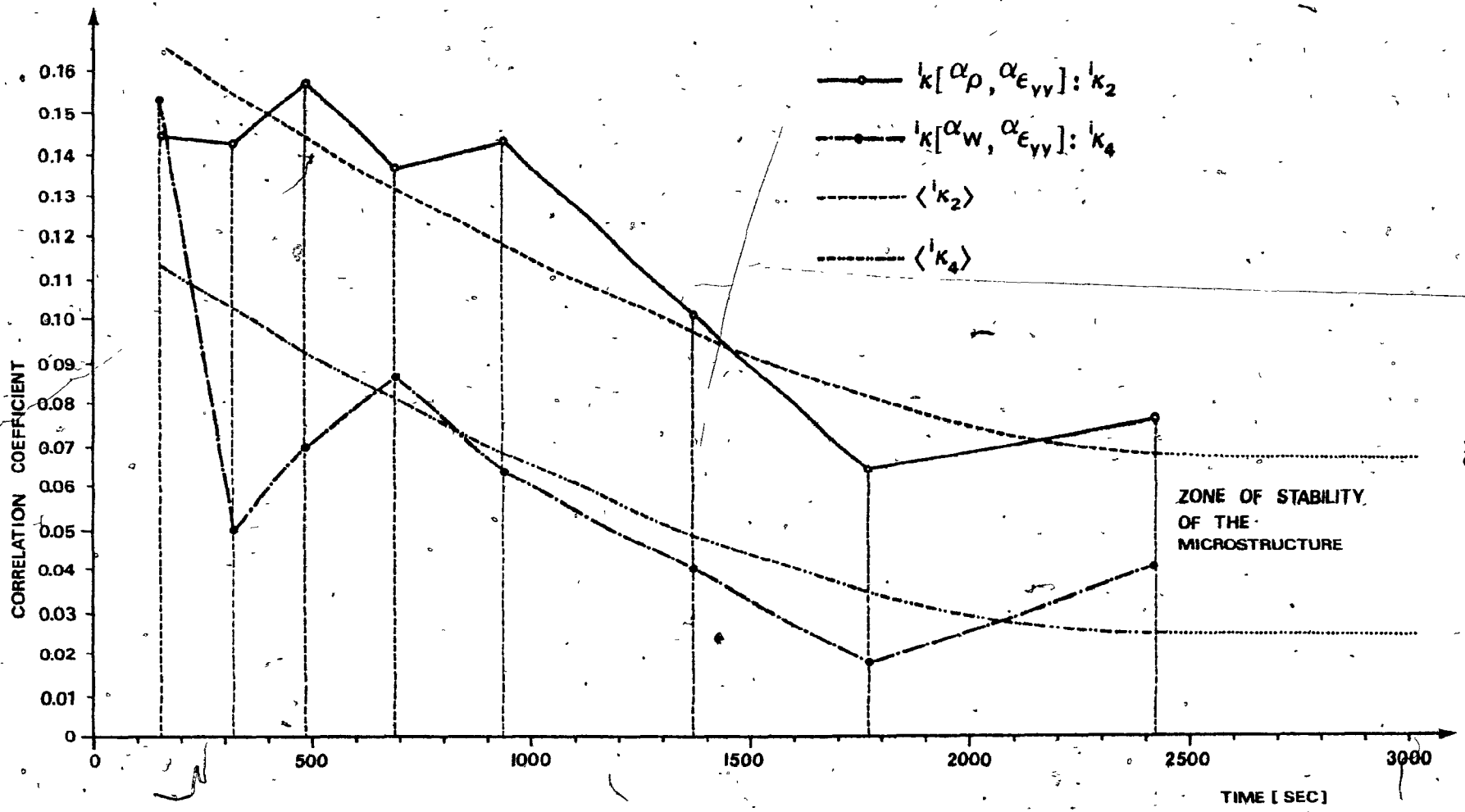

FIG. 5.17 VARIATIONS OF $\langle {}^{i}\kappa_2 \rangle$ AND $\langle {}^{i}\kappa_4 \rangle$ WITH TIME.

coefficients ${}^{\beta}k_1,\ldots,{}^{\beta}k_4$, as obtained for the β^{th} row of the sample ; $\beta=1,2,\ldots,19$, a similar discussion is valid. Moreover, it can be seen that the correlation coefficients in terms of their sign and magnitude differ for different rows of the paper, indicating clearly that strain-volumetric mass density relation is not the same over the entire paper sample and it is affected by the boundary conditions.

2. Another important conclusion that can be made concerns the signs of the quantities $\kappa_1,\ldots,\kappa_4$ and ${}^{\beta}k_1,\ldots,{}^{\beta}k_4$. It can be seen from Table (5.3) and similar tables of Appendix V, that most of the ${}^{\beta}k_1$, ${}^{\beta}k_3$, κ_1 and κ_3 quantities are negative-valued, which means that for the given newsprint paper sample, higher strains in the load direction are induced in the areas of lower mass density (${}^{\alpha}\rho$ or ${}^{\alpha}w$). In general, the above statement does not hold for all types of fibrous networks. Mechanical response behaviour of papers, among other factors, is significantly influenced by the formation process and the applied heat and pressure during the calendering process [71]. For example, it has been shown experimentally [19] that the fractured zone of an uncalendered newsprint paper occurs in the lower basis weight regions, whilst that of the calendered newsprint is associated with the higher basis weight regions.

On the other hand, quantities ${}^{\beta}k_2$, ${}^{\beta}k_4$, κ_2 and κ_4 are mostly

positive valued showing that higher values of the strains in the yy-direction (transverse direction) are accompanied by higher values of $^{\alpha}\rho$ and $^{\alpha}w$. This, however, can be ascribed by the excessive out-of-plane motion of the paper web during the load application. The areas possessing higher $^{\alpha}\rho$ or $^{\alpha}w$ contain a larger number of fibres and therefore the motion of these fibres produce higher out-of-plane motions at those areas of the paper web.

A better insight into the problem that is given here as a proposed future research is the one that also accounts for the microstructural quantities. It has been well observed [28] that the applied load to a fibrous network is carried by the fibres and their mutual bonding areas. The strength characteristics of the fibres are different from those of the bonds, thus each of them has a certain contribution towards the macroscopic response behaviour of the network. In general, the total bonding area in a sheet of paper is a function of the number of fibres, their orientation and other influencing factors. For a theoretical sheet, i.e. a sheet made of an ensemble of lines, comparable to the fibres in a real sheet, the total number of fibres in a unit area of a sheet as well as their relative bonding area has been derived in terms of the basis weight of a thin (2-dimensional) sheet and the number of thin plies in the sheet [32-36]. Therefore, by employing a similar procedure for actual paper sheets

using the local basis weight and the local thickness quantities or, more briefly, the volumetric mass density, it will become possible to evaluate the total number of fibres and the total bonding area as functions of ${}^{\alpha}w$, ${}^{\alpha}\tau$ and/or ${}^{\alpha}\rho$. Then, the response behaviour of the bonding area and the fibre segments towards the determination of the macroscopic response behaviour of the fibrous network will include the distributions of the quantities mentioned above.

In this context, when the fibrous material under consideration here is subjected to some external load application, all the field quantities ${}^{\alpha}\rho$, ${}^{\alpha}\varepsilon_{xx}$, ${}^{\alpha}\varepsilon_{yy}$,... must be regarded as stochastic processes, i.e.

$$
\begin{aligned}
{}^{\alpha}\rho &\rightarrow {}^{\alpha}\rho(t) \\
{}^{\alpha}\varepsilon_{xx} &\rightarrow {}^{\alpha}\varepsilon_{xx}(t) \\
{}^{\alpha}\varepsilon_{yy} &\rightarrow {}^{\alpha}\varepsilon_{yy}(t) \\
&\vdots
\end{aligned}
$$

Consequently, the correlation coefficients become time dependent and are then correlation functions defined by:

$\phi(X, t_i, Y, t_j)$: Cross-correlation function

$\phi(X, t_i, X, t_j)$: Auto-correlation function

where X(t) and Y(t) are two stochastic processes and can be substituted by the time dependent field quantities ${}^{\alpha}\rho(t)$, ${}^{\alpha}\varepsilon_{xx}(t)$,... These correlation functions, whose elements have partly been derived in this thesis, are of utmost importance in studying the random processes that are associated with the above field quantities. Finally, a general formulation of the constitutive relations containing ${}^{\alpha}\rho(t)$ and the corresponding random process will become possible.

It must be emphasized, however, that the actual formulation of the analytical procedure outlined above has not been within the scope of the present thesis.

Chapter VI

CONCLUDING REMARKS AND FUTURE RESEARCH

(A) Concluding remarks

Since the main aim of this thesis was to design an automated technique for the measurements of the deformation field on both sides of thin foils as illustrated by its application to the deformation of newsprint paper, the following conclusions can be made:

1) The sequential-DSHI technique has been shown to be an accurate procedure of producing interferograms of thin foil materials.

2) The reconstruction method including a new scanning procedure for the interferograms as well as the evaluation of fringe numbers has been demonstrated.

3) A general holographic-electro-optical technique has been designed and instrumented for the evaluation of the obtained interferograms in a self-consistent manner.

4) In the case of fibrous networks, as illustrated by newsprint paper, a new quantity has been defined, which is the "volumetric mass density". The latter has been established experimentally to a high accuracy.

5) Thus, the deformational behaviour and the creep-curve of the newsprint paper have been obtained by this new

holographic-electro-optical technique.

6) Correlation coefficients have been determined between the volumetric mass density and/or the basis weight and the induced strain field. It was then concluded that the VMD is a more appropriate material strength characteristic than the conventional basis weight used in the paper industry.

(B) Future research

The suitability of the technique in the present investigation has been demonstrated. However, it is proposed by this author that the testing procedure and future research may be further developed in the following way:

1) In order to produce even more accurate interferograms for various materials, it is suggested to fully automize and standardize the formation stage of the sequential-DSHI technique. This can be achieved by a proper monitoring device and digital shutter device for the "fully automatic" exposure of the holographic plates. This additional development would permit experimental studies that could include the observations of the transitional deformation behaviour. The latter is important since it is related to the changes in the microstructure of the material.

2) Apart from the remarks made in Section 5.5 of Chapter V, a faster technique could be used for the evaluation of the area

mass density distribution as suggested more recently in reference [46], but with a necessary rearrangement and synchronization for the holographic testing procedure.

STATEMENT OF ORIGINALITY AND CONTRIBUTION TO KNOWLEDGE

I) The author of this thesis believes that the new experimental method of the automatic evaluation of interferograms represents a distinct contribution to experimental mechanics. In particular, the new technique is of high accuracy in the assessment of the deformational behaviour of solids and of great advantage when dealing with thin foils of various structured media.

II) A further contribution consists in introducing the "volumetric mass density" even for very thin sheet materials and its accurate experimental determination.

III) It has been shown in this thesis for the first time that there exists a correlation between the volumetric mass density and the induced strain field caused by uniaxial loading of a newsprint paper to a greater extent than in the conventional test procedure using the "basis weight" concept.

REFERENCES

[1] Axelrad, D.R. "Micromechanics of Solids" PWN-Elsevier Publ. (1978)

[2] Haddad, Y.M. "Response Behaviour of a Two Dimensional Fibrous Network" Ph.D. Thesis, McGill University, Montreal (1975)

[3] Kalousek, J. "Experimental Investigation of Deformation of Structured Media" Ph.D. Thesis, McGill University, Montreal (1973)

[4] Peralta-Fabi, Ri "Experimental Investigation of Creep Behaviour of Bond Paper" Ph.D. Thesis, McGill University, Montreal (1978)

[5] Axelrad, D.R. Kalousek, J. "Stress Holographic Interferometry" Micromechanics Lab.Rep. No.71-7, McGill University, Montreal (1971)

[6] Kubat, J. Lindbergson, B. "Mechanical Relaxation in Paper Studied by Means of the Torsional Pendulum" Svensk Papperstidning, Vol.68, No.21: 743 (1965)

[7] Baum, G.A. Bornhoeft, L.R. "Estimating Poisson Ratios in Paper Using Ultrasonic Techniques" Tappi, Vol.62, No.5, 87 (1979)

[8] Mann, R.W. Baum, G.A. Habeger, C.C. "Determination of all Nine Orthotropic Elastic Constants for Machine-Made Paper" Tappi, Vol.63, No.2: 163 (1980)

[9] Jones, A.R. "An Experimental Investigation of the In-Plane Elastic Moduli of Paper" Tappi, Vol.51, No.5: 203 (1968)

[10] Craver, J.K. Taylor, D.L. "Non Destructive Sonic Measurements of Paper Elasticity" Tappi, Vol.48, No.3: 142 (1965)

[11] Page, D.H.
Seth, R.S.
De Grâce, J.H.
"The Elastic Modulus of Paper. Part I: The Controlling Mechanisms" Tappi, Vol.62, No.9: 99 (1979)

[12] Seth, R.S.
"Measurement of Fracture Resistance of Paper" Tappi, Vol.62, No.7: 92 (1979)

[13] Heckers, W.
Hart, D.
Göttsching, L.
"Fracture Mechanism of Paper. (1): Theory of Fracture Mechanics" Papier, Vol.34, No.3: 85 (1980)

[14] Page, D.H.
"A Theory for the Tensile Strength of Paper" Tappi, Vol.52, No.4: 674 (1969)

[15] Kallmes, O.J.
Perez, M.
"A New Theory for the Load/Elongation Properties of Paper" In Consolidation of the Paper Web. Transactions of the Cambridge Symp. (1965), Ed. F. Bolam, Tech. Sect. British Paper and Board Makers' Assoc. (Inc.), London, Vol.2: 779 (1966)

[16] Kallmes, O.J.
"Behaviour of Paper Under Strain" Paper Trade J. Vol.154: 54, July, (1970)

[17] Kallmes, O.J.
"New Approach of Measuring Formation - A Matter of Uniformity" Paper Trade Journal, Vol. 155, 43 (1971)

[18] Lyne, M.B.
Hazell, R.
"Formation Testing as a Means of Monitoring Strength Uniformity" In The Fundamental Properties of Paper Related to its Uses. Transactions of the Cambridge Symp. (1973), Ed. F. Bolam, Tech. Div. British Paper and Board Industry Federation, London, Vol.1: 74 (1976)

[19] Moffat, J.M.
Beath, L.R.
Mihelich, W.G.
"Major Factors Governing Newsprint Strength" In The Fundamental Properties of Paper Related to its Uses. Transactions of the Cambridge Symp. (1973), Ed. F. Bolam, Tech. Div. British Paper and Board Industry Federation, London, Vol.1: 104 (1976)

[20] Nissan, A.H.
"The Role of Hydrogen Bond in the Rheological Behaviour of Cellulose Sheets" Textile Res.J. Vol 9: 780 (1955)

[21] Nissan, A.H.
"The Rheological Behaviour of Hydrogen Bonded Solids" Parts 1 and 2, Trans. Faraday Soc., Vol.53, No.5: 700 (1957)

[22] Sternstein, S.S.
"Micromechanics of Fibre Networks" In Cellulose and Cellulose Derivatives. Ed. Bikales, N. and Segal, L., p.644 John Wiley and Sons, Inc. (1974)

[23] Brezinski, J.P.
"The Creep Properties of Paper" Tappi, Vol.39, No.2: 116 (1956)

[24] Page, D.H.
Tydeman, P.A.
"Fibre to Fibre Bonds, Part 2 - A Preliminary Study of Their Properties in Paper Sheets" Papper Tech. Vol.1, No.5: 519 (1960)

[25] Erickson, L.D.
"Physical Properties of Stratified Sheets" Tappi, Vol.60, No.10: 113 (1977)

[26] Stockmann, V.E.
"How Strong Can Paper be Made ?" Tappi, Vol.59, No.3: 97 (1976)

[27] Kallmes, O.J.
Stockel, I.H.
Bernier, G.A.
"The Elastic Behaviour of Paper" Pulp and Paper Mag. of Can. Vol.64, No.10: T449 (1963)

[28] Perkins, R.W.
Mark, R.E.
"On the Structural Theory of the Elastic Behaviour of Paper" Tappi, Vol.59, No.12: 118 (1976)

[29] Hollmark, H.
Andersson, H.
Perkins, R.W.
"Mechanical Properties of Low Density Sheets" Tappi, Vol.61, No.9: 69 (1978)

[30] Axelrad, D.R.
Atack, D.
Provan, J.W.
"Microrheology of Fibrous Systems" Rheol.Acta, Vol.12: 170 (1973)

[31] Haddad, Y.
"A Theoretical Approach to Inter-fibre Bonding of Cellulose" J. of Colloid and Interface Sc. Vol.76, No.2: 490 (1980)

[32] Kallmes, O.J.
Corte, H.
"The Structure of Paper: I. The Statistical Geometry of an Ideal Two Dimensional Fiber Network" Tappi, Vol.43, No.9: 737 (1960)

[33] Kallmes, O.J.
Corte, H.
Bernier, G.
"The Structure of Paper: II. The Statistical Geometry of a Multi-planar Fibre Network" Tappi, Vol.44, No.7: 519 (1961)

[34] Kallmes, O.J.
Bernier, G.
"The Structure of Paper: III. The Absolute, Relative, and Maximum Bonded Areas of Random Fibre Networks" Tappi, Vol.45, No.11: 867 (1962)

[35] Kallmes, O.J.
Bernier, G.
"The Structure of Paper: IV. The Free Fibre Length of a Multiplanar Sheet" Tappi, Vol.46, No.2: 108 (1963)

[36] Kallmes, O.J.
Corte, H.
Bernier, G.
"The Structure of Paper: V. The Bonding States of Fibers in Randomly Formed Papers" Tappi, Vol.46, No.8: 493 (1963)

[37] Andreichenko, V. Ya. "Structure and Mechanical Properties of the Paper Sheet: I. Mathematical Description of the Sheet Structure" Sb.Tr.VNII Tsellyul.-Bumazh. Prom. No.58: 80 (1971)

[38] Andreichenko, V. Ya. "Structure and Mechanical Properties of the Paper Sheet: II. Properties of the Sheet at Zero Span of the Sample" Sb.Tr. VNII Tsellyul.-Bumazh. Prom. No.58: 89 (1971)

[39] Hagland, L. Norman, B. Wahren, D. "Mass Distribution in Random Sheets - Theoretical Evaluation and Comparison with Real Sheets" Swedish Forest Products Research Laboratory, Stockholm, Sweden. (1974)

[40] Axelrad, D.R. "Theory of Bond Failure in Hydrogen-Bonded Solids" Advances in Molecular Relaxation and Interaction Processes, Vol.15: 51 Elsevier Scientific Pub.Co. (1979)

[41] Page, D.H. De Grâce, J.H. "The Determination of Fibre Walls by Beating and Refining" Tappi, Vol.50, No.10: 489 (1967)

[42] Page, D.H. "The Axial Compression of Fibres - A Newly Discovered Bonding Action" Pulp and Paper Mag. Can. Vol.67, No.1: T2 (1966)

[43] Norman, B. Wahren, D. "Mass Distribution and Sheet Properties of Paper" In The Fundamental Properties of Paper Related to its Uses. Transactions of the Cambridge Symp.(1973), Ed. F. Bolam, Tech. Div. British Paper and Board Industry Federation, London, Vol.1: 7 (1976)

[44] Corte, H.
Dodson, C.T.J.
"Über die verteilung der massendichte in Papier"
Das Papier, Vol.23, No.7: 381 (1969)

[45] Dodson, C.T.J.
"A Contribution to the Development of a Statistical Rheology of Bonded Fibrous Networks"
Ph.D. Thesis, Brunel University (1969)

[46] Herdman, P.T.
Corte, H.
"Comments on the Distribution of Mass Density in Paper"
Pulp and Paper Mag. Can. Vol.81, No.10: T261 (1980)

[47] Collier, R.J.
Bruchhardt, C.B.
Lin, L.H.
"Optical Holography"
Academic Press, New York (1971)

[48] Ostrovsky, Yu, I.
"Holography and Its Application"
Mir Publishers, Moscow (1977)

[49] Stroke, G.W.
"An Introduction to Coherent Optics and Holography"
2nd Ed. Academic Press, N.Y. (1969)

[50] Leigh, E.N.
Upatnieks, J.
"Wavefront Reconstruction with Diffused Illuminated Three-Dimensional Objects" J. Opt.Soc. Am. Vol.54, No.11: 1295 (1964)

[51] Ennos, A.E.
"Measurement of In-Plane Surface Strain by Hologram Interferometry"
J. Sc. Instr., Vol.2, No.1: 731 (1968)

[52] Alexandrov, E.B.
Bonch-Bruevich, A.M.
"Investigation of Surface Strain by Hologram Technique" Soviet Physics - Tech. Phys. Vol 12, No.2: 258 (1967)

[53] Fosati-Bellani, V. Sona, A. "Measurement of Three-Dimensional Displacement by Scanning a Double-Exposure Hologram" Appl. Opt. Vol.13, No.6: 1337 (1974)

[54] Ek, L. Biedermann, K. "Implementation of Hologram Interferometry with a Continuously Scanning Reconstruction Beam" Appl. Opt. Vol.17, No.11: 1727 (1978)

[55] Champagne, E.B. "Nonparaxial Imaging, Magnification, and Aberration Properties in Holography" J. Opt.Soc. Am. Vol.57, No.1: 51 (1967)

[56] Ek, L. Klaus, B. "Analysis of a System for Hologram Interferometry with a Continuously Scanning Reconstruction Beam" App. Opt. Vol.16, No.9, 2535 (1977)

[57] Norman, B. Wahren, D. "The Measurement of Mass Distribution in Paper Sheets Using a Beta Radiographic Method. Svensk Papperstidning, Vol.77, No.11: 397 (1974)

[58] Norman, B. Smith, D. "Beta Radiography of Paper" Int. Report, Swedish Forest Products Research Laboratory, Stockholm, Sweden. (1972)

[59] Herdman, P.T. "Measurement of the Distribution of Mass Density in Paper" Paper Technology and Industry, Vol.19, No.7: 246 (1978)

[60] Tydeman, P.A. "The Measurement and Automatic Print-Out of Small Scale Basis Weight Variations" BP & BIRA Bulletin, June (1965)

[61] Norman, B. "An Investigation of the Mass Distribution in Paper Sheets" Swedish Forest Product Research Laboratory, Stockholm, Sweden. (1975)

[62] Attwood, D.
Parker, J.R.
"Basis Weight Variations Over Small Areas of Paper" Paper Technology, No.3: 435 (1962)

[63] Norman, B.
Wahren, D.
"A Comprehensive Method for the Description of Mass Distribution in Sheets and Flocculation and Turbulence in Suspensions" Svensk Papperstidning, Vol. 75, No.20: 807 (1972)

[64] Herdman, P.T.
"Measurement of the Distribution of Mass Density in Paper" Paper Technology and Industry, Vol.19, No.7: 246 (1978)

[65] Ohrn, O.E.
"Thickness Variations of Paper on Stretching" Svensk Papperstidning, Vol.68, No.5: 141 (1965)

[66] Van Liew, G.P.
"The Z-Direction Deformation of Paper" Tappi, Vol.57, No.11: 121 (1974)

[67] Lyne, B.
"Measurement of the Distribution of Surface Void Sizes in Paper" Tappi, Vol.59, No.7: 102 (1976)

[68] Imamura, R.
Murakami, K.
Vesaka, T.
"Thickness Variation and Apparent Thickness in the Paper Sheet" Tappi, Vol.62, No.1: 35 (1979)

[69] Ranger, A.E.
Hopkins, L.F.
"A New Theory of the Tensile Behaviour of Paper" In The Formation and Structure of Paper. Transactions of the Oxford Symp. (1961), Ed. F. Bolam, Tech. Sect. British Paper and Board Makers' Assoc. (Inc.), London, Vol.1: 277 (1962)

[70] Axelrad, D.R.
Private Communications

[71] Papulis, A. "Probability, Random Variables and Stochastic Processes" McGraw-Hill Book Company (1965)

[72] Breiman, L. "Statistics with a View Toward Applications" Houghton Miffin Company (1973)

[73] Yaglom, A.M. "An Introduction to the Theory of Stationary Random Functions" Prentice-Hall, Inc. (1962)

[74] Bulmer, M.G. "Principles of Statistics" The M.I.T. Press (1967)

[75] Motorola Inc. "M6800 Microprocessor Application Manual" Motorola Inc. (1975)

[76] Motorola Inc. "MEK6800D2 Evaluation Kit II Manual" Motorola Inc. (1976)

[77] Motorola Inc. "M6800 Programming Reference Manual" Motorola Inc. (1976)

APPENDIX I

MICROCOMPUTER DESIGN

I.1 Introduction

The microcomputer designed to meet the requirements discussed in the present work (Chapter IV) is basically a Motorola MC6800-Kit II microprocessor system. This system consists of a microprocessor element MC6800 and some family devices that are shown in Fig. I.1. The elements ROM (Read Only Memory) and RAM (Random Access Memory) allocate memory locations to the program control routines and the input data. The microprocessor is permitted to communicate with the peripheral devices, i.e. X-Y positioner, scanning device, etc. Through PIA (Peripheral Interface Adaptor) for parallel data flow, and through ACIA (Asynchronous Communications Interface Adaptor), if serial data flow is needed. Both types have been used in the design of the microcomputer. It can be seen from Fig. I.1 that the communication of the MPU with its family devices are facilitated through a set of connections that are classified as follows:

1. DATA bus: It is an 8-bit bidirectional bus to facilitate the data flow throughout the system. This bus can run 7-10 family devices without buffering.

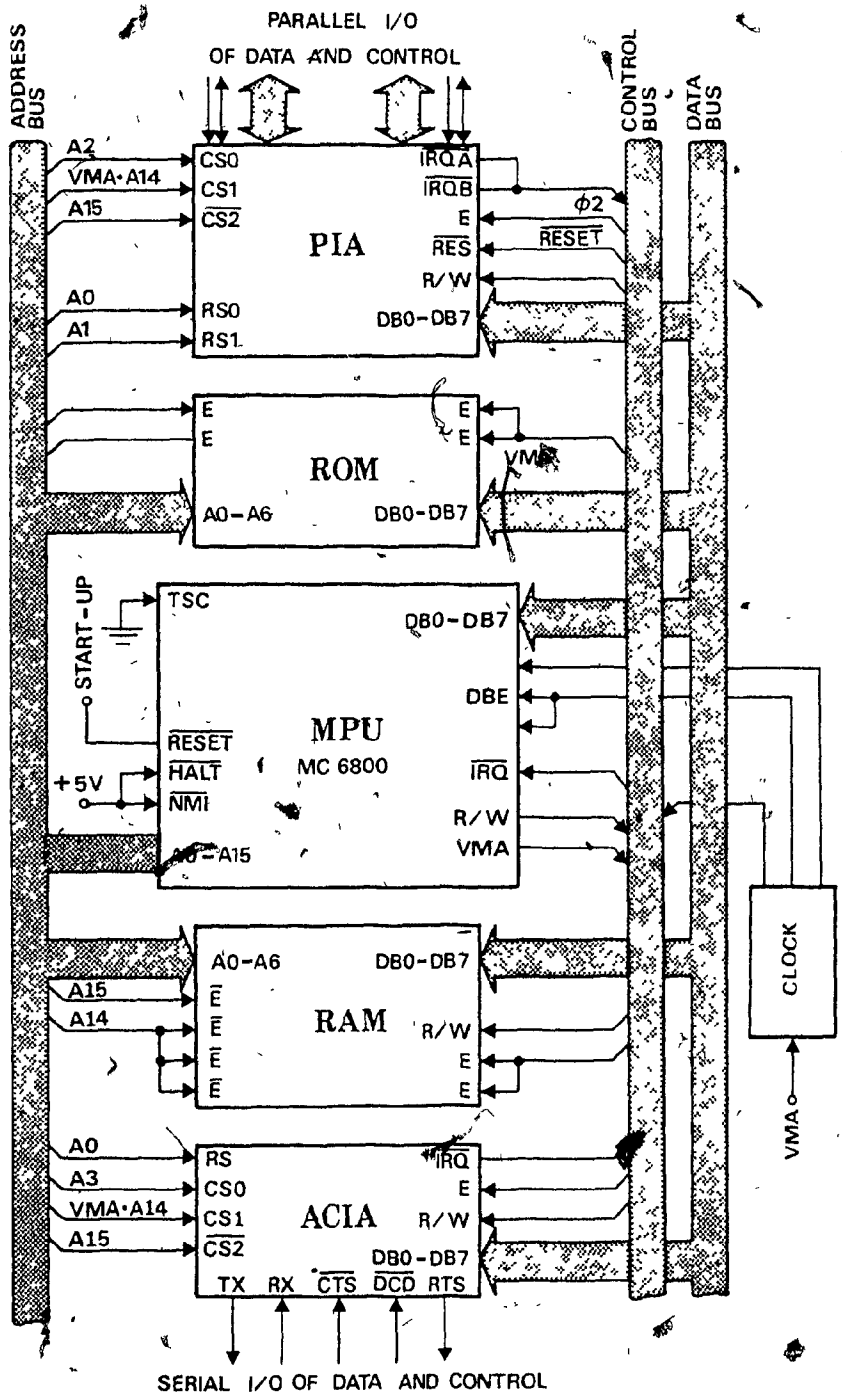

FIG. 1.1 MC 6800 MINIMUM SYSTEM - KIT II.

2. ADDRESS bus: The 16-bit ADDRESS bus is used, not only to specify memory locations, but also to simplify the input/output devices. Its special connections to the DATA bus and CONTROL bus permits the use of the input/output interfaces as memories.

3. CONTROL bus: The CONTROL bus contains a complicated mix of signals, in order to regulate the system operations. Details of these signals are not within the framework of the present thesis. However, the reader is referred to reference [75].

Among all the family devices, which are illustrated in Fig. I.1, perhaps PIA is the most important one. Briefly, PIA is a bidirectional programmable interface, which is equipped with two channels A and B (see the block diagram of Fig. I.2). Each channel is then equipped with three registers CRA(B), ORA(B) and DDRA(B), which control the data direction and flow. These registers themselves can be used as temporary memory locations. On each part of the "peripheral side" there is one pair of interrupt status control signals that can be used to synchronize the user's device to the MPU cycles. These signals are usually referred to as the "synchronization signals". The data is then allowed to flow through each of the 8-bit bidirectional lines PA0-PA7 and PB0-PB7. The MPU side of the PIA shows its connection to the MPU through the DATA, ADDRESS and CONTROL buses. A more comprehensive description of the PIA is given in the next section, where its application will be discussed.

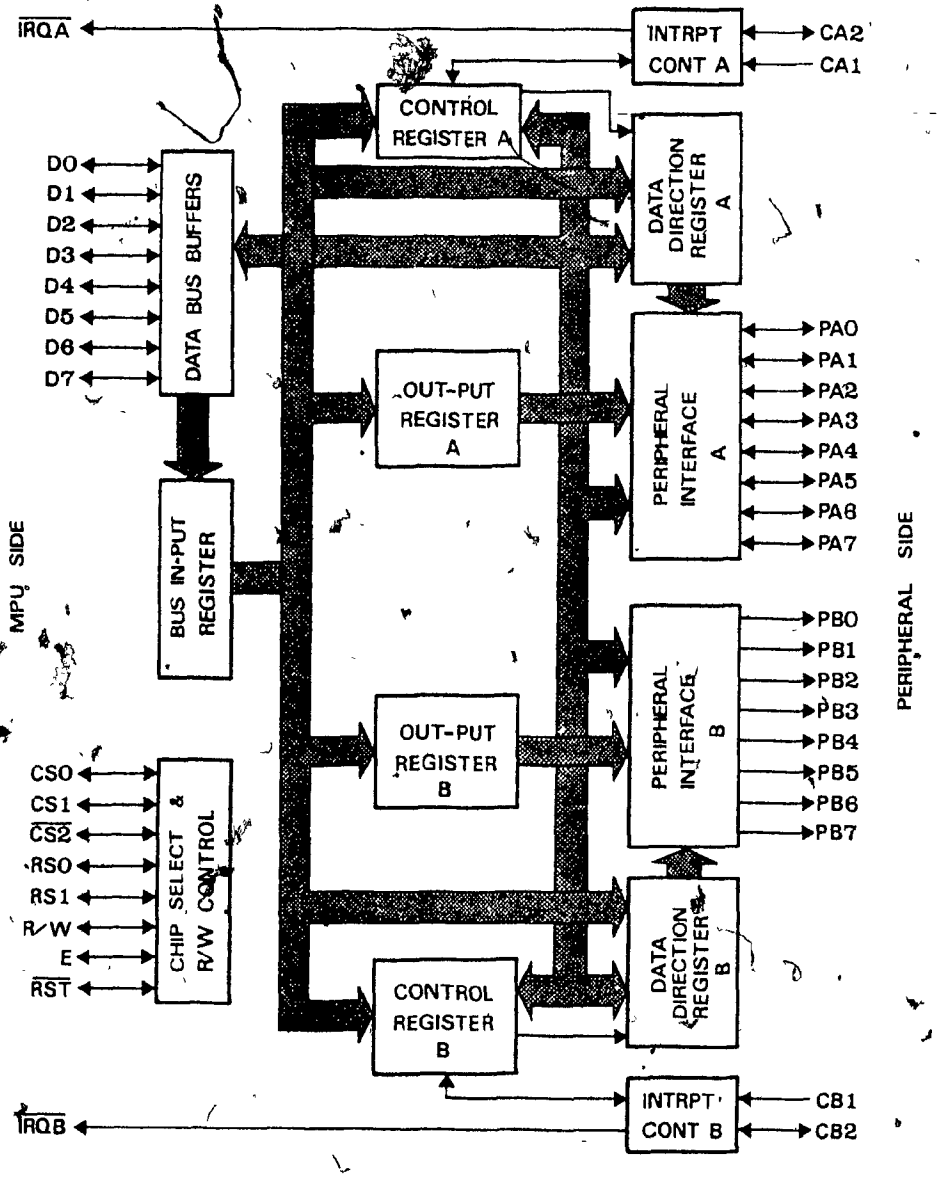

FIG. I.2 BLOCK DIAGRAM OF A PIA MC6821.

I.2 System Expansion

The MPU and its family devices shown in Fig. 1.1 form a minimum system. That is, for the design of a microcomputer a minimum system is the basic requirement. Thus, in order to automate the reconstruction stage of the holographic interferometry, the minimum system of Fig. 1.1 has been expanded to that whose block diagram is shown in Fig. 1.3. The minimum system is coupled to several peripheral devices by means of proper interfaces. The application and explanation of each is given in subsequent sections. The photograph of the microcomputer is also shown in Fig. 4.1.

I.2.1 4K Low-Power RAM Board

The MC6800 module board has been equipped with a port for memory expansion. For the purpose of holographic interferometry, a 4K-byte low-power RAM board has been employed to be used for the storage of the program and the raw data that is being received from the photometer-indicator. The connections are carried out in such a manner that the memory locations can be addressed from 2000 to 2FFF.

I.2.2 Keypunch and Display Monitor

KIT-II of MC6800 is equipped with a keypunch and display monitor board, by means of which a program can be punched into the memory. Eight of the 24 available keys are used for controlling purposes of the program execution. The main usage of the keypunch

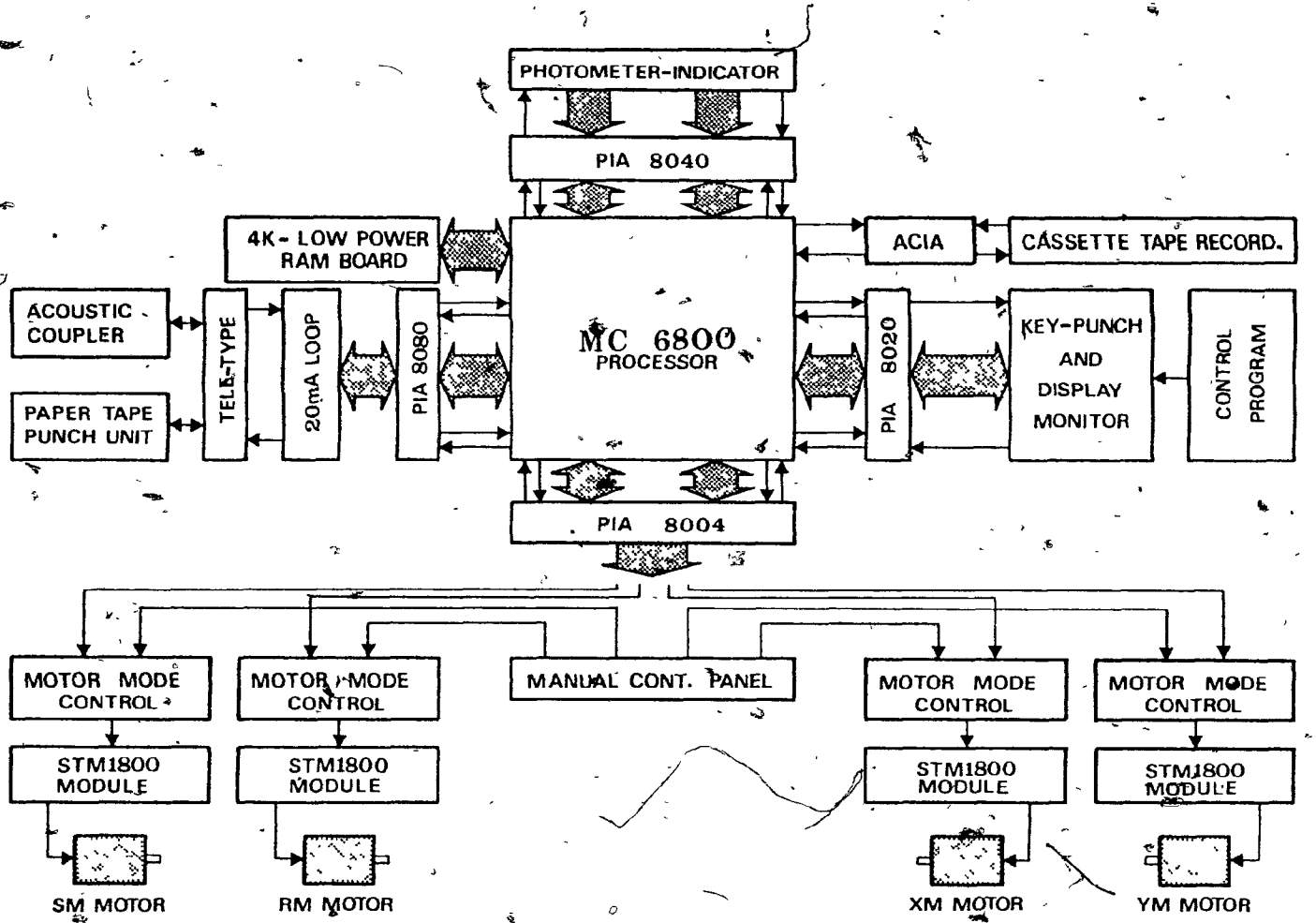

FIG. 1.3 MICROCOMPUTER - SYSTEM ORGANIZATION.

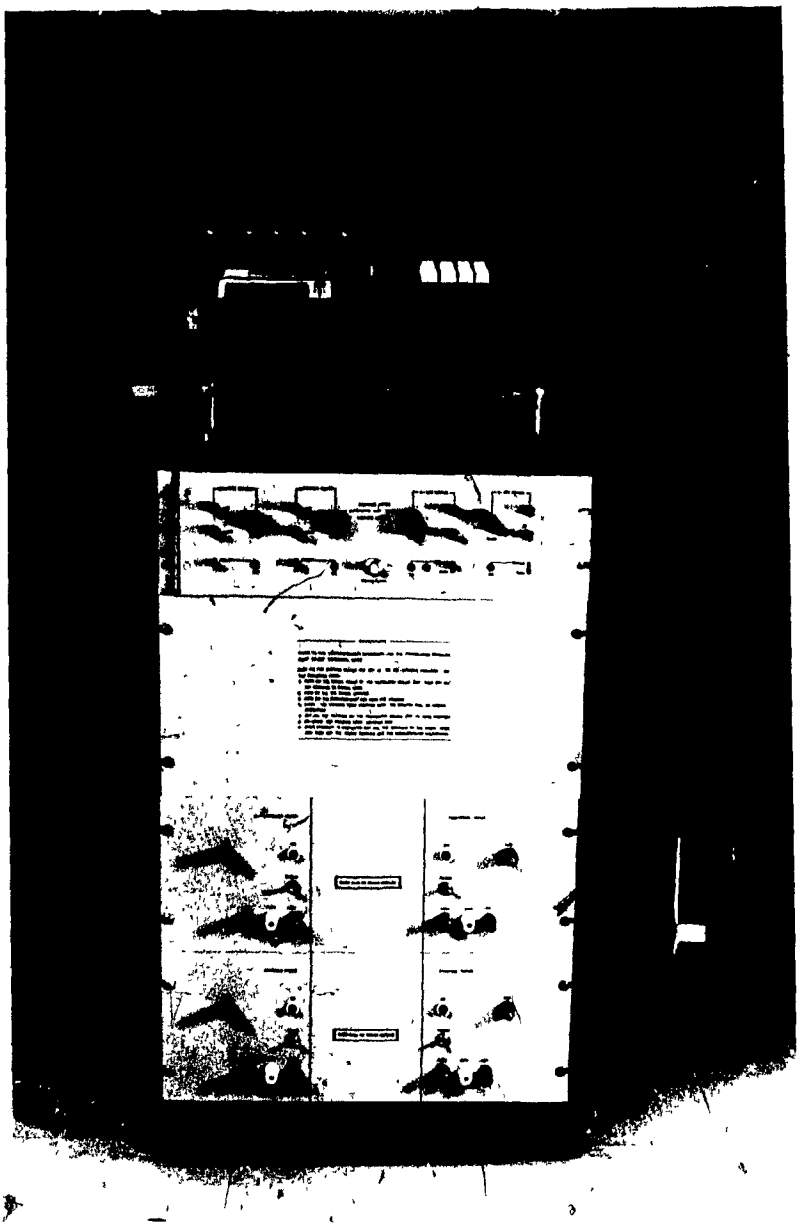

FIG. I.4 PHOTOGRAPH OF THE MICROCOMPUTER UNIT.

in the present work is to control the punching process of the program, i.e. from a cassette tape into the memory and vice-versa. It is also used to start the entire system and punch-in the information of the reconstruction stage as the "running time" of each motor, the number of observation points, etc. The monitor, however, is mainly used to check the contents of memory locations. It also indicates the beginning and the end of program execution. The cassette tape recorder and the keypunch are interfaced to the MPU by means of an ACIA and PIA 8020, respectively.

I.2.3 Teletype (TTY) Interface

A teletype unit (TTY) has been employed in the system expansion which is equipped with a paper tape punch device and an acoustic coupler unit. It should be mentioned that the programming language of the MC6800 used, is "Cross-Assembly". However, in the present investigation the program was written in "Assembly" language. It was then converted into cross-assembly language by the "Motorola Cross-Assembly" routine, which had been available in the Computer Library of McGill University. The converted program was then punched onto a paper tape by means of a PDP-11 computer unit. Therefore, the paper punch device on TTY was used to "READ" the program from the paper tape, then through the TTY, to punch it into the memory of the MPU. However, the acoustic

coupler has been in line with the TTY in order to facilitate the direct communication of the MPU and the computer system of this University called "MUSIC". Communications of this type were occasionally required in order to check the data manipulation of the entire system.

The TTY-MPU interface is shown in Fig. 1.5. This interface is geared to PIA 8080 as shown in the general schematics of the microcomputer in Fig. 1.7.

I.2.4 Photometer-Indicator Interface

The photometer-indicator is capable of converting the light intensity of the fringe patterns into an analoge out-put (0-1 volt) or into a 16-bit BCD output (Binary Coded Decimal). The BCD output port of the unit has several additional input/output lines, among which two should be specially mentioned. With reference to Fig. 1.7, it can be seen that the "SYNC" signal is coming out from this unit. A high to low transition on this line indicates the MPU that the light intensity process is completed and the data is ready to be "READ". The MPU then "READS" the data. The other signal is the "Transfer Inhibit" which is maintained at a high level. When the "READ" process of the data by MPU is finished, the latter sends a signal to pull this line to the low level. The occurring transition informs then, the PMI (photometer) that the "READ" process is completed and hence, PMI can send out the next data. These

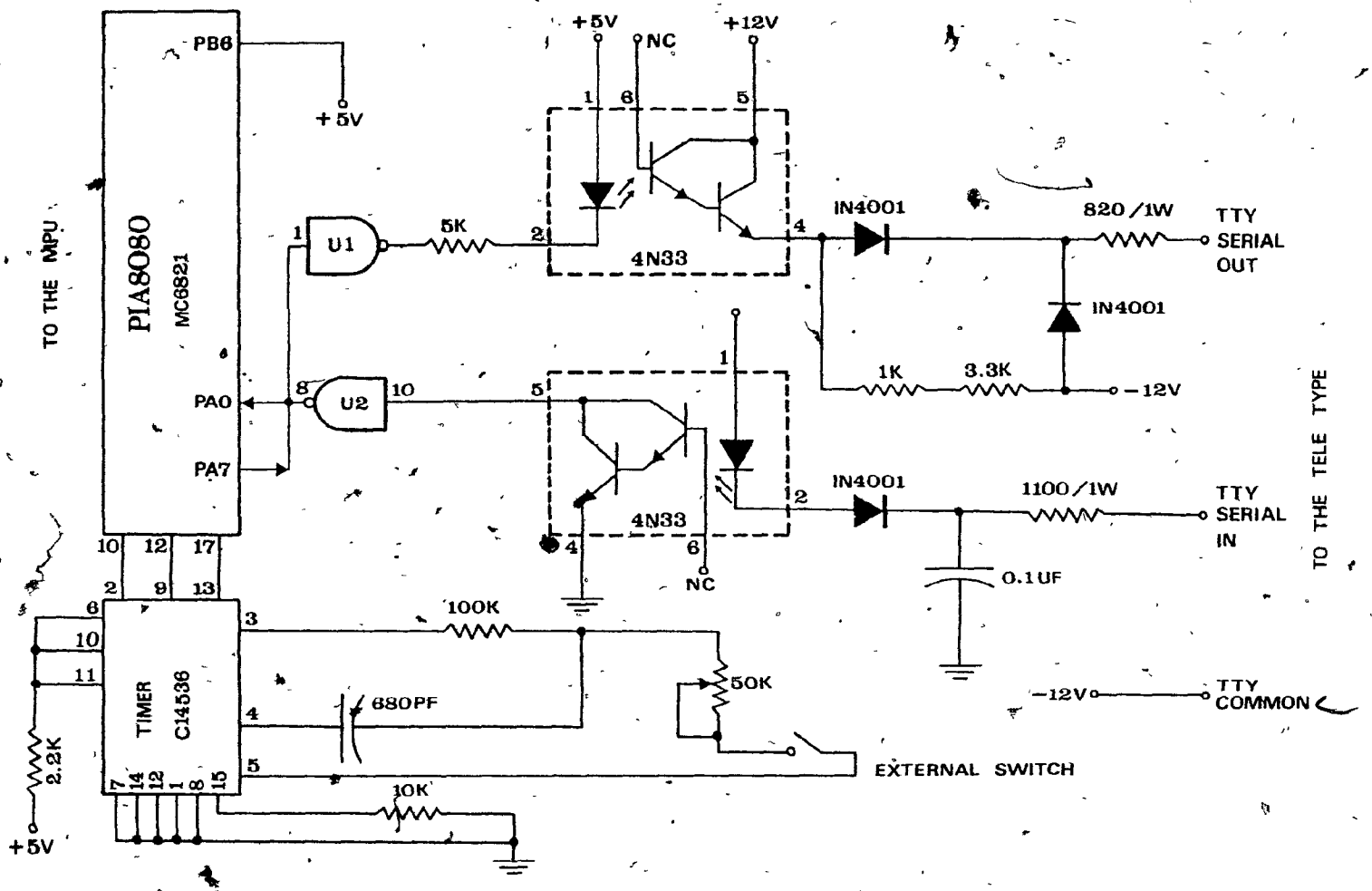

FIG. 1.5 CIRCUITRY OF MPU – TTY INTERFACE.

two lines are connected to the CA1 and CA2 lines of the PIA 8040. The 16-bit data lines are connected to the PA0-PA7 and PB0-PB7 of the PIA. It should be mentioned that normally a PIA on the MC6800 module does not accept both its channels as input or output simultaneously. However, by means of certain modifications to the PIA 8040, this difficulty was avoided.

It can be seen that the data flow from PMI to the MPU is synchronized by the "SYNC" and "Transfer Inhibit" signals. Also, no matter what sampling time (data rate) has been selected on the PMI unit, the synchronization is taken care of automatically. Fig.1.7 shows the connection of PMI to PIA 8040.

I.2.5 Stepping Motors Interface

The stepping motors employed in this investigation are SLO-SYN, model M092-FC08, 3V/4A motors, which perform 200 steps per revolution (1.9 degrees per step). The maximum output torque is 200 oz-in. The module stages that operate the motors are SLO-SYN, STM 1800DV, each of which consumes a power of ±15V/10A. The stepping-rate of the motors as well as the direction of their rotation are manually controlled. However, for the automatic control of these modules and hence the motors, it was necessary to interface the modules independently to the PIA 8004 of the microcomputer. The interfacing boards (Digital Mode Control) were made such that each of them receives three signals at points A,B and C (See Fig.1.6a) and then trigger the module stages through points R,S,K,L,...

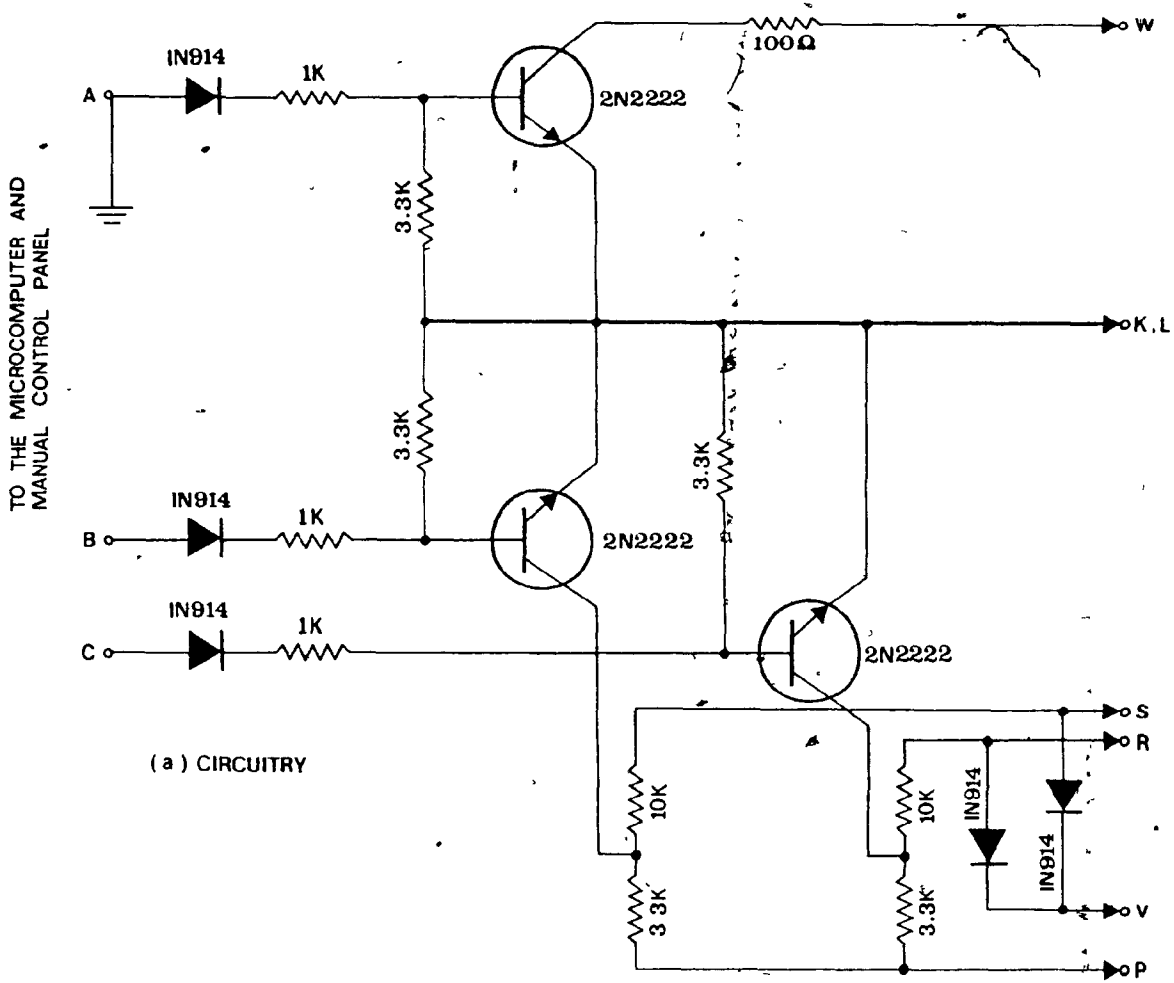

(a) CIRCUITRY

A = 0 MOTOR «ON»

A = 1 MOTOR «OFF»

A = 0

B	C	FUNCTION
0	0	INVALID CONDITION
0	1	C W. ROTATION
1	0	C C.W ROTATION
1	1	NO ROTATION

(b) TRUTH TABLE

FIG. I.8 MOTOR MODE CONTROL STAGE.

Another aspect of these interfaces is to take care of the difference between the load levels of the MPU (+5V TTL standard) and the translator module stages (±15V/10A). Any combination of signals reaching to points A,B and C will set the corresponding stepping motor in a certain mode. Thus, Fig. 1.6b shows the "truth table" of such combinations. Point A of all these interfaces have been grounded, in order to maintain the motors in the "ON" and "NO-RUNNING" modes. The points B and C of all the interfaces are connected to side A of the PIA 8004. Hence, by loading the output register of the PIA with a proper 8-bit number, one of the motors can be started up, whilst the other three are maintained in NO-RUNNING condition.

For the purpose of the reconstruction procedure, as discussed earlier (Chapter IV), a proper sequence of 8-bit numbers have been loaded to the PIA 8004. These numbers have been generated and sent to the PIA by a program which is listed in Appendix II.

I.2.6 Manual Control Panel

For the purpose of calibrating the reconstruction stage, a manual control panel has been designed in order to break the connection between the MPU and the translator module stages. This permits the control of the stepping-rate and the direction of rotation of each motor independently. For each motor a combination of 8 trimpot resistors of 5KΩ and 10KΩ have been employed. Each set of 8 trimpots, by means of a six contact rotary switch

is coupled to one translator module so that the stepping-rate of the corresponding motor is controlled. The rotary switch is used for quick selection of the stepping rates. Fine adjustment of the stepping rates are obtained by adjustment of the trimpots. Together with each set of trimpots, there are two microswitches in line, which connect the translator modules and their digital mode controls to an external power supply (+5V/100 mA). Each microswitch then, activates the motor in one direction.

From the sections discussed above, it can be seen that altogether three PIA's, a 4K RAM board and a 20mA-loop interface have been added to the minimum system of Fig. 1.1. The MC6800 module is designed such that no buffering was needed for this number of interfacing units.

Furthermore, it should be noted that the design details have not been discussed in detail, since the purpose of this Appendix was to assist in the understanding of the automatic technique and control as described in Chapter IV and Appendix II. However, further discussion on the MC6800-system is given in references [75-77].

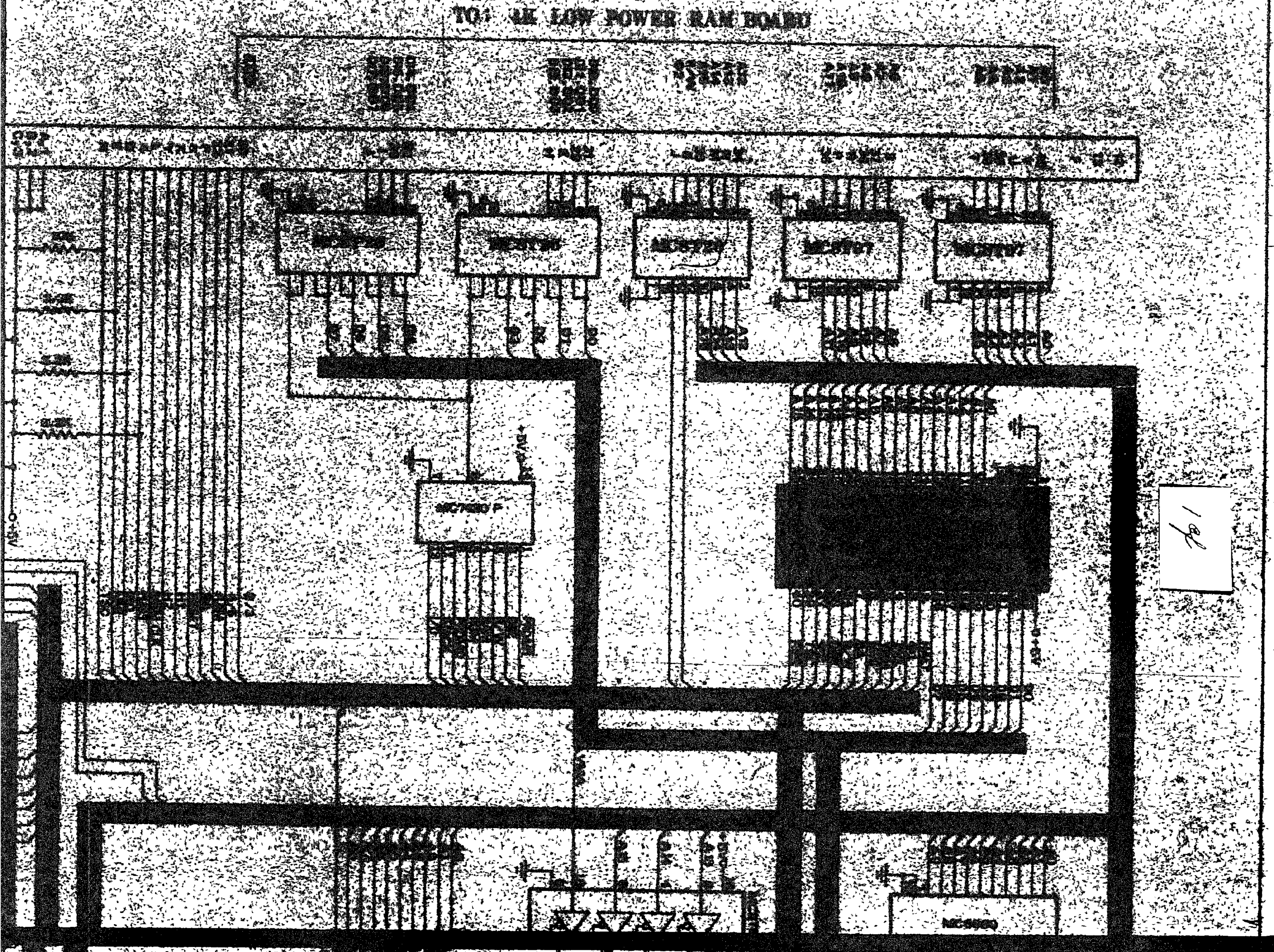
TO: 4K LOW POWER RAM BOARD
+5V
1 of

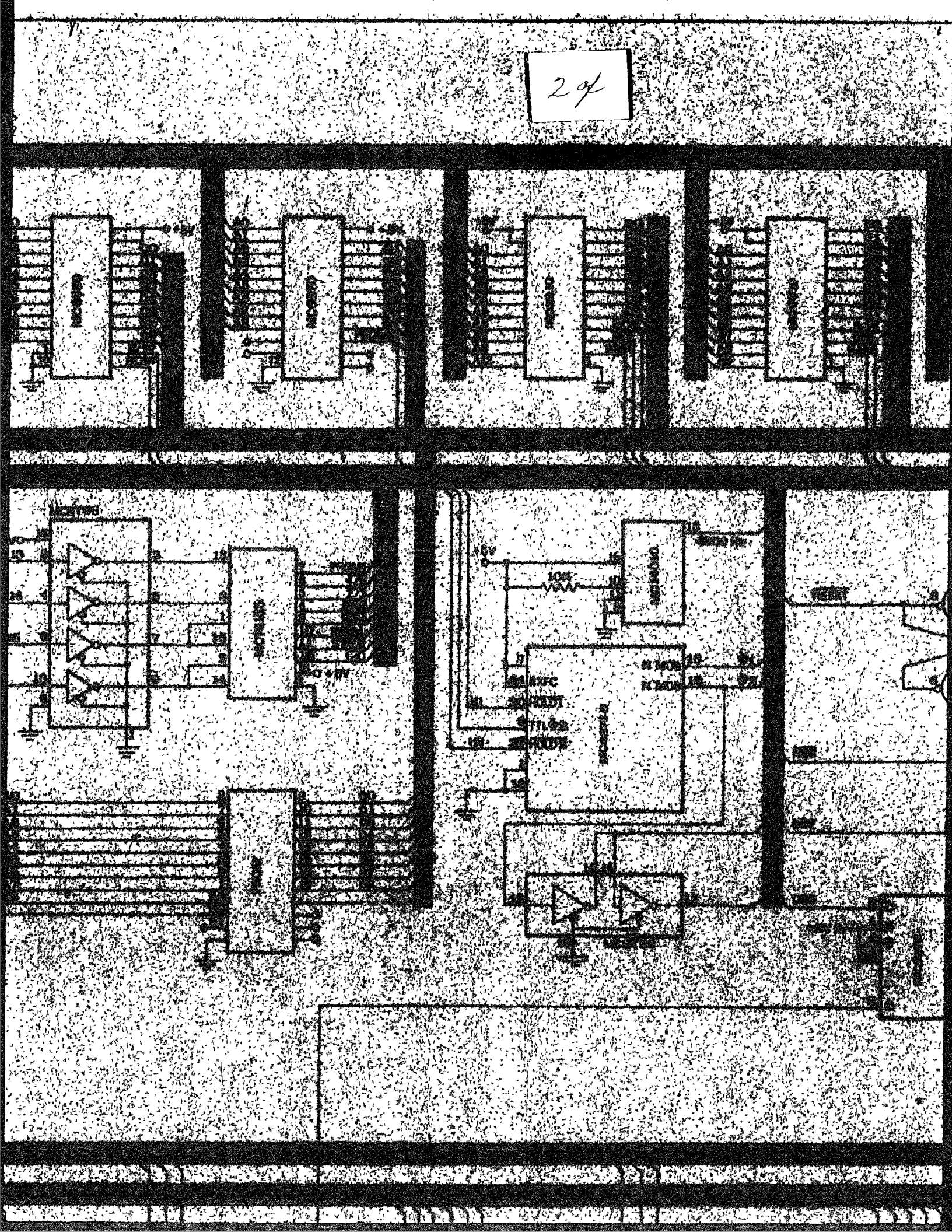

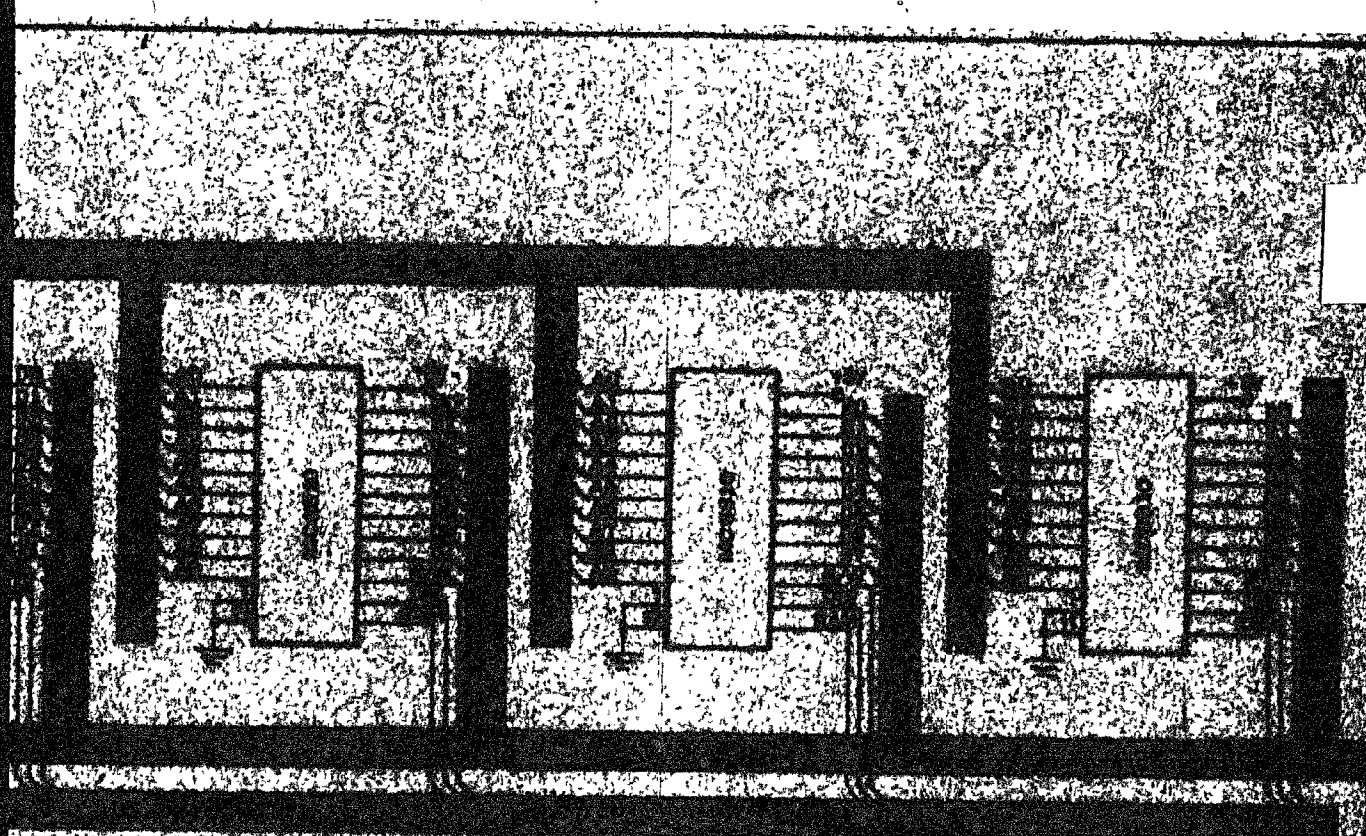

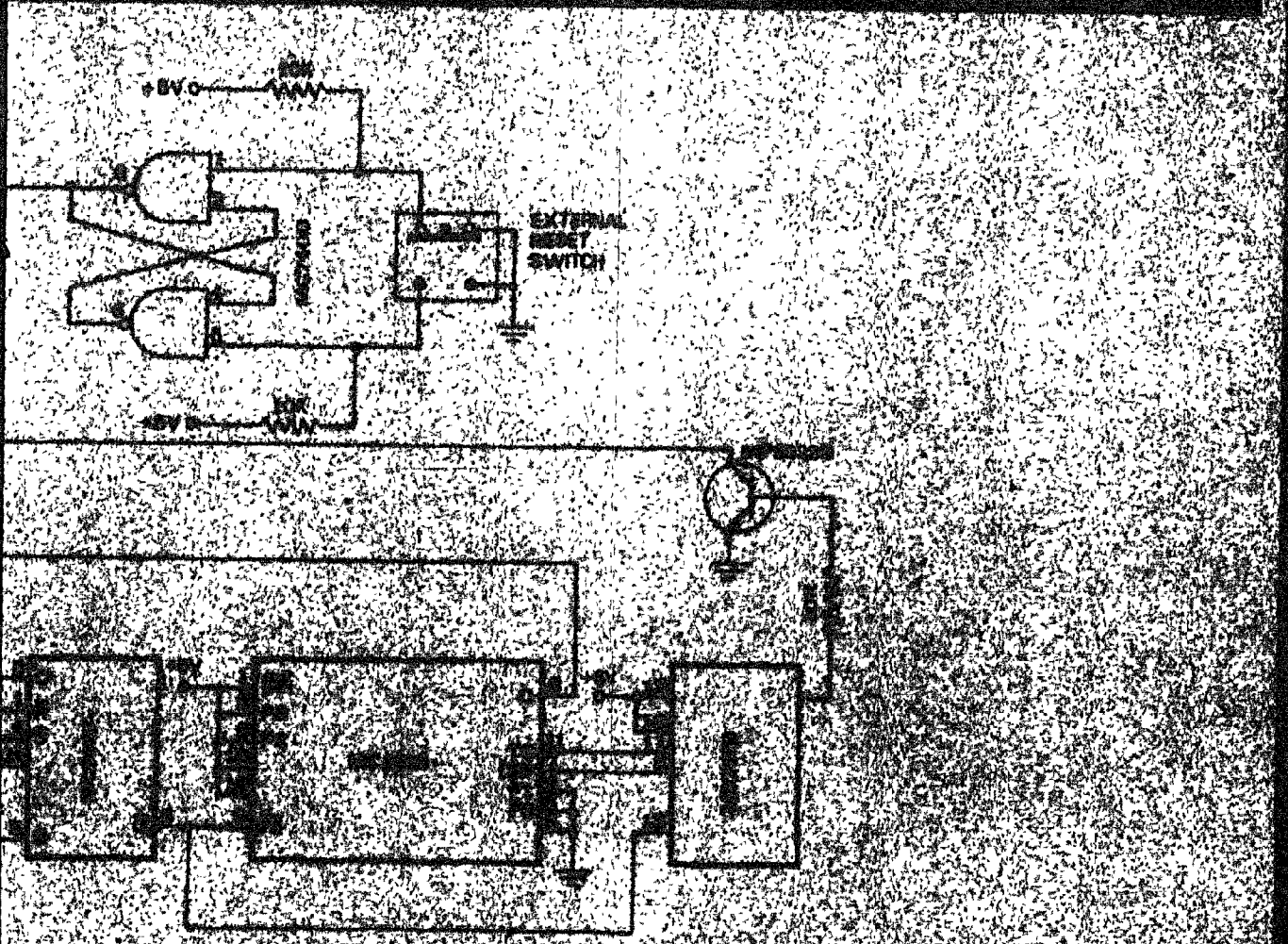
+5V
EXTERNAL
RESET
SWITCH

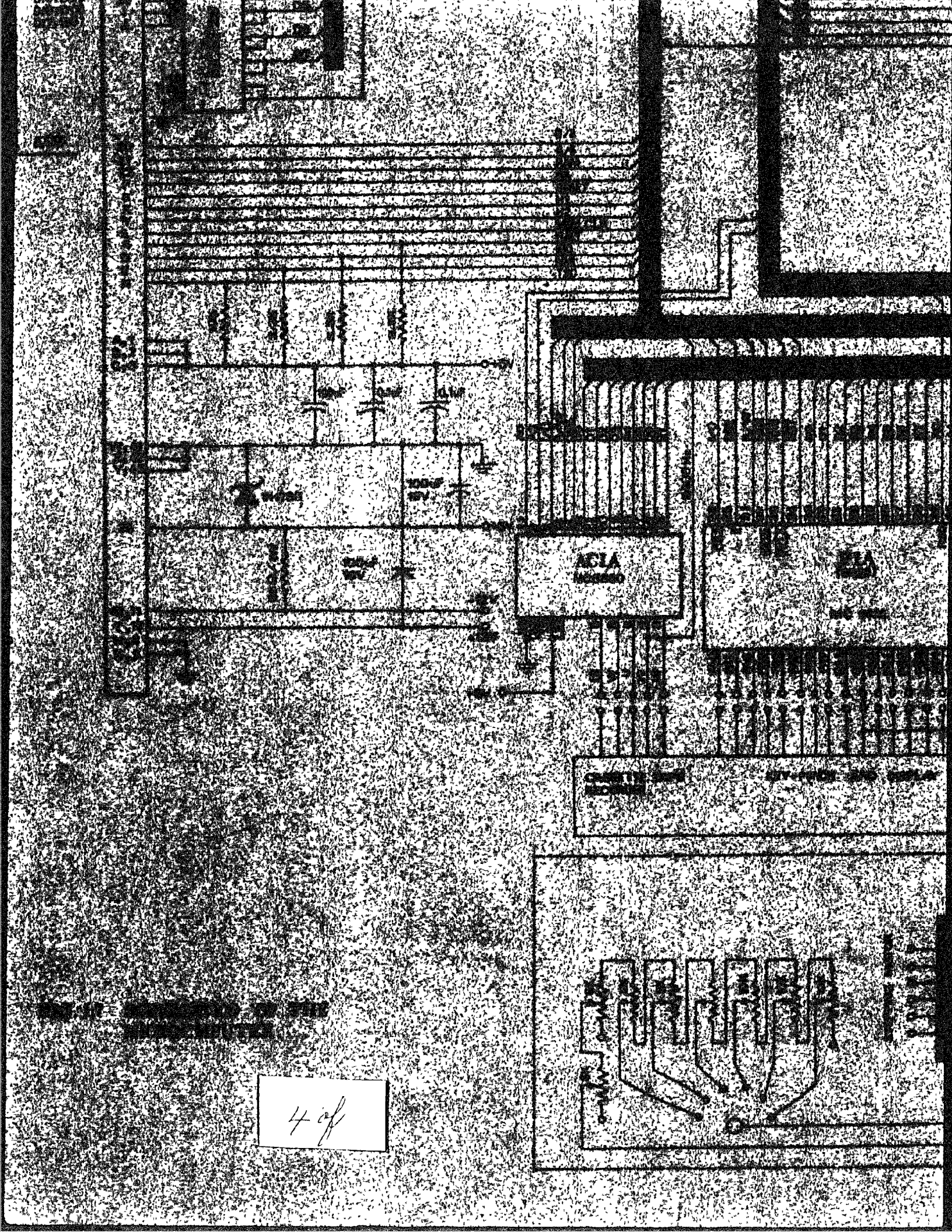

4 off

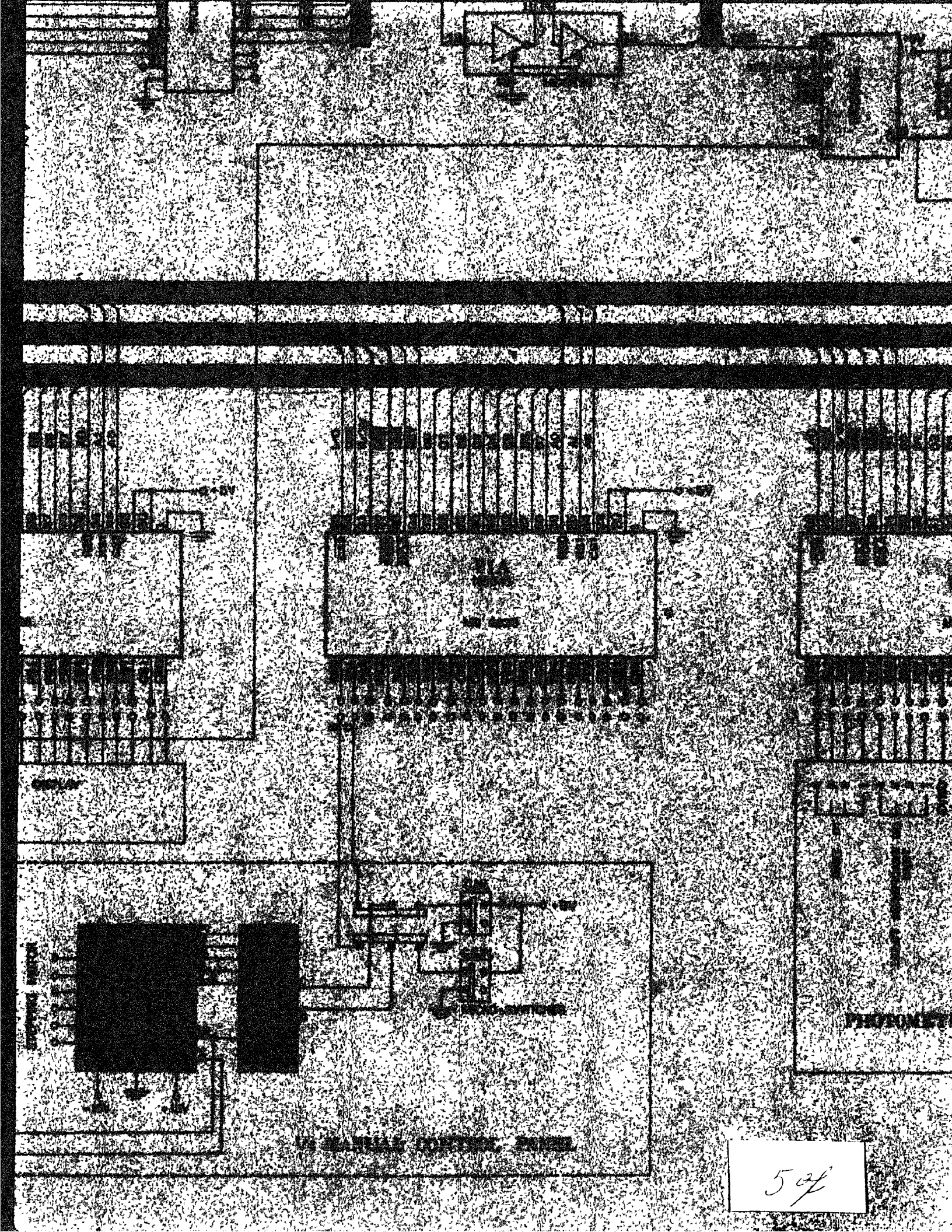

5 of

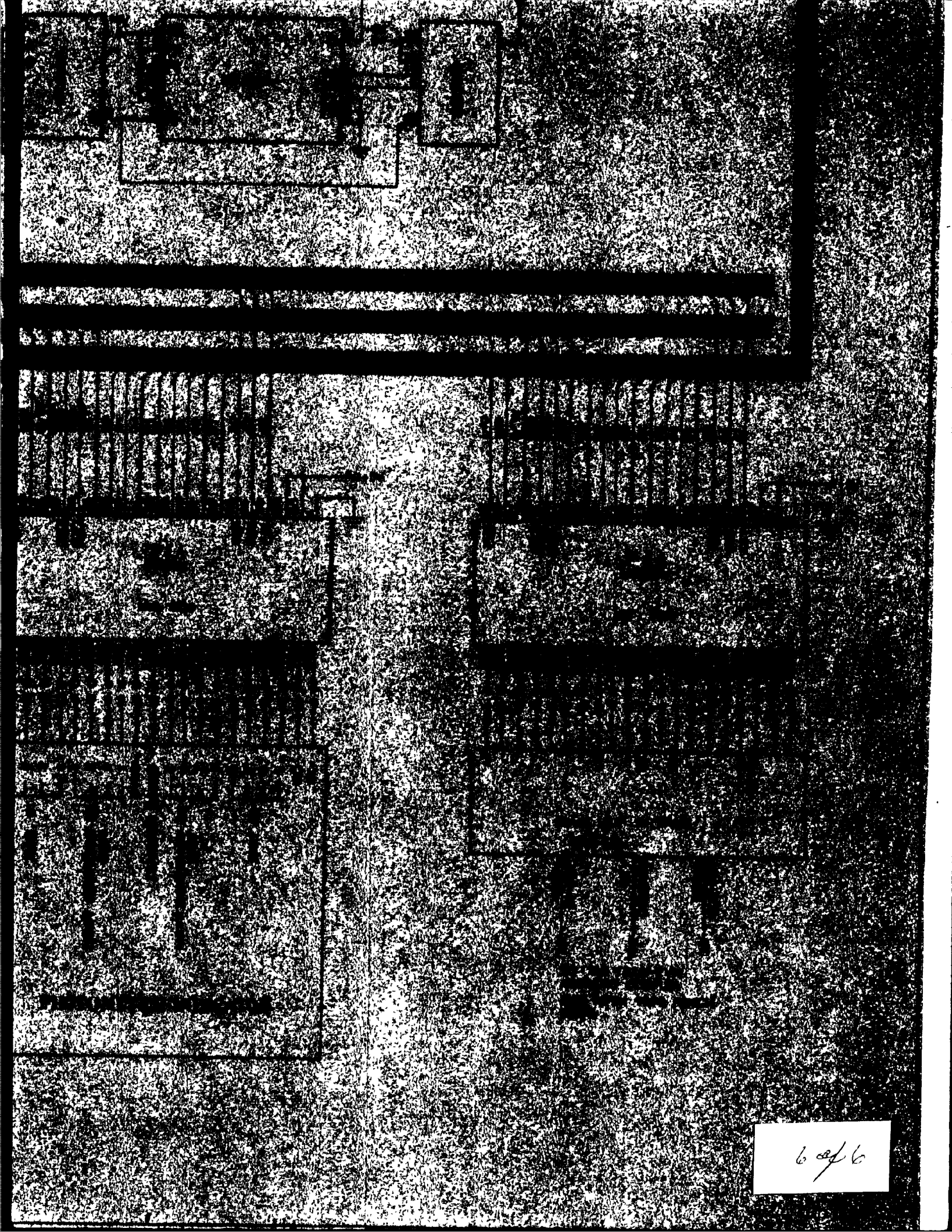

APPENDIX II

```
        MOTOROLA MC6800 CROSS ASSEMBLER, RELEASE 1,3

00001                           NAM   BEZAI



00003 0000                      ORG   $0000
00004 **
00005 **
00006 **
00007 **
00008 **    MICROCOMPUTER PROGRAM LISTING FOR THE
00009 **    HOLOGRAPHIC-ELECTRO-OPTICAL SCANNING METHOD.
00010 **
00011 **
00012 **    THE PROGRAM CONSISTS OF TWO PARTS :
00013 **    T 1: 005B- THIS SEGMENT TRIGGERS ALL THE
00014 **    STM1800DV TRANSLATOR MODULES AND SETS ALL
00015 **    THE STEPPING MOTORS TO THE 'ON' MODE.
00016 **      2: 00A7- THIS SEGMENT ACTIVATES THE
00017 **    SCANNING ROUTINE. THE BRIEF FLOW CHART HAS
00018 **    BEEN GIVEN IN FIGS 4.16-4.18 9
00019 **
00020 **    THE INPUT TO THIS PROGRAM IS AS FOLLOWS:
00021 **     LOCATION 0000: SCANNING MOTOR(SM) RUNNING
00022 **                    TIME .
00023 **     LOCATION 0001: SCANNING DIRECTION MOTOR(RM)
00024 **                    RUNNING TIME
00025 **     LOCATION 0002: X-POSITIONING MOTOR(XM)
00026 **                    RUNNING TIME .
00027 **     LOCATION 0003: Y-POSITIONING MOTOR(YM)
00028 **                    RUNNING TIME .
00029 **     LOCATION 0004: NUMBER OF COLUMNS OF THE
00030 **                    OBSERVATION POINTS .
00031 **     LOCATION 0005: NUMBER OF ROWS OF THE
00032 **                    OBSERVATION POINTS .
00033 **     LOCATION 0006: SAMPLING TIME OF THE
00034 **                    PHOTOMETER INDICATOR .
00035 **
00036 **
00037 **    THE ABOVE DATA SHOULD BE FED INTO THE
00038 **    MICROCOMPUTER BEFORE THE EXECUTION OF THE
00039 **    FIRST PROGRAM SEGMENT .
00040 **       THE PROGRAM THEN PERFORMS THE SCANNING
00041 **    ROUTINE AND STORES THE INTERFEROGRAM
00042 **    TRANSPARANCY MEASUREMENT RESULTS . WHENEVER
00043 **    THE MAXIMUM LIMIT OF THE MEMORY IS REACHED
00043 **    THE CONTENTS OF THE MEMORY IS PUNCHED ONTO
00045 **    PAPER TAPE AND THE UNIT CONTINUES EXECUTING
00046 **    THE PROGRAM UNTILL THE LAST OBSERVATION POINT
00047 **    IS ALSO CONSIDERED. FINALLY THE MICROCOMPUTER
00048 **    SETS THE SCANNING MIRROR AND THE FIBRE OPTIC
00049 **    BACK TO INITIAL CONDITIONS .
00050 **
00051 **
00052 0000 0001      SMOTOR RMB   1
00053 0001 0001      RMOTOR RMB   1
00054 0002 0001      XMOTOR RMB   1
00055 0002 0001      YMOTOR RMB   1
00056 0004 0001      XDPNTS RMB   1
00057 0005 0001      YDPNTS RMB   1
00058 0006 0001      STIME  RMB   1
00059                *
00060                *    TEMPORARY LOCATIONS RESERVED
```

```
00061                          *    FOR THE PROGRAM USAGE.
00062                          *
00063  0007 0002    TEMP    RMB   2
00064  0009 0002    FROM    RMB   2
00065  000B 0002    TO      RMB   2
00066  000D 0002    BEGA    RMB   2
00067  000F 0002    ENDA    RMB   2
00068                          *
00069                          *    PUNCHING ADDRESSES.
00070                          *
00071  0011 0002    TEMPA   RMB   2
00072  0013 0002    TEMPB   RMB   2
00073  0015 0002    TEMPC   RMB   2
00074  0017 0002    TEMPD   RMB   2
00075  0019 0002    TPONTS  RMB   2
00076                          *
00077                          *    TOTAL DATA BYTES FOR 1 POINT.
00078                          *
00079  001B 0001    FUTRE1  RMB   1
00080  001C 0001    FUTRE2  RMB   1
00081                          *
00082                          *    SAVE NO. OF ROWS.
00083                          *    SAVE NO. OF COLUMNS.
00084                          *
00085  001D 0002    TMPLOC  RMB   2
00086  001F 0001    TEMP1   RMB   1
00087  0020 0001    TEMP2   RMB   1
00088  0021 0001    NPNTS   RMB   1
00089                          *
00090                          *    NO. OF POINTS THAT CAN BE
00091                          *    EVALUATED BEFORE PUNCHING .
00092                          *
00093  0022 0002    TEMPX   RMB   2
00094  0024 0002    TEMPY   RMB   2
00095                          *
00096                          *    TOTAL NO. OF POINTS.
00097                          *
00098  0026 0010    LABLE1  RMB   $10
00099                          *
00100                          *    BEGINNING ADDRESS FOR STORING
00101                          *    WHILE SCANNING.
00102                          *
00103  0036 01F0    LABLE1  FDB   $01F0
00104  0038 0001    DIR     RMB   1
00105  0039 0001    XDIR    RMB   1
00106                          *
00107                          *    FLAG FOR X-MOTOR INDICATING
00108                          *    THE DIRECTION OF ROTATION.
00109                          *
00110  003A 0002    NUMBER  RMB   2
00111  003C 0001    NUMBR1  RMB   1
00112  003D 0001    NUMBR2  RMB   1
00113  003E 00      ZERO    FCB   $00
00114  003F 01      ONE     FCB   $01
00115  0040 01      TWO     FCB   $02
00116  0041 03      THREE   FCB   $03
00117  0042 04      FOUR    FCB   $04
00118  0043 05      FIVE    FCB   $05
00119  0044 06      SIX     FCB   $06
00120  0045 07      SEVEN   FCB   $07
00121  0046 08      EIGHT   FCB   $08
00122  0047 09      NINE    FCB   $09
00123  0048 FF      STOP    FCB   $FF
00124  0049 FB      CW1     FCB   $FB
00125  004A F7      CCW1    FCB   $F7
00126  004B FE      CW2     FCB   $FE
00127  004C FD      CCW2    FCB   $FD
00128  004D BF      CW3     FCB   $BF
00129  004E DF      CCW3    FCB   $DF
00130  004F 7F      CW4     FCB   $7F
00131  0050 EF      CW5     FCB   $EF
00132  0051 /A      TEN     FCB   10
```

```
00133 0052 12          TWEVE   FCB     $12
00134 0053 0F          FIFTEN  FCB     15
00135 0054 10          SIXTEN  FCB     16
00136 0055 20          TWENTY  FCB     $20
00137 0056 22          TWNTY2  FCB     $22
00138 0057 26          TWNTY6  FCB     $26
00139 0058 30          THIRTY  FCB     $30
00140 0059 34          THRTY4  FCB     $34
00141 005A 39          THRTY9  FCB     $39
00142                  *
00143                  *    I/O FOR THE PHOTOMETER
00144                  *    INDICATOR.
00145                  *
00146      8006        PIACRA  EQU     $8006
00147      8007        PIACRB  EQU     $8007
00148      8004        PIADRA  EQU     $8004
00149      8005        PIADRB  EQU     $8005
00150                  *
00151                  *    I/O PORT FOR MOTORS.
00152                  *
00153      8040        PIADR1  EQU     $8040
00154      8042        PIADR2  EQU     $8042
00155      8041        PIACR1  EQU     $8041
00156      8043        PIACR2  EQU     $8043
00157                  *
00158                  *    I/O PORT FOR TTY.
00159                  *
00160      8080        PIADA   EQU     $8080
00161      8082        PIADB   EQU     $8082
00162      8081        PIAAB   EQU     $8081
00163      8083        PIAAB   EQU     $8083
00164      E0AC        MONITR  EQU     $E0AC
00165                  *
00166                  *    FIRST SEGMENT OF PROGRAM.
00167                  *    SET ALL MOTORS TO 'ON' MODE.
00168                  *
00169 005B 7F 003A             CLR     NUMBER
00170 005E 7F 0009             CLR     FROM
00171 0061 7F 000A             CLR     FROM+1
00172 0064 7F 000B             CLR     TO
00173 0067 7F 000C             CLR     TO+1
00174 006A 4F                  CLR A
00175 006B B7 8006             STA A   PIACRA
00176 006E B7 8007             STA A   PIACRB
00177 0071 B7 8004             STA A   PIADRA
00178 0074 B7 8005             STA A   PIADRB
00179 0077 B7 8043             STA A   PIACR2
00180 007A 96 48               LDA A   STOP
00181 007C B7 8042             STA A   PIADR2
00182 007F 96 42               LDA A   FOUR
00183 0081 B7 8043             STA A   PIACR2
00184   000084 B7 8006           STA A PIACRA
00185 0087 B7 8007             STA A   PIACRB
00186 008A 96 48               LDA A   STOP
00187 008C B7 8042             STA A   PIADR2
00188 008F 4F                  CLR A
00189 0090 97 39               STA A   XDIR
00190 0092 97 38               STA A   DIR
00191 0094 96 49               LDA A   C 1
00192 0096 97 3C               STA A   NUMBR1
00193 0098 96 4A               LDA A   CCW1
00194 009A 97 3D               STA A   NUMBR2
00195 009C 96 05               LDA A   YDPNTS
00196 009E 97 1B               STA A   FUTRE1
00197 00A0 96 04               LDA A   XDPNTS
00198 00A2 97 1C               STA A   FUTRE2
00199                  *
00200                  *    SET THE MONITOR INDICATING
00201                  *    ALL MOTORS ARE 'ON'.
00202                  *
00203 00A4 BD E0AC             JSR     MONITR
00204                  *
```

```
00205                          *    SECOND SEGMENT OF THE PROGRAM
00206                          *    SCANNING ROUTINE .
00207                          *
00208                          *    NO. OF TRANSPARENCY READINGS.
00209                          *
00210  00A7  96 0b                    LDA A STIME
00211  00A9  d6 00                    LDA B SMOTOR
00212  00AB  5A                LOOP   DEC B
00213  00AC  D1 3E                    CMP B ZERO
00214  00AE  27 04                    BEQ   CUT
00215  00B0  9B 06                    ADD A STIME
00216  00B2  20 F7                    BRA   LOOP
00217  00B4  97 3B             OUT    STA A NUMBER+1
00218  00B6  7C 003B                  INC   NUMBER+1
00219  00B9  4F                       CLR A
00220  00BA  97 3A                    STA A NUMBER
00221  00BC  DE 3A                    LDX   NUMBER
00222  00BE  96 3B                    LDA A NUMBER+1
00223                          *
00224                          *    THE ABOVE LOCATION CONTAINS
00225                          *    TOTAL DATA POINT IN ONE
00226                          *    SCANNING DIRECTION.
00227                          *
00228  00C0  08                LOOPM  INX
00229  00C1  4A                       DEC A
00230  00C2  26 FC                    BNE   LOOPM
00231  00C4  96 3B                    LDA A NUMBER+1
00232  00C6  5A 3B                    DEC B
00233  00C7  26 F7                    BNE   LOOPM
00234  00C9  DF 19                    STX   TPONTS
00235  00C8  5F                       CLR B
00236  00CC  7F 0022                  CLR   TEMPX
00237  00CF  96 04                    LDA A XDPNTS
00238  00D1  97 23                    STA A TEMPX+1
00239  00D3  96 05                    LDA A YDPNTS
00240  00D5  97 25                    STA A TEMPY+1
00241  00D7  96 04             LOOPT  LDA A XDPNTS
00242  00D9  9B 23                    ADD A TEMPX+1
00243  00DB  97 23                    STA A TEMPX+1
00244  00DD  D9 22                    ADC B TEMPX
00245  00DF  D7 22                    STA B TEMPX
00246  00E1  5F                       CLR B
00247  00E2  96 25                    LDA A TEMPY+1
00248  00E4  4A                       DEC A
00249  00E5  97 25                    STA A TEMPY+1
00250  00E7  91 3F                    CMP A ONE
00251  00E9  26 EC                    BNE   LOOPT
00252  00EB  BD 2047                  JSR   INTZ
00253  00EE  CE 226F                  LDX   #ENND
00254  00F1  DF 26                    STX   LABEL1
00255  00F3  96 48                    LDA A STOP
00256  00F5  DE 26                    LDX   LABEL1
00257  00F7  A7 00                    STA A 0,X
00258  00F9  08                       INX
00259  00FA  DF 26                    STX   LABEL1
00260  00FC  96 4B             START  LDA A CW2
00261  00FE  BD 2005                  JSR   SCAN
00262  0101  BD 01A3                  JSR   MOTORR
00263  0104  96 4C                    LDA A CCW2
00264  0106  BD 2005                  JSR   SCAN
00265  0109  BD 01A3                  JSR   MOTORR
00266  010C  96 4B                    LDA A CW2
00267  010E  BD 2005                  JSR   SCAN
00268  0111  BD 01A3                  JSR   MOTORR
00269  0114  96 4CA3                  LDA A C"#2
00270  0116  B7 8042                  STA A PIADR2
00271  0119  BD 20C2                  JSR   SCAAN
00272  011C  96 48                    LDA A STOP
00273  011E  B7 8042                  STA A PIADR2
00274  0121  7A 0021                  DEC   NPNTS
00275                          *
00276                          *    THE ABOVE LOCATION CONTAINS THE
```

```
00277                    *    NUMBER OF POINTS THAT HAVE
00278                    *    BEEN EVALUATED.
00279                    *
00280                    *    PUNCH DATA ONTO PAPER TAPE.
00281                    *
00282 0124 27 02              BEQ    SEND
00283 0126 20 11              BRA    PRCED
00284 0128 BD 20FE   SEND     JSR    INFRM1
00285 012B DE 22              LDX    TEMPX
00286 012D 9C 3E              CPX    ZERO
00287 012F 27 05              BEQ    FEND
00288 0131 BD 2047            JSR    INTZ
00289 0134 20 03              BRA    PRCED
00290 0136 7E 0172   FEND     JMP    ENJOY
00291 0139 01        PRCED    NOP
00292 013A 96 04              LDA A  XDPNTS
00293 013C 4A                 DEC A
00294 013D 04                 STA A  XDPNTS
00295 013F 91 3E              CMP A  ZERO
00296 0141 27 06              BEQ    XFINIS
00297 0143 BD 01C9            JSR    MOTORX
00298 0146 7E 00FC            JMP    START
00299 0149 96 1C     XFINIS   LDA A  FUTRE2
00300 014B 97 04              STA A  XDPNTS
00301 014D 7A 0005            DEC    YDPNTS
00302 0150 27 20              BEQ    ENJOY
00303 0152 96 39              LDA A  XDIR
00304 0154 91 3E              CMP A  ZERO
00305 0156 26 05              BNE    EVEN
00306 0158 4C 05              INC A
00307 0159 97 39              STA A  XDIR
00308 015B 20 03              BRA    DONE
00309 015D 4F        EVEN     CLR A
00310 015E 97 39              STA A  XDIR
00311 0160 96 4D     DONE     LDA A  CW3
00312 0162 B7 8042            STA A  PIADR2
00313 0165 D6 03              LDA B  YMOTOR
00314 0167 BD 20B1            JSR    DELAY
00315 016A 96 48B1            LDA A  STOP
00316 016C B7 8042            STA A  PIADR2
00317 016F 7E 00FC            JMP    START
00318 0172 D6 1B     ENJOY    LDA B  FUTRE2
00319 0174 D4 3F              AND B  ONE
00320 0176 27 14              BEQ    EASY
00321 0178 96 4E     LOOP2    LDA A  CCW3
00322 017A B7 8042            STA A  PIADR2
00323 017D D6 02              LDA B  XMOTOR
00324 017F BD 20B1            JSR    DELAY
00325 0182 96 48              LDA A  STOP
00326 0184 B7 8042            STA A  PIADR2
00327 0187 7A 001C            DEC    FUTRE2
00328 018A 26 EC              BNE    LOOP2
00329 018C 96 4F     EASY     LDA A  CW4
00330 018E B7 8042            STA A  PIADR2
00331 0191 D6 03              LDA B  YMOTOR
00332 0193 BD 20B1            JSR    DELAY
00333 0196 96 48B1            LDA A  STOP
00334 0198 B7 8042            STA A  PIADR2
00335 019B 7A 001B            DEC    FUTRE1
00336 019E 26 EC              BNE    EASY
00337 01A0 BD E0AC   OVER     JSR    MONITR
00338 **
00339 **
00340 **
00341 **
00342 **
00343 **
00344 **    SUBROUTINE RMOTOR :
00345 **
00346 **    THIS ROUTINE IS USED TO SET THE RM-MOTOR IN
00347 **    THE 'RUN' MODE.WHEN 'DIR=0-2' ROTATION IS
00348 **    C.W. AND C.C.W. WHEN DIR=3-6.
```

```
00349 **
00350 **
00351 01A3 96 41     MOTORR LDA A THREE
00352 01A5 91 38            CMP A DIR
00353 01A7 2F 04            BLE   CHANGE
00354 01A9 96 3C            LDA A NUMBR1
00355 01AB 20 02            BRA   ROTATE
00356 01AD4 96 3D     CHANGE LDA A NUMB2
00357 01AF B7 4042  ROTATE  STA A PIADR2
00358 01B2 D6 01            LDA B RMOTOR
00359 01B4 BD 20B1          JSR   DELAY
00360 01B7 96 48            LDA A STOP
00361 01B9 B7 8042          STA A PIADR2
00362 01BC 96 38            LDA A DIR
00363 01BE 4C               INC A
00364 01BF 97 38            STA A DIR
00365 01C1 91 44            CMP A SIX
00366 01C3 2D 03            BLT   RETURN
00367 01C5 4F               CLR A
00368 01C6 97 38            STA A DIR
00369 01C8 39        RETURN RTS
00370 **
00371 **
00372 **
00373 **
00374 **
00375 **
00376 **    SUBROUTINE XMOTOR :
00377 **
00378 **    THIS ROUTINE IS USED FOR POSITIONING OF THE
00379 **    FIBRE OPTIC BY MEANS OF X-Y POSITIONER. IT
00380 **    ACTIVATES MOTORS XM AND YM.
00381 **
00382 **
00383 01C9 96 39     MOTORX LDA A XDIR
00384 01CB 91 3E            CMP A ZERO
00385 01CD 27 04            BEQ   CWISE
00386 01CF 96 50     ANTICW LDA A CW5
00387 01D1 20 02            BRA   SKIP
00388 01D3 96 4E     CWISE  LDA A CCW3
00389 01D5 B7 8042   SKIP   STA A PIADR2
00390 01D7 D6 02            LDA B XMOTOR
00391 01DA BD 20B1          JSR   DELAY
00392 01DD 96 48            LDA A STOP
00393 01DF B7 8042          STA A PIADR2
00394 01E2                  RTS
00395 **
00396 2000                  ORG   $2000
00397 2000 0001      CLEAR  RMB   1
00398 2001 7800      COUNTR FDB   $7800
00399 2003 0002      LINE   RMB   2
00400 **
00401 **
00402 **
00403 **
00404 **
00405 **
00406 **    SUBROUTINE SCAN :
00407 **    THIS ROUTINE IS USED TO SET THE SM-MOTOR
00408 **    INTO THE 'RUN' MODE AND TO STORE THE OUTPUT
00409 **    OF THE PHOTOMETER INDICATOR.
00410 **
00411 **
00412 2005 B7 8042  SCAN   STA A PIADR2
00413 2008 D6 3F            LDA B CNE
00414 200A 96 42            LDA A FOUR
00415 200C B7 8006          STA A PIACRA
00416 200F B7 8007          STA A PIACRB
00417 2012 B6 8006  WAIT    LDA A PIACRA
00418 2015 2A FB            BPL   WAIT
00419 2017 FE 8004          LDX   PIADRA
00420 201A DF 28            STX   LABEL1+2
```

```
00421 201C DE 26           LDX   LABEL1
00422 201E 96 28           LDA A LABEL1+2
00423 2020 A7 00           STA A 0,X
00424 2022 08              INX
00425 2023 96 29           LDA A LABEL1+3
00426 2025 A7 00           STA A 0,X
00427 2027 08              INX
00428 2028 DF 26           STX   LABEL1
00429 202A 5C              INC B
00430 202B D1 3B           CMP B NUMBER+1
00431 202D 26 E3           BNE   WAIT
00432 202F 96 48           LDA A STOP
00433 2031 DE 26           LDX   LABEL1
00434 2033 A7 00           STA A 0,X
00435 2035 08              INX
00436 2036 DF 26           STX   LABEL1
00437 2038 96 48           LDA A STOP
00438 203A B7 8042         STA A PIADR2
00439 203D 39              RTS
00440 203E 7D        PROMPT FCB   $D,$A,0,0,0,0,'S,'1,4
00441 203F 0A
00442 2040 00
00443 2041 00
00444 2042 00
00445 2043 00
00446 2044 53
00447 2045 31
00448 2046 04
00449                      *
00450                      *
00451 **    THE FOLLOWING ROUTINE IS USED TO :
00452 **      1: CALCULATE THE NUMBER OF POINTS THAT CAN
00453 **    BE SCANNED IN ORDER TO STAY WITHIN THE
00454 **    LIMITS OF THE AVAILABLE MEMORY AND
00455 **      2: TO SPECIFY THE STARTING AND THE ENDING
00456 **    LOCATIONS OF THE PUNCHING ROUTINE .
00457 **
00458 2047 7F 0021 INTZ    CLR   NPNTS
00459                      *     NUMBER OF POINT TO BE SCANNED.
00460 204A 7F 0020           CLR   TEMP2
00461                      *     TEMPORARY STORAGE .
00462 204D 7F 2000           CLR   CLEAR
00463 2050 CE 226F           LDX   #ENND
00464 2053 DF 1D             STX   TMPLOC
00465 2055 DF 0B             LDX   TO
00466 2057 DF 09             STX   FROM
00467 2059 5F          LPNPTS CLR B
00468 205A 96 1E             LDA A TMPLOC+1
00469 205C 9B 3B             ADD A NUMBER+1
00470 205E D9 1D             ADC B TMPLOC
00471 2060 D7 1D             STA B TMPLOC
00472 2062 97 1E             STA A TMPLOC+1
00473 2064 7C 0020           INC   TEMP2
00474 2067 0C                CLC
00475 2068 86 F0             LDA A #$F0
00476 206A 90 1E             SUB A TMPLOC+1
00477 206C B6 2F             LDA A #$2F
00478 206E 92 1D             SBC A TMPLOC
00479 2070 25 18             BCS   ADJ
00480 2072 96 20             LDA A TEMP2
00481 2074 81 03             CMP A #3
00482 2076 26 E1             BNE   LPNPTS
00483 2078 7F 0020           CLR   TEMP2
00484 207B 7C 0021           INC   NPNTS
00485 207E DE 0B             LDX   TO
00486 2080 08                INX
00487 2081 DF 0B             STX   TO
00488 2083 DE 22             LDX   TEMPX
00489 2085 09                DEX
00490 2086 DF 22             STX   TEMPX
00491 2088 26 CF             BNE   LPNPTS
00492 208A 96 20       ADJ   LDA A TEMP2
```

```
00493  208C 81 00            CMP A #0
00494  208E 27 15            BEQ   SET
00495  2090 5F               CLR B
00496  2091 96 1E            LDA A TMPLOC+1
00497  2093 D6 1D            LDA B TMPLOC
00498  2095 90 3B            SUB A NUMBER+1
00499  2097 F2 2000          SBC B CLEAR
00500  209A 97 1E            STA A TMPLOC+1
00501  209C D7 1D            STA B TMPLOC
00502  209E 96 20            LDA A TEMP2
00503  20A0 4A               DEC A
00504  20A1 97 20            STA A TEMP2
00505  20A3 20 E5            BRA   ADJ
00506  20A5 CE 226F   SET     LDX   #ENND
00507  20A8 DF 0D            STX   BEGA
00508  20AA DF 26            STX   LABEL1
00509  20AC DE 1D            LDX   TMPLOC
00510  20AE DF 0F            STX   ENDA
00511  20B0 39               RTS
00512                  *
00513                  *
00514                  *
00515  **    SUBROUTINE DELAY
00516  **
00517  **
00518  **    THIS ROUTINE GENERATES TIME INTERVALS FOR
00519  **    ALL THE MOTORS SUCH THAT DURING THIS TIME
00520  **    INTERVAL THE MOTORS REMAIN IN THE 'RUN'
00521  **    MODE. AN INPUT NUMBER 1 IN THE B-REGISTER
00522  **    CAUSES 1 SECOND OF TIME INTERVAL.
00523  **
00524  **
00525  20B1 FE 2001   DELAY  LDX   COUNTR
00526  20B4 09        LUUP   DEX
00527  20B5 A6 00            LDA A 0,X
00528  20B7 01               NOP
00529  20B8 01               NOP
00530  20B9 8C 0000          CPX   #00
00531  20BC 26 F6            BNE   LUUP
00532  20BE 5A               DEC B
00533  20BF 26 F0            BNE   DELAY
00534  20C1 39               RTS
00535                  *
00536                  *
00537  **    SUBROUTINE SCAAN
00538  **
00539  **
00540  **    THIS RCUTINE ENABLES THE SM-MOTOR TO BRING
00541  **    THE BEAM TO THE STARTING POINT OF THE
00542  **    SCANNING PROCEDURE, WHEN THE NEXT POINT IS
00543  **    TO BE CONSIDERED .
00544  **
00545  **
00546  20C2 B7 8042   SCAAN  STA A PIADR2
00547  20C5 D6 3F            LDA B ONE
00548  20C7 96 42            LDA A FOUR
00549  20C9 B7 8006          STA A PIACRA
00550  20CC B7 8007          STA A PIACRB
00551  20CF B6 8006   WAAIT  LDA A PIACRA
00552  20D2 2A FB            BPL   WAAIT
00553  20D4 FE 8004          LDX   PIADRA
00554  20D7 DF 28            STX   LABEL1+2
00555  20D9 DE 36            LDX   LABLE1
00556  20DB 96 28            LDA A LABEL1+2
00557  20DD A7 00            STA A 0,X
00558  20DF 01               NOP
00559  20E0 01               NOP
00560  20E1 96 29            LDA A LABEL1+3
00561  20E3 A7 00            STA A 0,X
00562  20E5 01               NOP
00563  20E6 01               NOP
00564  20E7 DF 36            STX   LABLE1
```

```
00565 20E9 5C            INC B
00566 20EA D1 3B         CMP B NUMBER+1
00567 20EC 26 E1         BNE   WAAIT
00568 20EE 96 48         LDA A STOP
00569 20F0 DE 36         LDX   LABLE1
00570 20F2 A7 00         STA A 0,X
00571 20F4 01            NOP
00572 20F5 01            NOP
00573 20F6 DF 36         STX   LABLE1
00574 20F8 96 48         LDA A STOP
00575 20FA B7 8042       STA A PIADR2
00576 20FD 39            RTS
00577                    *
00578                    *
00579 **    SUBROUTINE PUNCH
00580 **
00581 **
00582 **    THIS ROUTINE IS CALLED WHEN THE MEMORY
00583 **    LOCATIONS ARE OCCUPTED BY THE RAW DATA .
00584 **    IT THEN PUNCHES THE MEMORY CONTENTS ONTO
00585 **    PAPER TAPE .
00586 **
00587 **
00588 20FE CE 8080  INFRM1 LDX   #PIADA
00589 2101 6C 00         INC   0,X
00590 2103 96 45         LDA A SEVEN
00591 2105 A7 01         STA A 1,X
00592 2107 6C 00         INC   0,X
00593 2109 A7 02         STA A 2,X
00594 210B 96 59    SETUP LDA A THRTY4
00595 210D B7 8083       STA A PIACB
00596 2110 B7 8082       STA A PIADB
00597 2113 CE 221B       LDX   #MASGE1
00598 2116 D6 56         LDA B TWNTY2
00599 2118 BD 220F       JSR   SBRTNC
00600 211B CE 0009       LDX   #FROM
00601 211E BD 2202       JSR   SBRTNH
00602 2121 CE 223D       LDX   #MASGE3
00603 2124 D6 42         LDA B FOUR
00604 2126 BD 220F       JSR   SBRTNC
00605 2129 CE 000B       LDA   #TO
00606 212C BD 2202       JSR   SBRTNH
00607 212F CE 2241  INFRM2 LDX   #MASGE4
00608 2132 D6 57         LDA B TWNTY6
00609 2134 BD 220F       JSR   SBRTNC
00610 2137 CE 000D       LDX   #BEGA
00611 213A BD 2202       JSR   SBRTNH
00612 213D CE 2267       LDX   #MASGE6
00613 2140 D6 42         LDA B FOUR
00614 2142 BD 220F       JSR   SBRTNC
00615 2145 CE 000F       LDX   #ENDA
00616 2148 BD 2202       JSR   SBRTNH
00617 214B CE 226B       LDX   #MASGE7
00618 214E D6 42         LDA B FOUR
00619 2150 BD 220F       JSR   SBRTNC
00620 2153 96 52    PRNPUN LDA A TWELVE
00621 2155 BD 21C0       JSR   PRNBYT
00622 2158 DE 0D         LDX   BEGA
00623 215A DF 11         STX   TEMPA
00624 215C 96 10    PNPRN2 LDA A ENDA+1
00625 215E 90 12         SUB A TEMPA+1
00626 2160 D6 0F         LDA B ENDA
00627 2162 D2 11         SBC B TEMPA
00628 2164 26 04         BNE   PPRNT1
00629 2168 25 02         BCS   PPRNT2
00630 216A 96 53    PPRNT1 LDA A FIFTEN
00631 216C 9B 42    PPRNT2 ADD A FOUR
00632 216E B7 2003       STA A LINE
00633 2171 90 41         SUB A THREE
00634 2173 97 07         STA A TEMP
00635 2175 CE 203E       LDX   #PROMPT
00636 2178 BD 21B9       JSR   CHECK
```

```
00637 217B 5F                CLR B
00638 217C CE 2003           LDX  #LINE
00639 217F 8D 27             BSR  PPRNT4
00640 2181 CE 0011           LDX  #TEMPA
00641 2184 8D 22             BSR  PPRNT4
00642 2186 8D 20             BSR  PPRNT4
00643 2188 DE 11             LDX  TEMPA
00644 218A BD 21A8 PPRNT3    JSR  PPRNT4
00645 218D 7A 0007           DEC  TEMP
00646 2190 26 F8             BNE  PPRNT3
00647 2192 DF 11             STX  TEMPA
00648 2194 53                COM B
00649 2195 37                PSH B
00650 2196 30                TSX
00651 2197 8D 0F             BSR  PPRNT4
00652 2199 33                PUL B
00653 219A DE 11             LDX  TEMPA
00654 219C 09                DEX
00655 219D 9C 0F             CPX  ENDA
00656 219F 26 BB             BNE  PNPRN2
00657 21A1 39                RTS
00658 21A2 DF 13 INITSV      STX  TEMPB
00659 21A4 CE 8080           LDX  #PIADA
00660 21A7 39                RTS
00661 21A8 EB 00 PPRNT4      ADD B 0,X
00662 21AA 7E 21F1           JMP  TRMNL1
00663 21AD 6D 02 ADJSP1      TST  2,X
00664 21AF 2A FC             BPL  ADJSP1
00665 21B1 6C 02 ADJSP2      INC  2,X
00666 21B3 6A 02             DEC  2,X
00667 21B5 39                RTS
00668 21B6 8D 08 STPRNT      BSR  PRNBYT
00669 21B8 08                INX
00670 21B9 A6 00 CHECK       LDA A X
00671 21BB 91 42             CMP A FOUR
00672 21BD 26 F7             BNE  STPRNT
00673 21BF 39                RTS
00674                        *
00675                        *
00676 21C0 7E 21C3 PRNBYT    JMP  PRINT
00677 21C3 37      PRINT     PSH B
00678 21C4 8D DC             BSR  INITSV
00679 21C6 D6 51 PUNCH1      LDA B TEN
00680 21C8 6A 00             DEC  0,X
00681 21CA 8D E5             BSR  ADJSP2
00682 21CC 8D DF PUNCH2      BSR  ADJSP1
00683 21CE A7 00             STA A 0,X
00684 21D0 0D                SEC
00685 21D1 46                ROR A
00686 21D2 5A                DEC B
00687 21D3 26 F7             BNE  PUNCH2
00688 21D5 E6 02 PUNCH3      LDA B 2,X
00689 21D7 58                ASL B
00690 21D8 2A 02             BPL  PUNCH4
00691 21DA 8D D1             BSR  ADJSP1
00692 21DC DE 13 PUNCH4      LDX  TEMPB
00693 21DE 33                PUL B
00694 21DF 39                RTS
00695 21E0 44 PRNLHF         LSR A
00696 21E1 44                LSR A
00697 21E2 44                LSR A
00698 21E3 44                LSR A
00699 21E4 94 53 PRNRHF      AND A FIFTEN
00700 21E6 9B 58             ADD A THIRTY
00701 21E8 91 5A             CMP A THRTY9
00702 21EA 23 D4             BLS  PRNBYT
00703 21EC 9B 45             ADD A SEVEN
00704 21EE 7E 21C3           JMP  PRINT
00705 21F1 A6 00 TRMNL1      LDA A 0,X
00706 21F3 8D EB TRMNL2      BSR  PRNLHF
00707 21F5 A6 00             LDA A 0,X
00708 21F7 08                INX
```

```
00709 21F8 20 EA            BRA    PRNRHF
00710 21FA 8D F5    FCURBT  BSR    TRMNL1
00711 21FC 8D F3    TWOBYT  BSR    TRMNL1
00712 21FE 9o 55    BLANK   LDA A  TWENTY
00713 2200 20 BE            BRA    PRNBYT
00714                       *
00715                       *
00716 2202 D6 40    SBRTNH  LDA B  TWO
00717 2204 A6 00    LOOPH   LDA A  0,X
00718 2206 BD 21F1          JSR    TRMNL1
00719 2209 5A               DEC B
00720 220A D1 3E            CMP B  ZERO
00721 220C 26 F6            BNE    LOOPH
00722 220E 39               RTS
00723                       *
00724                       *
00725 220F A6 00    SBRTNC  LDA A  0,X
00726 2211 BD 21C3          JSR    PRINT
00727 2214 08               INX
00728 2215 5A               DEC B
00729 2216 D1 3E            CMP B  ZERO
00730 2218 26 F5            BNE    SBRTNC
00731 221A 39               RTS
00732                       *
00733                       *
00734 **    MESSAGES :
00735 **
00736 **
00737 **
00738 221B 0D       MASGE1  FCB    $D,$A,$A,$A
00739 221C 0A
00740 221D 0A
00741 221E 0A
00742 221F 20       MASGE2  FCC    '          '
00743 2220 20
00744 2221 20
00745 2222 20
00746 2223 20
00747 2224 20
00748 2225 20
00749 2226 20
00750 2227 20
00751 2228 20
00752 2229 50               FCC    'POINTS SCANNED FROM '
00753 222A 4F
00754 222B 49
00755 222C 4E
00756 222D 54
00757 222E 53
00758 222F 20
00759 2230 53
00760 2231 43
00761 2232 41
00762 2233 4E
00763 2234 4E
00764 2235 45
00765 2236 44
00766 2237 20
00767 2238 46
00768 2239 52
00769 223A 4F
00770 223B 4D
00771 223C 20
00772 223D 20       MASGE3  FCC    ' TO '
00773 223E 54
00774 223F 4F
00775 2240 20
00776 2241 0D       MASGE4  FCB    $D,$A,$A,$A,$A
00777 2242 0A
00778 2243 0A
00779 2244 0A
00780 2245 0A
```

```
00781  2246  20          MASGES FCC
00782  2247  20
00783  2248  20
00784  2249  20
00785  224A  20
00786  224B  20
00787  224C  20
00788  224D  20
00789  224E  20
00790  224F  20
       **
       **
       **
       **
       **
       **
       **
       **
       **
       **
       **
       **
       **
       **
       **
       **
       **
       **
       **
       **
       **
       **
       **
       **
       **
       **
       **
       **
       **
       **
       **
       **
       **
       **
       **
       **
       **
       **
       **
       **
       **
       **
       **
       **
       **
       **
       **
       **
       **
       **
       **
       **
       **
       **
       **
       **
       **
       **
       **
       **
       **
```

APPENDIX III

```
C
C
C
C
C
C
C             * CALCCMP ROUTINE :
C
C             *
C             * THIS ROUTINE IS DESIGNED TO CHECK THE CONTENTS
C             * OF ANY OF THE DATA FILES. THE OUTPUT OF THIS
C             * ROUIINE IS THE PLOTS ASSOCIATED TO THE FRINGE
C             * PATTERNS. FRINGE NUMBERS CAN ALSO BE EVALUATED
C             * FROM THESE PLOTS.
C             *
C      /LOAD FORTG1
C      /JOB FRINGE
C
C      REAL ITEMP(4),FDATA(32),XAXIS(32)
C      LOGICAL*1 SS,ONE,DATA(60),TDBYTE(2),CHAR1,EQUAL
C
C      DATA SS,ONE/'S','1'/
C      N=0;CALL PLOTON;10 :READ(5,20,END=80) DATA
C   20 FORMAT(60A1)
C      IF((EQUAL(DATA(1),SS,1)).AND.(EQUAL(DATA(2),ONE,1)))
C     .GO TO 30;GO TO 10;30 :TDBYTE(1)=DATA(3);TDBYTE(2)=DATA(4)
C      CALL CONVERT(IDBYTE,VALUE);NBYTES=VALUE-3
C      NCHAR=NBYTES*2+4;DO 40 I=1,32;XAXIS(I)=I
C      CALL SCALE(XAXIS,7.0,30,1)
C      DO 70 KK=8,NCHAR,4;DO 50 I=1,4;KKK=KK+I
C      CHAR1=DATA(KKK);ITEMP(I)=CNTINT(CHAR1)
C      IF(ITEMP(1).NE.15) GO TO 60
C      NN=N;CALL PPLOT(FDATA,XAXIS,NN);N=0;GO TO 70
C      FDATA(N)=ITEMP(1)*1000.0+ITEMP(2)*100.0+ITEMP(3)*10.0
C     <+ITEMP(4)
C   70 CONTINUE;GO TO 10
C   80 CALL PPLOT(FDATA,XAXIS,NN)
C   80 CALL ENDPLT;STOP;END
C
C
C      SUBROUTINE CONVERT(HEXVAL,DECIMAL)
C      LOGICAL*1 HEXVAL(2),HXCHAR(16),EQUAL
C      DIMENSION IDCIML(2)
C      DATA HXCHAR/'0','1','2','3','4','5','6','7','8','9',
C     <'A','B','C','D','E','F'/
C      DO 300 I=1,2;DO 100 J=1,16
C      IF(EQUAL(HEXVAL(I),HXCHAR(J),1)) GO TO 200
C  100 CONTINUE;200 :IDCIML(I)=J-I;300 :CONTINUE
C      DCIMAL=IDCIML(1)*16+IDCIML(2);RETURN;END
C
C
C      FUNCTION CNTINT(HXVAL)
C      REAL INTEQT(11)
C      LOGICAL*1 HXVAL,CHAR(11),EQUAL
C      DATA CHAR/'0','1','2','3','4','5','6','7','8','9','F'/
C      DATA INTEQT/0.0,1.0,2.0,3.0,4.0,5.0,6.0,7.0,8.0,9.0,15.0/
C      DO 400 I=1,11;II=I
C      IF(EQUAL(HXVAL,CHAR(I),1)) GO TO 500;400 :CONTINUE
C  500 CNTINT=INTEQT(II);RETURN;END
C
C
C      SUBROUTINE PPLOT(FDATA,XAXIS,NN)
C      DIMENSION FDATA(32),XAXIS(32)
C      DATA ORIG1,ORIG2/0.0,-1.0/
C      ORIG2=ORIG2+1.0
C      DO 600 I=1,NN;600 :FDATA(I)=FDATA(I)+ORIG2
C      FACTOR=1.0+ORIG2;CALL SCALE(FDATA,FACTOR,NN,1)
C      CALL PLOT(ORIG1,ORIG2,2);IF (ORIG2.EQ.6.0) ORIG2=0.0
C      CALL FLINE(XAXIS,FDATA,-NN,1,0,3);RETURN;END
C
C
C
C
C
C
```

```
$WATFIV ,TIME=300,PAGES=1000,LINES=76,NOEXT
C
C
C
C
C
C            * FRINGE NUMBER EVALUATION:
C
C
C            * THIS PROGRAM READS THE INTERFEROGRAM TRANSPARA-
C            * NCY MEASUREMENT RESULTS THAT HAVE BEEN SAVED
C            * BY THE 'PTREAD' ROUTINE AND EVALUATES THE
C            * CORRESPONDING FRINGE NUMBERS9 THE
C            * RESULTS OF THIS PROGRAM ARE THEN PUNCHED
C            * ONTO INDEX CARDS. THE LATTER WILL BE FED
C            * INTO THE MAIN COMPUTER PROGRAM OF APPENDIX V
C            * FOR THE EVALUATION OF THE REQUIRED QUANTITIES.
C
C
C
C
C     DIMENSION DATA(8,2790),RDATA(30,720),EL(3,3)
C     DIMENSION ARR1(3,30),ARR2(3,210),IL(10)
C     DIMENSION F1(240),F2(240),F3(240),LE(3),FN(3)
C     INTEGER DATA
C   8 FORMAT(9F6.1)
C     DO 7 I=1,3;7 :READ(5,8) (EL(I,J),J=1,3)
C     DO 10 J=1,2790;10 :READ(5,20) (DATA(I,J),I=1,8)
C  20 FORMAT(8X,8A4)
C     M=1;N=0;DO 50 I=1,2790;DO 40 J=1,8;N=N+1
C     IF(N.NE.31) GO TO 30;N=0;M=M+1;GO TO 40
C  30 RDATA(N,M)=FLOAT(DATA(J,I));40 :CONTINUE;50 :CONTINUE.
C
C
C     N=0;DO 70 I=1,720,3;DO 60 J=1,30
C     ARR1(1,J)=RDATA(I,J);ARR1(2,J)=RDATA(I+1,J)
C  60 ARR1(3,J)=RDATA(I+2,J);CALL FRINGE(ARR1,FN,EL)
C  60 N=N+1,F1(N)=FN(1);F2(N)=FN(I);F3(N)=FN(O)
C  70 CONTINUE;M=1;N=12;DO 80 I=1,20
C     PUNCH 90,(F1(K),K=M,N);PUNCH 90,(F2(K),K=M,N)
C     PUNCH 90,(F3NK),K=M,N);M=N+1,N=N+12
C  80 CONTINUE.
C  90 FORMAT(12F6.3)
C     STOP;END
C
C
C     SUBROUTINE FRINGE(ARR1,FN,EL)
C     DIMENSION ARR1(O
C     DIMENSION ARR1(3,30),ARR2(3,210),EL(3,3),LE(3),FN(3)
C
C     N=1;DO 140 I=1,3;DO 100 J=1,30
C     ARR2(I,N)=ARR1(I,J)
C     ARR2(I,N+2)=(ARR1(I,J)+ARR1(I,J+1))/2.0
C     ARR2(I,N+1)=(ARR1(I,J)+ARR2(I,N+2))/2.0
C     ARR2(I,N+3)=(ARR1(I,N+2)+ARR1(I,J+1))/2.0
C     N=N+4;100 :CONTINUE
C     IM=IK=IN=0;DO 110 J=1,119
C     DIF=ARR2(I,J+1)-ARR2(I,J)
C     IF(DIF.GT.0.0) NN(J)=1;IF(DIF.LT.0.0) NN(J)=-1
C     IF(DIF.EQ.0.0) NN(J)=0;110 :CONTINUE;M=NN(1)
C     DO 120 J=2,119;N=NN(J)
C     IF(M.EQ.N.AND.M.NE.0) GO TO 120
C     IN=IN+1;IF(IM.EQ.0) IM=J
C     IL(IN)=J;IK=IK+1;120 :CONTINUE
C     F1=IM/IL(1);F2=((119-IK)/IL(IN))
C     F=IN+F1+F2;DO 130 J=1,3
C 130 LE(J)=(119.0/(EL(I,1)+EL(I,2)+EL(I,3)))*EL(I,J)
C 130 F1M=LE(1)/IL(1);F2M=LE(3)/IL(IN);FN(I)=F-F1M-F2M
C 140 CONTINUE;RETURN;END
C
C             **
C             **
C             **
C             **
C             **
C             **
```

APPENDIX IV

```
C
C
C
C
C
C
C
C            ***    PROGRAM TO EVALUATE THE VOLUMETRIC MASS
C            ***    DENSITY AND THE LOCAL THICKNESS OF NEWSPRINT
C            **     PAPER SAMPLE NO.38 .
C
C
C            *      INPUT TO THIS PROGRAM IS AS FOLLOWING :
C            *       IATM(I,J): APPARENT THICKNESS MEASUREMENTS.
C            *       ABM(I,J) : APPARENT BASE LINE MEASUREMENTS.
C            *       SHIFT(I) : THE AMOUNT BY WHICH THE BASE LINE
C            *                  IS SHIFTED IN ORDER TO FALL WITHIN
C            *                  THE LINEAR RANGE OF THE FOTONIC
C            *                  SENSOR.
C            *      DT1,2(I) :  DIGITIZING REFERENCE POINTS OF THE
C            *                  APPARENT THICKNESS MEASUREMENTS.
C            *      DB1,2(I) :  DIGITIIZING REFERENCE PCINTS OF THE
C            *                  APPARENT BASE LINE MEASUREMENTS.
C            *      AMD(I,J) :  APPARENT GRAMMAGE MEASUREMENTS.
C            *      DM1,2(I) :  DIGITIZING REFERENCE POINTS OF THE
C            *                  APPARENT GRAMMAGE MEASUREMENTS.
C            *      BW(I)    :  BASIS WEIGHT AND ABSORBANCE VALUES
C            *                  OF THE MULTI STEP HANDSHEET.
      DIMENSION ATM(40,26),ABM(40,26),DT1(26),DT2(26),DB1(26)
      DIMENSION LNT(26),LNB(26),AMD(40,26),DM1(26),DM2(26)
      DIMENSION SHIFT(26),LND(26),DB2(26),TM(40,26),TMD(40,26)
      DIMENSION MT(40,26),MTD(40,26),BW(10),AB(10),IDEN(40,26)
      DIMENSION AR(40,26),KYP(10,15),KYN(10,15),STEP(10)
      DIMENSION IDAT(3),IPOS(150),ISTEP(10),DEN(40,26)
      DIMENSION IHIS(10),KZ1(10),KZ2(10),KZ3(10)
      DIMENSION DTM(40,26),TM1(40,26),SRT(40,26),ASRT(40)
      INTEGER IDAT /'|','*','-'/
      WRITE(6,1)
    1 FORMAT('1')
      DO 4000 J=1,26;READ(5,1000)  LNT(J),DT1(J),DT2(J)
 1000 FORMAT(I5,2F8.1)
      N=1;M=10;DO 3100 II=1,4;READ(5,2000) (ATM(I,J),I=N,M)
 2000 FORMAT(10F8.1)
      N=N+10;M=M+10;3100 :CONTINUE;4000 :CONTINUE;DO 6000 J=1,26
      READ(5,1100) LNB(J),DB1(J),DB2(J),SHIFT(J)
 1100 FORMAT(I5,3F8.1)
      N=1;M=10;DO 5100 II=1,4;READ(5,2000) (ABM(I,J),I=N,M)
      N=N+10;M=M+10;5100 :CONTINUE;6000 :CONTINUE;DO 8000 J=1,26
      READ(5,1000) LND(J),DM1(J),DM2(J);N=1;M=10;DO 7100 II=1,4
      READ(5,2000) (AMD(I,J),I=N,M);N=N+10;M=M+10;7100 :CONTINUE
 8000 CONTINUE;READ(5,8100) (BW(I),I=1,10);READ(5,8100) (AB(I),I=1,10)
 8100 FORMAT(10F8.1)
      READ(5,8110)  IHIS(1),(KZ1(I),I=1,10)
 8110 FORMAT(11I5)
      READ(5,8110)  IHIS(2),(KZ2(I),I=1,10)
      READ(5,8110)  IHIS(3),(KZ3(I),I=1,10)
      NH1=10;NH2=10;NH3=10;DO 8120 I=1,10
      IF(KZ1(I).EQ.0)  NH1=NH1-1;IF(KZ2(I).EQ.0)  NH2=NH2-1
      IF(KZ3(I).EQ.0)  NH3=NH3-1;8120 :CONTINUE;CALL SORT(ATM)
      CALL SORT(ABM);CALL SORT(AMD);M=1;N=20;DO 8595 L=1,2
 8585 FORMAT('1',///,49X,'APPARENT MASS DISTRIBUTION READINGS',
     .60X,'ROW',2X,'COLUMN',/,61X,I2,2X,I2)
      WRITE(6,8585) M,N;WRITE(6,8520) (IPOS(IK),IK=1,126),(I,I=M
     .,N),(IPOS(JK),JK=1,126);DO 8590 J=1,26
 8590 WRITE(6,8540) J,DM1(J),DM2(J),(AMD(I,J),I=M,N)
      M=21;N=40;8595 :CONTINUE
      WRITE(6,8600) (IPOS(J1),J1=1,43),(IPOS(J2),J2=1,43),(BW(I)
     .,AB(I),I,I=1,10),(IPOS(J3),J3=1,43)
 8600 FORMAT('1',/////////////,50X,'MASS DISTRIBUTION CALIBRAT',
     .'ION DATA',///,45X,43A1,/,45X,'ABSORBANCE',4X,
     .'BASIS WEIGHT (GR/M2)',4X,'POINT',/,45X,43A1,/,10(48X,
     .F4.1,15X,F4.1,12X,I2,/),//,45X,43A1)
      DO 9200 I=1,40;DO 9100 J=1,26
      ABM(I,J)=ABM(I,J)-SHIFT(J)-(DB1(J)+DB2(J))/2.0
      ATM(I,J)=ATM(I,J)-(DT1(J)+DT2(J))/2.0
      TM(I,J)=ABS(ATM(I,J)-ABM(I,J))*2.424;9100 :CONTINUE
```

```
C
C
C
C
 9200 CONTINUE;WRITE(6,9300)
 9300 FORMAT('1',//,52X,'THICKNESS MEASUREMENT RESULTS OF',/,
     .52X,'THE NEWSPRINT PAPER SAMPLE NO.38',/,64X,'(MICRONS)')
      WRITE(6,9500)(IPOS(JA),JA=1,108),(J,J=1,26),(IPOS(JB),JB=1,108)
 9500 FORMAT(' ',/,14X,108A1,/,20X,9(I1,3X),17(I2,2X),/,14X,108A1)
      DO 9540 I=1,40;DO 9530 J=1,26;MT(I,J)=TM(I,J)
 9530 TM1(I,J)=TM(I,J);9540 :CONTINUE;DO 9550 I=1,40
 9550 WRITE(6,9600) I,(MT(I,J),J=1,26)
 9600 FORMAT(' ',13X,I2,1X,'|',1X,26(I3,1X))
      IF(IHIS(1).EQ.0) GO TO 9655;NA=KZ1(NH1);NB=NA+1
      CALL HISTO(TM,40,26,0.0,KZ1,NH1,KYP,KYN,AMEAN,STEP)
      MEAN=AMEAN;IF(NB-10) 9609,9625,9628;9609 :DO 9620 I=1,NH1
      DO 9610 J=NB,10;KYP(I,J)=0;9610 :KYN(I,J)=0;9620 :CONTINUE
      GO TO 9628;9625 :DO 9626 I=1,NH1;KYP(I,10)=0
 9626 KYN(I,10)=0;9628 :WRITE(6,9630)(IPOS(I),I=1,108),MEAN
 9630 FORMAT(' ',13X,108A1,/,14X,'HISTOGRAMS INFORMATION :',
     .10X,'MEAN VALUE=',I4)
      DO 9640 I=1,NH1;ISTEP(I)=STEP(I)
 9640 WRITE(6,9650) ISTEP(I),(KYN(I,11-K),K=1,10),(KYP(I,L),L=1,10)
 9650 FORMAT(' ',8X,'STEP SIZE=',I3,10(2X,I3),2X,'MEAN',10(2X,I3))
 9655 DO 9700 I=1,40;DO 9690 J=1,26
      AMD(I,J)=100.0-AMD(I,J)*(100.0/(DM1(J)-DM2(J)))
      DO 9680 N=1,9
      IF(AMD(I,J).GE.AB(N).AND.AMD(I,J).LT.AB(N+1)) X1=BW(N)
      IF(AMD(I,J).GE.AB(N).AND.AMD(I,J).LT.AB(N+1)) X2=BW(N+1)
      IF(AMD(I,J).GE.AB(N).AND.AMD(I,J).LT.AB(N+1)) Y1=AB(N)
      IF(AMD(I,J).GE.AB(N).AND.AMD(I,J).LT.AB(N+1)) Y2=AB(N+1)
 9680 CONTINUE;TMD(I,J)=((X1-X2)/(Y1-Y2))*AMD(I,J)-0.5*(((
     .X1-X2)/Y1+Y2)-(X1+X2));9690 :CONTINUE;9700 :CONTINUE
      WRITE(6,9710)
 9710 FORMAT('1',//,52X,'GRAMMAGE DISTRIBUTION RESULTS OF',/,
     .52X,'THE NEWSPRINT PAPER SAMPLE NO.38',/,65X,'(GR/M2)')
      WRITE(6,9500)(IPOS(JA),JA=1,108),(J,J=1,26),(IPOS(JB),
     .JB=1,108);DO 9730 I=1,40;DO 9720 J=1,26;MTD(I,J)=TMD(I,J)
 9720 DTM(I,J)=TMD(I,J);9730 :CONTINUE;DO 9735 I=1,40
 9735 WRITE(6,9600) I,(MTD(I,J),J=1,26)
      IF(IHIS(2).EQ.0) GO TO 9745;NA=KZ2(NH2);NB=NA+1
      CALL HISTO(TMD,40,26,0.0,KZ2,NH2,KYP,KYN,AMEAN,STEP)
      MEAN=AMEAN;IF(NB-10) 9737,9741,9743;9737 :DO 9740 I=1,NH2
      DO 9738 J=NB,10;KYP(I,J)=0;9738 :KYN(I,J)=0;9740 :CONTINUE
      GO TO 9743;9741 :DO 9742 I=1,NH2;KYP(I,10)=0;9742 :KYN(I,10)=0
 9743 WRITE(6,9630)(IPOS(I),I=1,108),MEAN;DO 9744 I=1,NH2
      ISTEP(I)=STEP(I)
 9744 WRITE(6,9650) ISTEP(I),(KYN(I,11-K),K=1,10),(KYP(I,L),L=1,10)
 9745 DO 9760 I=1,40;DO 9750 J=1,26
      DEN(I,J)=(DTM(I,J)/TM1(I,J))*1000.0
 9750 IDEN(I,J)=DEN(I,J);9760 :CONTINUE;WRITE(6,9770)
 8520 FORMAT(' ',126A1,I20,126A1)
 8540 FORMAT(' ',I1,12F10.3)
 9770 FORMAT('1',//,52X,'3-D MASS DISTRIBUTION RESULTS OF',/,
     .52X,'THE NEWSPRINT PAPER SAMPLE NO.38',/,65X,'(KG/M3)')
      WRITE(6,9500)(IPOS(JA),JA=1,108),(J,J=1,26),(IPOS(JB),
     .JB=1,108);DO 9780 I=1,40
 9780 WRITE(6,9600) I,(IDEN(I,J),J=1,26)
      IF(IHIS(3).EQ.0) GO TO 9789;NA=KZ3(NH3);NB=NA+1
      CALL HISTO(DEN,40,26,0.0,KZ3,NH3,KYP,KYN,AMEAN,STEP)
      MEAN=AMEAN;IF(NB-10) 9781,9785,9787;9781 :DO 9784 I=1,NH3
      DO 9782 J=NB,10;KYP(I,J)=0;9782 :KYN(I,J)=0;9784 :CONTINUE
      GO TO 9787;9785 :DO 9786 I=1,NH3;KYP(I,10)=0;9786 :KYN(I,10)=0
 9787 WRITE(6,9630)(IPOS(I),I=1,108),MEAN;DO 9788 I=1,NH3
      ISTEP(I)=STEP(I)
 9788 WRITE(6,9650) ISTEP(I),(KYN(I,11-K),K=1,10),(KYP(I,L),L=1,10)
 9789 WRITE(6,9790)
 9790 FORMAT('1')
      STOP;END

      SUBROUTINE SORT(SRT)
      DIMENSION SRT(40,26),ASRT(40)
      DO 3 J=1,26;DO 1 I=1,40;1 :ASRT(41-I)=SRT(I,J)
C
C
```

```
C
C
197         DO 2 K=1,40;2 :SRT(K,J)=ASRT(K);3 :CONTINUE;RETURN;END


202         SUBROUTINE HISTO(AR,I,J,ST,KZ,N,KYP,KYN,AMEAN,STEP)
203         DIMENSION AR(40,26),KYP(10,15),KYN(10,15),STEP(10),KZ(10)
204         MAXI=0;DO 9 NI=1,N;IF(MAXI-KZ(NI)) 2,9,9;2 :MAXI=KZ(NI)
208       9 CONTINUE;SUM=0.0;DO 20 J1=1,J;DO 10 I1=1,I
212      10 SUM=SUM+AR(I1,J1);20 :CONTINUE;A=I*J;AMEAN=SUM/A;DO 40 J1=1,J
217         DO 30 I1=1,I;30 :AR(I1,J1)=AMEAN-AR(I1,J1)
219      40 CONTINUE;DO 200 MO=1,N;AMAX=0.0;DO 60 J1=1,J;DO 50 I1=1,I
224         IF(AMAX-ABS(AR(I1,J1))) 55,60,60;50 :CONTINUE
226      55 AMAX=ABS(AR(I1,J1));60 :CONTINUE;STEP(MO)=AMAX/KZ(MO)
229         IX=KZ(MO);BMIN=0.0;BMAX=STEP(MO);DO 110 MN=1,IX
233         MM=0;DO 100 J1=1,J;DO 90 I1=1,I
236      90 IF(AR(I1,J1).GT.BMIN.AND.AR(I1,J1).LE.BMAX) MM=MM+1
237     100 CONTINUE;KYP(MO,MN)=MM;BMIN=BMAX;BMAX=BMAX+STEP(MO)
241     110 CONTINUE;K2=KZ(MO)+1;IF(K2.LT.MAXI) GO TO 112
244         KYP(NO,K2)=0;GO TO 118;112 :DO 115 ME=K2,MAXI
247     115 KYP(NO,ME)=0;118 :BMAX=0.0;BMIN=-STEP(MO);DO 150 MN=1,IX
251         MM=0;DO 140 J1=1,J;DO 130 I1=1,I
254     130 IF(AR(I1,J1).GT.BMIN.AND.AR(I1,J1).LE.BMAX) MM=MM+1
255     140 CONTINUE;KYN(MO,MN)=MM;BMAX=BMIN;BMIN=BMIN-STEP(MO)
259     150 CONTINUE;IF(K2.LT.MAXI) GO TO 170;KYN(MO,K2)=0;GO TO 200
263     170 DO 180 ME=K2,MAXI;180 :KYN(MO,ME)=0;200 :CONTINUE
266         RETURN;END

$DATA
```

APPENDIX V

```
$WATFIV ,TIME=300,PAGES=1000,LINES=76,NOEXT
C
C
C
C
C
C
C
C
C
C
C
C
C
C
C
C
C  ****************************************************************
C  *****                                                     *****
C  *****                   MAIN PROGRAM                      *****
C  *****        ANALYSIS OF THE RECONSTRUCTED                *****
C  *****             - INTERFEROGRAMS                        *****
C  *****                                                     *****
C  **********----------------------------------------------**********
C  **                                                            **
C  **     THE MAIN PROGRAM IS CONSISTED OF THE                   **
C  **    FOLLOWING PARTS .ALL PARTS ,EXCEPT (1) AND              **
C  **    (2) ARE OPTIONAL AND CAN BE ACTIVATED VIA               **
C  **    INPUT CONTROL CARDS .                                   **
C  **      1): EVALUATION OF THE THREE-DIMENSIONAL               **
C  **          DEFORMATION FIELD :SUBROUTINE DEFORM .            **
C  **      2): CALCULATION OF THE STATISTICS OF THE              **
C  **          DEFORMATION FIELD ,STRAIN FIELD ,...              **
C  **          SUBROUTINE STATIS .                               **
C  **      3): CALCULATION OF THE PROBABILITY DENSI-             **
C  **          TIES OF THE DEFORMATION FIELD .                   **
C  **          SUBROUTINE PDENS .                                **
C  **      4): CALCULATION OF THE CUMMULATIVE DEFORM-            **
C  **          ATION FIELD :SUBROUTINE CUMU .                    **
C  **      5): EVALUATION OF THE STRAIN FIELD BASED ON**
C  **          THE CAUCHY CONCEPT :SUBROUTINE STRAIN .**
C  **      6): EVALUATION OF THE THICKNESS CHANGES               **
C  **          OF THE OBJECT :SUBROUTINE CHANGE .                **
C  **      7): CALCULATION OF A CORRELATION MATRIX               **
C  **          BETWEEN THE DEFORMATION FIELD AND                 **
C  **          THICKNESS CHANGES :SUBROUTINE CROLAT .            **
C  **      8): CONSTRUCTION OF SEVERAL HISTOGRAMS FOR            **
C  **          ANY GIVEN ARRAY SUCH AS DEFORMATION ,             **
C  **          STRAIN FIELD ,ECT .THE FREQUENCIES ARE            **
C  **          COMPUTED FOR THE CENTRAL DISTRIBUTIONS            **
C  **          SUBROUTINE HISTO .                                **
C  **                                                            **
C  **********----------------------------------------------**********
C  **                                                            **
C  **    INPUTS TO THIS PROGRAM ARE AS FOLLOWING :               **
C  **      1): THICKNESS MEASUREMENT RESULTS .                   **
C  **      2): AREA MASS DISTRIBUTION RESULTS .                  **
C  **      3): VOLUMETRIC MASS DISTRIBUTION RESULTS .            **
C  **      4): FRINGE NUMBER VECTOR .                            **
C  **      5): RECONSTRUCTION GEOMETRY DATA .                    **
C  **      6): INPUT CONTROL CARDS .                             **
C  **                                                            **
C  ****************************************************************
C
C
C
C
C
C
C
C
C
C
C
C
C
C
C
C
```

```
C
C
C
C
      DIMENSION F1(20,12),F2(20,12),F3(20,12),XMESH(20,12),X(4)
      DIMENSION YMESH(20,12),ZDEF(20,12),STY(20,12),AJP(20,12)
      DIMENSION B(3,1),A(3,3),WKAREA(18),AINV(3,3),DEFX(20,12)
      DIMENSION XDEF(20,12),YDEF(20,12),DEFY(20,12),Y(4),Z(4)
      DIMENSION STVAR(3,16),STMEAN(3,16),SVAR(3,16),SMEAN(3,16)
      DIMENSION TKNS(20,12),TK(20,12),TMD(20,12),AR(20,12)
      DIMENSION DL(4),DM(4),DN(4),C(1,3),CC(8,7),KZ5(5),SLOPE(2,8)
      DIMENSION IPOS(130),IDAT(3),JDAT(16),KDAT(6),ARRAY(20,12)
      DIMENSION KZ1(5),KZ2(5),KZ3(5),KZ4(5),KZ6(5),KZ7(5),KZ8(5)
      DIMENSION XPD(20,12),YPD(20,12),ZPD(20,12),STX(20,12)
      DIMENSION CCXD(2,20,12),CCYD(2,20,12),CCZD(2,20,12),ITIME(8)
      DIMENSION CXD(20,12),CYD(20,12),CZD(20,12),BR(20,12)
      DIMENSION COC(8,20,7),ARR1(20),ARR2(20),CLC(8,20,7)
      DIMENSION TMDA(20,12),SSM(2,16),SSV(2,16),TCC(3,16)
      DIMENSION ARR3(20,12),ARR4(20,12),A1R(19,11),A2R(19,11)
      DOUBLE PRECISION ARR1,ARR2,ARR3,ARR4,A1R,A2R
      DOUBLE PRECISION AINV,CXD,CYD,CZD,STX,STY,XPD,YPD,ZPD
      DOUBLE PRECISION XDEF,YDEF,ZDEF,STMEAN,STVAR,SMEAN,SVAR
      DOUBLE PRECISION SXV,SYV,SXM,SYM,WKAREA,TKNS,TK,B,A,DEFX
      DOUBLE PRECISION VRNCE,AMEAN,ARRAY,AR,AMN,BMN,CMN,DMN,DEFY
      DOUBLE PRECISION TMDA,TMD,TCC,CCXD,CCYD,CCZD,TCM
      INTEGER IDAT /' ',' ','-'/
      INTEGER KDAT /'X','Y','Z','XX','YY','MEAN'/
      INTEGER JDAT
      DO 5 I=1,110,5 :IPOS(I)=IDAT(3)
      READ(5,10) NUMBER,NOCUMU,IROW,ICOL,ISUM,LAR,JTK;KN=NUMBER/2
   10 FORMAT(7I3)
      READ(5,15)(ITIME(I),I=1,KN)
   15 FORMAT(8I5)
      READ(5,60) NH1,(KZ1(I),I=1,5);READ(5,60) NH2,(KZ2(I),I=1,5)
      READ(5,60) NH3,(KZ3(I),I=1,5);READ(5,60) NH4,(KZ4(I),I=1,5)
      READ(5,60) NH5,(KZ5(I),I=1,5);READ(5,60) NH6,(KZ6(I),I=1,5)
      READ(5,60) NH7,(KZ7(I),I=1,5);READ(5,60) NH8,(KZ8(I),I=1,5)
   40 FORMAT(12F6.1)
   60 FORMAT(6I3)
      DO 20 I=1,IROW,20 :READ(5,40)(TK(I,J),J=1,ICOL)
      DO 30 I=1,IROW,30 :READ(5,40)(TMD(I,J),J=1,ICOL)
      DO 35 I=1,IROW,35 :READ(5,40)(TMDA(I,J),J=1,ICOL)
C     ****
C     ****
C     **** IN ORDER TO IDENTIFY THE OBSERVATION POINTS ,A
C     **** MATRIX 'MESH(I,J)' ,WHICH IS ANALOGOUS TO THE MESH
C     **** OF POINTS ON THE REAL IMAGE PLANE IS GENERATED .
C     **** THIS MATRIX HAS THE LABLE OF THE OBSERVATION POINTS
C     **** AS WELL AS THEIR COORDINATE VALUES .
C     ****
C     ****
      DO 80 I=1,IROW;DO 70 J=1,ICOL;XMESH(I,J)=(48-4*I)
   70 YMESH(I,J)=(4*J-26);80 :CONTINUE;IROW1=IROW-1;ICOL1=ICOL-1
C     ****
C     ****
      WRITE(6,100);IY=0;DO 103 I=1,IROW;DO 101 J=1,ICOL
      TMD(I,J)=TMD(I,J)*1.7;TMDA(I,J)=TMD(I,J)*TK(I,J)/1000.0
  100 FORMAT('1',////,28X,'THICKNESS MEASUREMENT AND VOLUMETRIC',
     */,28X,'MASS DISTRIBUTION RESULTS :SAMPLE#38',/,16X,60('-'),
     */,16X,'*  CO-ORDINATES  * THICKNESS *',5X,'AREA',5X,'*  ',
     *'VOLUMETRIC  *',/,16X,'*',6X,'(MM)',6X,'*',11X,'*',
     *2(' MASS DENSITY *'),/,16X,'*',4X,'X',7X,'Y',3X,'* (MICRON',
     *'S) *',4X,'(GR/M2)   *',4X,'(KG/M3)   *',/,16X,'*',
     *16('-'),'*',11('-'),'*',2(14('-'),'*'))
      WRITE(6,102) XMESH(I,J),YMESH(I,J),TK(I,J),TMDA(I,J),
     .TMD(I,J);IY=IY+1;IF(IY.EQ.61.OR.IY.EQ.133.OR.IY.EQ.205.OR.
     .IY.EQ.277) WRITE(6,204);101 :CONTINUE;103 :CONTINUE
  102 FORMAT(' ',15X,'*',2(2X,F5.1),2X,'*',D10.3,' *',2(2X,D10.3,
     *2X,'*'))
      WRITE(6,128)(IPOS(I),I=1,60);WRITE(6,130)(IPOS(I),I=1,20)
      CALL STATIS(TK,AMN,BMN,IROW,ICOL,IROW,ICOL)
      SVAR(1,1)=AMN;SMEAN(1,1)=BMN
      CALL STATIS(TMDA,AMN,CMN,IROW,ICOL,IROW,ICOL)
      SVAR(1,2)=AMN;SMEAN(1,2)=CMN
      CALL STATIS(TMD,AMN,DMN,IROW,ICOL,IROW,ICOL)
      SVAR(1,3)=AMN;SMEAN(1,3)=DMN
```

```
      C
      C
      C
      C
   79       WRITE(6,105)(SMEAN(1,I),I=1,3);WRITE(6,106)(SVAR(1,I),I=1,3)
   81   105 FORMAT(' ',//,24X,'MEAN VALUE',D10.3,4X,D10.3,5X,D10.3)
   82   106 FORMAT(16X,'STANDARD DEVIATION',D10.3,4X,D10.3,5X,D10.3)
      C    ****
   83       DO 2222 NHLGRM=1,NUMBER
   84       READ(5,111) JDAT(NHLGRM),R1,R2,R3,ALPHA,BETA,EL
   85       READ(5,112) IS,ITK,IC,IP,JD,JS,JC,JP
   86   111 FORMAT(A4,3F6.1,2F6.3,F6.1)
   87   112 FORMAT(9I2)
      C    ****
      C    **** READING OF THE FRINGE NUMBERS :
      C    ****
   88       DO 114 I=1,IROW;READ(5,113)(F1(I,J),J=1,ICOL)
   90       READ(5,113)(F2(I,J),J=1,ICOL);READ(5,113)(F3(I,J),J=1,ICOL)
   92   113 FORMAT(12F6.3)
   93   114 CONTINUE
      C    ****
      C    **** CALCULATION OF THE COORDINATES OF THE TERMINAL
      C    **** POINTS ON THE SCANNING DIRECTIONS :
      C    ****
   94       X(1)=0.0;Y(1)=EL*COS(BETA);Z(1)=EL*SIN(BETA);X(2)=R1
   98       Y(2)=Y(1);Z(2)=Z(1);X(3)=0.5D0*R2;Y(3)=Y(1)-0.75D0*R2
  102       Z(3)=Z(1)+0.433D0*R2;X(4)=0.5D0*R3;Y(4)=Y(1)+0.75D0*R3
  105       Z(4)=Z(1)-0.433D0*R3
      C    ****
      C    **** IN THE FOLLOWING LOOP (LOOP 119) THE RECONSTRUCTION
      C    **** COORDINATES TRANSFORMATION MATRIX IS CONSTRUCTED
      C    **** FOR EACH INDIVIDUAL OBSERVATION POINT .THEN THE
      C    **** DEFORMATION VECTOR OF THAT POINT IS EVALUATED
      C    **** AND SAVED IN THE ARRAYS :XDEF(I,J),YDEF(I,J),
      C    **** ZDEF(I,J) ,WHERE INDICES I AND I ARE REFERRED TO
      C    **** THE LOCATION OF THE OBSERVATION POINT .
      C    ****
  106       DO 119 IM=1,IROW;DO 118 JM=1,ICOL;XOP=XMESH(IM,JM)
  109       YOP=YMESH(IM,JM);FN1=F1(IM,JM);FN2=F2(IM,JM);FN3=F3(IM,JM)
  113       CALL DEFORM(XOP,YOP,X,Y,Z,FN1,FN2,FN3,B,NHLGRM)
  114       XDEF(IM,JM)=B(1,1);YDEF(IM,JM)=B(2,1);118 :ZDEF(IM,JM)=
           -B(3,1);119 :CONTINUE
  118       IF(ITK.NE.0) CALL CHANGE(ZDEF,NHLGRM,TKNS,K2,IPOS,IROW,ICOL)
      C    ****
  119       IF(NOCUMU.EQ.0) GO TO 158
  120       WRITE(6,120) JDAT(NHLGRM),(IPOS(I),I=1,60),(IPOS(J),J=1,57)
  121   120 FORMAT('1',////,26X,'RECONSTRUCTION RESULTS OF ',
           *'INTERFEROGRAM',/,26X,A4,' OF THE NEWS-PRINT PAPER ',
           *'SAMPLE #38',//,30X,'(NON-CUMMULATIVE DEFORMATION)',//,
           *16X,60A1,/,16X,'*  CO-ORDINATES  *',14X,'DEFORMATIONS'
           *,15X,'*',/,16X,'*',4X,'X',7X,'Y',3X,'*',7X,'X',12X,'Y'
           *,12X,'Z',7X,'*',/,16X,'*',16A1,'*',41A1,'*')
  122       CALL STATIS(XDEF,VRNCE,AMEAN,IROW,ICOL,IROW,ICOL)
  123       STMEAN(1,NHLGRM)=AMEAN;STVAR(1,NHLGRM)=VRNCE
  125       CALL STATIS(YDEF,VRNCE,AMEAN,IROW,ICOL,IROW,ICOL)
  126       STMEAN(2,NHLGRM)=AMEAN;STVAR(2,NHLGRM)=VRNCE
  128       CALL STATIS(ZDEF,VRNCE,AMEAN,IROW,ICOL,IROW,ICOL)
  129       STMEAN(3,NHLGRM)=AMEAN;STVAR(3,NHLGRM)=VRNCE
  131       IY=0;DO 125 I=1,IROW;DO 123 J=1,ICOL
  134       WRITE(6,124) XMESH(I,J),YMESH(I,J),XDEF(I,J),YDEF(I,J)
           .,ZDEF(I,J);IY=IY+1;IF(IY.EQ.60.OR.IY.EQ.132.OR.IY.EQ.204
           -.OR.IY.EQ.276) WRITE(6,204);123 :CONTINUE
  138   124 FORMAT(' ',15X,'*',2(2X,F5.1),2X,'*',3(2X,D11.4),2X,'*')
  139   125 CONTINUE;WRITE(6,128)(IPOS(KNF),KNF=1,60)
  141       WRITE(6,126)(IPOS(I),I=1,20)
  142   126 FORMAT(' ',//,16X,'STATISTICAL RESULTS:',/,16X,20A1,//
           *,31X,'MEAN VALUE',5X,'STANDARD DEVIATION')
  143   129 WRITE(6,127)(KDAT(I),STMEAN(I,NHLGRM),STVAR(I,NHLGRM),I=1,3)
  144   127 FORMAT(' ',3(15X,A1,'-DIRECTION',2X,D11.3,4X,D11.3,/,1X))
  145   128 FORMAT(' ',15X,60A1)
  146   130 FORMAT(' ',//,16X,'STATISTICAL RESULTS:',/,16X,20A1)
  147       IF(JD.EQ.0) GO TO 132;BMN=STMEAN(1,NHLGRM)
  149       CMN=STMEAN(2,NHLGRM);DMN=STMEAN(3,NHLGRM)
  151       CALL HISTO(XDEF,BMN,IROW,ICOL,KZ1,NH1,IROW,ICOL)
  152       CALL HISTO(YDEF,CMN,IROW,ICOL,KZ2,NH2,IROW,ICOL)
  153       CALL HISTO(ZDEF,DMN,IROW,ICOL,KZ3,NH3,IROW,ICOL)
```

```
C
C
C
C
      IF(I2.EQ.0)  GO TO  139
  132 WRITE(6,133)  JDAT(NHLGRM),(IPOS(I),I=1,60),(IPOS(J),J=1,57)
  133 FORMAT('1',////,32X,'PROBABILITY DENSITIES OF THE',/,32X,
     *'DEFORMATION FIELD: PCINT ',A4,//,16X,60A1,/,16X,'*  CO-',
     *'ORDINATES  *',10X,'PROBABILITY DENSITIES',10X,'*',/,16X,
     *'*',4X,'X',7X,'Y',3X,'*',7X,'X',12X,'Y',12X,'Z',7X,'*',
     */,16X,'*',16A1,'*',41A1,'*')
      CALL PDENS(XDEF,YDEF,ZDEF,STVAR,STMEAN,XPD,YPD,ZPD,NHLGRM
     .,IROW,ICOL);IY=0;DO 135 I=1,IROW;DO 134 J=1,ICOL
      WRITE(6,124)  XMESH(I,J),YMESH(I,J),XPD(I,J),YPD(I,J)
     .ZPD(I,J);IY=IY+1;IF(IY.EQ.60.OR.IY.EQ.132.OR.IY.EQ.204.OR.
     .IY.EQ.276)  WRITE(6,204);134 :CONTINUE;135 :CONTINUE
      WRITE(6,128) (IPOS(KNF),KNF=1,60)
  139 IF(IS.EQ.0)  GO TO 205
      CALL STRAIN(XDEF,YDEF,STX,STY,IROW,ICOL)
      WRITE(6,140)  JDAT(NHLGRM),(IPOS(I1),I1=1,61),(IPOS(I2)
     .,I2=1,56);IY=0
  140 FORMAT('1',////,28X,'EVALUATED STRAIN FIELD AT POINT ',A4,
     *//,16X,61A1,/,16X,2('*ELEMENT*',4X,'EXX',7X,'EYY',4X),'*',
     */,16X,2('*',7A1,'*',21A1),'*')
      IROW2=(IROW+1/2)*2;DO 143 I=1,IROW2,2;DO 141 J=1,ICOL1;II=I+1
      WRITE(6,142)  I,J,STX(I,J),STY(I,J),II,J,STX(II,J),STY(II,J)
      IY=IY+1;IF(IY.EQ.63.OR.IY.EQ.135.OR.IY.EQ.207.OR.IY.EQ.
     .279)  WRITE(6,204);141 :CONTINUE
  142 FORMAT('  ',15X,2('* ',I2,',',I2,' * ',2(D9.2,1X)),'*')
  143 CONTINUE;IF(IROW2.EQ.IROW1) GO TO 146;DO 144 J=1,ICOL1
  144 WRITE(6,145)  IROW1,J,STX(IROW1,J),STY(IROW1,J)
  145 FORMAT('  ',15X,'* ',I2,',',I2,' * ',2(D9.2,1X),'*',7X,'*',
     *21X,'*')
  146 WRITE(6,147) (IPOS(I1),I1=1,61)
  147 FORMAT('  ',15X,61A1)
      CALL STATIS(STX,SXV,SXM,IROW,ICOL,IROW1,ICOL1)
      CALL STATIS(STY,SYV,SYM,IROW,ICOL,IROW1,ICOL1)
      SSM(1,NHLGRM)=SXM;SSM(2,NHLGRM)=SYM
      SSV(1,NHLGRM)=SXV;SSV(2,NHLGRM)=SYV
      WRITE(6,126) (IPOS(I),I=1,20);WRITE(6,148)  KDAT(4),SXM,SXV
      WRITE(6,148)  KDAT(5),SYM,SYV
  148 FORMAT('  ',16X,A2,'-STRAIN:',3X,D11.4,4X,D11.4)
      IF(JS.EQ.0)  GO TO 205
      CALL HISTO(STX,SXM,IROW,ICOL,KZ6,NH6,IROW1,ICOL1)
      CALL HISTO(STY,SYM,IROW,ICOL,KZ6,NH6,IROW1,ICOL1)
      GO TO 205
  158 NLR=(NHLGRM/2)*2;IF(NLR.EQ.NHLGRM)  LOR=2
      IF(NLR.NE.NHLGRM)  LOR=1
      WRITE(6,159)  JDAT(NHLGRM),(IPOS(I),I=1,60),(IPOS(J),J=1,57)
  159 FORMAT('1',////,26X,'RECONSTRUCTION RESULTS OF INTERFEROG'
     *,'RAM',/,26X,A4,'  OF THE NEWS-PRINT PAPER SAMPLE #38',/,
     *33X,'CUMMULATIVE DEFORMATION)',//,16X,60A1,/,16X,'*  CO-'
     *,'ORDINATES  *',14X,'DEFORMATIONS',15X,'*',/,16X,'*',4X,
     *'X',7X,'Y',3X,'*',7X,'X',12X,'Y',12X,'Z',7X,'*',/,16X,'*',
     *16A1,'*',41A1,'*')
      CALL CUMU(XDEF,YDEF,ZDEF,CCXD,CCYD,CCZD,NHLGRM,IROW,ICOL)
      DO 161 I=1,IROW;DO 160 J=1,ICOL;CXD(I,J)=CCXD(LOR,I,J)
      CYD(I,J)=CCYD(LOR,I,J);160 :CZD(I,J)=CCZD(LOR,I,J)
  161 CONTINUE
      CALL STATIS(CXD,VRNCE,AMEAN,IROW,ICOL,IROW,ICOL)
      STMEAN(1,NHLGRM)=AMEAN;STVAR(1,NHLGRM)=VRNCE
      CALL STATIS(CYD,VRNCE,AMEAN,IROW,ICOL,IROW,ICOL)
      STMEAN(2,NHLGRM)=AMEAN;STVAR(2,NHLGRM)=VRNCE
      CALL STATIS(CZD,VRNCE,AMEAN,IROW,ICOL,IROW,ICOL)
      STMEAN(3,NHLGRM)=AMEAN;STVAR(3,NHLGRM)=VRNCE
      IY=0;DO 163 I=1,IROW;DO 162 J=1,ICOL
      WRITE(6,124)  XMESH(I,J),YMESH(I,J),CXD(I,J),CYD(I,J)
     .CZD(I,J);IY=IY+1;IF(IY.EQ.60.OR.IY.EQ.132.OR.IY.EQ.204.OR.
     .IY.EQ.276)  WRITE(6,204);162 :CONTINUE;163 :CONTINUE;WRITE
     .(6,128) (IPOS(KNF),KNF=1,60);WRITE(6,126) (IPOS(I),I=1,20)
      WRITE(6,127) (KDAT(I),STMEAN(I,NHLGRM),STVAR(I,NHLGRM)
     .,I=1,3);IF(JD.EQ.0)  GO TO 165;BMN=STMEAN(1,NHLGRM)
      CALL HISTO(CXD,BMN,IROW,ICOL,KZ1,NH1,IROW,ICOL)
      CMN=STMEAN(2,NHLGRM);DMN=STMEAN(3,NHLGRM)
      CALL HISTO(CYD,CMN,IROW,ICOL,KZ2,NH2,IROW,ICOL)
      CALL HISTO(CZD,DMN,IROW,ICOL,KZ3,NH3,IROW,ICOL)
```

```
C
C
C
C
241       165 IF(IP.EQ.0) GO TO 170;CALL PDENS(CXD,CYD,CZD,STVAR,STMEAN
              .,XPD,YPD,ZPD,NHLGRM,IROW,ICOL)
243           WRITE(6,166) JDAT(NHLGRM),(IPOS(I),I=1,60),(IPOS(J),J=1,57)
244       166 FORMAT('1',////,32X,'PROBABILITY DENSITIES OF THE',//,32X,
              *'DEFORMATION FIELD;POINT ',A4,/,33X,'(CUMMULATIVE DEFORM'
              *,'ATION)',//,10X,60A1,/,16X,'*  CO-ORDINATES  *',10X,'PRO'
              *,'BABILITY DENSITIES',10X,'*',/,16X,'*',4X,'X',7X,'Y',3X,
              *'*',7X,'A',12X,'Y',12X,'Z',7X,'*',/,16X,'*',10A1,'*',41A1,'*')
245           IY=0;DO 168 I=1,IROW;DO 167 J=1,ICOL
248           WRITE(6,124) XMESH(I,J),YMESH(I,J),XPD(I,J),YPD(I,J),
              .ZPD(I,J);IY=IY+1;IF(IY.EQ.60.OR.IY.EQ.132.OR.IY.EQ.204.OR.
              .IY.EQ.276) WRITE(6,204);167 :CONTINUE;168 :CONTINUE;WRITE
              .(6,128)(IPOS(KNF),KNF=1,60)
254       170 IF(IS.EQ.0) GO TO 205
255           CALL STRAIN(CXD,CYD,STX,STY,IROW,ICOL);IY=0
257           WRITE(6,140) JDAT(NHLGRM),(IPOS(I1),I1=1,61),(IPOS(I2)
              .,I2=1,56);IROW2=(IROW1/2)*2;DO 172 I=1,IROW2,2;DO 171 J=1
              .,ICOL1;II=I+1
262           WRITE(6,142) I,J,STX(I,J),STY(I,J),II,J,STX(II,J),STY(II,J)
263           IY=IY+1;IF(IY.EQ.63.OR.IY.EQ.135.OR.IY.EQ.207.OR.IY.EQ.279)
              .WRITE(6,204);171 :CONTINUE
266       172 CONTINUE;IF(IROW2.EQ.IROW1) GO TO 174;DO 173 J=1,ICOL1
269       173 WRITE(6,145) IROW1,J,STX(IROW1,J),STY(IROW1,J)
270       174 WRITE(6,147)(IPOS(I1),I1=1,61)
271           CALL STATIS(STX,SXV,SXM,IROW,ICOL,IROW1,ICOL1)
272           CALL STATIS(STY,SYV,SYM,IROW,ICOL,IROW1,ICOL1)
273           SSM(1,NHLGRM)=SXM;SSM(2,NHLGRM)=SYM
275           SSV(1,NHLGRM)=SXV;SSV(2,NHLGRM)=SYV
277           WRITE(6,126)(IPOS(I),I=1,20);WRITE(6,148) KDAT(4),SXM,SXV
279           WRITE(6,148) KDAT(5),SYM,SYV;IF(JS.EQ.0) GO TO 205
281           CALL HISTO(STX,SXM,IROW,ICOL,KZ6,NH6,IROW1,ICOL1)
282           CALL HISTO(STY,SYM,IROW,ICOL,KZ6,NH6,IROW1,ICOL1)
283       203 FORMAT('1')
284       204 FORMAT('1',///)
285       205 NXY=NHLGRM/2;NYX=NXY*2;IF(NYX.EQ.NHLGRM) GO TO 248
288           DO 247 I=1,IROW1;DO 246 J=1,ICOL1;ARR3(I,J)=STX(I,J)
291       246 ARR4(I,J)=STY(I,J);247 :CONTINUE;GO TO 2222;248 :DO 250 I=
              .1,IROW1;DO 249 J=1,ICOL1;ARR3(I,J)=(ARR3(I,J)+STX(I,J))/
              .2.0;249 :ARR4(I,J)=(ARR4(I,J)+STY(I,J))/2.0;250 :CONTINUE
299           DO 262 I=1,IROW1;DO 255 J=1,ICOL1;ARR1(J)=TMD(I,J)
302       255 ARR2(J)=TKNS(I,J);CALL CROLAT(ARR1,ARR2,ICOL1,CRC)
304           COC(NXY,I,1)=CRC;DO 256 J=1,ICOL1;256 :ARR2(J)=ARR3(I,J)
307           CALL CROLAT(ARR1,ARR2,ICOL1,CRC);COC(NXY,I,6)=CRC
309           DO 257 J=1,ICOL1;257 :ARR2(J)=ARR4(I,J)
311           CALL CROLAT(ARR1,ARR2,ICOL1,CRC);COC(NXY,I,7)=CRC
313           DO 258 J=1,ICOL1;ARR1(J)=TKNS(I,J);258 :ARR2(J)=ARR3(I,J)
316           CALL CROLAT(ARR1,ARR2,ICOL1,CRC);COC(NXY,I,4)=CRC
318           DO 259 J=1,ICOL1;259 :ARR2(J)=ARR4(I,J)
320           CALL CROLAT(ARR1,ARR2,ICOL1,CRC);COC(NXY,I,5)=CRC
322           DO 260 J=1,ICOL1;260 :ARR1(J)=TMDA(I,J)
324           CALL CROLAT(ARR1,ARR2,ICOL1,CRC);COC(NXY,I,3)=CRC
326           DO 261 J=1,ICOL1;261 :ARR2(J)=ARR3(I,J)
328           CALL CROLAT(ARR1,ARR2,ICOL1,CRC);COC(NXY,I,2)=CRC
330       262 CONTINUE;DO 266 I1=1,IROW1;DO 265 I2=1,ICOL1;A1R(I1,I2)=
              .ARR3(I1,I2);265 :A2R(I1,I2)=TMD(I1,I2);266 :CONTINUE
336           CALL CROLI(A1R,A2R,CRC,IROW1,ICOL1);CC(NXY,6)=CRC
338           DO 268 I1=1,IROW1;DO 267 I2=1,ICOL1;267 :A1R(I1,I2)=ARR4(I1,I2)
341       268 CONTINUE;CALL CROLI(A1R,A2R,CRC,IROW1,ICOL1);CC(NXY,7)=CRC
344           DO 270 I1=1,IROW1;DO 269 I2=1,ICOL1;269 :A1R(I1,I2)=TKNS(I1,I2)
347       270 CONTINUE;CALL CROLI(A1R,A2R,CRC,IROW1,ICOL1);CC(NXY,1)=CRC
350           DO 272 I1=1,IROW1;DO 271 I2=1,ICOL1;271 :A2R(I1,I2)=ARR3(I1,I2)
353       272 CONTINUE;CALL CROLI(A1R,A2R,CRC,IROW1,ICOL1);CC(NXY,4)=CRC
356           DO 274 I1=1,IROW1;DO 273 I2=1,ICOL1;273 :A2R(I1,I2)=ARR4(I1,I2)
359       274 CONTINUE;CALL CROLI(A1R,A2R,CRC,IROW1,ICOL1);CC(NXY,5)=CRC
362           DO 276 I1=1,IROW1;DO 275 I2=1,ICOL1
364       275 A1R(I1,I2)=TMDA(I1,I2);276 :CONTINUE
366           CALL CROLI(A1R,A2R,CRC,IROW1,ICOL1);CC(NXY,3)=CRC
368           DO 278 I1=1,IROW1;DO 277 I2=1,ICOL1;277 :A2R(I1,I2)=ARR3(I1,I2)
371       278 CONTINUE;CALL CROLI(A1R,A2R,CRC,IROW1,ICOL1);CC(NXY,2)=CRC
374           DO 286 J=1,ICOL1;DO 279 I=1,IROW1;ARR1(I)=TMD(I,J)
377       279 ARR2(I)=TKNS(I,J);CALL CROLAT(ARR1,ARR2,IROW1,CRC)
379           CLC(NXY,J,1)=CRC;DO 280 I=1,IROW1;280 :ARR2(I)=ARR3(I,J)
```

```
C
C
C
382           CALL CROLAT(ARR1,ARR2,IROW1,CRC);CLC(NXY,J,6)=CRC
384           DO 281 I=1,IROW1;281 :ARR2(I)=ARR4(I,J)
386           CALL CROLAT(ARR1,ARR2,IROW1,CRC);CLC(NXY,J,7)=CRC
388           DO 282 I=1,IROW1;ARR1(I)=TKNS(I,J);282 :ARR2(I)=ARR3(I,J)
391           CALL CROLAT(ARR1,ARR2,IROW1,CRC);CLC(NXY,J,4)=CRC
393           DO 283 I=1,IROW1;283 :ARR2(I)=ARR4(I,J)
395           CALL CROLAT(ARR1,ARR2,IROW1,CRC);CLC(NXY,J,5)=CRC
397           DO 284 I=1,IROW1;284 :ARR1(I)=TMDA(I,J)
399           CALL CROLAT(ARR1,ARR2,IROW1,CRC);CLC(NXY,J,3)=CRC
401           DO 285 I=1,IROW1;285 :ARR2(I)=ARR3(I,J)
403           CALL CROLAT(ARR1,ARR2,IROW1,CRC);CLC(NXY,J,2)=CRC
405       286 CONTINUE;DO 288 I1=1,IROW1;DO 287 I2=1,ICOL1
408           TMD(I1,I2)=(TMD(I1,I2)*TK(I1,I2))/(TK(I1,I2)-TKNS(I1,I2))
409       287 TK(I1,I2)=TK(I1,I2)-TKNS(I1,I2);288 :CONTINUE
411      2222 CONTINUE;IF(ISUM.EQ.0) GO TO 3333
413           WRITE(6,210);WRITE(6,211);WRITE(6,212)(KDAT(I),I=1,3)
416       210 FORMAT('1',////,38X,'TABLES OF SUMMARY',/,38X,17('*'))
417       211 FORMAT(////,16X,'(I)  DEFORMATION FIELD :',/,16X,23('-'))
418       212 FORMAT(' ',15X,'MEAN VALUES',/,16X,'STANDARD DEVIATIONS',/,
     *16X,61('-'),/,16X,'*POINT*',3(3X,A1,'-DIRECTION',3X,'*'),
     */,16X,'*',5X,'*',3(4X,'R',7X,'L',4X,'*'),/,16X,'*',5('-'),
     *'*',3(17('-'),'*'))
419           N=0;DO 213 I=1,NUMBER,2;N=N+1;II=I+1;213 :WRITE(6,214) N,
     .(STMEAN(J,I),STMEAN(J,II),J=1,3),(STVAR(K,I),STVAR(K,II),
     .K=1,3);WRITE(6,215);IF(IP.EQ.0) GO TO 218
426       214 FORMAT(' ',15X,'*',I3,2X,'*',3(F7.2,F8.2,'  *'),/,16X,
     *'*',5X,'*',3(F7.2,F8.2,'  *'))
427       215 FORMAT(' ',15X,61('-'))
428           WRITE(6,216);WRITE(6,212)(KDAT(I),I=1,3)
430       216 FORMAT(////,16X,'(II)  PROBABILITY DENSITIES :',/,16X,28('-'))
431           N=0;DO 217 I=1,NUMBER,2;N=N+1;II=I+1;217 :WRITE(6,214) N,
     .(SMEAN(J,I),SMEAN(J,II),J=1,3),(SVAR(K,I),SVAR(K,II),K=1,3)
436           WRITE(6,215);218 :IF(IS.EQ.0) GO TO 223;WRITE(6,219) KDAT
     .(4),KDAT(5);N=0;DO 220 I=1,NUMBER,2;N=N+1;II=I+1
443       219 FORMAT('1',////,16X,'(III)  STRAIN FIELD :',/,16X,'MEAN V',
     *'ALUES',/,16X,'STANDARD DEVIATIONS',/,16X,53('-'),/,16X,
     *'* POINT *',2(6X,A2,'-STRAIN',6X,'*'),/,16X,'*',7X,'*',2(5X
     *,'R',9X,'L',5X,'*'),/,16X,'*',7('-'),'*',2(21('-'),'*'))
444       220 WRITE(6,221) N,(SSM(J,I),SSM(J,II),J=1,2),(SSV(K,I),
     .SSV(K,II),K=1,2);WRITE(6,222);223 :IF(LAR.EQ.0) GO TO 231
447       221 FORMAT(' ',15X,'*',I4,3X,'*',2(2D10.2,'  *'),/,16X,'*',7X,
     *'*',2(2D10.2,'  *'))
448       222 FORMAT(' ',15X,53('-'))
449           DO 225 I=1,3;DO 224 J=1,NUMBER,2;JJ=J+1;II=JJ/2
453           STMEAN(I,II)=(STMEAN(I,J)+STMEAN(I,JJ))/2.0D0
454           IF(I.EQ.3) GO TO 225
455       224 SSM(I,II)=(SSM(I,J)+SSM(I,JJ))/2.0D0;225 :CONTINUE
457           NHL=NUMBER/2;I=1;DO 226 J=2,NHL;JJ=J-1
461       226 SLOPE(I,J)=(SSM(I,J)-SSM(I,JJ))/FLOAT(ITIME(JJ))
462           SLOPE(1,1)=SLOPE(2,1)=0.0;WRITE(6,228)(KDAT(I),I=1,5)
464       228 FORMAT(////,16X,'(IV)  AVERAGED VALUES OF THE',/,21X,'TWO S',
     *'IDES:',///,16X,61('-'),/,16X,'*    *',6X,'DEFORMATION',7X,
     *2(8X,'STRAIN'),3X,'*',/,16X,'*',3X,'*',4X,3(A1,7X),1X,A2,
     *8X,A2,6X,'RATE',4X,'*',/,16X,'*---*',55('-'),'*')
465           DO 229 I=1,NHL;229 :WRITE(6,230) I,(STMEAN(J,I),J=1,3),
     .(SSM(K,I),K=1,2),SLOPE(1,I)
467       230 FORMAT(' ',15X,'*',I2,' *',F7.2,2F8.2,1X,3D10.2,' *')
468           WRITE(6,215)
469       231 IF(IC.EQ.0) GO TO 3333
470           KN=NUMBER/2
471           DO 236 I=1,KN
472           IM=ITIME(I)/60
473           IS=ITIME(I)-IM*60
474           KQ=(I/2)*2;IF(KQ.NE.I) WRITE(6,203)
476           WRITE(6,232) IM,IS,(IPOS(J),J=1,99)
477       232 FORMAT(' ',6(/),32X,'CORRELATION COEFFICIENTS',/,37X,
     *'AT TIME T=',I2,I3,//,20X,51A1,/,20X,'* ROW *',3('  VMD  ')
     *,2('   T   '),2('  BW  '),'*',/,20X,'*  NO.  *',
     *3('    EXX    EYY'),'  *',/,20X,'*',5A1,'*',43A1,'*')
478           DO 233 II=1,IROW1
479       233 WRITE(6,234) II,(COC(I,II,L),L=1,7)
480       234 FORMAT(' ',19X,'*',I3,' *',7F6.3,' *')
```

```
      C
      C
      C
      C
  481       WRITE(6,235)(IPOS(IX),IX=1,51)
  482   235 FORMAT(' ',19X,52A1)
  483       WRITE(6,237)(CC(I,J),J=1,7);236 :CONTINUE
  485   237 FORMAT(' ',//,20X,'ENTIRE',//,20X,'SAMPLE:',7F6.3)
  486       DO 240 I=1,KN;IM=ITIME(I)/60;IS=ITIME(I)-IM*60
  489       IF(I.EQ.1.OR.I.EQ.4.OR.I.EQ.7) WRITE(6,204)
  490       WRITE(6,238) IM,IS,(IPOS(J),J=1,99)
  491   238 FORMAT(' ',5(/),32X,'CORRELATION COEFFICIENTS',//,37X,
     *'AT TIME T=',I2,I3,//,20X,51A1,/,20X,'* COL *',3('  VMD ')
     *,2('   T   '),2('   BW  '),' *',/,20X,'* NO. *   T  ',
     *3('   EXX   EYY'),' *',/,20X,'*',5A1,'*',43A1,'*')
  492       DO 239 JJ=1,ICOL1;239 :WRITE(6,234) JJ,(CLC(I,JJ,L),L=1,7)
  494       WRITE(6,235)(IPOS(IX),IX=1,51);240 :CONTINUE
  496  3333 WRITE(6,203);STOP;END

  499       SUBROUTINE DEFORM(XOP,YOP,X,Y,Z,FN1,FN2,FN3,B,NHG)
  500       DIMENSION X(4),Y(4),Z(4),B(3,1),A(3,3),WKAREA(18)
  501       DIMENSION DL(4),DM(4),DN(4)
  502       DOUBLE PRECISION A,B,WKAREA
      C     ****
      C     **** CONSTRUCTION OF THE RECONSTRUCTION-COORDINATE
      C     **** TRANSFORMATION MATRIX .
      C     ****
  503       DO 300 I=1,4;TTT=SQRT((X(I)-XOP)**2+(Y(I)-YOP)**2+(Z(I))**2)
  505       DL(I)=(X(I)-XOP)/TTT;DM(I)=(Y(I)-YOP)/TTT;DN(I)=Z(I)/TTT
  508   300 CONTINUE;NH=(NHG/2)*2;DO 301 I=1,3;A(I,1)=DL(I+1)-DL(1)
  512       A(I,2)=DM(I+1)-DM(1);A(I,3)=DN(I+1)-DN(1)
  514       IF(NH.EQ.NHG) A(I,2)=-A(I,2);IF(NH.EQ.NHG) A(I,3)=-A(I,3)
  516   301 CONTINUE
      C     ****
      C     **** CONSTRUCTION OF THE FRINGE NUMBER VECTOR :
      C     ****
  517       B(1,1)=FN1*0.488D0;B(2,1)=FN2*0.488D0;B(3,1)=FN3*0.488D0
      C     ****
      C     **** SOLUTION OF THE DEFORMATION EVALUATION EQUATION :
      C     ****
  520       CALL LEQT2F(A,1,3,3,B,1,WKAREA,IER);RETURN;END

  523       SUBROUTINE STATIS(ARRAY,VRNCE,AMEAN,IR,IC,IR1,IC1)
  524       DIMENSION ARRAY(IR,IC)
  525       DOUBLE PRECISION VRNCE,AMEAN,ARRAY
  526       V=0.0D0;DO 401 I=1,IR1;DO 400 J=1,IC1;400 :V=V+ARRAY(I,J)
  530   401 CONTINUE;AMEAN=V/FLOAT(IR1*IC1);V=0.0D0;DO 403 I=1,IR1
  534       DO 402 J=1,IC1;402 :V=(ARRAY(I,J)-AMEAN)**2+V;403 :CONTINUE
  537       VRNCE=SQRT(V/FLOAT(IR1*IC1));RETURN;END

  540       SUBROUTINE PDENS(XDEF,YDEF,ZDEF,STVAR,STMEAN,XPD,YPD,
     .ZPD,INT,IR,IC)
  541       DIMENSION XDEF(IR,IC),YDEF(IR,IC),ZDEF(IR,IC),STVAR(3,16)
  542       DIMENSION XPD(IR,IC),YPD(IR,IC),ZPD(IR,IC),STMEAN(3,16)
  543       DOUBLE PRECISION XDEF,YDEF,ZDEF,STVAR,STMEAN,XPD,YPD,ZPD
      C     ****
  544       PIE=3.1415;DO 451 I=1,IR;DO 450 J=1,IC
  547       XPD(I,J)=(1.0D0/(SQRT(2*PIE)*STVAR(1,INT)))*DEXP(-((XDEF
     .(I,J)-STMEAN(1,INT))**2)/(2*STVAR(1,INT)**2))
  548       YPD(I,J)=(1.0D0/(SQRT(2*PIE)*STVAR(2,INT)))*DEXP(-((YDEF
     .(I,J)-STMEAN(2,INT))**2)/(2*STVAR(2,INT)**2))
  549       ZPD(I,J)=(1.0D0/(SQRT(2*PIE)*STVAR(3,INT)))*DEXP(-((ZDEF
     .(I,J)-STMEAN(3,INT))**2)/(2*STVAR(3,INT)**2));450 :CONTINUE
  551   451 CONTINUE;RETURN;END

  554       SUBROUTINE CUMU(XDEF,YDEF,ZDEF,CCXD,CCYD,CCZD,NN,IR,IC)
      C     ****
  555       DIMENSION XDEF(IR,IC),YDEF(IR,IC),ZDEF(IR,IC)
  556       DIMENSION CCXD(2,IR,IC),CCYD(2,IR,IC),CCZD(2,IR,IC)
  557       DOUBLE PRECISION XDEF,YDEF,ZDEF,CCXD,CCYD,CCZD
  558       IF(NN.NE.1.AND.NN.NE.2) GO TO 540;IF(NN.NE.1) GO TO 510
      C
```

```
      C
      C
      C
560         DO 505 I=1,IR;DO 500 J=1,IC;500 :CCXD(1,I,J)=CCYD(1,I,J)=
           .CCZD(1,I,J)=0.0D0;505 :CONTINUE;GO TO 540;510 :DO 530 I=1,IR
566         DO 520 J=1,IC;520 :CCXD(2,I,J)=CCYD(2,I,J)=CCZD(2,I,J)=0.0D0
568     530 CONTINUE;540 :N=(NN/2)*2;IF(N.EQ.NN) GO TO 570;DO 560 I=1,IR
572         DO 550 J=1,IC;CCXD(1,I,J)=CCXD(1,I,J)+XDEF(I,J)
574         CCYD(1,I,J)=CCYD(1,I,J)+YDEF(I,J);550 :CCZD(1,I,J)=CCZD(1,
           .I,J)+ZDEF(I,J);560 :CONTINUE;RETURN;570 :DO 590 I=1,IR
579         DO 580 J=1,IC;CCXD(2,I,J)=CCXD(2,I,J)+XDEF(I,J)
581         CCYD(2,I,J)=CCYD(2,I,J)+YDEF(I,J);580 :CCZD(2,I,J)=
           .CCZD(2,I,J)+ZDEF(I,J);590 :CONTINUE;RETURN;END


586         SUBROUTINE STRAIN(XDEF,YDEF,STX,STY,IR,IC)
      C     ****
587         DIMENSION XDEF(IR,IC),YDEF(IR,IC),STX(IR,IC),STY(IR,IC)
588         DOUBLE PRECISION XDEF,YDEF,STX,STY
      C     ****
      C     **** THE STRAIN TENSOR EVALUATED AS FOLLOWS IS BASED ON
      C     **** THE CAUCHY STRAIN CONCEPT :
      C     ****     STRAIN(I,J)=(DU(I)/DX(J)+DU(J)/DX(I))/2
      C     **** HOWEVER ,THE EVALUATION IS DONE BY A FINITE
      C     **** DIFFERENCE TECHNIQUE .
      C     ****
589         IR1=IR-1;IC1=IC-1;DO 710 I=1,IR1;DO 700 J=1,IC1
593         STX(I,J)=(XDEF(I,J)-XDEF(I+1,J))/4000.0D0
594     700 STY(I,J)=(YDEF(I,J)-YDEF(I,J+1))/4000.0D0
595     710 CONTINUE;RETURN;END


598         SUBROUTINE CHANGE(ZDEF,NHLGRM,TKNS,K2,IPOS,IR,IC)
      C     ****
599         DIMENSION ZDEF(IR,IC),TKNS(IR,IC),IPOS(70)
600         DOUBLE PRECISION ZDEF,TKNS
      C     ****
601         K1=NHLGRM/2;K2=K1*2;IF(K2.EQ.NHLGRM) GO TO 915
604         DO 910 I=1,IR;DO 905 J=1,IC;905 :TKNS(I,J)=ZDEF(I,J)
607     910 CONTINUE;RETURN;915 :DO 925 I=1,IR;DO 920 J=1,IC
611     920 TKNS(I,J)=TKNS(I,J)+ZDEF(I,J);925 :CONTINUE
613         WRITE(6,928)
614     928 FORMAT('1',////,28X,'EVALUATED THICKNESS CHANGES (MICRONS)')
615         JS=1;ICA=IC/6;ICB=IC-ICA*6;DO 942 I=1,ICA;JE=6*I
620         IF(I.NE.1) GO TO 934;WRITE(6,932) JS,JE,(IPOS(I1)
           .,I1=1,59),(J1,J1=JS,JE),(IPOS(I2),I2=1,56)
622     932 FORMAT(' ',39X,'(COLUMNS:',I2,'-',I2,')',/,17X,59A1,/,17
           *X,'*',6X,'*',4X,I2,5(6X,I2),4X,'*',/,17X,'*',6A1,'*',
           *50A1,'*')
623         GO TO 938;934 :WRITE(6,936)JS,JE,(IPOS(I1),I1=1,59),
           .(J1,J1=JS,JE),(IPOS(I2),I2=1,56)
625     936 FORMAT('1',16X,'*',21X,'(COLUMNS:',I2,'-',I2,')',21X,'*',/,
           *17X,59A1,/,17X,'*',6X,'*',4X,I2,5(6X,I2),4X,'*',/,17X,
           *'*',6A1,'*',50A1,'*')
626     938 DO 939 II=1,IR;939 :WRITE(6,940) II,(TKNS(II,JJ),JJ=JS,JE)
628     940 FORMAT(' ',16X,'*',I2,'*',6(2X,F6.2),'*')
629         WRITE(6,948)(IPOS(I1),I1=1,59)
630     942 JS=JS+6;IF(ICB.EQ.0) RETURN;JE=JE+ICB;JG=JE+6;JS=JS+6
635     948 FORMAT('1',16X,59A1)
636         WRITE(6,936) JE,JF,(IPOS(I1),I1=1,59),(J1,J1=JS,JG),(IPOS(I
           .2),I2=1,59);DO 944 II=1,IR;944 :WRITE(6,940) II,(TKNS(II,
           .JJ),JJ=JE,JF);SETURN;END


641         SUBROUTINE HISTO(AR,AMN,IR,IC,KZ,NH,IR1,IC1)
      C     ****
642         DIMENSION AR(IR,IC),KZ(5),NF(11)
643         DOUBLE PRECISION AR,AMN
644         WRITE(6,959);AMAX=0.0;DO 952 I=1,IR1;DO 951 J=1,IC1
648         AR(I,J)=AR(I,J)-AMN;951 :IF(DABS(AR(I,J)).GT.AMAX) AMAX=
           .DABS(AR(I,J));952 :CONTINUE;DO 960 I=1,NH;N=KZ(I);STEP=
           .AMAX/FLOAT(N);BMIN=-AMAX;BMAX=BMIN+STEP;M=N*2;DO 953 J=1,M
658     953 NF(J)=0;DO 956 J=1,M;DO 955 I1=1,IR1;DO 954 I2=1,IC1
662     954 IF(AR(I1,I2).GT.BMIN.AND.AR(I1,I2).LE.BMAX) NF(J)=NF(J)+1
663     955 CONTINUE;BMIN=BMAX;956 :BMAX=BMAX+STEP;WRITE(6,957) STEP,
           .(NF(I3),I3=1,N)
```

```
667      955 CONTINUE;BMIN=BMAX;956 :BMAX=BMAX+STEP;WRITE(6,957) STEP,
            -(NF(I3),I3=1,N)
C
C
C
671      957 FORMAT(' ',15X,'STEP SIZE= ',D11.4,6X,6I4)
672          NX=N+1;WRITE(6,958) (NF(I4),I4=NX,M)
674      958 FORMAT(' ',43X,6I4)
675      959 FORMAT(' ',15X,'FREQUENCY AROUND MEAN:',/,16X,22('-'))
676      960 CONTINUE;RETURN;END

679          SUBROUTINE CROLAT(ARR1,ARR2,N,CRC)
680          DIMENSION ARR1(N),ARR2(N)
681          DOUBLE PRECISION ARR1,ARR2
682          A1=A2=V1=V2=A=0.0;DO 970 I=1,N;A1=A1+ARR1(I)
685      970 A2=A2+ARR2(I);A1=A1/FLOAT(N);A2=A2/FLOAT(N);DO 971 I=1,N
689          V1=V1+(ARR1(I)-A1)**2;V2=V2+(ARR2(I)-A2)**2
691      971 A=A+(ARR1(I)-A1)*(ARR2(I)-A2);CRC=A/SQRT(V1*V2);RETURN;END

695          SUBROUTINE CROLI(A1R,A2R,CRC,L1,L2)
696          DIMENSION A1R(L1,L2),A2R(L1,L2)
697          DOUBLE PRECISION A1R,A2R
698          B1=B2=B=V1=V2=0.0;DO 981 I=1,L1;DO 980 J=1,L2
701          B1=B1+A1R(I,J);980 :B2=B2+A2R(I,J);981 :CONTINUE
704          B1=B1/FLOAT(L1*L2);B2=B2/FLOAT(L1*L2);DO 983 I=1,L1
707          DO 982 J=1,L2;982 :B=B+(A1R(I,J)-B1)*(A2R(I,J)-B2)
709      983 CONTINUE;DO 985 I=1,L1;DO 984 J=1,L2;V1=V1+((A1R(I,J)-B1)**2)
713      984 V2=V2+((A2R(I,J)-B2)**2);985 :CONTINUE
715          CRC=B/SQRT(V1*V2);RETURN;END

     $DATA
```

THICKNESS MEASUREMENT AND VOLUMETRIC MASS DISTRIBUTION RESULTS ;SAMPLE# 38

CO-ORDINATES (MM) X	Y	THICKNESS (MICRONS)	AREA MASS DENSITY (GR/M2)	VOLUMETRIC MASS DENSITY (KG/M3)
44.0	-22.0	0.825D 02	0.657D 02	0.796D 03
44.0	-18.0	0.797D 02	0.679D 02	0.851D 03
44.0	-14.0	0.797D 02	0.590D 02	0.741D 03
44.0	-10.0	0.949D 02	0.698D 02	0.735D 03
44.0	-6.0	0.932D 02	0.710D 02	0.762D 03
44.0	-2.0	0.858D 02	0.658D 02	0.767D 03
44.0	2.0	0.925D 02	0.501D 02	0.541D 03
44.0	6.0	0.875D 02	0.716D 02	0.819D 03
44.0	10.0	0.890D 02	0.591D 02	0.664D 03
44.0	14.0	0.921D 02	0.650D 02	0.705D 03
44.0	18.0	0.894D 02	0.715D 02	0.799D 03
44.0	22.0	0.808D 02	0.678D 02	0.839D 03
40.0	-22.0	0.808D 02	0.677D 02	0.838D 03
40.0	-18.0	0.793D 02	0.657D 02	0.829D 03
40.0	-14.0	0.856D 02	0.658D 02	0.768D 03
40.0	-10.0	0.956D 02	0.687D 02	0.719D 03
40.0	-6.0	0.896D 02	0.643D 02	0.717D 03
40.0	-2.0	0.938D 02	0.590D 02	0.629D 03
40.0	2.0	0.905D 02	0.754D 02	0.833D 03
40.0	6.0	0.894D 02	0.701D 02	0.784D 03
40.0	10.0	0.824D 02	0.638D 02	0.775D 03
40.0	14.0	0.994D 02	0.820D 02	0.824D 03
40.0	18.0	0.834D 02	0.578D 02	0.693D 03
40.0	22.0	0.847D 02	0.704D 02	0.831D 03
36.0	-22.0	0.842D 02	0.594D 02	0.706D 03
36.0	-18.0	0.875D 02	0.613D 02	0.700D 03
36.0	-14.0	0.800D 02	0.529D 02	0.662D 03
36.0	-10.0	0.898D 02	0.561D 02	0.625D 03
36.0	-6.0	0.721D 02	0.502D 02	0.696D 03
36.0	-2.0	0.870D 02	0.723D 02	0.831D 03
36.0	2.0	0.934D 02	0.725D 02	0.776D 03
36.0	6.0	0.897D 02	0.662D 02	0.738D 03
36.0	10.0	0.904D 02	0.695D 02	0.768D 03
36.0	14.0	0.865D 02	0.595D 02	0.688D 03
36.0	18.0	0.841D 02	0.634D 02	0.754D 03
36.0	22.0	0.825D 02	0.578D 02	0.701D 03
32.0	-22.0	0.842D 02	0.706D 02	0.839D 03
32.0	-18.0	0.797D 02	0.530D 02	0.666D 03
32.0	-14.0	0.827D 02	0.475D 02	0.575D 03
32.0	-10.0	0.881D 02	0.688D 02	0.781D 03
32.0	-6.0	0.837D 02	0.664D 02	0.793D 03
32.0	-2.0	0.875D 02	0.534D 02	0.610D 03
32.0	2.0	0.910D 02	0.747D 02	0.821D 03
32.0	6.0	0.863D 02	0.730D 02	0.846D 03
32.0	10.0	0.853D 02	0.557D 02	0.653D 03
32.0	14.0	0.919D 02	0.608D 02	0.661D 03
32.0	18.0	0.870D 02	0.589D 02	0.677D 03
32.0	22.0	0.942D 02	0.689D 02	0.731D 03
28.0	-22.0	0.842D 02	0.706D 02	0.838D 03
28.0	-18.0	0.877D 02	0.563D 02	0.642D 03
28.0	-14.0	0.831D 02	0.595D 02	0.716D 03
28.0	-10.0	0.964D 02	0.715D 02	0.742D 03
28.0	-6.0	0.833D 02	0.700D 02	0.840D 03
28.0	-2.0	0.766D 02	0.627D 02	0.819D 03
28.0	2.0	0.927D 02	0.615D 02	0.664D 03
28.0	6.0	0.868D 02	0.605D 02	0.697D 03
28.0	10.0	0.921D 02	0.644D 02	0.699D 03
28.0	14.0	0.894D 02	0.698D 02	0.781D 03
28.0	18.0	0.882D 02	0.545D 02	0.618D 03
28.0	22.0	0.947D 02	0.687D 02	0.726D 03
24.0	-22.0	0.847D 02	0.611D 02	0.721D 03

24.	-18.	0.751D 02	0.495D 02	0.660D 03
24.	-14.	0.877D 02	0.526D 02	0.599D 03
24.	-10.	0.932D 02	0.624D 02	0.670D 03
24.	-6.	0.920D 02	0.571D 02	0.621D 03
24.	-2.	0.853D 02	0.587D 02	0.688D 03
24.	2.	0.927D 02	0.573D 02	0.618D 03
24.	6.	0.834D 02	0.586D 02	0.702D 03
24.	10.	0.848D 02	0.623D 02	0.734D 03
24.	14.	0.824D 02	0.629D 02	0.764D 03
24.	18.	0.880D 02	0.540D 02	0.614D 03
24.	22.	0.908D 02	0.681D 02	0.750D 03
20.	-22.	0.908D 02	0.636D 02	0.701D 03
20.	-18.	0.851D 02	0.686D 02	0.806D 03
20.	-14.	0.902D 02	0.679D 02	0.752D 03
20.	-10.	0.934D 02	0.540D 02	0.578D 03
20.	-6.	0.854D 02	0.529D 02	0.620D 03
20.	-2.	0.814D 02	0.685D 02	0.842D 03
20.	2.	0.837D 02	0.635D 02	0.759D 03
20.	6.	0.887D 02	0.646D 02	0.728D 03
20.	10.	0.817D 02	0.663D 02	0.812D 03
20.	14.	0.928D 02	0.715D 02	0.770D 03
20.	18.	0.911D 02	0.656D 02	0.721D 03
20.	22.	0.947D 02	0.564D 02	0.596D 03
16.	-22.	0.915D 02	0.706D 02	0.771D 03
16.	-18.	0.887D 02	0.617D 02	0.695D 03
16.	-14.	0.834D 02	0.546D 02	0.654D 03
16.	-10.	0.927D 02	0.562D 02	0.606D 03
16.	-6.	0.871D 02	0.565D 02	0.649D 03
16.	-2.	0.877D 02	0.719D 02	0.820D 03
16.	2.	0.896D 02	0.693D 02	0.774D 03
16.	6.	0.911D 02	0.463D 02	0.509D 03
16.	10.	0.907D 02	0.594D 02	0.654D 03
16.	14.	0.919D 02	0.694D 02	0.755D 03
16.	18.	0.848D 02	0.505D 02	0.595D 03
16.	22.	0.922D 02	0.719D 02	0.780D 03
12.	-22.	0.816D 02	0.617D 02	0.756D 03
12.	-18.	0.856D 02	0.609D 02	0.711D 03
12.	-14.	0.788D 02	0.448D 02	0.569D 03
12.	-10.	0.876D 02	0.672D 02	0.767D 03
12.	-6.	0.825D 02	0.642D 02	0.779D 03
12.	-2.	0.882D 02	0.535D 02	0.606D 03
12.	2.	0.925D 02	0.586D 02	0.633D 03
12.	6.	0.870D 02	0.584D 02	0.671D 03
12.	10.	0.827D 02	0.696D 02	0.841D 03
12.	14.	0.938D 02	0.655D 02	0.699D 03
12.	18.	0.904D 02	0.568D 02	0.628D 03
12.	22.	0.917D 02	0.600D 02	0.655D 03
8.	-22.	0.852D 02	0.645D 02	0.756D 03
8.	-18.	0.868D 02	0.694D 02	0.799D 03
8.	-14.	0.793D 02	0.581D 02	0.733D 03
8.	-10.	0.833D 02	0.637D 02	0.765D 03
8.	-6.	0.901D 02	0.755D 02	0.838D 03
8.	-2.	0.887D 02	0.696D 02	0.784D 03
8.	2.	0.869D 02	0.666D 02	0.766D 03
8.	6.	0.875D 02	0.693D 02	0.792D 03
8.	10.	0.836D 02	0.566D 02	0.677D 03
8.	14.	0.950D 02	0.519D 02	0.546D 03
8.	18.	0.858D 02	0.504D 02	0.587D 03
8.	22.	0.845D 02	0.677D 02	0.801D 03
4.	-22.	0.830D 02	0.530D 02	0.638D 03
4.	-18.	0.904D 02	0.587D 02	0.649D 03
4.	-14.	0.861D 02	0.650D 02	0.755D 03
4.	-10.	0.905D 02	0.635D 02	0.702D 03
4.	-6.	0.760D 02	0.589D 02	0.775D 03
4.	-2.	0.873D 02	0.524D 02	0.601D 03
4.	2.	0.917D 02	0.608D 02	0.663D 03
4.	6.	0.747D 02	0.503D 02	0.673D 03
4.	10.	0.897D 02	0.613D 02	0.683D 03
4.	14.	0.916D 02	0.721D 02	0.787D 03
4.	18.	0.953D 02	0.635D 02	0.667D 03
0.	-22.	0.874D 02	0.675D 02	0.772D 03
		0.874D 02	0.530D 02	0.603D 03

0.0	-18.0	0.822D 02	0.629D 02	0.765D 03
0.0	-14.0	0.856D 02	0.544D 02	0.635D 03
0.0	-10.0	0.794D 02	0.611D 02	0.770D 03
0.0	-6.0	0.910D 02	0.744D 02	0.818D 03
0.0	-2.0	0.894D 02	0.664D 02	0.743D 03
0.0	2.0	0.833D 02	0.644D 02	0.773D 03
0.0	6.0	0.894D 02	0.751D 02	0.840D 03
0.0	10.0	0.914D 02	0.645D 02	0.705D 03
0.0	14.0	0.933D 02	0.686D 02	0.735D 03
0.0	18.0	0.902D 02	0.612D 02	0.678D 03
0.0	22.0	0.876D 02	0.733D 02	0.837D 03
-4.0	-22.0	0.816D 02	0.597D 02	0.731D 03
-4.0	-18.0	0.861D 02	0.734D 02	0.853D 03
-4.0	-14.0	0.880D 02	0.708D 02	0.804D 03
-4.0	-10.0	0.867D 02	0.735D 02	0.848D 03
-4.0	-6.0	0.886D 02	0.672D 02	0.758D 03
-4.0	-2.0	0.861D 02	0.539D 02	0.626D 03
-4.0	2.0	0.854D 02	0.581D 02	0.680D 03
-4.0	6.0	0.814D 02	0.539D 02	0.662D 03
-4.0	10.0	0.894D 02	0.607D 02	0.678D 03
-4.0	14.0	0.945D 02	0.684D 02	0.724D 03
-4.0	18.0	0.902D 02	0.615D 02	0.682D 03
-4.0	22.0	0.847D 02	0.682D 02	0.805D 03
-8.0	-22.0	0.884D 02	0.730D 02	0.826D 03
-8.0	-18.0	0.899D 02	0.648D 02	0.721D 03
-8.0	-14.0	0.756D 02	0.537D 02	0.710D 03
-8.0	-10.0	0.862D 02	0.613D 02	0.711D 03
-8.0	-6.0	0.862D 02	0.652D 02	0.756D 03
-8.0	-2.0	0.931D 02	0.600D 02	0.644D 03
-8.0	2.0	0.794D 02	0.557D 02	0.701D 03
-8.0	6.0	0.810D 02	0.534D 02	0.659D 03
-8.0	10.0	0.865D 02	0.680D 02	0.786D 03
-8.0	14.0	0.960D 02	0.624D 02	0.650D 03
-8.0	18.0	0.914D 02	0.754D 02	0.825D 03
-8.0	22.0	0.787D 02	0.570D 02	0.724D 03
-12.0	-22.0	0.837D 02	0.483D 02	0.576D 03
-12.0	-18.0	0.819D 02	0.649D 02	0.792D 03
-12.0	-14.0	0.739D 02	0.572D 02	0.773D 03
-12.0	-10.0	0.862D 02	0.722D 02	0.837D 03
-12.0	-6.0	0.787D 02	0.560D 02	0.711D 03
-12.0	-2.0	0.836D 02	0.698D 02	0.835D 03
-12.0	2.0	0.859D 02	0.729D 02	0.849D 03
-12.0	6.0	0.836D 02	0.537D 02	0.643D 03
-12.0	10.0	0.885D 02	0.693D 02	0.783D 03
-12.0	14.0	0.887D 02	0.656D 02	0.740D 03
-12.0	18.0	0.807D 02	0.638D 02	0.790D 03
-12.0	22.0	0.867D 02	0.706D 02	0.815D 03
-16.0	-22.0	0.765D 02	0.564D 02	0.737D 03
-16.0	-18.0	0.824D 02	0.672D 02	0.816D 03
-16.0	-14.0	0.802D 02	0.465D 02	0.580D 03
-16.0	-10.0	0.714D 02	0.402D 02	0.563D 03
-16.0	-6.0	0.854D 02	0.699D 02	0.819D 03
-16.0	-2.0	0.868D 02	0.681D 02	0.785D 03
-16.0	2.0	0.850D 02	0.686D 02	0.806D 03
-16.0	6.0	0.805D 02	0.620D 02	0.771D 03
-16.0	10.0	0.865D 02	0.612D 02	0.707D 03
-16.0	14.0	0.822D 02	0.621D 02	0.756D 03
-16.0	18.0	0.894D 02	0.750D 02	0.838D 03
-16.0	22.0	0.917D 02	0.690D 02	0.752D 03
-20.0	-22.0	0.743D 02	0.550D 02	0.740D 03
-20.0	-18.0	0.839D 02	0.650D 02	0.775D 03
-20.0	-14.0	0.800D 02	0.538D 02	0.672D 03
-20.0	-10.0	0.789D 02	0.554D 02	0.702D 03
-20.0	-6.0	0.782D 02	0.635D 02	0.811D 03
-20.0	-2.0	0.778D 02	0.568D 02	0.730D 03
-20.0	2.0	0.767D 02	0.630D 02	0.822D 03
-20.0	6.0	0.771D 02	0.601D 02	0.779D 03
-20.0	10.0	0.771D 02	0.649D 02	0.842D 03
-20.0	14.0	0.778D 02	0.502D 02	0.646D 03
		0.894D 02	0.554D 02	0.620D 03
		0.818D 02	0.620D 02	0.758D 03

-24.0	-18.0	0.810D 02	0.553D 02	0.682D 03
-24.0	-14.0	0.751D 02	0.624D 02	0.831D 03
-24.0	-10.0	0.794D 02	0.632D 02	0.796D 03
-24.0	-6.0	0.869D 02	0.737D 02	0.848D 03
-24.0	-2.0	0.742D 02	0.572D 02	0.771D 03
-24.0	2.0	0.869D 02	0.628D 02	0.722D 03
-24.0	6.0	0.834D 02	0.709D 02	0.850D 03
-24.0	10.0	0.814D 02	0.658D 02	0.808D 03
-24.0	14.0	0.875D 02	0.716D 02	0.818D 03
-24.0	18.0	0.911D 02	0.773D 02	0.848D 03
-24.0	22.0	0.913D 02	0.707D 02	0.774D 03
-28.0	-22.0	0.791D 02	0.524D 02	0.662D 03
-28.0	-18.0	0.819D 02	0.509D 02	0.622D 03
-28.0	-14.0	0.802D 02	0.527D 02	0.657D 03
-28.0	-10.0	0.741D 02	0.528D 02	0.713D 03
-28.0	-6.0	0.750D 02	0.500D 02	0.667D 03
-28.0	-2.0	0.834D 02	0.696D 02	0.835D 03
-28.0	2.0	0.791D 02	0.597D 02	0.754D 03
-28.0	6.0	0.822D 02	0.588D 02	0.715D 03
-28.0	10.0	0.817D 02	0.542D 02	0.663D 03
-28.0	14.0	0.868D 02	0.535D 02	0.617D 03
-28.0	18.0	0.916D 02	0.653D 02	0.713D 03
-28.0	22.0	0.891D 02	0.660D 02	0.741D 03
-32.0	-22.0	0.757D 02	0.562D 02	0.743D 03
-32.0	-18.0	0.824D 02	0.651D 02	0.790D 03
-32.0	-14.0	0.759D 02	0.571D 02	0.752D 03
-32.0	-10.0	0.835D 02	0.696D 02	0.833D 03
-32.0	-6.0	0.852D 02	0.703D 02	0.825D 03
-32.0	-2.0	0.771D 02	0.569D 02	0.738D 03
-32.0	2.0	0.762D 02	0.591D 02	0.775D 03
-32.0	6.0	0.749D 02	0.548D 02	0.732D 03
-32.0	10.0	0.797D 02	0.630D 02	0.790D 03
-32.0	14.0	0.829D 02	0.689D 02	0.831D 03
-32.0	18.0	0.701D 02	0.534D 02	0.761D 03
-32.0	22.0	0.874D 02	0.501D 02	0.573D 03

STATISTICAL RESULTS:

MEAN VALUE	0.856D 02	0.624D 02	0.731D 03
STANDARD DEVIATION	0.555D 01	0.732D 01	0.777D 02

RECONSTRUCTION RESULTS OF INTERFEROGRAM
(1R) OF THE NEWS-PRINT PAPER SAMPLE #38
CUMMULATIVE DEFORMATION)

CO-ORDINATES X	CO-ORDINATES Y	DEFORMATIONS X	DEFORMATIONS Y	DEFORMATIONS Z
44.0	-22.0	0.1311D 02	-0.1639D 02	0.3054D 01
44.0	-18.0	0.1306D 02	0.1993D 02	0.4319D 01
44.0	-14.0	0.1329D 02	-0.1610D 02	-0.1627D 01
44.0	-10.0	0.1293D 02	0.1461D 02	0.7541D 01
44.0	-6.0	0.1304D 02	0.1866D 02	0.4884D 01
44.0	-2.0	0.1386D 02	0.9608D 01	-0.1596D 02
44.0	2.0	0.1379D 02	-0.2260D 02	-0.1414D 02
44.0	6.0	0.1342D 02	0.6510D 01	-0.4829D 01
44.0	10.0	0.1384D 02	-0.1599D 02	-0.1526D 02
44.0	14.0	0.1343D 02	-0.2150D 01	-0.4864D 01
44.0	18.0	0.1282D 02	-0.1264D 02	0.1061D 02
44.0	22.0	0.1392D 02	0.2098D 01	-0.1749D 02
40.0	-22.0	0.1262D 02	0.1407D 02	0.9196D 01
40.0	-18.0	0.1294D 02	-0.1219D 01	0.1029D 01
40.0	-14.0	0.1371D 02	-0.1624D 02	-0.1835D 02
40.0	-10.0	0.1328D 02	-0.2076D 02	-0.7544D 01
40.0	-6.0	0.1373D 02	0.3747D 01	-0.1898D 02
40.0	-2.0	0.1348D 02	0.2575D 01	-0.1250D 02
40.0	2.0	0.1301D 02	-0.7715D 01	-0.6976D 00
40.0	6.0	0.1334D 02	-0.2125D 02	-0.9107D 01
40.0	10.0	0.1281D 02	-0.1852D 02	0.4324D 01
40.0	14.0	0.1310D 02	-0.6648D 01	-0.2914D 01
40.0	18.0	0.1307D 02	0.1351D 02	-0.2507D 01
40.0	22.0	0.1265D 02	-0.1344D 01	-0.1678D 02
36.0	-22.0	0.1298D 02	0.2187D 01	0.2359D 00
36.0	-18.0	0.1358D 02	0.1222D 02	-0.1521D 02
36.0	-14.0	0.1289D 02	-0.4097D 01	0.2335D 01
36.0	-10.0	0.1225D 02	-0.1596D 02	0.1538D 02
36.0	-6.0	0.1233D 02	0.1242D 02	0.1229D 02
36.0	-2.0	0.1206D 02	0.1143D 02	0.1035D 02
36.0	2.0	0.1352D 02	-0.2032D 02	0.1721D 02
36.0	6.0	0.1325D 02	0.7940D 01	-0.9969D 01
36.0	10.0	0.1352D 02	-0.9028D 00	-0.1307D 02
36.0	14.0	0.1322D 02	-0.2861D 01	-0.2001D 02
36.0	18.0	0.1253D 02	-0.1224D 02	-0.1234D 02
36.0	22.0	0.1254D 02	-0.5572D 00	0.5242D 01
32.0	-22.0	0.1192D 02	0.9686D 01	0.4792D 01
32.0	-18.0	0.1205D 02	0.1113D 02	-0.1183D 02
32.0	-14.0	0.1209D 02	-0.1766D 02	-0.5306D 01
32.0	-10.0	0.1187D 02	0.1356D 02	-0.8905D 01
32.0	-6.0	0.1280D 02	-0.1485D 02	-0.1692D 02
32.0	-2.0	0.1216D 02	0.1175D 02	0.1628D 01
32.0	2.0	0.1284D 02	0.9683D 01	0.3748D 01
32.0	6.0	0.1288D 02	-0.4638D 01	0.2050D 01
32.0	10.0	0.1306D 02	-0.2218D 01	-0.1281D 02
32.0	14.0	0.1262D 02	0.1001D 02	-0.8392D 01
32.0	18.0	0.1254D 02	-0.2241D 02	0.3276D 01
32.0	22.0	0.1249D 02	-0.1680D 02	0.1195D 02
28.0	-22.0	0.1237D 02	0.2967D 01	0.1317D 02
28.0	-16.0	0.1222D 02	-0.7557D 01	-0.4171D 01
28.0	-14.0	0.1277D 02	0.1314D 02	-0.4212D 01
28.0	-10.0	0.1225D 02	0.5554D 01	0.1714D 02
28.0	-6.0	0.1173D 02	-0.1134D 02	-0.1039D 02
28.0	-2.0	0.1262D 02	-0.6035D 01	-0.1176D 02
28.0	2.0	0.1183D 02	0.6385D 01	0.5521D 01
28.0	6.0	0.1246D 02	0.1234D 02	-0.1457D 02
28.0	10.0	0.1259D 02	0.6794D 01	-0.1019D 02
28.0	14.0	0.1200D 02	0.7740D 00	-0.4973D 01
28.0	18.0	0.1172D 02	0.1164D 02	0.7836D 01
28.0	22.0	0.1235D 02	-0.1515D 02	0.5601D 01

24.0	-22.0	0.1273D 02	-0.7775D 01	-0.5856D 01	
24.0	-18.0	0.1199D 02	-0.7405D 01	-0.7596D 01	
24.0	-14.0	0.1228D 02	-0.2112D 02	0.1757D 02	
24.0	-10.0	0.1235D 02	-0.1495D 02	-0.1274D 02	
24.0	-6.0	0.1267D 02	0.4951D 01	-0.1473D 02	
24.0	-2.0	0.1133D 02	0.2047D 02	0.1114D 02	
24.0	2.0	0.1143D 02	-0.1144D 02	-0.1957D 02	
24.0	6.0	0.1130D 02	-0.1088D 02	-0.4366D 01	
24.0	10.0	0.1131D 02	0.1477D 02	0.1107D 02	
24.0	14.0	0.1137D 02	-0.9708D 00	0.9981D 01	
24.0	18.0	0.1169D 02	-0.1745D 02	-0.1552D 02	
24.0	22.0	0.1242D 02	0.6860D 01	-0.8100D 01	
20.0	-22.0	0.1266D 02	-0.5187D 01	0.8312D 01	
20.0	-18.0	0.1217D 02	0.2075D 01	-0.9095D 01	
20.0	-14.0	0.1219D 02	-0.1836D 02	-0.1004D 02	
20.0	-10.0	0.1238D 02	0.6493D 00	0.4728D 01	
20.0	-6.0	0.1212D 02	-0.1808D 02	-0.3573D 01	
20.0	-2.0	0.1128D 02	0.1142D 02	-0.1420D 01	
20.0	2.0	0.1112D 02	-0.1533D 02	0.3652D 00	
20.0	6.0	0.1216D 02	0.1450D 02	0.2886D 01	
20.0	10.0	0.1125D 02	0.1126D 02	0.6831D 01	
20.0	14.0	0.1191D 02	-0.1256D 02	-0.8446D 01	
20.0	18.0	0.1114D 02	-0.1185D 02	0.5711D 01	
20.0	22.0	0.1150D 02	-0.4157D 00	-0.5836D 00	
16.0	-22.0	0.1172D 02	-0.1261D 01	-0.1953D 02	
16.0	-18.0	0.1113D 02	0.5299D 01	0.7367D 00	
16.0	-14.0	0.1212D 02	-0.2411D 00	0.1272D 02	
16.0	-10.0	0.1145D 02	-0.1580D 01	-0.9712D 01	
16.0	-6.0	0.1166D 02	-0.6019D 01	0.1021D 02	
16.0	-2.0	0.1164D 02	0.1404D 02	-0.5676D 01	
16.0	2.0	0.1085D 02	-0.1146D 02	-0.9069D 01	
16.0	6.0	0.1082D 02	-0.2165D 02	0.6020D 01	
16.0	10.0	0.1135D 02	0.7061D 01	0.1293D 02	
16.0	14.0	0.1207D 02	0.1241D 02	-0.2868D 01	
16.0	18.0	0.1223D 02	0.2557D 01	0.1474D 00	
16.0	22.0	0.1094D 02	0.5283D 00	-0.1888D 02	
12.0	-22.0	0.1136D 02	-0.1987D 02	-0.1505D 00	
12.0	-18.0	0.1076D 02	0.5248D 01	-0.7371D 01	
12.0	-14.0	0.1117D 02	0.2400D 01	0.9266D 01	
12.0	-10.0	0.1116D 02	0.2104D 02	0.1728D 02	
12.0	-6.0	0.1068D 02	-0.6988D 01	0.1254D 02	
12.0	-2.0	0.1127D 02	0.9518D-01	-0.4063D 01	
12.0	2.0	0.1137D 02	-0.7486D 01	-0.7993D 01	
12.0	6.0	0.1118D 02	0.1552D 01	0.7150D 01	
12.0	10.0	0.1155D 02	0.1148D 02	0.1556D 02	
12.0	14.0	0.1175D 02	-0.7691D 01	0.7419D 01	
12.0	18.0	0.1153D 02	-0.9991D 01	-0.1102D 02	
12.0	22.0	0.1083D 02	0.9262D 01	-0.1704D 02	
8.0	-22.0	0.1134D 02	-0.1611D 02	0.7379D 01	
8.0	-18.0	0.1105D 02	-0.1502D 02	-0.1106D 02	
8.0	-14.0	0.1073D 02	-0.1787D 02	-0.1160D 02	
8.0	-10.0	0.1083D 02	0.9548D 01	-0.1656D 02	
8.0	-6.0	0.1121D 02	-0.1464D 02	-0.9779D 01	
8.0	-2.0	0.1070D 02	-0.1299D 02	0.1139D 02	
8.0	2.0	0.1039D 02	-0.1937D 02	0.1560D 02	
8.0	6.0	0.1056D 02	0.2165D 02	-0.1083D 02	
8.0	10.0	0.1095D 02	0.1282D 02	0.1210D 02	
8.0	14.0	0.1108D 02	-0.1788D 02	-0.4395D 01	
8.0	18.0	0.1003D 02	0.8148D 01	0.1504D 02	
8.0	22.0	0.1137D 02	0.1194D 02	0.5842D 01	
4.0	-22.0	0.1024D 02	0.1967D 01	0.1414D 02	
4.0	-18.0	0.1072D 02	0.6296D 01	-0.6024D 01	
4.0	-14.0	0.1109D 02	-0.7214D 01	0.9064D 01	
4.0	-10.0	0.1102D 02	-0.3636D 01	-0.1627D 02	
4.0	-6.0	0.1032D 02	0.1296D 02	0.8357D 00	
4.0	-2.0	0.9918D 01	0.7505D 01	-0.4439D 01	
4.0	2.0	0.1048D 02	0.3549D 01	-0.3968D 01	
4.0	6.0	0.9877D 01	-0.6188D 01	0.1593D 02	
4.0	10.0	0.1030D 02	-0.1495D 02	0.1665D 02	
4.0	14.0	0.9954D 01	0.1039D 02	0.3329D 01	
4.0	18.0	0.1073D 02	0.1411D 02	-0.1484D 02	
4.0	22.0	0.1114D 02	0.7599D 01	-0.1890D 02	

0.0	-22.0	0.9952D 01	-0.1518D 02	0.1386D 02	
0.0	-18.0	0.9978D 01	-0.1183D 02	0.2987D 01	
0.0	-14.0	0.1020D 02	-0.6277D 01	-0.1895D 02	
0.0	-10.0	0.1040D 02	0.1097D 02	0.1186D 02	
0.0	-6.0	0.9774D 01	0.8477D 01	0.1478D 01	
0.0	-2.0	0.9568D 01	-0.1076D 01	0.1678D 01	
0.0	2.0	0.9694D 01	-0.2116D 02	0.1406D 02	
0.0	6.0	0.9876D 01	-0.2081D 02	-0.8857D 00	
0.0	10.0	0.1088D 02	0.1042D 02	-0.3443D 01	
0.0	14.0	0.1013D 02	-0.2282D 02	0.1432D 01	
0.0	18.0	0.9638D 01	-0.1348D 01	-0.7993D 01	
0.0	22.0	0.1095D 02	-0.3977D 01	-0.1313D 02	
-4.0	-22.0	0.1082D 02	-0.2120D 01	-0.7652D 01	
-4.0	-18.0	0.1002D 02	0.6682D 01	0.1009D 02	
-4.0	-14.0	0.1054D 02	-0.9208D 01	-0.2875D 01	
-4.0	-10.0	0.9872D 01	-0.1141D 02	0.1089D 02	
-4.0	-6.0	0.1055D 02	0.1334D 02	-0.8038D 01	
-4.0	-2.0	0.9716D 01	-0.2205D 02	-0.7475D-03	
-4.0	2.0	0.9316D 01	0.1208D 02	-0.2576D 01	
-4.0	6.0	0.1013D 02	-0.1932D 02	-0.1208D 02	
-4.0	10.0	0.9929D 01	0.1438D 02	0.9437D 00	
-4.0	14.0	0.1017D 02	-0.2685D 01	0.8534D 01	
-4.0	18.0	0.1022D 02	-0.1573D 02	0.4506D 01	
-4.0	22.0	0.9594D 01	-0.1478D 01	-0.5444D 01	
-6.0	-22.0	0.9387D 01	0.1923D 01	-0.8868D 01	
-8.0	-18.0	0.1049D 02	0.7711D 01	0.1785D 02	
-8.0	-14.0	0.1025D 02	-0.4619D 01	0.9184D 01	
-8.0	-10.0	0.9755D 01	-0.9442D 01	0.5934D 01	
-8.0	-6.0	0.1009D 02	-0.1591D 02	-0.1899D 02	
-8.0	-2.0	0.9858D 01	0.9713D 01	0.6193D 01	
-8.0	2.0	0.9058D 01	-0.3927D 01	-0.6105D 01	
-8.0	6.0	0.9766D 01	-0.1114D 02	-0.1534D 02	
-8.0	10.0	0.9218D 01	-0.6523D 01	-0.1363D 02	
-8.0	14.0	0.1029D 02	-0.4152D 01	0.4230D 01	
-8.0	18.0	0.9133D 01	0.1079D 02	0.1434D 02	
-8.0	22.0	0.9373D 01	0.1233D 02	0.3774D-01	
-12.0	-22.0	0.9749D 01	-0.1303D 02	0.1520D 02	
-12.0	-18.0	0.9566D 01	-0.1096D 02	0.4808D 01	
-12.0	-14.0	0.1020D 02	0.2875D 01	0.1336D 02	
-12.0	-10.0	0.1024D 02	0.1314D 02	-0.6361D 01	
-12.0	-6.0	0.9448D 01	-0.1919D 02	-0.1647D 02	
-12.0	-2.0	0.9024D 01	0.1035D 02	0.1359D 02	
-12.0	2.0	0.1004D 02	0.1474D 02	0.7334D 01	
-12.0	6.0	0.9512D 01	0.4970D 01	0.6547D 01	
-12.0	10.0	0.9581D 01	-0.6695D 01	0.6131D 00	
-12.0	14.0	0.9444D 01	-0.2015D 02	-0.1265D 01	
-12.0	18.0	0.9576D 01	0.6449D 01	0.1175D 02	
-12.0	22.0	0.8946D 01	-0.9087D 00	0.1672D 02	
-16.0	-22.0	0.1003D 02	-0.1595D 02	-0.1382D 02	
-16.0	-18.0	0.9571D 01	0.2373D 01	0.9173D 01	
-16.0	-14.0	0.8786D 01	0.5175D 01	-0.1710D 02	
-16.0	-10.0	0.9001D 01	0.8459D 01	0.2510D 01	
-16.0	-6.0	0.1001D 02	-0.2057D 01	0.1521D 02	
-16.0	-2.0	0.8856D 01	0.1271D 02	-0.1809D 02	
-16.0	2.0	0.9620D 01	-0.1374D 02	-0.1498D 02	
-16.0	6.0	0.9949D 01	-0.8068D 01	-0.5634D 01	
-16.0	10.0	0.8897D 01	0.1124D 02	-0.8031D 00	
-16.0	14.0	0.9392D 01	0.6228D 01	-0.1397D 02	
-16.0	18.0	0.9348D 01	-0.1346D 02	0.2627D 01	
-16.0	22.0	0.9888D 01	-0.1526D 02	-0.1437D 02	
-20.0	-22.0	0.9749D 01	-0.2230D 02	0.6925D 01	
-20.0	-18.0	0.9413D 01	-0.1283D 02	0.1689D 02	
-20.0	-14.0	0.8407D 01	-0.2531D 01	-0.3586D 01	
-20.0	-10.0	0.9533D 01	0.9333D 01	0.1481D 01	
-20.0	-6.0	0.9248D 01	0.9695D 01	-0.5004D 01	
-20.0	-2.0	0.8700D 01	-0.1951D 02	-0.6002D 01	
-20.0	2.0	0.8540D 01	-0.2218D 02	-0.9897D 01	
-20.0	6.0	0.9290D 01	0.2948D 01	-0.1454D 02	
-20.0	10.0	0.8423D 01	-0.5228D 01	0.8603D 01	
-20.0	14.0	0.8867D 01	-0.1026D 02	-0.1917D 02	
-20.0	18.0	0.9514D 01	0.9721D 01	-0.1314D 02	
-20.0	22.0	0.9408D 01	-0.1425D 02	-0.6366D 00	

*	-24.0	-22.0	*	0.9214D 01	0.9952D 01	-0.9019D 01	*
*	-24.0	-18.0	*	0.8939D 01	0.9829D 01	-0.3158D 01	*
*	-24.0	-14.0	*	0.8362D 01	-0.7036D 00	0.1698D 02	*
*	-24.0	-10.0	*	0.9251D 01	-0.1700D 02	-0.8356D 00	*
*	-24.0	-6.0	*	0.9288D 01	-0.8603D 00	0.1310D 02	*
*	-24.0	-2.0	*	0.8915D 01	-0.2004D 02	-0.1401D 02	*
*	-24.0	2.0	*	0.9607D 01	-0.2186D 01	0.1520D 02	*
*	-24.0	6.0	*	0.8286D 01	0.1461D 02	0.9145D 01	*
*	-24.0	10.0	*	0.8790D 01	0.4647D 01	-0.1938D 02	*
*	-24.0	14.0	*	0.9537D 01	-0.1028D 02	-0.6641D 01	*
*	-24.0	18.0	*	0.8503D 01	0.8052D 01	-0.1854D 01	*
*	-24.0	22.0	*	0.8961D 01	-0.8403D 01	-0.1815D 02	*
*	-28.0	-22.0	*	0.9284D 01	0.2607D 01	-0.1907D 02	*
*	-28.0	-18.0	*	0.9155D 01	0.4975D 01	0.9985D 01	*
*	-28.0	-14.0	*	0.9383D 01	-0.1082D 02	0.1191D 02	*
*	-28.0	-10.0	*	0.9110D 01	0.1331D 02	-0.1422D 02	*
*	-28.0	-6.0	*	0.8831D 01	-0.1334D 02	-0.4929D 00	*
*	-28.0	-2.0	*	0.8886D 01	0.1298D 02	-0.4927D 01	*
*	-28.0	2.0	*	0.8109D 01	-0.6451D 00	0.2984D 01	*
*	-28.0	6.0	*	0.8933D 01	-0.1011D 02	-0.2191D 01	*
*	-28.0	10.0	*	0.9771D 01	-0.7205D 01	0.1373D 02	*
*	-28.0	14.0	*	0.8572D 01	-0.1879D 02	-0.1424D 02	*
*	-28.0	18.0	*	0.9033D 01	-0.8450D 00	-0.2400D 01	*
*	-28.0	22.0	*	0.8806D 01	0.1122D 02	0.4264D 01	*
*	-32.0	-22.0	*	0.7890D 01	0.1111D 02	0.1138D 02	*
*	-32.0	-18.0	*	0.7826D 01	-0.1699D 02	0.5721D 01	*
*	-32.0	-14.0	*	0.8507D 01	0.1021D 02	-0.1960D 02	*
*	-32.0	-10.0	*	0.8547D 01	0.1194D 01	0.9593D 01	*
*	-32.0	-6.0	*	0.7868D 01	0.3174D 00	-0.9998D 01	*
*	-32.0	-2.0	*	0.9072D 01	0.1171D 02	-0.1812D 02	*
*	-32.0	2.0	*	0.8495D 01	0.1190D 02	0.8634D 01	*
*	-32.0	6.0	*	0.8615D 01	-0.1568D 02	-0.4066D 01	*
*	-32.0	10.0	*	0.8817D 01	-0.1062D 01	-0.3097D 01	*
*	-32.0	14.0	*	0.8017D 01	-0.1803D 02	-0.1673D 02	*
*	-32.0	18.0	*	0.8725D 01	-0.1096D 02	0.5156D 01	*
*	-32.0	22.0	*	0.8712D 01	-0.4185D 01	-0.8179D 01	*

STATISTICAL RESULTS:

	MEAN VALUE	STANDARD DEVIATION
X-DIRECTION	0.108D 02	0.156D 01
Y-DIRECTION	-0.189D 01	0.116D 02
Z-DIRECTION	-0.142D 01	0.107D 02

EVALUATED STRAIN FIELD AT POINT (1B)

ELEMENT	EXX	EYY	ELEMENT	EXX	EYY
1, 1	0.12D-03	-0.91D-02	2, 1	-0.89D-04	0.38D-02
1, 2	0.30D-04	0.90D-02	2, 2	-0.16D-03	0.38D-02
1, 3	-0.10D-03	-0.77D-02	2, 3	0.20D-03	0.11D-02
1, 4	-0.87D-04	-0.10D-02	2, 4	0.26D-03	-0.61D-02
1, 5	-0.17D-03	0.23D-02	2, 5	0.35D-03	0.29D-03
1, 6	0.97D-04	0.81D-02	2, 6	0.36D-03	0.26D-02
1, 7	0.20D-03	-0.73D-02	2, 7	-0.13D-03	0.34D-02
1, 8	0.20D-04	0.56D-02	2, 8	0.23D-04	-0.68D-03
1, 9	0.26D-03	-0.35D-02	2, 9	-0.18D-03	-0.30D-02
1,10	0.82D-04	0.26D-02	2,10	-0.30D-04	-0.50D-02
1,11	-0.64D-04	-0.37D-02	2,11	0.14D-03	0.37D-02
3, 1	0.26D-03	-0.25D-02	4, 1	-0.11D-03	-0.36D-03
3, 2	0.35D-03	0.41D-02	4, 2	-0.43D-04	0.72D-02
3, 3	0.20D-03	0.30D-02	4, 3	-0.17D-03	-0.78D-02
3, 4	0.94D-04	-0.71D-02	4, 4	-0.95D-04	0.71D-02
3, 5	-0.12D-03	0.25D-03	4, 5	0.27D-03	-0.66D-02
3, 6	-0.25D-04	0.79D-02	4, 6	-0.12D-03	0.52D-03
3, 7	0.17D-03	-0.71D-02	4, 7	0.25D-03	0.36D-02
3, 8	0.93D-04	0.22D-02	4, 8	0.11D-03	-0.60D-03
3, 9	0.11D-03	0.49D-03	4, 9	0.12D-03	-0.31D-02
3,10	0.15D-03	0.23D-02	4,10	0.16D-03	0.61D-02
3,11	-0.35D-05	-0.29D-02	4,11	0.20D-03	-0.14D-02
5, 1	-0.91D-04	0.26D-02	6, 1	0.19D-04	-0.93D-04
5, 2	0.57D-04	-0.52D-02	6, 2	-0.46D-04	0.34D-02
5, 3	0.12D-03	0.19D-02	6, 3	0.21D-04	-0.15D-02
5, 4	-0.25D-04	0.42D-02	6, 4	-0.84D-05	-0.50D-02
5, 5	-0.23D-03	-0.13D-02	6, 5	0.14D-03	-0.39D-02
5, 6	0.32D-03	-0.31D-02	6, 6	0.12D-04	0.80D-02
5, 7	0.10D-03	-0.15D-02	6, 7	0.77D-04	-0.14D-03
5, 8	0.29D-03	0.14D-02	6, 8	-0.22D-03	-0.64D-02
5, 9	0.32D-03	0.15D-02	6, 9	0.13D-04	0.39D-02
5,10	0.16D-03	-0.27D-02	6,10	-0.13D-03	0.41D-02
5,11	0.83D-05	0.67D-02	6,11	0.14D-03	-0.61D-02
7, 1	0.23D-03	-0.18D-02	8, 1	0.89D-04	-0.16D-02
7, 2	0.26D-03	0.51D-02	8, 2	0.91D-04	0.14D-02
7, 3	0.17D-04	-0.48D-02	8, 3	0.24D-03	0.33D-03
7, 4	0.23D-03	0.47D-02	8, 4	0.72D-04	0.11D-02
7, 5	0.12D-03	-0.74D-02	8, 5	0.24D-03	-0.50D-02
7, 6	-0.89D-04	0.67D-02	8, 6	0.92D-04	0.64D-02
7, 7	0.66D-04	-0.75D-02	8, 7	-0.13D-03	0.25D-02
7, 8	0.33D-03	0.81D-03	8, 8	-0.89D-04	-0.72D-02
7, 9	-0.25D-04	0.60D-02	8, 9	-0.49D-04	-0.13D-02
7,10	-0.41D-04	-0.18D-03	8,10	0.80D-04	0.25D-02
7,11	-0.27D-03	-0.29D-02	8,11	0.17D-03	0.51D-03
9, 1	0.45D-05	-0.63D-02	10, 1	0.28D-03	-0.27D-03
9, 2	-0.72D-04	0.71D-03	10, 2	0.82D-04	0.71D-03
9, 3	0.11D-03	-0.47D-02	10, 3	-0.88D-04	-0.69D-02
9, 4	0.84D-04	0.70D-02	10, 4	-0.49D-04	0.60D-02
9, 5	-0.13D-03	-0.18D-02	10, 5	0.22D-03	-0.41D-03
9, 6	0.14D-03	0.19D-02	10, 6	0.20D-03	0.16D-02
9, 7	0.24D-03	-0.23D-02	10, 7	-0.23D-04	-0.10D-01
9, 8	0.16D-03	-0.25D-02	10, 8	0.17D-03	0.22D-02
9, 9	0.15D-03	0.48D-02	10, 9	0.16D-03	0.77D-02
9,10	0.17D-03	0.57D-03	10,10	0.28D-03	-0.65D-02
9,11	0.38D-03	-0.48D-02	10,11	-0.18D-03	-0.95D-03
11, 1	0.73D-04	-0.11D-02	12, 1	-0.22D-03	-0.84D-03
11, 2	0.19D-03	0.34D-02	12, 2	-0.10D-04	-0.14D-02
11, 3	0.22D-03	-0.89D-03	12, 3	-0.84D-04	-0.43D-02
11, 4	0.16D-03	-0.41D-02	12, 4	0.13D-03	0.62D-03
11, 5	0.14D-03	0.14D-02	12, 5	-0.19D-03	0.24D-02
11, 6	0.88D-04	0.99D-03	12, 6	-0.37D-04	0.50D-02
11, 7	0.20D-03	0.24D-02	12, 7	0.95D-04	-0.89D-04
11, 8	0.29D-06	0.22D-02	12, 8	-0.64D-04	-0.78D-02

11, 9	-0.14D-03	-0.63D-02	12, 9	0.24D-03	0.83D-02
11,10	-0.45D-04	-0.93D-03	12,10	-0.98D-05	-0.54D-02
11,11	0.27D-03	0.16D-02	12,11	-0.14D-03	0.66D-03
13, 1	0.36D-03	-0.22D-02	14, 1	-0.90D-04	-0.14D-02
13, 2	-0.12D-03	0.40D-02	14, 2	0.23D-03	0.31D-02
13, 3	0.72D-04	0.55D-03	14, 3	0.12D-04	0.12D-02
13, 4	0.29D-04	-0.62D-02	14, 4	-0.12D-03	0.16D-02
13, 5	0.12D-03	0.88D-02	14, 5	0.16D-03	-0.64D-02
13, 6	-0.36D-04	-0.85D-02	14, 6	0.21D-03	0.34D-02
13, 7	0.65D-04	0.78D-02	14, 7	-0.25D-03	0.18D-02
13, 8	0.91D-04	-0.84D-02	14, 8	0.64D-04	-0.12D-02
13, 9	0.18D-03	0.43D-02	14, 9	-0.91D-04	-0.59D-03
13,10	-0.30D-04	0.33D-02	14,10	0.21D-03	-0.37D-02
13,11	0.27D-03	-0.36D-02	14,11	-0.11D-03	-0.38D-03
15, 1	-0.71D-04	-0.52D-03	16, 1	0.71D-04	-0.46D-02
15, 2	-0.13D-05	-0.35D-02	16, 2	0.40D-04	-0.70D-03
15, 3	0.35D-03	-0.26D-02	16, 3	0.95D-04	-0.82D-03
15, 4	0.31D-03	0.81D-02	16, 4	-0.13D-03	0.26D-02
15, 5	-0.14D-03	-0.74D-02	16, 5	0.19D-03	-0.37D-02
15, 6	0.42D-04	-0.11D-02	16, 6	0.39D-04	0.66D-02
15, 7	0.11D-03	0.24D-02	16, 7	0.27D-03	-0.14D-02
15, 8	-0.11D-03	0.29D-02	16, 8	0.16D-03	-0.48D-02
15, 9	0.17D-03	0.34D-02	16, 9	0.12D-03	0.13D-02
15,10	0.13D-04	-0.66D-02	16,10	0.13D-03	0.49D-02
15,11	0.57D-04	0.18D-02	16,11	-0.42D-04	0.45D-03
17, 1	0.13D-03	-0.24D-02	18, 1	-0.18D-04	0.31D-04
17, 2	0.12D-03	-0.26D-02	18, 2	-0.54D-04	0.26D-02
17, 3	0.11D-04	-0.30D-02	18, 3	-0.26D-03	0.41D-02
17, 4	0.71D-04	-0.90D-04	18, 4	0.35D-04	-0.40D-02
17, 5	-0.10D-04	0.73D-02	18, 5	0.11D-03	0.48D-02
17, 6	-0.54D-04	0.67D-03	18, 6	0.74D-05	-0.45D-02
17, 7	-0.27D-03	-0.63D-02	18, 7	0.37D-03	-0.42D-02
17, 8	0.25D-03	0.20D-02	18, 8	-0.16D-03	0.25D-02
17, 9	-0.92D-04	0.13D-02	18, 9	-0.25D-03	0.37D-02
17,10	-0.17D-03	-0.50D-02	18,10	0.24D-03	-0.46D-02
17,11	0.25D-03	0.60D-02	18,11	-0.13D-03	0.41D-02
19, 1	0.35D-03	-0.59D-03			
19, 2	0.33D-03	0.39D-02			
19, 3	0.22D-03	-0.60D-02			
19, 4	0.14D-03	0.67D-02			
19, 5	0.24D-03	-0.66D-02			
19, 6	-0.47D-04	0.34D-02			
19, 7	-0.96D-04	0.24D-02			
19, 8	0.80D-04	-0.73D-03			
19, 9	0.24D-03	0.29D-02			
19,10	0.14D-03	-0.45D-02			
19,11	0.77D-04	-0.30D-02			

STATISTICAL RESULTS:

	MEAN VALUE	STANDARD DEVIATION
XX-STRAIN:	0.6486D-04	0.1528D-03
YY-STRAIN:	-0.8742D-04	0.4348D-02

EVALUATED THICKNESS CHANGES (MICRONS)
(COLUMNS: 1- 6)

	1	2	3	4	5	6
1	0.84	-2.86	5.69	-4.09	-2.77	3.09
2	-3.65	2.68	-2.42	0.55	-2.96	1.89
3	1.12	2.28	-5.85	4.84	5.75	-5.64
4	4.43	3.29	-5.43	1.71	-0.45	1.28
5	0.93	-5.07	4.42	-3.12	5.19	-1.45
6	-2.50	7.07	-2.30	-2.01	1.15	-5.07
7	-4.35	1.20	1.36	2.33	-4.12	1.88
8	-2.11	2.06	2.21	-4.90	4.70	0.21
9	5.79	-0.11	6.07	-1.56	4.31	3.34
10	3.55	-2.09	2.23	1.11	6.38	-4.05
11	6.50	-2.29	-6.06	-5.73	3.92	-5.10
12	2.13	3.95	2.27	-3.33	5.73	-5.08
13	-5.13	-4.14	2.78	1.90	-4.23	5.14
14	4.92	-3.67	4.23	-2.70	2.89	4.88
15	-0.16	3.15	-5.43	2.14	0.92	-1.27
16	2.93	2.54	-5.49	1.59	1.99	2.69
17	6.51	5.81	-3.51	6.42	5.29	-1.60
18	2.00	-5.33	-3.23	0.32	1.55	-4.30
19	2.58	-2.24	-5.29	6.63	-0.75	1.97
20	1.86	6.70	0.99	-0.50	4.42	2.38

(COLUMNS: 7-12)

	7	8	9	10	11	12
1	-2.85	-2.66	-2.24	5.03	3.79	-5.38
2	7.03	-2.37	-1.82	4.54	-0.96	-2.22
3	1.74	4.76	-3.44	2.95	2.70	-2.58
4	2.53	-1.42	0.73	-3.74	-1.97	2.65
5	6.69	5.84	-5.47	-2.98	-1.34	6.25
6	-1.43	-0.57	0.51	-3.24	0.91	-3.17
7	4.72	1.11	-4.54	-2.77	5.59	5.49
8	1.76	-1.90	4.57	3.87	-1.54	6.81
9	5.03	-1.31	-0.39	6.82	5.94	-1.57
10	2.93	-4.75	5.71	-3.82	2.36	-1.82
11	-3.60	2.99	3.04	-1.88	6.68	-1.63
12	-6.05	6.63	-5.12	2.46	-0.23	4.49
13	-2.30	3.25	-0.00	4.90	-6.10	-1.90
14	-6.28	2.88	-5.42	-3.91	-1.45	2.15
15	3.01	4.40	5.69	6.22	-5.22	-4.23
16	6.58	-5.92	2.71	-5.71	-5.29	2.57
17	4.43	4.42	-0.50	1.17	-0.43	1.27
18	-0.43	4.45	-4.66	4.45	-5.75	-1.04
19	1.29	-3.63	-3.42	2.18	-0.27	-5.57
20	1.01	5.10	6.04	-2.33	5.10	2.43

RECONSTRUCTION RESULTS OF INTERFEROGRAM
(1L) OF THE NEWS-PRINT PAPER SAMPLE #38
CUMMULATIVE DEFORMATION)

CO-ORDINATES X	CO-ORDINATES Y	DEFORMATIONS X	DEFORMATIONS Y	DEFORMATIONS Z
44.0	-22.0	0.1313D 02	-0.7517D 01	-0.2217D 01
44.0	-18.0	0.1368D 02	0.1251D 01	-0.7183D 01
44.0	-14.0	0.1295D 02	-0.7177D 01	0.7314D 01
44.0	-10.0	0.1280D 02	0.2781D 01	-0.1163D 02
44.0	-6.0	0.1315D 02	0.1395D 02	-0.7652D 01
44.0	-2.0	0.1397D 02	0.6093D 00	0.1905D 02
44.0	2.0	0.1326D 02	-0.5028D 01	0.1129D 02
44.0	6.0	0.1333D 02	-0.1717D 02	0.2166D 01
44.0	10.0	0.1343D 02	0.7689D 01	0.1302D 02
44.0	14.0	0.1324D 02	0.1023D 02	0.9892D 01
44.0	18.0	0.1408D 02	0.1093D 02	-0.6817D 01
44.0	22.0	0.1284D 02	-0.1531D 02	0.1211D 02
40.0	-22.0	0.1229D 02	-0.1656D 02	-0.1285D 02
40.0	-18.0	0.1357D 02	-0.4911D 01	0.1649D 01
40.0	-14.0	0.1285D 02	0.7051D 01	0.1594D 02
40.0	-10.0	0.1308D 02	-0.8723D 01	0.8090D 01
40.0	-6.0	0.1375D 02	0.9524D 01	0.1602D 02
40.0	-2.0	0.1300D 02	-0.4968D 01	0.1440D 02
40.0	2.0	0.1365D 02	-0.1101D 02	0.7723D 01
40.0	6.0	0.1343D 02	0.1778D 01	0.6738D 01
40.0	10.0	0.1250D 02	-0.7690D 01	-0.6144D 01
40.0	14.0	0.1177D 02	0.4301D 00	0.7452D 01
40.0	18.0	0.1390D 02	0.5738D 01	0.1551D 01
40.0	22.0	0.1222D 02	0.7768D 01	0.1456D 02
36.0	-22.0	0.1406D 02	0.1872D 02	0.8852D 00
36.0	-18.0	0.1306D 02	-0.8507D 00	0.1749D 02
36.0	-14.0	0.1195D 02	-0.1703D 01	-0.8185D 01
36.0	-10.0	0.1340D 02	-0.7506D 01	-0.1053D 02
36.0	-6.0	0.1366D 02	0.5487D 01	-0.6534D 01
36.0	-2.0	0.1266D 02	0.1709D 02	-0.1599D 02
36.0	2.0	0.1273D 02	0.1759D 00	-0.1547D 02
36.0	6.0	0.1083D 02	-0.9050D 01	0.1473D 02
36.0	10.0	0.1200D 02	0.1485D 01	0.9629D 01
36.0	14.0	0.1362D 02	0.1313D 02	0.2296D 02
36.0	18.0	0.1212D 02	-0.9014D 01	0.1504D 02
36.0	22.0	0.1352D 02	-0.1742D 01	-0.7824D 01
32.0	-22.0	0.1007D 02	-0.2180D 01	-0.3649D 00
32.0	-18.0	0.1370D 02	-0.6930D 01	0.1512D 02
32.0	-14.0	0.1226D 02	0.1706D 01	-0.1260D 00
32.0	-10.0	0.1355D 02	0.1282D 02	0.1062D 02
32.0	-6.0	0.1261D 02	-0.4269D-01	0.1647D 02
32.0	-2.0	0.1232D 02	0.7647D 00	-0.3449D 00
32.0	2.0	0.1096D 02	-0.1408D 02	-0.1219D 01
32.0	6.0	0.1272D 02	-0.1619D 02	-0.3474D 01
32.0	10.0	0.1193D 02	-0.8338D 01	0.1354D 02
32.0	14.0	0.1255D 02	0.9235D 01	0.4650D 01
32.0	18.0	0.1372D 02	0.7034D 01	-0.5245D 01
32.0	22.0	0.1169D 02	-0.7372D 01	-0.9295D 01
28.0	-22.0	0.9985D 01	-0.1523D 02	-0.1225D 02
28.0	-18.0	0.1181D 02	-0.1661D 02	-0.8953D 00
28.0	-14.0	0.1302D 02	0.1253D 02	0.8633D 01
28.0	-10.0	0.9690D 01	-0.5258D 00	-0.2026D 02
28.0	-6.0	0.1275D 02	0.7198D 01	0.1558D 02
28.0	-2.0	0.1355D 02	0.1935D 02	0.1031D 02
28.0	2.0	0.9842D 01	-0.7026D 01	0.1165D 01
28.0	6.0	0.1344D 02	-0.1519D 02	0.2042D 02
28.0	10.0	0.1009D 02	-0.1289D 02	0.4720D 01
28.0	14.0	0.1120D 02	0.1521D 02	0.1997D 01
28.0	18.0	0.1214D 02	0.1626D 02	-0.9180D 01
28.0	22.0	0.1300D 02	-0.1075D 02	0.6521D 00

24.0	-22.0	0.1252D 02	0.2855D 01	0.3352D 01
24.0	-18.0	0.1316D 02	-0.1051D 02	0.1466D 02
24.0	-14.0	0.1237D 02	0.3743D 01	-0.1987D 02
24.0	-10.0	0.9473D 01	-0.7350D 01	0.1073D 02
24.0	-6.0	0.1057D 02	-0.9555D 01	0.1588D 02
24.0	-2.0	0.1231D 02	0.1202D 02	-0.1621D 02
24.0	2.0	0.1308D 02	0.3577D 01	0.1814D 02
24.0	6.0	0.1088D 02	-0.4942D 01	0.3795D 01
24.0	10.0	0.9790D 01	0.7059D 01	-0.1056D 02
24.0	14.0	0.1336D 02	-0.6915D 01	-0.1322D 02
24.0	18.0	0.9595D 01	-0.7737D 01	0.1643D 02
24.0	22.0	0.1333D 02	0.7621D 01	0.4925D 01
20.0	-22.0	0.1227D 02	0.1304D 02	-0.1266D 02
20.0	-18.0	0.1111D 02	-0.5098D 01	0.1029D 02
20.0	-14.0	0.1342D 02	0.1584D 02	0.1140D 02
20.0	-10.0	0.9615D 01	0.4253D 01	-0.2394D 01
20.0	-6.0	0.1167D 02	0.1396D 02	-0.5502D 00
20.0	-2.0	0.1201D 02	-0.4165D 01	0.3296D 01
20.0	2.0	0.1027D 02	0.2494D 01	0.4355D 01
20.0	6.0	0.1342D 02	-0.1220D 02	-0.1772D 01
20.0	10.0	0.1266D 02	-0.4771D 01	-0.1137D 02
20.0	14.0	0.1072D 02	0.1749D 02	0.5673D 01
20.0	18.0	0.1007D 02	0.3316D 01	-0.1215D 00
20.0	22.0	0.1214D 02	0.8336D 01	0.6069D 01
16.0	-22.0	0.1295D 02	0.1056D 02	0.1742D 02
16.0	-18.0	0.1090D 02	-0.1641D 01	0.1320D 01
16.0	-14.0	0.9321D 01	-0.9206D 01	-0.1051D 02
16.0	-10.0	0.1246D 02	0.8307D 01	0.4812D 01
16.0	-6.0	0.1166D 02	-0.1538D 02	-0.5508D 01
16.0	-2.0	0.1011D 02	0.1857D 01	0.5882D 01
16.0	2.0	0.1224D 02	-0.4186D 01	0.1083D 02
16.0	6.0	0.1037D 02	0.6595D 01	-0.7925D 01
16.0	10.0	0.9689D 01	0.6888D 01	-0.8366D 01
16.0	14.0	0.1248D 02	-0.1826D 02	0.6738D 01
16.0	18.0	0.1180D 02	-0.1007D 02	-0.1687D 01
16.0	22.0	0.1238D 02	0.1142D 02	0.2568D 02
12.0	-22.0	0.1122D 02	0.9312D-01	0.5945D 01
12.0	-18.0	0.9869D 01	-0.4274D 01	0.7261D 01
12.0	-14.0	0.1104D 02	-0.1434D 02	-0.3193D 01
12.0	-10.0	0.1353D 02	0.3553D 01	-0.1884D 02
12.0	-6.0	0.1116D 02	-0.1151D 02	-0.8232D 01
12.0	-2.0	0.1018D 02	0.6619D 01	0.7402D 01
12.0	2.0	0.1046D 02	0.1273D 00	0.1302D 02
12.0	6.0	0.1243D 02	-0.9977D 01	-0.8457D 01
12.0	10.0	0.9415D 01	-0.1834D 02	-0.1594D 02
12.0	14.0	0.1181D 02	0.6186D 01	-0.5994D 00
12.0	18.0	0.1108D 02	0.9271D 01	0.1695D 02
12.0	22.0	0.1373D 02	0.1867D 02	0.1547D 02
8.0	-22.0	0.1351D 02	0.1528D 02	-0.3833D 01
8.0	-18.0	0.9662D 01	-0.1618D 01	0.8973D 01
8.0	-14.0	0.1166D 02	0.7220D 01	0.1382D 02
8.0	-10.0	0.1235D 02	-0.6473D 00	0.1768D 02
8.0	-6.0	0.8657D 01	-0.1383D 02	0.1616D 02
8.0	-2.0	0.9868D 01	-0.1298D 02	-0.1544D 02
8.0	2.0	0.8578D 01	0.1544D 01	-0.1267D 02
8.0	6.0	0.1231D 02	-0.1792D 02	0.6074D 01
8.0	10.0	0.1210D 02	0.2433D 01	-0.6391D 01
8.0	14.0	0.9015D 01	-0.3461D 01	0.5734D 00
8.0	18.0	0.9403D 01	-0.6602D 01	-0.1268D 02
8.0	22.0	0.1256D 02	-0.4906D 01	-0.7658D 01
4.0	-22.0	0.8956D 01	-0.1076D 01	-0.7649D 01
4.0	-18.0	0.9048D 01	0.1096D 02	0.3730D 01
4.0	-14.0	0.8067D 01	-0.5163D 01	-0.1512D 02
4.0	-10.0	0.1240D 02	0.6999D 01	0.1054D 02
4.0	-6.0	0.8489D 01	-0.6117D 01	0.3081D 01
4.0	-2.0	0.1081D 02	0.1452D 02	-0.6605D 00
4.0	2.0	0.1314D 02	0.1530D 02	0.3726D 00
4.0	6.0	0.8030D 01	-0.8906D 01	-0.1294D 02
4.0	10.0	0.9512D 01	-0.9640D 01	-0.1360D 02
4.0	14.0	0.8754D 01	-0.1329D 02	-0.5211D 01
4.0	18.0	0.1205D 02	0.9605D 01	0.2152D 02
4.0	22.0	0.8974D 01	0.1610D 02	0.1727D 02

0.0	-22.0	0.8593D 01	-0.8911D 01	-0.1174D 02	
0.0	-18.0	0.8379D 01	0.7303D 01	0.9624D 00	
0.0	-14.0	0.9558D 01	-0.8567D 01	0.2122D 02	
0.0	-10.0	0.8112D 01	-0.1423D 02	-0.1520D 02	
0.0	-6.0	0.9055D 01	-0.1580D 01	0.4255D 01	
0.0	-2.0	0.1208D 02	0.1589D 02	-0.6755D 01	
0.0	2.0	0.9116D 01	-0.4052D 01	-0.2011D 02	
0.0	6.0	0.1265D 02	0.4754D 01	0.7519D 01	
0.0	10.0	0.8181D 01	-0.4795D 01	-0.1679D 01	
0.0	14.0	0.7901D 01	-0.1658D 02	0.1028D 01	
0.0	18.0	0.9960D 01	-0.1289D 02	0.7761D 01	
0.0	22.0	0.1046D 02	0.1006D 02	0.1762D 02	
-4.0	-22.0	0.8604D 01	-0.1787D 02	0.2521D 01	
-4.0	-18.0	0.8403D 01	0.9670D 01	-0.1423D 02	
-4.0	-14.0	0.8796D 01	-0.7237D 01	0.5654D 01	
-4.0	-10.0	0.1182D 02	0.9626D 01	-0.8985D 01	
-4.0	-6.0	0.8896D 01	0.3662D 01	0.3809D 01	
-4.0	-2.0	0.8679D 01	-0.1727D 02	0.5145D 01	
-4.0	2.0	0.9887D 01	-0.1359D 02	0.2802D 00	
-4.0	6.0	0.8113D 01	-0.9391D 01	0.1533D 02	
-4.0	10.0	0.8577D 01	0.3621D 01	-0.9466D 00	
-4.0	14.0	0.8939D 01	-0.5904D 01	-0.3636D 01	
-4.0	18.0	0.8013D 01	-0.6851D 01	-0.1060D 02	
-4.0	22.0	0.8584D 01	0.4495D 01	0.3541D 01	
-8.0	-22.0	0.8599D 01	-0.1680D 02	0.1379D 02	
-8.0	-18.0	0.1005D 02	0.8288D 00	-0.2151D 02	
-8.0	-14.0	0.1165D 02	-0.1316D 02	-0.4953D 01	
-8.0	-10.0	0.8895D 01	0.4607D 01	-0.8631D 01	
-8.0	-6.0	0.8348D 01	0.1252D 01	0.2188D 02	
-8.0	-2.0	0.8731D 01	-0.9125D 01	-0.1313D 01	
-8.0	2.0	0.8735D 01	0.1775D 02	-0.1743D 00	
-8.0	6.0	0.8753D 01	-0.7475D 01	0.1822D 02	
-8.0	10.0	0.8384D 01	0.1710D 02	0.8215D 01	
-8.0	14.0	0.9013D 01	-0.8848D 01	-0.8140D 01	
-8.0	18.0	0.8828D 01	-0.1905D 02	-0.1579D 02	
-8.0	22.0	0.1132D 02	-0.1783D 02	0.2111D 01	
-12.0	-22.0	0.8626D 01	-0.9413D 01	-0.2136D 02	
-12.0	-18.0	0.9606D 01	0.1626D 02	-0.1658D 01	
-12.0	-14.0	0.1139D 02	0.1113D 02	-0.1879D 02	
-12.0	-10.0	0.8827D 01	0.1747D 02	0.8506D 01	
-12.0	-6.0	0.8268D 01	-0.3961D 00	0.1739D 02	
-12.0	-2.0	0.8370D 01	-0.1516D 02	-0.1486D 02	
-12.0	2.0	0.8359D 01	0.4859D 01	-0.4319D 01	
-12.0	6.0	0.8188D 01	-0.1409D 02	-0.2150D 01	
-12.0	10.0	0.8623D 01	-0.1809D 02	0.5076D 01	
-12.0	14.0	0.7778D 01	-0.1393D 01	0.7485D 01	
-12.0	18.0	0.1052D 02	0.1702D 02	-0.1697D 02	
-12.0	22.0	0.9403D 01	0.1522D 02	-0.2095D 02	
-16.0	-22.0	0.8084D 01	0.4245D 01	0.1675D 02	
-16.0	-18.0	0.9095D 01	-0.1448D 01	-0.6633D 01	
-16.0	-14.0	0.7428D 01	0.1193D 02	0.1160D 02	
-16.0	-10.0	0.7775D 01	-0.7189D 01	-0.9182D 00	
-16.0	-6.0	0.1159D 02	0.8478D 01	-0.1322D 02	
-16.0	-2.0	0.8707D 01	-0.3591D 01	0.2078D 02	
-16.0	2.0	0.8140D 01	-0.6064D 01	0.2156D 02	
-16.0	6.0	0.7446D 01	0.8861D 01	-0.2821D 00	
-16.0	10.0	0.8663D 01	-0.1029D 02	0.3512D 01	
-16.0	14.0	0.9153D 01	0.7193D 01	0.8255D 01	
-16.0	18.0	0.9125D 01	-0.1436D 02	-0.7914D 01	
-16.0	22.0	0.7914D 01	-0.1656D 02	0.1693D 02	
-20.0	-22.0	0.8161D 01	0.4038D 01	-0.4109D 00	
-20.0	-18.0	0.9061D 01	0.6944D 01	-0.1108D 02	
-20.0	-14.0	0.7890D 01	0.1270D 02	0.7368D-01	
-20.0	-10.0	0.7601D 01	-0.1622D 02	0.4938D 01	
-20.0	-6.0	0.7480D 01	-0.1524D 02	0.1030D 02	
-20.0	-2.0	0.8595D 01	0.1340D 01	0.4403D 01	
-20.0	2.0	0.6797D 01	-0.1406D 02	0.1433D 02	
-20.0	6.0	0.9287D 01	-0.1316D 02	0.1896D 02	
-20.0	10.0	0.6981D 01	0.1341D 01	-0.9099D 01	
-20.0	14.0	0.7445D 01	0.1527D 02	0.2034D 02	
-20.0	18.0	0.8447D 01	0.1811D 02	0.1271D 02	
-20.0	22.0	0.6725D 01	-0.9553D 01	0.1904D 01	

-24.0	-22.0	0.7676D 01	-0.9479D 01	0.1102D 02	
-24.0	-18.0	0.8876D 01	-0.2262D 01	-0.2170D 01	
-24.0	-14.0	0.7274D 01	0.1357D 02	-0.2021D 02	
-24.0	-10.0	0.7895D 01	0.1437D 02	0.1159D 01	
-24.0	-6.0	0.6952D 01	-0.7780D 00	-0.1155D 02	
-24.0	-2.0	0.7751D 01	-0.1006D 02	0.9709D 01	
-24.0	2.0	0.7602D 01	-0.1771D 02	-0.1563D 02	
-24.0	6.0	0.7301D 01	0.8015D 01	-0.4696D 01	
-24.0	10.0	0.8603D 01	-0.1751D 02	0.1473D 02	
-24.0	14.0	0.8009D 01	0.4068D 01	0.1109D 02	
-24.0	18.0	0.8250D 01	-0.1333D 02	-0.3893D 01	
-24.0	22.0	0.7989D 01	-0.9162D 00	0.1711D 02	
-28.0	-22.0	0.6454D 01	0.1852D 02	0.2165D 02	
-28.0	-18.0	0.6903D 01	-0.7936D 01	-0.1223D 02	
-28.0	-14.0	0.7382D 01	-0.2072D 01	-0.1720D 02	
-28.0	-10.0	0.8469D 01	0.1440D 02	0.2085D 02	
-28.0	-6.0	0.7110D 01	-0.4234D 00	-0.2522D 00	
-28.0	-2.0	0.7838D 01	0.1076D 02	0.6893D 01	
-28.0	2.0	0.8502D 01	0.1566D 02	-0.1695D 01	
-28.0	6.0	0.7424D 01	-0.1202D 02	-0.1437D 01	
-28.0	10.0	0.6229D 01	-0.1282D 02	-0.1715D 02	
-28.0	14.0	0.6970D 01	-0.1501D 02	0.1642D 02	
-28.0	18.0	0.5940D 01	-0.1656D 02	0.2131D 01	
-28.0	22.0	0.8154D 01	-0.2291D 01	-0.9832D 01	
-32.0	-22.0	0.8306D 01	-0.9655D 01	-0.9521D 01	
-32.0	-18.0	0.7315D 01	0.9258D 01	0.9784D 00	
-32.0	-14.0	0.6525D 01	0.1766D 02	0.2059D 02	
-32.0	-10.0	0.7266D 01	-0.5169D 00	-0.1009D 02	
-32.0	-6.0	0.6824D 01	-0.5976D 01	0.1442D 02	
-32.0	-2.0	0.6020D 01	-0.6253D 01	0.2050D 02	
-32.0	2.0	0.7083D 01	-0.1370D 02	-0.7622D 01	
-32.0	6.0	0.6278D 01	-0.2366D 00	0.9167D 01	
-32.0	10.0	0.6715D 01	-0.1157D 02	0.9133D 01	
-32.0	14.0	0.6708D 01	-0.9991D 01	0.1440D 02	
-32.0	18.0	0.6110D 01	-0.1181D 02	-0.5173D-01	
-32.0	22.0	0.6706D 01	-0.1461D 02	0.1061D 02	

STATISTICAL RESULTS:

	MEAN VALUE	STANDARD DEVIATION
X-DIRECTION	0.102D 02	0.226D 01
Y-DIRECTION	-0.102D 01	0.106D 02
Z-DIRECTION	0.190D 01	0.114D 02

EVALUATED STRAIN FIELD AT POINT (1L)

ELEMENT	EXX	EYY	ELEMENT	EXX	EYY
1, 1	0.21D-03	-0.22D-02	2, 1	-0.44D-03	-0.29D-02
1, 2	0.27D-04	0.21D-02	2, 2	0.13D-03	-0.30D-02
1, 3	0.25D-04	-0.25D-02	2, 3	0.22D-03	0.39D-02
1, 4	-0.70D-04	-0.28D-02	2, 4	-0.80D-04	-0.46D-02
1, 5	-0.15D-03	0.33D-02	2, 5	0.21D-04	0.36D-02
1, 6	0.24D-03	0.14D-02	2, 6	0.84D-04	0.15D-02
1, 7	-0.98D-04	0.30D-02	2, 7	0.23D-03	-0.32D-02
1, 8	-0.27D-04	-0.62D-02	2, 8	0.65D-03	0.24D-02
1, 9	0.23D-03	-0.63D-03	2, 9	0.12D-03	-0.20D-02
1, 10	0.37D-03	-0.18D-03	2, 10	-0.46D-03	-0.13D-02
1, 11	0.44D-04	0.66D-02	2, 11	0.45D-03	-0.51D-03
3, 1	0.10D-02	0.49D-02	4, 1	0.21D-04	0.12D-02
3, 2	-0.16D-03	0.21D-03	4, 2	0.47D-03	-0.22D-02
3, 3	-0.79D-04	0.15D-02	4, 3	-0.19D-03	-0.28D-02
3, 4	-0.36D-04	-0.32D-02	4, 4	0.96D-03	0.32D-02
3, 5	-0.26D-03	-0.29D-02	4, 5	-0.36D-04	-0.20D-03
3, 6	0.86D-04	0.42D-02	4, 6	-0.31D-03	0.37D-02
3, 7	0.44D-03	0.23D-02	4, 7	0.28D-03	0.53D-03
3, 8	-0.47D-03	-0.20D-02	4, 8	-0.18D-03	-0.20D-02
3, 9	0.16D-04	-0.29D-02	4, 9	0.46D-03	-0.44D-02
3, 10	0.27D-03	0.55D-02	4, 10	0.34D-03	0.55D-03
3, 11	-0.40D-03	-0.16D-02	4, 11	0.40D-03	0.36D-02
5, 1	-0.63D-03	0.35D-03	6, 1	0.61D-04	0.33D-02
5, 2	-0.34D-03	-0.73D-02	6, 2	0.51D-03	-0.30D-02
5, 3	0.16D-03	0.33D-02	6, 3	-0.26D-03	0.28D-02
5, 4	0.54D-04	-0.19D-02	6, 4	-0.35D-04	0.55D-03
5, 5	0.54D-03	-0.30D-02	6, 5	-0.27D-03	-0.54D-02
5, 6	0.31D-03	0.66D-02	6, 6	0.76D-04	0.21D-02
5, 7	-0.81D-03	0.20D-02	6, 7	0.70D-03	0.21D-02
5, 8	0.64D-03	-0.58D-03	6, 8	-0.64D-03	-0.30D-02
5, 9	0.75D-04	-0.70D-02	6, 9	-0.72D-03	0.35D-02
5, 10	-0.54D-03	-0.26D-03	6, 10	0.66D-03	0.21D-03
5, 11	0.64D-03	0.68D-02	6, 11	-0.12D-03	-0.38D-02
7, 1	-0.17D-03	0.45D-02	8, 1	0.43D-03	0.31D-02
7, 2	0.52D-04	-0.52D-02	8, 2	0.26D-03	0.19D-02
7, 3	0.10D-02	0.29D-02	8, 3	-0.43D-03	-0.44D-02
7, 4	-0.71D-03	-0.24D-02	8, 4	-0.27D-03	0.59D-02
7, 5	0.16D-05	0.45D-02	8, 5	0.13D-03	-0.43D-02
7, 6	0.48D-03	-0.17D-02	8, 6	-0.18D-04	0.15D-02
7, 7	-0.49D-03	0.37D-02	8, 7	-0.45D-03	-0.27D-02
7, 8	0.70D-03	-0.19D-02	8, 8	-0.51D-03	-0.73D-04
7, 9	0.74D-03	-0.50D-02	8, 9	0.68D-04	0.63D-02
7, 10	-0.44D-03	0.35D-02	8, 10	0.17D-03	-0.20D-02
7, 11	-0.43D-03	-0.13D-02	8, 11	0.18D-03	-0.54D-02
9, 1	-0.57D-03	0.11D-02	10, 1	0.11D-02	0.42D-02
9, 2	0.52D-04	0.25D-02	10, 2	0.15D-03	-0.22D-02
9, 3	-0.16D-03	-0.45D-02	10, 3	0.90D-03	0.20D-02
9, 4	0.29D-03	0.38D-02	10, 4	-0.13D-04	0.33D-02
9, 5	0.63D-03	-0.45D-02	10, 5	0.42D-04	-0.21D-03
9, 6	0.78D-04	0.16D-02	10, 6	-0.23D-03	-0.36D-02
9, 7	0.47D-03	0.25D-02	10, 7	-0.11D-02	0.49D-02
9, 8	0.30D-04	0.21D-02	10, 8	0.11D-02	-0.51D-02
9, 9	-0.67D-03	-0.61D-02	10, 9	0.65D-03	0.15D-02
9, 10	0.70D-03	-0.77D-03	10, 10	0.65D-04	0.79D-03
9, 11	0.42D-03	-0.23D-02	10, 11	-0.66D-03	-0.42D-03
11, 1	0.41D-04	-0.30D-02	12, 1	-0.26D-05	-0.41D-02
11, 2	0.17D-03	0.40D-02	12, 2	-0.62D-05	0.40D-02
11, 3	-0.37D-03	-0.30D-02	12, 3	0.19D-03	0.14D-02
11, 4	0.11D-02	0.33D-02	12, 4	-0.93D-03	-0.32D-02
11, 5	-0.14D-03	-0.52D-02	12, 5	0.40D-04	-0.44D-02
11, 6	-0.32D-03	-0.19D-03	12, 6	0.85D-03	0.50D-02
11, 7	0.10D-02	0.61D-02	12, 7	-0.19D-03	-0.22D-02
11, 8	-0.12D-02	0.18D-03	12, 8	0.11D-02	-0.24D-02

11, 9	0.33D-03	0.91D-03	12, 9	-0.99D-04	0.29D-02
11,10	0.21D-03	-0.57D-02	12,10	-0.26D-03	-0.92D-03
11,11	0.52D-03	-0.16D-02	12,11	0.49D-03	-0.57D-02
13, 1	0.13D-05	-0.69D-02	14, 1	-0.69D-05	-0.44D-02
13, 2	-0.41D-03	0.42D-02	14, 2	0.11D-03	0.35D-02
13, 3	-0.71D-03	-0.42D-02	14, 3	0.66D-04	-0.44D-02
13, 4	0.73D-03	0.15D-02	14, 4	0.17D-04	0.84D-03
13, 5	0.14D-03	0.52D-02	14, 5	0.20D-04	0.26D-02
13, 6	-0.13D-04	-0.92D-03	14, 6	0.90D-04	-0.67D-02
13, 7	0.29D-03	-0.10D-02	14, 7	0.94D-04	0.63D-02
13, 8	-0.16D-03	-0.33D-02	14, 8	0.14D-03	-0.61D-02
13, 9	0.46D-04	0.24D-02	14, 9	-0.60D-04	0.65D-02
13,10	-0.19D-04	0.24D-03	14,10	0.31D-03	0.26D-02
13,11	-0.20D-03	-0.28D-02	14,11	-0.42D-03	-0.30D-03
15, 1	0.14D-03	-0.64D-02	16, 1	-0.19D-04	0.14D-02
15, 2	0.13D-03	0.13D-02	16, 2	0.85D-05	-0.33D-02
15, 3	0.99D-03	-0.16D-02	16, 3	-0.12D-03	0.48D-02
15, 4	0.26D-03	0.45D-02	16, 4	0.44D-04	-0.39D-02
15, 5	-0.83D-03	0.37D-02	16, 5	0.10D-02	0.30D-02
15, 6	-0.84D-04	-0.50D-02	16, 6	0.28D-04	-0.24D-02
15, 7	0.55D-04	0.47D-02	16, 7	0.34D-03	-0.70D-03
15, 8	0.19D-03	0.10D-02	16, 8	-0.46D-03	0.48D-02
15, 9	-0.10D-04	-0.42D-02	16, 9	0.42D-03	-0.44D-02
15,10	-0.34D-03	-0.46D-02	16,10	0.43D-03	0.54D-02
15,11	0.35D-03	0.45D-03	16,11	0.17D-03	0.55D-03
17, 1	0.12D-03	-0.73D-03	18, 1	0.31D-03	-0.18D-02
17, 2	0.46D-04	-0.14D-02	18, 2	0.49D-03	-0.40D-02
17, 3	0.15D-03	0.72D-02	18, 3	-0.27D-04	-0.20D-03
17, 4	-0.73D-04	-0.25D-03	18, 4	-0.14D-03	0.38D-02
17, 5	0.13D-03	-0.41D-02	18, 5	-0.40D-04	0.23D-02
17, 6	0.21D-03	0.38D-02	18, 6	-0.22D-04	0.19D-02
17, 7	-0.20D-03	-0.22D-03	18, 7	-0.23D-03	-0.64D-02
17, 8	0.50D-03	-0.36D-02	18, 8	-0.31D-04	0.64D-02
17, 9	-0.41D-03	-0.35D-02	18, 9	0.59D-03	-0.54D-02
17,10	-0.14D-03	-0.71D-03	18,10	0.26D-03	0.43D-02
17,11	0.49D-04	0.69D-02	18,11	0.58D-03	-0.31D-02
19, 1	-0.46D-03	0.66D-02			
19, 2	-0.10D-03	-0.15D-02			
19, 3	0.21D-03	-0.41D-02			
19, 4	0.30D-03	0.37D-02			
19, 5	0.72D-04	-0.28D-02			
19, 6	0.45D-03	-0.12D-02			
19, 7	0.35D-03	0.69D-02			
19, 8	0.29D-03	0.20D-03			
19, 9	-0.12D-03	0.55D-03			
19,10	0.65D-04	0.39D-03			
19,11	-0.43D-04	-0.36D-02			

STATISTICAL RESULTS:

	MEAN VALUE	STANDARD DEVIATION
XX-STRAIN:	0.8597D-04	0.4176D-03
YY-STRAIN:	-0.3602D-04	0.3610D-02

RECONSTRUCTION RESULTS OF INTERFEROGRAM
(2R) OF THE NEWS-PRINT PAPER SAMPLE #38
CUMMULATIVE DEFORMATION)

CO-ORDINATES X	CO-ORDINATES Y	DEFORMATIONS X	DEFORMATIONS Y	DEFORMATIONS Z
44.0	-22.0	0.2429D 02	-0.2677D 02	0.1393D 02
44.0	-18.0	0.2363D 02	0.2151D 02	0.3716D 01
44.0	-14.0	0.2515D 02	-0.2698D 02	-0.1785D 02
44.0	-10.0	0.2412D 02	0.2177D 02	0.5976D 01
44.0	-6.0	0.2439D 02	0.2470D 02	0.4992D 01
44.0	-2.0	0.2457D 02	0.5364D 01	0.2502D 01
44.0	2.0	0.2474D 02	-0.1823D 02	-0.1193D 02
44.0	6.0	0.2400D 02	0.1528D 02	-0.7112D 00
44.0	10.0	0.2531D 02	-0.3496D 02	-0.2701D 02
44.0	14.0	0.2436D 02	-0.1435D 01	-0.1933D 02
44.0	18.0	0.2376D 02	-0.1423D 02	0.1515D 02
44.0	22.0	0.2480D 02	-0.4397D 01	-0.1060D 02
40.0	-22.0	0.2289D 02	0.2212D 02	0.6319D 01
40.0	-18.0	0.2348D 02	0.1807D 02	-0.6189D 01
40.0	-14.0	0.2420D 02	-0.3164D 01	-0.3218D 02
40.0	-10.0	0.2425D 02	-0.3724D 02	-0.1358D 01
40.0	-6.0	0.2482D 02	-0.1359D 02	-0.5797D 01
40.0	-2.0	0.2440D 02	-0.1649D 02	-0.1914D 02
40.0	2.0	0.2377D 02	-0.1131D 02	-0.1753D 02
40.0	6.0	0.2439D 02	-0.1856D 02	-0.4682D 00
40.0	10.0	0.2293D 02	-0.9386D 01	0.6240D 01
40.0	14.0	0.2430D 02	-0.1148D 02	-0.1908D 02
40.0	18.0	0.2347D 02	0.2580D 02	-0.3514D 01
40.0	22.0	0.2266D 02	0.1223D 02	-0.1387D 02
36.0	-22.0	0.2375D 02	0.1914D 01	0.1116D 02
36.0	-18.0	0.2438D 02	0.4711D 01	-0.1407D 02
36.0	-14.0	0.2338D 02	-0.7651D 01	0.1518D 02
36.0	-10.0	0.2287D 02	-0.1547D 02	0.8208D 01
36.0	-6.0	0.2334D 02	0.2380D 02	-0.4359D 01
36.0	-2.0	0.2324D 02	0.1453D 01	0.4895D 01
36.0	2.0	0.2449D 02	-0.3824D 02	0.2427D 02
36.0	6.0	0.2435D 02	0.1331D 01	-0.1188D 02
36.0	10.0	0.2382D 02	0.3882D 00	0.2590D 01
36.0	14.0	0.2400D 02	-0.2369D 01	-0.8140D 01
36.0	18.0	0.2416D 02	-0.2221D 02	-0.1029D 02
36.0	22.0	0.2348D 02	0.2350D 01	-0.1230D 02
32.0	-22.0	0.2245D 02	-0.8095D 01	0.1264D 02
32.0	-18.0	0.2275D 02	-0.6943D 01	-0.2102D 02
32.0	-14.0	0.2273D 02	-0.3721D 02	-0.1941D 02
32.0	-10.0	0.2264D 02	0.1883D 02	-0.1272D 02
32.0	-6.0	0.2273D 02	-0.1066D 02	-0.7760D 01
32.0	-2.0	0.2341D 02	0.1317D 02	0.1115D 02
32.0	2.0	0.2390D 02	-0.5219D 01	0.1692D 01
32.0	6.0	0.2309D 02	-0.6261D 00	-0.5448D 01
32.0	10.0	0.2147D 02	0.1146D 02	-0.9551D 01
32.0	14.0	0.2208D 02	0.2331D 02	0.2941D 01
32.0	18.0	0.2297D 02	-0.3847D 02	-0.1139D 02
32.0	22.0	0.2226D 02	-0.2376D 02	0.3082D 02
28.0	-22.0	0.2309D 02	-0.7539D 01	0.3153D 02
28.0	-18.0	0.2216D 02	0.1176D 02	-0.4371D 01
28.0	-14.0	0.2175D 02	0.2436D 02	0.5278D 01
28.0	-10.0	0.2173D 02	0.2328D 02	0.5469D 01
28.0	-6.0	0.2108D 02	-0.8777D 01	-0.1485D 02
28.0	-2.0	0.2211D 02	-0.1688D 02	0.1071D 01
28.0	2.0	0.2274D 02	-0.9616D 01	0.1196D 01
28.0	6.0	0.2284D 02	0.1309D 02	-0.2970D 02
28.0	10.0	0.2177D 02	0.1682D 02	-0.2423D 02
28.0	14.0	0.2228D 02	-0.1997D 02	0.2641D 01
28.0	18.0	0.2133D 02	-0.5548D 01	0.2190D 02
28.0	22.0	0.2223D 02	-0.3503D 02	-0.6560D 00

24.0	-22.0	0.2230D 02	-0.7062D 01	0.1252D 02	
24.0	-18.0	0.2199D 02	0.5574D 01	0.3387D 01	
24.0	-14.0	0.2239D 02	-0.1277D 02	0.5936D 01	
24.0	-10.0	0.2137D 02	-0.1110D 01	-0.2695D 02	
24.0	-6.0	0.2208D 02	0.1957D 02	-0.1191D 02	
24.0	-2.0	0.2084D 02	0.3523D 02	0.1979D 02	
24.0	2.0	0.2043D 02	-0.7586D 00	-0.1519D 02	
24.0	6.0	0.2086D 02	0.7841D 01	-0.1318D 02	
24.0	10.0	0.2080D 02	0.1205D 02	0.2538D 01	
24.0	14.0	0.2131D 02	0.3182D 00	0.2715D 02	
24.0	18.0	0.2030D 02	-0.5688D 01	0.2833D 01	
24.0	22.0	0.2262D 02	-0.1309D 02	-0.6084D 01	
20.0	-22.0	0.2180D 02	-0.8692D 01	0.1687D 02	
20.0	-18.0	0.2134D 02	0.1242D 02	-0.1531D 02	
20.0	-14.0	0.2171D 02	-0.3772D 02	0.2533D 01	
20.0	-10.0	0.2312D 02	-0.1438D 02	0.2055D 02	
20.0	-6.0	0.2235D 02	-0.3527D 02	0.9255D 01	
20.0	-2.0	0.2194D 02	0.1068D 02	-0.1275D 02	
20.0	2.0	0.2100D 02	-0.1053D 02	-0.1455D 02	
20.0	6.0	0.2174D 02	0.2269D 02	-0.1616D 00	
20.0	10.0	0.2105D 02	-0.4324D 01	-0.2349D 01	
20.0	14.0	0.2251D 02	-0.3232D 02	-0.2542D 02	
20.0	18.0	0.2134D 02	-0.1409D 02	-0.1164D 02	
20.0	22.0	0.2011D 02	0.1657D 02	0.2202D 01	
16.0	-22.0	0.2105D 02	-0.1871D 02	-0.3430D 02	
16.0	-18.0	0.2070D 02	-0.1337D 02	-0.2389D 01	
16.0	-14.0	0.2141D 02	-0.2151D 02	0.2152D 02	
16.0	-10.0	0.1941D 02	0.5361D 01	-0.9982D 01	
16.0	-6.0	0.2087D 02	-0.5212D 01	-0.3691D 01	
16.0	-2.0	0.2060D 02	0.1199D 01	-0.1671D 02	
16.0	2.0	0.1950D 02	-0.2299D 02	-0.2628D 02	
16.0	6.0	0.1976D 02	-0.2804D 02	0.7890D 00	
16.0	10.0	0.1970D 02	0.2739D 00	0.1787D 02	
16.0	14.0	0.2071D 02	0.2528D 02	0.7606D-01	
16.0	18.0	0.2043D 02	0.2182D 02	-0.1056D 02	
16.0	22.0	0.1902D 02	0.1884D 02	-0.1522D 02	
12.0	-22.0	0.1992D 02	-0.2380D 02	-0.1770D 02	
12.0	-18.0	0.1873D 02	0.2446D 02	-0.1427D 02	
12.0	-14.0	0.1963D 02	0.5398D 01	0.1237D 02	
12.0	-10.0	0.1966D 02	0.3472D 02	0.5250D 01	
12.0	-6.0	0.1904D 02	-0.4672D 01	0.1266D 02	
12.0	-2.0	0.1902D 02	0.1203D 02	0.8195D 01	
12.0	2.0	0.1958D 02	-0.1225D 02	0.1036D 02	
12.0	6.0	0.2021D 02	-0.1812D 02	0.1513D 02	
12.0	10.0	0.1983D 02	0.1230D 02	0.4791D 01	
12.0	14.0	0.2043D 02	-0.1950D 02	-0.7106D 01	
12.0	18.0	0.2082D 02	-0.2827D 02	0.2478D 01	
12.0	22.0	0.2007D 02	-0.1213D 02	-0.3401D 02	
8.0	-22.0	0.1905D 02	-0.3228D 02	0.3497D 01	
8.0	-18.0	0.1979D 02	-0.1709D 02	-0.1623D 02	
8.0	-14.0	0.1944D 02	-0.3153D 02	0.2053D 01	
8.0	-10.0	0.1930D 02	0.2356D 01	-0.2265D 01	
8.0	-6.0	0.1827D 02	-0.2539D 00	-0.6013D 00	
8.0	-2.0	0.1815D 02	-0.8533D 01	-0.3709D 01	
8.0	2.0	0.1977D 02	-0.4019D 02	-0.1051D 01	
8.0	6.0	0.1884D 02	0.2297D 02	-0.6963D 01	
8.0	10.0	0.1956D 02	-0.8140D 01	0.2637D 02	
8.0	14.0	0.1887D 02	-0.6434D 01	0.1297D 02	
8.0	18.0	0.1816D 02	0.2777D 02	0.3119D 02	
8.0	22.0	0.2028D 02	-0.1860D 01	-0.1671D 01	
4.0	-22.0	0.1819D 02	0.1078D 02	0.5952D 01	
4.0	-18.0	0.1877D 02	0.2479D 02	-0.2245D 02	
4.0	-14.0	0.1847D 02	0.3643D 01	-0.1723D 01	
4.0	-10.0	0.2024D 02	-0.2181D 02	-0.1230D 01	
4.0	-6.0	0.1815D 02	0.1432D 01	0.1948D 02	
4.0	-2.0	0.1828D 02	-0.1043D 02	0.1266D 02	
4.0	2.0	0.1803D 02	0.1712D 02	-0.1195D 02	
4.0	6.0	0.1768D 02	0.9363D 01	0.4537D 00	
4.0	10.0	0.1807D 02	-0.1338D 02	0.1123D 02	
4.0	14.0	0.1817D 02	-0.3277D 01	0.7927D 01	
4.0	18.0	0.1773D 02	0.2619D 02	-0.2931D 02	
4.0	22.0	0.1944D 02	-0.1326D 02	-0.3422D 02	

0.0	-22.0	0.1711D 02	-0.1860D 02	0.2193D 02	
0.0	-18.0	0.1731D 02	-0.8995D 01	0.1305D 02	
0.0	-14.0	0.1767D 02	0.1253D 02	-0.1504D 02	
0.0	-10.0	0.1739D 02	0.2309D 02	0.2745D 01	
0.0	-6.0	0.1657D 02	0.2371D 02	0.9128D 01	
0.0	-2.0	0.1768D 02	-0.1595D 02	0.1488D 02	
0.0	2.0	0.1756D 02	-0.3137D 02	0.2058D 02	
0.0	6.0	0.1585D 02	-0.1829D 02	-0.4328D 00	
0.0	10.0	0.1778D 02	0.2204D 02	-0.1759D 02	
0.0	14.0	0.1784D 02	-0.1276D 02	-0.8817D 01	
0.0	18.0	0.1699D 02	0.1047D 01	-0.5808D 01	
0.0	22.0	0.1803D 02	0.1396D 02	-0.1342D 02	
-4.0	-22.0	0.1797D 02	-0.3862D 01	-0.9642D 01	
-4.0	-18.0	0.1741D 02	-0.1834D 01	-0.4541D 01	
-4.0	-14.0	0.1853D 02	-0.1909D 02	0.6862D 01	
-4.0	-10.0	0.1735D 02	-0.8245D 01	0.6704D 01	
-4.0	-6.0	0.1791D 02	0.5040D 01	-0.5764D 00	
-4.0	-2.0	0.1773D 02	-0.4251D 02	-0.1760D 02	
-4.0	2.0	0.1696D 02	0.4829D 01	0.3114D 00	
-4.0	6.0	0.1732D 02	-0.1546D 02	-0.2331D 02	
-4.0	10.0	0.1801D 02	0.4451D 01	-0.4788D 01	
-4.0	14.0	0.1738D 02	-0.8043D 01	-0.9516D 01	
-4.0	18.0	0.1650D 02	-0.2635D 02	0.9302D 01	
-4.0	22.0	0.1747D 02	-0.9207D 01	-0.5445D 01	
-8.0	-22.0	0.1669D 02	0.1805D 02	0.9263D 01	
-8.0	-18.0	0.1782D 02	-0.2625D 00	0.2892D 02	
-8.0	-14.0	0.1768D 02	-0.2009D 02	-0.3658D 01	
-8.0	-10.0	0.1768D 02	-0.6498D 01	0.2471D 02	
-8.0	-6.0	0.1711D 02	-0.1175D 02	-0.3041D 01	
-8.0	-2.0	0.1666D 02	0.1227D 02	0.2496D 02	
-8.0	2.0	0.1503D 02	0.9318D 01	-0.7705D 01	
-8.0	6.0	0.1690D 02	0.2838D 01	-0.1578D 01	
-8.0	10.0	0.1529D 02	0.1088D 02	-0.4299D 01	
-8.0	14.0	0.1838D 02	-0.5879D 01	-0.1020D 02	
-8.0	18.0	0.1674D 02	0.8217D 00	0.2097D 02	
-8.0	22.0	0.1704D 02	0.1122D 02	-0.8219D 01	
-12.0	-22.0	0.1671D 02	-0.1513D 02	0.1101D 02	
-12.0	-18.0	0.1610D 02	-0.2552D 02	-0.1178D 02	
-12.0	-14.0	0.1670D 02	-0.1863D 01	0.1546D 02	
-12.0	-10.0	0.1579D 02	0.1967D 02	-0.9172D 01	
-12.0	-6.0	0.1596D 02	-0.5208D 01	-0.4736D 01	
-12.0	-2.0	0.1666D 02	-0.3139D 01	0.2672D 01	
-12.0	2.0	0.1733D 02	0.1543D 02	0.2351D 01	
-12.0	6.0	0.1638D 02	0.8282D 01	0.2531D 02	
-12.0	10.0	0.1622D 02	-0.3289D 01	0.3526D 01	
-12.0	14.0	0.1527D 02	-0.2246D 02	-0.5118D 00	
-12.0	18.0	0.1604D 02	-0.1392D 02	0.6130D 01	
-12.0	22.0	0.1603D 02	-0.2189D 02	0.2767D 02	
-16.0	-22.0	0.1619D 02	-0.2459D 02	-0.3065D 02	
-16.0	-18.0	0.1537D 02	0.1294D 02	0.1532D 02	
-16.0	-14.0	0.1545D 02	0.1782D 02	-0.3432D 02	
-16.0	-10.0	0.1620D 02	0.1230D 02	0.4249D 01	
-16.0	-6.0	0.1649D 02	0.1307D 02	-0.1615D 01	
-16.0	-2.0	0.1573D 02	0.7547D 01	-0.2969D 02	
-16.0	2.0	0.1619D 02	-0.3112D 02	-0.2170D 02	
-16.0	6.0	0.1726D 02	-0.1404D 02	-0.1858D 02	
-16.0	10.0	0.1431D 02	0.2517D 02	-0.1091D 02	
-16.0	14.0	0.1662D 02	0.5494D 01	-0.2000D 02	
-16.0	18.0	0.1596D 02	-0.2446D 02	0.4771D 01	
-16.0	22.0	0.1722D 02	-0.1921D 02	0.2011D 01	
-20.0	-22.0	0.1578D 02	-0.4368D 02	0.1223D 01	
-20.0	-18.0	0.1551D 02	-0.7489D 01	0.1986D 02	
-20.0	-14.0	0.1452D 02	-0.2526D 00	-0.1134D 01	
-20.0	-10.0	0.1686D 02	-0.1166D 02	-0.7009D 01	
-20.0	-6.0	0.1542D 02	-0.1485D 01	-0.4053D 01	
-20.0	-2.0	0.1542D 02	-0.1686D 02	-0.1928D 02	
-20.0	2.0	0.1422D 02	-0.1644D 02	-0.2207D 02	
-20.0	6.0	0.1581D 02	0.2341D-01	-0.7130D 01	
-20.0	10.0	0.1562D 02	-0.3985D 01	0.7018D 01	
-20.0	14.0	0.1638D 02	-0.2409D 02	-0.1100D 02	
-20.0	18.0	0.1657D 02	-0.8722D 01	-0.2923D 02	
-20.0	22.0	0.1632D 02	-0.1888D 02	-0.5006D 01	

-24.0	-22.0	0.1623D 02	0.9915D 01	-0.6897D 01	
-24.0	-18.0	0.1506D 02	0.1551D 02	0.1212D 02	
-24.0	-14.0	0.1490D 02	-0.1192D 02	0.3040D 01	
-24.0	-10.0	0.1496D 02	-0.1987D 02	-0.1756D 02	
-24.0	-6.0	0.1517D 02	0.1818D 02	0.9480D 01	
-24.0	-2.0	0.1522D 02	-0.1394D 02	-0.9867D 01	
-24.0	2.0	0.1390D 02	0.1420D 02	0.8316D 01	
-24.0	6.0	0.1405D 02	0.1336D 02	0.2034D 02	
-24.0	10.0	0.1383D 02	-0.1424D 01	-0.1823D 02	
-24.0	14.0	0.1427D 02	-0.1811D 02	-0.1671D 02	
-24.0	18.0	0.1369D 02	0.1436D 02	-0.4038D 01	
-24.0	22.0	0.1386D 02	-0.1148D 02	-0.3623D 02	
-28.0	-22.0	0.1447D 02	0.1400D 02	-0.1890D 02	
-28.0	-18.0	0.1406D 02	0.7404D 00	0.1750D 02	
-28.0	-14.0	0.1381D 02	0.5828D 01	0.2832D 02	
-28.0	-10.0	0.1439D 02	0.8839D 01	-0.1209D 02	
-28.0	-6.0	0.1411D 02	-0.7518D 01	-0.3485D 01	
-28.0	-2.0	0.1297D 02	0.3135D 02	-0.4945D 01	
-28.0	2.0	0.1315D 02	0.1595D 02	-0.1315D 02	
-28.0	6.0	0.1353D 02	-0.8101D 01	0.1001D 02	
-28.0	10.0	0.1573D 02	-0.1311D 02	0.1015D 02	
-28.0	14.0	0.1389D 02	-0.2671D 02	0.9911D-01	
-28.0	18.0	0.1391D 02	-0.6735D 01	-0.9608D 01	
-28.0	22.0	0.1431D 02	-0.5147D 01	-0.1886D 01	
-32.0	-22.0	0.1341D 02	0.9070D 00	0.1215D 02	
-32.0	-18.0	0.1217D 02	-0.4002D-01	0.8267D 01	
-32.0	-14.0	0.1294D 02	0.2711D 02	-0.2766D 02	
-32.0	-10.0	0.1438D 02	0.2647D 01	-0.7731D 01	
-32.0	-6.0	0.1321D 02	-0.1186D 02	-0.1160D 02	
-32.0	-2.0	0.1413D 02	-0.3463D 01	-0.7850D 01	
-32.0	2.0	0.1279D 02	0.2166D 02	0.2118D 02	
-32.0	6.0	0.1336D 02	0.2048D 01	0.1423D 02	
-32.0	10.0	0.1350D 02	0.3593D 01	-0.1030D 02	
-32.0	14.0	0.1343D 02	-0.3265D 02	0.2372D 01	
-32.0	18.0	0.1398D 02	-0.9363D 01	0.5138D 01	
-32.0	22.0	0.1482D 02	-0.2556D 02	-0.1269D 02	

STATISTICAL RESULTS:

	MEAN VALUE	STANDARD DEVIATION
X-DIRECTION	0.190D 02	0.342D 01
Y-DIRECTION	-0.313D 01	0.172D 02
Z-DIRECTION	-0.194D 01	0.145D 02

EVALUATED STRAIN FIELD AT POINT (2 R)

ELEMENT	EXX	EYY	ELEMENT	EXX	EYY
1, 1	0.35D-03	-0.12D-01	2, 1	-0.21D-03	0.10D-02
1, 2	0.38D-04	0.12D-01	2, 2	-0.23D-03	0.53D-02
1, 3	0.24D-03	-0.12D-01	2, 3	0.20D-03	0.85D-02
1, 4	-0.31D-04	-0.73D-03	2, 4	0.34D-03	-0.59D-02
1, 5	-0.11D-03	0.48D-02	2, 5	0.37D-03	0.73D-03
1, 6	0.42D-04	0.59D-02	2, 6	0.29D-03	-0.13D-02
1, 7	0.24D-03	-0.84D-02	2, 7	-0.18D-03	0.18D-02
1, 8	-0.98D-04	0.13D-01	2, 8	0.10D-04	-0.23D-02
1, 9	0.59D-03	-0.84D-02	2, 9	-0.22D-03	0.52D-03
1,10	0.16D-04	0.32D-02	2,10	0.75D-04	-0.93D-02
1,11	0.71D-04	-0.25D-02	2,11	-0.17D-03	0.34D-02
3, 1	0.32D-03	-0.70D-03	4, 1	-0.16D-03	-0.29D-03
3, 2	0.41D-03	0.31D-02	4, 2	0.15D-03	0.76D-02
3, 3	0.16D-03	0.20D-02	4, 3	0.25D-03	-0.14D-01
3, 4	0.58D-04	-0.98D-02	4, 4	0.23D-03	0.74D-02
3, 5	0.15D-03	0.56D-02	4, 5	0.41D-03	-0.60D-02
3, 6	-0.42D-04	0.99D-02	4, 6	0.32D-03	0.46D-02
3, 7	0.15D-03	-0.99D-02	4, 7	0.29D-03	-0.11D-02
3, 8	0.32D-03	0.24D-03	4, 8	0.62D-04	-0.30D-02
3, 9	0.59D-03	0.69D-03	4, 9	-0.76D-04	-0.30D-02
3,10	0.48D-03	0.50D-02	4,10	-0.52D-04	0.15D-01
3,11	0.30D-03	-0.61D-02	4,11	0.41D-03	-0.37D-02
5, 1	0.20D-03	-0.48D-02	6, 1	0.12D-03	-0.32D-02
5, 2	0.42D-04	-0.31D-02	6, 2	0.16D-03	0.46D-02
5, 3	-0.16D-03	0.27D-03	6, 3	0.17D-03	-0.29D-02
5, 4	0.90D-04	0.80D-02	6, 4	-0.44D-03	-0.52D-02
5, 5	-0.25D-03	0.20D-02	6, 5	-0.69D-04	-0.39D-02
5, 6	0.32D-03	-0.18D-02	6, 6	-0.28D-03	0.90D-02
5, 7	0.58D-03	-0.57D-02	6, 7	-0.14D-03	-0.21D-02
5, 8	0.50D-03	-0.93D-03	6, 8	-0.22D-03	-0.11D-02
5, 9	0.24D-03	0.92D-02	6, 9	-0.63D-04	0.29D-02
5,10	0.24D-03	-0.36D-02	6,10	-0.30D-03	0.15D-02
5,11	0.26D-03	0.74D-02	6,11	-0.26D-03	0.18D-02
7, 1	0.19D-03	-0.53D-02	8, 1	0.28D-03	-0.13D-02
7, 2	0.16D-03	0.13D-01	8, 2	0.49D-03	0.20D-02
7, 3	0.74D-04	-0.58D-02	8, 3	0.44D-03	-0.67D-02
7, 4	0.93D-03	0.52D-02	8, 4	-0.64D-04	0.26D-02
7, 5	0.37D-03	-0.11D-01	8, 5	0.46D-03	-0.16D-02
7, 6	0.34D-03	0.53D-02	8, 6	0.40D-03	0.60D-02
7, 7	0.38D-03	-0.83D-02	8, 7	-0.20D-04	0.13D-02
7, 8	0.49D-03	0.68D-02	8, 8	-0.11D-03	-0.71D-02
7, 9	0.34D-03	0.70D-02	8, 9	-0.30D-04	-0.63D-02
7,10	0.45D-03	-0.46D-02	8,10	0.69D-04	0.86D-03
7,11	0.23D-03	-0.77D-02	8,11	-0.97D-04	0.75D-03
9, 1	0.22D-03	-0.12D-01	10, 1	0.22D-03	-0.38D-02
9, 2	-0.27D-03	0.48D-02	10, 2	0.25D-03	0.36D-02
9, 3	0.49D-04	-0.73D-02	10, 3	0.24D-03	-0.85D-02
9, 4	0.90D-04	0.98D-02	10, 4	-0.23D-03	0.65D-03
9, 5	0.19D-03	-0.42D-02	10, 5	0.30D-04	0.21D-02
9, 6	0.22D-03	0.61D-02	10, 6	-0.32D-04	0.79D-02
9, 7	-0.48D-04	0.15D-02	10, 7	0.43D-03	-0.16D-01
9, 8	0.34D-03	-0.76D-02	10, 8	0.29D-03	0.78D-02
9, 9	0.66D-04	0.79D-02	10, 9	0.37D-03	-0.43D-03
9,10	0.39D-03	0.22D-02	10,10	0.18D-03	-0.86D-02
9,11	0.67D-03	-0.40D-02	10,11	0.11D-03	0.74D-02
11, 1	0.27D-03	-0.35D-02	12, 1	-0.22D-03	-0.24D-02
11, 2	0.36D-03	0.53D-02	12, 2	-0.23D-04	-0.54D-02
11, 3	0.20D-03	0.64D-02	12, 3	-0.22D-03	-0.26D-02
11, 4	0.71D-03	-0.56D-02	12, 4	0.11D-04	-0.16D-03
11, 5	0.39D-03	0.30D-02	12, 5	-0.33D-03	0.99D-02
11, 6	0.15D-03	-0.69D-02	12, 6	-0.11D-04	0.39D-02
11, 7	0.12D-03	0.19D-02	12, 7	0.15D-03	-0.33D-02
11, 8	0.46D-03	0.57D-02	12, 8	-0.37D-03	-0.10D-01

11, 9	0.73D-04	-0.25D-02	12, 9	-0.59D-04	0.87D-02
11,10	0.83D-04	-0.74D-02	12,10	0.12D-03	-0.35D-02
11,11	0.19D-03	0.99D-02	12,11	0.12D-03	-0.32D-02
13, 1	0.32D-03	-0.51D-03	14, 1	-0.47D-05	0.46D-02
13, 2	-0.10D-03	0.43D-02	14, 2	0.43D-03	0.50D-02
13, 3	0.21D-03	-0.27D-02	14, 3	0.25D-03	-0.34D-02
13, 4	-0.84D-04	-0.33D-02	14, 4	0.47D-03	0.13D-02
13, 5	0.20D-03	0.12D-01	14, 5	0.29D-03	-0.60D-02
13, 6	0.27D-03	-0.12D-01	14, 6	0.43D-06	0.74D-03
13, 7	0.48D-03	0.51D-02	14, 7	-0.57D-03	0.16D-02
13, 8	0.10D-03	-0.50D-02	14, 8	0.13D-03	-0.20D-02
13, 9	0.68D-03	0.31D-02	14, 9	-0.23D-03	0.42D-02
13,10	-0.25D-03	0.46D-02	14,10	0.78D-03	-0.17D-02
13,11	-0.60D-04	-0.43D-02	14,11	0.17D-03	-0.26D-02
15, 1	0.13D-03	0.26D-02	16, 1	0.10D-03	-0.94D-02
15, 2	0.18D-03	-0.59D-02	16, 2	-0.33D-04	-0.12D-02
15, 3	0.31D-03	-0.54D-02	16, 3	0.23D-03	0.14D-02
15, 4	-0.10D-03	0.62D-02	16, 4	-0.17D-03	-0.15D-03
15, 5	-0.13D-03	-0.52D-03	16, 5	0.27D-03	0.14D-02
15, 6	0.23D-03	-0.46D-02	16, 6	0.78D-04	0.97D-02
15, 7	0.29D-03	0.18D-02	16, 7	0.49D-03	-0.43D-02
15, 8	-0.22D-03	0.29D-02	16, 8	0.36D-03	-0.98D-02
15, 9	0.48D-03	0.48D-02	16, 9	-0.33D-03	0.49D-02
15,10	-0.34D-03	-0.21D-02	16,10	0.60D-04	0.75D-02
15,11	0.20D-04	0.20D-02	16,11	-0.15D-03	-0.13D-02
17, 1	-0.11D-03	-0.90D-02	18, 1	0.44D-03	-0.14D-02
17, 2	0.11D-03	-0.18D-02	18, 2	0.25D-03	0.69D-02
17, 3	-0.94D-04	0.29D-02	18, 3	0.27D-03	0.20D-02
17, 4	0.48D-03	-0.25D-02	18, 4	0.14D-03	-0.95D-02
17, 5	0.62D-04	0.38D-02	18, 5	0.27D-03	0.80D-02
17, 6	0.50D-04	-0.11D-03	18, 6	0.56D-03	-0.70D-02
17, 7	0.80D-04	-0.41D-02	18, 7	0.19D-03	0.21D-03
17, 8	0.44D-03	0.10D-02	18, 8	0.13D-03	0.37D-02
17, 9	0.45D-03	0.50D-02	18, 9	-0.47D-03	0.42D-02
17,10	0.53D-03	-0.38D-02	18,10	0.94D-04	-0.81D-02
17,11	0.72D-03	0.25D-02	18,11	-0.55D-04	0.65D-02
19, 1	0.26D-03	0.33D-02			
19, 2	0.47D-03	-0.13D-02			
19, 3	0.22D-03	-0.75D-03			
19, 4	0.30D-05	0.41D-02			
19, 5	0.23D-03	-0.97D-02			
19, 6	-0.29D-03	0.38D-02			
19, 7	0.90D-04	0.60D-02			
19, 8	0.42D-04	0.13D-02			
19, 9	0.56D-03	0.34D-02			
19,10	0.11D-03	-0.50D-02			
19,11	-0.19D-04	-0.40D-03			

STATISTICAL RESULTS:

	MEAN VALUE	STANDARD DEVIATION
XX-STRAIN:	0.1448D-03	0.2551D-03
YY-STRAIN:	-0.5727D-04	0.5850D-02

EVALUATED STRAIN FIELD AT POINT (2L)

ELEMENT	EXX	EYY	ELEMENT	EXX	EYY
1, 1	0.30D-03	-0.33D-02	2, 1	-0.39D-03	-0.10D-03
1, 2	0.20D-03	0.48D-02	2, 2	0.83D-04	-0.59D-02
1, 3	0.23D-03	-0.95D-03	2, 3	0.42D-03	0.53D-02
1, 4	-0.28D-03	-0.65D-02	2, 4	-0.97D-04	-0.66D-02
1, 5	-0.20D-03	0.46D-02	2, 5	0.58D-04	0.71D-02
1, 6	0.37D-03	0.43D-02	2, 6	0.47D-03	0.13D-03
1, 7	-0.11D-03	0.44D-02	2, 7	0.74D-03	0.91D-04
1, 8	-0.38D-04	-0.75D-02	2, 8	0.11D-02	-0.95D-03
1, 9	0.32D-03	-0.52D-02	2, 9	0.56D-03	-0.33D-02
1, 10	0.26D-03	0.49D-02	2, 10	0.25D-03	0.18D-02
1, 11	0.93D-04	0.45D-02	2, 11	0.88D-03	-0.40D-02
3, 1	0.13D-02	0.56D-02	4, 1	-0.21D-04	0.23D-02
3, 2	0.20D-03	0.34D-02	4, 2	0.59D-03	-0.80D-02
3, 3	0.82D-04	-0.82D-03	4, 3	-0.29D-03	-0.26D-02
3, 4	0.35D-03	-0.47D-02	4, 4	0.12D-02	0.90D-02
3, 5	0.95D-03	0.19D-02	4, 5	0.25D-03	-0.18D-02
3, 6	0.18D-04	0.67D-02	4, 6	-0.30D-03	0.12D-02
3, 7	0.20D-03	0.15D-02	4, 7	0.84D-03	0.54D-02
3, 8	-0.43D-03	-0.56D-02	4, 8	0.70D-04	-0.40D-02
3, 9	-0.25D-03	0.24D-03	4, 9	0.58D-03	-0.76D-02
3, 10	0.22D-03	-0.37D-03	4, 10	0.11D-03	0.23D-03
3, 11	-0.61D-03	-0.14D-02	4, 11	0.12D-02	0.57D-02
5, 1	-0.53D-03	-0.23D-02	6, 1	0.42D-03	-0.28D-02
5, 2	0.31D-04	-0.92D-02	6, 2	0.11D-02	-0.28D-02
5, 3	0.70D-03	0.76D-02	6, 3	0.48D-04	0.51D-02
5, 4	-0.20D-03	-0.64D-04	6, 4	0.42D-03	-0.33D-03
5, 5	0.36D-03	-0.57D-02	6, 5	0.13D-03	-0.20D-02
5, 6	0.88D-03	0.52D-02	6, 6	0.14D-03	-0.10D-02
5, 7	-0.14D-02	0.98D-03	6, 7	0.14D-02	-0.83D-03
5, 8	0.58D-03	-0.14D-02	6, 8	-0.12D-03	0.41D-03
5, 9	0.39D-03	-0.24D-02	6, 9	-0.83D-03	0.31D-02
5, 10	-0.48D-04	-0.30D-02	6, 10	0.83D-03	-0.12D-02
5, 11	0.70D-03	0.10D-01	6, 11	0.45D-05	-0.23D-02
7, 1	-0.15D-03	0.64D-02	8, 1	0.73D-03	0.31D-02
7, 2	-0.48D-03	-0.74D-02	8, 2	0.49D-03	-0.36D-02
7, 3	0.11D-02	0.65D-03	8, 3	-0.78D-03	-0.18D-02
7, 4	-0.21D-03	-0.12D-02	8, 4	-0.17D-03	0.71D-02
7, 5	0.21D-03	0.83D-02	8, 5	-0.67D-05	-0.38D-02
7, 6	0.64D-03	-0.49D-02	8, 6	0.89D-04	-0.23D-02
7, 7	-0.76D-03	0.30D-02	8, 7	0.11D-02	-0.30D-03
7, 8	0.76D-03	-0.52D-02	8, 8	-0.38D-03	-0.35D-02
7, 9	0.12D-02	-0.43D-02	8, 9	0.28D-03	0.12D-01
7, 10	-0.11D-03	0.79D-02	8, 10	-0.13D-03	-0.68D-02
7, 11	-0.21D-03	-0.44D-02	8, 11	0.27D-03	-0.60D-02
9, 1	-0.65D-03	-0.19D-02	10, 1	0.13D-02	0.63D-02
9, 2	0.15D-03	0.52D-02	10, 2	0.18D-03	-0.37D-03
9, 3	0.16D-03	-0.78D-02	10, 3	0.11D-02	-0.13D-02
9, 4	0.10D-03	0.76D-02	10, 4	0.20D-03	0.69D-02
9, 5	0.81D-03	-0.40D-02	10, 5	-0.93D-04	0.87D-03
9, 6	0.11D-03	-0.22D-02	10, 6	-0.18D-03	-0.73D-02
9, 7	0.14D-03	0.23D-02	10, 7	-0.11D-02	0.56D-02
9, 8	-0.75D-05	0.40D-03	10, 8	0.92D-03	-0.88D-03
9, 9	-0.61D-03	-0.68D-02	10, 9	0.35D-03	-0.60D-03
9, 10	0.11D-02	0.65D-02	10, 10	-0.75D-04	-0.18D-02
9, 11	0.20D-03	-0.39D-02	10, 11	-0.73D-03	-0.23D-03
11, 1	0.44D-03	-0.50D-02	12, 1	-0.33D-03	-0.73D-02
11, 2	0.32D-03	0.62D-02	12, 2	-0.30D-04	0.76D-02
11, 3	0.13D-04	-0.77D-02	12, 3	0.46D-05	-0.19D-02
11, 4	0.89D-03	0.68D-02	12, 4	-0.56D-03	-0.33D-03
11, 5	0.27D-04	-0.89D-02	12, 5	0.41D-03	-0.82D-03
11, 6	-0.14D-04	-0.48D-03	12, 6	0.30D-03	-0.60D-03
11, 7	0.12D-02	0.11D-01	12, 7	-0.19D-03	0.11D-02
11, 8	-0.75D-03	-0.49D-02	12, 8	0.10D-02	-0.14D-02

11, 9	0.90D-03	0.46D-02	12, 9	-0.74D-04	0.38D-02
11,10	0.24D-03	-0.45D-02	12,10	-0.51D-04	0.39D-02
11,11	0.66D-03	-0.52D-02	12,11	0.98D-03	-0.86D-02
13, 1	0.21D-03	-0.60D-02	14, 1	0.29D-03	0.85D-03
13, 2	-0.31D-03	0.81D-02	14, 2	0.44D-03	-0.18D-02
13, 3	-0.67D-03	-0.76D-02	14, 3	-0.13D-03	0.18D-03
13, 4	0.78D-03	0.56D-02	14, 4	-0.59D-04	0.27D-02
13, 5	0.10D-04	0.33D-02	14, 5	-0.14D-03	0.18D-02
13, 6	0.73D-03	-0.13D-02	14, 6	-0.29D-03	-0.11D-01
13, 7	0.54D-03	0.22D-02	14, 7	0.12D-04	0.50D-02
13, 8	-0.24D-03	-0.83D-02	14, 8	0.35D-03	-0.45D-02
13, 9	-0.31D-03	0.38D-02	14, 9	0.45D-03	0.12D-01
13,10	-0.39D-03	-0.82D-04	14,10	0.68D-03	0.11D-02
13,11	-0.18D-03	0.44D-03	14,11	-0.82D-03	0.61D-03
15, 1	0.23D-03	-0.21D-02	16, 1	-0.11D-03	-0.24D-02
15, 2	-0.70D-04	-0.13D-02	16, 2	-0.11D-03	-0.29D-02
15, 3	0.13D-02	-0.44D-02	16, 3	-0.22D-03	0.34D-02
15, 4	0.17D-03	0.45D-02	16, 4	0.38D-03	-0.16D-02
15, 5	-0.62D-03	0.93D-02	16, 5	0.47D-03	0.49D-02
15, 6	0.12D-04	-0.51D-02	16, 6	0.34D-03	-0.56D-02
15, 7	0.17D-03	0.12D-02	16, 7	0.29D-03	-0.27D-02
15, 8	0.32D-03	0.30D-02	16, 8	-0.11D-02	0.80D-02
15, 9	-0.63D-03	-0.53D-02	16, 9	0.11D-02	-0.35D-02
15,10	-0.34D-03	-0.25D-02	16,10	0.38D-03	0.12D-02
15,11	0.65D-03	0.52D-03	16,11	0.51D-04	0.61D-02
17, 1	0.98D-05	-0.58D-02	18, 1	-0.14D-03	0.28D-02
17, 2	0.45D-03	-0.35D-02	18, 2	0.61D-03	-0.35D-02
17, 3	0.35D-03	0.11D-01	18, 3	-0.12D-03	-0.52D-02
17, 4	-0.41D-03	-0.32D-02	18, 4	0.44D-03	0.61D-02
17, 5	0.82D-03	0.13D-02	18, 5	0.20D-03	0.34D-02
17, 6	0.31D-03	0.35D-02	18, 6	0.80D-04	0.56D-02
17, 7	0.48D-03	-0.51D-02	18, 7	-0.23D-03	-0.82D-02
17, 8	0.15D-02	0.18D-02	18, 8	-0.14D-03	0.25D-02
17, 9	-0.34D-03	-0.78D-02	18, 9	0.50D-03	-0.66D-02
17,10	-0.24D-03	0.41D-02	18,10	0.22D-03	0.98D-02
17,11	0.60D-03	0.42D-02	18,11	0.59D-03	-0.37D-02
19, 1	0.25D-03	0.11D-01			
19, 2	-0.20D-03	-0.56D-02			
19, 3	0.42D-03	0.19D-02			
19, 4	0.39D-03	0.14D-02			
19, 5	-0.39D-03	-0.54D-02			
19, 6	0.44D-03	0.28D-02			
19, 7	0.83D-04	0.84D-02			
19, 8	0.21D-03	-0.43D-02			
19, 9	0.14D-03	-0.11D-02			
19,10	0.28D-03	0.64D-02			
19,11	-0.16D-03	-0.56D-02			

STATISTICAL RESULTS:

	MEAN VALUE	STANDARD DEVIATION
XX-STRAIN:	0.1878D-03	0.5094D-03
YY-STRAIN:	0.2514D-04	0.4962D-02

RECONSTRUCTION RESULTS OF INTERFEROGRAM
(3R) OF THE NEWS-PRINT PAPER SAMPLE #38
CUMMULATIVE DEFORMATION)

CO-ORDINATES X	CO-ORDINATES Y	DEFORMATIONS X	DEFORMATIONS Y	DEFORMATIONS Z
44.0	-22.0	0.3278D 02	-0.2443D 02	0.1705D 02
44.0	-18.0	0.3212D 02	0.1547D 02	-0.2591D 01
44.0	-14.0	0.3366D 02	-0.2845D 02	-0.2038D 02
44.0	-10.0	0.3327D 02	0.1069D 02	-0.4523D 01
44.0	-6.0	0.3274D 02	0.1766D 02	0.2069D 02
44.0	-2.0	0.3141D 02	0.1450D 02	0.1144D 02
44.0	2.0	0.3295D 02	-0.1353D 02	-0.1219D 02
44.0	6.0	0.3298D 02	0.1602D 00	0.4321D 01
44.0	10.0	0.3141D 02	-0.3189D 02	-0.2227D 02
44.0	14.0	0.3158D 02	-0.8362D 01	-0.1614D 02
44.0	18.0	0.3093D 02	-0.5089D 00	0.2626D 01
44.0	22.0	0.3205D 02	-0.1308D 02	-0.2135D 01
40.0	-22.0	0.3124D 02	0.2133D 02	0.9003D 01
40.0	-18.0	0.3175D 02	0.2840D 02	-0.1146D 02
40.0	-14.0	0.3259D 02	0.1468D 01	-0.4376D 02
40.0	-10.0	0.3294D 02	-0.4213D 02	-0.1355D 02
40.0	-6.0	0.3219D 02	-0.1503D 02	-0.1290D 02
40.0	-2.0	0.3316D 02	-0.3012D 02	-0.8002D 01
40.0	2.0	0.3024D 02	-0.2587D 02	-0.1364D 02
40.0	6.0	0.3267D 02	-0.1579D 02	0.9141D 01
40.0	10.0	0.3042D 02	-0.2827D 01	-0.6639D 00
40.0	14.0	0.3311D 02	-0.1325D 02	-0.2913D 02
40.0	18.0	0.3299D 02	0.2044D 02	0.5780D 01
40.0	22.0	0.3224D 02	0.4252D 01	0.1805D 01
36.0	-22.0	0.3129D 02	0.8030D 01	0.2292D 02
36.0	-18.0	0.3217D 02	0.1346D 02	-0.2151D 02
36.0	-14.0	0.3075D 02	-0.6927D 01	0.1657D 02
36.0	-10.0	0.3144D 02	-0.3041D 02	0.2127D 02
36.0	-6.0	0.3251D 02	0.1070D 02	-0.4118D 01
36.0	-2.0	0.3125D 02	-0.1342D 00	-0.7232D 01
36.0	2.0	0.3100D 02	-0.4674D 02	0.1348D 02
36.0	6.0	0.3328D 02	-0.8562D 01	-0.1456D 02
36.0	10.0	0.3172D 02	0.8066D 01	-0.1364D 02
36.0	14.0	0.3186D 02	-0.1427D 02	-0.2133D 02
36.0	18.0	0.3201D 02	-0.2792D 02	-0.1505D 02
36.0	22.0	0.3160D 02	-0.3395D 01	-0.2679D 02
32.0	-22.0	0.3093D 02	-0.1385D 02	0.1072D 02
32.0	-18.0	0.3128D 02	-0.4807D 01	-0.5224D 01
32.0	-14.0	0.3039D 02	-0.3345D 02	-0.1087D 02
32.0	-10.0	0.3100D 02	0.1442D 02	-0.1177D-01
32.0	-6.0	0.2918D 02	-0.2308D 02	-0.9173D 01
32.0	-2.0	0.3128D 02	0.8372D 01	0.2827D 02
32.0	2.0	0.3147D 02	0.6720D 01	0.1646D 01
32.0	6.0	0.3024D 02	-0.1394D 02	-0.5126D 01
32.0	10.0	0.2897D 02	0.2131D 02	-0.4411D 01
32.0	14.0	0.3048D 02	0.2082D 02	0.5395D 01
32.0	18.0	0.3087D 02	-0.4543D 02	-0.1951D 02
32.0	22.0	0.3013D 02	-0.1821D 02	0.1399D 02
28.0	-22.0	0.3036D 02	0.2875D 01	0.4529D 02
28.0	-18.0	0.2953D 02	0.2129D 02	-0.1719D 02
28.0	-14.0	0.2929D 02	0.3846D 02	-0.1048D 01
28.0	-10.0	0.2927D 02	0.3539D 02	0.1236D 02
28.0	-6.0	0.2892D 02	-0.1637D 02	-0.1190D 02
28.0	-2.0	0.2998D 02	-0.2422D 02	0.2375D 01
28.0	2.0	0.3032D 02	-0.8977D 01	0.2482D 01
28.0	6.0	0.3132D 02	0.1930D 02	-0.3917D 02
28.0	10.0	0.2957D 02	0.1558D 02	-0.3152D 02
28.0	14.0	0.3004D 02	-0.2318D 02	0.9073D 01
28.0	18.0	0.2898D 02	-0.1719D 02	0.3788D 02
28.0	22.0	0.2978D 02	-0.2934D 02	-0.1805D 02

24.0	-22.0	0.2986D 02	0.2314D 01	-0.1208D 01	
24.0	-18.0	0.2952D 02	0.1039D 02	0.1082D 02	
24.0	-14.0	0.2895D 02	-0.1812D 02	0.2246D 02	
24.0	-10.0	0.2869D 02	0.2105D 00	-0.3510D 02	
24.0	-6.0	0.2873D 02	0.1853D 02	-0.1962D 02	
24.0	-2.0	0.2816D 02	0.2677D 02	0.1309D 02	
24.0	2.0	0.2804D 02	-0.1274D 02	-0.1195D 02	
24.0	6.0	0.2839D 02	-0.4882D 01	-0.1328D 02	
24.0	10.0	0.2933D 02	0.7596D 01	0.1393D 02	
24.0	14.0	0.2836D 02	-0.1351D 02	0.1973D 02	
24.0	18.0	0.2679D 02	-0.1711D 00	0.5654D 01	
24.0	22.0	0.3055D 02	-0.1906D 02	-0.9307D 01	
20.0	-22.0	0.2850D 02	-0.7548D 01	0.1740D 02	
20.0	-18.0	0.2871D 02	0.1567D 02	-0.1818D 02	
20.0	-14.0	0.2926D 02	-0.2736D 02	-0.3158D 00	
20.0	-10.0	0.3072D 02	-0.2794D 02	0.1110D 02	
20.0	-6.0	0.2882D 02	-0.2433D 02	0.1531D 01	
20.0	-2.0	0.2845D 02	0.2282D 02	-0.1554D 01	
20.0	2.0	0.2792D 02	0.1160D 01	-0.1641D 01	
20.0	6.0	0.2894D 02	0.2222D 02	0.1315D 01	
20.0	10.0	0.2930D 02	0.6567D-01	-0.3840D 01	
20.0	14.0	0.3005D 02	-0.2398D 02	-0.1043D 02	
20.0	18.0	0.2850D 02	-0.1313D 01	-0.1684D 02	
20.0	22.0	0.2685D 02	0.2233D 02	0.1653D 02	
16.0	-22.0	0.2786D 02	-0.2431D 02	-0.3695D 02	
16.0	-18.0	0.2761D 02	-0.1502D 02	0.1144D 01	
16.0	-14.0	0.2655D 02	-0.1828D 02	0.2827D 02	
16.0	-10.0	0.2662D 02	-0.6038D 01	-0.6472D 01	
16.0	-6.0	0.2722D 02	0.5004D 01	-0.9881D 01	
16.0	-2.0	0.2718D 02	-0.9615D 00	-0.2938D 02	
16.0	2.0	0.2572D 02	-0.1340D 02	-0.4221D 02	
16.0	6.0	0.2672D 02	-0.3094D 02	0.2951D 01	
16.0	10.0	0.2582D 02	0.5810D 01	0.3006D 02	
16.0	14.0	0.2745D 02	0.1188D 02	-0.1719D 02	
16.0	18.0	0.2465D 02	0.1629D 02	-0.1730D 02	
16.0	22.0	0.2484D 02	0.2249D 02	0.1069D 01	
12.0	-22.0	0.2679D 02	-0.2121D 02	-0.2273D 02	
12.0	-18.0	0.2481D 02	0.2773D 02	-0.1054D 02	
12.0	-14.0	0.2617D 02	0.2001D 00	-0.2117D 01	
12.0	-10.0	0.2814D 02	0.3346D 02	-0.2390D 01	
12.0	-6.0	0.2611D 02	-0.1057D 02	0.2167D 02	
12.0	-2.0	0.2571D 02	0.1289D 01	-0.4939D 01	
12.0	2.0	0.2574D 02	-0.1259D 02	0.1369D 02	
12.0	6.0	0.2499D 02	-0.2417D 02	0.3050D 02	
12.0	10.0	0.2682D 02	0.2345D 02	-0.1249D 02	
12.0	14.0	0.2710D 02	-0.2967D 02	-0.2314D 02	
12.0	18.0	0.2693D 02	-0.2979D 02	0.2070D 01	
12.0	22.0	0.2545D 02	-0.2763D 02	-0.4882D 02	
8.0	-22.0	0.2527D 02	-0.4053D 02	0.2010D 02	
8.0	-18.0	0.2632D 02	-0.5870D 01	-0.1507D 01	
8.0	-14.0	0.2505D 02	-0.3649D 02	0.3912D 01	
8.0	-10.0	0.2516D 02	0.1591D 02	-0.6268D 01	
8.0	-6.0	0.2423D 02	0.6645D 01	0.1288D 02	
8.0	-2.0	0.2355D 02	-0.9091D 01	0.2653D 01	
8.0	2.0	0.2628D 02	-0.5560D 02	-0.1262D 02	
8.0	6.0	0.2553D 02	0.2631D 02	-0.1927D 02	
8.0	10.0	0.2589D 02	-0.1641D 02	0.2843D 02	
8.0	14.0	0.2387D 02	0.3941D 01	0.1851D 02	
8.0	18.0	0.2464D 02	-0.1994D 02	0.2917D 02	
8.0	22.0	0.2648D 02	-0.4069D 01	0.1496D 02	
4.0	-22.0	0.2517D 02	0.3211D 01	-0.7349D 01	
4.0	-18.0	0.2257D 02	0.2603D 02	-0.3772D 02	
4.0	-14.0	0.2489D 02	0.4570D 01	-0.1642D 02	
4.0	-10.0	0.2601D 02	-0.2157D 02	-0.1510D 01	
4.0	-6.0	0.2498D 02	0.8147D 01	0.2081D 02	
4.0	-2.0	0.2503D 02	-0.2742D 01	0.1933D 02	
4.0	2.0	0.2371D 02	0.2483D 02	-0.2153D 02	
4.0	6.0	0.2356D 02	0.7070D 01	-0.5652D 01	
4.0	10.0	0.2224D 02	-0.2374D 02	0.1140D 02	
4.0	14.0	0.2362D 02	0.6406D 01	0.8014D 01	
4.0	18.0	0.2327D 02	0.2565D 02	-0.1379D 02	
4.0	22.0	0.2401D 02	-0.1748D 02	-0.1711D 02	

0.0	-22.0	0.23020 02	-0.19090 02	0.16950 02
0.0	-18.0	0.21730 02	-0.15720 02	0.26150 02
0.0	-14.0	0.23770 02	0.14830 02	-0.32590 02
0.0	-10.0	0.22660 02	0.28070 02	0.82320 01
0.0	-6.0	0.22180 02	0.22100 02	-0.69190 01
0.0	-2.0	0.23530 02	-0.30340 02	0.31210 01
0.0	2.0	0.23510 02	-0.21370 02	0.34990 02
0.0	6.0	0.21360 02	-0.62420 01	-0.40920 01
0.0	10.0	0.23920 02	0.11360 02	-0.25840 02
0.0	14.0	0.22660 02	-0.14850 02	-0.32270 01
0.0	18.0	0.26680 02	0.63270 01	0.21410 01
0.0	22.0	0.23830 02	0.38130 01	-0.15690 02
-4.0	-22.0	0.24290 02	-0.55940 01	-0.46160 01
-4.0	-18.0	0.22820 02	0.10170 02	-0.12970 02
-4.0	-14.0	0.23860 02	-0.13390 02	-0.65520 01
-4.0	-10.0	0.21440 02	-0.19850 02	0.11540 02
-4.0	-6.0	0.23900 02	-0.82970 01	0.94830 01
-4.0	-2.0	0.23130 02	-0.45290 02	-0.11400 02
-4.0	2.0	0.23430 02	0.93910 01	0.10030 02
-4.0	6.0	0.21860 02	-0.78200 01	-0.40600 02
-4.0	10.0	0.22260 02	0.22910 01	-0.50870 01
-4.0	14.0	0.23580 02	-0.32560 01	0.52290 01
-4.0	18.0	0.22040 02	-0.37230 02	0.55310 01
-4.0	22.0	0.23310 02	-0.22650 02	-0.21580 02
-8.0	-22.0	0.22990 02	0.12840 02	0.19390 01
-8.0	-18.0	0.23370 02	-0.19540 00	0.15920 02
-8.0	-14.0	0.22820 02	-0.16910 02	-0.20640 02
-8.0	-10.0	0.23150 02	-0.13560 01	0.29270 02
-8.0	-6.0	0.20930 02	0.65450-01	-0.80110 01
-8.0	-2.0	0.21690 02	0.15350 02	0.25750 02
-8.0	2.0	0.20780 02	0.88970 01	0.84250 01
-8.0	6.0	0.22870 02	-0.10810 02	-0.13920 02
-8.0	10.0	0.20230 02	0.18400 02	0.12810 02
-8.0	14.0	0.23660 02	-0.75890 01	-0.17970 02
-8.0	18.0	0.20510 02	0.10610 02	0.36200 02
-8.0	22.0	0.23000 02	0.51350 01	-0.94710 01
-12.0	-22.0	0.22030 02	-0.22170 02	0.99000 01
-12.0	-18.0	0.21600 02	-0.27930 02	0.52610 01
-12.0	-14.0	0.21860 02	-0.88370 01	0.13260 02
-12.0	-10.0	0.22360 02	0.74850 01	-0.27080 02
-12.0	-6.0	0.21330 02	0.87550 01	-0.21370 02
-12.0	-2.0	0.22340 02	-0.31720 01	0.49930 00
-12.0	2.0	0.22320 02	0.28350 02	-0.11500 02
-12.0	6.0	0.21180 02	-0.16540 01	0.10210 02
-12.0	10.0	0.21880 02	-0.16010 02	-0.32700 01
-12.0	14.0	0.18890 02	-0.83430 01	-0.10840 02
-12.0	18.0	0.20200 02	-0.26050 02	0.10030 02
-12.0	22.0	0.20720 02	-0.19020 02	0.30580 02
-16.0	-22.0	0.20730 02	-0.22540 02	-0.18980 02
-16.0	-18.0	0.20750 02	0.26080 01	0.27460 02
-16.0	-14.0	0.20570 02	0.21570 02	-0.28270 02
-16.0	-10.0	0.20820 02	0.10480 02	-0.87740 01
-16.0	-6.0	0.22360 02	0.17150 01	-0.51530 01
-16.0	-2.0	0.21830 02	-0.70140 01	-0.46630 02
-16.0	2.0	0.21350 02	-0.26490 02	-0.38880 02
-16.0	6.0	0.22100 02	-0.45790 01	-0.32340 02
-16.0	10.0	0.18940 02	0.21150 02	-0.20180 02
-16.0	14.0	0.20660 02	0.19830 02	-0.22520 02
-16.0	18.0	0.19990 02	-0.16880 02	0.10900 02
-16.0	22.0	0.21750 02	-0.19230 02	0.11660 02
-20.0	-22.0	0.21100 02	-0.36390 02	-0.67880 01
-20.0	-18.0	0.20770 02	-0.21980 02	0.13600 02
-20.0	-14.0	0.19850 02	-0.10870 02	0.15950 02
-20.0	-10.0	0.21300 02	-0.10400 02	0.79790 01
-20.0	-6.0	0.19510 02	0.13560 02	0.13790 02
-20.0	-2.0	0.21200 02	-0.21820 02	-0.19800 02
-20.0	2.0	0.16860 02	-0.27250 02	-0.30100 02
-20.0	6.0	0.20330 02	-0.11820 02	0.68580 01
-20.0	10.0	0.20830 02	0.49490 01	-0.41570 01
-20.0	14.0	0.21410 02	-0.16460 02	-0.19090 01
-20.0	18.0	0.20970 02	-0.78490 01	-0.19640 02
-20.0	22.0	0.20770 02	-0.27860 02	-0.10930 02

*	-24.0	-22.0	*	0.2248D 02	0.1332D 02	0.8752D 01	*
*	-24.0	-18.0	*	0.1963D 02	0.4148D 01	0.2892D 02	*
*	-24.0	-14.0	*	0.1924D 02	-0.1419D 02	0.6103D 01	*
*	-24.0	-10.0	*	0.2210D 02	-0.3473D 02	-0.2660D 02	*
*	-24.0	-6.0	*	0.1961D 02	0.2227D 02	-0.3401D 01	*
*	-24.0	-2.0	*	0.2065D 02	-0.1515D 02	-0.2347D 02	*
*	-24.0	2.0	*	0.1912D 02	0.7483D 01	0.1671D 02	*
*	-24.0	6.0	*	0.1847D 02	0.1774D 02	0.8433D 01	*
*	-24.0	10.0	*	0.1808D 02	0.1346D 02	-0.1621D 02	*
*	-24.0	14.0	*	0.1894D 02	-0.1348D 02	-0.2034D 02	*
*	-24.0	18.0	*	0.1901D 02	0.2204D 02	0.1274D 02	*
*	-24.0	22.0	*	0.1884D 02	-0.2418D 02	-0.4083D 02	*
*	-28.0	-22.0	*	0.1920D 02	0.5966D-01	-0.1919D 02	*
*	-28.0	-18.0	*	0.1828D 02	0.1326D 02	0.3544D 02	*
*	-28.0	-14.0	*	0.1820D 02	0.5109D 01	0.2950D 02	*
*	-28.0	-10.0	*	0.1887D 02	0.2130D 02	-0.1257D 02	*
*	-28.0	-6.0	*	0.1835D 02	0.7126D 01	-0.1078D 02	*
*	-28.0	-2.0	*	0.1756D 02	0.2053D 02	-0.2062D 02	*
*	-28.0	2.0	*	0.1855D 02	0.1538D 02	-0.2289D 02	*
*	-28.0	6.0	*	0.1727D 02	0.9992D 00	-0.4634D 01	*
*	-28.0	10.0	*	0.1971D 02	0.6059D 00	0.1163D 02	*
*	-28.0	14.0	*	0.1806D 02	-0.2674D 02	0.4214D 01	*
*	-28.0	18.0	*	0.1947D 02	-0.1258D 02	-0.1209D 02	*
*	-28.0	22.0	*	0.1876D 02	0.6172D 01	0.1222D 01	*
*	-32.0	-22.0	*	0.1724D 02	-0.9471D 00	0.2663D 02	*
*	-32.0	-18.0	*	0.1703D 02	-0.8182D 01	0.1446D 02	*
*	-32.0	-14.0	*	0.1649D 02	0.3407D 02	-0.4160D 02	*
*	-32.0	-10.0	*	0.1928D 02	-0.6874D 01	-0.8678D 01	*
*	-32.0	-6.0	*	0.1737D 02	-0.1060D 02	-0.8975D 01	*
*	-32.0	-2.0	*	0.1785D 02	0.3315D 01	-0.6972D 01	*
*	-32.0	2.0	*	0.1653D 02	0.3291D 02	0.3405D 01	*
*	-32.0	6.0	*	0.1807D 02	0.7703D 01	0.3042D 02	*
*	-32.0	10.0	*	0.1702D 02	0.1203D 02	-0.1253D 02	*
*	-32.0	14.0	*	0.1711D 02	-0.2839D 02	0.2398D 01	*
*	-32.0	18.0	*	0.1773D 02	-0.3997D 01	-0.6560D 01	*
*	-32.0	22.0	*	0.1876D 02	-0.4138D 02	-0.2903D 02	*

STATISTICAL RESULTS:

	MEAN VALUE	STANDARD DEVIATION
X-DIRECTION	0.251D 02	0.472D 01
Y-DIRECTION	-0.364D 01	0.187D 02
Z-DIRECTION	-0.269D 01	0.182D 02

EVALUATED STRAIN FIELD AT POINT (3R)

ELEMENT	EXX	EYY	ELEMENT	EXX	EYY
1, 1	0.38D-03	-0.10D-01	2, 1	-0.12D-04	-0.18D-02
1, 2	0.91D-04	0.11D-01	2, 2	-0.10D-03	0.75D-02
1, 3	0.27D-03	-0.98D-02	2, 3	0.46D-03	0.10D-01
1, 4	0.63D-04	-0.17D-02	2, 4	0.38D-03	-0.68D-02
1, 5	0.14D-03	0.79D-03	2, 5	-0.80D-04	0.38D-02
1, 6	-0.44D-03	0.70D-02	2, 6	0.48D-03	-0.11D-02
1, 7	0.68D-03	-0.34D-02	2, 7	-0.19D-03	-0.25D-02
1, 8	0.77D-04	0.80D-02	2, 8	-0.15D-03	-0.32D-02
1, 9	0.25D-03	-0.59D-02	2, 9	-0.33D-03	0.26D-02
1,10	-0.38D-03	-0.20D-02	2,10	0.31D-03	-0.84D-02
1,11	-0.51D-03	0.31D-02	2,11	0.25D-03	0.40D-02
3, 1	0.90D-04	-0.14D-02	4, 1	0.14D-03	-0.23D-02
3, 2	0.22D-03	0.51D-02	4, 2	0.44D-03	0.72D-02
3, 3	0.92D-04	0.59D-02	4, 3	0.27D-03	-0.12D-01
3, 4	0.11D-03	-0.10D-01	4, 4	0.43D-03	0.94D-02
3, 5	0.83D-03	0.27D-02	4, 5	0.66D-04	-0.79D-02
3, 6	-0.89D-05	0.12D-01	4, 6	0.33D-03	0.41D-03
3, 7	-0.12D-03	-0.95D-02	4, 7	0.29D-03	0.52D-02
3, 8	0.76D-03	-0.42D-02	4, 8	-0.27D-03	-0.88D-02
3, 9	0.69D-03	0.56D-02	4, 9	-0.15D-03	0.12D-03
3,10	0.35D-03	-0.34D-02	4,10	0.11D-03	0.17D-01
3,11	0.28D-03	-0.61D-02	4,11	0.47D-03	-0.68D-02
5, 1	0.12D-03	-0.46D-02	6, 1	0.34D-03	-0.20D-02
5, 2	0.36D-06	-0.43D-02	6, 2	0.20D-03	0.71D-02
5, 3	0.84D-04	0.77D-03	6, 3	-0.78D-04	-0.46D-02
5, 4	0.14D-03	0.13D-01	6, 4	-0.51D-03	-0.46D-02
5, 5	0.46D-04	0.20D-02	6, 5	-0.21D-04	-0.21D-02
5, 6	0.45D-03	-0.38D-02	6, 6	-0.71D-04	0.99D-02
5, 7	0.57D-03	-0.71D-02	6, 7	0.30D-04	-0.20D-02
5, 8	0.73D-03	0.93D-03	6, 8	-0.14D-03	-0.31D-02
5, 9	0.60D-04	0.97D-02	6, 9	0.90D-05	0.53D-02
5,10	0.42D-03	-0.15D-02	6,10	-0.42D-03	-0.33D-02
5,11	0.55D-03	0.30D-02	6,11	-0.43D-03	0.47D-02
7, 1	0.16D-03	-0.58D-02	8, 1	0.27D-03	-0.23D-02
7, 2	0.28D-03	0.11D-01	8, 2	0.70D-03	0.81D-03
7, 3	0.68D-03	0.14D-03	8, 3	0.94D-04	-0.31D-02
7, 4	0.10D-02	-0.90D-03	8, 4	-0.38D-03	-0.28D-02
7, 5	0.40D-03	-0.12D-01	8, 5	0.28D-03	0.15D-02
7, 6	0.32D-03	0.54D-02	8, 6	0.37D-03	0.31D-02
7, 7	0.55D-03	-0.53D-02	8, 7	-0.55D-05	0.44D-02
7, 8	0.55D-03	0.55D-02	8, 8	0.43D-03	-0.92D-02
7, 9	0.87D-03	0.60D-02	8, 9	-0.25D-03	-0.15D-02
7,10	0.65D-03	-0.57D-02	8,10	0.87D-04	-0.11D-02
7,11	0.96D-03	-0.59D-02	8,11	-0.57D-03	-0.16D-02
9, 1	0.38D-03	-0.12D-01	10, 1	0.26D-04	-0.87D-02
9, 2	-0.38D-03	0.69D-02	10, 2	0.94D-03	0.77D-02
9, 3	0.28D-03	-0.83D-02	10, 3	0.41D-04	-0.13D-01
9, 4	0.74D-03	0.11D-01	10, 4	-0.21D-03	0.23D-02
9, 5	0.47D-03	-0.30D-02	10, 5	-0.19D-03	0.39D-02
9, 6	0.54D-03	0.35D-02	10, 6	-0.37D-03	0.12D-01
9, 7	-0.13D-03	0.29D-02	10, 7	0.64D-03	-0.20D-01
9, 8	-0.13D-03	-0.12D-01	10, 8	0.49D-03	0.11D-01
9, 9	0.23D-03	0.13D-01	10, 9	0.91D-03	-0.51D-02
9,10	0.81D-03	0.30D-04	10,10	0.64D-04	-0.40D-02
9,11	0.57D-03	-0.54D-03	10,11	0.34D-03	0.60D-02
11, 1	0.54D-03	-0.57D-02	12, 1	-0.32D-03	-0.84D-03
11, 2	0.21D-03	0.54D-02	12, 2	-0.27D-03	-0.76D-02
11, 3	0.28D-03	0.65D-02	12, 3	-0.24D-04	-0.33D-02
11, 4	0.84D-03	-0.74D-02	12, 4	0.30D-03	0.15D-02
11, 5	0.70D-03	0.27D-02	12, 5	-0.43D-03	0.13D-01
11, 6	0.37D-03	-0.69D-02	12, 6	0.10D-03	-0.22D-02
11, 7	0.51D-04	0.44D-02	12, 7	0.21D-04	-0.38D-02
11, 8	0.55D-03	0.77D-02	12, 8	-0.12D-03	-0.44D-02

11, 9	-0.42D-03	-0.75D-02	12, 9	0.41D-03	0.66D-02
11,10	0.24D-03	-0.48D-02	12,10	-0.23D-03	-0.53D-02
11,11	0.65D-03	0.11D-01	12,11	-0.34D-03	0.63D-03
13, 1	0.32D-03	-0.59D-02	14, 1	0.24D-03	0.33D-02
13, 2	-0.14D-03	0.59D-02	14, 2	0.44D-03	0.42D-02
13, 3	0.26D-03	0.16D-02	14, 3	0.24D-03	-0.39D-02
13, 4	-0.43D-03	-0.29D-02	14, 4	0.20D-03	-0.36D-03
13, 5	0.74D-03	0.92D-02	14, 5	-0.10D-03	-0.38D-02
13, 6	0.36D-03	-0.14D-01	14, 6	-0.16D-03	0.16D-02
13, 7	0.66D-03	0.43D-02	14, 7	-0.39D-03	0.49D-02
13, 8	-0.25D-03	-0.25D-02	14, 8	0.42D-03	-0.73D-02
13, 9	0.51D-03	0.14D-02	14, 9	-0.41D-03	0.65D-02
13,10	-0.20D-04	0.85D-02	14,10	0.12D-02	-0.45D-02
13,11	0.38D-03	-0.36D-02	14,11	0.79D-04	0.14D-02
15, 1	0.32D-03	0.14D-02	16, 1	-0.92D-04	-0.63D-02
15, 2	0.21D-03	-0.48D-02	16, 2	-0.73D-05	-0.47D-02
15, 3	0.32D-03	-0.41D-02	16, 3	0.18D-03	0.28D-02
15, 4	0.39D-03	-0.32D-03	16, 4	-0.12D-03	0.22D-02
15, 5	-0.26D-03	0.30D-02	16, 5	0.71D-03	0.22D-02
15, 6	0.15D-03	-0.79D-02	16, 6	0.16D-03	0.49D-02
15, 7	0.24D-03	0.75D-02	16, 7	0.62D-03	-0.55D-02
15, 8	-0.23D-03	0.36D-02	16, 8	0.44D-03	-0.64D-02
15, 9	0.74D-03	-0.19D-02	16, 9	-0.47D-03	0.33D-03
15,10	-0.44D-03	0.44D-02	16,10	-0.19D-03	0.92D-02
15,11	0.51D-04	-0.18D-02	16,11	-0.24D-03	0.59D-03
17, 1	-0.34D-03	-0.36D-02	18, 1	0.82D-03	0.23D-02
17, 2	0.29D-03	-0.28D-02	18, 2	0.34D-03	0.46D-02
17, 3	0.15D-03	-0.12D-03	18, 3	0.26D-03	0.51D-02
17, 4	-0.20D-03	-0.60D-02	18, 4	0.81D-03	-0.14D-01
17, 5	-0.25D-04	0.88D-02	18, 5	0.32D-03	0.94D-02
17, 6	0.14D-03	0.14D-02	18, 6	0.77D-03	-0.57D-02
17, 7	-0.66D-04	-0.39D-02	18, 7	0.14D-03	-0.26D-02
17, 8	0.46D-03	-0.42D-02	18, 8	0.30D-03	0.11D-02
17, 9	0.69D-03	0.54D-02	18, 9	-0.41D-03	0.67D-02
17,10	0.62D-03	-0.22D-02	18,10	0.22D-03	-0.89D-02
17,11	0.49D-03	0.50D-02	18,11	-0.12D-03	0.12D-01
19, 1	0.49D-03	-0.33D-02			
19, 2	0.31D-03	0.20D-02			
19, 3	0.43D-03	-0.40D-02			
19, 4	-0.10D-03	0.35D-02			
19, 5	0.24D-03	-0.34D-02			
19, 6	-0.73D-04	0.13D-02			
19, 7	0.50D-03	0.36D-02			
19, 8	-0.20D-03	0.98D-04			
19, 9	0.67D-03	0.68D-02			
19,10	0.24D-03	-0.35D-02			
19,11	0.43D-03	-0.47D-02			

STATISTICAL RESULTS:

	MEAN VALUE	STANDARD DEVIATION
XX-STRAIN:	0.1963D-03	0.3615D-03
YY-STRAIN:	0.8772D-05	0.6252D-02

EVALUATED THICKNESS CHANGES (MICRONS)
(COLUMNS: 1- 6)

	1	2	3	4	5	6
1	-5.34	-5.10	-6.41	-4.18	1.49	-3.32
2	-2.44	-5.60	-4.07	-2.22	0.61	3.42
3	-2.74	-0.42	2.11	0.21	2.58	-5.48
4	-2.81	-3.99	2.52	-2.63	-5.90	-3.60
5	-0.61	3.32	1.30	-4.41	0.07	-1.79
6	-0.75	-1.95	-0.92	-2.25	-1.36	1.09
7	-4.35	-1.76	-1.88	1.16	-2.26	-4.62
8	0.05	-4.75	-5.64	-1.12	-0.90	-1.18
9	-6.41	0.08	-1.26	-0.77	-6.31	0.86
10	-2.25	0.19	-2.96	-0.65	1.58	-5.90
11	-5.88	-4.74	-4.45	1.19	-2.97	-4.28
12	3.34	-1.68	-4.77	-2.71	-4.41	1.78
13	-4.18	2.88	-1.60	1.85	-5.93	-6.48
14	-3.14	1.90	-5.50	-4.33	0.34	5.02
15	-3.52	-0.35	-6.44	0.06	1.47	0.91
16	3.10	2.19	3.29	-2.15	3.01	-4.89
17	-4.10	3.18	-3.38	0.25	1.65	-3.63
18	-5.35	-3.30	1.47	-0.36	1.79	-0.79
19	3.20	-5.30	0.01	-2.01	-0.53	-0.08
20	2.04	0.31	-5.19	-4.77	3.08	1.61

(COLUMNS: 7-12)

	7	8	9	10	11	12
1	-2.94	3.38	-2.62	2.54	-1.16	-2.78
2	-0.05	-0.87	-0.80	-1.15	-2.51	2.18
3	-1.43	1.49	-3.74	-2.12	2.89	1.42
4	-0.82	-4.72	0.12	-3.80	-2.91	-0.61
5	0.51	1.57	-1.17	3.08	0.41	-4.74
6	-2.21	-2.25	1.03	1.64	-1.84	-1.32
7	-4.50	-1.39	2.54	0.34	-2.06	-0.90
8	-3.63	2.83	-5.90	1.11	-5.46	1.45
9	-0.63	-2.90	0.71	-4.18	-6.12	-1.07
10	-6.45	-1.41	1.90	-2.38	1.80	0.38
11	-2.77	-1.49	-5.75	-4.78	-5.33	2.36
12	-3.01	1.11	-4.02	-1.28	-2.74	-1.52
13	-0.32	1.97	-2.68	1.62	-5.12	-0.62
14	-6.22	3.37	-0.39	1.57	2.90	-3.33
15	-0.44	-3.26	-0.17	-0.62	0.65	-4.20
16	0.20	-4.82	-4.39	-2.14	0.42	2.54
17	-1.50	-5.86	-3.79	3.02	-0.70	-0.15
18	-4.06	-4.24	-3.89	-4.42	-4.57	0.05
19	-5.04	1.58	3.36	0.71	-6.19	-2.03
20	-2.84	0.67	-1.36	-1.44	0.32	-1.84

RECONSTRUCTION RESULTS OF INTERFEROGRAM
(3L) OF THE NEWS-PRINT PAPER SAMPLE #38
CUMMULATIVE DEFORMATION)

CO-ORDINATES X	CO-ORDINATES Y	DEFORMATIONS X	DEFORMATIONS Y	DEFORMATIONS Z
44.0	-22.0	0.3338D 02	-0.1417D 02	-0.1994D 02
44.0	-18.0	0.3441D 02	0.3940D 00	-0.5428D 01
44.0	-14.0	0.3431D 02	0.8089D 01	0.1789D 02
44.0	-10.0	0.3162D 02	-0.3590D 00	-0.6908D 01
44.0	-6.0	0.3368D 02	0.2960D 02	-0.2022D 02
44.0	-2.0	0.3462D 02	-0.2252D 01	-0.1075D 02
44.0	2.0	0.3314D 02	-0.1275D 02	0.2862D 01
44.0	6.0	0.3281D 02	-0.2668D 02	-0.4351D 01
44.0	10.0	0.3330D 02	-0.8720D 01	0.2092D 02
44.0	14.0	0.3329D 02	0.3856D 01	0.2150D 02
44.0	18.0	0.3531D 02	0.1103D 02	0.2877D 01
44.0	22.0	0.3383D 02	-0.2876D 02	-0.8791D 01
40.0	-22.0	0.3237D 02	0.5080D 01	-0.1199D 02
40.0	-18.0	0.3362D 02	-0.6680D 01	0.1243D 02
40.0	-14.0	0.3311D 02	0.2651D 02	0.4149D 02
40.0	-10.0	0.3338D 02	-0.5124D 01	0.8186D 01
40.0	-6.0	0.3456D 02	0.3119D 02	0.7118D 01
40.0	-2.0	0.3298D 02	-0.1483D 02	0.1591D 02
40.0	2.0	0.3367D 02	-0.8370D 01	0.1753D 02
40.0	6.0	0.3358D 02	-0.1844D 02	-0.1074D 02
40.0	10.0	0.3188D 02	-0.1444D 02	-0.4736D 01
40.0	14.0	0.3239D 02	0.4605D 01	0.3351D 02
40.0	18.0	0.3412D 02	0.3866D 01	-0.7991D 01
40.0	22.0	0.3227D 02	0.1080D 02	-0.3170D 01
36.0	-22.0	0.3326D 02	0.3194D 02	-0.2108D 02
36.0	-18.0	0.3326D 02	0.1592D 02	0.2574D 02
36.0	-14.0	0.3141D 02	0.9780D 01	-0.1911D 02
36.0	-10.0	0.3249D 02	0.8874D 01	-0.1278D 02
36.0	-6.0	0.3389D 02	0.2017D 02	0.9437D 01
36.0	-2.0	0.3115D 02	0.9017D 01	-0.1360D 01
36.0	2.0	0.3161D 02	-0.4391D 01	-0.1504D 02
36.0	6.0	0.2890D 02	-0.2565D 02	0.2389D 02
36.0	10.0	0.3117D 02	-0.9732D 01	0.3458D 01
36.0	14.0	0.3139D 02	0.9392D 01	0.2364D 02
36.0	18.0	0.3096D 02	0.6533D 01	0.1771D 02
36.0	22.0	0.3088D 02	-0.1589D 00	0.2526D 02
32.0	-22.0	0.2822D 02	-0.9631D 01	-0.6747D 01
32.0	-18.0	0.3237D 02	-0.1178D 02	0.1827D 01
32.0	-14.0	0.2966D 02	0.2143D 02	0.8380D 01
32.0	-10.0	0.3238D 02	0.3781D 02	-0.4368D 01
32.0	-6.0	0.3002D 02	-0.4575D 01	0.5163D 01
32.0	-2.0	0.3031D 02	-0.1701D 02	-0.2972D 02
32.0	2.0	0.2960D 02	0.6579D 01	0.3230D 01
32.0	6.0	0.3056D 02	-0.1788D 02	0.1501D 01
32.0	10.0	0.2994D 02	-0.2756D 02	0.1459D 01
32.0	14.0	0.2972D 02	0.6047D 01	-0.1244D 02
32.0	18.0	0.3296D 02	0.1413D 02	0.1550D 02
32.0	22.0	0.2957D 02	0.1751D 01	-0.1398D 02
28.0	-22.0	0.2798D 02	-0.1946D 02	-0.4078D 02
28.0	-18.0	0.2986D 02	-0.5492D 01	0.1422D 02
28.0	-14.0	0.3186D 02	0.4075D 02	0.1066D 02
28.0	-10.0	0.2698D 02	-0.8910D 01	-0.1704D 02
28.0	-6.0	0.2821D 02	-0.1347D 02	0.1545D 02
28.0	-2.0	0.3081D 02	0.1644D 02	-0.4816D 01
28.0	2.0	0.2587D 02	0.7703D 01	0.9124D 01
28.0	6.0	0.3140D 02	0.1721D 01	0.5001D 02
28.0	10.0	0.2829D 02	0.1384D 02	0.2390D 02
28.0	14.0	0.2930D 02	0.4864D 01	-0.1020D 02
28.0	18.0	0.2803D 02	0.3072D 02	-0.3733D 02
28.0	22.0	0.2939D 02	-0.2116D 02	0.2324D 02

24.0	-22.0	0.3002D 02	-0.1122D 02	-0.4083D 01
24.0	-18.0	0.2862D 02	0.1098D 02	-0.4449D 01
24.0	-14.0	0.2846D 02	0.2565D 02	-0.2586D 02
24.0	-10.0	0.2746D 02	-0.1859D 02	0.3160D 02
24.0	-6.0	0.2626D 02	-0.2290D 02	0.1923D 02
24.0	-2.0	0.2804D 02	-0.7038D 01	-0.1541D 02
24.0	2.0	0.3217D 02	0.1914D 02	0.5763D 01
24.0	6.0	0.2726D 02	0.5420D 01	0.9265D 01
24.0	10.0	0.2622D 02	0.1228D 02	-0.1408D 02
24.0	14.0	0.2898D 02	-0.2082D 02	-0.2302D 02
24.0	18.0	0.2556D 02	0.9527D 01	-0.8925D 01
24.0	22.0	0.3194D 02	0.1065D 02	0.2357D 01
20.0	-22.0	0.2837D 02	0.1632D 02	-0.2355D 02
20.0	-18.0	0.2478D 02	-0.1164D 02	0.2182D 02
20.0	-14.0	0.2775D 02	0.4442D 01	0.3669D 01
20.0	-10.0	0.2644D 02	0.1353D 02	-0.3222D 01
20.0	-6.0	0.2599D 02	0.1178D 02	-0.1139D 02
20.0	-2.0	0.2727D 02	-0.1184D 02	-0.3235D 01
20.0	2.0	0.2473D 02	-0.2515D 00	0.2187D 01
20.0	6.0	0.2729D 02	-0.2693D 02	-0.5255D 01
20.0	10.0	0.2958D 02	0.2357D 02	0.6147D 01
20.0	14.0	0.2661D 02	0.2558D 02	0.8174D 01
20.0	18.0	0.2495D 02	0.2336D 01	0.1720D 02
20.0	22.0	0.2623D 02	0.2100D 01	-0.7711D 01
16.0	-22.0	0.2822D 02	-0.5389D 01	0.3354D 02
16.0	-18.0	0.2588D 02	-0.2922D 02	-0.1675D 01
16.0	-14.0	0.2359D 02	0.1529D 02	-0.2851D 02
16.0	-10.0	0.2663D 02	0.1716D 02	0.5764D 00
16.0	-6.0	0.2520D 02	-0.1256D 02	0.1335D 02
16.0	-2.0	0.2433D 02	-0.4342D 01	0.2589D 02
16.0	2.0	0.2878D 02	0.2023D 02	0.3742D 02
16.0	6.0	0.2447D 02	-0.9119D 01	-0.7593D 00
16.0	10.0	0.2444D 02	0.2554D 02	-0.3198D 02
16.0	14.0	0.2600D 02	-0.3891D 02	0.1949D 02
16.0	18.0	0.2541D 02	0.9829D 00	0.8980D 01
16.0	22.0	0.2695D 02	0.3521D 02	0.8750D 01
12.0	-22.0	0.2523D 02	-0.8980D 01	0.2620D 02
12.0	-18.0	0.2479D 02	-0.1268D 02	0.8119D 01
12.0	-14.0	0.2645D 02	-0.9177D 01	0.6635D 01
12.0	-10.0	0.2709D 02	0.1667D 02	0.3272D 01
12.0	-6.0	0.2441D 02	-0.3439D 02	-0.2596D 02
12.0	-2.0	0.2417D 02	-0.1649D 01	0.5824D 01
12.0	2.0	0.2358D 02	0.1656D 01	-0.4552D 01
12.0	6.0	0.2553D 02	-0.1034D 02	-0.3058D 02
12.0	10.0	0.2332D 02	-0.1729D 02	0.1077D 02
12.0	14.0	0.2625D 02	0.1462D 02	0.2919D 02
12.0	18.0	0.2382D 02	-0.9824D 01	0.1959D 01
12.0	22.0	0.2960D 02	0.1940D 02	0.4371D 02
8.0	-22.0	0.2731D 02	0.1902D 02	-0.1459D 02
8.0	-18.0	0.2330D 02	0.3583D 01	-0.1798D 01
8.0	-14.0	0.2560D 02	0.1728D 02	-0.7648D 01
8.0	-10.0	0.2650D 02	0.1893D 02	0.1057D 02
8.0	-6.0	0.2161D 02	-0.1374D 02	-0.5020D 01
8.0	-2.0	0.2333D 02	-0.2060D 02	-0.1651D 02
8.0	2.0	0.2298D 02	-0.4062D 01	0.1298D 02
8.0	6.0	0.2588D 02	-0.6498D 01	0.1740D 02
8.0	10.0	0.2521D 02	-0.1213D 02	-0.2119D 02
8.0	14.0	0.2170D 02	-0.2142D 02	-0.2272D 02
8.0	18.0	0.2346D 02	0.7271D 01	-0.2722D 02
8.0	22.0	0.2555D 02	-0.6905D 01	-0.1916D 02
4.0	-22.0	0.2270D 02	-0.7392D 01	0.1163D 02
4.0	-18.0	0.2230D 02	-0.4882D 00	0.2685D 02
4.0	-14.0	0.2108D 02	-0.8300D 01	0.6094D 01
4.0	-10.0	0.2521D 02	0.1588D 02	0.1494D 01
4.0	-6.0	0.2161D 02	-0.2303D 02	-0.2257D 02
4.0	-2.0	0.2361D 02	0.1850D 02	-0.2939D 02
4.0	2.0	0.2737D 02	0.3655D 02	0.1551D 02
4.0	6.0	0.2148D 02	-0.2835D 02	0.9393D 01
4.0	10.0	0.2375D 02	0.8580D 00	-0.1553D 02
4.0	14.0	0.2125D 02	-0.1004D 02	-0.1299D 02
4.0	18.0	0.2574D 02	-0.1265D 01	0.1294D 02
4.0	22.0	0.2135D 02	0.1433D 02	0.1388D 02

0.0	-22.0	0.2050D 02	-0.1473D 02	-0.1390D 02	
0.0	-18.0	0.2120D 02	0.6951D 01	-0.2014D 02	
0.0	-14.0	0.2097D 02	-0.5197D 01	0.3080D 02	
0.0	-10.0	0.2141D 02	-0.2092D 02	-0.1430D 02	
0.0	-6.0	0.2138D 02	-0.9410D 01	0.1199D 02	
0.0	-2.0	0.2335D 02	-0.8139D 01	-0.8707D 01	
0.0	2.0	0.2210D 02	0.1662D 02	-0.4358D 02	
0.0	6.0	0.2427D 02	0.1178D 02	0.1349D 02	
0.0	10.0	0.1931D 02	-0.1072D 02	0.1495D 02	
0.0	14.0	0.2025D 02	-0.5829D 01	0.8138D 01	
0.0	18.0	0.2377D 02	-0.1104D 02	-0.7630D 01	
0.0	22.0	0.2197D 02	0.4440D 01	0.1899D 02	
-4.0	-22.0	0.2159D 02	-0.1686D 01	-0.1722D 01	
-4.0	-18.0	0.2110D 02	0.1781D 02	0.9008D 01	
-4.0	-14.0	0.2021D 02	-0.2574D 02	0.1026D 02	
-4.0	-10.0	0.2310D 02	0.5603D 01	-0.3763D 01	
-4.0	-6.0	0.1903D 02	-0.1145D 02	-0.3523D 01	
-4.0	-2.0	0.2186D 02	-0.2664D 02	0.1362D 02	
-4.0	2.0	0.2237D 02	-0.1502D 02	-0.1105D 02	
-4.0	6.0	0.1974D 02	-0.3775D 02	0.4291D 02	
-4.0	10.0	0.1961D 02	0.2375D 01	0.4558D 01	
-4.0	14.0	0.2047D 02	0.4057D 01	0.1218D 01	
-4.0	18.0	0.1855D 02	-0.4772D 01	-0.1891D 02	
-4.0	22.0	0.2123D 02	-0.2184D 00	0.2190D 02	
-8.0	-22.0	0.2025D 02	-0.2987D 01	0.4293D 01	
-8.0	-18.0	0.2162D 02	-0.2033D 02	-0.2090D 02	
-8.0	-14.0	0.2270D 02	0.3502D 01	0.1805D 02	
-8.0	-10.0	0.2015D 02	0.2976D 01	-0.3202D 02	
-8.0	-6.0	0.1922D 02	0.6849D 00	0.1224D 02	
-8.0	-2.0	0.1887D 02	-0.3252D 02	-0.1929D 02	
-8.0	2.0	0.2062D 02	0.3621D 02	-0.2404D 02	
-8.0	6.0	0.2080D 02	0.2685D 01	0.2189D 02	
-8.0	10.0	0.2042D 02	0.1381D 02	-0.2074D 02	
-8.0	14.0	0.2185D 02	-0.1041D 02	0.1839D 02	
-8.0	18.0	0.1880D 02	-0.4019D 02	-0.3495D 02	
-8.0	22.0	0.2223D 02	-0.1926D 02	0.9383D 01	
-12.0	-22.0	0.1888D 02	-0.1291D 01	-0.1737D 02	
-12.0	-18.0	0.1994D 02	0.1088D 02	-0.5337D 01	
-12.0	-14.0	0.2316D 02	0.2174D 02	-0.2702D 02	
-12.0	-10.0	0.2005D 02	0.2452D 02	0.3033D 02	
-12.0	-6.0	0.1912D 02	0.2005D 01	0.2041D 02	
-12.0	-2.0	0.1980D 02	-0.3246D 02	0.3521D 01	
-12.0	2.0	0.2028D 02	-0.4745D 01	0.1155D 02	
-12.0	6.0	0.1947D 02	-0.8574D 00	-0.9803D 01	
-12.0	10.0	0.1925D 02	-0.2138D 02	0.9560D 01	
-12.0	14.0	0.1894D 02	0.1203D 02	0.2104D 02	
-12.0	18.0	0.2196D 02	0.3980D 01	-0.1648D 02	
-12.0	22.0	0.2058D 02	0.1851D 02	-0.4277D 02	
-16.0	-22.0	0.1834D 02	-0.8647D 01	0.2812D 02	
-16.0	-18.0	0.2019D 02	-0.1170D 02	-0.2456D 02	
-16.0	-14.0	0.1760D 02	0.7211D 01	0.3011D 02	
-16.0	-10.0	0.1901D 02	-0.9853D 01	0.6017D 01	
-16.0	-6.0	0.2185D 02	0.1554D 02	0.1098D 02	
-16.0	-2.0	0.1980D 02	-0.3076D 02	0.4215D 02	
-16.0	2.0	0.1881D 02	-0.5731D 01	0.4634D 02	
-16.0	6.0	0.1800D 02	0.3290D 02	0.2131D 02	
-16.0	10.0	0.2111D 02	-0.1263D 02	0.2059D 02	
-16.0	14.0	0.1974D 02	-0.3521D 00	0.1665D 02	
-16.0	18.0	0.1921D 02	-0.2065D 02	-0.1784D 02	
-16.0	22.0	0.1969D 02	-0.4185D 02	-0.8519D 01	
-20.0	-22.0	0.1799D 02	-0.1210D 02	0.1319D 02	
-20.0	-18.0	0.2010D 02	0.9939D 01	-0.3505D 01	
-20.0	-14.0	0.1821D 02	0.2595D 02	-0.2428D 02	
-20.0	-10.0	0.1807D 02	-0.5136D 01	-0.1092D 01	
-20.0	-6.0	0.1938D 02	-0.1685D 02	-0.9459D 01	
-20.0	-2.0	0.1842D 02	0.2337D 01	0.1688D 02	
-20.0	2.0	0.1745D 02	-0.3296D 02	0.3600D 02	
-20.0	6.0	0.2141D 02	-0.8426D 01	-0.1178D 02	
-20.0	10.0	0.1694D 02	-0.2794D 01	-0.2355D 01	
-20.0	14.0	0.1784D 02	0.4944D 01	0.6505D 01	
-20.0	18.0	0.1644D 02	-0.5789D 01	0.1504D 02	
-20.0	22.0	0.1674D 02	-0.2292D 02	0.1315D 02	

* -24.0	-22.0 *	0.1792D 02	-0.9979D 01	-0.1512D 02	*
* -24.0	-18.0 *	0.1824D 02	-0.1077D 02	-0.3750D 02	*
* -24.0	-14.0 *	0.1651D 02	0.1175D 02	-0.6073D 01	*
* -24.0	-10.0 *	0.1879D 02	0.3017D 02	0.2941D 02	*
* -24.0	-6.0 *	0.1605D 02	0.1561D 02	0.4706D 01	*
* -24.0	-2.0 *	0.1655D 02	-0.1614D 02	0.1803D 02	*
* -24.0	2.0 *	0.1594D 02	-0.2160D 02	-0.1936D 02	*
* -24.0	6.0 *	0.1563D 02	0.1493D 02	-0.5073D 01	*
* -24.0	10.0 *	0.1799D 02	0.1074D 01	0.7281D 01	*
* -24.0	14.0 *	0.1887D 02	0.1560D 02	0.1761D 02	*
* -24.0	18.0 *	0.1682D 02	-0.1187D 02	-0.2274D 02	*
* -24.0	22.0 *	0.1673D 02	-0.1585D 02	0.4136D 02	*
* -28.0	-22.0 *	0.1799D 02	0.1884D 02	0.2193D 02	*
* -28.0	-18.0 *	0.1522D 02	-0.3002D 02	-0.4210D 02	*
* -28.0	-14.0 *	0.1665D 02	-0.1445D 01	-0.3101D 02	*
* -28.0	-10.0 *	0.1700D 02	-0.6078D 01	0.1421D 02	*
* -28.0	-6.0 *	0.1516D 02	-0.1287D 01	0.9988D 01	*
* -28.0	-2.0 *	0.1605D 02	0.1526D 02	0.2321D 02	*
* -28.0	2.0 *	0.1638D 02	0.2709D 00	0.1898D 02	*
* -28.0	6.0 *	0.1612D 02	-0.1687D 02	0.1875D 01	*
* -28.0	10.0 *	0.1525D 02	-0.2562D 02	-0.9382D 01	*
* -28.0	14.0 *	0.1757D 02	-0.1691D 02	0.4291D 00	*
* -28.0	18.0 *	0.1394D 02	-0.2535D 02	0.3050D 01	*
* -28.0	22.0 *	0.1647D 02	-0.1526D 02	-0.1157D 02	*
* -32.0	-22.0 *	0.1728D 02	0.1106D-01	-0.1909D 02	*
* -32.0	-18.0 *	0.1604D 02	-0.1212D 02	-0.7934D 01	*
* -32.0	-14.0 *	0.1453D 02	0.1080D 02	0.3711D 02	*
* -32.0	-10.0 *	0.1547D 02	0.8569D 00	0.4128D 01	*
* -32.0	-6.0 *	0.1700D 02	0.8635D 01	0.1884D 02	*
* -32.0	-2.0 *	0.1427D 02	0.8948D 00	0.9607D 01	*
* -32.0	2.0 *	0.1605D 02	-0.3456D 02	-0.4289D 01	*
* -32.0	6.0 *	0.1489D 02	-0.4391D 01	-0.2052D 02	*
* -32.0	10.0 *	0.1431D 02	-0.1305D 02	0.1934D 02	*
* -32.0	14.0 *	0.1666D 02	-0.2480D 02	-0.1881D 01	*
* -32.0	18.0 *	0.1434D 02	-0.3810D 02	0.8597D 01	*
* -32.0	22.0 *	0.1521D 02	-0.1464D 02	0.3388D 02	*

STATISTICAL RESULTS:

	MEAN VALUE	STANDARD DEVIATION
X-DIRECTION	0.241D 02	0.570D 01
Y-DIRECTION	-0.183D 01	0.169D 02
Z-DIRECTION	0.203D 01	0.189D 02

EVALUATED STRAIN FIELD AT POINT (3L)

ELEMENT	EXX	EYY	ELEMENT	EXX	EYY
1, 1	0.25D-03	-0.36D-02	2, 1	-0.22D-03	0.29D-02
1, 2	0.20D-03	-0.19D-02	2, 2	0.92D-04	-0.83D-02
1, 3	0.30D-03	0.21D-02	2, 3	0.42D-03	0.79D-02
1, 4	-0.44D-03	-0.75D-02	2, 4	0.22D-03	-0.91D-02
1, 5	-0.22D-03	0.80D-02	2, 5	0.17D-03	0.12D-01
1, 6	0.41D-03	0.26D-02	2, 6	0.46D-03	-0.16D-02
1, 7	-0.13D-03	0.35D-02	2, 7	0.52D-03	0.25D-02
1, 8	-0.19D-03	-0.45D-02	2, 8	0.12D-02	-0.10D-02
1, 9	0.36D-03	-0.31D-02	2, 9	0.18D-03	-0.48D-02
1,10	0.22D-03	-0.18D-02	2,10	0.25D-03	0.18D-03
1,11	0.30D-03	0.99D-02	2,11	0.79D-03	-0.17D-02
3, 1	0.13D-02	0.40D-02	4, 1	0.60D-04	0.54D-03
3, 2	0.22D-03	0.15D-02	4, 2	0.63D-03	-0.83D-02
3, 3	0.44D-03	0.23D-03	4, 3	-0.55D-03	-0.41D-02
3, 4	0.28D-04	-0.28D-02	4, 4	0.13D-02	0.11D-01
3, 5	0.97D-03	0.28D-02	4, 5	0.45D-03	0.31D-02
3, 6	0.21D-03	0.34D-02	4, 6	-0.13D-03	-0.59D-02
3, 7	0.50D-03	0.53D-02	4, 7	0.93D-03	0.61D-02
3, 8	-0.42D-03	-0.40D-02	4, 8	-0.21D-03	0.24D-02
3, 9	0.31D-03	-0.48D-02	4, 9	0.41D-03	-0.84D-02
3,10	0.42D-03	0.71D-03	4,10	0.11D-03	-0.20D-02
3,11	-0.50D-03	0.17D-02	4,11	0.12D-02	0.31D-02
5, 1	-0.51D-03	-0.35D-02	6, 1	0.41D-03	-0.55D-02
5, 2	0.31D-03	-0.12D-01	6, 2	0.96D-03	-0.37D-02
5, 3	0.85D-03	0.12D-01	6, 3	0.18D-03	0.11D-01
5, 4	-0.12D-03	0.11D-02	6, 4	0.25D-03	0.11D-02
5, 5	0.49D-03	-0.75D-02	6, 5	0.67D-04	-0.40D-02
5, 6	0.69D-03	0.22D-02	6, 6	0.19D-03	-0.65D-02
5, 7	-0.16D-02	0.15D-02	6, 7	0.19D-02	0.34D-02
5, 8	0.10D-02	-0.30D-02	6, 8	-0.77D-05	-0.17D-02
5, 9	0.52D-03	0.22D-02	6, 9	-0.84D-03	0.83D-02
5,10	0.80D-04	-0.65D-02	6,10	0.59D-03	-0.75D-02
5,11	0.62D-03	0.13D-01	6,11	0.15D-03	-0.33D-03
7, 1	0.36D-04	0.70D-02	8, 1	0.75D-03	0.60D-02
7, 2	-0.26D-03	-0.40D-02	8, 2	0.27D-03	-0.11D-01
7, 3	0.10D-02	-0.23D-02	8, 3	-0.72D-03	-0.47D-03
7, 4	-0.48D-04	0.44D-03	8, 4	-0.11D-03	0.74D-02
7, 5	0.20D-03	0.59D-02	8, 5	0.20D-03	-0.21D-02
7, 6	0.74D-03	-0.29D-02	8, 6	0.39D-04	-0.61D-02
7, 7	-0.10D-02	0.67D-02	8, 7	0.13D-02	0.73D-02
7, 8	0.70D-03	-0.13D-01	8, 8	-0.26D-03	-0.87D-02
7, 9	0.13D-02	-0.50D-03	8, 9	0.28D-03	0.16D-01
7,10	0.15D-03	0.58D-02	8,10	-0.64D-04	-0.10D-01
7,11	-0.11D-03	0.59D-04	8,11	0.40D-03	-0.86D-02
9, 1	-0.52D-03	0.92D-03	10, 1	0.12D-02	0.39D-02
9, 2	0.37D-03	-0.88D-03	10, 2	0.25D-03	-0.34D-02
9, 3	0.21D-03	-0.65D-02	10, 3	0.11D-02	-0.41D-03
9, 4	0.15D-03	0.13D-01	10, 4	0.32D-03	0.82D-02
9, 5	0.70D-03	-0.82D-02	10, 5	0.10D-05	0.17D-02
9, 6	0.21D-03	-0.83D-03	10, 6	-0.72D-04	-0.41D-02
9, 7	0.15D-03	0.30D-02	10, 7	-0.11D-02	0.61D-03
9, 8	-0.87D-04	0.17D-02	10, 8	0.11D-02	0.14D-02
9, 9	-0.47D-03	-0.80D-02	10, 9	0.36D-03	0.23D-02
9,10	0.11D-02	0.61D-02	10,10	0.11D-03	-0.72D-02
9,11	0.89D-04	-0.73D-02	10,11	-0.57D-03	0.35D-02
11, 1	0.55D-03	-0.17D-02	12, 1	-0.27D-03	-0.54D-02
11, 2	0.27D-03	0.20D-02	12, 2	0.26D-04	0.30D-02
11, 3	0.28D-04	-0.60D-02	12, 3	0.19D-03	0.39D-02
11, 4	0.95D-03	0.97D-02	12, 4	-0.42D-03	-0.29D-02
11, 5	0.56D-04	-0.10D-01	12, 5	0.59D-03	-0.32D-03
11, 6	0.67D-04	-0.45D-02	12, 6	0.37D-03	-0.62D-02
11, 7	0.13D-02	0.10D-01	12, 7	-0.68D-04	0.12D-02
11, 8	-0.70D-03	-0.73D-02	12, 8	0.11D-02	0.56D-02

11, 9	0.11D-02	0.27D-02	12, 9	-0.75D-04	-0.12D-02
11,10	0.25D-03	-0.22D-02	12,10	-0.54D-04	0.13D-02
11,11	0.49D-03	-0.39D-02	12,11	0.13D-02	-0.39D-02
13, 1	0.34D-03	-0.49D-02	14, 1	0.34D-03	0.43D-02
13, 2	-0.13D-03	0.11D-01	14, 2	0.42D-03	-0.60D-02
13, 3	-0.62D-03	-0.78D-02	14, 3	-0.12D-03	0.13D-03
13, 4	0.74D-03	0.43D-02	14, 4	0.23D-04	0.57D-03
13, 5	-0.47D-04	0.38D-02	14, 5	0.25D-04	0.83D-02
13, 6	0.75D-03	-0.29D-02	14, 6	-0.23D-03	-0.17D-01
13, 7	0.44D-03	0.57D-02	14, 7	0.85D-04	0.83D-02
13, 8	-0.26D-03	-0.10D-01	14, 8	0.33D-03	-0.27D-02
13, 9	-0.20D-03	-0.42D-03	14, 9	0.29D-03	0.61D-02
13,10	-0.35D-03	0.22D-02	14,10	0.73D-03	0.74D-02
13,11	-0.65D-04	-0.11D-02	14,11	-0.79D-03	-0.52D-02
15, 1	0.14D-03	-0.30D-02	16, 1	0.86D-04	0.76D-03
15, 2	-0.63D-04	-0.27D-02	16, 2	0.22D-04	-0.47D-02
15, 3	0.14D-02	-0.70D-03	16, 3	-0.15D-03	0.43D-02
15, 4	0.26D-03	0.56D-02	16, 4	0.23D-03	-0.63D-02
15, 5	-0.68D-03	0.86D-02	16, 5	0.62D-03	0.12D-01
15, 6	-0.24D-06	-0.69D-02	16, 6	0.35D-03	-0.63D-02
15, 7	0.37D-03	-0.97D-03	16, 7	0.34D-03	-0.97D-02
15, 8	0.37D-03	0.51D-02	16, 8	-0.85D-03	0.11D-01
15, 9	-0.46D-03	-0.84D-02	16, 9	0.10D-02	-0.31D-02
15,10	-0.20D-03	0.20D-02	16,10	0.47D-03	0.51D-02
15,11	0.69D-03	-0.36D-02	16,11	0.19D-03	0.53D-02
17, 1	0.17D-04	-0.55D-02	18, 1	-0.16D-04	0.20D-03
17, 2	0.47D-03	-0.40D-02	18, 2	0.76D-03	-0.56D-02
17, 3	0.42D-03	0.78D-02	18, 3	-0.35D-04	-0.46D-02
17, 4	-0.18D-03	0.29D-02	18, 4	0.45D-03	0.36D-02
17, 5	0.83D-03	-0.48D-02	18, 5	0.22D-03	0.79D-02
17, 6	0.47D-03	0.88D-02	18, 6	0.13D-03	0.14D-02
17, 7	0.38D-03	-0.61D-02	18, 7	-0.11D-03	-0.91D-02
17, 8	0.14D-02	-0.14D-02	18, 8	-0.12D-03	0.35D-02
17, 9	-0.26D-03	-0.19D-02	18, 9	0.68D-03	-0.36D-02
17,10	-0.26D-03	0.27D-02	18,10	0.33D-03	0.69D-02
17,11	0.40D-03	0.43D-02	18,11	0.72D-03	0.10D-02
19, 1	0.18D-03	0.12D-01			
19, 2	-0.21D-03	-0.71D-02			
19, 3	0.53D-03	0.12D-02			
19, 4	0.38D-03	-0.12D-02			
19, 5	-0.46D-03	-0.41D-02			
19, 6	0.45D-03	0.37D-02			
19, 7	0.84D-04	0.43D-02			
19, 8	0.31D-03	0.22D-02			
19, 9	0.24D-03	-0.22D-02			
19,10	0.23D-03	0.21D-02			
19,11	-0.99D-04	-0.25D-02			

STATISTICAL RESULTS:

	MEAN VALUE	STANDARD DEVIATION
XX-STRAIN:	0.2381D-03	0.5132D-03
YY-STRAIN:	0.2236D-04	0.5931D-02

RECONSTRUCTION RESULTS OF INTERFEROGRAM
(4B) OF THE NEWS-PRINT PAPER SAMPLE #38
CUMULATIVE DEFORMATION)

CO-ORDINATES X	CO-ORDINATES Y	DEFORMATIONS X	DEFORMATIONS Y	DEFORMATIONS Z
44.0	-22.0	0.4098D 02	-0.2203D 02	0.2020D 02
44.0	-18.0	0.4033D 02	0.9446D 01	-0.8894D 01
44.0	-14.0	0.4189D 02	-0.2989D 02	-0.2290D 02
44.0	-10.0	0.4213D 02	-0.3042D 00	-0.1499D 02
44.0	-6.0	0.4081D 02	0.1059D 02	0.3635D 02
44.0	-2.0	0.3798D 02	0.2360D 02	0.2036D 02
44.0	2.0	0.4088D 02	-0.8845D 01	-0.1247D 02
44.0	6.0	0.4168D 02	-0.1493D 02	0.9363D 01
44.0	10.0	0.3724D 02	-0.2882D 02	-0.1753D 02
44.0	14.0	0.3852D 02	-0.1531D 02	-0.1296D 02
44.0	18.0	0.3783D 02	0.1323D 02	-0.9896D 01
44.0	22.0	0.3902D 02	-0.2174D 02	0.6336D 01
40.0	-22.0	0.3931D 02	0.2066D 02	0.1173D 02
40.0	-18.0	0.3975D 02	0.3879D 02	-0.1671D 02
40.0	-14.0	0.4070D 02	0.2903D 00	-0.5532D 02
40.0	-10.0	0.4135D 02	-0.4700D 02	-0.2573D 02
40.0	-6.0	0.3928D 02	-0.1649D 02	-0.2002D 02
40.0	-2.0	0.4164D 02	-0.4376D 02	0.3131D 01
40.0	2.0	0.3643D 02	-0.4038D 02	-0.9730D 01
40.0	6.0	0.4067D 02	-0.1299D 02	0.1875D 02
40.0	10.0	0.3763D 02	0.3757D 01	-0.7562D 01
40.0	14.0	0.4165D 02	-0.1500D 02	-0.3917D 02
40.0	18.0	0.4223D 02	0.1512D 02	0.1508D 02
40.0	22.0	0.4153D 02	-0.3745D 01	0.1747D 02
36.0	-22.0	0.3856D 02	0.1424D 02	0.3469D 02
36.0	-18.0	0.3968D 02	0.2219D 02	-0.2897D 02
36.0	-14.0	0.3786D 02	-0.6265D 01	0.1793D 02
36.0	-10.0	0.3973D 02	-0.4536D 02	0.3433D 02
36.0	-6.0	0.4140D 02	-0.2378D 01	-0.3880D 01
36.0	-2.0	0.3698D 02	-0.1696D 01	-0.1935D 02
36.0	2.0	0.3723D 02	-0.5526D 02	0.2684D 01
36.0	6.0	0.4192D 02	-0.1845D 02	-0.1725D 02
36.0	10.0	0.3935D 02	0.1575D 02	-0.2986D 02
36.0	14.0	0.3944D 02	-0.2617D 02	-0.3452D 02
36.0	18.0	0.3958D 02	-0.3365D 02	-0.1983D 02
36.0	22.0	0.3945D 02	-0.9144D 01	-0.4129D 02
32.0	-22.0	0.3913D 02	-0.1966D 02	0.8764D 01
32.0	-18.0	0.3954D 02	-0.2593D 01	0.1060D 02
32.0	-14.0	0.3776D 02	-0.2972D 02	-0.2341D 01
32.0	-10.0	0.3909D 02	0.1004D 02	0.1270D 02
32.0	-6.0	0.3536D 02	-0.3551D 02	-0.1060D 02
32.0	-2.0	0.3889D 02	0.3625D 01	0.4540D 02
32.0	2.0	0.3876D 02	0.1867D 02	0.1602D 01
32.0	6.0	0.3712D 02	-0.2724D 02	-0.4800D 01
32.0	10.0	0.3620D 02	0.3118D 02	0.7363D 00
32.0	14.0	0.3860D 02	0.1833D 02	0.7842D 01
32.0	18.0	0.3850D 02	-0.5239D 02	-0.2762D 02
32.0	22.0	0.3773D 02	-0.1266D 02	-0.2844D 01
28.0	-22.0	0.3735D 02	0.1334D 02	0.5905D 02
28.0	-18.0	0.3662D 02	0.3087D 02	-0.3000D 02
28.0	-14.0	0.3655D 02	0.5257D 02	-0.7381D 01
28.0	-10.0	0.3654D 02	0.4746D 02	0.1922D 02
28.0	-6.0	0.3648D 02	-0.2394D 02	-0.8952D 01
28.0	-2.0	0.3757D 02	-0.3152D 02	0.3689D 01
28.0	2.0	0.3763D 02	-0.8342D 01	0.3762D 01
28.0	6.0	0.3951D 02	0.2547D 02	-0.4867D 02
28.0	10.0	0.3710D 02	0.1436D 02	-0.3881D 02
28.0	14.0	0.3752D 02	-0.2635D 02	0.1552D 02
28.0	18.0	0.3634D 02	-0.2883D 02	0.5385D 02
28.0	22.0	0.3706D 02	-0.2366D 02	-0.3545D 02

24.0	-22.0	0.3716D 02	0.1172D 02	-0.1493D 02	
24.0	-18.0	0.3678D 02	-0.1512D 02	0.1822D 02	
24.0	-14.0	0.3524D 02	-0.2343D 02	0.3900D 02	
24.0	-10.0	0.3574D 02	0.1521D 01	-0.4325D 02	
24.0	-6.0	0.3512D 02	0.1749D 02	-0.2734D 02	
24.0	-2.0	0.3522D 02	0.1835D 02	0.6408D 01	
24.0	2.0	0.3537D 02	-0.2471D 02	-0.8704D 01	
24.0	6.0	0.3566D 02	-0.1759D 02	-0.1338D 02	
24.0	10.0	0.3759D 02	0.3171D 01	0.2533D 02	
24.0	14.0	0.3513D 02	-0.2733D 02	0.1231D 02	
24.0	18.0	0.3302D 02	0.5414D 01	0.8502D 01	
24.0	22.0	0.3821D 02	-0.2495D 02	-0.1250D 02	
20.0	-22.0	0.3492D 02	-0.6400D 01	0.1793D 02	
20.0	-18.0	0.3581D 02	0.1892D 02	-0.2105D 02	
20.0	-14.0	0.3655D 02	-0.1699D 02	-0.3160D 01	
20.0	-10.0	0.3805D 02	-0.4154D 02	0.1635D 01	
20.0	-6.0	0.3501D 02	-0.1337D 02	-0.6183D 01	
20.0	-2.0	0.3468D 02	0.3495D 02	0.9628D 01	
20.0	2.0	0.3456D 02	0.1285D 02	0.1126D 02	
20.0	6.0	0.3586D 02	0.2179D 02	0.2807D 01	
20.0	10.0	0.3727D 02	0.4463D 01	-0.5335D 01	
20.0	14.0	0.3731D 02	-0.1562D 02	0.4566D 01	
20.0	18.0	0.3539D 02	0.1145D 02	-0.2206D 02	
20.0	22.0	0.3332D 02	0.2811D 02	0.3086D 02	
16.0	-22.0	0.3439D 02	-0.3001D 02	-0.3963D 02	
16.0	-18.0	0.3425D 02	-0.1662D 02	0.4691D 01	
16.0	-14.0	0.3142D 02	-0.1505D 02	0.3501D 02	
16.0	-10.0	0.3356D 02	-0.1738D 02	-0.2944D 01	
16.0	-6.0	0.3331D 02	0.1527D 02	-0.1606D 02	
16.0	-2.0	0.3350D 02	-0.3110D 01	-0.4204D 02	
16.0	2.0	0.3167D 02	-0.3787D 01	-0.5814D 02	
16.0	6.0	0.3341D 02	-0.3385D 02	0.5100D 01	
16.0	10.0	0.3167D 02	0.1137D 02	0.4225D 02	
16.0	14.0	0.3393D 02	-0.1534D 01	-0.3447D 02	
16.0	18.0	0.2859D 02	0.1075D 02	-0.2405D 02	
16.0	22.0	0.3039D 02	0.2614D 02	0.1736D 02	
12.0	-22.0	0.3340D 02	-0.1860D 02	-0.2776D 02	
12.0	-18.0	0.3063D 02	0.3096D 02	-0.6831D 01	
12.0	-14.0	0.3244D 02	-0.4974D 01	-0.1660D 02	
12.0	-10.0	0.3634D 02	0.3219D 02	-0.1004D 02	
12.0	-6.0	0.3292D 02	-0.1644D 02	0.3069D 02	
12.0	-2.0	0.3214D 02	-0.9420D 01	-0.1806D 02	
12.0	2.0	0.3163D 02	-0.1293D 02	0.1702D 02	
12.0	6.0	0.2951D 02	-0.3019D 02	0.4587D 02	
12.0	10.0	0.3354D 02	0.3461D 02	-0.2977D 02	
12.0	14.0	0.3350D 02	-0.3982D 02	-0.3917D 02	
12.0	18.0	0.3276D 02	-0.3130D 02	0.1663D 01	
12.0	22.0	0.3057D 02	-0.4311D 02	-0.6363D 02	
8.0	-22.0	0.3121D 02	-0.4885D 02	0.3667D 02	
8.0	-18.0	0.3257D 02	0.5351D 01	0.1321D 02	
8.0	-14.0	0.3040D 02	-0.4140D 02	0.5787D 01	
8.0	-10.0	0.3074D 02	0.2941D 02	-0.1030D 02	
8.0	-6.0	0.2993D 02	0.1361D 02	0.2629D 02	
8.0	-2.0	0.2867D 02	-0.9628D 01	0.9018D 01	
8.0	2.0	0.3252D 02	-0.7095D 02	-0.2417D 02	
8.0	6.0	0.3195D 02	0.2968D 02	-0.3157D 02	
8.0	10.0	0.3196D 02	-0.2462D 02	0.3051D 02	
8.0	14.0	0.2860D 02	0.1434D 02	0.2406D 02	
8.0	18.0	0.3085D 02	0.1212D 02	0.2714D 02	
8.0	22.0	0.3240D 02	-0.6306D 01	0.3157D 02	
4.0	-22.0	0.3187D 02	-0.4386D 01	-0.2067D 02	
4.0	-18.0	0.2610D 02	0.2724D 02	-0.5302D 02	
4.0	-14.0	0.3102D 02	0.5421D 01	-0.3115D 02	
4.0	-10.0	0.3150D 02	-0.2129D 02	-0.1778D 01	
4.0	-6.0	0.3154D 02	0.1490D 02	0.2214D 02	
4.0	-2.0	0.3151D 02	0.4946D 01	0.2599D 02	
4.0	2.0	0.2911D 02	0.3251D 02	-0.3113D 02	
4.0	6.0	0.2917D 02	0.4782D 01	-0.1176D 02	
4.0	10.0	0.2615D 02	-0.3409D 02	0.1156D 02	
4.0	14.0	0.2879D 02	0.1607D 02	0.8085D 01	
4.0	18.0	0.2854D 02	0.2513D 02	0.1728D 01	
4.0	22.0	0.2830D 02	-0.2171D 02	-0.3608D-02	

0.0	-22.0	0.2866D 02	-0.1957D 02	0.1197D 02	
0.0	-18.0	0.2587D 02	-0.2251D 02	0.3922D 02	
0.0	-14.0	0.2960D 02	0.1720D 02	-0.5011D 02	
0.0	-10.0	0.2765D 02	0.3308D 02	0.1372D 02	
0.0	-6.0	0.2751D 02	0.2051D 02	-0.2296D 02	
0.0	-2.0	0.2912D 02	-0.4472D 02	-0.8639D 01	
0.0	2.0	0.2918D 02	-0.1139D 02	0.4939D 02	
0.0	6.0	0.2661D 02	0.5831D 01	-0.7744D 01	
0.0	10.0	0.2980D 02	0.7091D 00	-0.3408D 02	
0.0	14.0	0.2721D 02	-0.1696D 02	0.2352D 01	
0.0	18.0	0.2410D 02	0.1160D 02	0.1008D 02	
0.0	22.0	0.2935D 02	-0.6337D 01	-0.1797D 02	
-4.0	-22.0	0.3033D 02	-0.7350D 01	0.3925D 00	
-4.0	-18.0	0.2795D 02	0.2211D 02	-0.2143D 02	
-4.0	-14.0	0.2893D 02	-0.7637D 01	-0.1995D 02	
-4.0	-10.0	0.2525D 02	-0.3151D 02	0.1634D 02	
-4.0	-6.0	0.2961D 02	-0.2163D 02	-0.1839D 02	
-4.0	-2.0	0.2828D 02	-0.4803D 02	-0.5182D 01	
-4.0	2.0	0.2961D 02	0.1392D 02	0.1973D 02	
-4.0	6.0	0.2612D 02	-0.1703D 00	-0.5788D 02	
-4.0	10.0	0.2626D 02	0.1751D 00	-0.5371D 01	
-4.0	14.0	0.2953D 02	0.1576D 01	0.1999D 02	
-4.0	18.0	0.2730D 02	-0.4813D 02	0.1743D 01	
-4.0	22.0	0.2887D 02	-0.3611D 02	-0.3773D 02	
-8.0	-22.0	0.2902D 02	0.7642D 01	-0.5386D 01	
-8.0	-18.0	0.2867D 02	0.6278D-02	0.2964D 01	
-8.0	-14.0	0.2769D 02	-0.1370D 02	-0.3761D 02	
-8.0	-10.0	0.2835D 02	0.3804D 01	0.3383D 02	
-8.0	-6.0	0.2447D 02	0.1186D 02	-0.1300D 02	
-8.0	-2.0	0.2646D 02	0.1846D 02	0.2654D 02	
-8.0	2.0	0.2626D 02	0.8503D 01	0.2456D 02	
-8.0	6.0	0.2855D 02	-0.2450D 02	-0.2630D 02	
-8.0	10.0	0.2490D 02	0.2595D 02	0.2992D 02	
-8.0	14.0	0.2868D 02	-0.9305D 01	-0.2574D 02	
-8.0	18.0	0.2402D 02	0.2039D 02	0.5142D 02	
-8.0	22.0	0.2869D 02	-0.9551D 00	-0.1073D 02	
-12.0	-22.0	0.2708D 02	-0.2920D 02	0.8786D 01	
-12.0	-18.0	0.2685D 02	-0.3024D 02	0.2234D 02	
-12.0	-14.0	0.2676D 02	-0.1581D 02	0.1105D 02	
-12.0	-10.0	0.2867D 02	-0.4701D 01	-0.4499D 02	
-12.0	-6.0	0.2644D 02	0.2272D 02	-0.3800D 02	
-12.0	-2.0	0.2775D 02	-0.3200D 01	-0.1679D 01	
-12.0	2.0	0.2704D 02	0.4123D 02	-0.2538D 02	
-12.0	6.0	0.2572D 02	-0.1158D 02	-0.4881D 01	
-12.0	10.0	0.2728D 02	-0.2868D 02	-0.1005D 02	
-12.0	14.0	0.2224D 02	0.5786D 01	-0.2117D 02	
-12.0	18.0	0.2408D 02	-0.3817D 02	0.1394D 02	
-12.0	22.0	0.2513D 02	-0.1614D 02	0.3348D 02	
-16.0	-22.0	0.2502D 02	-0.2046D 02	-0.7293D 01	
-16.0	-18.0	0.2585D 02	-0.7694D 01	0.3961D 02	
-16.0	-14.0	0.2542D 02	0.2531D 02	-0.2223D 02	
-16.0	-10.0	0.2518D 02	0.8699D 01	-0.2179D 02	
-16.0	-6.0	0.2796D 02	-0.9616D 01	-0.8685D 01	
-16.0	-2.0	0.2767D 02	-0.2154D 02	-0.6356D 02	
-16.0	2.0	0.2625D 02	-0.2186D 02	-0.5608D 02	
-16.0	6.0	0.2667D 02	0.4876D 01	-0.4611D 02	
-16.0	10.0	0.2329D 02	0.1712D 02	-0.2946D 02	
-16.0	14.0	0.2442D 02	0.3415D 02	-0.2504D 02	
-16.0	18.0	0.2376D 02	-0.9279D 01	0.1704D 02	
-16.0	22.0	0.2601D 02	-0.1925D 02	0.2131D 02	
-20.0	-22.0	0.2614D 02	-0.2914D 02	-0.1482D 02	
-20.0	-18.0	0.2578D 02	-0.3645D 02	0.7333D 01	
-20.0	-14.0	0.2491D 02	-0.2148D 02	0.3304D 02	
-20.0	-10.0	0.2549D 02	-0.9079D 01	0.2299D 02	
-20.0	-6.0	0.2333D 02	0.2863D 02	0.3164D 02	
-20.0	-2.0	0.2672D 02	-0.2676D 02	-0.2032D 02	
-20.0	2.0	0.2323D 02	-0.3807D 02	-0.3814D 02	
-20.0	6.0	0.2459D 02	-0.2360D 02	0.2086D 02	
-20.0	10.0	0.2578D 02	0.1390D 02	-0.1533D 02	
-20.0	14.0	0.2618D 02	-0.8819D 01	0.7186D 01	
-20.0	18.0	0.2508D 02	-0.7022D 01	-0.1009D 02	
-20.0	22.0	0.2496D 02	-0.3683D 02	-0.1686D 02	

*	-24.0	-22.0 *	0.2847D 02	0.1676D 02	0.2441D 02	*
*	-24.0	-18.0 *	0.2395D 02	-0.7100D 01	0.4572D 02	*
*	-24.0	-14.0 *	0.2333D 02	-0.1643D 02	0.9178D 01	*
*	-24.0	-10.0 *	0.2899D 02	-0.4954D 02	-0.3562D 02	*
*	-24.0	-6.0 *	0.2578D 02	0.2636D 02	-0.1628D 02	*
*	-24.0	-2.0 *	0.2582D 02	-0.1635D 02	-0.3708D 02	*
*	-24.0	2.0 *	0.2407D 02	0.7645D 00	0.2510D 02	*
*	-24.0	6.0 *	0.2264D 02	0.2215D 02	-0.3467D 01	*
*	-24.0	10.0 *	0.2202D 02	0.2836D 02	-0.1420D 02	*
*	-24.0	14.0 *	0.2335D 02	-0.8855D 01	-0.2397D 02	*
*	-24.0	18.0 *	0.2406D 02	0.2973D 02	0.2952D 02	*
*	-24.0	22.0 *	0.2354D 02	-0.3687D 02	-0.4543D 02	*
*	-28.0	-22.0 *	0.2367D 02	-0.1390D 02	-0.1949D 02	*
*	-28.0	-18.0 *	0.2223D 02	0.2581D 02	0.5339D 02	*
*	-28.0	-14.0 *	0.2233D 02	0.4374D 01	0.3067D 02	*
*	-28.0	-10.0 *	0.2307D 02	0.3373D 02	-0.1306D 02	*
*	-28.0	-6.0 *	0.2232D 02	0.2180D 02	-0.1806D 02	*
*	-28.0	-2.0 *	0.2187D 02	0.9699D 01	-0.3632D 02	*
*	-28.0	2.0 *	0.2368D 02	0.1484D 02	-0.3263D 02	*
*	-28.0	6.0 *	0.2074D 02	0.1009D 02	-0.1928D 02	*
*	-28.0	10.0 *	0.2342D 02	0.1431D 02	0.1311D 02	*
*	-28.0	14.0 *	0.2195D 02	-0.2678D 02	0.8318D 01	*
*	-28.0	18.0 *	0.2477D 02	-0.1842D 02	-0.1458D 02	*
*	-28.0	22.0 *	0.2296D 02	0.1751D 02	0.4335D 01	*
*	-32.0	-22.0 *	0.2080D 02	-0.2841D 01	0.4108D 02	*
*	-32.0	-18.0 *	0.2161D 02	-0.1631D 02	0.2065D 02	*
*	-32.0	-14.0 *	0.1977D 02	0.4103D 02	-0.5553D 02	*
*	-32.0	-10.0 *	0.2391D 02	-0.1638D 02	-0.9624D 01	*
*	-32.0	-6.0 *	0.2127D 02	-0.9316D 01	-0.6349D 01	*
*	-32.0	-2.0 *	0.2131D 02	0.1011D 02	-0.6092D 01	*
*	-32.0	2.0 *	0.2001D 02	0.4418D 02	-0.1437D 02	*
*	-32.0	6.0 *	0.2249D 02	0.1333D 02	0.4658D 02	*
*	-32.0	10.0 *	0.2026D 02	0.2044D 02	-0.1477D 02	*
*	-32.0	14.0 *	0.2050D 02	-0.2415D 02	0.2411D 01	*
*	-32.0	18.0 *	0.2123D 02	0.1411D 01	-0.1824D 02	*
*	-32.0	22.0 *	0.2244D 02	-0.5720D 02	-0.4536D 02	*

STATISTICAL RESULTS:

	MEAN VALUE	STANDARD DEVIATION
X-DIRECTION	0.310D 02	0.610D 01
Y-DIRECTION	-0.414D 01	0.235D 02
Z-DIRECTION	-0.344D 01	0.258D 02

EVALUATED STRAIN FIELD AT POINT (4R)

ELEMENT	EXX	EYY	ELEMENT	EXX	EYY
1, 1	0.42D-03	-0.79D-02	2, 1	0.19D-03	-0.45D-02
1, 2	0.14D-03	0.98D-02	2, 2	0.17D-04	0.96D-02
1, 3	0.30D-03	-0.74D-02	2, 3	0.71D-03	0.12D-01
1, 4	0.19D-03	-0.27D-02	2, 4	0.41D-03	-0.76D-02
1, 5	0.38D-03	-0.33D-02	2, 5	-0.53D-03	0.68D-02
1, 6	-0.91D-03	0.81D-02	2, 6	0.66D-03	-0.85D-03
1, 7	0.11D-02	0.15D-02	2, 7	-0.20D-03	-0.68D-02
1, 8	0.25D-03	0.35D-02	2, 8	-0.31D-03	-0.42D-02
1, 9	-0.96D-04	-0.34D-02	2, 9	-0.43D-03	0.47D-02
1,10	-0.78D-03	-0.71D-02	2,10	0.55D-03	-0.75D-02
1,11	-0.11D-02	0.87D-02	2,11	0.66D-03	0.47D-02
3, 1	-0.14D-03	-0.20D-02	4, 1	0.44D-03	-0.43D-02
3, 2	0.37D-04	0.71D-02	4, 2	0.73D-03	0.68D-02
3, 3	0.24D-04	0.98D-02	4, 3	0.30D-03	-0.99D-02
3, 4	0.16D-03	-0.11D-01	4, 4	0.64D-03	0.11D-01
3, 5	0.15D-02	-0.17D-03	4, 5	-0.28D-03	-0.98D-02
3, 6	0.24D-04	0.13D-01	4, 6	0.33D-03	-0.38D-02
3, 7	-0.38D-03	-0.92D-02	4, 7	0.28D-03	0.11D-01
3, 8	0.12D-02	-0.86D-02	4, 8	-0.60D-03	-0.15D-01
3, 9	0.79D-03	0.10D-01	4, 9	-0.23D-03	0.32D-02
3,10	0.21D-03	0.19D-02	4,10	0.27D-03	0.18D-01
3,11	0.27D-03	-0.61D-02	4,11	0.54D-03	-0.99D-02
5, 1	0.49D-04	-0.44D-02	6, 1	0.56D-03	-0.85D-03
5, 2	-0.41D-04	-0.54D-02	6, 2	0.24D-03	0.96D-02
5, 3	0.33D-03	0.13D-02	6, 3	-0.33D-03	-0.62D-02
5, 4	0.20D-03	0.18D-01	6, 4	-0.58D-03	-0.40D-02
5, 5	0.34D-03	0.19D-02	6, 5	0.27D-04	-0.21D-03
5, 6	0.59D-03	-0.58D-02	6, 6	0.13D-03	0.11D-01
5, 7	0.57D-03	-0.85D-02	6, 7	0.20D-03	-0.18D-02
5, 8	0.96D-03	0.28D-02	6, 8	-0.52D-04	-0.52D-02
5, 9	-0.12D-03	0.10D-01	6, 9	0.80D-04	0.76D-02
5,10	0.60D-03	0.62D-03	6,10	-0.54D-03	-0.82D-02
5,11	0.83D-03	-0.13D-02	6,11	-0.59D-03	0.76D-02
7, 1	0.13D-03	-0.63D-02	8, 1	0.25D-03	-0.33D-02
7, 2	0.39D-03	0.90D-02	8, 2	0.90D-03	-0.39D-03
7, 3	0.13D-02	0.61D-02	8, 3	-0.26D-03	0.58D-03
7, 4	0.11D-02	-0.70D-02	8, 4	-0.69D-03	-0.82D-02
7, 5	0.43D-03	-0.12D-01	8, 5	0.97D-04	0.46D-02
7, 6	0.30D-03	0.55D-02	8, 6	0.34D-03	0.17D-03
7, 7	0.72D-03	-0.22D-02	8, 7	0.99D-05	0.75D-02
7, 8	0.61D-03	0.43D-02	8, 8	0.98D-03	-0.11D-01
7, 9	0.14D-02	0.50D-02	8, 9	-0.47D-03	0.32D-02
7,10	0.84D-03	-0.68D-02	8,10	0.11D-03	-0.31D-02
7,11	0.17D-02	-0.42D-02	8,11	-0.10D-02	-0.38D-02
9, 1	0.55D-03	-0.12D-01	10, 1	-0.17D-03	-0.14D-01
9, 2	-0.49D-03	0.90D-02	10, 2	0.16D-02	0.12D-01
9, 3	0.51D-03	-0.93D-02	10, 3	-0.16D-03	-0.18D-01
9, 4	0.14D-02	0.12D-01	10, 4	-0.19D-03	0.40D-02
9, 5	0.75D-03	-0.18D-02	10, 5	-0.40D-03	0.58D-02
9, 6	0.87D-03	0.88D-03	10, 6	-0.71D-03	0.15D-01
9, 7	-0.22D-03	0.43D-02	10, 7	0.85D-03	-0.25D-01
9, 8	-0.61D-03	-0.16D-01	10, 8	0.69D-03	0.14D-01
9, 9	0.40D-03	0.19D-01	10, 9	0.15D-02	-0.97D-02
9,10	0.12D-02	-0.21D-02	10,10	-0.47D-04	0.56D-03
9,11	0.48D-03	0.30D-02	10,11	0.58D-03	0.46D-02
11, 1	0.80D-03	-0.79D-02	12, 1	-0.42D-03	0.73D-03
11, 2	0.56D-04	0.55D-02	12, 2	-0.52D-03	-0.99D-02
11, 3	0.36D-03	0.67D-02	12, 3	0.17D-03	-0.40D-02
11, 4	0.96D-03	-0.90D-02	12, 4	0.60D-03	0.31D-02
11, 5	0.10D-02	0.25D-02	12, 5	-0.52D-03	0.16D-01
11, 6	0.60D-03	-0.69D-02	12, 6	0.21D-03	-0.83D-02
11, 7	-0.17D-04	0.69D-02	12, 7	-0.11D-03	-0.43D-02
11, 8	0.84D-03	0.97D-02	12, 8	0.12D-03	0.13D-02

11, 9	-0.91D-03	-0.13D-01	12, 9	0.89D-03	0.44D-02
11,10	0.39D-03	-0.23D-02	12,10	-0.58D-03	-0.71D-02
11,11	0.11D-02	0.12D-01	12,11	-0.80D-03	0.45D-02
13, 1	0.33D-03	-0.74D-02	14, 1	0.49D-03	0.19D-02
13, 2	-0.18D-03	0.74D-02	14, 2	0.45D-03	0.34D-02
13, 3	0.31D-03	0.60D-02	14, 3	0.23D-03	-0.44D-02
13, 4	-0.77D-03	-0.25D-02	14, 4	-0.79D-04	-0.20D-02
13, 5	0.13D-02	0.66D-02	14, 5	-0.49D-03	-0.16D-02
13, 6	0.45D-03	-0.15D-01	14, 6	-0.32D-03	0.25D-02
13, 7	0.84D-03	0.35D-02	14, 7	-0.19D-03	0.83D-02
13, 8	-0.61D-03	-0.86D-04	14, 8	0.71D-03	-0.13D-01
13, 9	0.34D-03	-0.35D-03	14, 9	-0.60D-03	0.88D-02
13,10	0.21D-03	0.12D-01	14,10	0.16D-02	-0.74D-02
13,11	0.82D-03	-0.30D-02	14,11	-0.16D-04	0.53D-02
15, 1	0.52D-03	0.26D-03	16, 1	-0.28D-03	-0.32D-02
15, 2	0.25D-03	-0.36D-02	16, 2	0.19D-04	-0.83D-02
15, 3	0.33D-03	-0.28D-02	16, 3	0.13D-03	0.42D-02
15, 4	0.87D-03	-0.69D-02	16, 4	-0.78D-04	0.46D-02
15, 5	-0.36D-03	0.65D-02	16, 5	0.12D-02	0.30D-02
15, 6	0.18D-04	-0.11D-01	16, 6	0.24D-03	0.80D-04
15, 7	0.20D-03	0.13D-01	16, 7	0.76D-03	-0.67D-02
15, 8	-0.24D-03	0.43D-02	16, 8	0.52D-03	-0.31D-02
15, 9	0.10D-02	-0.86D-02	16, 9	-0.62D-03	-0.43D-02
15,10	-0.55D-03	0.11D-01	16,10	-0.44D-03	0.11D-01
15,11	0.81D-04	-0.55D-02	16,11	-0.33D-03	0.25D-02
17, 1	-0.56D-03	0.18D-02	18, 1	0.12D-02	0.60D-02
17, 2	0.46D-03	-0.37D-02	18, 2	0.43D-03	0.23D-02
17, 3	0.39D-03	-0.31D-02	18, 3	0.25D-03	0.63D-02
17, 4	-0.87D-03	-0.94D-02	18, 4	0.15D-02	-0.19D-01
17, 5	-0.11D-03	0.14D-01	18, 5	0.36D-03	0.11D-01
17, 6	0.23D-03	0.28D-02	18, 6	0.99D-03	-0.43D-02
17, 7	-0.21D-03	-0.36D-02	18, 7	0.98D-04	-0.53D-02
17, 8	0.49D-03	-0.94D-02	18, 8	0.48D-03	-0.16D-02
17, 9	0.93D-03	0.57D-02	18, 9	-0.34D-03	0.93D-02
17,10	0.71D-03	-0.45D-03	18,10	0.35D-03	-0.96D-02
17,11	0.26D-03	0.75D-02	18,11	-0.18D-03	0.17D-01
19, 1	0.72D-03	-0.99D-02			
19, 2	0.16D-03	0.54D-02			
19, 3	0.64D-03	-0.73D-02			
19, 4	-0.21D-03	0.30D-02			
19, 5	0.26D-03	0.30D-02			
19, 6	0.14D-03	-0.13D-02			
19, 7	0.92D-03	0.12D-02			
19, 8	-0.44D-03	-0.11D-02			
19, 9	0.79D-03	0.10D-01			
19,10	0.36D-03	-0.21D-02			
19,11	0.88D-03	-0.90D-02			

STATISTICAL RESULTS:

	MEAN VALUE	STANDARD DEVIATION
AX-STRAIN:	0.2477D-03	0.5713D-03
AY-STRAIN:	0.7481D-04	0.7898D-02

EVALUATED THICKNESS CHANGES (MICRONS)
(COLUMNS: 1- 6)

	1	2	3	4	5	6
1	-7.76	-5.59	-8.14	-3.47	-1.15	-6.27
2	-2.49	-6.48	-3.13	-0.55	2.23	2.39
3	-5.97	0.88	2.50	-2.34	3.39	-4.93
4	-3.44	-8.49	1.65	-6.08	-7.65	-8.23
5	-3.60	7.03	3.03	-7.30	-0.49	-2.67
6	1.75	-4.17	-4.50	-1.41	-0.27	2.79
7	-6.01	-1.80	-1.95	3.42	-1.49	-8.49
8	0.58	-7.07	-8.98	-2.18	0.06	0.97
9	-7.59	-0.66	1.16	0.48	-10.26	3.78
10	-0.31	-2.71	-4.36	-0.10	-0.54	-9.20
11	-5.29	-3.32	-3.07	1.64	-4.26	-7.07
12	5.46	-4.86	-2.88	-4.69	-2.72	4.75
13	-6.64	5.54	0.55	1.47	-6.15	-9.89
14	-2.74	5.23	-4.02	-6.75	1.41	6.60
15	-4.50	-3.88	-8.23	3.67	5.29	1.69
16	1.79	0.55	3.19	-0.27	4.74	-3.15
17	-3.97	5.55	-7.96	-2.62	-1.31	-4.77
18	-10.27	-7.75	1.37	1.32	4.95	1.68
19	4.39	-10.69	-0.21	-2.63	0.75	3.02
20	-0.15	-0.78	-4.21	-6.21	3.63	1.99

(COLUMNS: 7-12)

	7	8	9	10	11	12
1	-3.93	3.52	-4.47	2.74	0.95	-5.43
2	-0.81	-3.10	0.28	0.46	-5.24	-0.24
3	0.20	2.54	-1.78	-0.21	4.83	4.81
4	-1.12	-6.41	-0.86	-5.58	-2.29	2.54
5	0.39	3.97	-0.12	2.87	-2.67	-2.91
6	-3.65	-3.02	-0.88	3.67	-3.03	-1.12
7	-8.64	-2.15	3.72	-2.57	-1.77	-4.06
8	-1.71	3.37	-10.33	4.97	-6.00	-1.32
9	-1.53	-6.95	4.40	-2.42	-8.13	1.54
10	-6.30	0.58	2.19	-4.30	2.80	-2.84
11	-1.89	-0.77	-7.75	-6.47	-10.27	-0.26
12	-6.94	2.23	-3.72	-2.83	-5.29	-1.60
13	-1.55	6.09	-3.51	-0.74	-6.17	2.37
14	-11.58	6.99	-3.95	3.65	0.84	-4.22
15	2.16	-1.38	1.18	1.23	0.13	-6.22
16	4.51	-3.75	-4.07	-2.40	-0.64	1.49
17	-0.41	-10.65	-2.86	2.24	-2.86	1.00
18	-7.15	-3.30	-5.65	-5.21	-9.50	1.01
19	-4.80	5.03	4.21	0.13	-7.83	-3.35
20	-0.26	-2.34	-1.36	-1.94	2.78	0.81

RECONSTRUCTION RESULTS OF INTERFEROGRAM
(4L) OF THE NEWS-PRINT PAPER SAMPLE #38
CUMMULATIVE DEFORMATION)

CO-ORDINATES X	CO-ORDINATES Y	DEFORMATIONS X	DEFORMATIONS Y	DEFORMATIONS Z
44.0	-22.0	0.4089D 02	-0.2992D 02	-0.3085D 02
44.0	-18.0	0.4206D 02	-0.1392D 02	-0.4713D 01
44.0	-14.0	0.4262D 02	0.2424D 02	0.1227D 02
44.0	-10.0	0.3884D 02	0.2047D 01	0.8745D-01
44.0	-6.0	0.4171D 02	0.3641D 02	-0.3705D 02
44.0	-2.0	0.4228D 02	-0.1067D 02	-0.2594D 02
44.0	2.0	0.4107D 02	-0.1370D 02	-0.7869D 00
44.0	6.0	0.3989D 02	-0.2342D 02	-0.5871D 01
44.0	10.0	0.4100D 02	-0.1915D 02	0.1170D 02
44.0	14.0	0.4089D 02	-0.1572D 02	0.2107D 02
44.0	18.0	0.4370D 02	0.2176D 02	0.1635D 02
44.0	22.0	0.4254D 02	-0.4241D 02	-0.2269D 02
40.0	-22.0	0.4041D 02	0.1718D 02	-0.1222D 02
40.0	-18.0	0.4133D 02	-0.8330D 01	0.1121D 02
40.0	-14.0	0.4118D 02	0.3573D 02	0.4992D 02
40.0	-10.0	0.4120D 02	-0.7484D 01	0.1982D 02
40.0	-6.0	0.4272D 02	-0.3989D 02	0.1646D 02
40.0	-2.0	0.4051D 02	-0.2584D 02	0.7172D 01
40.0	2.0	0.4167D 02	-0.1155D 02	0.1281D 02
40.0	6.0	0.4111D 02	-0.3265D 02	-0.2345D 02
40.0	10.0	0.3946D 02	-0.2847D 02	0.2442D 01
40.0	14.0	0.4021D 02	-0.2744D 01	0.4401D 02
40.0	18.0	0.4162D 02	0.4041D 01	-0.2253D 02
40.0	22.0	0.3906D 02	0.7971D 00	-0.1907D 02
36.0	-22.0	0.4060D 02	0.2934D 02	-0.3882D 02
36.0	-18.0	0.4098D 02	0.2045D 02	0.3407D 02
36.0	-14.0	0.3949D 02	0.2254D 02	-0.1797D 02
36.0	-10.0	0.3913D 02	0.1701D 02	-0.2817D 02
36.0	-6.0	0.4160D 02	0.1984D 02	0.1259D 02
36.0	-2.0	0.3880D 02	0.4618D 01	0.5829D 01
36.0	2.0	0.4051D 02	0.6397D 01	-0.4039D 01
36.0	6.0	0.3641D 02	-0.3213D 02	0.2912D 02
36.0	10.0	0.4015D 02	-0.2377D 02	0.1791D 02
36.0	14.0	0.3930D 02	0.1804D 02	0.3662D 02
36.0	18.0	0.3886D 02	0.1028D 02	0.2731D 02
36.0	22.0	0.3759D 02	-0.1021D 02	0.4456D 02
32.0	-22.0	0.3569D 02	-0.1138D 02	-0.8239D 01
32.0	-18.0	0.3996D 02	-0.5518D 01	-0.2249D 02
32.0	-14.0	0.3638D 02	0.2895D 02	0.1502D 01
32.0	-10.0	0.4022D 02	0.5223D 02	-0.2316D 02
32.0	-6.0	0.3767D 02	0.2659D 01	-0.1068D 01
32.0	-2.0	0.3712D 02	-0.3208D 02	-0.5508D 02
32.0	2.0	0.3738D 02	0.2347D 02	0.2153D 01
32.0	6.0	0.3808D 02	-0.4308D 01	-0.5239D 01
32.0	10.0	0.3681D 02	-0.4304D 02	-0.4548D 01
32.0	14.0	0.3674D 02	-0.5806D 01	-0.2047D 02
32.0	18.0	0.4042D 02	0.1242D 02	0.2132D 02
32.0	22.0	0.3739D 02	0.1178D 02	0.5396D 01
28.0	-22.0	0.3512D 02	-0.1931D 02	-0.5814D 02
28.0	-18.0	0.3739D 02	-0.3614D-01	0.3406D 02
28.0	-14.0	0.3960D 02	0.5718D 02	0.2002D 02
28.0	-10.0	0.3401D 02	-0.1432D 02	-0.3120D 02
28.0	-6.0	0.3505D 02	-0.2438D 02	0.1201D 02
28.0	-2.0	0.3708D 02	0.1376D 02	-0.8801D 01
28.0	2.0	0.3327D 02	0.1873D 02	0.8237D 01
28.0	6.0	0.3997D 02	0.1044D 02	0.6348D 02
28.0	10.0	0.3595D 02	0.2981D 02	0.3107D 02
28.0	14.0	0.3637D 02	-0.3159D 00	-0.1377D 02
28.0	18.0	0.3519D 02	0.4107D 02	-0.5597D 02
28.0	22.0	0.3670D 02	-0.2424D 02	0.3773D 02

24.0	-22.0	0.3715D 02	-0.1283D 02	0.1138D 02	
24.0	-18.0	0.3508D 02	0.2176D 02	-0.1601D 02	
24.0	-14.0	0.3558D 02	0.4065D 02	-0.4690D 02	
24.0	-10.0	0.3421D 02	-0.3063D 02	0.3834D 02	
24.0	-6.0	0.3264D 02	-0.4124D 02	0.2668D 02	
24.0	-2.0	0.3499D 02	-0.1668D 02	-0.5932D 01	
24.0	2.0	0.4021D 02	0.3442D 02	-0.1132D 01	
24.0	6.0	0.3407D 02	0.1484D 01	0.6343D 01	
24.0	10.0	0.3331D 02	0.1802D 02	-0.2637D 02	
24.0	14.0	0.3556D 02	-0.3834D 02	-0.1192D 02	
24.0	18.0	0.3306D 02	0.2035D 02	-0.1480D 02	
24.0	22.0	0.4112D 02	0.1262D 02	0.4426D 01	
20.0	-22.0	0.3551D 02	0.2398D 02	-0.3009D 02	
20.0	-18.0	0.3168D 02	-0.6492D 01	0.2290D 02	
20.0	-14.0	0.3431D 02	-0.5781D 01	0.4563D 01	
20.0	-10.0	0.3389D 02	0.1647D 02	0.9666D 01	
20.0	-6.0	0.3267D 02	0.7542D 01	-0.5170D 01	
20.0	-2.0	0.3404D 02	-0.5192D 01	-0.2291D 02	
20.0	2.0	0.3089D 02	-0.2468D 01	-0.1936D 02	
20.0	6.0	0.3362D 02	-0.4566D 02	-0.8900D 01	
20.0	10.0	0.3679D 02	0.3858D 02	0.1136D 02	
20.0	14.0	0.3407D 02	0.2323D 02	-0.9389D 01	
20.0	18.0	0.3192D 02	0.9416D 01	0.2066D 02	
20.0	22.0	0.3255D 02	-0.1113D 02	-0.2610D 02	
16.0	-22.0	0.3464D 02	-0.1158D 02	0.3680D 02	
16.0	-18.0	0.3190D 02	-0.4853D 02	-0.1229D 02	
16.0	-14.0	0.3035D 02	0.3014D 02	-0.4423D 02	
16.0	-10.0	0.3345D 02	0.2600D 02	-0.5133D 01	
16.0	-6.0	0.3200D 02	-0.5120D 01	0.1958D 02	
16.0	-2.0	0.3077D 02	-0.4656D 01	0.3953D 02	
16.0	2.0	0.3597D 02	0.3730D 02	0.5164D 02	
16.0	6.0	0.3104D 02	-0.2653D 02	0.4658D 00	
16.0	10.0	0.3103D 02	0.3135D 02	-0.5450D 02	
16.0	14.0	0.3255D 02	-0.5038D 02	0.4174D 02	
16.0	18.0	0.3200D 02	0.3791D 01	0.9725D 01	
16.0	22.0	0.3367D 02	0.4972D 02	-0.8861D 01	
12.0	-22.0	0.3157D 02	-0.1112D 02	0.2364D 02	
12.0	-18.0	0.3163D 02	-0.2777D 02	0.3751D 01	
12.0	-14.0	0.3303D 02	0.3062D 01	0.2228D 02	
12.0	-10.0	0.3371D 02	0.2300D 02	0.1140D 02	
12.0	-6.0	0.3029D 02	-0.5127D 02	-0.4525D 02	
12.0	-2.0	0.3062D 02	0.4743D 00	0.2273D 02	
12.0	2.0	0.2983D 02	-0.2334D 01	-0.9412D 01	
12.0	6.0	0.3165D 02	-0.1730D 02	-0.5291D 02	
12.0	10.0	0.2993D 02	-0.3025D 02	0.3246D 02	
12.0	14.0	0.3255D 02	0.6816D 01	0.4281D 02	
12.0	18.0	0.2988D 02	-0.1596D 02	-0.5766D 01	
12.0	22.0	0.3646D 02	0.2865D 02	0.6006D 02	
8.0	-22.0	0.3313D 02	0.8448D 01	-0.3148D 02	
8.0	-18.0	0.2937D 02	0.3896D 01	-0.1923D 02	
8.0	-14.0	0.3196D 02	0.3139D 02	-0.1388D 02	
8.0	-10.0	0.3294D 02	0.2897D 02	0.1450D 02	
8.0	-6.0	0.2802D 02	-0.9275D 01	-0.1902D 02	
8.0	-2.0	0.2951D 02	-0.2000D 02	-0.3208D 02	
8.0	2.0	0.2914D 02	-0.1757D 02	0.1823D 02	
8.0	6.0	0.3243D 02	0.2632D 01	0.3027D 02	
8.0	10.0	0.3132D 02	-0.1337D 02	-0.2108D 02	
8.0	14.0	0.2795D 02	-0.3591D 02	-0.3257D 02	
8.0	18.0	0.3005D 02	0.1711D 02	-0.2239D 02	
8.0	22.0	0.3132D 02	-0.1414D 02	-0.3861D 02	
4.0	-22.0	0.2905D 02	-0.3187D 01	0.1965D 02	
4.0	-18.0	0.2809D 02	-0.1092D 02	0.3882D 02	
4.0	-14.0	0.2729D 02	0.5688D 00	0.1776D 02	
4.0	-10.0	0.3118D 02	0.1710D 02	0.3404D 01	
4.0	-6.0	0.2762D 02	-0.3493D 02	-0.2817D 02	
4.0	-2.0	0.2938D 02	0.1338D 02	-0.4313D 02	
4.0	2.0	0.3378D 02	0.4957D 02	0.2323D 02	
4.0	6.0	0.2728D 02	-0.3742D 02	0.1473D 02	
4.0	10.0	0.2981D 02	0.2776D 01	-0.2344D 02	
4.0	14.0	0.2694D 02	0.1835D 00	-0.1954D 02	
4.0	18.0	0.3161D 02	-0.1470D 01	-0.1285D 02	
4.0	22.0	0.2727D 02	0.8404D 01	-0.3486D 01	

0.0	-22.0	0.2639D 02	-0.2022D 02	-0.3457D 01	
0.0	-18.0	0.2711D 02	-0.7126D 01	-0.3808D 02	
0.0	-14.0	0.2712D 02	0.1422D 01	0.4544D 02	
0.0	-10.0	0.2704D 02	-0.4053D 02	-0.2449D 02	
0.0	-6.0	0.2733D 02	-0.1756D 02	0.2532D 02	
0.0	-2.0	0.2685D 02	-0.1655D 02	0.7801D 01	
0.0	2.0	0.2787D 02	0.3145D 02	-0.6492D 02	
0.0	6.0	0.2999D 02	0.2619D 02	0.1937D 02	
0.0	10.0	0.2454D 02	-0.2817D 02	0.1948D 02	
0.0	14.0	0.2587D 02	-0.7575D 00	-0.2702D 00	
0.0	18.0	0.3033D 02	0.5686D 01	-0.2085D 02	
0.0	22.0	0.2750D 02	-0.1141D-01	0.1967D 02	
-4.0	-22.0	0.2729D 02	0.1695D 01	-0.1337D 02	
-4.0	-18.0	0.2689D 02	0.1624D 02	0.2301D 02	
-4.0	-14.0	0.2559D 02	-0.3981D 02	0.2420D 02	
-4.0	-10.0	0.2829D 02	-0.7260D 01	-0.7092D 01	
-4.0	-6.0	0.2428D 02	-0.1804D 02	-0.7664D 00	
-4.0	-2.0	0.2703D 02	-0.3551D 02	-0.2489D 01	
-4.0	2.0	0.2764D 02	-0.1677D 02	-0.2230D 02	
-4.0	6.0	0.2487D 02	-0.5508D 02	0.6629D 02	
-4.0	10.0	0.2487D 02	-0.6943D 01	0.1335D 01	
-4.0	14.0	0.2611D 02	0.1404D 02	-0.1428D 02	
-4.0	18.0	0.2387D 02	-0.5225D 01	-0.2129D 02	
-4.0	22.0	0.2693D 02	0.6523D 01	0.4041D 02	
-8.0	-22.0	0.2548D 02	-0.3503D 01	0.8881D 01	
-8.0	-18.0	0.2669D 02	-0.3657D 02	-0.2713D 01	
-8.0	-14.0	0.2797D 02	0.5893D 01	0.3101D 02	
-8.0	-10.0	0.2553D 02	0.5572D 01	-0.4333D 02	
-8.0	-6.0	0.2477D 02	0.1287D 02	0.1864D 02	
-8.0	-2.0	0.2399D 02	-0.4959D 02	-0.1348D 02	
-8.0	2.0	0.2629D 02	0.4624D 02	-0.5176D 02	
-8.0	6.0	0.2606D 02	-0.2120D 01	0.4126D 02	
-8.0	10.0	0.2528D 02	0.9031D 00	-0.4180D 02	
-8.0	14.0	0.2738D 02	0.2204D 01	0.2981D 02	
-8.0	18.0	0.2362D 02	-0.5612D 02	-0.4934D 02	
-8.0	22.0	0.2769D 02	-0.8746D 01	0.6419D 01	
-12.0	-22.0	0.2390D 02	-0.9208D 00	-0.2075D 02	
-12.0	-18.0	0.2516D 02	0.1556D 02	-0.2629D 02	
-12.0	-14.0	0.2839D 02	0.3274D 02	-0.3304D 02	
-12.0	-10.0	0.2511D 02	0.1893D 02	0.5191D 02	
-12.0	-6.0	0.2399D 02	-0.8531D 01	0.4233D 02	
-12.0	-2.0	0.2473D 02	-0.3969D 02	0.7385D 01	
-12.0	2.0	0.2568D 02	-0.3788D 01	0.2758D 02	
-12.0	6.0	0.2488D 02	0.9858D 01	0.3911D 01	
-12.0	10.0	0.2476D 02	-0.2040D 02	0.1752D 02	
-12.0	14.0	0.2429D 02	0.2682D 02	0.3260D 02	
-12.0	18.0	0.2670D 02	-0.1474D 01	-0.2025D 02	
-12.0	22.0	0.2594D 02	0.3175D 02	-0.5189D 02	
-16.0	-22.0	0.2372D 02	-0.7563D 01	0.1822D 02	
-16.0	-18.0	0.2531D 02	-0.2491D 02	-0.3616D 02	
-16.0	-14.0	0.2255D 02	0.2352D 01	0.2725D 02	
-16.0	-10.0	0.2373D 02	-0.1869D 02	0.1876D 02	
-16.0	-6.0	0.2704D 02	0.2809D 02	0.1925D 02	
-16.0	-2.0	0.2475D 02	-0.4854D 02	0.5593D 02	
-16.0	2.0	0.2343D 02	-0.2034D 02	0.6805D 02	
-16.0	6.0	0.2321D 02	0.4981D 02	0.3132D 02	
-16.0	10.0	0.2604D 02	-0.1101D 02	0.2579D 02	
-16.0	14.0	0.2454D 02	-0.6889D 00	0.1678D 02	
-16.0	18.0	0.2378D 02	-0.3850D 02	-0.2462D 02	
-16.0	22.0	0.2443D 02	-0.5597D 02	-0.1668D 02	
-20.0	-22.0	0.2264D 02	-0.1530D 02	0.1725D 02	
-20.0	-18.0	0.2476D 02	0.5475D 01	0.8304D 01	
-20.0	-14.0	0.2294D 02	0.2370D 02	-0.4932D 02	
-20.0	-10.0	0.2337D 02	0.6777D 01	-0.1872D 02	
-20.0	-6.0	0.2391D 02	-0.3283D 02	-0.2862D 02	
-20.0	-2.0	0.2342D 02	0.1385D 02	0.1263D 02	
-20.0	2.0	0.2187D 02	-0.4530D 02	0.4363D 02	
-20.0	6.0	0.2570D 02	-0.1618D 02	-0.3644D 02	
-20.0	10.0	0.2205D 02	0.3977D 01	0.5959D 01	
-20.0	14.0	0.2222D 02	-0.1494D 02	-0.3502D 00	
-20.0	18.0	0.2249D 02	-0.1930D 02	0.2628D 01	
-20.0	22.0	0.2033D 02	-0.3661D 02	0.2007D 02	

*	-24.0	-22.0	0.2250D 02	-0.2676D 02	-0.4105D 02 *
*	-24.0	-18.0	0.2286D 02	-0.1598D 02	-0.6206D 02 *
*	-24.0	-14.0	0.2099D 02	0.1609D 02	-0.7778D 01 *
*	-24.0	-10.0	0.2323D 02	0.3202D 02	0.3976D 02 *
*	-24.0	-6.0	0.2066D 02	0.2846D 02	0.2254D 02 *
*	-24.0	-2.0	0.2090D 02	-0.2366D 02	0.3332D 02 *
*	-24.0	2.0	0.2081D 02	-0.9910D 01	-0.3489D 02 *
*	-24.0	6.0	0.2032D 02	0.3079D 02	0.3522D 01 *
*	-24.0	10.0	0.2285D 02	0.1270D 02	-0.3864D 00 *
*	-24.0	14.0	0.2339D 02	0.1389D 02	0.1602D 02 *
*	-24.0	18.0	0.2171D 02	-0.3351D 00	-0.4902D 02 *
*	-24.0	22.0	0.2114D 02	-0.2523D 02	0.4696D 02 *
*	-28.0	-22.0	0.2208D 02	0.7147D 01	0.2662D 02 *
*	-28.0	-18.0	0.1928D 02	-0.4954D 02	-0.7074D 02 *
*	-28.0	-14.0	0.2075D 02	-0.1372D 02	-0.3240D 02 *
*	-28.0	-10.0	0.2140D 02	-0.1514D 02	0.1208D 02 *
*	-28.0	-6.0	0.1964D 02	0.1565D 01	0.1802D 02 *
*	-28.0	-2.0	0.2025D 02	0.1220D 02	0.4192D 02 *
*	-28.0	2.0	0.2074D 02	-0.7025D 01	0.2391D 02 *
*	-28.0	6.0	0.2072D 02	-0.5574D 01	0.2155D 02 *
*	-28.0	10.0	0.1933D 02	-0.4354D 02	-0.6649D 01 *
*	-28.0	14.0	0.2164D 02	-0.3012D 02	-0.3541D 01 *
*	-28.0	18.0	0.1833D 02	-0.1924D 02	-0.2294D 01 *
*	-28.0	22.0	0.2057D 02	-0.2320D 02	-0.1804D 02 *
*	-32.0	-22.0	0.2169D 02	-0.4084D 01	-0.3370D 02 *
*	-32.0	-18.0	0.2013D 02	-0.1958D 02	-0.1491D 02 *
*	-32.0	-14.0	0.1821D 02	-0.6759D 01	0.4684D 02 *
*	-32.0	-10.0	0.1995D 02	0.1227D 02	-0.1135D 01 *
*	-32.0	-6.0	0.2174D 02	0.1986D 02	0.1985D 02 *
*	-32.0	-2.0	0.1848D 02	0.1348D 02	0.1072D 02 *
*	-32.0	2.0	0.2040D 02	-0.4504D 02	0.1321D 02 *
*	-32.0	6.0	0.1904D 02	-0.2357D 02	-0.3902D 02 *
*	-32.0	10.0	0.1805D 02	-0.2664D 02	0.2022D 02 *
*	-32.0	14.0	0.2095D 02	-0.3468D 02	-0.3830D 01 *
*	-32.0	18.0	0.1839D 02	-0.5427D 02	0.2306D 02 *
*	-32.0	22.0	0.1963D 02	-0.4674D 01	0.5102D 02 *

STATISTICAL RESULTS:

	MEAN VALUE	STANDARD DEVIATION
X-DIRECTION	0.301D 02	0.688D 01
Y-DIRECTION	-0.319D 01	0.242D 02
Z-DIRECTION	0.105D 01	0.283D 02

EVALUATED STRAIN FIELD AT POINT (4L)

ELEMENT	EXX	EYY	ELEMENT	EXX	EYY
1, 1	0.12D-03	-0.40D-02	2, 1	-0.45D-04	0.64D-02
1, 2	0.18D-03	-0.95D-02	2, 2	0.88D-04	-0.11D-01
1, 3	0.36D-03	0.55D-02	2, 3	0.42D-03	0.11D-01
1, 4	-0.59D-03	-0.86D-02	2, 4	0.52D-03	-0.12D-01
1, 5	-0.25D-03	0.12D-01	2, 5	0.28D-03	0.16D-01
1, 6	0.44D-03	0.76D-03	2, 6	0.43D-03	-0.36D-02
1, 7	-0.15D-03	0.24D-02	2, 7	0.29D-03	0.53D-02
1, 8	-0.30D-03	-0.11D-02	2, 8	0.12D-02	-0.10D-02
1, 9	0.38D-03	-0.86D-03	2, 9	-0.17D-03	-0.64D-02
1, 10	0.17D-03	-0.94D-02	2, 10	0.23D-03	-0.17D-02
1, 11	0.52D-03	0.16D-01	2, 11	0.69D-03	0.81D-03
3, 1	0.12D-02	0.22D-02	4, 1	0.14D-03	-0.15D-02
3, 2	0.26D-03	-0.52D-03	4, 2	0.64D-03	-0.86D-02
3, 3	0.78D-03	0.14D-02	4, 3	-0.81D-03	-0.58D-02
3, 4	-0.27D-03	-0.71D-03	4, 4	0.16D-02	0.12D-01
3, 5	0.98D-03	0.38D-02	4, 5	0.65D-03	0.87D-02
3, 6	0.42D-03	-0.44D-03	4, 6	0.92D-05	-0.14D-01
3, 7	0.78D-03	0.96D-02	4, 7	0.10D-02	0.69D-02
3, 8	-0.42D-03	-0.21D-02	4, 8	-0.47D-03	0.97D-02
3, 9	0.84D-03	-0.10D-01	4, 9	0.21D-03	-0.93D-02
3, 10	0.64D-03	0.19D-02	4, 10	0.93D-04	-0.46D-02
3, 11	-0.39D-03	0.51D-02	4, 11	0.13D-02	0.16D-03
5, 1	-0.51D-03	-0.48D-02	6, 1	0.41D-03	-0.86D-02
5, 2	0.58D-03	-0.14D-01	6, 2	0.85D-03	-0.47D-02
5, 3	0.10D-02	0.18D-01	6, 3	0.32D-03	0.18D-01
5, 4	-0.49D-04	0.25D-02	6, 4	0.81D-04	0.27D-02
5, 5	0.60D-03	-0.95D-02	6, 5	-0.85D-05	-0.61D-02
5, 6	0.52D-03	-0.12D-02	6, 6	0.24D-03	-0.13D-01
5, 7	-0.17D-02	0.21D-02	6, 7	0.23D-02	0.82D-02
5, 8	0.15D-02	-0.48D-02	6, 8	0.11D-03	-0.41D-02
5, 9	0.66D-03	0.75D-02	6, 9	-0.87D-03	0.14D-01
5, 10	0.20D-03	-0.10D-01	6, 10	0.37D-03	-0.15D-01
5, 11	0.53D-03	0.16D-01	6, 11	0.29D-03	0.19D-02
7, 1	0.22D-03	0.76D-02	8, 1	0.77D-03	0.92D-02
7, 2	-0.54D-04	-0.18D-03	8, 2	0.68D-04	-0.20D-01
7, 3	0.99D-03	-0.56D-02	8, 3	-0.67D-03	0.10D-02
7, 4	0.11D-03	0.22D-02	8, 4	-0.64D-04	0.78D-02
7, 5	0.17D-03	0.32D-02	8, 5	0.43D-03	-0.12D-03
7, 6	0.82D-03	-0.68D-03	8, 6	-0.11D-04	-0.10D-01
7, 7	-0.13D-02	0.11D-01	8, 7	0.15D-02	0.16D-01
7, 8	0.65D-03	-0.21D-01	8, 8	-0.15D-03	-0.14D-01
7, 9	0.14D-02	0.38D-02	8, 9	0.28D-03	0.20D-01
7, 10	0.38D-03	0.35D-02	8, 10	-0.16D-05	-0.14D-01
7, 11	-0.19D-04	0.51D-02	8, 11	0.53D-03	-0.11D-01
9, 1	-0.39D-03	0.42D-02	10, 1	0.10D-02	0.11D-02
9, 2	0.57D-03	-0.77D-02	10, 2	0.32D-03	-0.69D-02
9, 3	0.27D-03	-0.50D-02	10, 3	0.12D-02	0.61D-03
9, 4	0.19D-03	0.19D-01	10, 4	0.44D-03	0.96D-02
9, 5	0.57D-03	-0.13D-01	10, 5	0.99D-04	0.27D-02
9, 6	0.33D-03	0.70D-03	10, 6	0.33D-04	-0.61D-03
9, 7	0.17D-03	0.37D-02	10, 7	-0.12D-02	-0.51D-02
9, 8	-0.20D-03	0.32D-02	10, 8	0.13D-02	0.40D-02
9, 9	-0.35D-03	-0.93D-02	10, 9	0.38D-03	0.56D-02
9, 10	0.12D-02	0.57D-02	10, 10	0.25D-03	-0.13D-01
9, 11	-0.43D-04	-0.11D-01	10, 11	-0.39D-03	0.78D-02
11, 1	0.66D-03	0.19D-02	12, 1	-0.22D-03	-0.33D-02
11, 2	0.24D-03	-0.29D-02	12, 2	0.56D-04	-0.21D-02
11, 3	0.43D-04	-0.41D-02	12, 3	0.38D-03	0.10D-01
11, 4	0.10D-02	0.13D-01	12, 4	-0.31D-03	-0.57D-02
11, 5	0.73D-04	-0.12D-01	12, 5	0.76D-03	0.25D-03
11, 6	0.13D-03	-0.90D-02	12, 6	0.46D-03	-0.13D-01
11, 7	0.15D-02	0.22D-01	12, 7	0.58D-04	0.13D-02
11, 8	-0.68D-03	-0.10D-01	12, 8	0.13D-02	0.14D-01

11, 9	0.13D-02	0.65D-03	12, 9	-0.81D-04	-0.69D-02
11,10	0.27D-03	0.41D-03	12,10	-0.59D-04	-0.16D-02
11,11	0.32D-03	-0.25D-02	12,11	0.16D-02	0.14D-02
13, 1	0.45D-03	-0.30D-02	14, 1	0.39D-03	0.83D-02
13, 2	0.49D-04	0.14D-01	14, 2	0.38D-03	-0.11D-01
13, 3	-0.59D-03	-0.81D-02	14, 3	-0.11D-03	0.80D-04
13, 4	0.69D-03	0.27D-02	14, 4	0.10D-03	-0.18D-02
13, 5	-0.12D-03	0.44D-02	14, 5	0.19D-03	0.16D-01
13, 6	0.76D-03	-0.47D-02	14, 6	-0.19D-03	-0.24D-01
13, 7	0.34D-03	0.96D-02	14, 7	0.15D-03	0.12D-01
13, 8	-0.30D-03	-0.12D-01	14, 8	0.29D-03	-0.76D-03
13, 9	-0.10D-03	-0.52D-02	14, 9	0.13D-03	-0.33D-03
13,10	-0.52D-03	0.48D-02	14,10	0.77D-03	0.15D-01
13,11	0.62D-04	-0.29D-02	14,11	-0.77D-03	-0.12D-01
15, 1	0.46D-04	-0.41D-02	16, 1	0.27D-03	0.43D-02
15, 2	-0.39D-04	-0.43D-02	16, 2	0.14D-03	-0.68D-02
15, 3	0.15D-02	0.35D-02	16, 3	-0.98D-04	0.53D-02
15, 4	0.35D-03	0.69D-02	16, 4	0.88D-04	-0.12D-01
15, 5	-0.76D-03	0.78D-02	16, 5	0.78D-03	0.19D-01
15, 6	-0.45D-05	-0.90D-02	16, 6	0.33D-03	-0.70D-02
15, 7	0.56D-03	-0.34D-02	16, 7	0.39D-03	-0.18D-01
15, 8	0.42D-03	0.76D-02	16, 8	-0.62D-03	0.15D-01
15, 9	-0.32D-03	-0.12D-01	16, 9	0.10D-02	-0.26D-02
15,10	-0.62D-04	0.71D-02	16,10	0.58D-03	0.95D-02
15,11	0.73D-03	-0.83D-02	16,11	0.32D-03	0.44D-02
17, 1	0.36D-04	-0.52D-02	18, 1	0.10D-03	-0.27D-02
17, 2	0.48D-03	-0.46D-02	18, 2	0.89D-03	-0.80D-02
17, 3	0.49D-03	0.42D-02	18, 3	0.60D-04	-0.40D-02
17, 4	0.36D-04	0.99D-02	18, 4	0.46D-03	0.89D-03
17, 5	0.81D-03	-0.12D-01	18, 5	0.25D-03	0.13D-01
17, 6	0.63D-03	0.15D-01	18, 6	0.16D-03	-0.34D-02
17, 7	0.26D-03	-0.73D-02	18, 7	0.18D-04	-0.10D-01
17, 8	0.15D-02	-0.50D-02	18, 8	-0.10D-03	0.45D-02
17, 9	-0.20D-03	0.47D-02	18, 9	0.88D-03	-0.30D-03
17,10	-0.29D-03	0.11D-02	18,10	0.44D-03	0.36D-02
17,11	0.19D-03	0.43D-02	18,11	0.85D-03	0.62D-02
19, 1	0.98D-04	0.14D-01			
19, 2	-0.21D-03	-0.90D-02			
19, 3	0.63D-03	0.36D-03			
19, 4	0.36D-03	-0.42D-02			
19, 5	-0.52D-03	-0.27D-02			
19, 6	0.44D-03	0.48D-02			
19, 7	0.86D-04	-0.36D-03			
19, 8	0.42D-03	0.95D-02			
19, 9	0.32D-03	-0.34D-02			
19,10	0.17D-03	-0.27D-02			
19,11	-0.16D-04	0.99D-03			

STATISTICAL RESULTS:

	MEAN VALUE	STANDARD DEVIATION
XX-STRAIN:	0.2846D-03	0.5509D-03
YY-STRAIN:	0.1898D-04	0.8671D-02

RECONSTRUCTION RESULTS OF INTERFEROGRAM
(5m) OF THE NEWS-PRINT PAPER SAMPLE #38
CUMMULATIVE DEFORMATION)

CO-ORDINATES X	CO-ORDINATES Y	DEFORMATIONS X	DEFORMATIONS Y	DEFORMATIONS Z
44.0	-22.0	0.5137D 02	-0.2173D 02	0.1004D 02
44.0	-18.0	0.5121D 02	0.8271D 01	-0.9430D 01
44.0	-14.0	0.5204D 02	-0.4345D 02	-0.2298D 02
44.0	-10.0	0.5237D 02	0.4700D 01	-0.1258D 02
44.0	-6.0	0.5189D 02	0.2304D 01	0.3017D 02
44.0	-2.0	0.4855D 02	0.1747D 02	0.2738D 02
44.0	2.0	0.5102D 02	-0.7108D 01	-0.2868D 01
44.0	6.0	0.5255D 02	-0.2236D 02	0.3214D 00
44.0	10.0	0.4823D 02	-0.1981D 02	-0.1286D 02
44.0	14.0	0.4909D 02	-0.2411D 02	-0.1351D 02
44.0	18.0	0.4849D 02	0.1787D 02	-0.1529D 02
44.0	22.0	0.4950D 02	-0.1410D 02	0.1518D 02
40.0	-22.0	0.5023D 02	0.7773D 01	0.7796D 01
40.0	-18.0	0.4931D 02	0.4289D 02	-0.1651D 02
40.0	-14.0	0.5135D 02	0.1134D 02	-0.6290D 02
40.0	-10.0	0.5225D 02	-0.5533D 02	-0.2692D 02
40.0	-6.0	0.4959D 02	-0.1743D 02	-0.1639D 02
40.0	-2.0	0.5091D 02	-0.3554D 02	0.6290D 00
40.0	2.0	0.4720D 02	-0.5296D 02	-0.8388D 01
40.0	6.0	0.5091D 02	-0.1608D 02	0.2487D 02
40.0	10.0	0.4786D 02	0.2141D 01	-0.1223D 02
40.0	14.0	0.5126D 02	-0.9142D 01	-0.4118D 02
40.0	18.0	0.5263D 02	0.1757D 02	0.2062D 02
40.0	22.0	0.5190D 02	0.1677D 01	0.2303D 02
36.0	-22.0	0.4856D 02	-0.1430D 00	0.2820D 02
36.0	-18.0	0.4938D 02	0.2011D 02	-0.3022D 02
36.0	-14.0	0.4872D 02	-0.1555D 02	0.1803D 02
36.0	-10.0	0.4923D 02	-0.5145D 02	0.3051D 02
36.0	-6.0	0.5241D 02	-0.1637D 02	-0.3990D 01
36.0	-2.0	0.4802D 02	0.4071D 01	-0.1747D 02
36.0	2.0	0.4819D 02	-0.6311D 02	0.1727D 01
36.0	6.0	0.5050D 02	-0.2059D 02	-0.1539D 02
36.0	10.0	0.4853D 02	0.1801D 02	-0.3867D 02
36.0	14.0	0.4987D 02	-0.2906D 02	-0.3538D 02
36.0	18.0	0.4814D 02	-0.3769D 02	-0.1403D 02
36.0	22.0	0.5006D 02	-0.1019D 02	-0.5230D 02
32.0	-22.0	0.4802D 02	-0.1142D 02	0.4806D 01
32.0	-18.0	0.4761D 02	0.1756D 01	0.1574D 02
32.0	-14.0	0.4794D 02	-0.2239D 02	0.2382D 01
32.0	-10.0	0.4944D 02	0.4529D 01	0.2851D 01
32.0	-6.0	0.4491D 02	-0.2957D 02	-0.1187D 02
32.0	-2.0	0.4946D 02	0.8229D 01	0.4245D 02
32.0	2.0	0.4807D 02	0.7954D 01	0.1070D 02
32.0	6.0	0.4524D 02	-0.2797D 02	-0.1222D 02
32.0	10.0	0.4567D 02	0.3057D 02	0.1109D 02
32.0	14.0	0.4893D 02	0.2737D 02	-0.8596D 00
32.0	18.0	0.4823D 02	-0.6069D 02	-0.1819D 02
32.0	22.0	0.4739D 02	-0.9340D 01	-0.1131D 02
28.0	-22.0	0.4604D 02	0.1171D 02	0.5447D 02
28.0	-18.0	0.4648D 02	0.3939D 02	-0.2541D 02
28.0	-14.0	0.4593D 02	0.4057D 02	-0.1440D 02
28.0	-10.0	0.4628D 02	0.3341D 02	0.1659D 02
28.0	-6.0	0.4574D 02	-0.2803D 02	-0.4883D 01
28.0	-2.0	0.4617D 02	-0.3176D 02	0.3221D 01
28.0	2.0	0.4675D 02	-0.6819D 01	0.1069D 02
28.0	6.0	0.4848D 02	0.3631D 02	-0.5430D 02
28.0	10.0	0.4580D 02	0.1322D 01	-0.3064D 02
28.0	14.0	0.4827D 02	-0.4065D 02	0.2311D 02
28.0	18.0	0.4479D 02	-0.1961D 02	0.4811D 02
28.0	22.0	0.4681D 02	-0.3358D 02	-0.3558D 02

24.0	-22.0	0.4540D 02	0.1269D 02	-0.7334D 01	
24.0	-18.0	0.4618D 02	0.9844D 00	0.1582D 02	
24.0	-14.0	0.4489D 02	-0.3623D 02	0.4226D 02	
24.0	-10.0	0.4550D 02	-0.7678D 01	-0.3807D 02	
24.0	-6.0	0.4359D 02	0.2115D 02	-0.3601D 02	
24.0	-2.0	0.4495D 02	0.9589D 01	0.9165D 01	
24.0	2.0	0.4523D 02	-0.1374D 02	-0.6799D 01	
24.0	6.0	0.4457D 02	-0.7230D 01	-0.1793D 02	
24.0	10.0	0.4601D 02	0.7781D 00	0.3560D 02	
24.0	14.0	0.4333D 02	-0.2323D 02	0.1803D 02	
24.0	18.0	0.4244D 02	-0.1423D 01	0.3154D 01	
24.0	22.0	0.4746D 02	-0.1706D 02	-0.1417D 02	
20.0	-22.0	0.4548D 02	-0.9011D 01	0.2541D 02	
20.0	-18.0	0.4406D 02	0.1673D 02	-0.1627D 02	
20.0	-14.0	0.4606D 02	-0.1021D 02	-0.5086D 01	
20.0	-10.0	0.4494D 02	-0.4894D 02	0.8950D 01	
20.0	-6.0	0.4573D 02	-0.2491D 02	-0.3565D 01	
20.0	-2.0	0.4189D 02	0.3834D 02	0.9010D 01	
20.0	2.0	0.4388D 02	0.1830D 02	0.1982D 02	
20.0	6.0	0.4408D 02	0.1282D 02	0.8769D 01	
20.0	10.0	0.4540D 02	0.1589D 01	-0.4774D 01	
20.0	14.0	0.4559D 02	-0.6896D 01	0.3297D 01	
20.0	18.0	0.4393D 02	0.2338D 00	-0.1177D 02	
20.0	22.0	0.4313D 02	0.2103D 02	0.2973D 02	
16.0	-22.0	0.4228D 02	-0.2096D 02	-0.5014D 02	
16.0	-18.0	0.4488D 02	-0.2045D 02	0.5022D 01	
16.0	-14.0	0.3923D 02	-0.3867D 01	0.3716D 02	
16.0	-10.0	0.4155D 02	-0.1852D 02	-0.3635D 01	
16.0	-6.0	0.4230D 02	0.1273D 02	-0.8309D 01	
16.0	-2.0	0.4169D 02	0.5603D 01	-0.4697D 02	
16.0	2.0	0.3995D 02	-0.4453D 01	-0.6317D 02	
16.0	6.0	0.4188D 02	-0.4504D 02	0.5537D 01	
16.0	10.0	0.3938D 02	0.1943D 02	0.5192D 02	
16.0	14.0	0.4254D 02	-0.1563D 02	-0.3982D 02	
16.0	18.0	0.3679D 02	0.4379D 01	-0.1875D 02	
16.0	22.0	0.3969D 02	0.1764D 02	0.1590D 02	
12.0	-22.0	0.4110D 02	-0.2377D 02	-0.3679D 02	
12.0	-18.0	0.3880D 02	0.2205D 02	-0.9426D 01	
12.0	-14.0	0.4025D 02	0.1388D 01	-0.1621D 02	
12.0	-10.0	0.4318D 02	0.3607D 02	-0.1416D 02	
12.0	-6.0	0.4131D 02	-0.2637D 02	0.3360D 02	
12.0	-2.0	0.4070D 02	-0.1779D 02	-0.2154D 02	
12.0	2.0	0.3906D 02	-0.6979D 01	0.1211D 02	
12.0	6.0	0.3780D 02	-0.4011D 02	0.5422D 02	
12.0	10.0	0.4090D 02	0.3281D 02	-0.3715D 02	
12.0	14.0	0.4041D 02	-0.5296D 02	-0.4047D 02	
12.0	18.0	0.3948D 02	-0.2964D 02	0.1184D 02	
12.0	22.0	0.3993D 02	-0.3222D 02	-0.7202D 02	
8.0	-22.0	0.3887D 02	-0.5764D 02	0.4283D 02	
8.0	-18.0	0.4205D 02	0.4828D 01	0.1955D 02	
8.0	-14.0	0.3825D 02	-0.3067D 02	-0.6236D 01	
8.0	-10.0	0.3865D 02	0.1656D 02	-0.1583D 02	
8.0	-6.0	0.3668D 02	0.2167D 02	0.3015D 02	
8.0	-2.0	0.3819D 02	-0.8602D 01	0.9119D 01	
8.0	2.0	0.4010D 02	-0.6816D 02	-0.3633D 02	
8.0	6.0	0.4029D 02	0.3366D 02	-0.3802D 02	
8.0	10.0	0.3870D 02	-0.3385D 02	0.3863D 02	
8.0	14.0	0.3677D 02	0.1308D 02	0.1753D 02	
8.0	18.0	0.3804D 02	0.8794D 01	0.3517D 02	
8.0	22.0	0.4164D 02	0.9051D 00	0.3923D 02	
4.0	-22.0	0.3800D 02	-0.2907D 01	-0.2155D 02	
4.0	-18.0	0.3296D 02	0.2502D 02	-0.4838D 02	
4.0	-14.0	0.3738D 02	0.1238D 02	-0.4027D 02	
4.0	-10.0	0.3768D 02	-0.2247D 02	-0.1369D 02	
4.0	-6.0	0.3907D 02	0.2000D 01	0.2937D 02	
4.0	-2.0	0.3768D 02	0.5482D 01	0.3547D 02	
4.0	2.0	0.3512D 02	0.2115D 02	-0.2210D 02	
4.0	6.0	0.3463D 02	0.8855D 01	-0.1323D 02	
4.0	10.0	0.3232D 02	-0.3317D 02	0.9781D 01	
4.0	14.0	0.3549D 02	0.2050D 02	0.9831D 01	
4.0	18.0	0.3544D 02	0.2190D 02	0.7627D 01	
4.0	22.0	0.3420D 02	-0.1708D 02	-0.7421D 01	

0.0	-22.0	0.3544D 02	-0.3179D 02	0.1720D 02	
0.0	-18.0	0.3271D 02	-0.2258D 02	0.4065D 02	
0.0	-14.0	0.3557D 02	0.6077D 01	-0.6267D 02	
0.0	-10.0	0.3431D 02	0.2141D 02	0.2359D 02	
0.0	-6.0	0.3371D 02	0.1519D 02	-0.1448D 02	
0.0	-2.0	0.3631D 02	-0.4904D 02	-0.1272D 02	
0.0	2.0	0.3449D 02	-0.1387D 01	0.4073D 02	
0.0	6.0	0.3296D 02	0.1043D 02	-0.6536D 00	
0.0	10.0	0.3548D 02	0.9529D 01	-0.4346D 02	
0.0	14.0	0.3286D 02	-0.1952D 02	0.1941D 01	
0.0	18.0	0.3053D 02	0.2599D 01	0.2059D 02	
0.0	22.0	0.3583D 02	-0.1963D 01	-0.8081D 01	
-4.0	-22.0	0.3759D 02	-0.1240D 02	-0.4203D 00	
-4.0	-18.0	0.3377D 02	0.1061D 02	-0.2337D 02	
-4.0	-14.0	0.3540D 02	-0.7038D 01	-0.1980D 02	
-4.0	-10.0	0.3152D 02	-0.3202D 02	0.2589D 02	
-4.0	-6.0	0.3649D 02	-0.3286D 02	-0.2758D 02	
-4.0	-2.0	0.3425D 02	-0.5192D 02	-0.1407D 02	
-4.0	2.0	0.3549D 02	0.2166D 02	0.1089D 02	
-4.0	6.0	0.3242D 02	-0.7306D 01	-0.5317D 02	
-4.0	10.0	0.3167D 02	0.9570D 01	-0.9097D 01	
-4.0	14.0	0.3487D 02	0.1342D 02	0.2048D 02	
-4.0	18.0	0.3304D 02	-0.3801D 02	-0.1007D 02	
-4.0	22.0	0.3460D 02	-0.4261D 02	-0.4082D 02	
-8.0	-22.0	0.3583D 02	-0.5313D 01	0.2756D 01	
-8.0	-18.0	0.3566D 02	-0.5575D 01	-0.9189D 01	
-8.0	-14.0	0.3304D 02	-0.8555D 01	-0.3219D 02	
-8.0	-10.0	0.3477D 02	0.2871D 01	0.3925D 02	
-8.0	-6.0	0.3094D 02	0.1038D 02	-0.2298D 02	
-8.0	-2.0	0.3196D 02	0.2747D 02	0.3030D 02	
-8.0	2.0	0.3185D 02	0.6021D 01	0.2078D 02	
-8.0	6.0	0.3369D 02	-0.1876D 02	-0.1797D 02	
-8.0	10.0	0.3113D 02	0.1767D 02	0.2588D 02	
-8.0	14.0	0.3597D 02	-0.2034D 02	-0.3467D 02	
-8.0	18.0	0.2950D 02	0.1992D 02	0.5160D 02	
-8.0	22.0	0.3423D 02	0.5903D 01	-0.1365D 02	
-12.0	-22.0	0.3347D 02	-0.3757D 02	0.1816D 02	
-12.0	-18.0	0.3171D 02	-0.2214D 02	0.2158D 02	
-12.0	-14.0	0.3313D 02	-0.1866D 02	0.2000D 02	
-12.0	-10.0	0.3391D 02	-0.1479D 02	-0.3962D 02	
-12.0	-6.0	0.3180D 02	0.2720D 02	-0.4306D 02	
-12.0	-2.0	0.3313D 02	0.6222D 01	-0.3708D 01	
-12.0	2.0	0.3134D 02	0.2818D 02	-0.2502D 02	
-12.0	6.0	0.3050D 02	-0.8034D 01	-0.7395D 01	
-12.0	10.0	0.3294D 02	-0.2259D 02	-0.7545D 01	
-12.0	14.0	0.2964D 02	-0.1589D 01	-0.1787D 02	
-12.0	18.0	0.2976D 02	-0.5177D 02	0.1220D 02	
-12.0	22.0	0.3006D 02	-0.1033D 02	0.2739D 02	
-16.0	-22.0	0.3126D 02	-0.1924D 02	0.4314D 00	
-16.0	-18.0	0.3151D 02	-0.1634D 02	0.3894D 02	
-16.0	-14.0	0.3125D 02	0.1874D 02	-0.1204D 02	
-16.0	-10.0	0.3047D 02	0.5964D 00	-0.2551D 02	
-16.0	-6.0	0.3245D 02	-0.6119D 01	-0.1664D 02	
-16.0	-2.0	0.3337D 02	-0.2009D 02	-0.5801D 02	
-16.0	2.0	0.3209D 02	-0.2919D 02	-0.6313D 02	
-16.0	6.0	0.3160D 02	0.1294D 02	-0.3532D 02	
-16.0	10.0	0.2913D 02	0.1331D 02	-0.2584D 02	
-16.0	14.0	0.2893D 02	0.4066D 02	-0.2920D 02	
-16.0	18.0	0.2849D 02	-0.8179D 01	0.1080D 02	
-16.0	22.0	0.3102D 02	-0.1367D 02	0.1742D 02	
-20.0	-22.0	0.3063D 02	-0.4186D 02	-0.5442D 01	
-20.0	-18.0	0.3277D 02	-0.5013D 02	0.3268D 01	
-20.0	-14.0	0.2978D 02	-0.1733D 02	0.4038D 02	
-20.0	-10.0	0.3035D 02	-0.2160D 01	0.2397D 02	
-20.0	-6.0	0.2928D 02	0.1442D 02	0.2242D 02	
-20.0	-2.0	0.3190D 02	-0.3714D 02	-0.1203D 02	
-20.0	2.0	0.2804D 02	-0.3508D 02	-0.4375D 02	
-20.0	6.0	0.3008D 02	-0.2275D 02	0.2776D 02	
-20.0	10.0	0.2997D 02	0.2739D 00	-0.2470D 02	
-20.0	14.0	0.3094D 02	0.2730D 01	0.8896D 01	
-20.0	18.0	0.2975D 02	-0.1489D 01	0.2668D 00	
-20.0	22.0	0.2906D 02	-0.4007D 02	-0.1811D 02	

* -24.0	-22.0 *	0.3317D 02	0.2942D 01	0.3135D 02	*
* -24.0	-18.0 *	0.2954D 02	-0.2676D 01	0.3449D 02	*
* -24.0	-14.0 *	0.2740D 02	-0.6369D 01	0.1304D 02	*
* -24.0	-10.0 *	0.3334D 02	-0.4385D 02	-0.4484D 02	*
* -24.0	-6.0 *	0.2884D 02	0.1397D 02	-0.1070D 02	*
* -24.0	-2.0 *	0.3007D 02	-0.2457D 02	-0.3609D 02	*
* -24.0	2.0 *	0.2908D 02	0.1030D 02	0.1709D 02	*
* -24.0	6.0 *	0.2678D 02	0.1920D 02	0.2585D 01	*
* -24.0	10.0 *	0.2718D 02	0.2726D 02	-0.2584D 02	*
* -24.0	14.0 *	0.2765D 02	-0.1498D 02	-0.3264D 02	*
* -24.0	18.0 *	0.2863D 02	0.3903D 02	0.2747D 02	*
* -24.0	22.0 *	0.2771D 02	-0.3511D 02	-0.4604D 02	*
* -28.0	-22.0 *	0.2861D 02	-0.1339D 02	-0.1367D 02	*
* -28.0	-18.0 *	0.2680D 02	0.2523D 02	0.4821D 02	*
* -28.0	-14.0 *	0.2816D 02	-0.1978D 01	0.3533D 02	*
* -28.0	-10.0 *	0.2695D 02	0.4422D 02	-0.1960D 02	*
* -28.0	-6.0 *	0.2601D 02	0.3259D 02	-0.2956D 02	*
* -28.0	-2.0 *	0.2674D 02	0.9548D 01	-0.3398D 02	*
* -28.0	2.0 *	0.2868D 02	0.1153D 02	-0.3560D 02	*
* -28.0	6.0 *	0.2481D 02	0.3982D 01	-0.1333D 02	*
* -28.0	10.0 *	0.2734D 02	0.2370D 02	0.1885D 02	*
* -28.0	14.0 *	0.2738D 02	-0.1538D 02	0.7178D 01	*
* -28.0	18.0 *	0.3022D 02	-0.2264D 02	-0.1971D 02	*
* -28.0	22.0 *	0.2863D 02	0.2150D 02	0.7825D 01	*
* -32.0	-22.0 *	0.2572D 02	-0.1017D 02	0.4060D 02	*
* -32.0	-18.0 *	0.2634D 02	-0.9070D 01	0.1852D 02	*
* -32.0	-14.0 *	0.2366D 02	0.3138D 02	-0.6445D 02	*
* -32.0	-10.0 *	0.2772D 02	-0.2061D 02	-0.6300D 01	*
* -32.0	-6.0 *	0.2616D 02	-0.6892D 01	-0.1622D 02	*
* -32.0	-2.0 *	0.2632D 02	-0.4025D 01	-0.9660D 01	*
* -32.0	2.0 *	0.2381D 02	0.4538D 02	-0.1263D 02	*
* -32.0	6.0 *	0.2801D 02	0.2012D 02	0.3830D 02	*
* -32.0	10.0 *	0.2529D 02	0.2534D 02	-0.1660D 02	*
* -32.0	14.0 *	0.2427D 02	-0.2532D 02	-0.8599D 01	*
* -32.0	18.0 *	0.2500D 02	-0.3080D 01	-0.1781D 02	*
* -32.0	22.0 *	0.2617D 02	-0.5671D 02	-0.5325D 02	*

STATISTICAL RESULTS:

	MEAN VALUE	STANDARD DEVIATION
X-DIRECTION	0.383D 02	0.806D 01
Y-DIRECTION	-0.536D 01	0.240D 02
Z-DIRECTION	-0.368D 01	0.272D 02

EVALUATED STRAIN FIELD AT POINT (5R)

ELEMENT	EXX	EYY	ELEMENT	EXX	EYY
1, 1	0.26D-03	-0.75D-02	2, 1	0.42D-03	-0.88D-02
1, 2	0.47D-03	0.13D-01	2, 2	-0.18D-04	0.79D-02
1, 3	0.17D-03	-0.12D-01	2, 3	0.66D-03	0.17D-01
1, 4	0.28D-04	0.60D-03	2, 4	0.76D-03	-0.95D-02
1, 5	0.58D-03	-0.36D-02	2, 5	-0.70D-03	0.45D-02
1, 6	-0.59D-03	0.61D-02	2, 6	0.72D-03	0.44D-02
1, 7	0.96D-03	0.38D-02	2, 7	-0.25D-03	-0.92D-02
1, 8	0.41D-03	-0.64D-03	2, 8	0.10D-03	-0.46D-02
1, 9	0.92D-04	0.11D-02	2, 9	-0.17D-03	0.28D-02
1,10	-0.54D-03	-0.10D-01	2,10	0.35D-03	-0.67D-02
1,11	-0.10D-02	0.80D-02	2,11	0.11D-02	0.40D-02
3, 1	0.14D-03	-0.51D-02	4, 1	0.49D-03	-0.33D-02
3, 2	0.44D-03	0.89D-02	4, 2	0.28D-03	0.60D-02
3, 3	0.20D-03	0.90D-02	4, 3	0.50D-03	-0.67D-02
3, 4	-0.52D-04	-0.88D-02	4, 4	0.79D-03	0.85D-02
3, 5	0.19D-02	-0.51D-02	4, 5	-0.21D-03	-0.94D-02
3, 6	-0.36D-03	0.17D-01	4, 6	0.82D-03	0.69D-04
3, 7	0.30D-04	-0.11D-01	4, 7	0.33D-03	0.90D-02
3, 8	0.13D-02	-0.97D-02	4, 8	-0.81D-03	-0.15D-01
3, 9	0.72D-03	0.12D-01	4, 9	-0.32D-04	0.80D-03
3,10	0.23D-03	0.22D-02	4,10	0.17D-03	0.22D-01
3,11	-0.23D-04	-0.69D-02	4,11	0.86D-03	-0.13D-01
5, 1	0.10D-03	-0.69D-02	6, 1	-0.18D-04	0.29D-02
5, 2	0.73D-04	-0.18D-02	6, 2	0.53D-03	0.93D-02
5, 3	0.26D-03	0.33D-02	6, 3	-0.29D-03	-0.71D-02
5, 4	0.20D-03	0.15D-01	6, 4	0.14D-03	-0.72D-02
5, 5	0.54D-03	0.93D-03	6, 5	-0.53D-03	0.29D-02
5, 6	0.31D-03	-0.62D-02	6, 6	0.76D-03	0.58D-02
5, 7	0.38D-03	-0.11D-01	6, 7	0.34D-03	-0.16D-02
5, 8	0.98D-03	0.87D-02	6, 8	0.12D-03	-0.20D-02
5, 9	-0.53D-04	0.10D-01	6, 9	0.15D-03	0.60D-02
5,10	0.12D-02	-0.53D-02	6,10	-0.57D-03	-0.55D-02
5,11	0.59D-03	0.35D-02	6,11	-0.37D-03	0.39D-02
7, 1	0.80D-03	-0.64D-02	8, 1	0.29D-03	-0.13D-03
7, 2	-0.20D-03	0.67D-02	8, 2	0.15D-02	-0.41D-02
7, 3	0.17D-02	0.97D-02	8, 3	-0.25D-03	0.37D-02
7, 4	0.85D-03	-0.60D-02	8, 4	-0.41D-03	-0.78D-02
7, 5	0.86D-03	-0.16D-01	8, 5	0.25D-03	0.18D-02
7, 6	0.51D-04	0.50D-02	8, 6	0.25D-03	0.25D-02
7, 7	0.98D-03	0.14D-02	8, 7	0.22D-03	0.10D-01
7, 8	0.55D-03	0.28D-02	8, 8	0.10D-02	-0.16D-01
7, 9	0.15D-02	0.21D-02	8, 9	-0.38D-03	0.88D-02
7,10	0.76D-03	-0.18D-02	8,10	0.53D-03	-0.50D-02
7,11	0.18D-02	-0.52D-02	8,11	-0.67D-03	-0.33D-02
9, 1	0.56D-03	-0.11D-01	10, 1	0.22D-03	-0.16D-01
9, 2	-0.81D-03	0.52D-02	10, 2	0.23D-02	0.89D-02
9, 3	0.50D-03	-0.87D-02	10, 3	0.22D-03	-0.12D-01
9, 4	0.11D-02	0.16D-01	10, 4	0.24D-03	-0.13D-02
9, 5	0.12D-02	-0.21D-02	10, 5	-0.60D-03	0.76D-02
9, 6	0.93D-03	-0.27D-02	10, 6	0.13D-03	0.15D-01
9, 7	-0.26D-03	0.83D-02	10, 7	0.12D-02	-0.25D-01
9, 8	-0.62D-03	-0.18D-01	10, 8	0.14D-02	0.17D-01
9, 9	0.55D-03	0.21D-01	10, 9	0.16D-02	-0.12D-01
9,10	0.91D-03	-0.58D-02	10,10	0.32D-03	0.11D-02
9,11	0.36D-03	0.84D-03	10,11	0.65D-03	0.20D-02
11, 1	0.64D-03	-0.70D-02	12, 1	-0.54D-03	-0.23D-02
11, 2	0.64D-04	0.32D-02	12, 2	-0.27D-03	-0.72D-02
11, 3	0.45D-03	0.87D-02	12, 3	0.42D-04	-0.38D-02
11, 4	0.84D-03	-0.61D-02	12, 4	0.70D-03	0.16D-02
11, 5	0.13D-02	-0.87D-03	12, 5	-0.70D-03	0.16D-01
11, 6	0.34D-03	-0.39D-02	12, 6	0.51D-03	-0.12D-01
11, 7	0.16D-03	0.31D-02	12, 7	-0.25D-03	-0.30D-02
11, 8	0.42D-03	0.11D-01	12, 8	0.13D-03	0.23D-03

11, 9	-0.79D-03	-0.13D-01	12, 9	0.95D-03	0.73D-02
11,10	0.66D-03	-0.35D-03	12,10	-0.50D-03	-0.55D-02
11,11	0.12D-02	0.97D-02	12,11	-0.63D-03	0.11D-02
13, 1	0.44D-03	-0.58D-02	14, 1	0.59D-03	0.65D-04
13, 2	-0.47D-03	0.44D-02	14, 2	0.99D-03	0.74D-03
13, 3	0.59D-03	0.62D-02	14, 3	-0.23D-04	-0.29D-02
13, 4	-0.81D-03	0.21D-03	14, 4	0.22D-03	-0.19D-02
13, 5	0.14D-02	0.48D-02	14, 5	-0.22D-03	-0.43D-02
13, 6	0.57D-03	-0.18D-01	14, 6	-0.29D-03	0.54D-02
13, 7	0.91D-03	0.72D-02	14, 7	0.13D-03	0.62D-02
13, 8	-0.32D-03	-0.42D-02	14, 8	0.80D-03	-0.91D-02
13, 9	0.14D-03	-0.96D-03	14, 9	-0.45D-03	0.95D-02
13,10	-0.27D-03	0.13D-01	14,10	0.16D-02	-0.10D-01
13,11	0.89D-03	0.11D-02	14,11	-0.66D-04	0.35D-02
15, 1	0.55D-03	-0.39D-02	16, 1	0.16D-03	-0.73D-03
15, 2	0.49D-04	-0.87D-03	16, 2	-0.31D-03	-0.88D-02
15, 3	0.47D-03	-0.97D-03	16, 3	0.37D-03	0.45D-02
15, 4	0.86D-03	-0.10D-01	16, 4	0.30D-04	0.17D-02
15, 5	-0.16D-03	0.52D-02	16, 5	0.79D-03	0.35D-02
15, 6	-0.62D-04	-0.55D-02	16, 6	0.37D-03	0.23D-02
15, 7	-0.19D-03	0.91D-02	16, 7	0.10D-02	-0.11D-01
15, 8	-0.28D-03	0.36D-02	16, 8	0.38D-03	-0.93D-04
15, 9	0.95D-03	-0.52D-02	16, 9	-0.21D-03	-0.68D-02
15,10	0.18D-03	0.13D-01	16,10	-0.50D-03	0.12D-01
15,11	0.32D-03	-0.10D-01	16,11	-0.32D-03	0.14D-02
17, 1	-0.63D-03	0.21D-02	18, 1	0.11D-02	0.14D-02
17, 2	0.81D-03	-0.82D-02	18, 2	0.68D-03	0.92D-03
17, 3	0.59D-03	-0.38D-02	18, 3	-0.19D-03	0.94D-02
17, 4	-0.75D-03	-0.41D-02	18, 4	0.16D-02	-0.14D-01
17, 5	0.11D-03	0.13D-01	18, 5	0.71D-03	0.96D-02
17, 6	0.40D-03	-0.52D-03	18, 6	0.83D-03	-0.87D-02
17, 7	-0.26D-03	-0.31D-02	18, 7	0.10D-03	-0.22D-02
17, 8	0.82D-03	-0.58D-02	18, 8	0.49D-03	-0.20D-02
17, 9	0.70D-03	-0.61D-03	18, 9	-0.40D-04	0.11D-01
17,10	0.82D-03	0.11D-02	18,10	0.66D-04	-0.14D-01
17,11	0.28D-03	0.96D-02	18,11	-0.40D-03	0.19D-01
19, 1	0.72D-03	-0.97D-02			
19, 2	0.12D-03	0.68D-02			
19, 3	0.11D-02	-0.12D-01			
19, 4	-0.19D-03	0.29D-02			
19, 5	-0.39D-04	0.58D-02			
19, 6	0.10D-03	-0.50D-03			
19, 7	0.12D-02	0.19D-02			
19, 8	-0.80D-03	-0.49D-02			
19, 9	0.51D-03	0.98D-02			
19,10	0.78D-03	0.18D-02			
19,11	0.13D-02	-0.11D-01			

STATISTICAL RESULTS:

	MEAN VALUE	STANDARD DEVIATION
XX-STRAIN:	0.3283D-03	0.6041D-03
YY-STRAIN:	-0.7819D-04	0.8222D-02

EVALUATED THICKNESS CHANGES (MICRONS)
(COLUMNS: 1- 6)

	1	2	3	4	5	6
1	-0.51	-1.39	1.04	-3.43	2.76	-3.99
2	-2.36	2.93	-3.75	2.59	-4.44	-2.07
3	1.98	-2.12	1.47	3.84	-2.07	-2.61
4	0.70	-2.05	-2.44	1.11	3.58	-2.18
5	1.68	3.58	-2.83	-2.14	-1.47	0.48
6	-4.89	0.08	-4.25	1.50	-1.35	3.51
7	-0.71	1.39	-3.16	-2.60	0.70	-4.64
8	-3.47	1.28	2.52	-1.11	3.25	-4.03
9	-1.43	0.23	2.34	-1.38	-1.62	0.11
10	2.74	-2.18	3.09	-3.57	-2.48	2.45
11	1.40	-3.44	-0.14	3.61	-3.68	0.29
12	3.62	-3.56	-2.77	-1.83	3.59	-2.54
13	3.74	-4.59	-3.49	-1.74	0.06	-1.89
14	3.19	3.02	-2.99	2.47	-3.97	-0.80
15	-2.06	-3.08	2.32	-1.36	1.11	-2.61
16	0.40	-3.21	3.97	-1.76	-1.20	-0.27
17	-3.25	-2.53	-0.55	-0.18	0.42	-3.91
18	0.45	-0.33	-1.10	-2.61	1.46	1.58
19	2.08	-2.82	-2.70	-3.30	3.21	-4.16
20	0.67	-4.18	-2.83	1.97	-2.98	-4.19

(COLUMNS: 7-12)

	7	8	9	10	11	12
1	0.32	-4.89	-0.24	3.51	0.59	-0.30
2	-1.67	2.89	2.92	-4.74	-4.94	1.63
3	0.75	-3.76	3.18	-1.73	-2.05	-0.97
4	3.22	-2.27	-1.48	-1.11	3.94	-2.42
5	-4.54	-4.29	0.89	-2.55	1.56	-3.64
6	-0.75	-0.03	3.52	1.59	-3.61	-1.52
7	-1.62	-4.73	2.98	-4.08	0.51	-0.39
8	2.17	2.72	-2.58	1.17	3.77	-3.32
9	-2.26	1.48	-0.70	1.71	-3.94	1.98
10	-1.55	3.11	-4.33	-3.48	3.57	-2.34
11	-2.13	-4.97	2.37	-2.25	3.11	-1.01
12	-2.09	0.03	0.29	-4.53	1.34	-3.28
13	2.06	1.57	-4.94	-4.74	1.01	-3.87
14	1.30	-0.03	1.98	-0.62	-1.15	2.12
15	-4.41	-0.84	2.13	-2.02	1.11	-1.31
16	2.26	-3.02	-1.19	3.01	-2.57	2.25
17	-5.01	-0.70	-0.08	1.12	-1.02	-2.84
18	-3.30	-0.69	-4.01	-4.44	-0.35	-0.17
19	3.77	-1.78	2.43	-1.59	-3.00	-3.34
20	0.20	-2.19	-2.38	1.86	-0.88	-2.59

RECONSTRUCTION RESULTS OF INTERFEROGRAM (5L) OF THE NEWS-PRINT PAPER SAMPLE #38 (CUMMULATIVE DEFORMATION).

CO-ORDINATES X	CO-ORDINATES Y	DEFORMATIONS X	DEFORMATIONS Y	DEFORMATIONS Z
44.0	-22.0	0.5090D 02	-0.1898D 02	-0.2121D 02
44.0	-18.0	0.5220D 02	-0.1619D 02	-0.5474D 01
44.0	-14.0	0.5281D 02	0.1958D 02	-0.1340D 02
44.0	-10.0	0.4893D 02	0.2030D 01	-0.5741D 01
44.0	-6.0	0.5167D 02	0.4463D 02	-0.2811D 02
44.0	-2.0	0.5212D 02	-0.2706D 01	-0.3695D 02
44.0	2.0	0.5079D 02	-0.2111D 02	-0.1007D 02
44.0	6.0	0.4857D 02	-0.2866D 02	-0.1720D 01
44.0	10.0	0.4950D 02	-0.1504D 02	0.6799D 01
44.0	14.0	0.5136D 02	-0.9625D 01	0.2513D 02
44.0	18.0	0.5381D 02	0.1389D 02	0.2233D 02
44.0	22.0	0.5215D 02	-0.5368D 02	-0.3183D 02
40.0	-22.0	0.4957D 02	0.2648D 02	-0.1065D 02
40.0	-18.0	0.5093D 02	-0.1603D 02	0.1393D 02
40.0	-14.0	0.5123D 02	0.3187D 02	-0.5375D 02
40.0	-10.0	0.5139D 02	-0.2089D 01	0.2361D 02
40.0	-6.0	0.5254D 02	0.4353D 02	0.8385D 01
40.0	-2.0	0.4939D 02	-0.1462D 02	0.7606D 01
40.0	2.0	0.5091D 02	-0.1847D 02	0.9801D 01
40.0	6.0	0.5126D 02	-0.2413D 02	-0.2667D 02
40.0	10.0	0.4774D 02	-0.3824D 02	0.1003D 02
40.0	14.0	0.4970D 02	-0.1034D 02	0.4128D 02
40.0	18.0	0.5198D 02	0.1591D 02	-0.3301D 02
40.0	22.0	0.4911D 02	0.7746D 01	-0.2300D 02
36.0	-22.0	0.4976D 02	0.4239D 02	-0.3035D 02
36.0	-18.0	0.5085D 02	0.2457D 02	0.3320D 02
36.0	-14.0	0.4923D 02	0.1226D 02	-0.1661D 02
36.0	-10.0	0.4813D 02	0.2591D 02	-0.2051D 02
36.0	-6.0	0.4956D 02	0.1284D 02	0.1063D 02
36.0	-2.0	0.4667D 02	-0.3991D 01	0.1337D 01
36.0	2.0	0.5075D 02	0.1817D 02	-0.2330D 01
36.0	6.0	0.4542D 02	-0.3046D 02	0.2350D 02
36.0	10.0	0.5055D 02	-0.1996D 02	0.2989D 02
36.0	14.0	0.4778D 02	0.1174D 02	0.3575D 02
36.0	18.0	0.4796D 02	0.2217D 02	0.1947D 02
36.0	22.0	0.4603D 02	-0.1569D 02	0.5460D 02
32.0	-22.0	0.4580D 02	-0.1865D 02	-0.3583D 01
32.0	-18.0	0.4819D 02	-0.2254D 01	-0.3028D 02
32.0	-14.0	0.4650D 02	0.4258D 02	-0.5659D 01
32.0	-10.0	0.5023D 02	0.6275D 02	-0.1220D 02
32.0	-6.0	0.4691D 02	-0.6528D 01	0.3788D 01
32.0	-2.0	0.4675D 02	-0.4030D 02	-0.5430D 02
32.0	2.0	0.4588D 02	0.3466D 02	-0.3728D 01
32.0	6.0	0.4669D 02	-0.1162D 02	-0.9487D-01
32.0	10.0	0.4549D 02	-0.3929D 02	-0.1639D 02
32.0	14.0	0.4515D 02	-0.1118D 02	-0.1288D 02
32.0	18.0	0.5056D 02	0.1914D 02	0.1583D 02
32.0	22.0	0.4653D 02	0.3416D 01	0.1145D 02
28.0	-22.0	0.4402D 02	-0.3102D 02	-0.5188D 02
28.0	-18.0	0.4069D 02	0.6537D 01	0.3305D 02
28.0	-14.0	0.4878D 02	0.5561D 02	0.2421D 02
28.0	-10.0	0.4208D 02	-0.2625D 02	-0.3072D 02
28.0	-6.0	0.4254D 02	-0.2203D 02	0.6475D 01
28.0	-2.0	0.4048D 02	0.2247D 02	-0.7856D 01
28.0	2.0	0.4270D 02	0.2279D 02	-0.3236D 01
28.0	6.0	0.5002D 02	0.7121D 01	0.6482D 02
28.0	10.0	0.4526D 02	0.2991D 02	0.2379D 02
28.0	14.0	0.4578D 02	0.1329D 02	-0.2391D 02
28.0	18.0	0.4380D 02	0.3814D 02	-0.4867D 02
28.0	22.0	0.4534D 02	-0.1887D 02	0.3423D 02

24.0	-22.0	0.4552D 02	-0.2478D 02	-0.1099D 01	
24.0	-18.0	0.4364D 02	0.1195D 02	-0.1354D 02	
24.0	-14.0	0.4485D 02	0.4571D 02	-0.5441D 02	
24.0	-10.0	0.4151D 02	-0.3590D 02	0.3465D 02	
24.0	-6.0	0.4223D 02	-0.3686D 02	0.3400D 02	
24.0	-2.0	0.4344D 02	-0.2766D 02	-0.5181D 01	
24.0	2.0	0.4664D 02	0.3135D 02	-0.3789D 01	
24.0	6.0	0.4198D 02	0.1401D 02	0.1086D 02	
24.0	10.0	0.4320D 02	0.2874D 02	-0.3312D 02	
24.0	14.0	0.4496D 02	-0.2424D 02	-0.1605D 02	
24.0	18.0	0.4225D 02	0.1952D 02	-0.1306D 02	
24.0	22.0	0.5008D 02	0.2701D 02	0.4572D 01	
20.0	-22.0	0.4449D 02	0.2134D 02	-0.3828D 02	
20.0	-18.0	0.3899D 02	-0.1729D 02	0.1950D 02	
20.0	-14.0	0.4320D 02	0.2331D 01	0.3333D 01	
20.0	-10.0	0.4312D 02	0.1325D 02	-0.2525D 00	
20.0	-6.0	0.4234D 02	-0.1270D 01	-0.7085D 01	
20.0	-2.0	0.4232D 02	-0.5893D 01	-0.2693D 02	
20.0	2.0	0.4048D 02	0.1092D 02	-0.2954D 02	
20.0	6.0	0.4286D 02	-0.3793D 02	-0.1959D 02	
20.0	10.0	0.4553D 02	0.3209D 02	0.1378D 02	
20.0	14.0	0.4231D 02	0.1658D 02	-0.1220D 02	
20.0	18.0	0.4126D 02	0.1343D 02	0.1087D 02	
20.0	22.0	0.4203D 02	-0.1288D 01	-0.2536D 02	
16.0	-22.0	0.4238D 02	-0.1227D 02	0.4385D 02	
16.0	-18.0	0.3955D 02	-0.4336D 02	-0.1135D 02	
16.0	-14.0	0.3869D 02	0.3045D 02	-0.4386D 02	
16.0	-10.0	0.4107D 02	0.1471D 02	-0.5549D 01	
16.0	-6.0	0.4013D 02	-0.3559D 01	0.1508D 02	
16.0	-2.0	0.3800D 02	-0.1190D 02	0.4042D 02	
16.0	2.0	0.4553D 02	0.4647D 02	0.5884D 02	
16.0	6.0	0.3881D 02	-0.3748D 02	0.2753D 01	
16.0	10.0	0.3958D 02	0.2113D 02	-0.6675D 02	
16.0	14.0	0.4050D 02	-0.4878D 02	0.4825D 02	
16.0	18.0	0.4047D 02	0.1318D 02	0.8197D 01	
16.0	22.0	0.4253D 02	0.4375D 02	-0.1073D 02	
12.0	-22.0	0.3896D 02	-0.2163D 02	0.3125D 02	
12.0	-18.0	0.3930D 02	-0.2085D 02	0.6576D 01	
12.0	-14.0	0.4129D 02	0.8868D 01	0.2423D 02	
12.0	-10.0	0.4187D 02	0.2338D 02	0.1414D 02	
12.0	-6.0	0.3868D 02	-0.5839D 02	-0.4977D 02	
12.0	-2.0	0.3864D 02	0.1232D 02	0.2632D 02	
12.0	2.0	0.3802D 02	-0.1007D 02	-0.6765D 01	
12.0	6.0	0.3971D 02	-0.1505D 02	-0.5978D 02	
12.0	10.0	0.3815D 02	-0.3186D 02	0.3914D 02	
12.0	14.0	0.4046D 02	0.2000D 02	0.4581D 02	
12.0	18.0	0.3743D 02	-0.2217D 02	-0.1988D 02	
12.0	22.0	0.4372D 02	0.4073D 02	0.7043D 02	
8.0	-22.0	0.4156D 02	0.1567D 01	-0.3489D 02	
8.0	-18.0	0.3599D 02	0.6344D 01	-0.2775D 02	
8.0	-14.0	0.3909D 02	0.2440D 02	0.1234D 01	
8.0	-10.0	0.4127D 02	0.2479D 02	0.1646D 02	
8.0	-6.0	0.3587D 02	-0.2100D 02	-0.2537D 02	
8.0	-2.0	0.3703D 02	-0.1226D 02	-0.2973D 02	
8.0	2.0	0.3768D 02	-0.6307D 01	0.2885D 02	
8.0	6.0	0.4084D 02	0.1573D 02	0.3983D 02	
8.0	10.0	0.3838D 02	-0.2024D 02	-0.3354D 02	
8.0	14.0	0.3489D 02	-0.2946D 02	-0.2952D 02	
8.0	18.0	0.3769D 02	0.1291D 02	-0.2686D 02	
8.0	22.0	0.3982D 02	-0.2644D 02	-0.4861D 02	
4.0	-22.0	0.3628D 02	-0.2631D 01	0.2193D 02	
4.0	-18.0	0.3468D 02	-0.2004D 02	0.3074D 02	
4.0	-14.0	0.3701D 02	0.1396D 02	0.2674D 02	
4.0	-10.0	0.3907D 02	0.1901D 02	0.1892D 02	
4.0	-6.0	0.3400D 02	-0.3844D 02	-0.3908D 02	
4.0	-2.0	0.3630D 02	0.1828D 02	-0.5231D 02	
4.0	2.0	0.4135D 02	0.4298D 02	0.1208D 02	
4.0	6.0	0.3859D 02	-0.4526D 02	0.1123D 02	
4.0	10.0	0.3660D 02	0.1272D 02	-0.1929D 02	
4.0	14.0	0.3487D 02	0.3015D 01	-0.2353D 02	
4.0	18.0	0.3892D 02	-0.1087D 02	-0.1564D 02	
4.0	22.0	0.3426D 02	0.1130D 02	0.2920D 01	

0.0	-22.0	0.3367D 02	-0.7086D 01	-0.5068D 01	
0.0	-18.0	0.3498D 02	-0.3091D 00	-0.4307D 02	
0.0	-14.0	0.3367D 02	-0.7732D 01	0.5523D 02	
0.0	-10.0	0.3579D 02	-0.2848D 02	-0.3618D 02	
0.0	-6.0	0.3424D 02	-0.2359D 02	0.2042D 02	
0.0	-2.0	0.3523D 02	-0.3111D 02	0.9336D 01	
0.0	2.0	0.3483D 02	0.3496D 02	-0.5835D 02	
0.0	6.0	0.3818D 02	0.3469D 02	0.1231D 02	
0.0	10.0	0.3186D 02	-0.1921D 02	0.2914D 02	
0.0	14.0	0.3274D 02	-0.9217D 01	-0.4387D 01	
0.0	18.0	0.3775D 02	0.1945D 02	-0.3002D 02	
0.0	22.0	0.3393D 02	0.1824D 01	0.6501D 01	
-4.0	-22.0	0.3368D 02	-0.1092D 02	-0.8821D 01	
-4.0	-18.0	0.3468D 02	0.1556D 02	0.2037D 02	
-4.0	-14.0	0.3305D 02	-0.3024D 02	0.2057D 02	
-4.0	-10.0	0.3481D 02	-0.1501D 02	-0.1839D 02	
-4.0	-6.0	0.3074D 02	-0.1903D 02	0.8474D 01	
-4.0	-2.0	0.3468D 02	-0.3242D 02	0.4518D 01	
-4.0	2.0	0.3440D 02	-0.2496D 02	-0.1141D 02	
-4.0	6.0	0.3165D 02	-0.4411D 02	0.6315D 02	
-4.0	10.0	0.3164D 02	-0.9545D 01	0.1171D 00	
-4.0	14.0	0.3289D 02	0.6585D 01	-0.1951D 02	
-4.0	18.0	0.3156D 02	-0.1611D 01	-0.8479D 01	
-4.0	22.0	0.3371D 02	0.6965D-01	0.3964D 02	
-8.0	-22.0	0.3457D 02	-0.8048D 01	0.3929D 01	
-8.0	-18.0	0.3340D 02	-0.2831D 02	0.1246D 02	
-8.0	-14.0	0.3437D 02	0.2237D 01	0.2260D 02	
-8.0	-10.0	0.3364D 02	0.1831D 02	-0.4628D 02	
-8.0	-6.0	0.3216D 02	0.8837D 01	0.2465D 02	
-8.0	-2.0	0.3008D 02	-0.5822D 02	-0.1805D 02	
-8.0	2.0	0.3308D 02	0.4867D 02	-0.4667D 02	
-8.0	6.0	0.3178D 02	-0.8442D 01	0.3291D 02	
-8.0	10.0	0.3259D 02	0.1482D 02	-0.3577D 02	
-8.0	14.0	0.3422D 02	-0.2464D 01	0.3812D 02	
-8.0	18.0	0.3102D 02	-0.6627D 02	-0.5067D 02	
-8.0	22.0	0.3388D 02	-0.1439D 02	0.1146D 02	
-12.0	-22.0	0.2976D 02	0.3400D 01	-0.3219D 02	
-12.0	-18.0	0.3242D 02	0.2976D 02	-0.2861D 02	
-12.0	-14.0	0.3421D 02	0.3154D 02	-0.3967D 02	
-12.0	-10.0	0.3118D 02	0.2724D 02	-0.4519D 02	
-12.0	-6.0	0.2954D 02	-0.1984D 02	0.4849D 02	
-12.0	-2.0	0.3187D 02	-0.2767D 02	0.6807D 01	
-12.0	2.0	0.3245D 02	-0.1750D 01	0.2282D 02	
-12.0	6.0	0.3158D 02	-0.4363D-01	0.5586D 01	
-12.0	10.0	0.3033D 02	-0.2007D 02	0.1715D 02	
-12.0	14.0	0.2974D 02	0.1805D 02	0.2728D 02	
-12.0	18.0	0.3334D 02	-0.1342D 02	-0.1740D 02	
-12.0	22.0	0.3238D 02	0.4032D 02	-0.4711D 02	
-16.0	-22.0	0.3053D 02	-0.6982D 01	0.1090D 02	
-16.0	-18.0	0.3027D 02	-0.1888D 02	-0.3870D 02	
-16.0	-14.0	0.2873D 02	-0.2213D 01	0.2103D 02	
-16.0	-10.0	0.2961D 02	-0.2435D 02	0.2072D 02	
-16.0	-6.0	0.3364D 02	0.3051D 02	0.2600D 02	
-16.0	-2.0	0.3220D 02	-0.5460D 02	0.5012D 02	
-16.0	2.0	0.2844D 02	-0.1935D 02	0.7736D 02	
-16.0	6.0	0.3007D 02	0.4804D 02	0.1752D 02	
-16.0	10.0	0.3243D 02	-0.1828D 01	0.2098D 02	
-16.0	14.0	0.3042D 02	0.1319D 01	0.2396D 02	
-16.0	18.0	0.3016D 02	-0.2795D 02	-0.2095D 02	
-16.0	22.0	0.3045D 02	-0.6805D 02	-0.1053D 02	
-20.0	-22.0	0.2819D 02	-0.1416D 02	0.4623D 01	
-20.0	-18.0	0.3177D 02	0.1974D 02	0.9842D 01	
-20.0	-14.0	0.2824D 02	0.2133D 02	-0.5721D 02	
-20.0	-10.0	0.2919D 02	0.3270D 01	-0.1988D 02	
-20.0	-6.0	0.3038D 02	-0.2403D 02	-0.1898D 02	
-20.0	-2.0	0.2888D 02	0.2169D 02	0.4182D 00	
-20.0	2.0	0.2726D 02	-0.4438D 02	-0.4423D 02	
-20.0	6.0	0.3261D 02	-0.2125D 02	-0.4403D 02	
-20.0	10.0	0.2784D 02	-0.4542D 01	0.1525D 02	
-20.0	14.0	0.2825D 02	-0.1466D 02	-0.9446D 00	
-20.0	18.0	0.2730D 02	-0.3185D 02	-0.8748D 01	
-20.0	22.0	0.2488D 02	-0.2526D 02	0.1848D 02	

-24.0	-22.0	0.2766D 02	-0.1926D 02	-0.4754D 02
-24.0	-18.0	0.2803D 02	-0.1027D 02	-0.5115D 02
-24.0	-14.0	0.2603D 02	0.1311D 02	-0.1274D 02
-24.0	-10.0	0.2894D 02	0.2093D 02	0.4637D 02
-24.0	-6.0	0.2480D 02	0.1955D 02	0.1842D 02
-24.0	-2.0	0.2650D 02	-0.1483D 02	0.3391D 02
-24.0	2.0	0.2547D 02	0.3122D 01	-0.3018D 02
-24.0	6.0	0.2420D 02	0.1912D 02	-0.3216D 01
-24.0	10.0	0.2771D 02	0.5519D 01	0.7242D 01
-24.0	14.0	0.2746D 02	0.9637D 01	0.2025D 02
-24.0	18.0	0.2768D 02	0.5655D 01	-0.4732D 02
-24.0	22.0	0.2616D 02	-0.3312D 02	0.4740D 02
-28.0	-22.0	0.2648D 02	0.1599D 02	0.2288D 02
-28.0	-18.0	0.2387D 02	-0.4141D 02	-0.6838D 02
-28.0	-14.0	0.2665D 02	-0.1619D 02	-0.3976D 02
-28.0	-10.0	0.2562D 02	-0.2386D 02	0.1532D 02
-28.0	-6.0	0.2460D 02	-0.1135D 02	0.3273D 02
-28.0	-2.0	0.2456D 02	0.1496D 02	0.3542D 02
-28.0	2.0	0.2590D 02	-0.3209D 01	0.3065D 02
-28.0	6.0	0.2582D 02	-0.1015D 01	0.1382D 02
-28.0	10.0	0.2356D 02	-0.5111D 02	-0.9956D 01
-28.0	14.0	0.2658D 02	-0.1739D 02	-0.3991D 01
-28.0	18.0	0.2275D 02	-0.2239D 02	-0.1680D 00
-28.0	22.0	0.2630D 02	-0.3622D 02	-0.2486D 02
-32.0	-22.0	0.2647D 02	0.4013D 01	-0.3254D 02
-32.0	-18.0	0.2450D 02	-0.2463D 02	-0.1696D 02
-32.0	-14.0	0.2280D 02	-0.4049D 01	0.5293D 02
-32.0	-10.0	0.2465D 02	0.2394D 02	-0.2491D 01
-32.0	-6.0	0.2623D 02	0.6676D 01	0.2674D 02
-32.0	-2.0	0.2361D 02	0.2989D 01	0.1010D 02
-32.0	2.0	0.2476D 02	-0.4317D 02	0.1167D 02
-32.0	6.0	0.2338D 02	-0.3591D 02	-0.3293D 02
-32.0	10.0	0.2441D 02	-0.1739D 02	0.1967D 02
-32.0	14.0	0.2513D 02	-0.8394D 02	0.9036D 01
-32.0	18.0	0.2254D 02	-0.6464D 02	0.2175D 02
-32.0	22.0	0.2432D 02	-0.7199D 01	0.5632D 02

STATISTICAL RESULTS:

	MEAN VALUE	STANDARD DEVIATION
X-DIRECTION	0.376D 02	0.844D 01
Y-DIRECTION	-0.299D 01	0.254D 02
Z-DIRECTION	0.597D 00	0.295D 02

EVALUATED STRAIN FIELD AT POINT (5 L).

ELEMENT	EXX	EYY	ELEMENT	EXX	EYY
1, 1	0.33D-03	-0.70D-03	2, 1	-0.48D-04	0.11D-01
1, 2	0.32D-03	-0.89D-02	2, 2	0.18D-04	-0.12D-01
1, 3	0.40D-03	0.44D-02	2, 3	0.50D-03	0.85D-02
1, 4	-0.61D-03	-0.11D-01	2, 4	0.81D-03	-0.11D-01
1, 5	-0.22D-03	0.12D-01	2, 5	0.74D-03	0.15D-01
1, 6	0.68D-03	0.46D-02	2, 6	0.68D-03	0.96D-03
1, 7	-0.30D-04	0.19D-02	2, 7	0.42D-04	0.14D-02
1, 8	-0.67D-03	-0.33D-02	2, 8	0.15D-02	0.35D-02
1, 9	0.44D-03	-0.15D-02	2, 9	-0.70D-03	-0.70D-02
1,10	0.41D-03	-0.59D-02	2,10	0.48D-03	-0.66D-02
1,11	0.46D-03	0.17D-01	2,11	0.10D-02	0.20D-02
3, 1	0.99D-03	0.45D-02	4, 1	0.44D-03	-0.41D-02
3, 2	0.66D-03	0.31D-02	4, 2	0.38D-03	-0.11D-01
3, 3	0.68D-03	-0.34D-02	4, 3	-0.57D-03	-0.50D-02
3, 4	-0.53D-03	0.33D-02	4, 4	0.20D-02	0.17D-01
3, 5	0.66D-03	0.42D-02	4, 5	0.11D-02	0.84D-02
3, 6	-0.20D-04	-0.55D-02	4, 6	0.65D-04	-0.19D-01
3, 7	0.12D-02	0.12D-01	4, 7	0.80D-03	0.12D-01
3, 8	-0.32D-03	-0.26D-02	4, 8	-0.83D-03	0.69D-02
3, 9	0.13D-02	-0.79D-02	4, 9	0.59D-04	-0.70D-02
3,10	0.66D-03	-0.26D-02	4,10	-0.16D-03	-0.76D-02
3,11	-0.65D-03	0.95D-02	4,11	0.17D-02	0.39D-02
5, 1	-0.37D-03	-0.94D-02	6, 1	0.26D-03	-0.92D-02
5, 2	0.76D-03	-0.12D-01	6, 2	0.12D-02	-0.84D-02
5, 3	0.98D-03	0.20D-01	6, 3	0.41D-03	0.20D-01
5, 4	0.14D-03	-0.11D-02	6, 4	-0.40D-03	0.24D-03
5, 5	0.78D-04	-0.11D-01	6, 5	-0.27D-04	-0.23D-02
5, 6	0.76D-03	-0.79D-04	6, 6	0.28D-03	-0.15D-01
5, 7	-0.15D-02	0.39D-02	6, 7	0.20D-02	0.43D-02
5, 8	0.20D-02	-0.57D-02	6, 8	-0.22D-03	-0.37D-02
5, 9	0.51D-03	0.42D-02	6, 9	-0.58D-03	0.13D-01
5,10	0.20D-03	-0.62D-02	6,10	0.66D-03	-0.11D-01
5,11	0.39D-03	0.14D-01	6,11	0.25D-03	-0.19D-02
7, 1	0.53D-03	0.97D-02	8, 1	0.85D-03	0.78D-02
7, 2	-0.14D-03	-0.49D-02	8, 2	0.63D-04	-0.18D-01
7, 3	0.11D-02	-0.27D-02	8, 3	-0.65D-03	0.39D-02
7, 4	0.51D-03	0.36D-02	8, 4	-0.20D-03	0.46D-02
7, 5	0.55D-03	0.12D-02	8, 5	0.36D-03	0.21D-02
7, 6	0.11D-02	-0.42D-02	8, 6	-0.16D-03	-0.15D-01
7, 7	-0.13D-02	0.12D-01	8, 7	-0.19D-02	0.21D-01
7, 8	0.10D-02	-0.18D-01	8, 8	-0.22D-03	-0.15D-01
7, 9	0.15D-02	0.39D-02	8, 9	0.36D-03	0.17D-01
7,10	0.45D-03	0.79D-03	8,10	0.11D-04	-0.15D-01
7,11	0.20D-03	0.30D-02	8,11	0.76D-03	-0.76D-02
9, 1	-0.65D-03	-0.19D-03	10, 1	0.13D-02	-0.12D-02
9, 2	0.83D-03	-0.74D-02	10, 2	0.33D-03	-0.45D-02
9, 3	0.55D-03	-0.36D-02	10, 3	0.52D-03	-0.97D-04
9, 4	0.15D-03	0.20D-01	10, 4	0.55D-03	0.11D-01
9, 5	0.70D-03	-0.18D-01	10, 5	0.47D-03	-0.22D-02
9, 6	0.40D-03	0.56D-02	10, 6	0.18D-03	-0.15D-02
9, 7	0.86D-04	0.14D-02	10, 7	-0.92D-03	-0.55D-02
9, 8	-0.28D-03	0.41D-02	10, 8	0.18D-02	0.90D-02
9, 9	-0.57D-04	-0.13D-01	10, 9	0.45D-03	0.23D-02
9,10	0.14D-02	0.11D-01	10,10	0.65D-05	-0.11D-01
9,11	-0.66D-04	-0.16D-01	10,11	-0.31D-03	0.98D-02
11, 1	0.65D-03	0.44D-02	12, 1	-0.36D-05	-0.17D-02
11, 2	-0.76D-04	-0.85D-02	12, 2	0.75D-04	0.19D-02
11, 3	0.83D-03	-0.13D-02	12, 3	0.16D-03	0.52D-02
11, 4	0.82D-03	0.14D-01	12, 4	0.25D-03	-0.12D-02
11, 5	-0.60D-04	-0.14D-01	12, 5	0.87D-03	0.19D-02
11, 6	0.27D-03	-0.62D-02	12, 6	0.14D-03	-0.17D-01
11, 7	0.16D-02	0.22D-01	12, 7	0.11D-03	0.69D-04
11, 8	-0.11D-02	-0.14D-01	12, 8	0.16D-02	0.13D-01

*	11, 9	0.12D-02	0.24D-02	12, 9	0.56D-04	-0.25D-02	*
*	11,10	0.53D-03	0.35D-02	12,10	-0.38D-04	-0.72D-02	*
*	11,11	0.29D-03	-0.55D-02	12,11	0.15D-02	0.44D-02	*
*	13, 1	-0.22D-03	-0.66D-02	14, 1	0.12D-02	0.51D-02	*
*	13, 2	0.32D-03	0.11D-01	14, 2	0.24D-03	-0.76D-02	*
*	13, 3	-0.33D-03	-0.38D-02	14, 3	0.40D-04	-0.40D-02	*
*	13, 4	0.29D-03	0.10D-02	14, 4	0.61D-03	0.24D-02	*
*	13, 5	-0.35D-03	0.33D-02	14, 5	0.65D-03	0.17D-01	*
*	13, 6	0.11D-02	-0.19D-02	14, 6	-0.45D-03	-0.27D-01	*
*	13, 7	0.33D-03	0.48D-02	14, 7	0.16D-03	0.14D-01	*
*	13, 8	-0.32D-04	-0.86D-02	14, 8	0.51D-04	-0.58D-02	*
*	13, 9	-0.24D-03	-0.40D-02	14, 9	0.57D-03	0.43D-02	*
*	13,10	-0.33D-03	0.20D-02	14,10	0.11D-02	0.16D-01	*
*	13,11	0.13D-03	-0.42D-03	14,11	-0.58D-03	-0.13D-01	*
*	15, 1	-0.19D-03	-0.68D-02	16, 1	0.58D-03	0.30D-02	*
*	15, 2	0.54D-03	-0.45D-03	16, 2	-0.37D-03	-0.42D-02	*
*	15, 3	0.14D-02	0.11D-02	16, 3	0.12D-03	0.55D-02	*
*	15, 4	0.39D-03	0.12D-01	16, 4	0.11D-03	-0.14D-01	*
*	15, 5	-0.10D-02	0.20D-02	16, 5	0.82D-03	0.21D-01	*
*	15, 6	-0.83D-04	-0.65D-02	16, 6	0.83D-03	-0.88D-02	*
*	15, 7	0.10D-02	-0.43D-03	16, 7	0.29D-03	-0.17D-01	*
*	15, 8	0.38D-03	0.50D-02	16, 8	-0.63D-03	0.12D-01	*
*	15, 9	-0.53D-03	-0.95D-02	16, 9	0.11D-02	-0.79D-03	*
*	15,10	-0.17D-03	0.79D-02	16,10	0.54D-03	0.73D-02	*
*	15,11	0.80D-03	-0.13D-01	16,11	0.71D-03	0.10D-01	*
*	17, 1	0.13D-03	-0.85D-02	18, 1	0.30D-03	-0.22D-02	*
*	17, 2	0.93D-03	-0.40D-03	18, 2	0.10D-02	-0.58D-02	*
*	17, 3	0.55D-03	0.45D-02	18, 3	-0.16D-03	-0.20D-02	*
*	17, 4	0.60D-04	0.68D-02	18, 4	0.83D-03	0.35D-03	*
*	17, 5	0.14D-02	-0.11D-01	18, 5	0.49D-04	0.86D-02	*
*	17, 6	0.59D-03	-0.17D-01	18, 6	0.48D-03	-0.45D-02	*
*	17, 7	0.45D-03	-0.58D-02	18, 7	-0.11D-03	-0.40D-02	*
*	17, 8	0.21D-02	-0.42D-02	18, 8	-0.41D-03	0.34D-02	*
*	17, 9	0.32D-04	0.25D-02	18, 9	0.10D-02	-0.10D-02	*
*	17,10	0.20D-03	0.43D-02	18,10	0.22D-03	0.10D-02	*
*	17,11	-0.94D-04	-0.16D-02	18,11	0.12D-02	0.97D-02	*
*	19, 1	0.63D-06	0.14D-01				*
*	19, 2	-0.16D-03	-0.63D-02				*
*	19, 3	0.96D-03	0.19D-02				*
*	19, 4	0.24D-03	-0.31D-02				*
*	19, 5	-0.41D-03	-0.66D-02				*
*	19, 6	0.24D-03	0.45D-02				*
*	19, 7	0.28D-03	-0.55D-03				*
*	19, 8	0.61D-03	0.13D-01				*
*	19, 9	-0.21D-03	-0.84D-02				*
*	19,10	0.36D-03	0.12D-02				*
*	19,11	0.52D-04	0.35D-02				*

STATISTICAL RESULTS:

	MEAN VALUE	STANDARD DEVIATION
XX-STRAIN:	0.3519D-03	0.6386D-03
YY-STRAIN:	0.3468D-04	0.9041D-02

RECONSTRUCTION RESULTS OF INTERFEROGRAM
(6E) OF THE NEWS-PRINT PAPER SAMPLE #38
CUMMULATIVE DEFORMATION)

CO-ORDINATES X	CO-ORDINATES Y	DEFORMATIONS X	DEFORMATIONS Y	DEFORMATIONS Z
44.0	-22.0	0.6318D 02	-0.4036D 02	0.4823D 01
44.0	-18.0	0.6282D 02	-0.4886D-01	-0.1894D 01
44.0	-14.0	0.6330D 02	-0.3934D 02	-0.2121D 02
44.0	-10.0	0.6313D 02	-0.1469D 01	-0.1936D 02
44.0	-6.0	0.6237D 02	0.1835D 01	0.4097D 02
44.0	-2.0	0.5975D 02	0.2330D 02	0.2901D 02
44.0	2.0	0.6223D 02	0.1217D 01	-0.1142D 02
44.0	6.0	0.6332D 02	-0.2770D 02	-0.7911D 01
44.0	10.0	0.6004D 02	-0.3140D 02	-0.6140D 01
44.0	14.0	0.5960D 02	-0.3705D 02	-0.1924D 02
44.0	18.0	0.6026D 02	0.4282D 01	-0.1619D 02
44.0	22.0	0.6103D 02	-0.1769D 02	0.2287D 02
40.0	-22.0	0.6045D 02	0.1331D 02	0.4011D 00
40.0	-18.0	0.5948D 02	0.4654D 02	-0.8464D 01
40.0	-14.0	0.6303D 02	0.5897D 01	-0.7168D 02
40.0	-10.0	0.6411D 02	-0.7244D 02	-0.3422D 02
40.0	-6.0	0.6113D 02	-0.3271D 02	-0.4910D 01
40.0	-2.0	0.6098D 02	-0.3583D 02	0.3987D 01
40.0	2.0	0.5730D 02	-0.4479D 02	-0.1378D 02
40.0	6.0	0.6229D 02	-0.1447D 02	0.3519D 02
40.0	10.0	0.5890D 02	0.1657D 01	-0.1563D 02
40.0	14.0	0.6249D 02	-0.2013D 02	-0.4628D 02
40.0	18.0	0.6401D 02	0.3704D 01	0.2980D 02
40.0	22.0	0.6207D 02	-0.3955D 01	0.2665D 02
36.0	-22.0	0.5986D 02	0.7657D 01	0.1779D 02
36.0	-18.0	0.5852D 02	0.2464D 02	-0.1879D 02
36.0	-14.0	0.5863D 02	-0.2487D 02	0.2118D 02
36.0	-10.0	0.6067D 02	-0.6509D 02	0.2265D 02
36.0	-6.0	0.6269D 02	-0.1662D 01	0.6465D 01
36.0	-2.0	0.5803D 02	-0.1078D 02	-0.2557D 02
36.0	2.0	0.5792D 02	-0.7126D 02	-0.2333D 01
36.0	6.0	0.6152D 02	-0.1268D 02	-0.1106D 02
36.0	10.0	0.5956D 02	0.2699D 02	-0.3969D 02
36.0	14.0	0.6106D 02	-0.4501D 02	-0.3810D 02
36.0	18.0	0.5860D 02	-0.5246D 02	-0.1318D 02
36.0	22.0	0.6118D 02	-0.3123D 01	-0.6404D 02
32.0	-22.0	0.5770D 02	-0.1143D 02	0.1463D 02
32.0	-18.0	0.5846D 02	-0.7016D 01	0.2790D 02
32.0	-14.0	0.5909D 02	-0.4077D 02	-0.4678D 01
32.0	-10.0	0.5897D 02	-0.6372D 01	0.1199D 02
32.0	-6.0	0.5586D 02	-0.2379D 02	-0.9313D 00
32.0	-2.0	0.5925D 02	0.6294D 01	0.4866D 02
32.0	2.0	0.5768D 02	0.1529D 02	0.3150D 00
32.0	6.0	0.5478D 02	-0.1341D 02	-0.1444D 02
32.0	10.0	0.5500D 02	0.3398D 02	0.1984D 02
32.0	14.0	0.5857D 02	0.2087D 02	0.1162D 02
32.0	18.0	0.5902D 02	-0.5226D 02	-0.1528D 02
32.0	22.0	0.5742D 02	-0.1080D 02	-0.2146D 02
28.0	-22.0	0.5672D 02	-0.3231D 00	0.6644D 02
28.0	-18.0	0.5739D 02	0.2661D 02	-0.2973D 02
28.0	-14.0	0.5577D 02	0.2939D 02	-0.1831D 02
28.0	-10.0	0.5608D 02	0.1546D 02	0.1677D 02
28.0	-6.0	0.5562D 02	-0.3588D 02	-0.1154D 02
28.0	-2.0	0.5695D 02	-0.2390D 02	0.4763D 01
28.0	2.0	0.5701D 02	0.7681D 01	-0.6011D-02
28.0	6.0	0.5926D 02	0.3749D 02	-0.5857D 02
28.0	10.0	0.5562D 02	0.8853D 01	-0.4080D 02
28.0	14.0	0.5711D 02	-0.2619D 02	0.3056D 02
28.0	18.0	0.5556D 02	-0.2485D 02	0.5424D 02
28.0	22.0	0.5662D 02	-0.3187D 02	-0.4396D 02

24.0	-22.0	0.5677D 02	-0.3491D 01	-0.1842D 02	
24.0	-18.0	0.5588D 02	-0.1287D 02	0.1987D 02	
24.0	-14.0	0.5432D 02	-0.3150D 02	0.4821D 02	
24.0	-10.0	0.5678D 02	-0.1554D 02	-0.4062D 02	
24.0	-6.0	0.5317D 02	0.7258D 01	-0.2493D 02	
24.0	-2.0	0.5619D 02	-0.1000D 02	0.5263D 00	
24.0	2.0	0.5482D 02	-0.1337D 02	-0.5355D 01	
24.0	6.0	0.5496D 02	-0.2429D 02	-0.2763D 02	
24.0	10.0	0.5551D 02	0.5710D 01	0.2892D 02	
24.0	14.0	0.5443D 02	-0.2649D 02	0.1765D 02	
24.0	18.0	0.5161D 02	-0.5405D 01	0.6088D 01	
24.0	22.0	0.5829D 02	-0.2379D 02	-0.1039D 02	
20.0	-22.0	0.5410D 02	0.5260D 01	0.3674D 02	
20.0	-18.0	0.5399D 02	-0.2256D 02	-0.1643D 02	
20.0	-14.0	0.5605D 02	0.2758D 01	-0.1512D 02	
20.0	-10.0	0.5431D 02	-0.5492D 02	0.1089D 02	
20.0	-6.0	0.5450D 02	-0.1471D 02	0.1859D 00	
20.0	-2.0	0.5204D 02	0.3423D 02	0.5562D 01	
20.0	2.0	0.5433D 02	-0.1116D 01	0.2240D 02	
20.0	6.0	0.5333D 02	0.1364D 02	-0.4445D-01	
20.0	10.0	0.5610D 02	-0.6899D 01	-0.5974D 01	
20.0	14.0	0.5497D 02	-0.2328D 02	0.5228D 00	
20.0	18.0	0.5243D 02	0.4037D 01	-0.1035D 02	
20.0	22.0	0.5306D 02	0.1061D 02	0.2415D 02	
16.0	-22.0	0.5076D 02	-0.2402D 02	-0.3923D 02	
16.0	-18.0	0.5542D 02	-0.1267D 02	-0.1907D 01	
16.0	-14.0	0.4929D 02	-0.1065D 02	0.4705D 02	
16.0	-10.0	0.5066D 02	-0.2820D 02	-0.9434D 01	
16.0	-6.0	0.5106D 02	0.1484D 02	-0.1989D 00	
16.0	-2.0	0.5165D 02	-0.9483D 01	-0.5133D 02	
16.0	2.0	0.4998D 02	-0.2152D 02	-0.7100D 02	
16.0	6.0	0.5043D 02	-0.2972D 02	0.1441D 02	
16.0	10.0	0.4901D 02	0.3228D 02	0.5574D 02	
16.0	14.0	0.5292D 02	-0.9062D 00	-0.4769D 02	
16.0	18.0	0.4654D 02	-0.4781D 01	-0.2006D 02	
16.0	22.0	0.4989D 02	0.5395D 01	0.6174D 01	
12.0	-22.0	0.5032D 02	-0.3829D 02	-0.3604D 02	
12.0	-18.0	0.4753D 02	0.2409D 02	-0.1557D 02	
12.0	-14.0	0.5055D 02	0.2365D 01	-0.4745D 01	
12.0	-10.0	0.5335D 02	0.1970D 02	-0.1936D 02	
12.0	-6.0	0.5028D 02	-0.1398D 02	0.2186D 02	
12.0	-2.0	0.4923D 02	-0.2444D 02	-0.1159D 02	
12.0	2.0	0.4776D 02	-0.9781D 01	0.5644D 01	
12.0	6.0	0.4822D 02	-0.3052D 02	0.6199D 02	
12.0	10.0	0.4944D 02	0.2645D 02	-0.2624D 02	
12.0	14.0	0.5007D 02	-0.5025D 02	-0.4913D 02	
12.0	18.0	0.4855D 02	-0.3068D 02	0.6906D 00	
12.0	22.0	0.4897D 02	-0.2725D 02	-0.8423D 02	
8.0	-22.0	0.4809D 02	-0.7601D 02	0.3308D 02	
8.0	-18.0	0.5135D 02	-0.4899D 01	0.2363D 02	
8.0	-14.0	0.4854D 02	-0.3054D 02	0.5034D 01	
8.0	-10.0	0.4762D 02	0.2960D 02	-0.2485D 02	
8.0	-6.0	0.4577D 02	0.9693D 01	0.2438D 02	
8.0	-2.0	0.4687D 02	-0.8066D 00	0.8497D 01	
8.0	2.0	0.4963D 02	-0.5477D 02	-0.2452D 02	
8.0	6.0	0.4932D 02	0.3931D 02	-0.3800D 02	
8.0	10.0	0.4706D 02	-0.3585D 02	0.2774D 02	
8.0	14.0	0.4542D 02	0.4860D 01	0.2559D 02	
8.0	18.0	0.4728D 02	0.9718D 01	0.3373D 02	
8.0	22.0	0.5122D 02	-0.4970D 01	0.3376D 02	
4.0	-22.0	0.4830D 02	0.1071D 02	-0.1176D 02	
4.0	-18.0	0.4202D 02	0.2144D 02	-0.3679D 02	
4.0	-14.0	0.4555D 02	0.6312D 01	-0.4633D 02	
4.0	-10.0	0.4664D 02	-0.3455D 02	-0.5594D 01	
4.0	-6.0	0.4840D 02	0.7257D 01	0.1738D 02	
4.0	-2.0	0.4663D 02	0.1844D 02	0.2636D 02	
4.0	2.0	0.4342D 02	0.2890D 02	-0.1721D 02	
4.0	6.0	0.4450D 02	-0.3923D 00	-0.1726D 02	
4.0	10.0	0.4141D 02	-0.3216D 02	0.1403D 02	
4.0	14.0	0.4564D 02	0.7142D 01	-0.1035D 01	
4.0	18.0	0.4448D 02	0.1671D 02	0.9686D 01	
4.0	22.0	0.4220D 02	-0.4224D 01	-0.1181D 02	

0.0	-22.0	0.4518D 02	-0.3983D 02	0.2567D 02	
0.0	-18.0	0.4203D 02	-0.1965D 02	0.3801D 02	
0.0	-14.0	0.4431D 02	0.1107D 01	-0.6100D 02	
0.0	-10.0	0.4241D 02	0.3332D 02	0.1267D 02	
0.0	-6.0	0.4297D 02	0.8033D 01	-0.2624D 02	
0.0	-2.0	0.4523D 02	-0.5159D 02	-0.1104D 02	
0.0	2.0	0.4486D 02	0.3655D 01	0.3760D 02	
0.0	6.0	0.4108D 02	0.4736D 01	0.1015D 02	
0.0	10.0	0.4337D 02	0.1791D 02	-0.4631D 02	
0.0	14.0	0.4081D 02	-0.7775D 01	0.9358D 01	
0.0	18.0	0.3884D 02	0.4722D 01	0.2465D 02	
0.0	22.0	0.4425D 02	-0.4852D 01	-0.1049D 02	
-4.0	-22.0	0.4541D 02	-0.1849D 01	-0.1185D 02	
-4.0	-18.0	0.4255D 02	0.1778D 01	-0.2484D 02	
-4.0	-14.0	0.4353D 02	-0.1720D 02	-0.7462D 01	
-4.0	-10.0	0.3954D 02	-0.2792D 02	0.3537D 02	
-4.0	-6.0	0.4496D 02	-0.4143D 02	-0.3234D 02	
-4.0	-2.0	0.4267D 02	-0.6175D 02	-0.1916D 02	
-4.0	2.0	0.4430D 02	0.1722D 02	0.1960D 02	
-4.0	6.0	0.4028D 02	0.2508D 01	-0.5408D 02	
-4.0	10.0	0.3979D 02	0.1049D 02	-0.2173D 01	
-4.0	14.0	0.4332D 02	0.1616D 02	0.3096D 02	
-4.0	18.0	0.4151D 02	-0.5295D 02	-0.1305D 02	
-4.0	22.0	0.4250D 02	-0.4354D 02	-0.3128D 02	
-8.0	-22.0	0.4351D 02	0.2287D 01	-0.8347D 01	
-8.0	-18.0	0.4318D 02	-0.1356D 02	-0.1813D 02	
-8.0	-14.0	0.4009D 02	-0.1717D 00	-0.4081D 02	
-8.0	-10.0	0.4309D 02	-0.8690D 01	0.4029D 02	
-8.0	-6.0	0.3860D 02	0.1597D 02	-0.2451D 02	
-8.0	-2.0	0.4008D 02	0.1743D 02	0.2497D 02	
-8.0	2.0	0.4050D 02	-0.1039D 01	0.2401D 02	
-8.0	6.0	0.4099D 02	-0.1374D 02	-0.5098D 01	
-8.0	10.0	0.3913D 02	0.1155D 02	0.2733D 02	
-8.0	14.0	0.4379D 02	-0.1909D 02	-0.4441D 02	
-8.0	18.0	0.3692D 02	0.9778D 01	0.5428D 02	
-8.0	22.0	0.4184D 02	-0.5639D 01	-0.1433D 02	
-12.0	-22.0	0.4142D 02	-0.4775D 02	0.2039D 02	
-12.0	-18.0	0.3935D 02	-0.3773D 02	0.1240D 02	
-12.0	-14.0	0.4059D 02	-0.1268D 02	0.8951D 01	
-12.0	-10.0	0.4114D 02	-0.2508D 01	-0.3761D 02	
-12.0	-6.0	0.3977D 02	0.1766D 02	-0.5092D 02	
-12.0	-2.0	0.4199D 02	-0.3741D 00	0.3923D 01	
-12.0	2.0	0.3813D 02	0.3151D 02	-0.2499D 02	
-12.0	6.0	0.3777D 02	-0.3544D 01	0.4805D 01	
-12.0	10.0	0.4064D 02	-0.3282D 02	-0.1759D 02	
-12.0	14.0	0.3788D 02	0.4194D 01	-0.1430D 02	
-12.0	18.0	0.3707D 02	-0.5701D 02	0.9123D 01	
-12.0	22.0	0.3792D 02	-0.2385D 02	0.1861D 02	
-16.0	-22.0	0.3911D 02	-0.1958D 02	0.4284D 01	
-16.0	-18.0	0.3916D 02	-0.1189D 02	0.4632D 02	
-16.0	-14.0	0.3845D 02	0.2747D 02	-0.7762D 01	
-16.0	-10.0	0.3857D 02	0.1362D 02	-0.3288D 02	
-16.0	-6.0	0.4045D 02	-0.1385D 02	-0.1065D 02	
-16.0	-2.0	0.4036D 02	-0.1659D 02	-0.6985D 02	
-16.0	2.0	0.3981D 02	-0.3710D 02	-0.6695D 02	
-16.0	6.0	0.3862D 02	0.7486D 01	-0.3884D 02	
-16.0	10.0	0.3638D 02	0.2309D 00	-0.3733D 02	
-16.0	14.0	0.3741D 02	0.5432D 02	-0.2892D 02	
-16.0	18.0	0.3527D 02	0.5582D 01	0.1557D 02	
-16.0	22.0	0.3763D 02	-0.2225D 01	0.1468D 02	
-20.0	-22.0	0.3917D 02	-0.5334D 02	-0.2267D 01	
-20.0	-18.0	0.4038D 02	-0.4258D 02	0.1277D 01	
-20.0	-14.0	0.3639D 02	-0.2569D 02	0.5080D 02	
-20.0	-10.0	0.3703D 02	0.8005D 01	0.2745D 02	
-20.0	-6.0	0.3665D 02	0.1925D 02	0.1083D 02	
-20.0	-2.0	0.3951D 02	-0.4085D 02	-0.2060D 02	
-20.0	2.0	0.3482D 02	-0.2837D 02	-0.5562D 02	
-20.0	6.0	0.3713D 02	-0.3771D 02	0.3536D 02	
-20.0	10.0	0.3770D 02	0.2464D 01	-0.1387D 02	
-20.0	14.0	0.3745D 02	0.1530D 02	0.3267D 01	
-20.0	18.0	0.3683D 02	-0.2324D 01	-0.3425D 01	
-20.0	22.0	0.3534D 02	-0.3977D 02	-0.1430D 02	

* -24.0	-22.0 *	0.4005D 02	0.4204D 01	0.2131D 02	*
* -24.0	-18.0 *	0.3663D 02	-0.1061D 01	0.4215D 02	*
* -24.0	-14.0 *	0.3609D 02	-0.1064D 02	0.9687D 01	*
* -24.0	-10.0 *	0.4043D 02	-0.5798D 02	-0.3752D 02	*
* -24.0	-6.0 *	0.3510D 02	0.1415D 02	-0.2239D 02	*
* -24.0	-2.0 *	0.3742D 02	-0.2236D 02	-0.4100D 02	*
* -24.0	2.0 *	0.3556D 02	0.3267D 01	0.2411D 02	*
* -24.0	6.0 *	0.3389D 02	0.1391D 02	-0.2891D 01	*
* -24.0	10.0 *	0.3450D 02	0.3984D 02	-0.2126D 02	*
* -24.0	14.0 *	0.3401D 02	-0.2295D 02	-0.3090D 02	*
* -24.0	18.0 *	0.3441D 02	0.4774D 02	0.1658D 02	*
* -24.0	22.0 *	0.3480D 02	-0.4542D 02	-0.5239D 02	*
* -28.0	-22.0 *	0.3576D 02	-0.2031D 02	-0.1410D 02	*
* -28.0	-18.0 *	0.3315D 02	0.2472D 02	0.3685D 02	*
* -28.0	-14.0 *	0.3566D 02	-0.7357D 01	0.3960D 02	*
* -28.0	-10.0 *	0.3536D 02	0.4078D 02	-0.1974D 02	*
* -28.0	-6.0 *	0.3256D 02	0.4501D 02	-0.4024D 02	*
* -28.0	-2.0 *	0.3292D 02	0.5882D 01	-0.3036D 02	*
* -28.0	2.0 *	0.3509D 02	0.3511D 00	-0.2798D 02	*
* -28.0	6.0 *	0.3226D 02	-0.8867D 01	-0.1982D 02	*
* -28.0	10.0 *	0.3345D 02	0.2872D 02	0.2735D 02	*
* -28.0	14.0 *	0.3330D 02	-0.7826D 01	-0.1687D 01	*
* -28.0	18.0 *	0.3796D 02	-0.3487D 02	-0.7170D 01	*
* -28.0	22.0 *	0.3549D 02	0.2076D 02	0.6472D 01	*
* -32.0	-22.0 *	0.3165D 02	-0.3936D 01	0.3340D 02	*
* -32.0	-18.0 *	0.3325D 02	-0.1276D 02	0.2384D 02	*
* -32.0	-14.0 *	0.3131D 02	0.2508D 02	-0.5608D 02	*
* -32.0	-10.0 *	0.3377D 02	-0.3046D 02	-0.1736D 02	*
* -32.0	-6.0 *	0.3242D 02	-0.9344D 01	-0.2036D 02	*
* -32.0	-2.0 *	0.3227D 02	0.7217D 01	-0.8601D 01	*
* -32.0	2.0 *	0.2974D 02	0.5520D 02	-0.2411D 02	*
* -32.0	6.0 *	0.3407D 02	0.1718D 02	0.4798D 02	*
* -32.0	10.0 *	0.3172D 02	0.1047D 02	-0.1700D 02	*
* -32.0	14.0 *	0.3252D 02	-0.1975D 02	-0.4271D 01	*
* -32.0	18.0 *	0.3118D 02	-0.4826D 01	-0.1025D 02	*
* -32.0	22.0 *	0.3307D 02	-0.5855D 02	-0.6218D 02	*

STATISTICAL RESULTS:

	MEAN VALUE	STANDARD DEVIATION
X-DIRECTION	0.472D 02	0.945D 01
Y-DIRECTION	-0.714D 01	0.254D 02
Z-DIRECTION	-0.406D 01	0.286D 02

EVALUATED STRAIN FIELD AT POINT (6R)

ELEMENT	EXX	EYY	ELEMENT	EXX	EYY
1, 1	0.68D-03	-0.10D-01	2, 1	0.15D-03	-0.83D-02
1, 2	0.83D-03	0.96D-02	2, 2	0.24D-03	0.10D-01
1, 3	0.67D-04	-0.92D-02	2, 3	0.11D-02	0.20D-01
1, 4	-0.25D-03	-0.83D-03	2, 4	0.86D-03	-0.99D-02
1, 5	0.31D-03	-0.54D-02	2, 5	-0.39D-03	0.78D-03
1, 6	-0.31D-03	0.55D-02	2, 6	0.74D-03	0.22D-02
1, 7	0.12D-02	0.72D-02	2, 7	-0.15D-03	-0.76D-02
1, 8	0.26D-03	0.92D-03	2, 8	0.19D-03	-0.40D-02
1, 9	0.28D-03	0.14D-02	2, 9	-0.16D-03	0.54D-02
1,10	-0.72D-03	-0.10D-01	2,10	0.36D-03	-0.60D-02
1,11	-0.94D-03	0.55D-02	2,11	0.14D-02	0.19D-02
3, 1	0.54D-03	-0.42D-02	4, 1	0.24D-03	-0.11D-02
3, 2	0.17D-04	0.12D-01	4, 2	0.27D-03	0.84D-02
3, 3	-0.12D-03	0.10D-01	4, 3	0.83D-03	-0.86D-02
3, 4	0.42D-03	-0.16D-01	4, 4	0.72D-03	0.44D-02
3, 5	0.17D-02	-0.31D-02	4, 5	0.59D-04	-0.75D-02
3, 6	-0.30D-03	0.21D-01	4, 6	0.57D-03	-0.22D-02
3, 7	0.59D-04	-0.15D-01	4, 7	0.17D-03	0.72D-02
3, 8	0.17D-02	-0.99D-02	4, 8	-0.11D-02	-0.12D-01
3, 9	0.11D-02	0.18D-01	4, 9	-0.15D-03	0.33D-02
3,10	0.62D-03	0.19D-02	4,10	0.37D-03	0.18D-01
3,11	-0.10D-03	-0.12D-01	4,11	0.86D-03	-0.10D-01
5, 1	-0.12D-04	-0.67D-02	6, 1	0.67D-03	0.23D-02
5, 2	0.38D-03	-0.70D-03	6, 2	0.47D-03	0.47D-02
5, 3	0.36D-03	0.35D-02	6, 3	-0.43D-03	-0.40D-02
5, 4	-0.18D-03	0.13D-01	6, 4	0.62D-03	-0.57D-02
5, 5	0.61D-03	-0.30D-02	6, 5	-0.33D-03	0.43D-02
5, 6	0.19D-03	-0.79D-02	6, 6	0.10D-02	0.84D-03
5, 7	0.55D-03	-0.75D-02	6, 7	0.12D-03	0.27D-02
5, 8	0.11D-02	0.72D-02	6, 8	0.41D-03	-0.75D-02
5, 9	0.26D-04	0.88D-02	6, 9	-0.15D-03	0.81D-02
5,10	0.67D-03	-0.33D-03	6,10	-0.14D-03	-0.53D-02
5,11	0.99D-03	0.18D-02	6,11	-0.21D-03	0.46D-02
7, 1	0.83D-03	-0.43D-02	8, 1	0.11D-03	-0.28D-02
7, 2	-0.36D-03	0.50D-02	8, 2	0.20D-02	-0.50D-03
7, 3	0.17D-02	0.14D-01	8, 3	-0.31D-03	0.44D-02
7, 4	0.91D-03	-0.10D-01	8, 4	-0.67D-03	-0.11D-01
7, 5	0.86D-03	-0.12D-01	8, 5	0.20D-03	0.61D-02
7, 6	0.98D-04	0.88D-02	8, 6	0.61D-03	0.30D-02
7, 7	0.11D-02	-0.37D-02	8, 7	0.55D-03	0.20D-02
7, 8	0.73D-03	0.51D-02	8, 8	0.55D-03	-0.15D-01
7, 9	0.18D-02	0.41D-02	8, 9	-0.11D-03	0.83D-02
7,10	0.51D-03	-0.68D-02	8,10	0.71D-03	0.97D-03
7,11	0.15D-02	-0.16D-02	8,11	-0.50D-03	-0.25D-02
9, 1	0.56D-03	-0.16D-01	10, 1	-0.52D-04	-0.18D-01
9, 2	-0.95D-03	0.54D-02	10, 2	0.23D-02	0.64D-02
9, 3	0.50D-03	-0.43D-02	10, 3	0.75D-03	-0.15D-01
9, 4	0.14D-02	0.84D-02	10, 4	0.25D-03	0.50D-02
9, 5	0.11D-02	0.26D-02	10, 5	-0.66D-03	-0.26D-02
9, 6	0.59D-03	-0.37D-02	10, 6	0.60D-04	0.13D-01
9, 7	-0.47D-03	0.52D-02	10, 7	0.16D-02	-0.24D-01
9, 8	-0.28D-03	-0.14D-01	10, 8	0.12D-02	0.19D-01
9, 9	0.60D-03	0.19D-01	10, 9	0.14D-02	-0.10D-01
9,10	0.12D-02	-0.49D-02	10,10	-0.54D-04	-0.12D-02
9,11	0.32D-03	-0.86D-03	10,11	0.70D-03	0.37D-02
11, 1	0.78D-03	-0.27D-02	12, 1	-0.59D-04	-0.50D-02
11, 2	-0.38D-05	0.38D-02	12, 2	-0.13D-03	-0.52D-02
11, 3	0.31D-03	0.10D-01	12, 3	0.20D-03	-0.81D-02
11, 4	0.11D-02	-0.10D-01	12, 4	0.72D-03	0.63D-02
11, 5	0.14D-02	-0.23D-02	12, 5	-0.50D-03	0.15D-01
11, 6	0.35D-03	-0.26D-02	12, 6	0.64D-03	-0.14D-01
11, 7	-0.36D-03	0.73D-02	12, 7	0.14D-03	-0.27D-03
11, 8	0.85D-03	0.79D-02	12, 8	0.20D-03	-0.33D-02

* 11, 9 *	-0.49D-03	-0.98D-03	*	12, 9 *	0.90D-03	0.64D-02	*
* 11,10 *	0.12D-02	-0.24D-02	*	12,10 *	-0.63D-03	-0.31D-02	*
* 11,11 *	0.14D-02	0.52D-02	*	12,11 *	-0.67D-03	0.24D-02	*
* 13, 1 *	0.48D-03	-0.91D-03	*	14, 1 *	0.52D-03	0.40D-02	*
* 13, 2 *	-0.16D-03	0.47D-02	*	14, 2 *	0.96D-03	-0.33D-02	*
* 13, 3 *	0.86D-03	0.27D-02	*	14, 3 *	-0.13D-03	0.21D-02	*
* 13, 4 *	-0.89D-03	0.34D-02	*	14, 4 *	0.49D-03	-0.62D-02	*
* 13, 5 *	0.16D-02	0.51D-02	*	14, 5 *	-0.29D-03	-0.36D-03	*
* 13, 6 *	0.65D-03	-0.20D-01	*	14, 6 *	-0.48D-03	0.46D-02	*
* 13, 7 *	0.95D-03	0.37D-02	*	14, 7 *	0.59D-03	0.32D-02	*
* 13, 8 *	-0.18D-03	-0.20D-02	*	14, 8 *	0.81D-03	-0.63D-02	*
* 13, 9 *	0.16D-03	-0.15D-02	*	14, 9 *	-0.38D-03	0.77D-02	*
* 13,10 *	-0.12D-03	0.17D-01	*	14,10 *	0.15D-02	-0.72D-02	*
* 13,11 *	0.11D-02	-0.24D-02	*	14,11 *	-0.38D-04	0.39D-02	*
* 15, 1 *	0.58D-03	-0.25D-02	*	16, 1 *	-0.14D-04	-0.19D-02	*
* 15, 2 *	0.48D-04	-0.63D-02	*	16, 2 *	-0.31D-03	-0.98D-02	*
* 15, 3 *	0.54D-03	-0.25D-02	*	16, 3 *	0.52D-03	0.35D-02	*
* 15, 4 *	0.64D-03	-0.50D-02	*	16, 4 *	0.38D-03	0.69D-02	*
* 15, 5 *	-0.17D-03	0.45D-02	*	16, 5 *	0.95D-03	0.68D-03	*
* 15, 6 *	0.41D-03	-0.80D-02	*	16, 6 *	0.21D-03	0.51D-02	*
* 15, 7 *	-0.42D-03	0.88D-02	*	16, 7 *	0.12D-02	-0.11D-01	*
* 15, 8 *	-0.21D-03	0.73D-02	*	16, 8 *	0.37D-03	0.18D-02	*
* 15, 9 *	0.11D-02	-0.93D-02	*	16, 9 *	-0.33D-03	-0.14D-01	*
* 15,10 *	0.12D-03	0.15D-01	*	16,10 *	-0.95D-05	0.12D-01	*
* 15,11 *	0.45D-03	-0.83D-02	*	16,11 *	-0.39D-03	0.20D-02	*
* 17, 1 *	-0.22D-03	-0.27D-02	*	18, 1 *	0.11D-02	0.13D-02	*
* 17, 2 *	0.94D-03	-0.42D-02	*	18, 2 *	0.87D-03	0.24D-02	*
* 17, 3 *	0.73D-04	-0.84D-02	*	18, 3 *	0.11D-03	0.12D-01	*
* 17, 4 *	-0.85D-03	-0.28D-02	*	18, 4 *	0.13D-02	-0.18D-01	*
* 17, 5 *	0.39D-03	0.15D-01	*	18, 5 *	0.64D-03	0.91D-02	*
* 17, 6 *	0.52D-03	-0.31D-02	*	18, 6 *	0.11D-02	-0.64D-02	*
* 17, 7 *	-0.18D-03	0.23D-02	*	18, 7 *	0.12D-03	-0.27D-02	*
* 17, 8 *	0.81D-03	-0.10D-01	*	18, 8 *	0.41D-03	-0.65D-02	*
* 17, 9 *	0.80D-03	-0.32D-02	*	18, 9 *	0.26D-03	0.16D-01	*
* 17,10 *	0.86D-03	0.44D-02	*	18,10 *	0.18D-03	-0.18D-01	*
* 17,11 *	0.01D-03	0.94D-02	*	18,11 *	-0.89D-03	0.23D-01	*
* 19, 1 *	0.10D-02	-0.11D-01	*				*
* 19, 2 *	-0.26D-04	0.80D-02	*				*
* 19, 3 *	0.11D-02	-0.12D-01	*				*
* 19, 4 *	0.40D-03	-0.11D-02	*				*
* 19, 5 *	0.37D-04	0.98D-02	*				*
* 19, 6 *	0.16D-03	0.14D-02	*				*
* 19, 7 *	0.13D-02	0.23D-02	*				*
* 19, 8 *	-0.45D-03	-0.94D-02	*				*
* 19, 9 *	0.43D-03	0.91D-02	*				*
* 19,10 *	0.19D-03	0.68D-02	*				*
* 19,11 *	0.17D-02	-0.14D-01	*				*

STATISTICAL RESULTS:

	MEAN VALUE	STANDARD DEVIATION
XX-STRAIN:	0.3901D-03	0.6278D-03
YY-STRAIN:	-0.9204D-04	0.8583D-02

EVALUATED THICKNESS CHANGES (MICRONS)
(COLUMNS: 1- 6)

	1	2	3	4	5	6
1	-2.14	4.32	3.69	-4.04	5.91	4.43
2	-7.08	-6.50	5.46	-0.37	-3.44	0.99
3	2.43	-0.73	2.42	-3.41	0.42	5.98
4	0.83	-7.02	-3.48	2.77	-2.98	2.13
5	-0.37	2.49	-1.14	3.85	4.25	0.56
6	3.87	2.79	-1.51	3.70	-3.34	-3.01
7	1.04	-2.26	2.39	5.99	-0.67	3.78
8	2.80	-1.36	0.60	5.11	-1.32	1.67
9	-6.49	-2.26	2.04	5.54	-0.90	-4.62
10	-4.79	-1.86	3.19	-6.66	-3.50	1.75
11	1.63	4.69	-5.02	-6.01	1.66	0.91
12	3.80	-4.41	3.01	2.53	-5.70	-6.79
13	0.39	-6.33	3.20	-4.47	-3.96	-0.27
14	0.94	6.17	-5.06	-4.61	1.74	3.71
15	1.07	-5.02	5.52	-1.92	5.79	-1.37
16	-3.16	3.80	-0.68	-4.58	3.72	-5.13
17	-2.87	-5.59	0.43	1.36	4.70	-5.80
18	4.92	3.61	-1.36	2.39	-5.37	0.95
19	0.03	-0.57	-1.21	2.58	-0.14	5.50
20	-1.34	-3.40	3.51	1.58	-4.54	6.27

(COLUMNS: 7-12)

	7	8	9	10	11	12
1	-2.64	-3.06	-5.34	5.85	1.04	3.58
2	-6.88	1.21	4.30	-0.67	1.66	-5.74
3	-1.48	4.23	-1.59	0.61	4.87	-2.89
4	4.06	-2.64	4.93	0.46	-5.08	4.39
5	-2.02	-1.93	-5.50	4.84	-0.70	-6.60
6	1.58	3.58	3.13	-4.32	-5.95	-3.60
7	-2.23	-4.67	-3.74	3.62	-1.39	5.77
8	3.04	-1.89	-7.03	0.13	5.97	-4.95
9	3.87	-0.18	-5.30	1.39	-4.89	3.49
10	-3.13	-7.49	5.27	1.36	4.11	-7.26
11	-3.85	6.04	-1.49	3.99	-3.78	0.50
12	-4.57	0.87	-6.74	5.71	-1.44	-5.34
13	5.44	3.71	0.01	0.80	-4.42	-5.22
14	-3.91	-5.37	4.28	-1.07	-4.77	2.86
15	-6.46	-4.19	-1.72	0.08	-1.84	2.40
16	1.96	5.87	-5.68	2.45	1.80	-1.26
17	2.03	-3.84	4.98	-2.73	3.27	-5.24
18	-0.13	-6.28	0.18	-4.85	1.24	5.70
19	3.83	-3.53	3.22	-2.42	2.95	2.28
20	-3.08	-7.11	-1.26	-3.42	-1.88	-5.55

RECONSTRUCTION RESULTS OF INTERFEROGRAM
(6L) OF THE NEWS-PRINT PAPER SAMPLE #38
CUMMULATIVE DEFORMATION)

CO-ORDINATES X	CO-ORDINATES Y	DEFORMATIONS X	DEFORMATIONS Y	DEFORMATIONS Z
44.0	-22.0	0.6340D 02	-0.2292D 02	-0.1813D 02
44.0	-18.0	0.6456D 02	-0.6890D 01	-0.8694D 01
44.0	-14.0	0.6482D 02	0.1607D 02	0.1533D 02
44.0	-10.0	0.6041D 02	-0.1224D 02	-0.3007D 01
44.0	-6.0	0.6395D 02	0.5656D 02	-0.3298D 02
44.0	-2.0	0.6489D 02	0.7747D 01	-0.3415D 02
44.0	2.0	0.6240D 02	-0.3364D 02	-0.4158D 01
44.0	6.0	0.6047D 02	-0.3541D 02	0.3455D 01
44.0	10.0	0.6198D 02	-0.9210D 01	-0.5257D 01
44.0	14.0	0.6420D 02	0.1900D 01	0.3671D 02
44.0	18.0	0.6478D 02	0.1723D 02	0.2427D 02
44.0	22.0	0.6442D 02	-0.6062D 02	-0.3593D 02
40.0	-22.0	0.6107D 02	0.3626D 02	-0.1033D 02
40.0	-18.0	0.6338D 02	-0.1066D 02	-0.6170D 00
40.0	-14.0	0.6211D 02	0.4048D 02	0.6799D 02
40.0	-10.0	0.6419D 02	0.7813D 01	0.3128D 02
40.0	-6.0	0.6469D 02	0.4476D 02	-0.6528D 01
40.0	-2.0	0.6178D 02	-0.1777D 02	0.5240D 01
40.0	2.0	0.6310D 02	-0.2973D 02	0.8312D 01
40.0	6.0	0.6317D 02	-0.1176D 02	-0.3579D 02
40.0	10.0	0.5858D 02	-0.3919D 02	0.1773D 02
40.0	14.0	0.6083D 02	-0.2294D 02	0.4571D 02
40.0	18.0	0.6470D 02	0.1496D 02	-0.4052D 02
40.0	22.0	0.6185D 02	0.1973D 02	-0.3237D 02
36.0	-22.0	0.6128D 02	0.4994D 02	-0.1752D 02
36.0	-18.0	0.6300D 02	0.1800D 02	0.2104D 02
36.0	-14.0	0.6039D 02	0.2145D 02	-0.1733D 02
36.0	-10.0	0.5871D 02	0.1600D 02	-0.1605D 02
36.0	-6.0	0.6059D 02	-0.1463D 01	0.5975D 00
36.0	-2.0	0.5937D 02	-0.2248D 01	0.1542D 02
36.0	2.0	0.6087D 02	0.1295D 02	0.2483D 00
36.0	6.0	0.5813D 02	-0.1661D 02	0.2340D 02
36.0	10.0	0.6211D 02	-0.3083D 02	0.2932D 02
36.0	14.0	0.6044D 02	0.1678D 02	0.3908D 02
36.0	18.0	0.5928D 02	0.2058D 02	0.2349D 02
36.0	22.0	0.5640D 02	-0.2605D 02	0.6345D 02
32.0	-22.0	0.5672D 02	-0.1161D 02	-0.1258D 02
32.0	-18.0	0.6093D 02	0.1146D 02	-0.4896D 02
32.0	-14.0	0.5851D 02	0.5961D 02	-0.2083D 01
32.0	-10.0	0.6108D 02	0.5970D 02	-0.1857D 02
32.0	-6.0	0.5866D 02	0.3914D 01	-0.1014D 02
32.0	-2.0	0.5836D 02	-0.2329D 02	-0.5833D 02
32.0	2.0	0.5806D 02	0.3513D 02	0.1072D 02
32.0	6.0	0.5655D 02	0.2593D 01	-0.5096D 00
32.0	10.0	0.5658D 02	-0.2353D 02	-0.2021D 02
32.0	14.0	0.5584D 02	-0.1121D 02	-0.2490D 02
32.0	18.0	0.6091D 02	0.4956D 01	0.7837D 01
32.0	22.0	0.5631D 02	-0.8878D 01	0.2599D 02
28.0	-22.0	0.5446D 02	-0.2818D 02	-0.6421D 02
28.0	-18.0	0.5883D 02	0.1401D 02	0.3986D 02
28.0	-14.0	0.5963D 02	0.5019D 02	0.2697D 02
28.0	-10.0	0.5336D 02	-0.1697D 02	-0.2705D 02
28.0	-6.0	0.5222D 02	-0.3694D 02	0.1738D 02
28.0	-2.0	0.5866D 02	0.1294D 02	-0.8836D 01
28.0	2.0	0.5406D 02	0.2660D 02	0.5445D 01
28.0	6.0	0.6000D 02	0.1879D 02	0.6716D 02
28.0	10.0	0.5610D 02	0.3087D 02	-0.2846D 02
28.0	14.0	0.5576D 02	-0.1287D 01	-0.2652D 02
28.0	18.0	0.5527D 02	-0.4025D 02	-0.5550D 02
28.0	22.0	0.5755D 02	-0.2433D 02	0.3601D 02

24.0	-22.0	0.5042D 02	-0.4002D 02	0.1386D 02	
24.0	-18.0	0.5409D 02	0.1916D 02	-0.1480D 02	
24.0	-14.0	0.5600D 02	0.4604D 02	-0.6187D 02	
24.0	-10.0	0.5259D 02	-0.4801D 02	0.4091D 02	
24.0	-6.0	0.5217D 02	-0.2986D 02	0.1958D 02	
24.0	-2.0	0.5482D 02	-0.2056D 02	0.4492D 00	
24.0	2.0	0.5776D 02	0.2078D 02	-0.3650D 01	
24.0	6.0	0.5200D 02	0.4124D 02	0.2414D 02	
24.0	10.0	0.5565D 02	0.2613D 02	-0.2332D 02	
24.0	14.0	0.5463D 02	-0.3258D 02	-0.2000D 02	
24.0	18.0	0.5272D 02	0.1009D 02	-0.2195D 02	
24.0	22.0	0.6251D 02	0.3710D 02	-0.2811D 01	
20.0	-22.0	0.5703D 02	0.3220D 02	-0.4856D 02	
20.0	-18.0	0.5096D 02	0.5803D 00	0.1740D 02	
20.0	-14.0	0.5361D 02	0.2419D 01	0.1576D 02	
20.0	-10.0	0.5389D 02	0.7754D 01	0.3799D 01	
20.0	-6.0	0.5360D 02	0.2586D 01	-0.1151D 02	
20.0	-2.0	0.5237D 02	-0.1129D 02	-0.1970D 02	
20.0	2.0	0.5256D 02	0.2790D 01	-0.3434D 02	
20.0	6.0	0.5259D 02	-0.4806D 02	-0.1545D 02	
20.0	10.0	0.5593D 02	0.3866D 02	0.1123D 02	
20.0	14.0	0.5213D 02	0.3476D 01	-0.5809D 01	
20.0	18.0	0.5192D 02	0.1003D 02	0.8062D 01	
20.0	22.0	0.5194D 02	0.7158D 01	-0.1401D 02	
16.0	-22.0	0.5223D 02	-0.5354D 01	0.3573D 02	
16.0	-18.0	0.4926D 02	-0.2713D 02	-0.5778D 01	
16.0	-14.0	0.4857D 02	0.2715D 02	-0.5315D 02	
16.0	-10.0	0.5247D 02	0.1262D 02	0.5358D 01	
16.0	-6.0	0.4958D 02	-0.1799D 02	0.5657D 01	
16.0	-2.0	0.4808D 02	-0.1026D 02	0.4645D 02	
16.0	2.0	0.5509D 02	0.5371D 02	0.6971D 02	
16.0	6.0	0.4919D 02	-0.4504D 02	-0.8009D 01	
16.0	10.0	0.4850D 02	0.2853D 02	-0.7760D 02	
16.0	14.0	0.4985D 02	-0.5704D 02	0.5626D 02	
16.0	18.0	0.5228D 02	0.1587D 02	0.1548D 02	
16.0	22.0	0.5219D 02	0.3454D 02	-0.5954D 01	
12.0	-22.0	0.4951D 02	-0.3683D 02	0.2400D 02	
12.0	-18.0	0.4978D 02	-0.1674D 02	0.1046D 02	
12.0	-14.0	0.4960D 02	-0.1059D 00	0.1481D 02	
12.0	-10.0	0.5060D 02	0.1789D 02	0.2488D 02	
12.0	-6.0	0.4918D 02	-0.4697D 02	-0.3893D 02	
12.0	-2.0	0.4889D 02	0.2966D 02	0.1175D 02	
12.0	2.0	0.4948D 02	0.5443D 01	0.3569D 01	
12.0	6.0	0.4897D 02	-0.2091D 02	-0.6774D 02	
12.0	10.0	0.4813D 02	-0.2356D 02	0.2293D 02	
12.0	14.0	0.4858D 02	0.7150D 01	0.5586D 02	
12.0	18.0	0.4651D 02	-0.2368D 02	-0.1362D 02	
12.0	22.0	0.5276D 02	0.5311D 02	0.6614D 02	
8.0	-22.0	0.5058D 02	0.1579D 02	-0.2994D 02	
8.0	-18.0	0.4558D 02	-0.2228D 01	-0.3369D 02	
8.0	-14.0	0.4966D 02	0.1672D 02	-0.6850D 01	
8.0	-10.0	0.5181D 02	0.3013D 02	0.1883D 02	
8.0	-6.0	0.4494D 02	-0.4288D 01	-0.2309D 02	
8.0	-2.0	0.4497D 02	-0.2373D 02	-0.2736D 02	
8.0	2.0	0.4886D 02	-0.1488D 02	0.1391D 02	
8.0	6.0	0.4926D 02	0.2327D 02	0.3232D 02	
8.0	10.0	0.4722D 02	-0.3236D 02	-0.1737D 02	
8.0	14.0	0.4579D 02	-0.1502D 02	-0.3622D 02	
8.0	18.0	0.4885D 02	0.2243D 02	-0.2131D 02	
8.0	22.0	0.4855D 02	-0.3357D 02	-0.5040D 02	
4.0	-22.0	0.4421D 02	-0.1614D 02	0.1377D 02	
4.0	-18.0	0.4359D 02	-0.1597D 02	0.2384D 02	
4.0	-14.0	0.4567D 02	0.7094D 01	0.2778D 02	
4.0	-10.0	0.4707D 02	0.1571D 02	0.4818D 01	
4.0	-6.0	0.4474D 02	-0.3384D 02	-0.2543D 02	
4.0	-2.0	0.4501D 02	0.1073D 02	-0.4228D 02	
4.0	2.0	0.4793D 02	0.2944D 02	0.3336D 01	
4.0	6.0	0.4271D 02	-0.5566D 02	0.2129D 02	
4.0	10.0	0.4512D 02	0.2283D 02	-0.2502D 02	
4.0	14.0	0.4536D 02	0.1502D 02	-0.8679D 01	
4.0	18.0	0.4902D 02	-0.1590D 02	-0.2148D 02	
4.0	22.0	0.4381D 02	0.2781D 02	0.7807D 01	

0.0	-22.0	0.4249D 02	-0.6118D 01	-0.9731D 01	
0.0	-18.0	0.4319D 02	-0.8130D 01	-0.4483D 02	
0.0	-14.0	0.4101D 02	0.8588D 00	0.5657D 02	
0.0	-10.0	0.4467D 02	-0.4207D 02	-0.2273D 02	
0.0	-6.0	0.4428D 02	-0.1738D 02	0.2649D 02	
0.0	-2.0	0.4387D 02	-0.3022D 02	0.8609D 00	
0.0	2.0	0.4401D 02	0.2158D 02	-0.5979D 02	
0.0	6.0	0.4506D 02	0.3770D 02	0.2377D 01	
0.0	10.0	0.4063D 02	-0.1869D 02	0.2526D 02	
0.0	14.0	0.4094D 02	-0.1487D 02	-0.6095D 01	
0.0	18.0	0.4591D 02	0.1895D 02	-0.3523D 02	
0.0	22.0	0.4242D 02	-0.1172D 02	0.3574D 01	
-4.0	-22.0	0.4132D 02	-0.2267D 01	0.2998D 01	
-4.0	-18.0	0.4336D 02	0.1356D 02	0.1551D 02	
-4.0	-14.0	0.4096D 02	-0.3978D 02	0.1142D 02	
-4.0	-10.0	0.4402D 02	-0.1176D 02	-0.3234D 02	
-4.0	-6.0	0.4146D 02	-0.5981D 01	0.9271D 01	
-4.0	-2.0	0.4281D 02	-0.3106D 02	0.9334D 01	
-4.0	2.0	0.4312D 02	-0.3928D 02	-0.1467D 02	
-4.0	6.0	0.3867D 02	-0.4511D 02	0.6776D 02	
-4.0	10.0	0.4033D 02	-0.4227D 01	-0.6798D 01	
-4.0	14.0	0.4125D 02	0.1462D 02	-0.2919D 02	
-4.0	18.0	0.4031D 02	-0.8851D 01	-0.9915D 01	
-4.0	22.0	0.4192D 02	0.2760D 01	0.2488D 02	
-8.0	-22.0	0.4452D 02	-0.1877D 02	0.1597D 02	
-8.0	-18.0	0.4072D 02	-0.2320D 02	0.2757D 02	
-8.0	-14.0	0.4388D 02	0.1819D 02	0.2615D 02	
-8.0	-10.0	0.4242D 02	0.5774D 01	-0.5193D 02	
-8.0	-6.0	0.4006D 02	0.8298D 01	0.2792D 02	
-8.0	-2.0	0.3818D 02	-0.4339D 02	-0.8997D 01	
-8.0	2.0	0.4203D 02	0.5594D 02	-0.5381D 02	
-8.0	6.0	0.4049D 02	-0.2020D 02	0.1466D 02	
-8.0	10.0	0.3939D 02	0.1193D 01	-0.3295D 02	
-8.0	14.0	0.4290D 02	-0.3328D 01	0.4680D 02	
-8.0	18.0	0.3916D 02	-0.5800D 02	-0.5811D 02	
-8.0	22.0	0.4259D 02	-0.2416D 02	0.1500D 02	
-12.0	-22.0	0.3866D 02	0.9122D 01	-0.3336D 02	
-12.0	-18.0	0.4245D 02	0.3430D 02	-0.2444D 02	
-12.0	-14.0	0.4196D 02	0.1735D 02	-0.2310D 02	
-12.0	-10.0	0.3809D 02	0.2316D 02	0.4126D 02	
-12.0	-6.0	0.3876D 02	-0.1589D 02	0.6214D 02	
-12.0	-2.0	0.3875D 02	-0.3618D 02	-0.2193D 01	
-12.0	2.0	0.4004D 02	-0.1279D 02	0.1632D 02	
-12.0	6.0	0.3908D 02	-0.9485D 01	-0.1081D 02	
-12.0	10.0	0.3813D 02	-0.1792D 02	0.2547D 02	
-12.0	14.0	0.3823D 02	0.2858D 01	0.2379D 02	
-12.0	18.0	0.4000D 02	-0.5683D 01	-0.1616D 02	
-12.0	22.0	0.4006D 02	0.5795D 02	-0.3592D 02	
-16.0	-22.0	0.3870D 02	0.4568D 01	0.3889D 01	
-16.0	-18.0	0.3911D 02	-0.2076D 02	-0.4229D 02	
-16.0	-14.0	0.3859D 02	-0.1705D 02	0.1607D 02	
-16.0	-10.0	0.3693D 02	-0.1852D 02	0.2352D 02	
-16.0	-6.0	0.4234D 02	0.3171D 02	0.2374D 02	
-16.0	-2.0	0.3971D 02	-0.6558D 02	0.5682D 02	
-16.0	2.0	0.3573D 02	-0.1442D 02	0.8315D 02	
-16.0	6.0	0.3654D 02	0.5785D 02	0.2691D 02	
-16.0	10.0	0.4000D 02	-0.6600D 01	0.2680D 02	
-16.0	14.0	0.3938D 02	0.1033D 02	0.2612D 02	
-16.0	18.0	0.3815D 02	-0.1131D 02	-0.2391D 02	
-16.0	22.0	0.3742D 02	-0.6562D 02	-0.9061D 01	
-20.0	-22.0	0.3719D 02	-0.2476D 02	-0.1418D 01	
-20.0	-18.0	0.4062D 02	0.1644D 02	0.6243D 01	
-20.0	-14.0	0.3512D 02	0.3431D 02	-0.6719D 02	
-20.0	-10.0	0.3645D 02	-0.3485D 01	-0.2200D 02	
-20.0	-6.0	0.3842D 02	-0.1822D 02	-0.2689D 01	
-20.0	-2.0	0.3911D 02	0.3001D 02	0.3188D 01	
-20.0	2.0	0.3394D 02	-0.5606D 02	0.5813D 02	
-20.0	6.0	0.4129D 02	-0.3531D 02	-0.5547D 02	
-20.0	10.0	0.3414D 02	-0.4712D-01	0.9395D 01	
-20.0	14.0	0.3464D 02	-0.1869D 02	0.1958D 01	
-20.0	18.0	0.3508D 02	-0.3949D 02	-0.1785D 01	
-20.0	22.0	0.3102D 02	-0.2774D 02	0.9433D 01	

*	-24.0	-22.0	* 0.3476D 02	-0.3837D 01	-0.3257D 02 *
*	-24.0	-18.0	* 0.3511D 02	-0.1512D 01	-0.5521D 02 *
*	-24.0	-14.0	* 0.3374D 02	0.8447D 01	-0.1074D 02 *
*	-24.0	-10.0	* 0.3486D 02	0.2353D 02	0.4143D 02 *
*	-24.0	-6.0	* 0.3190D 02	0.2369D 02	0.2474D 02 *
*	-24.0	-2.0	* 0.3248D 02	-0.2648D 02	0.3976D 02 *
*	-24.0	2.0	* 0.3286D 02	0.3308D 01	-0.3734D 02 *
*	-24.0	6.0	* 0.3023D 02	0.5963D 01	-0.4025D 01 *
*	-24.0	10.0	* 0.3457D 02	0.4639D 01	0.2846D 01 *
*	-24.0	14.0	* 0.3510D 02	-0.5287D 01	0.1366D 02 *
*	-24.0	18.0	* 0.3413D 02	0.1233D 02	-0.3518D 02 *
*	-24.0	22.0	* 0.3292D 02	-0.1874D 02	0.5945D 02 *
*	-28.0	-22.0	* 0.3238D 02	0.1083D 00	0.2334D 02 *
*	-28.0	-18.0	* 0.3098D 02	-0.4214D 02	-0.5759D 02 *
*	-28.0	-14.0	* 0.3272D 02	-0.2295D 02	-0.4524D 02 *
*	-28.0	-10.0	* 0.3299D 02	-0.1167D 02	0.1804D 02 *
*	-28.0	-6.0	* 0.3107D 02	-0.9382D 01	0.4326D 02 *
*	-28.0	-2.0	* 0.3107D 02	0.1890D 02	0.3731D 02 *
*	-28.0	2.0	* 0.3312D 02	-0.4367D 01	0.2687D 02 *
*	-28.0	6.0	* 0.3233D 02	0.1313D 02	0.1678D 02 *
*	-28.0	10.0	* 0.2989D 02	-0.4219D 02	-0.1523D 02 *
*	-28.0	14.0	* 0.3479D 02	-0.8019D 00	0.2451D 01 *
*	-28.0	18.0	* 0.2867D 02	-0.3166D 02	-0.9764D 01 *
*	-28.0	22.0	* 0.3266D 02	-0.3748D 02	-0.2123D 02 *
*	-32.0	-22.0	* 0.3295D 02	0.4804D 01	-0.2669D 02 *
*	-32.0	-18.0	* 0.3233D 02	-0.2122D 02	-0.2569D 02 *
*	-32.0	-14.0	* 0.2879D 02	-0.1441D 02	0.4807D 02 *
*	-32.0	-10.0	* 0.3042D 02	0.2017D 02	0.1015D 02 *
*	-32.0	-6.0	* 0.3262D 02	0.1012D 02	0.2634D 02 *
*	-32.0	-2.0	* 0.3109D 02	0.1018D 02	0.1531D 02 *
*	-32.0	2.0	* 0.3058D 02	-0.5413D 02	0.2007D 02 *
*	-32.0	6.0	* 0.3003D 02	-0.3028D 02	-0.4973D 02 *
*	-32.0	10.0	* 0.3101D 02	-0.2612D 02	0.1881D 02 *
*	-32.0	14.0	* 0.3140D 02	-0.3629D 02	0.1292D 01 *
*	-32.0	18.0	* 0.2881D 02	-0.7227D 02	0.1230D 02 *
*	-32.0	22.0	* 0.3008D 02	-0.2142D 02	0.5970D 02 *

STATISTICAL RESULTS:

	MEAN VALUE	STANDARD DEVIATION
X-DIRECTION	0.469D 02	0.102D 02
Y-DIRECTION	-0.303D 01	0.271D 02
Z-DIRECTION	0.650D 00	0.310D 02

EVALUATED STRAIN FIELD AT POINT (6L)

ELEMENT	EXX	EYY	ELEMENT	EXX	EYY
1, 1	0.56D-03	-0.40D-02	2, 1	-0.50D-04	0.13D-01
1, 2	0.30D-03	-0.57D-02	2, 2	0.93D-04	-0.14D-01
1, 3	0.68D-03	0.71D-02	2, 3	0.43D-03	0.82D-02
1, 4	-0.95D-03	-0.17D-01	2, 4	0.14D-02	-0.92D-02
1, 5	-0.19D-03	0.12D-01	2, 5	0.10D-02	0.16D-01
1, 6	0.78D-03	0.10D-01	2, 6	0.60D-03	0.30D-02
1, 7	-0.17D-03	0.44D-03	2, 7	0.56D-03	-0.45D-02
1, 8	-0.67D-03	-0.66D-02	2, 8	0.13D-02	0.69D-02
1, 9	0.85D-03	-0.28D-02	2, 9	-0.88D-03	-0.41D-02
1,10	0.84D-03	-0.38D-02	2,10	0.97D-04	-0.95D-02
1,11	0.20D-04	0.19D-01	2,11	0.14D-02	-0.12D-02
3, 1	0.11D-02	0.80D-02	4, 1	0.56D-03	-0.58D-02
3, 2	0.52D-03	-0.86D-03	4, 2	0.52D-03	-0.12D-01
3, 3	0.47D-03	0.14D-02	4, 3	-0.28D-03	-0.23D-04
3, 4	-0.59D-03	0.44D-02	4, 4	0.19D-02	0.14D-01
3, 5	0.48D-03	0.20D-03	4, 5	0.16D-02	0.68D-02
3, 6	0.25D-03	-0.38D-02	4, 6	-0.77D-04	-0.15D-01
3, 7	0.70D-03	0.74D-02	4, 7	0.10D-02	0.81D-02
3, 8	0.40D-03	0.36D-02	4, 8	-0.86D-03	0.65D-02
3, 9	0.14D-02	-0.12D-01	4, 9	0.12D-03	-0.31D-02
3,10	0.12D-02	-0.95D-03	4,10	0.20D-04	-0.40D-02
3,11	-0.41D-03	0.12D-01	4,11	0.14D-02	0.35D-02
5, 1	-0.49D-03	-0.11D-01	6, 1	-0.15D-03	-0.15D-01
5, 2	0.12D-02	-0.90D-02	6, 2	0.78D-03	-0.69D-02
5, 3	0.91D-03	0.17D-01	6, 3	0.60D-03	0.24D-01
5, 4	0.19D-03	0.50D-02	6, 4	-0.32D-03	-0.20D-02
5, 5	0.11D-04	-0.12D-01	6, 5	-0.36D-03	-0.48D-02
5, 6	0.96D-03	-0.34D-02	6, 6	0.61D-03	-0.10D-01
5, 7	-0.92D-03	0.20D-02	6, 7	0.13D-02	-0.11D-03
5, 8	0.20D-02	-0.30D-02	6, 8	-0.15D-03	-0.12D-02
5, 9	0.11D-03	0.80D-02	6, 9	-0.70D-04	0.15D-01
5,10	0.28D-03	-0.10D-01	6,10	0.62D-03	-0.11D-01
5,11	0.64D-03	0.16D-01	6,11	0.20D-03	-0.68D-02
7, 1	0.12D-02	0.79D-02	8, 1	0.68D-03	0.54D-02
7, 2	0.42D-03	-0.46D-03	8, 2	-0.13D-03	-0.14D-01
7, 3	0.13D-02	-0.13D-02	8, 3	-0.26D-03	0.36D-02
7, 4	0.36D-03	0.13D-02	8, 4	0.47D-03	0.77D-02
7, 5	0.10D-02	0.35D-02	8, 5	0.10D-03	-0.19D-02
7, 6	0.11D-02	-0.35D-02	8, 6	-0.20D-03	-0.16D-01
7, 7	-0.63D-03	0.13D-01	8, 7	0.14D-02	0.25D-01
7, 8	0.85D-03	-0.22D-01	8, 8	0.55D-04	-0.18D-01
7, 9	0.19D-02	0.88D-02	8, 9	0.93D-04	0.21D-01
7,10	0.57D-03	-0.16D-02	8,10	0.32D-03	-0.18D-01
7,11	-0.89D-04	0.72D-03	8,11	0.14D-02	-0.47D-02
9, 1	-0.27D-03	-0.50D-02	10, 1	0.16D-02	0.45D-02
9, 2	0.11D-02	-0.42D-02	10, 2	0.50D-03	-0.47D-02
9, 3	-0.16D-04	-0.45D-02	10, 3	0.10D-02	-0.34D-02
9, 4	-0.30D-03	0.16D-01	10, 4	0.12D-02	0.86D-02
9, 5	0.11D-02	-0.19D-01	10, 5	0.48D-04	0.49D-02
9, 6	0.98D-03	0.61D-02	10, 6	-0.10D-04	-0.22D-02
9, 7	0.16D-03	0.66D-02	10, 7	0.23D-03	-0.95D-02
9, 8	-0.73D-04	0.66D-03	10, 8	0.16D-02	0.14D-01
9, 9	0.23D-03	-0.77D-02	10, 9	0.53D-03	-0.43D-02
9,10	0.70D-03	-0.77D-02	10,10	0.11D-03	-0.94D-02
9,11	-0.58D-03	-0.19D-01	10,11	-0.42D-04	0.14D-01
11, 1	0.43D-03	-0.44D-04	12, 1	0.29D-03	0.50D-03
11, 2	0.10D-03	-0.58D-02	12, 2	-0.43D-04	-0.22D-02
11, 3	0.12D-02	-0.22D-02	12, 3	0.12D-04	0.11D-01
11, 4	0.60D-03	0.12D-01	12, 4	0.16D-03	-0.62D-02
11, 5	0.12D-03	-0.13D-01	12, 5	0.71D-03	0.32D-02
11, 6	0.29D-03	-0.32D-02	12, 6	0.27D-03	-0.13D-01
11, 7	0.98D-03	-0.21D-01	12, 7	0.22D-03	-0.40D-02
11, 8	-0.59D-03	-0.20D-01	12, 8	0.16D-02	0.14D-01

11, 9	0.11D-02	0.20D-02	12, 9	-0.74D-04	-0.96D-03
11,10	0.11D-02	0.77D-02	12,10	-0.79D-04	-0.85D-02
11,11	0.78D-03	-0.11D-01	12,11	0.14D-02	0.77D-02
13, 1	-0.80D-03	-0.40D-02	14, 1	0.15D-02	0.11D-02
13, 2	0.66D-03	0.13D-01	14, 2	-0.43D-03	-0.10D-01
13, 3	-0.73D-03	-0.70D-02	14, 3	0.48D-03	0.31D-02
13, 4	0.40D-03	-0.14D-02	14, 4	0.11D-02	-0.63D-03
13, 5	0.35D-03	0.63D-02	14, 5	0.33D-03	0.13D-01
13, 6	0.12D-02	0.21D-02	14, 6	-0.14D-03	-0.25D-01
13, 7	0.27D-03	0.15D-02	14, 7	0.50D-03	0.19D-01
13, 8	-0.45D-03	-0.10D-01	14, 8	0.35D-03	-0.53D-02
13, 9	0.24D-03	-0.47D-02	14, 9	0.32D-03	0.11D-02
13,10	-0.41D-03	0.59D-02	14,10	0.12D-02	0.14D-01
13,11	0.29D-03	-0.29D-02	14,11	-0.21D-03	-0.85D-02
15, 1	-0.96D-05	-0.63D-02	16, 1	0.38D-03	0.63D-02
15, 2	0.84D-03	0.42D-02	16, 2	-0.38D-03	-0.93D-03
15, 3	0.84D-03	-0.15D-02	16, 3	0.87D-03	0.37D-03
15, 4	0.29D-03	0.98D-02	16, 4	0.12D-03	-0.13D-01
15, 5	-0.90D-03	0.51D-02	16, 5	0.98D-03	0.24D-01
15, 6	-0.24D-03	-0.58D-02	16, 6	0.15D-03	-0.13D-01
15, 7	0.11D-02	-0.83D-03	16, 7	0.45D-03	-0.18D-01
15, 8	0.63D-03	0.21D-02	16, 8	-0.12D-02	0.16D-01
15, 9	-0.47D-03	-0.52D-02	16, 9	0.15D-02	-0.42D-02
15,10	-0.29D-03	0.21D-02	16,10	0.12D-02	0.54D-02
15,11	0.46D-03	-0.16D-01	16,11	0.77D-03	0.14D-01
17, 1	0.61D-03	-0.10D-01	18, 1	0.59D-03	-0.58D-03
17, 2	0.14D-02	-0.45D-02	18, 2	0.10D-02	-0.25D-02
17, 3	0.35D-03	0.94D-02	18, 3	0.25D-03	-0.38D-02
17, 4	0.40D-03	0.37D-02	18, 4	0.47D-03	-0.38D-04
17, 5	0.16D-02	-0.12D-01	18, 5	0.21D-03	0.13D-01
17, 6	0.17D-02	0.22D-01	18, 6	0.35D-03	-0.74D-02
17, 7	0.27D-03	-0.52D-02	18, 7	-0.64D-04	-0.66D-03
17, 8	0.28D-02	-0.88D-02	18, 8	-0.52D-03	0.33D-03
17, 9	-0.11D-03	0.47D-02	18, 9	0.12D-02	0.25D-02
17,10	-0.11D-03	0.52D-02	18,10	0.76D-04	-0.44D-02
17,11	0.24D-03	-0.29D-02	18,11	0.14D-02	0.78D-02
19, 1	-0.14D-03	0.11D-01			
19, 2	-0.34D-03	-0.48D-02			
19, 3	0.98D-03	-0.28D-02			
19, 4	0.64D-03	-0.57D-03			
19, 5	-0.39D-03	-0.71D-02			
19, 6	-0.69D-05	0.58D-02			
19, 7	0.64D-03	-0.44D-02			
19, 8	0.57D-03	0.14D-01			
19, 9	-0.28D-03	-0.10D-01			
19,10	0.85D-03	0.77D-02			
19,11	-0.37D-04	0.15D-02			

STATISTICAL RESULTS:

	MEAN VALUE	STANDARD DEVIATION
XX-STRAIN:	0.4256D-03	0.6557D-03
YY-STRAIN:	0.3577D-04	0.9564D-02

RECONSTRUCTION RESULTS OF INTERFEROGRAM (7R) OF THE NEWS-PRINT PAPER SAMPLE #38 CUMMULATIVE DEFORMATION).

CO-ORDINATES X	CO-ORDINATES Y	DEFORMATIONS X	DEFORMATIONS Y	DEFORMATIONS Z
44.0	-22.0	0.7376D 02	-0.4352D 02	0.1450D 02
44.0	-18.0	0.7334D 02	0.1012D 02	-0.2524D 00
44.0	-14.0	0.7403D 02	-0.3969D 02	-0.2374D 02
44.0	-10.0	0.7373D 02	-0.7091D 01	-0.2986D 02
44.0	-6.0	0.7290D 02	0.9581D 01	0.4399D 02
44.0	-2.0	0.7007D 02	0.3558D 02	0.1537D 02
44.0	2.0	0.7256D 02	0.4989D 01	-0.7536D 01
44.0	6.0	0.7398D 02	-0.3724D 02	-0.1601D 01
44.0	10.0	0.6963D 02	-0.3161D 02	-0.2084D 01
44.0	14.0	0.7008D 02	-0.4523D 02	-0.2785D 02
44.0	18.0	0.7009D 02	0.7066D-01	-0.1391D 02
44.0	22.0	0.7157D 02	-0.2946D 02	0.2721D 02
40.0	-22.0	0.7096D 02	0.1550D 02	-0.1003D 02
40.0	-18.0	0.6931D 02	0.3866D 02	-0.2078D 02
40.0	-14.0	0.7248D 02	0.9863D 01	-0.6983D 02
40.0	-10.0	0.7414D 02	-0.7150D 02	-0.3170D 02
40.0	-6.0	0.7132D 02	-0.1982D 02	-0.6161D 01
40.0	-2.0	0.7101D 02	0.3081D 02	0.8259D 01
40.0	2.0	0.6694D 02	-0.4256D 02	-0.2549D 02
40.0	6.0	0.7263D 02	-0.1526D 02	0.3789D 02
40.0	10.0	0.6801D 02	0.5766D 01	-0.3180D 01
40.0	14.0	0.7307D 02	-0.3242D 02	-0.5972D 02
40.0	18.0	0.7331D 02	0.5803D 01	0.3030D 02
40.0	22.0	0.7185D 02	0.7108D 01	0.3669D 02
36.0	-22.0	0.7057D 02	0.4444D 01	0.7947D 01
36.0	-18.0	0.6776D 02	0.3170D 02	-0.2309D 02
36.0	-14.0	0.6804D 02	-0.2350D 02	0.1985D 02
36.0	-10.0	0.7010D 02	-0.7335D 02	0.2529D 02
36.0	-6.0	0.7353D 02	-0.1610D 02	0.1923D 02
36.0	-2.0	0.6782D 02	0.1714D 02	-0.1224D 02
36.0	2.0	0.6720D 02	-0.6948D 02	-0.2744D 01
36.0	6.0	0.7100D 02	-0.1470D 02	-0.1052D 02
36.0	10.0	0.6973D 02	0.3895D 02	-0.4761D 02
36.0	14.0	0.7055D 02	-0.4485D 02	-0.4658D 02
36.0	18.0	0.6827D 02	-0.4198D 02	0.1472D 00
36.0	22.0	0.7145D 02	-0.4630D 01	-0.7036D 02
32.0	-22.0	0.6775D 02	-0.2036D 02	0.3619D 01
32.0	-18.0	0.6784D 02	-0.5065D 01	0.3267D 02
32.0	-14.0	0.6927D 02	-0.3341D 02	-0.6972D 01
32.0	-10.0	0.6861D 02	-0.1214D 02	0.5326D 00
32.0	-6.0	0.6453D 02	-0.1473D 02	0.7380D 01
32.0	-2.0	0.6828D 02	0.1125D 02	0.5656D 02
32.0	2.0	0.6818D 02	0.1251D 02	-0.1321D 02
32.0	6.0	0.6378D 02	-0.1232D 02	-0.1695D 02
32.0	10.0	0.6526D 02	0.2310D 02	0.2735D 02
32.0	14.0	0.6909D 02	0.8028D 01	0.1604D 01
32.0	18.0	0.6877D 02	-0.5140D 02	-0.1236D 02
32.0	22.0	0.6721D 02	-0.1255D 02	-0.3183D 02
28.0	-22.0	0.6587D 02	0.7805D 01	0.6651D 02
28.0	-18.0	0.6677D 02	0.2190D 02	-0.3534D 02
28.0	-14.0	0.6575D 02	0.3292D 02	-0.1578D 02
28.0	-10.0	0.6510D 02	0.2493D 02	0.7223D 01
28.0	-6.0	0.6490D 02	-0.2301D 02	-0.2482D 02
28.0	-2.0	0.6716D 02	-0.3124D 02	0.9073D 00
28.0	2.0	0.6709D 02	0.2830D-01	0.1275D 02
28.0	6.0	0.6936D 02	0.2715D 02	-0.6658D 02
28.0	10.0	0.6447D 02	0.1275D 02	-0.3819D 02
28.0	14.0	0.6639D 02	-0.2309D 02	0.4259D 02
28.0	18.0	0.6498D 02	-0.3815D 02	0.5385D 02
28.0	22.0	0.6693D 02	-0.3161D 02	-0.3843D 02

24.0	-22.0	0.6065D 02	0.9521D 01	-0.2782D 02	
24.0	-18.0	0.6533D 02	-0.1142D 02	0.1219D 02	
24.0	-14.0	0.6323D 02	-0.3223D 02	0.6128D 02	
24.0	-10.0	0.6046D 02	-0.5997D 01	-0.5287D 02	
24.0	-6.0	0.6204D 02	0.7586D 01	-0.2017D 02	
24.0	-2.0	0.6525D 02	0.4151D 01	0.4114D 01	
24.0	2.0	0.6452D 02	-0.1425D 02	0.6860D 01	
24.0	6.0	0.6383D 02	-0.2279D 02	-0.2958D 02	
24.0	10.0	0.6543D 02	-0.3919D 01	0.3877D 02	
24.0	14.0	0.6366D 02	-0.3472D 02	0.5007D 01	
24.0	18.0	0.5955D 02	-0.1458D 02	0.1504D 01	
24.0	22.0	0.6737D 02	-0.2766D 02	-0.1894D 02	
20.0	-22.0	0.6285D 02	0.1920D 02	0.3749D 02	
20.0	-18.0	0.6239D 02	0.2025D 02	-0.7900D 01	
20.0	-14.0	0.6376D 02	0.2708D 01	-0.8651D 01	
20.0	-10.0	0.6294D 02	-0.6037D 02	0.9985D 01	
20.0	-6.0	0.6329D 02	-0.8075D 01	0.8253D 01	
20.0	-2.0	0.6049D 02	0.3793D 02	-0.7484D 01	
20.0	2.0	0.6371D 02	-0.1470D 02	0.2108D 02	
20.0	6.0	0.6166D 02	0.1130D 02	0.1421D 01	
20.0	10.0	0.6382D 02	0.5095D 00	-0.6234D 00	
20.0	14.0	0.6281D 02	-0.1708D 02	-0.4877D 01	
20.0	18.0	0.6092D 02	0.1375D 02	-0.9451D 00	
20.0	22.0	0.6238D 02	0.6940D 01	0.1589D 02	
16.0	-22.0	0.6024D 02	-0.3582D 02	-0.4910D 02	
16.0	-18.0	0.6285D 02	-0.1775D 02	0.2772D 01	
16.0	-14.0	0.5738D 02	-0.1189D 01	0.4568D 02	
16.0	-10.0	0.5903D 02	-0.1512D 02	-0.3454D 01	
16.0	-6.0	0.5950D 02	0.1306D 02	-0.6530D 01	
16.0	-2.0	0.5858D 02	0.6154D 00	-0.4619D 02	
16.0	2.0	0.5875D 02	-0.1065D 02	-0.6200D 02	
16.0	6.0	0.5840D 02	-0.1778D 02	0.1015D 02	
16.0	10.0	0.5822D 02	0.1815D 02	0.4329D 02	
16.0	14.0	0.6120D 02	-0.1288D 02	-0.4182D 02	
16.0	18.0	0.5521D 02	-0.8875D 00	-0.9216D 01	
16.0	22.0	0.5922D 02	-0.9419D 01	-0.6728D 01	
12.0	-22.0	0.5787D 02	-0.4295D 02	-0.3547D 02	
12.0	-18.0	0.5562D 02	0.3698D 02	-0.1274D 02	
12.0	-14.0	0.5907D 02	0.1190D 02	-0.1360D 02	
12.0	-10.0	0.6178D 02	0.1432D 02	-0.2687D 02	
12.0	-6.0	0.5802D 02	-0.3029D 01	0.3059D 02	
12.0	-2.0	0.5872D 02	-0.2058D 02	-0.1724D 02	
12.0	2.0	0.5639D 02	-0.1379D 02	0.6964D 01	
12.0	6.0	0.5683D 02	-0.4547D 02	0.7140D 02	
12.0	10.0	0.5835D 02	0.1415D 02	-0.2974D 02	
12.0	14.0	0.5782D 02	-0.6396D 02	-0.4522D 02	
12.0	18.0	0.5727D 02	-0.2457D 02	-0.3870D 01	
12.0	22.0	0.5714D 02	-0.2698D 02	-0.6122D 02	
8.0	-22.0	0.5562D 02	-0.8923D 02	0.4028D 02	
8.0	-18.0	0.5935D 02	-0.3598D 00	0.1568D 02	
8.0	-14.0	0.5692D 02	-0.3595D 02	0.2846D 01	
8.0	-10.0	0.5497D 02	-0.1556D 02	-0.1429D 02	
8.0	-6.0	0.5474D 02	-0.5288D 01	0.2911D 02	
8.0	-2.0	0.5534D 02	-0.6013D 00	0.4974D 01	
8.0	2.0	0.5766D 02	-0.4619D 02	-0.3104D 02	
8.0	6.0	0.5703D 02	0.2628D 02	-0.3446D 02	
8.0	10.0	0.5556D 02	-0.4009D 02	0.2051D 02	
8.0	14.0	0.5332D 02	0.7815D 01	0.1161D 02	
8.0	18.0	0.5486D 02	0.1293D 01	0.3871D 02	
8.0	22.0	0.5949D 02	0.5872D 01	0.4495D 02	
4.0	-22.0	0.5660D 02	0.2110D 02	-0.2462D 02	
4.0	-18.0	0.4956D 02	0.1537D 02	-0.3672D 02	
4.0	-14.0	0.5342D 02	0.8302D 01	-0.4194D 02	
4.0	-10.0	0.5561D 02	-0.3946D 02	-0.1688D 02	
4.0	-6.0	0.5638D 02	0.1922D 02	-0.1642D 02	
4.0	-2.0	0.5467D 02	0.3236D 02	-0.3044D 02	
4.0	2.0	0.5104D 02	0.2182D 02	-0.2975D 02	
4.0	6.0	0.5286D 02	-0.5893D 01	-0.1003D 02	
4.0	10.0	0.4819D 02	-0.2046D 02	0.2545D 02	
4.0	14.0	0.5379D 02	0.2418D 01	0.1031D 01	
4.0	18.0	0.5268D 02	0.3203D 02	0.4531D 01	
4.0	22.0	0.5065D 02	-0.7895D 01	-0.2408D 02	

0.0	-22.0	0.5413D 02	-0.4770D 02	0.1211D 02
0.0	-18.0	0.4999D 02	-0.6641D 01	0.4000D 02
0.0	-14.0	0.5136D 02	0.1555D 02	-0.5033D 02
0.0	-10.0	0.5049D 02	0.2022D 02	0.2020D 02
0.0	-6.0	0.5051D 02	-0.2640D 01	-0.3299D 02
0.0	-2.0	0.5218D 02	-0.5253D 02	-0.1074D 02
0.0	2.0	0.5331D 02	0.1687D 02	0.3007D 02
0.0	6.0	0.4829D 02	0.1994D 02	-0.3326D 01
0.0	10.0	0.5035D 02	0.1303D 02	-0.4193D 02
0.0	14.0	0.4771D 02	-0.5022D 01	0.1554D 02
0.0	18.0	0.4656D 02	-0.1216D 01	0.1181D 02
0.0	22.0	0.5148D 02	-0.1582D 02	-0.7169D 01
-4.0	-22.0	0.5175D 02	0.2616D 01	-0.1434D 02
-4.0	-18.0	0.4935D 02	-0.9843D 01	-0.1010D 02
-4.0	-14.0	0.5099D 02	-0.1456D 02	-0.1129D 02
-4.0	-10.0	0.4631D 02	-0.2138D 02	0.3202D 02
-4.0	-6.0	0.5122D 02	-0.3140D 02	-0.3905D 02
-4.0	-2.0	0.4986D 02	-0.6758D 02	-0.6688D 01
-4.0	2.0	0.5106D 02	0.3195D 02	0.2406D 02
-4.0	6.0	0.4671D 02	-0.3153D 01	-0.4032D 02
-4.0	10.0	0.4663D 02	0.1271D 01	-0.1026D 02
-4.0	14.0	0.5072D 02	0.1190D 02	0.3814D 02
-4.0	18.0	0.4764D 02	-0.4238D 02	-0.3153D 01
-4.0	22.0	0.4973D 02	-0.5084D 02	-0.3300D 02
-8.0	-22.0	0.5115D 02	-0.2117D 01	-0.2235D 02
-8.0	-18.0	0.4985D 02	-0.2298D 02	-0.1369D 02
-8.0	-14.0	0.4635D 02	0.7569D 01	-0.4722D 02
-8.0	-10.0	0.5007D 02	0.1283D 01	0.2821D 02
-8.0	-6.0	0.4465D 02	0.3171D 02	-0.1955D 02
-8.0	-2.0	0.4656D 02	0.1636D 02	0.1116D 02
-8.0	2.0	0.4778D 02	-0.1225D 02	0.1475D 02
-8.0	6.0	0.4788D 02	-0.2553D 02	-0.1145D 02
-8.0	10.0	0.4628D 02	0.1864D 02	0.3774D 02
-8.0	14.0	0.5042D 02	-0.6184D 01	-0.3058D 02
-8.0	18.0	0.4310D 02	-0.2224D 01	0.4227D 02
-8.0	22.0	0.4901D 02	-0.1496D 02	-0.6518D 01
-12.0	-22.0	0.4810D 02	-0.5442D 02	0.1210D 02
-12.0	-18.0	0.4634D 02	-0.2498D 02	0.2672D 02
-12.0	-14.0	0.4664D 02	-0.1840D 02	0.4030D 01
-12.0	-10.0	0.4843D 02	0.5955D 01	-0.4654D 02
-12.0	-6.0	0.4667D 02	0.2076D 02	-0.5138D 02
-12.0	-2.0	0.4968D 02	-0.1080D 02	0.1766D 02
-12.0	2.0	0.4482D 02	0.4020D 02	-0.1200D 02
-12.0	6.0	0.4445D 02	0.1260D 02	0.1989D 02
-12.0	10.0	0.4670D 02	-0.4158D 02	-0.7913D 01
-12.0	14.0	0.4391D 02	0.1492D 02	-0.1070D 02
-12.0	18.0	0.4386D 02	-0.6633D 02	0.6834D 00
-12.0	22.0	0.4453D 02	-0.1944D 02	0.2118D 02
-16.0	-22.0	0.4560D 02	-0.3444D 02	-0.5232D 01
-16.0	-18.0	0.4437D 02	-0.1063D 02	0.3251D 02
-16.0	-14.0	0.4436D 02	0.3860D 02	-0.4772D 01
-16.0	-10.0	0.4580D 02	0.1024D 02	-0.2786D 02
-16.0	-6.0	0.4670D 02	-0.2863D 02	-0.2545D 02
-16.0	-2.0	0.4701D 02	-0.1877D 02	-0.6707D 02
-16.0	2.0	0.4544D 02	-0.2233D 02	-0.6629D 02
-16.0	6.0	0.4377D 02	0.2125D 02	-0.4267D 02
-16.0	10.0	0.4178D 02	-0.8161D 01	-0.2240D 02
-16.0	14.0	0.4366D 02	0.4413D 02	-0.2539D 02
-16.0	18.0	0.4228D 02	0.7796D-01	0.1161D 02
-16.0	22.0	0.4362D 02	0.5762D 01	0.1917D 02
-20.0	-22.0	0.4511D 02	-0.4472D 02	-0.1243D 02
-20.0	-18.0	0.4611D 02	-0.2819D 02	-0.1192D 02
-20.0	-14.0	0.4362D 02	-0.3322D 02	0.6125D 02
-20.0	-10.0	0.4408D 02	-0.6381D 01	0.4208D 02
-20.0	-6.0	0.4289D 02	0.2622D 02	0.1493D 02
-20.0	-2.0	0.4566D 02	-0.3150D 02	-0.3289D 02
-20.0	2.0	0.4045D 02	-0.4034D 02	-0.5519D 02
-20.0	6.0	0.4335D 02	-0.5051D 02	0.2766D 02
-20.0	10.0	0.4407D 02	0.1806D 02	-0.9161D 01
-20.0	14.0	0.4350D 02	0.2212D 02	0.1551D 02
-20.0	18.0	0.4235D 02	-0.3843D-01	-0.1074D 02
-20.0	22.0	0.4217D 02	-0.5446D 02	-0.5645D 01

*	-24.0	-22.0	*	0.4674D 02	0.2289D 00	0.7500D 01	*
*	-24.0	-18.0	*	0.4268D 02	0.9879D 01	0.4912D 02	*
*	-24.0	-14.0	*	0.4309D 02	0.2863D 01	0.1998D 02	*
*	-24.0	-10.0	*	0.4593D 02	-0.5082D 02	-0.4141D 02	*
*	-24.0	-6.0	*	0.4107D 02	0.1163D 02	-0.1070D 02	*
*	-24.0	-2.0	*	0.4311D 02	-0.7186D 01	-0.5436D 02	*
*	-24.0	2.0	*	0.4112D 02	-0.5365D 01	0.1452D 02	*
*	-24.0	6.0	*	0.3884D 02	0.1183D 02	-0.2560D 01	*
*	-24.0	10.0	*	0.3950D 02	0.5524D 02	-0.3440D 02	*
*	-24.0	14.0	*	0.3955D 02	-0.1794D 02	-0.2004D 02	*
*	-24.0	18.0	*	0.4023D 02	0.3478D 02	0.9897D 01	*
*	-24.0	22.0	*	0.4031D 02	-0.5477D 02	-0.6668D 02	*
*	-28.0	-22.0	*	0.4009D 02	-0.1602D 02	-0.1294D 02	*
*	-28.0	-18.0	*	0.3845D 02	0.2493D 02	0.4187D 02	*
*	-28.0	-14.0	*	0.4086D 02	0.1286D 01	0.3919D 02	*
*	-28.0	-10.0	*	0.3997D 02	0.3571D 02	-0.2593D 02	*
*	-28.0	-6.0	*	0.3801D 02	0.6074D 02	-0.2820D 02	*
*	-28.0	-2.0	*	0.3791D 02	0.2037D 02	-0.2388D 02	*
*	-28.0	2.0	*	0.3939D 02	-0.1902D 01	-0.3474D 02	*
*	-28.0	6.0	*	0.3776D 02	-0.2856D 01	-0.1880D 02	*
*	-28.0	10.0	*	0.3862D 02	0.4142D 02	0.1534D 02	*
*	-28.0	14.0	*	0.3853D 02	-0.9682D 01	-0.9737D 01	*
*	-28.0	18.0	*	0.4236D 02	-0.2437D 02	-0.7036D 01	*
*	-28.0	22.0	*	0.4003D 02	0.1679D 02	-0.7877D 01	*
*	-32.0	-22.0	*	0.3653D 02	-0.1603D 02	0.3916D 02	*
*	-32.0	-18.0	*	0.3792D 02	-0.2610D 02	0.1176D 02	*
*	-32.0	-14.0	*	0.3661D 02	0.4076D 02	-0.6022D 02	*
*	-32.0	-10.0	*	0.3921D 02	-0.4186D 02	-0.1226D 02	*
*	-32.0	-6.0	*	0.3702D 02	-0.2360D 02	-0.1910D 02	*
*	-32.0	-2.0	*	0.3782D 02	-0.1749D 01	-0.1988D 02	*
*	-32.0	2.0	*	0.3381D 02	0.6999D 02	-0.3821D 02	*
*	-32.0	6.0	*	0.3821D 02	0.3191D 02	0.5807D 02	*
*	-32.0	10.0	*	0.3631D 02	0.2457D 02	-0.1715D 02	*
*	-32.0	14.0	*	0.3728D 02	-0.5616D 01	-0.1036D 01	*
*	-32.0	18.0	*	0.3610D 02	-0.2001D 02	-0.1111D 02	*
*	-32.0	22.0	*	0.3853D 02	-0.4654D 02	-0.5166D 02	*

STATISTICAL RESULTS:

	MEAN VALUE	STANDARD DEVIATION
X-DIRECTION	0.550D 02	0.111D 02
Y-DIRECTION	-0.661D 01	0.272D 02
Z-DIRECTION	-0.458D 01	0.293D 02

EVALUATED STRAIN FIELD AT POINT (7B)

ELEMENT	EXX	EYY	ELEMENT	EXX	EYY
1, 1	0.70D-03	-0.13D-01	2, 1	0.99D-04	-0.58D-02
1, 2	0.10D-02	0.12D-01	2, 2	0.39D-03	0.72D-02
1, 3	0.39D-03	-0.81D-02	2, 3	0.11D-02	0.20D-01
1, 4	-0.10D-03	-0.42D-02	2, 4	0.10D-02	0.13D-01
1, 5	0.39D-03	-0.65D-02	2, 5	-0.55D-03	0.27D-02
1, 6	-0.23D-03	0.76D-02	2, 6	0.80D-03	0.29D-02
1, 7	0.14D-02	0.11D-01	2, 7	-0.66D-04	-0.68D-02
1, 8	0.34D-03	-0.14D-02	2, 8	0.41D-03	-0.53D-02
1, 9	0.40D-03	0.34D-02	2, 9	-0.43D-03	0.95D-02
1,10	-0.75D-03	-0.11D-01	2,10	0.63D-03	-0.96D-02
1,11	-0.81D-03	0.74D-02	2,11	0.13D-02	-0.33D-03
3, 1	0.70D-03	-0.68D-02	4, 1	0.47D-03	-0.38D-02
3, 2	-0.20D-04	0.14D-01	4, 2	0.27D-03	0.71D-02
3, 3	-0.31D-03	0.12D-01	4, 3	0.88D-03	-0.53D-02
3, 4	0.37D-03	-0.14D-01	4, 4	0.88D-03	0.65D-03
3, 5	0.22D-02	-0.83D-02	4, 5	-0.92D-04	-0.65D-02
3, 6	-0.11D-03	0.22D-01	4, 6	0.28D-03	-0.32D-03
3, 7	-0.25D-03	-0.14D-01	4, 7	0.27D-03	0.62D-02
3, 8	0.18D-02	-0.13D-01	4, 8	-0.14D-02	-0.89D-02
3, 9	0.11D-02	0.21D-01	4, 9	0.20D-03	0.38D-02
3,10	0.37D-03	-0.72D-03	4,10	0.68D-03	0.15D-01
3,11	-0.13D-03	-0.93D-02	4,11	0.95D-03	-0.97D-02
5, 1	-0.20D-03	-0.35D-02	6, 1	0.95D-03	0.52D-02
5, 2	0.36D-03	-0.28D-02	6, 2	0.74D-03	0.52D-02
5, 3	0.63D-03	0.20D-02	6, 3	-0.13D-03	-0.66D-02
5, 4	-0.34D-03	0.12D-01	6, 4	0.88D-03	-0.34D-02
5, 5	0.71D-03	0.21D-02	6, 5	-0.31D-03	0.86D-03
5, 6	0.48D-03	-0.78D-02	6, 6	0.12D-02	0.46D-02
5, 7	0.64D-03	-0.68D-02	6, 7	0.20D-03	0.21D-02
5, 8	0.14D-02	0.36D-02	6, 8	0.54D-03	-0.47D-02
5, 9	-0.24D-03	0.90D-02	6, 9	0.40D-03	0.77D-02
5,10	0.68D-03	0.38D-02	6,10	0.21D-03	-0.50D-02
5,11	0.14D-02	-0.16D-02	6,11	-0.34D-03	0.33D-02
7, 1	0.65D-03	-0.26D-03	8, 1	0.59D-03	-0.45D-02
7, 2	-0.12D-03	0.44D-02	8, 2	0.18D-02	-0.41D-02
7, 3	0.16D-02	0.16D-01	8, 3	-0.42D-03	0.35D-02
7, 4	0.98D-03	-0.13D-01	8, 4	-0.69D-03	-0.70D-02
7, 5	0.95D-03	-0.12D-01	8, 5	0.37D-03	0.31D-02
7, 6	0.48D-03	0.13D-01	8, 6	0.46D-03	0.28D-02
7, 7	0.12D-02	-0.65D-02	8, 7	0.59D-03	0.18D-02
7, 8	0.82D-03	0.27D-02	8, 8	0.39D-03	-0.90D-02
7, 9	0.14D-02	0.44D-02	8, 9	-0.34D-04	-0.78D-02
7,10	0.40D-03	-0.77D-02	8,10	0.85D-03	-0.30D-02
7,11	0.14D-02	0.17D-02	8,11	-0.52D-03	0.21D-02
9, 1	0.56D-03	-0.20D-01	10, 1	-0.25D-03	-0.22D-01
9, 2	-0.93D-03	0.63D-02	10, 2	0.24D-02	0.89D-02
9, 3	0.54D-03	-0.61D-03	10, 3	0.87D-03	-0.13D-01
9, 4	0.17D-02	0.43D-02	10, 4	-0.16D-03	0.52D-02
9, 5	0.82D-03	0.44D-02	10, 5	-0.41D-03	-0.12D-02
9, 6	0.35D-03	-0.17D-02	10, 6	0.17D-03	0.11D-01
9, 7	-0.32D-03	0.79D-02	10, 7	0.17D-02	-0.18D-01
9, 8	-0.51D-04	-0.15D-01	10, 8	0.10D-02	0.17D-01
9, 9	0.70D-03	0.20D-01	10, 9	0.18D-02	-0.12D-01
9,10	0.11D-02	-0.98D-02	10,10	-0.12D-03	0.16D-02
9,11	0.60D-03	0.60D-03	10,11	0.55D-03	-0.11D-02
11, 1	0.62D-03	0.14D-02	12, 1	0.59D-03	-0.10D-01
11, 2	-0.11D-03	0.18D-02	12, 2	0.16D-03	-0.55D-02
11, 3	0.51D-03	0.12D-01	12, 3	0.94D-04	-0.12D-02
11, 4	0.13D-02	-0.15D-01	12, 4	0.10D-02	0.44D-02
11, 5	0.15D-02	-0.33D-02	12, 5	-0.18D-03	0.14D-01
11, 6	0.62D-03	0.26D-02	12, 6	0.58D-03	-0.17D-01
11, 7	-0.57D-03	0.69D-02	12, 7	0.56D-03	-0.77D-03
11, 8	0.11D-02	0.36D-02	12, 8	0.39D-03	0.17D-02

11, 9	-0.54D-03	-0.97D-02	12, 9	0.93D-03	0.45D-02
11,10	0.15D-02	-0.74D-02	12,10	-0.75D-03	-0.95D-03
11,11	0.15D-02	0.10D-01	12,11	-0.27D-03	0.37D-02
13, 1	0.15D-03	0.31D-02	14, 1	0.76D-03	0.52D-02
13, 2	-0.13D-03	0.12D-02	14, 2	0.88D-03	-0.76D-02
13, 3	0.12D-02	0.17D-02	14, 3	-0.73D-04	0.16D-02
13, 4	-0.94D-03	0.25D-02	14, 4	0.41D-03	-0.76D-02
13, 5	0.16D-02	0.90D-02	14, 5	-0.50D-03	0.38D-02
13, 6	0.82D-03	-0.25D-01	14, 6	-0.78D-03	0.72D-02
13, 7	0.82D-03	0.88D-02	14, 7	0.74D-03	0.33D-02
13, 8	-0.28D-03	-0.11D-02	14, 8	0.86D-03	-0.11D-01
13, 9	0.85D-04	-0.27D-02	14, 9	-0.11D-03	0.62D-02
13,10	0.75D-04	0.14D-01	14,10	0.16D-02	-0.99D-03
13,11	0.11D-02	0.21D-02	14,11	-0.19D-03	0.32D-02
15, 1	0.62D-03	-0.74D-02	16, 1	0.12D-03	-0.60D-02
15, 2	0.49D-03	-0.16D-02	16, 2	-0.44D-03	-0.12D-01
15, 3	0.57D-03	-0.61D-02	16, 3	0.19D-03	0.71D-02
15, 4	0.66D-03	-0.37D-02	16, 4	0.43D-03	0.97D-02
15, 5	-0.80D-05	0.79D-02	16, 5	0.95D-03	-0.25D-02
15, 6	0.67D-03	-0.13D-01	16, 6	0.34D-03	0.89D-03
15, 7	-0.16D-03	0.69D-02	16, 7	0.12D-02	-0.11D-01
15, 8	0.17D-03	0.14D-01	16, 8	0.10D-03	0.74D-02
15, 9	0.12D-02	-0.14D-01	16, 9	-0.57D-03	-0.13D-01
15,10	0.61D-04	0.20D-01	16,10	0.42D-04	0.11D-01
15,11	0.39D-03	-0.12D-01	16,11	-0.16D-04	-0.14D-02
17, 1	-0.41D-03	-0.41D-02	18, 1	0.17D-02	-0.24D-02
17, 2	-0.86D-03	0.13D-02	18, 2	0.11D-02	0.18D-02
17, 3	-0.13D-03	-0.67D-02	18, 3	0.56D-03	0.13D-01
17, 4	-0.46D-03	-0.81D-02	18, 4	0.15D-02	-0.16D-01
17, 5	0.45D-03	0.14D-01	18, 5	0.76D-03	0.47D-02
17, 6	0.64D-03	0.22D-02	18, 6	0.13D-02	-0.46D-03
17, 7	-0.17D-03	0.25D-02	18, 7	0.43D-03	-0.43D-02
17, 8	0.11D-02	-0.17D-01	18, 8	0.27D-03	-0.11D-01
17, 9	0.11D-02	-0.10D-02	18, 9	0.22D-03	0.18D-01
17,10	0.99D-03	0.55D-02	18,10	0.26D-03	-0.13D-01
17,11	0.53D-03	0.14D-01	18,11	-0.53D-03	0.22D-01
19, 1	0.89D-03	-0.10D-01			
19, 2	0.13D-03	0.59D-02			
19, 3	0.11D-02	-0.86D-02			
19, 4	0.19D-03	-0.63D-02			
19, 5	0.25D-03	0.10D-01			
19, 6	0.24D-04	0.56D-02			
19, 7	0.14D-02	0.24D-03			
19, 8	-0.11D-03	-0.11D-01			
19, 9	0.58D-03	0.13D-01			
19,10	0.31D-03	0.37D-02			
19,11	0.16D-02	-0.10D-01			

STATISTICAL RESULTS:

	MEAN VALUE	STANDARD DEVIATION
XX-STRAIN:	0.4633D-03	0.6564D-03
YY-STRAIN:	-0.3933D-04	0.9055D-02

EVALUATED THICKNESS CHANGES (MICRONS)
(COLUMNS: 1- 6)

	1	2	3	4	5	6
1	-4.07	-0.32	2.89	6.34	-2.95	1.46
2	4.17	-2.77	-6.07	4.44	4.89	-4.33
3	-2.71	-2.32	-1.36	-5.13	1.52	-6.08
4	-0.93	2.60	-0.15	0.93	-4.85	-2.76
5	-5.62	2.77	-5.71	-1.94	4.96	-0.28
6	4.58	-0.11	-2.36	1.51	-0.70	-2.91
7	-3.56	-7.37	-6.56	-5.76	3.04	5.33
8	3.70	-3.93	-4.11	-1.36	1.65	2.34
9	-5.67	2.79	2.23	-2.74	1.35	5.64
10	-1.17	3.48	4.41	-7.34	-0.80	5.97
11	-2.29	5.22	-1.11	-3.94	3.85	0.10
12	5.87	-5.34	-2.95	-1.43	-3.63	2.90
13	-3.49	0.56	-2.73	-4.69	5.19	-7.39
14	-3.08	3.32	3.06	-3.28	-2.27	7.39
15	-1.35	0.97	3.46	0.44	4.70	-8.74
16	-2.37	5.32	-5.90	1.99	1.91	2.45
17	-3.41	1.29	-0.15	-3.38	2.70	-0.56
18	6.81	-1.35	-4.45	-3.00	0.49	3.30
19	3.83	-2.18	-4.83	5.22	-2.95	-2.11
20	-6.11	3.08	1.39	-1.95	-3.51	4.00

(COLUMNS: 7-12)

	7	8	9	10	11	12
1	3.98	-0.23	-5.51	4.72	-4.31	2.87
2	6.50	-2.72	1.24	1.38	-1.81	-0.25
3	2.58	-4.26	5.61	-0.32	1.30	1.75
4	-1.57	-2.86	3.60	1.33	-1.73	4.77
5	-8.50	-3.01	0.78	-0.77	-1.98	-6.07
6	1.03	1.97	0.24	4.81	4.04	4.97
7	-0.29	4.62	-6.88	0.82	2.37	-3.99
8	2.15	-0.86	3.23	2.46	-0.37	0.53
9	-6.63	-7.51	3.39	-5.44	-4.82	2.65
10	-4.00	-6.50	1.83	0.19	2.01	1.44
11	2.06	-4.43	-0.29	-2.71	4.08	7.69
12	0.86	0.57	1.53	-6.20	5.91	-1.05
13	-2.15	1.11	-1.37	-1.34	0.91	-3.54
14	6.02	-0.98	0.86	-6.43	2.62	-3.06
15	0.81	-1.95	-2.97	-6.86	4.08	4.47
16	-0.22	1.25	-5.83	-3.42	3.53	1.73
17	-4.12	6.16	2.14	-3.01	6.10	-3.25
18	-0.50	-4.30	3.20	1.53	0.93	0.83
19	1.64	0.79	-0.64	-0.77	3.53	6.57
20	1.60	-7.46	-2.76	-6.40	4.66	-7.79

RECONSTRUCTION RESULTS OF INTERFEROGRAM
(7L) OF THE NEWS-PRINT PAPER SAMPLE #38
CUMMULATIVE DEFORMATION)

CO-ORDINATES X	CO-ORDINATES Y	DEFORMATIONS X	DEFORMATIONS Y	DEFORMATIONS Z
44.0	-22.0	0.7571D 02	-0.2897D 02	-0.3187D 02
44.0	-18.0	0.7702D 02	-0.1852D 02	-0.1065D 02
44.0	-14.0	0.7779D 02	0.1638D 02	0.2074D 02
44.0	-10.0	0.7253D 02	-0.5043D 01	0.1384D 02
44.0	-6.0	0.7591D 02	0.4739D 02	-0.3895D 02
44.0	-2.0	0.7791D 02	0.4278D 01	-0.1906D 02
44.0	2.0	0.7479D 02	-0.2421D 02	-0.4066D 01
44.0	6.0	0.7364D 02	-0.1955D 02	-0.3082D 01
44.0	10.0	0.7425D 02	0.1461D 00	-0.1483D 02
44.0	14.0	0.7601D 02	-0.9589D 01	0.5004D 02
44.0	18.0	0.7317D 02	0.2950D 02	0.1768D 02
44.0	22.0	0.7671D 02	-0.5748D 02	-0.3741D 02
40.0	-22.0	0.7276D 02	0.2544D 02	0.4265D 01
40.0	-18.0	0.7574D 02	-0.1485D 02	0.8930D 01
40.0	-14.0	0.7357D 02	0.2913D 02	0.6006D 02
40.0	-10.0	0.7654D 02	0.3168D 01	0.3320D 02
40.0	-6.0	0.7692D 02	0.3087D 02	-0.3877D 00
40.0	-2.0	0.7404D 02	-0.1618D 02	-0.3359D 01
40.0	2.0	0.7486D 02	-0.3499D 02	0.2652D 02
40.0	6.0	0.7617D 02	-0.1274D 01	-0.4121D 02
40.0	10.0	0.7003D 02	-0.4384D 02	0.6514D 01
40.0	14.0	0.7302D 02	-0.3399D 02	0.6052D 02
40.0	18.0	0.7749D 02	0.1871D 02	-0.4284D 02
40.0	22.0	0.7441D 02	0.8011D 01	-0.4266D 02
36.0	-22.0	0.7252D 02	0.3404D 02	-0.1038D 02
36.0	-18.0	0.7494D 02	0.5379D 01	0.2303D 02
36.0	-14.0	0.7196D 02	0.2298D 02	-0.1737D 02
36.0	-10.0	0.7067D 02	0.7216D 01	-0.2382D 02
36.0	-6.0	0.7215D 02	-0.1670D 02	-0.1065D 02
36.0	-2.0	0.7019D 02	0.4059D 01	-0.3992D 01
36.0	2.0	0.7174D 02	0.3042D 02	0.3245D 01
36.0	6.0	0.6919D 02	-0.2962D 01	0.1859D 02
36.0	10.0	0.7249D 02	-0.3081D 02	0.4284D 02
36.0	14.0	0.7126D 02	0.3095D 02	0.4724D 02
36.0	18.0	0.6953D 02	0.8270D 01	0.1146D 02
36.0	22.0	0.6646D 02	-0.3699D 02	0.7152D 02
32.0	-22.0	0.6788D 02	-0.3288D 01	-0.2499D 01
32.0	-18.0	0.7246D 02	0.2485D 02	-0.5163D 02
32.0	-14.0	0.6855D 02	0.4615D 02	0.6013D-01
32.0	-10.0	0.7167D 02	0.4732D 02	-0.1807D 00
32.0	-6.0	0.6897D 02	0.1771D 02	-0.2330D 02
32.0	-2.0	0.6972D 02	-0.1664D 02	-0.6899D 02
32.0	2.0	0.6881D 02	0.3004D 02	0.2267D 02
32.0	6.0	0.6760D 02	0.1940D 02	-0.8623D 00
32.0	10.0	0.6807D 02	-0.1576D 02	-0.2412D 02
32.0	14.0	0.6585D 02	-0.1827D 02	-0.1356D 02
32.0	18.0	0.7202D 02	-0.3426D 01	0.3186D 01
32.0	22.0	0.6695D 02	-0.7899D 01	0.4113D 02
28.0	-22.0	0.6566D 02	-0.2145D 02	-0.6992D 02
28.0	-18.0	0.6924D 02	0.8495D 01	0.4824D 02
28.0	-14.0	0.7016D 02	0.3635D 02	0.1873D 02
28.0	-10.0	0.6376D 02	-0.1158D 02	-0.1943D 02
28.0	-6.0	0.6159D 02	-0.2327D 02	0.3561D 02
28.0	-2.0	0.6999D 02	0.1509D 02	-0.5261D 01
28.0	2.0	0.6221D 02	0.2228D 02	-0.1582D 02
28.0	6.0	0.6878D 02	0.9575D 01	0.7217D 02
28.0	10.0	0.6593D 02	0.1792D 02	0.2662D 02
28.0	14.0	0.6711D 02	0.0662D 01	-0.3931D 02
28.0	18.0	0.6392D 02	0.3538D 02	-0.5709D 02
28.0	22.0	0.6688D 02	-0.1454D 02	0.2442D 02

24.0	-22.0	0.6782D 02	-0.2420D 02	0.2784D 02	
24.0	-18.0	0.6281D 02	0.7065D 01	-0.7226D 01	
24.0	-14.0	0.6441D 02	0.3814D 02	-0.7730D 02	
24.0	-10.0	0.6393D 02	-0.4564D 02	0.5467D 02	
24.0	-6.0	0.6137D 02	-0.4191D 02	0.1412D 02	
24.0	-2.0	0.6422D 02	-0.7412D 01	-0.6053D 01	
24.0	2.0	0.6871D 02	0.2001D 02	-0.1483D 02	
24.0	6.0	0.6087D 02	0.6788D 01	0.2806D 02	
24.0	10.0	0.6488D 02	0.2711D 02	-0.3293D 02	
24.0	14.0	0.6407D 02	-0.3322D 02	-0.2540D 01	
24.0	18.0	0.6122D 02	0.2888D 01	-0.1332D 02	
24.0	22.0	0.7202D 02	0.3688D 02	-0.1071D 02	
20.0	-22.0	0.6627D 02	0.3756D 02	-0.5287D 02	
20.0	-18.0	0.5816D 02	0.1411D 02	0.1499D 01	
20.0	-14.0	0.6151D 02	0.6059D 01	0.2733D 01	
20.0	-10.0	0.6310D 02	0.1368D 01	-0.1057D 01	
20.0	-6.0	0.6136D 02	0.1769D 01	-0.1653D 02	
20.0	-2.0	0.6173D 02	0.5477D 01	-0.1329D 01	
20.0	2.0	0.6084D 02	0.4875D 01	-0.3332D 02	
20.0	6.0	0.6011D 02	-0.4915D 02	-0.1230D 02	
20.0	10.0	0.6474D 02	0.2283D 02	-0.9962D 00	
20.0	14.0	0.5989D 02	-0.6760D 01	0.4142D 00	
20.0	18.0	0.6013D 02	0.1929D 02	0.1027D 01	
20.0	22.0	0.5946D 02	0.1986D 01	-0.9741D 01	
16.0	-22.0	0.6170D 02	0.8147D 01	0.4931D 02	
16.0	-18.0	0.5868D 02	-0.1402D 02	-0.1439D 02	
16.0	-14.0	0.5568D 02	0.1530D 02	-0.5588D 02	
16.0	-10.0	0.5983D 02	0.1239D 02	-0.1980D 01	
16.0	-6.0	0.5660D 02	-0.1265D 02	0.1363D 02	
16.0	-2.0	0.5621D 02	-0.2453D 01	0.4364D 02	
16.0	2.0	0.6396D 02	0.4456D 02	0.6286D 02	
16.0	6.0	0.5676D 02	-0.4364D 02	-0.4606D 01	
16.0	10.0	0.5625D 02	0.1436D 02	-0.6192D 02	
16.0	14.0	0.5752D 02	-0.4442D 02	0.5284D 02	
16.0	18.0	0.5874D 02	0.6972D 01	0.4269D 01	
16.0	22.0	0.5976D 02	0.2323D 02	0.7477D 01	
12.0	-22.0	0.5742D 02	-0.2731D 02	0.1776D 02	
12.0	-18.0	0.5762D 02	-0.2106D 02	0.1043D 02	
12.0	-14.0	0.5904D 02	0.7796D 01	0.2588D 02	
12.0	-10.0	0.5726D 02	0.1076D 02	0.2966D 02	
12.0	-6.0	0.5694D 02	-0.3709D 02	-0.4631D 02	
12.0	-2.0	0.5713D 02	0.4203D 02	0.2304D 02	
12.0	2.0	0.5627D 02	0.3036D 00	-0.4379D 01	
12.0	6.0	0.5561D 02	-0.2686D 02	-0.8465D 02	
12.0	10.0	0.5487D 02	-0.3662D 02	0.2982D 02	
12.0	14.0	0.5580D 02	-0.9092D 01	0.4651D 02	
12.0	18.0	0.5410D 02	-0.7614D 01	-0.1388D 02	
12.0	22.0	0.6220D 02	0.6282D 02	0.6578D 02	
8.0	-22.0	0.5800D 02	0.1937D 01	-0.3831D 02	
8.0	-18.0	0.5311D 02	-0.6350D 01	-0.2225D 02	
8.0	-14.0	0.5770D 02	0.2038D 02	-0.2520D 00	
8.0	-10.0	0.5911D 02	0.1841D 02	0.9175D 00	
8.0	-6.0	0.5181D 02	0.5334D 00	-0.2863D 02	
8.0	-2.0	0.5275D 02	-0.1309D 02	-0.1786D 02	
8.0	2.0	0.5675D 02	-0.2062D 02	0.1644D 02	
8.0	6.0	0.5622D 02	0.2008D 02	-0.2228D 02	
8.0	10.0	0.5524D 02	-0.1647D 02	-0.8319D 01	
8.0	14.0	0.5279D 02	-0.8436D 01	-0.2205D 02	
8.0	18.0	0.5637D 02	0.1695D 02	-0.2427D 02	
8.0	22.0	0.5550D 02	-0.3783D 02	-0.6015D 02	
4.0	-22.0	0.5222D 02	-0.3097D 01	0.2434D 02	
4.0	-18.0	0.5127D 02	-0.1203D 02	0.2899D 02	
4.0	-14.0	0.5306D 02	0.2049D 02	0.2229D 02	
4.0	-10.0	0.5383D 02	0.7660D 01	0.1217D 02	
4.0	-6.0	0.5241D 02	-0.2607D 02	-0.2062D 02	
4.0	-2.0	0.5186D 02	0.7380D 01	-0.4626D 02	
4.0	2.0	0.5556D 02	0.2000D 02	0.1793D 02	
4.0	6.0	0.5084D 02	-0.4170D 02	0.9639D 01	
4.0	10.0	0.5290D 02	0.1364D 02	-0.3673D 02	
4.0	14.0	0.5260D 02	0.2221D 02	-0.1346D 02	
4.0	18.0	0.5748D 02	-0.2347D 01	-0.1224D 02	
4.0	22.0	0.5028D 02	0.2533D 02	0.2776D 02	

0.0	-22.0	0.4885D 02	-0.4015D 01	0.9700D 01	
0.0	-18.0	0.4964D 02	-0.2138D 02	-0.5216D 02	
0.0	-14.0	0.4851D 02	0.3808D 01	0.4295D 02	
0.0	-10.0	0.5186D 02	-0.5316D 02	-0.3169D 02	
0.0	-6.0	0.5087D 02	-0.1592D 02	0.2961D 02	
0.0	-2.0	0.5058D 02	-0.1319D 02	0.3468D 01	
0.0	2.0	0.5116D 02	0.1388D 02	-0.5140D 02	
0.0	6.0	0.5157D 02	-0.4529D 02	0.1643D 02	
0.0	10.0	0.4613D 02	-0.2855D 02	0.2240D 02	
0.0	14.0	0.4738D 02	-0.2124D 02	-0.1848D 02	
0.0	18.0	0.5412D 02	0.3472D 02	-0.1647D 02	
0.0	22.0	0.4862D 02	-0.9304D 01	-0.7953D 00	
-4.0	-22.0	0.4823D 02	-0.1610D 02	0.1988D 01	
-4.0	-18.0	0.4995D 02	0.3478D 01	0.1335D 01	
-4.0	-14.0	0.4742D 02	-0.3254D 02	0.1252D 02	
-4.0	-10.0	0.4995D 02	-0.1907D 02	-0.3367D 02	
-4.0	-6.0	0.4701D 02	0.5045D 01	0.2117D 02	
-4.0	-2.0	0.5087D 02	-0.2836D 02	-0.1053D 02	
-4.0	2.0	0.5051D 02	-0.3893D 02	-0.2129D 02	
-4.0	6.0	0.4585D 02	-0.2984D 02	0.5512D 02	
-4.0	10.0	0.4594D 02	-0.1113D 02	-0.7500D-01	
-4.0	14.0	0.4715D 02	0.1431D 02	-0.3770D 02	
-4.0	18.0	0.4558D 02	-0.1163D 02	-0.1890D 02	
-4.0	22.0	0.4960D 02	0.1551D 02	0.2305D 02	
-8.0	-22.0	0.5063D 02	-0.3437D 02	0.2688D 02	
-8.0	-18.0	0.4769D 02	-0.1543D 02	0.2645D 02	
-8.0	-14.0	0.4932D 02	0.3165D 01	0.3563D 02	
-8.0	-10.0	0.4872D 02	0.1061D 02	-0.4313D 02	
-8.0	-6.0	0.4611D 02	0.2084D 02	0.2069D 02	
-8.0	-2.0	0.4385D 02	-0.3364D 02	0.1219D 02	
-8.0	2.0	0.4808D 02	0.4619D 02	-0.3853D 02	
-8.0	6.0	0.4687D 02	-0.3658D 02	0.2004D 02	
-8.0	10.0	0.4638D 02	-0.8079D 01	-0.4250D 02	
-8.0	14.0	0.5090D 02	0.1164D 02	0.2654D 02	
-8.0	18.0	0.4491D 02	-0.4930D 02	-0.4348D 02	
-8.0	22.0	0.4869D 02	-0.1156D 02	0.4127D 01	
-12.0	-22.0	0.4384D 02	0.1396D 01	-0.2642D 02	
-12.0	-18.0	0.4816D 02	0.4583D 02	-0.3780D 02	
-12.0	-14.0	0.4874D 02	0.1722D 02	-0.1472D 02	
-12.0	-10.0	0.4400D 02	0.1065D 02	0.5063D 02	
-12.0	-6.0	0.4450D 02	-0.2904D 02	0.6730D 02	
-12.0	-2.0	0.4585D 02	-0.2349D 02	-0.2466D 02	
-12.0	2.0	0.4717D 02	-0.8256D 00	0.4142D 01	
-12.0	6.0	0.4503D 02	-0.1465D 02	-0.2784D 02	
-12.0	10.0	0.4358D 02	-0.1340D 02	0.1282D 02	
-12.0	14.0	0.4425D 02	0.2688D 01	0.1334D 02	
-12.0	18.0	0.4732D 02	0.4661D 01	-0.3649D 01	
-12.0	22.0	0.4654D 02	0.6741D 02	-0.3402D 02	
-16.0	-22.0	0.4433D 02	0.2201D 02	0.1103D 02	
-16.0	-18.0	0.4521D 02	-0.2136D 02	-0.2316D 02	
-16.0	-14.0	0.4406D 02	-0.1546D 02	0.7189D 01	
-16.0	-10.0	0.4347D 02	-0.2403D 02	0.2048D 02	
-16.0	-6.0	0.4786D 02	0.3817D 02	0.4045D 02	
-16.0	-2.0	0.4648D 02	-0.5176D 02	0.5649D 02	
-16.0	2.0	0.4196D 02	-0.1499D 02	0.8227D 02	
-16.0	6.0	0.4180D 02	0.4876D 02	0.3198D 02	
-16.0	10.0	0.4789D 02	-0.2047D 01	0.6028D 01	
-16.0	14.0	0.4572D 02	0.1909D 02	0.1917D 02	
-16.0	18.0	0.4347D 02	-0.2155D 02	-0.1642D 02	
-16.0	22.0	0.4521D 02	-0.5160D 02	-0.1183D 02	
-20.0	-22.0	0.4312D 02	-0.8421D 01	0.5337D 01	
-20.0	-18.0	0.4699D 02	0.9600D 01	0.2073D 02	
-20.0	-14.0	0.4042D 02	0.1699D 02	-0.7779D 02	
-20.0	-10.0	0.4187D 02	-0.4023D 01	-0.4001D 02	
-20.0	-6.0	0.4551D 02	-0.3206D 02	-0.4092D 01	
-20.0	-2.0	0.4457D 02	0.4206D 02	0.1492D 02	
-20.0	2.0	0.4076D 02	-0.4608D 02	0.5357D 02	
-20.0	6.0	0.4892D 02	-0.4777D 02	-0.4161D 02	
-20.0	10.0	0.3962D 02	0.1169D 02	0.6829D 01	
-20.0	14.0	0.4056D 02	-0.2749D 02	-0.1329D 02	
-20.0	18.0	0.4180D 02	-0.2449D 02	0.1162D 02	
-20.0	22.0	0.3780D 02	-0.2620D 02	-0.2469D 01	

*	-24.0	-22.0	*	0.4009D 02	-0.1893D 02	-0.1196D 02 *
*	-24.0	-18.0	*	0.4021D 02	0.2249D 01	-0.8353D 02 *
*	-24.0	-14.0	*	0.3907D 02	0.1535D 02	-0.2548D 02 *
*	-24.0	-10.0	*	0.4117D 02	0.9067D 01	0.4233D 02 *
*	-24.0	-6.0	*	0.3653D 02	0.1790D 02	0.1354D 02 *
*	-24.0	-2.0	*	0.3710D 02	-0.2641D 02	0.5642D 02 *
*	-24.0	2.0	*	0.3718D 02	0.2051D 02	-0.2825D 02 *
*	-24.0	6.0	*	0.3441D 02	0.1361D 02	-0.8657D 01 *
*	-24.0	10.0	*	0.3904D 02	-0.3789D 01	0.1918D 02 *
*	-24.0	14.0	*	0.4123D 02	-0.1975D 02	0.4327D 01 *
*	-24.0	18.0	*	0.3846D 02	0.2295D 02	-0.2757D 02 *
*	-24.0	22.0	*	0.3779D 02	-0.9486D 01	0.7458D 02 *
*	-28.0	-22.0	*	0.3971D 02	-0.1160D 02	0.2606D 02 *
*	-28.0	-18.0	*	0.3568D 02	-0.3694D 02	-0.6479D 02 *
*	-28.0	-14.0	*	0.3772D 02	-0.3643D 02	-0.4967D 02 *
*	-28.0	-10.0	*	0.3777D 02	0.3014D 01	0.2946D 02 *
*	-28.0	-6.0	*	0.3510D 02	-0.5867D 01	0.2828D 02 *
*	-28.0	-2.0	*	0.3511D 02	0.1055D 02	0.2871D 02 *
*	-28.0	2.0	*	0.3726D 02	0.7097D 01	0.3527D 02 *
*	-28.0	6.0	*	0.3719D 02	0.2944D 02	0.1656D 02 *
*	-28.0	10.0	*	0.3495D 02	-0.4463D 02	-0.3870D 01 *
*	-28.0	14.0	*	0.4113D 02	-0.1190D 02	0.9726D 01 *
*	-28.0	18.0	*	0.3316D 02	-0.1498D 02	-0.6365D 01 *
*	-28.0	22.0	*	0.3738D 02	-0.2947D 02	-0.3115D 00 *
*	-32.0	-22.0	*	0.3745D 02	-0.1033D 02	-0.3857D 02 *
*	-32.0	-18.0	*	0.3762D 02	-0.3680D 01	-0.1052D 02 *
*	-32.0	-14.0	*	0.3314D 02	-0.2322D 02	0.5360D 02 *
*	-32.0	-10.0	*	0.3490D 02	0.3089D 02	0.3099D 01 *
*	-32.0	-6.0	*	0.3820D 02	0.5020D 01	0.2157D 02 *
*	-32.0	-2.0	*	0.3543D 02	-0.1495D 02	0.3059D 02 *
*	-32.0	2.0	*	0.3568D 02	-0.4068D 02	0.3577D 02 *
*	-32.0	6.0	*	0.3429D 02	-0.4606D 02	-0.6728D 02 *
*	-32.0	10.0	*	0.3482D 02	-0.3755D 02	0.1620D 02 *
*	-32.0	14.0	*	0.3750D 02	-0.3038D 02	-0.8347D 01 *
*	-32.0	18.0	*	0.3365D 02	-0.5857D 02	0.1782D 02 *
*	-32.0	22.0	*	0.3492D 02	-0.1166D 02	0.4139D 02 *

STATISTICAL RESULTS:

	MEAN VALUE	STANDARD DEVIATION
X-DIRECTION	0.548D 02	0.125D 02
Y-DIRECTION	-0.253D 01	0.252D 02
Z-DIRECTION	0.945D 00	0.322D 02

EVALUATED STRAIN FIELD AT POINT (7L)

ELEMENT	EXX	EYY	ELEMENT	EXX	EYY
1, 1	0.74D-03	-0.26D-02	2, 1	0.59D-04	0.10D-01
1, 2	0.32D-03	-0.87D-02	2, 2	0.20D-03	-0.11D-01
1, 3	0.11D-02	0.54D-02	2, 3	0.40D-03	-0.65D-02
1, 4	-0.10D-02	-0.13D-01	2, 4	0.15D-02	-0.69D-02
1, 5	-0.25D-03	0.11D-01	2, 5	0.12D-02	0.12D-01
1, 6	0.97D-03	0.71D-02	2, 6	0.96D-03	0.47D-02
1, 7	-0.17D-04	-0.12D-02	2, 7	0.78D-03	-0.84D-02
1, 8	-0.63D-03	-0.49D-02	2, 8	0.17D-02	0.11D-01
1, 9	0.11D-02	0.24D-02	2, 9	-0.62D-03	-0.25D-02
1,10	0.75D-03	-0.98D-02	2,10	0.44D-03	-0.13D-01
1,11	0.17D-03	0.22D-01	2,11	0.20D-02	0.27D-02
3, 1	0.12D-02	0.72D-02	4, 1	0.56D-03	-0.70D-02
3, 2	0.62D-03	-0.44D-02	4, 2	0.80D-03	-0.53D-02
3, 3	0.85D-03	0.39D-02	4, 3	-0.40D-03	-0.29D-03
3, 4	-0.25D-03	0.60D-02	4, 4	0.20D-02	0.74D-02
3, 5	0.79D-03	-0.52D-02	4, 5	0.18D-02	0.86D-02
3, 6	0.12D-03	-0.66D-02	4, 6	-0.66D-04	-0.12D-01
3, 7	0.73D-03	0.83D-02	4, 7	0.16D-02	0.27D-02
3, 8	0.40D-03	0.70D-02	4, 8	-0.29D-03	0.38D-02
3, 9	0.11D-02	-0.15D-01	4, 9	0.53D-03	0.63D-03
3,10	0.14D-02	0.57D-02	4,10	-0.32D-03	-0.37D-02
3,11	-0.62D-03	0.11D-01	4,11	0.20D-02	0.11D-02
5, 1	-0.54D-03	-0.75D-02	6, 1	0.39D-03	-0.78D-02
5, 2	0.16D-02	-0.70D-02	6, 2	0.12D-02	-0.78D-02
5, 3	0.14D-02	0.12D-01	6, 3	0.73D-03	0.21D-01
5, 4	-0.42D-04	0.29D-02	6, 4	0.21D-03	-0.93D-03
5, 5	0.56D-04	-0.96D-02	6, 5	0.94D-06	-0.86D-02
5, 6	0.14D-02	-0.18D-02	6, 6	0.62D-03	-0.69D-02
5, 7	-0.16D-02	0.32D-02	6, 7	0.20D-02	0.33D-02
5, 8	0.20D-02	-0.21D-02	6, 8	0.19D-03	-0.51D-02
5, 9	0.26D-03	0.28D-02	6, 9	0.34D-04	0.15D-01
5,10	0.76D-03	-0.72D-02	6,10	0.10D-02	-0.90D-02
5,11	0.68D-03	0.12D-01	6,11	0.27D-03	-0.85D-02
7, 1	0.11D-02	0.59D-02	8, 1	0.11D-02	0.55D-02
7, 2	-0.13D-03	0.20D-02	8, 2	0.27D-03	-0.73D-02
7, 3	0.15D-02	0.12D-02	8, 3	-0.84D-03	0.73D-03
7, 4	0.92D-03	-0.10D-03	8, 4	0.64D-03	0.63D-02
7, 5	0.12D-02	-0.93D-03	8, 5	-0.83D-04	-0.25D-02
7, 6	0.14D-02	0.15D-03	8, 6	-0.23D-03	-0.12D-01
7, 7	-0.78D-03	0.14D-01	8, 7	0.19D-02	0.22D-01
7, 8	0.84D-03	-0.18D-01	8, 8	0.29D-03	-0.15D-01
7, 9	-0.21D-02	0.74D-02	8, 9	0.34D-03	0.15D-01
7,10	0.59D-03	-0.65D-02	8,10	0.43D-03	-0.13D-01
7,11	0.35D-03	0.43D-02	8,11	0.12D-02	-0.41D-02
9, 1	-0.14D-03	-0.16D-02	10, 1	0.14D-02	0.21D-02
9, 2	0.11D-02	-0.72D-02	10, 2	0.46D-03	-0.67D-02
9, 3	0.33D-03	-0.74D-03	10, 3	0.12D-02	0.49D-03
9, 4	-0.46D-03	0.12D-01	10, 4	0.13D-02	0.45D-02
9, 5	0.13D-02	-0.20D-01	10, 5	-0.15D-03	0.34D-02
9, 6	0.11D-02	0.10D-01	10, 6	0.22D-03	0.19D-02
9, 7	-0.12D-03	0.68D-02	10, 7	0.30D-03	-0.10D-01
9, 8	-0.15D-03	0.24D-02	10, 8	0.13D-02	0.91D-02
9, 9	-0.93D-04	-0.69D-02	10, 9	0.58D-03	-0.20D-02
9,10	0.75D-03	-0.37D-03	10,10	0.31D-04	-0.63D-02
9,11	-0.57D-03	-0.18D-01	10,11	-0.28D-03	0.14D-01
11, 1	0.84D-03	0.22D-02	12, 1	0.15D-03	0.43D-02
11, 2	0.41D-03	-0.81D-02	12, 2	-0.77D-04	-0.63D-02
11, 3	0.16D-02	0.32D-02	12, 3	-0.23D-03	0.14D-01
11, 4	0.49D-03	0.84D-02	12, 4	0.48D-03	-0.93D-02
11, 5	0.38D-03	-0.84D-02	12, 5	0.97D-03	-0.68D-03
11, 6	0.32D-03	-0.32D-02	12, 6	-0.71D-04	-0.63D-02
11, 7	0.11D-02	0.15D-01	12, 7	0.16D-03	-0.79D-02
11, 8	-0.19D-03	-0.14D-01	12, 8	0.14D-02	0.18D-01

11, 9	0.17D-02	-0.21D-02	12, 9	0.47D-04	-0.18D-02
11,10	0.13D-02	0.61D-02	12,10	0.58D-04	-0.14D-01
11,11	0.84D-03	-0.69D-02	12,11	0.21D-02	0.11D-01
13, 1	-0.60D-03	-0.49D-02	14, 1	0.17D-02	-0.47D-02
13, 2	0.56D-03	0.90D-02	14, 2	-0.12D-03	-0.46D-02
13, 3	-0.47D-03	-0.34D-02	14, 3	0.15D-03	-0.19D-02
13, 4	0.31D-03	-0.60D-02	14, 4	0.12D-02	-0.26D-02
13, 5	0.22D-03	0.84D-02	14, 5	0.40D-03	0.14D-01
13, 6	0.18D-02	0.26D-02	14, 6	-0.50D-03	-0.20D-01
13, 7	0.61D-03	-0.23D-02	14, 7	0.23D-03	0.21D-01
13, 8	-0.26D-03	-0.47D-02	14, 8	0.46D-03	-0.71D-02
13, 9	-0.11D-03	-0.64D-02	14, 9	0.70D-03	-0.49D-02
13,10	-0.94D-03	0.65D-02	14,10	0.17D-02	0.15D-01
13,11	0.17D-03	-0.68D-02	14,11	-0.60D-03	-0.94D-02
15, 1	-0.12D-03	-0.11D-01	16, 1	0.30D-03	0.11D-01
15, 2	0.74D-03	0.72D-02	16, 2	-0.45D-03	-0.15D-02
15, 3	0.12D-02	0.16D-02	16, 3	0.91D-03	0.21D-02
15, 4	0.13D-03	0.99D-02	16, 4	0.40D-03	-0.16D-01
15, 5	-0.84D-03	-0.14D-02	16, 5	0.59D-03	0.22D-01
15, 6	-0.16D-03	-0.57D-02	16, 6	0.48D-03	-0.92D-02
15, 7	0.13D-02	0.35D-02	16, 7	0.30D-03	-0.16D-01
15, 8	0.81D-03	-0.31D-03	16, 8	-0.18D-02	0.13D-01
15, 9	-0.11D-02	-0.40D-02	16, 9	0.21D-02	-0.53D-02
15,10	-0.37D-03	-0.49D-03	16,10	0.13D-02	0.10D-01
15,11	0.96D-03	-0.16D-01	16,11	0.42D-03	-0.75D-02
17, 1	0.76D-03	-0.45D-02	18, 1	0.95D-04	-0.53D-02
17, 2	0.17D-02	-0.18D-02	18, 2	0.11D-02	-0.33D-02
17, 3	0.34D-03	0.53D-02	18, 3	0.34D-03	0.16D-02
17, 4	0.18D-03	0.70D-02	18, 4	0.85D-03	-0.22D-02
17, 5	0.22D-02	-0.19D-01	18, 5	0.36D-03	0.11D-01
17, 6	0.19D-02	0.22D-01	18, 6	0.50D-03	-0.12D-01
17, 7	0.89D-03	0.42D-03	18, 7	-0.21D-04	0.17D-02
17, 8	0.36D-02	-0.15D-01	18, 8	-0.70D-03	0.43D-02
17, 9	0.15D-03	0.98D-02	18, 9	0.10D-02	0.40D-02
17,10	-0.17D-03	-0.75D-03	18,10	0.24D-04	-0.11D-01
17,11	0.83D-03	0.43D-03	18,11	0.13D-02	0.81D-02
19, 1	0.57D-03	0.63D-02			
19, 2	-0.48D-03	-0.13D-03			
19, 3	0.11D-02	-0.99D-02			
19, 4	0.72D-03	0.22D-02			
19, 5	-0.78D-03	-0.41D-02			
19, 6	-0.80D-04	0.86D-03			
19, 7	0.40D-03	-0.56D-02			
19, 8	0.72D-03	0.19D-01			
19, 9	0.31D-04	-0.82D-02			
19,10	0.91D-03	0.77D-03			
19,11	-0.12D-03	0.36D-02			

STATISTICAL RESULTS:

	MEAN VALUE	STANDARD DEVIATION
XX-STRAIN:	0.5275D-03	0.7847D-03
YY-STRAIN:	-0.2402D-04	0.8914D-02

RECONSTRUCTION RESULTS OF INTERFEROGRAM
(8R) OF THE NEWS-PRINT PAPER SAMPLE #38
CUMMULATIVE DEFORMATION)

CO-ORDINATES X	CO-ORDINATES Y	DEFORMATIONS X	DEFORMATIONS Y	DEFORMATIONS Z
44.0	-22.0	0.8634D 02	-0.4861D 02	-0.2131D 01
44.0	-18.0	0.8607D 02	-0.1912D 01	-0.6220D 00
44.0	-14.0	0.8648D 02	-0.2674D 02	-0.3914D 02
44.0	-10.0	0.8579D 02	0.1017D 02	-0.1618D 02
44.0	-6.0	0.8470D 02	0.2049D 02	0.5328D 02
44.0	-2.0	0.8252D 02	0.4088D 02	0.2700D 02
44.0	2.0	0.8559D 02	-0.1345D 02	-0.2213D 02
44.0	6.0	0.8614D 02	-0.1616D 02	-0.1481D 02
44.0	10.0	0.8229D 02	-0.4196D 02	0.7640D 01
44.0	14.0	0.8312D 02	-0.7481D 02	-0.2454D 02
44.0	18.0	0.8167D 02	0.3002D 02	-0.2269D 02
44.0	22.0	0.8487D 02	-0.4616D 02	0.1111D 02
40.0	-22.0	0.8291D 02	0.9619D 01	-0.1642D 02
40.0	-18.0	0.8134D 02	0.4147D 02	-0.2654D 02
40.0	-14.0	0.8455D 02	0.7393D 00	-0.7173D 02
40.0	-10.0	0.8059D 02	-0.7614D 02	-0.1956D 02
40.0	-6.0	0.8349D 02	-0.3445D 02	0.1164D 02
40.0	-2.0	0.8244D 02	-0.1224D 02	-0.2700D 01
40.0	2.0	0.7863D 02	-0.4408D 02	-0.1977D 02
40.0	6.0	0.8414D 02	0.3234D 01	0.3728D 02
40.0	10.0	0.8112D 02	0.1093D 02	-0.9556D 01
40.0	14.0	0.8511D 02	-0.4292D 02	-0.6430D 02
40.0	18.0	0.8512D 02	0.8077D 01	0.3093D 02
40.0	22.0	0.8358D 02	-0.6278D 00	0.4233D 02
36.0	-22.0	0.8163D 02	0.1769D 02	0.2401D 02
36.0	-18.0	0.7995D 02	0.1593D 02	-0.2008D 02
36.0	-14.0	0.7999D 02	-0.4012D 02	0.3212D 02
36.0	-10.0	0.8209D 02	-0.8727D 02	0.3026D 02
36.0	-6.0	0.8513D 02	-0.3261D 02	0.3311D 02
36.0	-2.0	0.7976D 02	0.6827D 01	-0.2314D 02
36.0	2.0	0.7842D 02	-0.5670D 02	0.1466D 00
36.0	6.0	0.8213D 02	-0.3845D 01	-0.3223D 01
36.0	10.0	0.8018D 02	0.4970D 02	-0.6005D 02
36.0	14.0	0.8204D 02	-0.3939D 02	-0.6569D 02
36.0	18.0	0.8003D 02	-0.4354D 02	-0.9167D 01
36.0	22.0	0.8283D 02	-0.5334D 01	-0.7576D 02
32.0	-22.0	0.7901D 02	-0.2509D 02	0.1725D 02
32.0	-18.0	0.7974D 02	-0.2537D 02	0.3105D 02
32.0	-14.0	0.8022D 02	-0.3297D 02	-0.2749D 01
32.0	-10.0	0.8137D 02	-0.2309D 02	-0.3933D 01
32.0	-6.0	0.7554D 02	-0.7801D 01	0.5622D 01
32.0	-2.0	0.7903D 02	0.3016D 02	0.4840D 02
32.0	2.0	0.7939D 02	0.2066D 02	-0.1854D 02
32.0	6.0	0.7528D 02	-0.2994D 02	-0.2026D 02
32.0	10.0	0.7668D 02	0.1337D 02	0.2078D 02
32.0	14.0	0.8020D 02	0.1104D 02	-0.8237D 01
32.0	18.0	0.7971D 02	-0.4132D 02	0.1474D 01
32.0	22.0	0.7915D 02	-0.3600D 02	-0.4244D 02
28.0	-22.0	0.7638D 02	0.4730D 01	0.8259D 02
28.0	-18.0	0.7762D 02	0.2227D 02	-0.3161D 02
28.0	-14.0	0.7885D 02	0.3569D 02	-0.2064D 02
28.0	-10.0	0.7585D 02	0.4453D 02	0.1896D 02
28.0	-6.0	0.7588D 02	-0.2422D 02	-0.2902D 02
28.0	-2.0	0.7834D 02	-0.4145D 02	-0.1892D 02
28.0	2.0	0.7697D 02	-0.4624D 01	0.1765D 02
28.0	6.0	0.7982D 02	0.4597D 02	-0.7278D 02
28.0	10.0	0.7537D 02	0.1495D 01	-0.3722D 02
28.0	14.0	0.7794D 02	-0.2662D 02	0.4091D 02
28.0	18.0	0.7598D 02	-0.3744D 02	0.3904D 02
28.0	22.0	0.7729D 02	-0.2201D 02	-0.2636D 02

24.0	-22.0	0.7727D 02	-0.8250D 01	-0.3447D 02	
24.0	-18.0	0.7533D 02	-0.1858D 01	-0.2292D 02	
24.0	-14.0	0.7328D 02	-0.1404D 02	-0.4864D 02	
24.0	-10.0	0.7674D 02	0.1010D 02	-0.6764D 02	
24.0	-6.0	0.7366D 02	-0.2598D 01	-0.3554D 02	
24.0	-2.0	0.7621D 02	-0.1816D 02	-0.1383D 02	
24.0	2.0	0.7536D 02	-0.3119D 02	-0.9032D 00	
24.0	6.0	0.7423D 02	-0.2890D 02	-0.1836D 02	
24.0	10.0	0.7556D 02	-0.1411D 01	0.4906D 02	
24.0	14.0	0.7420D 02	-0.4408D 02	0.1790D 02	
24.0	18.0	0.7012D 02	-0.1920D 02	-0.3104D 01	
24.0	22.0	0.7693D 02	-0.9336D 01	-0.3803D 01	
20.0	-22.0	0.7292D 02	0.2713D 02	0.4892D 02	
20.0	-18.0	0.7268D 02	0.8928D 01	-0.1027D 02	
20.0	-14.0	0.7426D 02	-0.4583D 01	-0.2299D 02	
20.0	-10.0	0.7240D 02	-0.4537D 02	0.2463D 02	
20.0	-6.0	0.7342D 02	-0.9524D 01	0.1602D 02	
20.0	-2.0	0.7088D 02	0.3515D 02	-0.1831D 02	
20.0	2.0	0.7378D 02	-0.2004D 02	0.2661D 02	
20.0	6.0	0.7247D 02	-0.8126D 01	-0.1143D 02	
20.0	10.0	0.7392D 02	0.4120D 01	0.4989D 00	
20.0	14.0	0.7358D 02	-0.2760D 02	-0.2238D 02	
20.0	18.0	0.7165D 02	-0.3424D 01	-0.1048D 02	
20.0	22.0	0.7201D 02	0.1255D 02	0.3063D 02	
16.0	-22.0	0.7038D 02	-0.2315D 02	-0.5952D 02	
16.0	-18.0	0.7322D 02	-0.2297D 02	0.2987D 01	
16.0	-14.0	0.6775D 02	-0.1157D 02	0.4728D 02	
16.0	-10.0	0.6919D 02	-0.1128D 02	0.2799D 01	
16.0	-6.0	0.6919D 02	0.1321D 02	-0.2212D 02	
16.0	-2.0	0.6888D 02	-0.2231D 02	-0.4462D 02	
16.0	2.0	0.6851D 02	-0.8760D 01	-0.7128D 02	
16.0	6.0	0.6863D 02	-0.2651D 02	0.2479D 02	
16.0	10.0	0.6762D 02	0.2959D 02	0.2633D 02	
16.0	14.0	0.7026D 02	0.2928D 01	-0.3277D 02	
16.0	18.0	0.6432D 02	-0.3100D 01	0.8468D 01	
16.0	22.0	0.6932D 02	-0.2229D 02	-0.4989D 01	
12.0	-22.0	0.6752D 02	-0.4037D 02	-0.4166D 02	
12.0	-18.0	0.6468D 02	0.5384D 02	-0.1464D 02	
12.0	-14.0	0.6825D 02	0.2393D 02	-0.3264D 02	
12.0	-10.0	0.7104D 02	0.2189D 02	-0.8011D 01	
12.0	-6.0	0.6708D 02	-0.4247D 01	0.4726D 02	
12.0	-2.0	0.6615D 02	-0.3442D 02	-0.2306D 01	
12.0	2.0	0.6601D 02	-0.3089D 02	-0.8427D 01	
12.0	6.0	0.6617D 02	-0.4599D 02	0.7283D 02	
12.0	10.0	0.6717D 02	0.2203D 02	-0.1793D 02	
12.0	14.0	0.6684D 02	-0.5042D 02	-0.3764D 02	
12.0	18.0	0.6664D 02	-0.2178D 02	-0.2166D 02	
12.0	22.0	0.6638D 02	-0.3459D 02	-0.4979D 02	
8.0	-22.0	0.6526D 02	-0.1003D 03	0.2853D 02	
8.0	-18.0	0.6850D 02	0.6567D 01	0.2498D 02	
8.0	-14.0	0.6552D 02	-0.3537D 02	0.2047D 01	
8.0	-10.0	0.6365D 02	0.1540D 02	-0.7173D 01	
8.0	-6.0	0.6354D 02	-0.1827D 02	0.2469D 02	
8.0	-2.0	0.6491D 02	-0.1870D 02	0.1476D 02	
8.0	2.0	0.6663D 02	-0.6121D 02	-0.3615D 02	
8.0	6.0	0.6634D 02	0.6160D 01	-0.4892D 02	
8.0	10.0	0.6500D 02	-0.5479D 02	0.1333D 02	
8.0	14.0	0.6164D 02	-0.2120D 01	0.1602D 02	
8.0	18.0	0.6337D 02	-0.2493D 01	0.4624D 02	
8.0	22.0	0.6816D 02	-0.1273D 01	0.6048D 02	
4.0	-22.0	0.6468D 02	-0.2075D 02	-0.9941D 01	
4.0	-18.0	0.5768D 02	0.2664D 02	-0.5126D 02	
4.0	-14.0	0.6154D 02	0.8144D 01	-0.5493D 02	
4.0	-10.0	0.6365D 02	-0.3127D 02	-0.2662D 02	
4.0	-6.0	0.6464D 02	0.1782D 02	0.6781D 01	
4.0	-2.0	0.6316D 02	0.2409D 02	0.1906D 02	
4.0	2.0	0.5956D 02	0.2210D 01	-0.3360D 02	
4.0	6.0	0.6141D 02	-0.2226D 02	0.3059D 01	
4.0	10.0	0.5625D 02	-0.2578D 02	0.3736D 02	
4.0	14.0	0.6181D 02	0.2956D 01	-0.8475D 01	
4.0	18.0	0.6043D 02	0.4141D 02	0.1413D 02	
4.0	22.0	0.5903D 02	-0.1319D 02	-0.1415D 02	

0.0	-22.0	0.6272D 02	-0.6733D 02	0.2749D 02	
0.0	-18.0	0.5830D 02	-0.1320D 02	0.3210D 02	
0.0	-14.0	0.5915D 02	0.1597D 02	-0.5948D 02	
0.0	-10.0	0.5799D 02	0.3222D 02	0.2870D 02	
0.0	-6.0	0.5865D 02	-0.7781D 01	-0.3406D 02	
0.0	-2.0	0.6041D 02	-0.5759D 02	-0.6446D 00	
0.0	2.0	0.6148D 02	0.2058D 02	0.3975D 02	
0.0	6.0	0.5659D 02	0.7671D 01	-0.8254D 01	
0.0	10.0	0.5830D 02	0.9772D 01	-0.5930D 02	
0.0	14.0	0.5521D 02	0.4375D 01	0.9246D 01	
0.0	18.0	0.5442D 02	0.4333D 01	-0.5343D 01	
0.0	22.0	0.5904D 02	-0.3235D 01	-0.2751D 00	
-4.0	-22.0	0.5978D 02	-0.1558D 01	-0.7740D 01	
-4.0	-18.0	0.5699D 02	-0.2054D 02	0.1237D 01	
-4.0	-14.0	0.5880D 02	-0.2566D 02	0.2946D 01	
-4.0	-10.0	0.5361D 02	-0.1606D 02	0.2762D 02	
-4.0	-6.0	0.5870D 02	-0.3041D 02	-0.2171D 02	
-4.0	-2.0	0.5810D 02	-0.7934D 02	-0.2022D 02	
-4.0	2.0	0.5913D 02	0.1164D 02	0.1649D 02	
-4.0	6.0	0.5399D 02	0.6206D 00	-0.3217D 02	
-4.0	10.0	0.5422D 02	0.9942D 01	-0.2007D 02	
-4.0	14.0	0.5813D 02	0.1309D 02	0.2652D 02	
-4.0	18.0	0.5513D 02	-0.3414D 02	-0.1319D 02	
-4.0	22.0	0.5699D 02	-0.4581D 02	-0.2650D 02	
-8.0	-22.0	0.5850D 02	-0.1210D 02	-0.1169D 02	
-8.0	-18.0	0.5719D 02	-0.3128D 02	-0.2967D 01	
-8.0	-14.0	0.5294D 02	0.2585D 02	-0.3184D 02	
-8.0	-10.0	0.5681D 02	0.1707D 02	0.3137D 02	
-8.0	-6.0	0.5171D 02	0.3728D 02	-0.2883D 02	
-8.0	-2.0	0.5371D 02	0.1938D 02	0.2873D 02	
-8.0	2.0	0.5553D 02	-0.2666D 01	0.4458D 01	
-8.0	6.0	0.5523D 02	-0.3509D 02	-0.1325D 02	
-8.0	10.0	0.5379D 02	-0.1815D 01	0.2676D 02	
-8.0	14.0	0.5760D 02	-0.1402D 02	-0.3999D 02	
-8.0	18.0	0.5014D 02	0.5349D 01	0.3050D 02	
-8.0	22.0	0.5625D 02	-0.2328D 02	-0.2470D 02	
-12.0	-22.0	0.5477D 02	-0.4984D 02	0.1279D 02	
-12.0	-18.0	0.5297D 02	-0.2938D 02	0.3370D 02	
-12.0	-14.0	0.5370D 02	-0.3539D 02	-0.3185D 01	
-12.0	-10.0	0.5509D 02	0.4307D 01	-0.3173D 02	
-12.0	-6.0	0.5389D 02	0.5034D 01	-0.5572D 02	
-12.0	-2.0	0.5657D 02	-0.1858D 02	-0.1935D 01	
-12.0	2.0	0.5123D 02	0.5690D 02	-0.2782D 01	
-12.0	6.0	0.5065D 02	0.3039D 02	0.3517D 02	
-12.0	10.0	0.5326D 02	-0.2748D 02	0.1129D 02	
-12.0	14.0	0.5056D 02	0.7480D 01	-0.1321D 02	
-12.0	18.0	0.5087D 02	-0.8321D 02	-0.4102D 01	
-12.0	22.0	0.5065D 02	-0.7487D 01	0.2969D 02	
-16.0	-22.0	0.5253D 02	-0.3605D 02	-0.1018D 02	
-16.0	-18.0	0.5096D 02	-0.2291D 02	0.4144D 02	
-16.0	-14.0	0.5052D 02	0.5160D 02	-0.3577D 01	
-16.0	-10.0	0.5233D 02	0.1285D 02	-0.1975D 02	
-16.0	-6.0	0.5286D 02	-0.2999D 02	-0.7624D 01	
-16.0	-2.0	0.5379D 02	-0.3118D 02	-0.5298D 02	
-16.0	2.0	0.5175D 02	-0.3181D 02	-0.8611D 02	
-16.0	6.0	0.4975D 02	0.2316D 02	-0.4359D 02	
-16.0	10.0	0.4788D 02	0.7379D 01	-0.3300D 02	
-16.0	14.0	0.5002D 02	0.4940D 02	-0.1272D 02	
-16.0	18.0	0.4818D 02	0.1060D 02	0.1848D 02	
-16.0	22.0	0.4968D 02	0.1828D 02	0.1012D 02	
-20.0	-22.0	0.5105D 02	-0.2807D 02	-0.1323D 02	
-20.0	-18.0	0.5219D 02	-0.3405D 02	-0.2904D 01	
-20.0	-14.0	0.4951D 02	-0.2501D 02	0.7727D 02	
-20.0	-10.0	0.5030D 02	-0.1277D 02	0.5717D 02	
-20.0	-6.0	0.4914D 02	0.1662D 02	0.1257D 02	
-20.0	-2.0	0.5189D 02	-0.2924D 02	-0.4293D 02	
-20.0	2.0	0.4614D 02	-0.2294D 02	-0.6681D 02	
-20.0	6.0	0.4960D 02	-0.5984D 02	0.1575D 02	
-20.0	10.0	0.4994D 02	0.2619D 02	-0.1283D 02	
-20.0	14.0	0.4960D 02	0.2791D 02	0.2671D 02	
-20.0	18.0	0.4820D 02	0.1463D 02	0.5828D 01	
-20.0	22.0	0.4842D 02	-0.5707D 02	0.5507D 01	

*	-24.0	-22.0	0.5258D 02	-0.1962D 02	0.2202D 01
*	-24.0	-18.0	0.4838D 02	0.2284D 02	0.6058D 02
*	-24.0	-14.0	0.4873D 02	0.1518D 01	0.1474D 02
*	-24.0	-10.0	0.5215D 02	-0.7116D 02	-0.4654D 02
*	-24.0	-6.0	0.4673D 02	0.2659D 02	-0.3046D 02
*	-24.0	-2.0	0.4887D 02	0.5039D 01	-0.6137D 02
*	-24.0	2.0	0.4689D 02	0.1416D 02	0.3177D 02
*	-24.0	6.0	0.4515D 02	0.9000D 01	0.2048D 01
*	-24.0	10.0	0.4536D 02	0.4761D 02	-0.2787D 02
*	-24.0	14.0	0.4502D 02	-0.3004D 01	-0.3092D 02
*	-24.0	18.0	0.4646D 02	0.2936D 02	0.2168D 02
*	-24.0	22.0	0.4602D 02	-0.6084D 02	-0.7810D 02
*	-28.0	-22.0	0.4573D 02	0.3868D 01	0.5916D 01
*	-28.0	-18.0	0.4475D 02	0.3381D 02	0.5849D 02
*	-28.0	-14.0	0.4646D 02	-0.5032D 01	0.3884D 02
*	-28.0	-10.0	0.4504D 02	0.4498D 02	-0.7282D 01
*	-28.0	-6.0	0.4337D 02	0.7373D 02	-0.4271D 02
*	-28.0	-2.0	0.4347D 02	0.2432D 02	-0.5524D 01
*	-28.0	2.0	0.4491D 02	0.9756D-01	-0.3019D 02
*	-28.0	6.0	0.4292D 02	0.1390D 02	-0.9023D 01
*	-28.0	10.0	0.4414D 02	-0.3509D 02	0.1553D 02
*	-28.0	14.0	0.4417D 02	-0.2401D 02	-0.2320D 02
*	-28.0	18.0	0.4803D 02	-0.4022D 02	-0.1727D 02
*	-28.0	22.0	0.4560D 02	0.2131D 02	-0.8231D 01
*	-32.0	-22.0	0.4175D 02	-0.9678D-01	0.4895D 02
*	-32.0	-18.0	0.4343D 02	-0.4699D 02	-0.1159D 01
*	-32.0	-14.0	0.4180D 02	0.3322D 02	-0.5815D 02
*	-32.0	-10.0	0.4438D 02	-0.4161D 02	-0.1635D 02
*	-32.0	-6.0	0.4253D 02	-0.2773D 02	-0.3194D 02
*	-32.0	-2.0	0.4301D 02	-0.6404D 01	-0.1010D 02
*	-32.0	2.0	0.3906D 02	0.8630D 02	-0.3131D 02
*	-32.0	6.0	0.4314D 02	0.4554D 02	0.5648D 02
*	-32.0	10.0	0.4154D 02	0.3648D 02	-0.2763D 02
*	-32.0	14.0	0.4273D 02	-0.1044D 02	0.1013D 02
*	-32.0	18.0	0.4161D 02	-0.2518D 02	-0.1751D 02
*	-32.0	22.0	0.4353D 02	-0.3334D 02	-0.4920D 02

STATISTICAL RESULTS:

	MEAN VALUE	STANDARD DEVIATION
X-DIRECTION	0.637D 02	0.133D 02
Y-DIRECTION	-0.716D 01	0.306D 02
Z-DIRECTION	-0.437D 01	0.321D 02

EVALUATED STRAIN FIELD AT POINT (8B)

ELEMENT	EXX	EYY	ELEMENT	EXX	EYY
1, 1	0.86D-03	-0.12D-01	2, 1	0.32D-03	-0.80D-02
1, 2	0.12D-02	0.62D-02	2, 2	0.47D-03	0.10D-01
1, 3	0.48D-03	-0.82D-02	2, 3	0.11D-02	0.19D-01
1, 4	-0.20D-03	-0.26D-02	2, 4	0.11D-02	-0.10D-01
1, 5	0.30D-03	-0.51D-02	2, 5	-0.41D-03	-0.56D-02
1, 6	0.19D-04	0.14D-01	2, 6	0.67D-03	0.80D-02
1, 7	0.17D-02	0.12D-02	2, 7	0.53D-04	-0.12D-01
1, 8	0.50D-03	0.60D-02	2, 8	0.50D-03	-0.19D-02
1, 9	0.29D-03	0.82D-02	2, 9	0.23D-03	0.13D-01
1, 10	-0.50D-03	-0.26D-01	2, 10	0.77D-03	-0.13D-01
1, 11	-0.86D-03	0.19D-01	2, 11	0.13D-02	0.22D-02
3, 1	0.05D-03	0.44D-03	4, 1	0.66D-03	0.71D-04
3, 2	-0.73D-04	0.14D-01	4, 2	0.53D-03	0.19D-02
3, 3	-0.57D-04	0.12D-01	4, 3	0.97D-03	-0.25D-02
3, 4	0.18D-03	-0.14D-01	4, 4	0.14D-02	-0.38D-02
3, 5	0.24D-02	-0.99D-02	4, 5	-0.84D-04	-0.95D-02
3, 6	0.18D-03	0.16D-01	4, 6	0.17D-03	0.24D-02
3, 7	-0.24D-03	-0.13D-01	4, 7	0.61D-03	0.13D-01
3, 8	0.17D-02	-0.13D-01	4, 8	-0.11D-02	-0.11D-01
3, 9	0.88D-03	0.22D-01	4, 9	0.33D-03	0.58D-03
3, 10	0.46D-03	0.10D-02	4, 10	0.56D-03	0.13D-01
3, 11	0.82D-04	-0.96D-02	4, 11	0.93D-03	-0.13D-02
5, 1	-0.22D-03	-0.44D-02	6, 1	0.11D-02	0.25D-02
5, 2	0.57D-03	-0.34D-02	6, 2	0.66D-03	0.32D-02
5, 3	0.77D-03	-0.22D-02	6, 3	-0.25D-03	-0.62D-02
5, 4	-0.22D-03	0.17D-01	6, 4	0.11D-02	0.32D-02
5, 5	0.56D-03	0.43D-02	6, 5	0.59D-04	0.39D-02
5, 6	0.53D-03	-0.92D-02	6, 6	0.13D-02	0.33D-02
5, 7	0.40D-03	-0.13D-01	6, 7	0.40D-03	-0.57D-03
5, 8	0.14D-02	0.11D-01	6, 8	0.44D-03	-0.69D-02
5, 9	-0.47D-04	0.70D-02	6, 9	0.41D-03	0.11D-01
5, 10	0.94D-03	0.27D-02	6, 10	0.15D-03	-0.62D-02
5, 11	0.15D-02	-0.39D-02	6, 11	-0.38D-03	-0.25D-02
7, 1	0.64D-03	0.46D-02	8, 1	0.71D-03	-0.47D-04
7, 2	-0.13D-03	0.34D-02	8, 2	0.21D-02	-0.29D-02
7, 3	0.16D-02	0.10D-01	8, 3	-0.13D-03	-0.72D-04
7, 4	0.80D-03	-0.90D-02	8, 4	-0.46D-03	-0.61D-02
7, 5	0.11D-02	-0.11D-01	8, 5	0.53D-03	0.89D-02
7, 6	0.50D-03	0.14D-01	8, 6	0.68D-03	-0.34D-02
7, 7	0.13D-02	-0.30D-02	8, 7	0.63D-03	0.44D-02
7, 8	0.96D-03	-0.31D-02	8, 8	0.62D-03	-0.14D-01
7, 9	0.16D-02	0.79D-02	8, 9	0.11D-03	0.67D-02
7, 10	0.83D-03	-0.60D-02	8, 10	0.85D-03	0.15D-02
7, 11	0.18D-02	-0.40D-02	8, 11	-0.58D-03	0.48D-02
9, 1	0.57D-03	-0.24D-01	10, 1	0.15D-03	-0.27D-01
9, 2	-0.95D-03	0.75D-02	10, 2	0.27D-02	0.10D-01
9, 3	0.68D-03	0.51D-03	10, 3	0.99D-03	-0.13D-01
9, 4	0.18D-02	-0.65D-02	10, 4	-0.22D-05	0.84D-02
9, 5	0.88D-03	0.75D-02	10, 5	-0.28D-03	0.11D-03
9, 6	0.31D-03	-0.88D-03	10, 6	0.44D-03	0.11D-01
9, 7	-0.15D-03	0.38D-02	10, 7	0.18D-02	-0.17D-01
9, 8	-0.41D-04	-0.17D-01	10, 8	0.12D-02	0.15D-01
9, 9	0.54D-03	0.18D-01	10, 9	0.22D-02	-0.13D-01
9, 10	0.13D-02	-0.72D-02	10, 10	-0.43D-04	0.93D-04
9, 11	0.82D-03	0.32D-02	10, 11	0.74D-03	-0.30D-03
11, 1	0.49D-03	-0.15D-02	12, 1	0.74D-03	-0.14D-01
11, 2	-0.16D-03	0.46D-02	12, 2	0.33D-03	-0.73D-02
11, 3	0.60D-03	0.99D-02	12, 3	0.87D-04	-0.41D-02
11, 4	0.14D-02	-0.12D-01	12, 4	0.11D-02	0.10D-01
11, 5	0.15D-02	-0.16D-02	12, 5	-0.11D-04	0.12D-01
11, 6	0.69D-03	0.55D-02	12, 6	0.58D-03	-0.20D-01
11, 7	-0.48D-03	0.61D-02	12, 7	0.59D-03	0.32D-02
11, 8	0.12D-02	0.68D-03	12, 8	0.65D-03	-0.53D-03

* 11, 9 *	-0.51D-03	-0.72D-02 *	12, 9 *	0.10D-02	0.13D-02 *
* 11,10 *	0.16D-02	-0.96D-02 *	12,10 *	-0.73D-03	0.11D-04 *
* 11,11 *	0.15D-02	0.14D-01 *	12,11 *	-0.18D-03	0.19D-02 *
* 13, 1 *	0.32D-03	0.47D-02 *	14, 1 *	0.93D-03	0.48D-02 *
* 13, 2 *	-0.50D-04	0.13D-02 *	14, 2 *	0.11D-02	-0.14D-01 *
* 13, 3 *	0.15D-02	-0.24D-02 *	14, 3 *	-0.19D-03	0.22D-02 *
* 13, 4 *	-0.80D-03	0.36D-02 *	14, 4 *	0.43D-03	-0.51D-02 *
* 13, 5 *	0.17D-02	0.12D-01 *	14, 5 *	-0.54D-03	0.45D-02 *
* 13, 6 *	0.11D-02	-0.23D-01 *	14, 6 *	-0.71D-03	0.42D-02 *
* 13, 7 *	0.90D-03	0.28D-02 *	14, 7 *	0.11D-02	0.94D-02 *
* 13, 8 *	-0.31D-03	-0.23D-02 *	14, 8 *	0.11D-02	-0.83D-02 *
* 13, 9 *	0.11D-03	-0.79D-03 *	14, 9 *	0.13D-03	0.31D-02 *
* 13,10 *	0.13D-03	0.12D-01 *	14,10 *	0.18D-02	-0.48D-02 *
* 13,11 *	0.12D-02	0.29D-02 *	14,11 *	-0.18D-03	0.72D-02 *
* 15, 1 *	0.56D-03	-0.51D-02 *	16, 1 *	0.37D-03	-0.33D-02 *
* 15, 2 *	0.50D-03	0.15D-02 *	16, 2 *	-0.31D-03	-0.19D-01 *
* 15, 3 *	0.79D-03	-0.99D-02 *	16, 3 *	0.25D-03	0.97D-02 *
* 15, 4 *	0.69D-03	-0.18D-03 *	16, 4 *	0.51D-03	0.11D-01 *
* 15, 5 *	0.26D-03	0.59D-02 *	16, 5 *	0.93D-03	0.30D-03 *
* 15, 6 *	0.69D-03	-0.19D-01 *	16, 6 *	0.48D-03	0.16D-03 *
* 15, 7 *	-0.13D-03	0.66D-02 *	16, 7 *	0.14D-02	-0.14D-01 *
* 15, 8 *	0.22D-03	0.14D-01 *	16, 8 *	0.39D-04	0.39D-02 *
* 15, 9 *	0.13D-02	-0.87D-02 *	16, 9 *	-0.51D-03	-0.11D-01 *
* 15,10 *	0.14D-03	0.23D-01 *	16,10 *	0.10D-03	0.97D-02 *
* 15,11 *	0.67D-03	-0.19D-01 *	16,11 *	-0.47D-05	-0.19D-02 *
* 17, 1 *	-0.38D-03	0.15D-02 *	18, 1 *	0.17D-02	-0.11D-01 *
* 17, 2 *	0.95D-03	-0.23D-02 *	18, 2 *	0.91D-03	0.53D-02 *
* 17, 3 *	0.19D-03	-0.31D-02 *	18, 3 *	0.57D-03	0.18D-01 *
* 17, 4 *	-0.46D-03	-0.73D-02 *	18, 4 *	0.18D-02	-0.24D-01 *
* 17, 5 *	0.60D-03	0.11D-01 *	18, 5 *	0.84D-03	0.54D-02 *
* 17, 6 *	0.75D-03	-0.16D-02 *	18, 6 *	0.14D-02	-0.23D-02 *
* 17, 7 *	-0.19D-03	0.92D-02 *	18, 7 *	0.49D-03	0.13D-02 *
* 17, 8 *	0.11D-02	-0.22D-01 *	18, 8 *	0.56D-03	-0.97D-02 *
* 17, 9 *	0.11D-02	-0.43D-03 *	18, 9 *	0.30D-03	0.13D-01 *
* 17,10 *	0.11D-02	0.33D-02 *	18,10 *	0.21D-03	-0.81D-02 *
* 17,11 *	0.43D-03	0.18D-01 *	18,11 *	-0.39D-03	0.23D-01 *
* 19, 1 *	0.10D-02	-0.75D-02 *			
* 19, 2 *	0.33D-03	0.97D-02 *			
* 19, 3 *	0.12D-02	-0.13D-01 *			
* 19, 4 *	0.16D-03	-0.72D-02 *			
* 19, 5 *	0.21D-03	0.12D-01 *			
* 19, 6 *	0.11D-03	0.61D-02 *			
* 19, 7 *	0.15D-02	-0.34D-02 *			
* 19, 8 *	-0.56D-04	-0.53D-02 *			
* 19, 9 *	0.65D-03	0.15D-01 *			
* 19,10 *	0.36D-03	0.41D-02 *			
* 19,11 *	0.16D-02	-0.15D-01 *			

STATISTICAL RESULTS:

	MEAN VALUE	STANDARD DEVIATION
XX-STRAIN:	0.5571D-03	0.6726D-03
YY-STRAIN:	-0.2828D-04	0.9890D-02

EVALJATED THICKNESS CHANGES (MICRONS)
(COLUMNS: 1- 6)

	1	2	3	4	5	6
1	2.33	4.07	-4.50	2.8o	1.87	-6.57
2	o.3o	-2.33	3.55	-3.12	0.32	-1.46
3	-4.6o	-3.63	5.56	-7.35	-10.38	9.87
4	-8.61	-4.05	6.52	-1.32	1.02	-0.01
5	-4.40	6.16	-4.90	1.94	-6.07	5.98
6	4.77	-11.55	5.74	5.72	1.55	10.49
7	3.6d	-1.0b	1.19	-5.99	4.14	-0.32
8	5.13	-2.80	-3.40	5.52	-3.27	-0.55
9	-6.48	0.64	-4.44	-1.70	-9.22	-7.36
10	2.32	1.03	-2.69	-2.77	-7.78	3.28
11	-11.77	6.21	10.61	9.90	-3.38	9.25
12	-6.21	-3.68	-1.08	2.57	-7.53	4.88
13	5.45	3.22	-6.63	-1.70	2.32	-4.40
14	-6.92	2.52	-8.96	3.04	-1.79	-10.26
15	7.87	-5.5o	8.58	-5.61	-0.25	5.28
16	-2.83	-5.44	7.52	-3.93	-6.47	-6.32
17	-8.56	-9.90	1.67	-11.94	-6.81	4.21
18	-1.79	4.85	5.23	0.57	1.65	7.27
19	-6.73	-0.57	6.86	-12.41	3.88	-6.24
20	-4.76	-6.62	-1.45	1.22	-3.41	-5.02

(COLUMNS: 7-12)

	7	8	9	10	11	12
1	6.73	6.26	0.93	-7.40	-3.31	14.86
2	-10.43	3.27	3.82	-5.14	1.16	1.77
3	-2.76	-7.83	7.11	-0.22	-1.78	4.65
4	-2.2o	2.67	0.34	7.01	-0.01	-1.34
5	-9.92	-6.50	7.20	4.39	4.91	-10.72
6	3.57	-1.43	-2.69	1.81	-0.26	1.39
7	-7.43	1.04	5.90	7.4b	-5.59	-10.20
8	-0.45	-0.41	-2.69	-o.95	-1.46	-9.34
9	-3.67	1.41	-2.01	-10.62	-4.26	0.08
10	-3.0b	9.20	-6.28	4.21	-4.83	-0.75
11	5.73	-6.92	-6.71	4.31	-10.67	0.52
12	6.04	-7.95	10.35	-2.19	3.75	-7.13
13	4.42	-5.92	2.04	-4.45	10.10	1.35
14	10.76	-3.45	9.67	6.93	3.96	0.50
15	-5.91	-9.14	-11.65	-7.92	7.79	3.85
16	-4.73	8.24	-1.59	5.31	5.49	-1.59
17	-3.60	-3.60	1.25	-3.52	-2.50	-4.06
18	-3.25	-7.07	4.97	-3.71	5.20	3.79
19	-2.72	2.81	4.15	-0.27	2.25	7.33
20	-3.00	-6.54	-6.15	1.00	-5.80	-3.77

RECONSTRUCTION RESULTS OF INTERFEROGRAM
(8L) OF THE NEWS-PRINT PAPER SAMPLE #38
CUMMULATIVE DEFORMATION)

CO-ORDINATES X	CO-ORDINATES Y	DEFORMATIONS X	DEFORMATIONS Y	DEFORMATIONS Z
44.0	-22.0	0.8721D 02	-0.3809D 02	-0.1291D 02
44.0	-18.0	0.8899D 02	-0.1704D 02	-0.6208D 01
44.0	-14.0	0.8899D 02	0.7945D 01	0.3164D 02
44.0	-10.0	0.8360D 02	-0.2235D 01	0.3016D 01
44.0	-6.0	0.8737D 02	0.6292D 02	-0.4637D 02
44.0	-2.0	0.8973D 02	0.5505D 01	-0.3725D 02
44.0	2.0	0.8636D 02	-0.3026D 02	0.1726D 02
44.0	6.0	0.8527D 02	-0.3945D 02	0.1638D 02
44.0	10.0	0.8573D 02	0.9079D 01	-0.2363D 02
44.0	14.0	0.8733D 02	0.2214D 01	0.3933D 02
44.0	18.0	0.9059D 02	0.4145D 02	0.2316D 02
44.0	22.0	0.8877D 02	-0.6524D 02	-0.6440D 01
40.0	-22.0	0.8347D 02	0.6092D 01	0.1702D 02
40.0	-18.0	0.8752D 02	-0.2060D 02	0.1235D 02
40.0	-14.0	0.8464D 02	0.3704D 02	0.6551D 02
40.0	-10.0	0.8762D 02	-0.6556D 01	0.1795D 02
40.0	-6.0	0.8861D 02	0.4195D 02	-0.1787D 02
40.0	-2.0	0.8517D 02	-0.2185D 02	0.7354D 00
40.0	2.0	0.8643D 02	-0.4726D 02	0.1037D 02
40.0	6.0	0.8781D 02	0.5853D 00	-0.3733D 02
40.0	10.0	0.8094D 02	-0.5294D 02	0.1671D 02
40.0	14.0	0.8306D 02	-0.3359D 02	0.5996D 02
40.0	18.0	0.8959D 02	0.2505D 02	-0.4231D 02
40.0	22.0	0.8478D 02	0.1691D 02	-0.4653D 02
36.0	-22.0	0.8466D 02	0.5520D 02	-0.3111D 02
36.0	-18.0	0.8604D 02	0.4497D 01	0.1638D 02
36.0	-14.0	0.8225D 02	0.2086D 02	-0.2407D 02
36.0	-10.0	0.8222D 02	-0.1539D 01	-0.3614D 02
36.0	-6.0	0.8386D 02	-0.1049D 02	-0.3491D 02
36.0	-2.0	0.8157D 02	0.2281D 02	0.1678D 02
36.0	2.0	0.8284D 02	0.3020D 02	-0.2404D 01
36.0	6.0	0.7810D 02	-0.1308D 02	0.3473D 01
36.0	10.0	0.8295D 02	-0.2939D 02	0.6240D 02
36.0	14.0	0.8312D 02	0.4568D 02	0.6613D 02
36.0	18.0	0.7984D 02	-0.2001D 01	0.1899D 02
36.0	22.0	0.7839D 02	-0.3934D 02	0.8158D 02
32.0	-22.0	0.7624D 02	-0.5781D 01	-0.2475D 02
32.0	-18.0	0.8417D 02	0.1693D 02	-0.5406D 02
32.0	-14.0	0.7916D 02	0.4790D 02	0.2352D 01
32.0	-10.0	0.8343D 02	0.6161D 02	0.2968D 01
32.0	-6.0	0.7974D 02	0.1755D 02	-0.2052D 02
32.0	-2.0	0.8044D 02	-0.1603D 02	-0.6084D 02
32.0	2.0	0.7816D 02	0.1393D 02	0.2574D 02
32.0	6.0	0.7861D 02	0.8260D 00	0.5122D 01
32.0	10.0	0.7823D 02	-0.2533D 02	-0.1720D 02
32.0	14.0	0.7688D 02	-0.8090D 01	0.3296D 01
32.0	18.0	0.8387D 02	0.4351D 01	-0.1066D 02
32.0	22.0	0.7718D 02	-0.1651D 02	0.5040D 02
28.0	-22.0	0.7399D 02	-0.3877D 02	-0.9039D 02
28.0	-18.0	0.7935D 02	-0.1058D 02	0.5068D 02
28.0	-14.0	0.8142D 02	0.5830D 02	0.1870D 02
28.0	-10.0	0.7206D 02	-0.1238D 02	-0.2923D 02
28.0	-6.0	0.7249D 02	-0.1538D 02	0.3375D 02
28.0	-2.0	0.8201D 02	0.3669D 02	0.2055D 02
28.0	2.0	0.7036D 02	0.1422D 02	-0.3063D 02
28.0	6.0	0.8015D 02	-0.7789D 01	0.7186D 02
28.0	10.0	0.7446D 02	0.3182D 01	0.3286D 02
28.0	14.0	0.7684D 02	0.2371D 02	-0.3324D 02
28.0	18.0	0.7482D 02	0.5354D 02	-0.3737D 02
28.0	22.0	0.7779D 02	-0.2686D 02	0.1627D 01

24.0	-22.0	0.7872D 02	-0.2120D 02	-0.3927D 02	
24.0	-18.0	0.7384D 02	-0.5180D 01	-0.2951D 02	
24.0	-14.0	0.7544D 02	0.4232D 02	-0.5892D 02	
24.0	-10.0	0.7201D 02	-0.5418D 02	0.7516D 02	
24.0	-6.0	0.7037D 02	-0.5291D 02	0.3103D 02	
24.0	-2.0	0.7536D 02	0.6081D 01	0.2239D 02	
24.0	2.0	0.8000D 02	0.2384D 02	-0.3503D 01	
24.0	6.0	0.6998D 02	0.9427D 00	0.1542D 02	
24.0	10.0	0.7319D 02	0.3491D 02	-0.4591D 02	
24.0	14.0	0.7563D 02	-0.4123D 02	-0.1362D 02	
24.0	18.0	0.6917D 02	-0.6071D 01	-0.8976D 01	
24.0	22.0	0.8340D 02	0.4523D 02	-0.2969D 01	
20.0	-22.0	0.7695D 02	0.5208D 02	-0.6063D 02	
20.0	-18.0	0.6758D 02	0.8107D 01	0.2808D 01	
20.0	-14.0	0.7328D 02	0.2377D 02	0.1826D 02	
20.0	-10.0	0.7109D 02	0.5886D 01	-0.2170D 02	
20.0	-6.0	0.7144D 02	0.1726D 02	-0.2016D 02	
20.0	-2.0	0.7214D 02	0.6040D 00	0.9177D 01	
20.0	2.0	0.6943D 02	0.7360D 01	-0.4628D 02	
20.0	6.0	0.7186D 02	-0.6306D 02	0.1596D 01	
20.0	10.0	0.7583D 02	0.1740D 02	0.3783D 01	
20.0	14.0	0.6938D 02	0.1299D 02	0.2588D 02	
20.0	18.0	0.6876D 02	0.2285D 02	0.4972D 01	
20.0	22.0	0.6960D 02	0.1099D 02	-0.3468D 02	
16.0	-22.0	0.7296D 02	0.1982D 02	0.6486D 02	
16.0	-18.0	0.6797D 02	-0.1614D 02	-0.1740D 02	
16.0	-14.0	0.6356D 02	0.4818D 01	-0.6088D 02	
16.0	-10.0	0.7058D 02	0.2150D 02	-0.2717D 01	
16.0	-6.0	0.6672D 02	-0.2996D 02	0.2596D 02	
16.0	-2.0	0.6475D 02	-0.6052D 00	0.4152D 02	
16.0	2.0	0.7448D 02	0.3963D 02	0.7169D 02	
16.0	6.0	0.6556D 02	-0.3643D 02	-0.1966D 02	
16.0	10.0	0.6473D 02	0.2227D 02	-0.4765D 02	
16.0	14.0	0.6796D 02	-0.6552D 02	0.3684D 02	
16.0	18.0	0.6864D 02	-0.4791D 01	-0.1487D 02	
16.0	22.0	0.7010D 02	0.3546D 02	-0.3598D 01	
12.0	-22.0	0.6700D 02	-0.2753D 02	0.1747D 02	
12.0	-18.0	0.6595D 02	-0.2610D 02	0.1296D 02	
12.0	-14.0	0.6857D 02	-0.8308D 01	0.4049D 02	
12.0	-10.0	0.6900D 02	0.1454D 02	0.9095D 01	
12.0	-6.0	0.6630D 02	-0.5054D 02	-0.7219D 02	
12.0	-2.0	0.6557D 02	0.4886D 02	0.7484D 00	
12.0	2.0	0.6519D 02	0.2596D 00	0.7341D 01	
12.0	6.0	0.6637D 02	-0.3813D 02	-0.8466D 02	
12.0	10.0	0.6275D 02	-0.5740D 02	0.1600D 02	
12.0	14.0	0.6582D 02	-0.2549D 01	0.2832D 02	
12.0	18.0	0.6362D 02	0.2590D 01	-0.3528D 00	
12.0	22.0	0.7395D 02	0.8326D 02	0.5442D 02	
8.0	-22.0	0.6989D 02	0.1921D 02	-0.2388D 02	
8.0	-18.0	0.6118D 02	-0.8692D 01	-0.3052D 02	
8.0	-14.0	0.6767D 02	0.2795D 02	-0.2147D 01	
8.0	-10.0	0.6957D 02	0.1689D 02	-0.8965D 01	
8.0	-6.0	0.5887D 02	-0.1565D 02	-0.3199D 02	
8.0	-2.0	0.6113D 02	-0.2763D 02	-0.2437D 02	
8.0	2.0	0.6408D 02	-0.1873D 02	0.1849D 02	
8.0	6.0	0.6690D 02	0.5322D-01	0.4594D 02	
8.0	10.0	0.6575D 02	-0.1371D 02	-0.7421D 01	
8.0	14.0	0.6036D 02	-0.1252D 02	-0.2224D 02	
8.0	18.0	0.6428D 02	0.9398D 01	-0.3663D 02	
8.0	22.0	0.6625D 02	-0.4371D 02	-0.7644D 02	
4.0	-22.0	0.5965D 02	-0.4895D 01	-0.2107D 01	
4.0	-18.0	0.5906D 02	0.5234D 00	0.4974D 02	
4.0	-14.0	0.6001D 02	0.1552D 02	0.4589D 02	
4.0	-10.0	0.6464D 02	0.1555D 02	0.3181D 02	
4.0	-6.0	0.5953D 02	-0.3307D 02	-0.1436D 02	
4.0	-2.0	0.6132D 02	0.2418D 02	-0.2562D 02	
4.0	2.0	0.6709D 02	0.3734D 02	0.2751D 02	
4.0	6.0	0.5744D 02	-0.5208D 02	-0.1038D 02	
4.0	10.0	0.6087D 02	0.2518D 01	-0.5535D 02	
4.0	14.0	0.6012D 02	0.7504D 01	0.3620D 00	
4.0	18.0	0.6758D 02	0.7235D 01	-0.3250D 02	
4.0	22.0	0.5769D 02	0.4272D 02	0.1835D 02	

0.0	-22.0	0.5596D 02	-0.1437D 02	-0.1190D 02
0.0	-18.0	0.5670D 02	-0.1312D 02	-0.4794D 02
0.0	-14.0	0.5451D 02	-0.6475D 01	0.5103D 02
0.0	-10.0	0.5862D 02	-0.6907D 02	-0.3762D 02
0.0	-6.0	0.5845D 02	-0.1816D 02	0.2315D 02
0.0	-2.0	0.6108D 02	0.4652D 01	-0.1750D 01
0.0	2.0	0.5894D 02	0.9686D 01	-0.5504D 02
0.0	6.0	0.6247D 02	0.5021D 02	0.1340D 02
0.0	10.0	0.5315D 02	-0.3327D 02	0.5012D 02
0.0	14.0	0.5391D 02	-0.3999D 02	-0.1438D 02
0.0	18.0	0.6264D 02	0.2036D 02	0.4427D 01
0.0	22.0	0.5737D 02	-0.9735D 00	-0.1482D 02
-4.0	-22.0	0.5537D 02	-0.3660D 02	0.8433D 00
-4.0	-18.0	0.5705D 02	0.1454D 02	-0.6788D 01
-4.0	-14.0	0.5468D 02	-0.4173D 02	-0.8353D 01
-4.0	-10.0	0.6022D 02	-0.7958D 01	-0.3098D 02
-4.0	-6.0	0.5443D 02	0.8469D 01	0.6161D 01
-4.0	-2.0	0.5811D 02	-0.4791D 02	-0.1391D 01
-4.0	2.0	0.5892D 02	-0.5406D 02	-0.9299D 01
-4.0	6.0	0.5242D 02	-0.4153D 02	0.4105D 02
-4.0	10.0	0.5323D 02	-0.6719D 01	0.1177D 02
-4.0	14.0	0.5472D 02	0.7873D 01	-0.3053D 02
-4.0	18.0	0.5242D 02	-0.1846D 02	0.1232D 01
-4.0	22.0	0.5677D 02	0.2024D 02	0.1791D 02
-8.0	-22.0	0.5770D 02	-0.5471D 02	0.7306D 01
-8.0	-18.0	0.5629D 02	-0.1405D 02	0.1825D 02
-8.0	-14.0	0.5923D 02	-0.1248D 02	0.1128D 02
-8.0	-10.0	0.5626D 02	0.1601D 02	-0.4325D 02
-8.0	-6.0	0.5305D 02	0.2158D 02	0.2819D 02
-8.0	-2.0	0.5105D 02	-0.4494D 02	-0.1563D 02
-8.0	2.0	0.5559D 02	0.6685D 02	-0.1747D 02
-8.0	6.0	0.5412D 02	-0.4589D 02	0.1839D 02
-8.0	10.0	0.5354D 02	0.1153D 02	-0.2184D 02
-8.0	14.0	0.5858D 02	0.2409D 01	0.4289D 02
-8.0	18.0	0.5241D 02	-0.6980D 02	-0.2775D 02
-8.0	22.0	0.5841D 02	-0.3125D 02	0.2281D 02
-12.0	-22.0	0.5110D 02	-0.8212D 01	-0.1924D 02
-12.0	-18.0	0.5635D 02	0.6370D 02	-0.5034D 02
-12.0	-14.0	0.5863D 02	0.3106D 02	0.1075D 01
-12.0	-10.0	0.5146D 02	0.2908D 02	0.3020D 02
-12.0	-6.0	0.5139D 02	-0.3016D 02	0.7139D 02
-12.0	-2.0	0.5289D 02	-0.3919D 02	0.2091D 00
-12.0	2.0	0.5417D 02	0.4182D 01	-0.1099D 02
-12.0	6.0	0.5176D 02	-0.3148D 02	-0.5227D 02
-12.0	10.0	0.5065D 02	-0.3535D 02	-0.1803D 02
-12.0	14.0	0.5067D 02	0.5386D 00	0.7932D 01
-12.0	18.0	0.5649D 02	0.2497D 02	0.8925D 01
-12.0	22.0	0.5463D 02	0.8523D 02	-0.3869D 02
-16.0	-22.0	0.5108D 02	0.2607D 02	0.1316D 02
-16.0	-18.0	0.5288D 02	-0.2340D 02	-0.3753D 02
-16.0	-14.0	0.5024D 02	-0.2317D 01	0.1351D 02
-16.0	-10.0	0.4989D 02	-0.3264D 02	0.8439D 01
-16.0	-6.0	0.5785D 02	0.4731D 02	0.1615D 02
-16.0	-2.0	0.5376D 02	-0.5771D 02	0.3608D 02
-16.0	2.0	0.4878D 02	-0.8624D 01	0.9735D 02
-16.0	6.0	0.4801D 02	0.5908D 02	0.4115D 02
-16.0	10.0	0.5515D 02	-0.1361D 02	0.1505D 02
-16.0	14.0	0.5346D 02	0.2648D 02	0.1181D 02
-16.0	18.0	0.5113D 02	-0.3754D 02	-0.1780D 02
-16.0	22.0	0.5171D 02	-0.7086D 02	-0.4363D 01
-20.0	-22.0	0.4997D 02	-0.4290D 01	-0.2424D 01
-20.0	-18.0	0.5469D 02	0.1703D 02	0.1817D 01
-20.0	-14.0	0.4705D 02	0.3064D 02	-0.9215D 02
-20.0	-10.0	0.4813D 02	-0.2379D 02	-0.6704D 02
-20.0	-6.0	0.5165D 02	-0.4999D 02	-0.8540D 01
-20.0	-2.0	0.5180D 02	0.4385D 02	0.2917D 02
-20.0	2.0	0.4628D 02	-0.2242D 02	0.6161D 02
-20.0	6.0	0.5673D 02	-0.6329D 02	-0.3329D 02
-20.0	10.0	0.4537D 02	0.1376D 02	0.1174D 02
-20.0	14.0	0.4677D 02	-0.1182D 02	-0.2801D 02
-20.0	18.0	0.4896D 02	-0.5492D 01	-0.7444D 01
-20.0	22.0	0.4325D 02	-0.3774D 02	-0.1768D 02

*	-24.0	-22.0	0.4645D 02	-0.3011D 02	-0.8450D 01
*	-24.0	-18.0	0.4769D 02	-0.5631D 00	-0.7014D 02
*	-24.0	-14.0	0.4507D 02	0.3207D 02	-0.1504D 02
*	-24.0	-10.0	0.4778D 02	0.2544D 02	0.4803D 02
*	-24.0	-6.0	0.4220D 02	0.1842D 02	0.3495D 02
*	-24.0	-2.0	0.4354D 02	-0.3776D 02	0.7069D 02
*	-24.0	2.0	0.4343D 02	0.3449D 00	-0.4875D 02
*	-24.0	6.0	0.4048D 02	0.2233D 02	-0.2033D 02
*	-24.0	10.0	0.4622D 02	-0.2445D 02	0.1762D 02
*	-24.0	14.0	0.4793D 02	-0.1545D 02	0.1150D 02
*	-24.0	18.0	0.4532D 02	0.7742D 01	-0.3415D 02
*	-24.0	22.0	0.4445D 02	-0.1074D 02	0.8978D 02
*	-28.0	-22.0	0.4518D 02	0.6934D 01	0.4705D 00
*	-28.0	-18.0	0.4135D 02	-0.4615D 02	-0.8198D 02
*	-28.0	-14.0	0.4377D 02	-0.3769D 02	-0.4245D 02
*	-28.0	-10.0	0.4509D 02	0.1671D 02	-0.1603D 01
*	-28.0	-6.0	0.4088D 02	-0.5528D 01	0.4667D 02
*	-28.0	-2.0	0.4178D 02	0.2117D 02	0.4124D 01
*	-28.0	2.0	0.4446D 02	0.2454D 02	0.2799D 02
*	-28.0	6.0	0.4331D 02	0.1558D 02	0.9596D 01
*	-28.0	10.0	0.3989D 02	-0.5810D 02	0.9000D-01
*	-28.0	14.0	0.4680D 02	-0.2913D 02	0.2291D 02
*	-28.0	18.0	0.3786D 02	-0.3329D 02	0.6112D 01
*	-28.0	22.0	0.4416D 02	-0.3133D 02	0.7372D 01
*	-32.0	-22.0	0.4439D 02	-0.2143D 02	-0.5311D 02
*	-32.0	-18.0	0.4366D 02	0.6993D 01	-0.4221D 01
*	-32.0	-14.0	0.3863D 02	-0.4603D 01	0.5008D 02
*	-32.0	-10.0	0.4083D 02	0.3104D 02	0.8410D 01
*	-32.0	-6.0	0.4380D 02	-0.2126D 01	0.3100D 02
*	-32.0	-2.0	0.4043D 02	0.6033D 01	0.1578D 02
*	-32.0	2.0	0.4147D 02	-0.5624D 02	0.2586D 02
*	-32.0	6.0	0.3944D 02	-0.4706D 02	-0.7222D 02
*	-32.0	10.0	0.4029D 02	-0.5093D 02	0.2054D 02
*	-32.0	14.0	0.4306D 02	-0.4294D 02	-0.1851D 02
*	-32.0	18.0	0.3852D 02	-0.7185D 02	0.1843D 02
*	-32.0	22.0	0.4042D 02	-0.2904D 02	0.3516D 02

STATISTICAL RESULTS:

	MEAN VALUE	STANDARD DEVIATION
X-DIRECTION	0.636D 02	0.143D 02
Y-DIRECTION	-0.386D 01	0.319D 02
Z-DIRECTION	0.587D-01	0.350D 02

EVALUATED STRAIN FIELD AT POINT (8L)

ELEMENT	EXX	EYY	ELEMENT	EXX	EYY
1, 1	0.93D-03	-0.51D-02	2, 1	-0.30D-03	0.67D-02
1, 2	0.37D-03	-0.64D-02	2, 2	0.37D-03	-0.14D-01
1, 3	0.11D-02	0.25D-02	2, 3	0.60D-03	0.11D-01
1, 4	-0.10D-02	-0.16D-01	2, 4	0.13D-02	-0.12D-01
1, 5	-0.31D-03	0.14D-01	2, 5	0.12D-02	0.16D-01
1, 6	0.11D-02	0.89D-02	2, 6	0.90D-03	0.64D-02
1, 7	-0.18D-04	0.23D-02	2, 7	0.90D-03	-0.12D-01
1, 8	-0.63D-03	-0.12D-01	2, 8	0.24D-02	0.13D-01
1, 9	0.12D-02	0.17D-02	2, 9	-0.50D-03	-0.48D-02
1, 10	0.11D-02	-0.98D-02	2, 10	-0.16D-04	-0.15D-01
1, 11	0.25D-03	0.27D-01	2, 11	0.24D-02	0.20D-02
3, 1	0.21D-02	0.13D-01	4, 1	0.56D-03	-0.57D-02
3, 2	0.47D-03	-0.41D-02	4, 2	0.12D-02	-0.77D-02
3, 3	0.77D-03	0.56D-02	4, 3	-0.56D-03	-0.34D-02
3, 4	-0.30D-03	0.22D-02	4, 4	0.28D-02	0.11D-01
3, 5	0.10D-02	-0.83D-02	4, 5	0.18D-02	0.84D-02
3, 6	0.28D-03	-0.18D-02	4, 6	-0.39D-03	-0.75D-02
3, 7	0.12D-02	0.11D-01	4, 7	0.20D-02	0.33D-02
3, 8	-0.13D-03	0.41D-02	4, 8	-0.39D-03	0.65D-02
3, 9	0.12D-02	-0.19D-01	4, 9	0.94D-03	-0.43D-02
3, 10	0.16D-02	0.12D-01	4, 10	0.11D-04	-0.31D-02
3, 11	-0.10D-02	0.93D-02	4, 11	0.23D-02	0.52D-02
5, 1	-0.12D-02	-0.70D-02	6, 1	0.44D-03	-0.40D-02
5, 2	0.14D-02	-0.15D-01	6, 2	0.16D-02	-0.12D-01
5, 3	0.15D-02	0.16D-01	6, 3	0.54D-03	0.24D-01
5, 4	0.11D-04	0.75D-03	6, 4	0.23D-03	-0.32D-03
5, 5	0.53D-03	-0.13D-01	6, 5	-0.27D-03	-0.15D-01
5, 6	0.17D-02	0.56D-02	6, 6	0.80D-03	-0.44D-02
5, 7	-0.24D-02	0.55D-02	6, 7	0.26D-02	0.57D-02
5, 8	0.25D-02	-0.27D-02	6, 8	-0.47D-03	-0.85D-02
5, 9	0.32D-03	-0.51D-02	6, 9	-0.66D-03	0.19D-01
5, 10	0.30D-03	-0.75D-02	6, 10	0.16D-02	-0.88D-02
5, 11	0.14D-02	0.20D-01	6, 11	0.10D-03	-0.13D-01
7, 1	0.10D-02	0.11D-01	8, 1	0.15D-02	0.90D-02
7, 2	-0.98D-04	-0.39D-02	8, 2	0.51D-03	-0.52D-02
7, 3	0.24D-02	0.45D-02	8, 3	-0.13D-02	-0.42D-02
7, 4	0.13D-03	-0.28D-02	8, 4	0.39D-03	0.13D-01
7, 5	0.12D-02	0.42D-02	8, 5	0.10D-03	-0.73D-02
7, 6	0.18D-02	-0.17D-02	8, 6	-0.21D-03	-0.10D-01
7, 7	-0.13D-02	0.18D-01	8, 7	0.23D-02	0.19D-01
7, 8	0.16D-02	-0.20D-01	8, 8	-0.20D-03	-0.15D-01
7, 9	0.28D-02	0.11D-02	8, 9	0.50D-03	0.22D-01
7, 10	0.35D-03	-0.25D-02	8, 10	0.54D-03	-0.15D-01
7, 11	0.31D-04	0.30D-02	8, 11	0.13D-02	-0.10D-01
9, 1	-0.72D-03	-0.38D-03	10, 1	0.26D-02	0.70D-02
9, 2	0.12D-02	-0.44D-02	10, 2	0.53D-03	-0.92D-02
9, 3	-0.23D-03	-0.57D-02	10, 3	0.19D-02	0.28D-02
9, 4	-0.14D-03	0.16D-01	10, 4	0.12D-02	0.81D-02
9, 5	0.19D-02	-0.25D-01	10, 5	-0.16D-03	0.30D-02
9, 6	0.11D-02	0.12D-01	10, 6	-0.47D-04	-0.22D-02
9, 7	0.28D-03	0.96D-02	10, 7	-0.75D-03	-0.47D-02
9, 8	-0.13D-03	0.48D-02	10, 8	0.24D-02	0.34D-02
9, 9	-0.75D-03	-0.14D-01	10, 9	0.12D-02	-0.30D-03
9, 10	0.14D-02	-0.13D-02	10, 10	0.61D-04	-0.55D-02
9, 11	-0.17D-03	-0.20D-01	10, 11	-0.82D-03	0.13D-01
11, 1	0.92D-03	-0.14D-02	12, 1	0.15D-03	-0.31D-03
11, 2	0.59D-03	-0.37D-02	12, 2	-0.88D-04	-0.17D-02
11, 3	0.14D-02	-0.76D-05	12, 3	-0.43D-04	0.16D-01
11, 4	0.15D-02	0.12D-01	12, 4	-0.40D-03	-0.13D-01
11, 5	0.27D-03	-0.14D-01	12, 5	0.10D-02	-0.57D-02
11, 6	0.60D-04	-0.33D-02	12, 6	0.74D-03	-0.13D-02
11, 7	0.20D-02	-0.22D-01	12, 7	0.56D-05	-0.10D-01
11, 8	-0.13D-02	-0.14D-01	12, 8	0.25D-02	0.21D-01

11, 9	0.19D-02	-0.12D-02	12, 9	-0.20D-04	0.17D-02
11,10	0.16D-02	0.67D-04	12,10	-0.20D-03	-0.15D-01
11,11	0.12D-02	-0.89D-02	12,11	0.26D-02	0.48D-02
13, 1	-0.58D-03	-0.13D-01	14, 1	0.16D-02	-0.10D-01
13, 2	0.19D-03	0.14D-01	14, 2	-0.14D-04	-0.39D-03
13, 3	-0.11D-02	-0.84D-02	14, 3	0.15D-03	-0.71D-02
13, 4	0.99D-03	-0.41D-02	14, 4	0.12D-02	-0.14D-02
13, 5	0.34D-03	0.14D-01	14, 5	0.42D-03	0.17D-01
13, 6	0.18D-02	0.15D-02	14, 6	-0.46D-03	-0.28D-01
13, 7	0.83D-03	-0.31D-02	14, 7	0.35D-03	0.28D-01
13, 8	-0.43D-03	-0.87D-02	14, 8	0.59D-03	-0.14D-01
13, 9	-0.77D-04	-0.36D-02	14, 9	0.72D-03	0.23D-02
13,10	-0.96D-03	0.66D-02	14,10	0.20D-02	0.18D-01
13,11	0.25D-05	-0.97D-02	14,11	-0.10D-02	-0.96D-02
15, 1	0.55D-05	-0.18D-01	16, 1	0.28D-03	0.12D-01
15, 2	0.87D-03	0.82D-02	16, 2	-0.45D-03	-0.53D-02
15, 3	0.21D-02	0.49D-03	16, 3	0.80D-03	0.76D-02
15, 4	0.39D-03	0.15D-01	16, 4	0.44D-03	-0.20D-01
15, 5	-0.16D-02	0.23D-02	16, 5	0.16D-02	0.26D-01
15, 6	-0.22D-03	-0.11D-01	16, 6	0.49D-03	-0.12D-01
15, 7	0.13D-02	0.89D-02	16, 7	0.62D-03	-0.17D-01
15, 8	0.94D-03	0.97D-03	16, 8	-0.22D-02	0.18D-01
15, 9	-0.11D-02	-0.90D-02	16, 9	0.24D-02	-0.10D-01
15,10	-0.70D-03	-0.61D-02	16,10	0.17D-02	0.16D-01
15,11	0.13D-02	-0.15D-01	16,11	0.54D-03	0.83D-02
17, 1	0.88D-03	-0.53D-02	18, 1	0.32D-03	-0.74D-02
17, 2	0.17D-02	-0.34D-02	18, 2	0.16D-02	-0.82D-02
17, 3	0.50D-03	0.14D-01	18, 3	0.33D-03	0.17D-02
17, 4	0.87D-04	0.65D-02	18, 4	0.67D-03	0.18D-02
17, 5	0.24D-02	-0.25D-01	18, 5	0.33D-03	0.14D-01
17, 6	0.21D-02	0.27D-01	18, 6	0.43D-03	-0.95D-02
17, 7	0.71D-03	0.22D-03	18, 7	-0.26D-03	-0.55D-02
17, 8	0.41D-02	-0.19D-01	18, 8	-0.71D-03	0.12D-01
17, 9	-0.21D-03	0.64D-02	18, 9	0.16D-02	-0.23D-02
17,10	-0.29D-03	-0.16D-02	18,10	0.28D-03	-0.58D-02
17,11	0.91D-03	0.81D-02	18,11	0.19D-02	0.46D-02
19, 1	0.20D-03	0.13D-01			
19, 2	-0.58D-03	-0.21D-02			
19, 3	0.13D-02	-0.14D-01			
19, 4	0.11D-02	0.56D-02			
19, 5	-0.73D-03	-0.67D-02			
19, 6	0.34D-03	-0.84D-03			
19, 7	0.75D-03	0.22D-02			
19, 8	0.97D-03	0.18D-01			
19, 9	-0.10D-03	-0.72D-02			
19,10	0.94D-03	0.10D-02			
19,11	-0.17D-03	-0.49D-03			

STATISTICAL RESULTS:

	MEAN VALUE	STANDARD DEVIATION
XX-STRAIN:	0.6060D-03	0.1023D-02
YY-STRAIN:	-0.7965D-04	0.1103D-01

TABLES OF SUMMARY
****

(I) DEFORMATION FIELD :

MEAN VALUES
STANDARD DEVIATIONS

POINT	X-DIRECTION R	X-DIRECTION L	Y-DIRECTION R	Y-DIRECTION L	Z-DIRECTION R	Z-DIRECTION L
1	10.81	10.25	-1.89	-1.02	-1.42	1.90
	1.5o	2.26	11.64	10.55	10.66	11.36
2	18.97	18.25	-3.13	-0.66	-1.94	2.07
	3.42	4.46	17.16	14.24	14.51	15.22
3	25.14	24.08	-3.64	-1.83	-2.69	2.03
	4.72	5.70	18.75	16.89	18.21	18.92
4	31.03	30.15	-4.14	-3.19	-3.44	1.05
	6.10	6.88	23.46	24.21	25.77	28.31
5	38.34	37.62	-5.36	-2.99	-3.68	0.60
	8.06	8.44	24.02	25.43	27.16	29.52
6	47.21	46.95	-7.14	-3.03	-4.06	0.65
	9.45	10.18	25.43	27.06	28.56	31.00
7	54.99	54.83	-6.61	-2.53	-4.58	0.95
	11.08	12.45	27.21	25.16	29.34	32.24
8	63.68	63.56	-7.16	-3.86	-4.37	0.06
	13.32	14.31	30.64	31.92	32.12	34.96

(III) STRAIN FIELD :
MEAN VALUES
STANDARD DEVIATIONS

POINT	XX-STRAIN R	XX-STRAIN L	YY-STRAIN R	YY-STRAIN L
1	0.66E-04	0.86E-04	-0.87E-04	-0.36E-04
	0.15E-03	0.42E-03	0.43E-02	0.36E-02
2	0.14E-03	0.19E-03	-0.57E-04	0.25E-04
	0.26E-03	0.51E-03	0.59E-02	0.50E-02
3	0.20E-03	0.24E-03	0.88E-05	0.22E-04
	0.36E-03	0.51E-03	0.63E-02	0.59E-02
4	0.25E-03	0.28E-03	0.75E-04	0.19E-04
	0.57E-03	0.55E-03	0.79E-02	0.87E-02
5	0.33E-03	0.35E-03	-0.78E-04	0.35E-04
	0.60E-03	0.64E-03	0.82E-02	0.90E-02
6	0.39E-03	0.43E-03	-0.92E-04	0.36E-04
	0.63E-03	0.66E-03	0.86E-02	0.96E-02
7	0.46E-03	0.53E-03	-0.39E-04	-0.24E-04
	0.66E-03	0.78E-03	0.91E-02	0.89E-02
8	0.56E-03	0.61E-03	-0.28E-04	-0.80E-04
	0.67E-03	0.10E-02	0.99E-02	0.11E-01

(IV) AVERAGED VALUES OF THE TWO SIDES:

	DEFORMATION X	DEFORMATION Y	DEFORMATION Z	STRAIN XX	STRAIN YY	STRAIN RATE
1	10.53	-1.46	0.24	0.75E-04	-0.62E-04	0.00E 00
2	18.61	-1.89	1.90	0.17E-03	-0.16E-04	0.63E-06
3	24.61	-2.74	-1.94	0.22E-03	0.16E-04	0.17E-06
4	30.59	-3.66	2.67	0.27E-03	0.47E-04	0.11E-06
5	37.98	-4.18	-2.69	0.34E-03	-0.22E-04	0.11E-06
6	47.08	-5.03	2.03	0.41E-03	-0.28E-04	0.73E-07
7	54.91	-4.57	-3.44	0.50E-03	-0.32E-04	0.65E-07
8	63.62	-5.51	1.05	0.58E-03	-0.54E-04	0.49E-07

CORRELATION COEFFICIENTS
AT TIME T= 2 25

ROW NO.	VMD T	VMD EXX	VMD EYY	T EXX	T EYY	BW EXX	BW EYY
1	0.112	-0.355	0.428	0.308	-0.087	-0.224	0.350
2	0.219	-0.540	-0.489	-0.238	-0.280	-0.642	-0.213
3	-0.397	-0.058	0.149	-0.072	-0.543	-0.111	0.322
4	0.473	0.274	0.275	0.185	0.365	0.202	0.152
5	0.118	-0.359	-0.181	0.042	0.273	-0.131	-0.070
6	-0.251	-0.185	0.282	0.030	-0.384	-0.150	0.462
7	0.051	0.217	0.242	-0.281	-0.373	0.340	0.205
8	0.282	0.578	0.574	0.296	-0.202	0.616	0.506
9	-0.445	-0.037	0.428	0.324	-0.655	-0.388	0.231
10	0.089	0.111	-0.023	-0.080	0.430	0.171	0.106
11	-0.080	0.489	-0.345	-0.198	-0.253	-0.039	-0.549
12	0.170	0.377	0.049	0.142	-0.549	0.189	0.028
13	-0.181	-0.162	0.432	-0.164	-0.315	-0.127	0.296
14	-0.013	-0.461	0.035	0.167	-0.877	-0.735	0.064
15	0.208	0.097	0.402	-0.405	0.155	0.272	0.390
16	0.146	0.418	-0.025	0.335	-0.618	0.365	-0.091
17	0.384	-0.149	-0.226	0.135	-0.496	-0.242	-0.493
18	0.189	0.118	0.483	-0.184	0.301	-0.319	0.692
19	0.289	0.064	0.058	-0.054	0.567	0.331	0.312
ENTIRE SAMPLE:	0.058	0.059	0.148	-0.011	-0.165	0.016	0.151

CORRELATION COEFFICIENTS
AT TIME T= 7 39

ROW NO.	VMD T	VMD EXX	VMD EYY	T EXX	T EYY	BW EXX	BW EYY
1	-0.009	-0.727	0.384	-0.569	0.350	-0.254	0.328
2	-0.435	-0.126	-0.332	-0.088	-0.076	-0.273	-0.104
3	-0.334	-0.431	0.016	-0.071	-0.422	-0.183	0.008
4	-0.425	0.164	0.512	-0.102	-0.251	0.103	0.317
5	-0.230	-0.378	-0.133	0.163	-0.533	-0.122	-0.230
6	0.392	-0.358	-0.358	-0.339	0.078	-0.149	-0.117
7	-0.139	0.130	0.388	0.617	0.104	0.030	0.036
8	-0.154	0.565	0.383	0.111	-0.388	0.496	0.337
9	-0.467	0.101	0.540	-0.294	0.556	0.033	0.144
10	0.013	-0.026	0.275	0.405	0.402	0.061	0.110
11	0.036	0.265	0.160	0.301	0.239	-0.037	-0.288
12	-0.088	0.433	0.464	-0.090	-0.630	0.188	0.455
13	0.460	-0.417	0.618	-0.619	0.391	-0.350	0.191
14	-0.145	-0.160	0.273	0.097	-0.615	-0.193	0.170
15	0.530	0.036	-0.231	-0.621	-0.002	-0.087	-0.194
16	0.168	0.335	0.050	0.165	-0.019	0.493	-0.253
17	-0.052	0.292	-0.270	-0.209	-0.046	-0.163	-0.728
18	0.217	-0.390	0.607	0.133	0.109	-0.383	0.290
19	-0.136	0.020	0.191	0.332	0.433	-0.047	0.447
ENTIRE SAMPLE:	-0.022	-0.008	0.201	-0.055	0.011	-0.004	0.072

CORRELATION COEFFICIENTS
AT TIME T=10 54

ROW NO.	VMD T	VMD EXX	VMD EYY	T EXX	T EYY	BW EXX	BW EYY
1	0.304	-0.677	0.193	-0.562	0.168	-0.557	0.295
2	-0.143	-0.113	-0.346	-0.308	-0.028	-0.237	-0.204
3	0.248	-0.318	-0.002	0.055	-0.091	-0.094	-0.324
4	-0.063	0.130	0.595	-0.129	-0.108	0.104	0.423
5	-0.125	-0.340	-0.056	0.319	-0.443	-0.029	-0.291
6	0.500	-0.306	-0.378	-0.215	-0.014	-0.263	-0.267
7	-0.100	0.223	0.411	0.640	-0.206	0.270	0.693
8	0.275	0.428	-0.306	0.414	-0.369	0.405	0.235
9	-0.064	0.167	0.528	0.132	0.565	0.083	0.444
10	0.205	-0.079	0.255	0.487	0.332	0.101	0.130
11	0.191	0.178	0.283	0.109	0.331	0.117	-0.034
12	0.050	0.339	0.275	0.075	-0.140	0.113	0.319
13	0.600	-0.309	0.649	-0.850	0.413	-0.581	0.367
14	0.215	-0.190	0.183	0.295	-0.645	-0.180	-0.020
15	0.586	0.149	-0.273	-0.528	0.154	-0.073	-0.197
16	0.416	0.428	0.001	0.547	-0.059	0.581	-0.179
17	0.476	0.312	-0.231	-0.299	-0.033	-0.195	-0.495
18	0.641	-0.431	0.612	0.055	0.012	-0.276	0.270
19	0.468	0.254	0.079	0.104	0.708	0.120	0.448
ENTIRE SAMPLE:	0.257	0.015	0.180	0.013	-0.008	0.002	0.091

CORRELATION COEFFICIENTS
AT TIME T=15 33

ROW NO.	VMD T	VMD EXX	VMD EYY	T EXX	T EYY	BW EXX	BW EYY
1	-0.065	-0.670	0.144	0.268	-0.043	-0.595	0.206
2	-0.045	-0.212	-0.507	-0.232	-0.502	-0.469	-0.343
3	-0.756	-0.190	0.188	0.023	-0.040	0.016	-0.322
4	0.501	0.053	0.543	0.643	0.393	0.042	0.374
5	-0.469	-0.242	-0.317	-0.146	-0.178	0.185	-0.397
6	0.581	-0.397	-0.337	0.057	-0.130	-0.165	-0.383
7	0.251	0.013	0.425	0.070	0.157	0.178	0.511
8	-0.399	0.394	0.276	0.118	-0.195	0.384	0.041
9	-0.074	0.177	0.435	0.164	-0.060	0.163	0.640
10	-0.164	0.159	0.225	0.079	0.255	0.265	0.114
11	-0.206	0.534	0.392	0.495	0.126	0.157	0.101
12	0.062	0.375	0.267	0.149	0.582	0.254	0.239
13	-0.455	-0.477	0.689	0.381	-0.344	-0.718	0.405
14	-0.150	0.036	0.144	0.345	0.150	-0.008	-0.420
15	-0.267	0.217	-0.020	0.116	-0.331	-0.120	0.123
16	-0.025	0.237	0.101	0.321	0.050	0.422	-0.092
17	-0.320	0.323	-0.434	0.218	0.202	-0.024	-0.501
18	0.102	-0.390	0.615	0.186	0.275	-0.265	0.164
19	-0.010	0.190	0.054	-0.055	0.209	-0.167	0.485
ENTIRE SAMPLE:	-0.124	0.033	0.181	0.129	0.005	0.002	0.068

CORRELATION COEFFICIENTS
AT TIME T=22 25

ROW NO.	VMD T	VMD EXX	VMD EYY	T EXX	T EYY	BW EXX	BW EYY
1	0.455	-0.637	-0.002	0.060	0.295	-0.451	0.167
2	-0.539	-0.285	-0.511	0.298	0.327	-0.646	-0.426
3	0.249	-0.055	0.135	-0.188	0.417	0.003	-0.512
4	0.302	-0.018	0.488	-0.003	0.417	0.093	0.347
5	0.217	-0.574	-0.335	-0.007	-0.421	0.007	-0.626
6	0.124	-0.177	-0.274	0.145	0.095	0.136	-0.281
7	-0.331	-0.043	0.394	-0.090	-0.067	0.231	0.596
8	0.027	0.374	0.252	0.149	-0.158	0.389	-0.023
9	0.028	0.311	0.377	0.066	0.531	0.291	0.639
10	-0.611	0.058	0.218	-0.260	-0.307	0.238	0.224
11	-0.228	0.698	0.396	-0.362	-0.450	0.574	-0.044
12	-0.050	0.253	0.228	-0.252	0.014	0.283	0.263
13	-0.092	-0.233	0.684	-0.228	-0.310	-0.665	0.347
14	0.233	-0.095	0.012	-0.287	-0.179	-0.088	-0.428
15	-0.296	0.164	-0.039	-0.325	0.015	-0.197	0.076
16	0.344	-0.022	0.095	-0.172	0.463	0.343	-0.114
17	0.017	0.356	-0.316	-0.470	0.151	0.049	-0.250
18	-0.696	-0.625	0.420	0.735	0.024	-0.355	0.049
19	0.405	0.176	-0.041	0.139	-0.201	-0.133	0.277
ENTIRE SAMPLE:	-0.045	-0.018	0.143	-0.064	0.037	-0.001	0.045

CORRELATION COEFFICIENTS
AT TIME T=29 9

ROW NO.	VMD T	VMD EXX	VMD EYY	T EXX	T EYY	BW EXX	BW EYY
1	-0.260	-0.689	-0.057	-0.241	-0.434	-0.431	0.070
2	0.057	-0.194	-0.636	-0.327	-0.518	-0.523	-0.329
3	0.012	-0.259	0.213	0.284	-0.142	-0.078	-0.311
4	-0.141	0.067	0.317	0.283	0.457	0.208	0.189
5	0.104	-0.565	-0.155	0.276	-0.193	0.073	-0.617
6	0.132	-0.004	-0.084	-0.065	-0.459	0.301	-0.006
7	-0.603	-0.149	0.469	-0.114	-0.342	0.118	0.544
8	0.473	0.483	0.211	0.316	0.308	0.435	-0.084
9	0.030	0.209	0.102	-0.419	0.360	0.223	0.591
10	-0.161	0.082	0.165	-0.078	-0.105	0.209	-0.039
11	-0.528	0.661	0.230	-0.237	0.086	0.504	-0.400
12	-0.220	0.164	0.158	0.623	0.111	0.168	0.276
13	-0.134	-0.286	0.551	0.009	0.625	-0.597	0.221
14	-0.178	-0.021	0.000	-0.754	-0.149	-0.087	-0.406
15	-0.233	0.074	0.072	0.290	-0.028	-0.434	0.125
16	0.251	-0.069	-0.047	-0.484	-0.072	0.125	-0.080
17	-0.231	0.437	-0.123	0.710	-0.217	-0.029	-0.070
18	-0.480	-0.630	0.392	0.280	-0.011	-0.081	0.067
19	0.101	0.054	0.063	0.286	-0.090	-0.091	0.214

ENTIRE SAMPLE: -0.125 -0.040 0.095 0.056 -0.059 -0.026 0.023

CORRELATION COEFFICIENTS
AT TIME T=41 59

ROW NO.	VMD T	VMD EXX	VMD EYY	T EXX	T EYY	BW EXX	BW EYY
1	-0.553	-0.695	0.106	-0.001	-0.080	-0.390	-0.041
2	-0.315	-0.275	-0.683	-0.012	0.718	-0.594	-0.569
3	-0.241	-0.260	0.173	-0.239	0.715	-0.069	-0.432
4	-0.538	0.158	0.476	-0.365	0.129	0.362	0.478
5	-0.280	-0.535	-0.136	0.267	0.033	0.084	-0.517
6	-0.255	-0.007	0.146	0.134	0.167	0.158	0.032
7	0.094	0.095	0.303	0.482	-0.044	0.212	0.237
8	-0.137	0.554	0.294	0.065	0.238	0.478	0.003
9	0.091	0.137	0.107	-0.708	0.314	0.120	0.595
10	-0.559	0.077	0.140	0.245	0.360	0.325	-0.110
11	-0.287	0.839	0.135	0.117	0.409	0.364	-0.580
12	-0.760	0.314	0.247	-0.074	-0.220	0.524	0.270
13	-0.494	-0.272	0.594	0.224	0.178	-0.605	0.189
14	-0.466	-0.101	0.019	0.285	0.613	-0.349	-0.567
15	-0.307	0.025	0.127	0.359	-0.678	-0.352	0.187
16	-0.418	0.029	-0.089	-0.379	0.579	0.148	-0.108
17	-0.473	0.366	-0.269	0.149	0.445	0.102	-0.310
18	0.110	-0.496	0.561	0.630	0.373	-0.079	0.193
19	-0.507	0.176	-0.101	-0.010	-0.261	0.051	0.305

ENTIRE SAMPLE: -0.333 0.009 0.089 0.071 0.190 0.020 -0.036